

**Investigating determinants of
sensitivity and resistance to T cell
redirecting antibodies in
colorectal cancer through patient
derived organoid models**

Maria Semiannikova

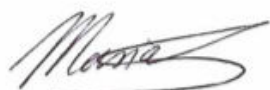
The Institute of Cancer Research
University of London

A thesis submitted for the degree of
Doctor of Philosophy
May 2023

Declaration

This thesis was completed under the supervision of Dr Marco Gerlinger and the work described here was carried out at Translational Oncogenomics Lab, Division of Molecular Pathology, The Institute of Cancer Research, 237 Fulham Road, SW3 6JB.

I, Maria Semiannikova, confirm that the work presented in this thesis is my own. Where others have made contributions or information has been derived from other sources this has been clearly referenced and acknowledged.

A handwritten signature in black ink, appearing to read 'Maria', with a long horizontal stroke extending to the right.

Signed: Maria Semiannikova

May 2023

COVID Statement of Impact

COVID-19 pandemic interrupted my studies in my third and fourth year of my PhD. Due to the shutting down of the institute because of the pandemic I was unable to perform experiments from 18/03/2020 until 08/06/2020 totalling 12 weeks. Additionally upon reopening in line with government safety guidelines the institute implemented social distancing rules which severely limited my ability to work. The nature of my project is such that all of my experiments are performed in tissue culture as I work with co-culturing of patient derived organoids and immune cells. Due to the new social distancing rules my lab only had access to one tissue culture hood instead of 3. Additionally, at the time my lab was processing samples from three clinical trials which meant that I had to dedicate a portion of my time to processing those and also these clinical samples were prioritised therefore I very frequently had to give up my already very limited time in tissue culture for those to be processed. Social distancing rules also affected access to core facilities such as flow cytometry and microscopy units further limiting my productivity. The social distancing rules were in place from 06/2020 to 08/2021 which is longer than a year therefore having a significant negative effect on my experimental work. The negative impact of the pandemic was further exacerbated by my lab relocating from the Institute of Cancer Research (ICR) to Barts Cancer Institute (BCI) at Queen Mary University of London as there were several months delay before I had access to the labs due to time needed for administrative approvals, mandatory health and safety training, getting access to institute/email/intranet/equipment booking systems. Additionally, BCI did not have some essential pieces of equipment that I require for my work while ICR no longer had any wet lab space available for me therefore I had to spend several months shuttling between the two institutes which further negatively affected my productivity. Due to the factors listed in this statement I received a 4 month extension from ICR.

Maria Semiannikova



Dr Marco Gerlinger



Abstract

Most colorectal cancers (CRCs) do not respond to treatment with immune-checkpoint-inhibitors due to modest mutation loads, low cytotoxic T cell infiltrates, and immunosuppressive microenvironments. The CEA-TCB bispecific antibody is a novel therapeutic agent that can help overcome the unfavourable immune landscape in CRC. CEA-TCB binds CD3 on T cells and targets them to the carcinoembryonic antigen (CEA) which is overexpressed on the cell surface of many CRC cells. Recent clinical trial data has shown that despite pre-selecting patients with CEA positive tumours only 11% treated with CEA-TCB monotherapy responded to the treatment. Mechanisms of resistance to T cell redirecting antibodies remain poorly understood, indicating a need for pre-clinical model systems that can be used to dissect the determinants of CEA-TCB response and resistance. It has been demonstrated that patient-derived organoids (PDO) may more accurately represent patient tumours than established cell lines.

The aim of my thesis was to use PDOs to investigate factors determining sensitivity and resistance to CEA-TCB therapy. After characterising CEA expression of eight PDOs generated from multi-drug resistant metastatic CRCs, three PDOs with persistently high CEA expression and good CEA-TCB response were selected to develop a co-culture technology of PDOs and allogeneic T cells which can be used to screen for microenvironmental factors that influence CEA-TCB activity. This model allowed me to evaluate the effect of different immunosuppressive cytokines and immune and stromal cell types commonly present in the CRC tumour microenvironment on CEA-TCB response. This screen revealed that TGF β , commonly overexpressed in CRCs, confers resistance to CEA-TCB by suppression of T cell cytolytic and proliferative abilities. I was able to reverse immunosuppressive effects of TGF β using a TGF β receptor inhibitor galunisertib, IL-2, and tumour targeted CEA-4-1BBL and stroma targeted FAP-IL2v bispecific T cell co-stimulatory agents, thus informing rational combination therapies for

clinical testing. The 3D configuration of this co-culture model was used to assess T cell infiltration into the PDOs and evaluate the impact of different PDO sizes and morphologies on CEA-TCB mediated killing of tumour cells. Distinct PDO morphologies as well as large organoid size did not impair T cell infiltration as CD8 T cells were able to penetrate into the centre of large organoids growing in different architectural patterns and showed strong killing activity. The versatile *in vitro* organoid and T-cell co-culture screening platform I developed can be used for identification of resistance mechanisms and rational combination therapies.

Acknowledgements

First and foremost, I would like to thank my supervisor, Marco Gerlinger, for adopting me into his lab after I lost my first lab at the ICR and giving me the opportunity to pursue a challenging but interesting project in his lab. Even during the most challenging times Marco was always full of enthusiasm and encouragement. I am thankful to him for his expertise, guidance, and passion for science which I found to be very contagious.

I would also like to thank all members of my lab, both past and present, for all of their help, support, scientific discussions, and practical advice over the past 4 years. In particular I would like to thank Beatrice Griffiths for teaching me how to work with organoids and for mentoring me which allowed me to become more independent in the lab. A massive thank you to Louise Barber for all of her help with sequencing, for inspiring me to always do good science, and for being instrumental to the good functioning of the lab. I am grateful to Reyes Gonzalez-Exposito as her work was the foundation for my PhD project. A special thank you to Alice and Marta, not only for useful scientific discussion but for always cheering me on and being my best supporters.

I also would like to extend my gratitude to the wider community at the ICR for creating such a wonderful environment to work in. I am grateful to Clare Isacke, Pascal Meier, Joanna Fearn, and Clare Gardner for supporting me during personally challenging times and ensuring I can still successfully complete this PhD. I want to thank all of the friends I had made at the ICR for always having my back, supporting me when experiments failed, and making working at the ICR a lot of fun.

I also want to thank my mom, who has always believed in me, even when I didn't believe in myself and for providing support even from thousands of miles away. Finally, I would like to thank my husband Damir for being with me through thick and thin, for your love and persistent encouragement. Without your unwavering belief in me and unconditional support I would not have been able to finish this PhD.

Table of contents

Declaration	2
COVID Statement of impact	3
Abstract	4
Acknowledgements	6
List of figures	12
List of tables	14
Abbreviations	15
1. Introduction	21
1.1 Colorectal cancer	21
1.1.1 Colorectal cancer carcinogenesis	21
1.1.2 Colorectal cancer subtyping	24
1.1.3 Colorectal cancer screening	25
1.1.4 Colorectal cancer staging	26
1.1.5 Current treatments of CRC	27
1.1.5.1 Chemotherapy	27
1.1.5.2 Targeted therapy	28
1.1.5.3 Immunotherapy	33
1.2 Immune system overview	34
1.2.1 The innate immune system	34
1.2.2 The adaptive immune system	36
1.3 The role of the adaptive immune system in cancer	40
1.4 Cancer immunoediting	45
1.5 The cancer-immunity cycle	47
1.5.1 Mechanisms of immune evasion	49
1.6 Cancer immunotherapy	56
1.6.1 Immune checkpoint blockade	57
1.6.2 Adoptive cell transfer/CAR T cell therapy	62
1.6.3 Bispecific antibodies	65
1.6.4 Immunotherapy in colorectal cancer	67
1.6.4.1 Immune checkpoint inhibitors	67
1.6.4.2 Immune checkpoint inhibitors in combination with chemotherapy	70
1.6.4.3 Immune checkpoint inhibitors in combination with anti-EGFR targeted therapy	71
1.6.4.4 Targeting LAG3 in colorectal cancer immunotherapy	71
1.6.4.5 CAR T cell therapy	72

1.6.4.6 T cell redirecting bispecific antibodies	73
1.7 PhD aims.....	77
2. Materials and methods	76
2.1 Materials.....	78
2.1.1 Tissue culture reagents	78
2.1.2 Advanced media supplements.....	79
2.1.3 Cytokines/Growth factors.....	80
2.1.4 Bispecific antibodies	80
2.1.5 Drugs	80
2.1.6 Flow cytometry.....	80
2.1.6.1 Antibodies	80
2.1.6.2 Viability dyes	81
2.1.6.3 Cell proliferation assay.....	81
2.1.7 Blocking antibodies.....	81
2.1.8 Commercial kits	82
2.1.9 Real-time quantitative polymerase chain reaction (RTqPCR) primers	82
2.1.10 Immunohistochemistry reagents.....	82
2.2 Methods	83
2.2.1 Patient samples	83
2.2.2 Tissue culture	83
2.2.2.1 Generation of patient derived organoids.....	83
2.2.2.2 Organoid passaging (3D configuration)	84
2.2.2.3 Adaptation of organoids to different media and 2D growth.....	85
2.2.2.4 Organoid passaging (2D configuration)	85
2.2.2.5 Organoid freezing	85
2.2.2.6 Organoid thawing.....	86
2.2.2.7 Labelling PDO with nuclear GFP	86
2.2.2.8 PBMC isolation	87
2.2.2.9 T cell isolation from PBMCs.....	88
2.2.2.10 T cell activation and expansion.....	88
2.2.2.11 CAF culture	89
2.2.2.12 Macrophage culture	89
2.2.3 2D co-culture assay	90
2.2.3.1 Calculating tumour cell growth in 2D co-culture assay	90
2.2.3.2 2D co-culture assay with tankyrase inhibitor Compound 21	91
2.2.3.3 2D co-culture assay: IFN γ and FasL blocking	91
2.2.3.4 TME soluble factors screen using 2D co-culture	91

2.2.3.5 Treatment of co-cultures with agents countering TGF β induced immunosuppression.....	92
2.2.3.6 2D co-culture assay with the addition of macrophages	92
2.2.3.7 2D co-culture assay with the addition of CAF conditioned media	93
2.2.3.8 2D co-culture assay with the addition of CAFs	93
2.2.3.9 2D co-culture assay under hypoxic conditions.....	94
2.2.4 Sensitivity of PDOs to IFN γ growth assay	94
2.2.5 Validation of IFN γ blocking antibody.....	95
2.2.6 Validation of FasL blocking antibody	95
2.2.7 Flow cytometry.....	95
2.2.7.1 Surface CEA expression.....	95
2.2.7.2 Flow cytometry analysis of T cells recovered from 2D co-culture assay.....	97
2.2.7.3 Surface Fas expression in PDOs.....	98
2.2.7.4 Analysis of M2 macrophage markers.....	98
2.2.8 3D PDO-T cell co-culture assay	99
2.2.9 Real-time quantitative polymerase chain reaction (RTqPCR)	101
2.2.10 RNA sequencing.....	102
2.2.11 Immunohistochemistry: CEA staining of FFPE tissue sections	103
2.2.11.1 CRC xenografts	103
2.2.11.2 PDO preparation for FFPE slides	103
2.2.11.3 CEA immunohistochemical staining of FFPE slides	103
2.2.12 Measuring patient tumour nest size.....	104
2.2.13 Statistics	105
3. Investigating factors regulating CEA expression in CRC patient derived organoids	106
3.1 Introduction	106
3.2 CEA expression in patient derived organoids (PDOs) grown in 2D	107
3.3 CEA expression in PDOs grown in 3D.....	112
3.4 Immunohistochemical analysis of CEA expression in PDOs and tumour tissue	114
3.5 Effect of PDO-T cell co-culturing conditions of CEA expression in 2D PDO..	116
3.6 Effect of cell growth density on CEA expression.....	118
3.7 IFN γ increases CEA expression in CEA-mixed PDOs.....	119
3.8 Advanced media downregulates CEA expression in CEA-high PDOs	121
3.9 Identifying advanced media components responsible for CEA downregulation in CEA-high PDOs	125

3.10 Gene set enrichment analysis (GSEA) reveals pathways enriched in p38 inhibitor and nicotinamide treated PDOs.....	132
3.11 Discussion.....	133
4. Developing and validating a robust and versatile T cell and CRC PDO co-culture platform for pre-clinical CEA-TCB research	137
4.1 Introduction	137
4.2 Optimisation and validation of PDO-T cell co-culture model.....	139
4.2.1 Co-culture model experimental set-up.....	139
4.2.2 CEA-TCB activity against PDOs with different CEA expression profiles	141
4.2.3 Inter- and intra-donor variability as a caveat of co-culture assay	143
4.2.4 Comparing PDO growth inhibition efficacy of in vitro pre-activated and non-activated CD8 T cells	146
4.3 Investigating whether Wnt/ β -catenin inhibition increases CEA expression and sensitivity to CEA-TCB therapy	148
4.3.1 Treatment of CEA-mixed PDOs with tankyrase inhibitor increases CEA expression	148
4.3.2 Tankyrase inhibition sensitises CEA-mixed PDOs to CEA-TCB treatment	151
4.3 Assessing the contribution of CD8 and CD4 T cells to CEA-TCB mediated tumour cell growth control	154
4.4 Investigating effector mechanisms of CD8 versus CD4 T cells	157
4.4.1 Granzyme B expression in CD8 and CD4 T cells activated by CEA-TCB	158
4.4.2 Role of Fas/FasL axis in CD8 and CD4 T cells mediated PDO growth control	165
4.4.3 Role of IFN γ in CD8 and CD4 T cell mediated PDO growth control.....	168
4.5 Discussion	172
5. Investigating effect of microenvironmental factors commonly found in CRC on CEA-TCB activity	178
5.1 Introduction	178
5.2 Investigating effect of IL-10 on CEA-TCB activity using PDO-T cell co-culture model	180
5.3 Investigating effect of VEGF on CEA-TCB activity using PDO-T cell co-culture model	185
5.4 Investigating effect of hypoxia on CEA-TCB activity using PDO-T cell co-culture model.....	188
5.5 Investigating effect of TGF β on CEA-TCB activity using PDO-T cell co-culture model	192
5.5.1 TGF β confers resistance to CEA-TCB	194
5.5.2 TGF β inhibits CD8 T cell proliferation and reduces granzyme expression	197

5.6 TGF β blockade and IL-2 overcome TGF β mediated CEA-TCB resistance ...	199
5.7 Novel stroma-targeted IL2v and tumour-targeted 4-1BBL bispecific antibody reverse TGF β induced immunosuppression	201
5.8 Incorporation of macrophages into the PDO-T cell co-culture model	208
5.8.1 Macrophage polarization towards M2 phenotype	210
5.8.2 Effect of M2 macrophages on CEA-TCB activity	212
5.9 Incorporation of CAFs into the PDO-T cell co-culture model	214
5.10 Discussion.....	220
6. Establishing a 3D PDO-T cell co-culture model to investigate T cell infiltration and killing of organoids in response to CEA-TCB	226
6.1 Introduction	226
6.2 Establishment of 3D PDO-T cell co-culture model.....	229
6.2.1 Optimisation of organoid harvesting	230
6.2.2 Matrix selection.....	231
6.2.3 T cell infiltration analysis.....	233
6.3 Investigating T cell infiltration into PDOs using 3D co-culture model.....	236
6.4 Establishment of cancer cell death readout	241
6.5 Effect of organoid size and morphology on T cell infiltration.....	244
6.5.1 T cell infiltration into organoids of different sizes	247
6.5.2 Effect of organoid size on T cell mediated killing of tumour cells	249
6.6 Increasing complexity of 3D co-culture model by adding a stromal component	251
6.7 Discussion.....	254
7. Final discussion and future perspectives.....	261
8. References	278

List of figures

Figure 1.1 Adenoma to carcinoma sequence in CRC	23
Figure 1.2 The cancer-immunity cycle.....	48
Figure 1.3 Four main phenotypes of anticancer immunity: hot, cold, excluded, and immunosuppressed	68
Figure 3.1 Patient derived organoid (PDO) growth in 2D and 3D	108
Figure 3.2 CEA antibody titration	109
Figure 3.3 CEA expression in PDOs grown in 2D	110
Figure 3.4 CEA expression in PDOs grown in 3D	113
Figure 3.5 Immunohistochemistry (IHC) analysis of CEA expression in PDOs and tumour tissue	115
Figure 3.6 Effect of PDO-T cell co-culture conditions on CEA expression of 2D PDOs	117
Figure 3.7 Effect of cell density on CEA expression in PDOs	118
Figure 3.8 Effect of IFN γ on CEA expression in PDOs	120
Figure 3.9 Effect of advanced media on CEA expression in 2D PDOs	122
Figure 3.10 Effect of FCS on CEA surface expression in CEA-high PDOs.....	125
Figure 3.11 Effect of different advanced media components on CEA expression in CEA-high PDOs	127
Figure 3.12 Effect of nicotinamide and p38 MAP kinase inhibitor SB202190 on CEA expression in 2D PDOs	129
Figure 3.13 Temporal regulation of CEA surface expression.....	131
Figure 3.14 GSEA of SB202190 and nicotinamide treated CEA-high PDOs	132
Figure 4.1 PDO-T cell co-culture experimental set-up	140
Figure 4.2 Assessment of CEA-TCB efficacy in CEA-high and CEA-mixed PDOs.....	142
Figure 4.3 Donor variability in ability to inhibit PDO growth.....	144
Figure 4.4 Comparison of pre-activated and non-activated CD8 T cell PDO growth control.....	147
Figure 4.5 Wnt/ β -catenin signalling pathway.....	149
Figure 4.6 Effect of tankyrase inhibition on CEA expression in CEA-mixed PDOs	150
Figure 4.7 Effect of tankyrase inhibitor Compound 21 on sensitivity of PDOs to CEA-TCB treatment	153
Figure 4.8 Comparing CD8 and CD4 T cell mediated PDO growth inhibition	156
Figure 4.9 Granzyme B expression in CD8 and CD4 T cells treated with CEA-TCB ..	160
Figure 4.10 Role of Fas/FasL pathway in CEA-TCB mediated killing of PDOs.....	167

Figure 4.11 Sensitivity of PDOs to IFN γ	169
Figure 4.12 IFN γ blocking in PDO-T cell co-culture assay	171
Figure 5.1 Effect of IL-10 on CEA-TCB activity	183
Figure 5.2 Effect of VEGF on CEA-TCB activity.....	186
Figure 5.3 Effect of hypoxia on CEA-TCB activity	190
Figure 5.4 Effect of TGF β on CEA-TCB activity	195
Figure 5.5 TGF β decreases granzyme expression and inhibits proliferation of CD8 T cells	198
Figure 5.6 Galunisertib and IL-2 reverse immunosuppressive effects of TGF β	200
Figure 5.7 Effect of FAP-IL2v and 4-1BBL-CEA on CEA-TCB activity	202
Figure 5.8 FAP-IL2v and 4-1BBL-CEA in combination with CEA-TCB reverse immunosuppressive TGF β effect	205
Figure 5.9 FAP-IL2v and 4-1BBL-CEA differentially increase TGF β inhibited proliferation and granzyme B expression	207
Figure 5.10 Macrophage polarisation to M2 phenotype	211
Figure 5.11 Macrophages enhance CEA-TCB mediated PDO growth inhibition by T cells	213
Figure 5.12 Effect of CAF conditioned media and CAFs on CEA-TCB activity	218
Figure 6.1 Experimental workflow of setting up a 3D CRC PDO and T cell co-culture model.....	229
Figure 6.2 Different methods of organoids harvesting.....	230
Figure 6.3 Collagen-Matrigel matrix supports PDO growth and T cell migration.....	232
Figure 6.4 T cell migration analysis	234
Figure 6.5 T cell infiltration analysis	235
Figure 6.6 CD8 T cell infiltration into PDOs quantification.....	238
Figure 6.7 Images of T cell infiltration into PDOs and T cell mediated tumour cell death	240
Figure 6.8 Quantifying cancer cell death in 3D co-culture assay	243
Figure 6.9 Effect of organoid morphology on T cell infiltration	245
Figure 6.10 Comparison of patient tumour nest and PDO size	246
Figure 6.11 Quantification of T cell infiltration into organoids of different size	248
Figure 6.12 Tumour cell killing by CD8 T cells	250
Figure 6.13 Incorporation of CAFs to 3D PDO-T cell co-culture	253

List of tables

Table 2.1 Tissue culture reagents	78
Table 2.2 Advanced media supplements	79
Table 2.3 Cytokines/growth factors	80
Table 2.4 Bispecific antibodies	80
Table 2.5 Drugs	80
Table 2.6 Flow cytometry antibodies	80
Table 2.7 Viability dyes	81
Table 2.8 Blocking antibodies.....	81
Table 2.9 Commercial kits	82
Table 2.10 Real-time quantitative polymerase chain reaction (RTqPCR) primers	82
Table 2.11 Immunohistochemistry reagents.....	82

List of abbreviations

ACK	Ammonium–chloride–potassium
ACT	Adoptive cell transfer
ADCC	Antibody-dependent cellular cytotoxicity
AICD	Activation induced cell death
ALL	Acute lymphoblastic leukemia
APC	Antigen presenting cell
APM	Antigen processing machinery
BCMA	B-cell maturation antigen
BCN	Breast cancer now
BCR	B cell receptor
BiTEs	Bi-specific T cell engager
BSA	Bovine serum albumin
C21	Compound 21
CAC	Colitis-associated cancer
CAF	Cancer associated fibroblast
CAR	Chimeric antigen receptor
CCL	Chemokine (C-C motif) ligand
CCR	Chemokine (C-C motif) receptor
CD	Crohn's disease
CD	Cluster of differentiation
CDK	Cyclin-dependent kinase
CEA	Carcinoembryonic antigen
CEA-TCB	Carcinoembryonic antigen T cell bispecific
CIMP	CpG island methylator phenotype
CIN	Chromosomal instability
CK1	Casein kinase 1
CM	Conditioned media
CMS	Consensus molecular subtype
COX	Cyclooxygenase
CRC	Colorectal cancer
CSF	Colony stimulating factor

CTA	Cancer testis antigen
CTB	Cell Titer Blue
CTL	Cytotoxic T lymphocyte
CTLA-4	Cytotoxic T lymphocyte associated protein
CXCL	Chemokine (C-X-C motif) ligand
DAB	3,3'-Diaminobenzidine
DC	Dendritic cell
DI	Deionised
DLL3	Delta-like ligand 3
DMEM	Dulbecco's Modified Eagle Medium
DMSO	Dimethyl sulfoxide
DNA	Deoxyribonucleic acid
DR	Death receptor
DRAQ7	Deep Red Anthraquinone 7
ECM	Extracellular matrix
EDTA	Ethylenediaminetetraacetic acid
EGF	Epidermal growth factor
EGFR	Epidermal growth factor receptor
EMT	Epithelial to mesenchymal transition
EpCAM	Epithelial cell adhesion molecule
ETbR	Endothelin B receptor
FACS	Fluorescence-activated cell sorting
FADD	FAS-associated death domain protein
FAP	Fibroblast activation protein
Fas-L	Fas ligand
FBS	Foetal bovine serum
Fc	Fragment crystallisable
FcR	Fragment crystallisable receptor
FcRn	neonatal Fc receptor
FCS	Foetal calf serum
FDA	Food and drug administration
FFPE	Formalin-fixed paraffin-embedded

FGF	Fibroblast growth factor
FIT	Faecal immunochemical test
FMO	Fluorescence minus one
Foxp3	Forkhead box P3
GAGs	Glycosaminoglycans
GAPDH	Glyceraldehyde 3-phosphate dehydrogenase
GFP	Green fluorescent protein
GM-CSF	Granulocyte-macrophage colony-stimulating factor
GSEA	Gene set enrichment analysis
GZMA	Granzyme A
GZMB	Granzyme B
HDAC	Histone deacetylases
HER	Human epidermal growth factor receptor
HGF	Hepatocyte growth factor
HIF-1a	Hypoxia Inducible Factor 1 Subunit Alpha
HLA	Human leukocyte antigens
HPV	Human papilloma virus
HRP	Horseradish peroxidase
HSC	Hematopoietic stem cells
IBD	Inflammatory bowel disease
ICAM	Intercellular adhesion molecule
ICI	Immune checkpoint inhibitor
IDO	Indoleamine 2,3-dioxygenase
IFN	Interferon
IL	Interleukin
irAEs	Immune related adverse events
ITAMs	Immunoreceptor tyrosine-based activation motif
ITS	Insulin-Transferrin-Selenium
JAK	Janus kinase
LAG-3	Lymphocyte-activation protein 3
LAP	Latency-associated protein
LEF	Lymphoid enhancer factor

LFA-1	Lymphocyte function-associated antigen 1
LGR5	Leucine-rich repeat-containing G-protein coupled receptor 5
LOH	Loss of heterozygosity
LOX	Lysyl oxidase
LPS	Lipopolysaccharides
LRS	Leukocyte reduction system
LTBP	Latent-TGF- β -binding protein
LV	Leucovorin
M- CSF	Macrophage colony-stimulating factor
MAPK	Mitogen-activated protein kinases
MCL	Mantle cell lymphoma
mCRC	Metastatic colorectal cancer
mCRPC	Metastatic castration-resistant prostate cancer
MCTS	Multicellular tumour spheroids
MDSC	Myeloid derived suppressor cells
MFI	Mean fluorescence intensity
MHC	Major histocompatibility complex
MMP	matrix metalloproteinases
MMR	Mismatch repair
mRNA	Messenger ribonucleic acid
MSI	Microsatellite instable
MSS	Microsatellite stable
NAC	N-Acetyl-L-cysteine
NHL	Non Hodgkin lymphoma
NHS	National health service
NK	Natural killer
NO	Nitric oxide
ORR	Objective response rate
OS	Overall survival
PAMPs	Pathogen associated molecular patterns
PBMCs	Peripheral blood mononuclear cells
PBS	Phosphate buffered saline

PD	Progressive disease
PD-1	Programmed cell death protein 1
PD-L1	Programmed death ligand-1
PDO	Patient derived organoid
PFS	Progression free survival
PGE2	Prostaglandin E ₂
PGs	Proteoglycans
PHA	Phytohemagglutinin
PI3K	Phosphoinositide 3-kinase
PIGF	Placental growth factor
PMSA	Prostate specific membrane antigen
PRRs	Pattern recognition receptors
PSA	Prostate specific antigen
qPCR	Quantitative polymerase chain reaction
RNA	Ribonucleic acid
ROS	Reactive oxygen species
RPMI	Roswell Park Memorial Institute
RR	Response rate
SOC	Standard of care
TAM	Tumour associated macrophage
TAP	Transporter associated with antigen processing
TBS	Tris buffered saline
Tcm	Central memory T cell
TCR	T cell receptor
TGFβ	Transforming growth factor beta
TGF-βR	Transforming growth factor beta receptor
Th	T helper cell
TIGIT	T-cell immunoreceptor with immunoglobulin and ITIM domains
TIL	Tumour infiltrating lymphocyte
TIM3	T cell immunoglobulin and mucin-domain containing-3
TKI	Tyrosine kinase inhibitor
TLR	Toll like receptor

TMB	Tumour mutational burden
TME	Tumour microenvironment
TNF α	Tumour necrosis factor alpha
TNM	Tumour, node, metastasis
TRAIL	Tumour necrosis factor-related apoptosis-inducing ligand
Treg	Regulatory T cell
TRUCK	CAR T cells redirected for universal cytokine killing
UC	Ulcerative colitis
VCAM	Vascular cell adhesion molecule
VEGF	Vascular endothelial growth factor
VEGFR	Vascular endothelial growth factor receptor
VLA-1	Very late antigen-1
WT	Wild type

Chapter 1 Introduction

1.1 Colorectal cancer

Colorectal cancer is the third most commonly diagnosed cancer in males and the second most common in females and the second leading cause of cancer mortality worldwide accounting for approximately 880,000 deaths in 2018 (Bray et al., 2018; Torre et al., 2015). The global burden of CRC is expected to increase by 60% to more than 2.2 million new cases and 1.1 million deaths by 2030 (Ferlay et al., 2015).

1.1.1 Colorectal cancer carcinogenesis

CRC develops when intestinal epithelial cells acquire a series of genetic and epigenetic changes that enable them to escape normal restraints on cell growth, leading to uncontrolled proliferation. In 1990 Vogelstein and Fearon described an adenoma to carcinoma carcinogenesis model that outlines sequential acquisition of genetic and epigenetic alterations allowing tumours to evolve from benign to malignant lesions (Fearon & Vogelstein, 1990) (Figure 1.1). Their proposed model is a combination of the following features: mutational activation and/or inactivation of tumour suppressor genes, somatic mutations of at least four or five genes must occur for the tumour to become malignantly transformed, and it is the accumulation of multiple genetic mutations rather than the order that is important. First, a gatekeeping mutation usually in the *APC* gene, gives a normal epithelial cell a growth advantage allowing it to outgrow its surrounding cells and become a small adenoma. Through its interaction with transcriptional factor β -catenin, APC regulates the transcription of a number of cell proliferation genes, therefore a mutation in this gene leads to uncontrolled cell proliferation and adenoma growth. Acquisition of a second mutation in a proto-oncogene such as KRAS results in a constitutively active oncogene signalling leading to further increased proliferation and clonal expansion. The second key genetic step in the transition of large adenomas into invasive carcinomas is inactivation of the p53 pathway by mutation of *TP53*. In most

tumours, both TP53 alleles are inactivated, usually by a combination of a missense mutation that inactivates the transcriptional activity of p53 and a 17p chromosomal deletion that eliminates the second TP53 allele (Baker et al., 1989, 1990; Grady & Markowitz, 2003). P53 regulates cell growth and division and can be activated by multiple cellular stresses. TP53 normally acts as a tumour suppressor gene by inducing genes that can cause cell cycle arrest or apoptosis therefore its inactivation leads to unrestrained proliferation. Subsequent mutations in genes such as *PIK3CA* and *SMAD4* occur eventually generating a malignant tumour. Although the exact amount of time for an adenoma to progress to a carcinoma has not been established it has been estimated to take over 10 years on average (Nguyen & Duong, 2018). The two main mechanisms responsible for accumulation of mutations are chromosomal instability and microsatellite instability. Chromosomal instability is observed in 70% of sporadic colorectal cancers and results in gains or losses of whole or large portions of chromosomes leading to aneuploidy and loss of heterozygosity (LOH). Microsatellite instability occurs in about 15% of CRC and results from mutations in DNA mismatch repair (MMR) genes such as *MLH1*, *MSH2*, *MSH6*, and *PMS2* or hypermethylation of *MLH1*. Inactivation of these genes can result in a DNA defect during DNA replication in repetitive sequences (microsatellites) resulting in the accumulation of frameshift mutations and base-pair substitutions. Another molecular pathway leading to development and progression of CRC is the hypermethylation of CpG islands commonly found in gene promotor regions resulting in silencing of tumour suppressor genes and these tumours are classified as the CpG island methylator phenotype (CIMP). Sporadic CRC is the most common type of CRC accounting for about 75% of cases. Of the remaining 25% about 20% are familial CRC with familial history of CRC but no inherited syndrome and 5% is inherited predisposition to CRC. Inherited CRC occurs in people with syndromes characterised by germline mutations in genes such as *APC* and MMR genes (most commonly *MLH1*, *MSH2*, or *MSH6*) that increase the risk of CRC development such as familial adenomatous polyposis (FAP) and Lynch Syndrome respectively (Valle et al., 2019).

Individuals with FAP start to develop hundreds of colon polyps in their mid-teens that with a high probability will develop into cancer. Individuals with unrecognised or untreated FAP will be diagnosed with CRC before the age 35-40.

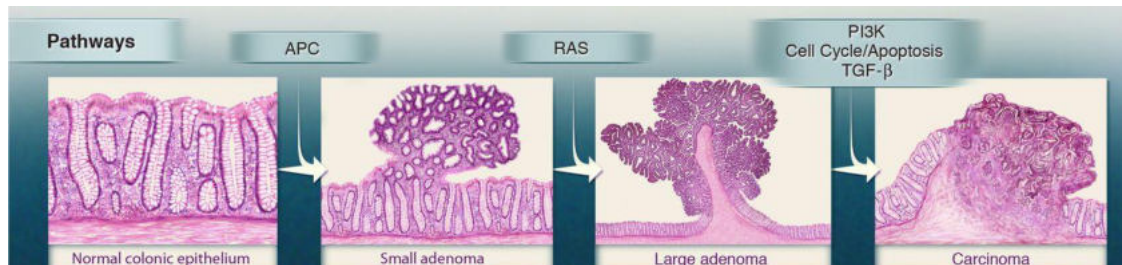


Figure 1.1 Adenoma to carcinoma sequence in CRC. Image taken from (Volgelstein et al., 2013)

Transformation of a normal cell into cancer is not only dependant on genetic aberrations in tumour cells but can also be promoted by microenvironmental factors such as inflammation. Chronic inflammation is a hallmark of cancer and 1-2% of CRC arise in patients with inflammatory bowel disease (IBD) such as ulcerative colitis (UC) and Crohn's disease (CD) known as colitis-associated cancer (CAC) ((Hanahan & Weinberg, 2011; Waldner & Neurath, 2009). Although that comprises a small fraction of CRC cases patients are among those at greatest risk of CRC in the general population. The molecular mechanisms by which inflammation promotes cancer development are not yet well characterised and may differ between CAC and other forms of colorectal cancer, but roles of specific cytokines and immune cells in the initiation and progression of CRC have been elucidated. IL-6 is an inflammatory cytokine secreted by cancer associated fibroblasts and several types of immune cells including macrophages in CRC (Nagasaki et al., 2013; Naugler & Karin, 2008; B. Zhong et al., 2021). IL-6 is overexpressed in CRC tissues and elevated in serum of CRC patients and it has been associated with larger tumour size, occurrence of liver metastasis, and reduced survival (Chung & Chang, 2003; Galizia et al., 2002; Knüpfner & Preiss, 2010; Komoda et al., 1998). Using an AOM+DSS mouse model of CAC in which repeated DSS administration causes chronic inflammation, thereby mimicking IBD, it has been demonstrated that IL-6 secreted by

lamina propria T cells and myeloid cells is a critical tumour promoter during early CAC tumorigenesis (Becker et al., 2004; Grivennikov et al., 2009). Treatment with anti-IL-6R antibodies or generation of *il6*^{-/-} mice protected mice from colon carcinogenesis. IL-6 enhanced the proliferation of intestinal epithelial cells and increased their resistance to apoptosis (Grivennikov et al., 2009). STAT3, transcription factor downstream of IL-6R, has been shown to drive *IL6* gene expression resulting in a feedforward autocrine feedback loop further promoting tumour growth (Q. Chang et al., 2013). Ablation of STAT3, in intestinal epithelial cells effectively inhibits CAC induction and growth, demonstrating the critical oncogenic function of this inflammatory cytokine in CRC and that tumour microenvironment also makes a major contribution to tumour development and progression (Grivennikov et al., 2009).

1.1.2 Colorectal cancer subtyping

CRC is a molecularly heterogeneous disease that can be classified based on key genetic mutations. Roughly 40% of patients with metastatic colorectal cancer have somatic activating KRAS mutations (Cunningham et al., 2010). KRAS is a member of the Ras family of small GTPases. Mutations in KRAS leads to constitutive activation resulting in activation of both RAF-MEK-ERK1/2 (mitogen-activated protein kinase, MAPK) and PI3K-AKT-mTOR signalling pathways promoting cell survival and apoptosis suppression (Downward, 1998). Patients with KRAS mutated mCRC, especially those with a G12D mutation, have a significantly worse progression free survival (PFS) in response to chemotherapy (Zocche et al., 2015). Mutations that activate BRAF, the main downstream effector of KRAS, arise in 8-10% of metastatic CRC and are mutually exclusive with *KRAS* mutations (Cunningham et al., 2010). A missense mutation leading to a valine to glutamic acid amino acid substitution (V600E) is the most frequent BRAF mutation (Ikenoue et al., 2003). Mutations in BRAF lead to constitutive activation of the MAPK signalling pathway mimicking the biological consequences of KRAS mutation. BRAF V600E mutations are more prevalent in microsatellite instable (MSI) tumours than

in microsatellite stable (MSS) tumours (Dienstmann et al., 2017). Patients with *BRAF* and *KRAS* mutation positive tumours have a significantly worse survival than that for patients with wild-type *KRAS* and *BRAF* when treated with chemotherapy (Souglakos et al., 2009; Yokota et al., 2011). A more recent molecular classification of CRC was created using gene expression profiling called consensus molecular subtypes (CMS) which identified four CRC subgroups with distinguishing features (Guinney et al., 2015). Tumours in the CSM1 (MSI, 14%) subgroup are hypermutated, microsatellite unstable, have a defective DNA MMR system, are strongly immunogenic, have *BRAF* mutations, and have a CpG island methylator phenotype (CIMP). CMS2 (canonical, 37%) group is characterised by high chromosomal instability (CIN), activation of Wnt and c-Myc signalling, and epithelial differentiation. CMS3 (metabolic, 13%) tumours have marked metabolic deregulation and contain *KRAS* mutations. Tumours in the CMS4 (mesenchymal, 23%) exhibit high TGF β signalling, upregulation of genes implicated in epithelial-to-mesenchymal transition (EMT), angiogenesis, and stromal infiltration. Guinney and colleagues also found clinical and prognostic associations with the four CMS. For example, patients with CMS4 tumours tended to be diagnosed at more advanced stages (III and IV) and have a worse overall survival (OS) than the other three groups. This classification system allows for a better understanding of a heterogeneous disease like colorectal cancer and can have several potential applications in clinical practice such as guiding treatment decisions and predicting prognosis.

1.1.3 Colorectal cancer screening

In a cancer that is characterised by gradual development such as CRC screening is essential in order to catch it at an early enough stage for successful treatment and better prognosis. Most colorectal cancers develop from adenomas (polyps), but only about 5% of polyps progress to colorectal cancer. Approximately 40% of people at age 50 or older have one or more adenomatous polyps therefore it is important to identify those polyps and remove them prior to cancer transition (Shussman & Wexner, 2014). Colorectal

cancer screening in the UK is offered to individuals between the ages 50 and 74 every two years and usually conducted through the use of faecal immunochemical test (FIT) which detects haemoglobin in the stool. FIT is the preferred method for CRC screening due to its good sensitivity, low cost, ease of use, and non-invasiveness. If the FIT is positive then people are offered a colonoscopy which is a more invasive but more robust as it allows an examination of the whole colon and can be used to immediately remove pre-cancerous polyps. However, studies shown that because of the invasiveness of a colonoscopy more people participate in screening when FIT is offered instead of a colonoscopy (Quintero 2012). Screening with FIT (annually or biannually) reduces CRC incidence and decreases mortality by about 30% further emphasizing the value of screening CRC (Mandel et al., 2000; Saito et al., 1995; Shaukat et al., 2013). Other effective strategies for screening include identifying and monitoring high-risk populations including families with hereditary CRC syndrome and individuals with inflammatory bowel disease.

1.1.4 Colorectal cancer staging

CRC staging determines the extent of cancer in the body which is essential for determining appropriate treatment options and predicting patient's prognosis. One of the commonly used staging systems is the number stages system classifying cancers into stage I-IV based on the extent of tumour invasion, lymph node involvement, and presence of distant metastasis. Stage I is characterised by the invasion of cancer cells into the deeper layers of the colon and rectum, but not the surrounding tissue. At this stage the cancer is localised and has not spread to nearby lymph nodes or other parts of the body. Tumours at stage II are larger and has spread into the outer wall of the colon or rectum or into tissue and organs next to them. Tumours classified as stage III have spread to nearby lymph nodes, but not other parts of the body. Finally, stage IV CRC is characterised by spread of cancer cells to other parts of the body (distant metastasis) most frequently to the liver, but also to the lungs. Tumour staging is further detailed with

the TNM staging system which stands for Tumour, Node, Metastasis. The Tumour component of TNM refers to the extent of the primary tumour, the Node component to the presence of cancer cells in the lymph nodes near the primary tumour, and the Metastasis component describes the spread of cancer to other parts of the body(Compton et al., 2004).

1.1.5 Current treatments of CRC

1.1.5.1 Chemotherapy

While many stage I- III cancers are curable with surgery which is combined with adjuvant chemotherapy for high risk stage II and for stage III CRCs, with survival rates ranging from 70-90%, the 5-year survival rate for metastatic CRCs remains below 10% (O'Connell et al., 2004). About 25% of patients present with metastasis at initial diagnosis and almost 50% of patients with CRC will develop metastasis (Van Cutsem et al., 2014). Some patients with metastatic disease receive chemotherapy treatment prior to metastasis resection to reduce the number and size of metastasis and enable subsequent surgical resection. Patients with disseminated unresectable CRC receive chemotherapy treatment. The standard of care treatment for mCRC consists of 5-fluorouracil (5-FU) in different combinations and schedules. Combination of 5-FU with leucovorin (LV) and oxaliplatin (FOLFOX) or with LV and irinotecan (FOLFIRI) remain the mainstream approaches in first-line treatment of mCRC (Van Cutsem et al., 2014). 5-FU is an antimetabolite drug that exerts its anticancer effects in conjunction with LV by inhibiting thymidylate synthase and incorporation of its metabolites into RNA and DNA thus inhibiting protein synthesis and cell division (Longley et al., 2003). Irinotecan inhibits the action of topoisomerase I preventing religation of the DNA strand causing double strand DNA breakage (Fujita et al., 2015). Oxaliplatin leads to G2/M arrest and apoptosis by forming intra-strand links between adjacent guanine residues, thus disrupting DNA replication and transcription (Arango et al., 2004). Each of these chemotherapy mechanisms results in cell death in CRC cells that are sensitive to these agents.

1.1.5.2 Targeted therapy

However, chemotherapy treatment has several important limitations such as systemic toxicity, unsatisfying response rates, and innate and acquired resistance. Therefore, a lot of research has been conducted to develop new treatment strategies. Targeted therapy drugs selectively target cancer cells while minimising damage to normal cells. One of the most common targets for targeted therapy is EGFR (epidermal growth factor receptor) which is overexpressed in about 70% of CRCs (Porębska et al., 2000). Binding of ligands to EGFR results in activation of the tyrosine kinase domain and subsequent activation of various downstream intracellular signalling pathways, including the RAS/RAF/MEK/ERK, PI3K/AKT, and JAK/STAT3 pathways, that promote cell growth, survival, and migration. Due to its overexpression it makes it an attractive target for cancer therapy. Monoclonal antibodies such as cetuximab and panitumumab bind the extracellular part of the receptor inhibiting ligand binding and subsequent signal transduction. Although as monotherapy cetuximab was effective, combination therapy of FOLFIRI/FOLFOX with cetuximab or panitumumab has shown increased response rates, overall survival, and progression free survival compared with cetuximab alone or chemotherapy alone (Cunningham et al., 2004; Douillard et al., 2010, 2014; Qin et al., 2018; Van Cutsem et al., 2009).

However, only patients with wild-type KRAS, a small G-protein downstream of EGFR, benefit from this therapy. Mutations in this gene, commonly at codons 12 and 13, cause constitutive activation of KRAS-signalling in about 35% of CRC making EGFR targeting therapies ineffective (Amado et al., 2015; Cunningham et al., 2004; Karapetis et al., 2008; Lièvre et al., 2008; Siena et al., 2009). These findings further highlight the value in molecularly stratifying patients. Another addition to combination targeted therapy are agents inhibiting BRAF, mutations in which lead to constitutive activation of the MAPK signalling pathway making EGFR targeting therapy ineffective (Benvenuti et al.,

2007; Di Nicolantonio et al., 2008). Although BRAF V600E inhibitors such as vemurafenib have proven effective in the treatment of BRAF-mutant melanoma, they have been surprisingly ineffective in BRAF-mutant colorectal cancers (Kopetz et al., 2015). It has been subsequently shown that BRAF V600E inhibitors trigger the reactivation of the MAPK pathway via EGFR through a feedback loop (Corcoran et al., 2012). This informed the development of combined BRAF V600E and EGFR inhibition which effectively prevents activation of the feedback loop in CRCs and hence suppresses MAPK pathway signalling. Combination of vemurafenib, irinotecan, and cetuximab in metastatic treatment refractory CRCs containing BRAF V600E mutation showed increased response rate and prolonged OS compared to treatment with irinotecan and cetuximab alone (Hong et al., 2016; Kopetz et al., 2017). In phase III clinical trial BEACON, BRAF V600E mutant mCRC patients were treated with either an anti-BRAF/MEK/EGFR triplet (encorafenib, binimetinib, and cetuximab), anti-BRAF/EGFR doublet (encorafenib and cetuximab), or control (investigators' choice of cetuximab plus irinotecan or FOLFIRI) regimens. The objective response rate (ORR) was 26.8% for the triplet arm, 19.5% for the doublet arm, and 1.8% for the control arm. Targeting BRAF and its downstream kinase MEK increased survival benefit with median OS for both the triplet and doublet arms being 9.3 months but only 5.9 months for the control arm (Tabernero et al., 2021).

Another receptor identified as driving resistance to EGFR targeting therapy is HER2 which belongs to the same ErbB (erythroblastosis oncogene B)/HER (human epidermal growth factor receptor) family as EGFR. Its homodimerization or heterodimerization with any other receptor of the HER family activates its intracellular kinase which activates the downstream signalling pathway RAS-RAF-ERK and PI3K-PTEN-AKT, which regulate cell proliferation and apoptosis. Through pre-clinical models it was shown that HER2 genomic amplification induced resistance to cetuximab in colorectal cancer and inhibition of HER2 signalling restored cetuximab sensitivity

(Yonesaka et al., 2011). Evaluation of clinical samples showed that HER2 was overexpressed in 2% of mCRC and was mutually exclusive with KRAS and BRAF mutations (Richman et al., 2016). Additionally HER2 amplification was found in cetuximab resistant tumours (Yonesaka et al., 2011). PFS as well as OS was shorter for patients with HER2 amplification than those without when treated with cetuximab alone or in combination with chemotherapy (Yonesaka et al., 2011). These findings proposed HER2 a new actionable target for mCRC therapy. In a phase II trial patients with HER2-amplified mCRC were treated with a combination of trastuzumab and pertuzumab, both inhibiting HER2 signalling, and 32% of patients achieved an ORR with an estimated median OS of 11.5 months (Meric-Bernstam et al., 2019). In another phase II trial in which HER2-positive mCRC patients were treated with trastuzumab and lapatinib (a tyrosine kinase inhibitor targeting both EGFR and HER2) 30% of patients achieved an ORR and the median PFS and OS were 5 and 11 months respectively (Sartore-Bianchi et al., 2016). Findings from the latest phase II trial MOUNTAINEER which investigated the combination of tucatinib, a highly selective HER2 targeting TKI, and trastuzumab in HER2 positive mCRC patients resulted in an accelerated approval by the FDA of this combination for this subgroup of patients (Strickler et al., 2022). This dual combination treatment reached a 38.1% ORR, a PFS of 8.2 months, and OS of 24.1 months. These are very promising findings demonstrating that chemotherapy refractory mCRC patients have other viable therapeutic options through targeted therapy. Although for a long time KRAS mutant CRC was considered untreatable, novel targeting therapies are emerging. While treatment of patients with KRASG12C-mutated advanced CRC (3% of tumours) with sotorasib, a specific, irreversible KRASG12C protein inhibitor, showed very modest results as monotherapy only achieving a 9.7% ORR, combining it with panitumumab resulted in 3-fold higher response rate of 30% (Fakih et al., 2022; Kuboki et al., 2022). A novel non-covalent inhibitor of KRAS with a G12D mutation, the most common KRAS mutation in CRC occurring in about 40% of KRAS mutations, MRTX1133 showed

significant preclinical antitumour activity and is now being investigated in a phase 1/2 clinical trial (NCT05737706) (Tang & Kang, 2022; Zhu et al., 2021).

Another targeted CRC treatment is antiangiogenic therapy inhibiting VEGF/VEGFR signalling. VEGF is a potent angiogenic factor that stimulates the growth of new blood vessels in tumours necessary for tumour growth and metastasis. VEGF levels and VEGFR activity are elevated in CRCs and are predictive of liver and lung metastasis and are associated with poor prognosis (Divella et al., 2017; Liu et al., 2014). The initial theory was that anti-VEGF therapy works by inhibiting activity of VEGF thereby preventing formation of new blood vessels and starving the tumour of oxygen and nutrients. However, it has been suggested that VEGF targeted therapy results in normalisation of blood vessels thus enhancing the delivery and effectiveness of chemotherapy agents (Jain, 2001). Several randomized control trials have demonstrated efficacy of anti-VEGF therapy in treatment of mCRC. Bevacizumab, a recombinant humanized monoclonal antibody that binds to all isoforms of VEGF-A and interferes with VEGF-VEGFR interactions, in combination with FOLFIRI showed increased OS and PFS and prolonged duration of response in mCRC patients compared with the chemotherapy regimen alone (Hurwitz et al., 2004). Although only bevacizumab has been approved as a first-line targeted agent, other anti-VEGF agents have been approved for second-line treatment. Aflibercept is a recombinant fusion protein that acts a decoy receptor for VEGF and PlGF (placental growth factor) and has a stronger affinity to VEGF-A than bevacizumab (Ferrara et al., 2004; Holash et al., 2002; Tang et al., 2012). While aflibercept showed limited single agent activity in patients with pre-treated mCRC, in combination with FOLFIRI it showed a better response, longer PFS, and longer OS than FOLFIRI treatment alone in mCRC patients who have previously received oxaliplatin or bevacizumab treatment (Tang et al., 2012; Van Cutsem et al., 2012). However, in the AFFIRM study where aflibercept was combined with FOLFOX as a first-line treatment no difference in PFS was observed, but there was higher toxicity suggesting that aflibercept

might be better in second-line treatment (Folprecht et al., 2016). Another drug targeting the VEGF pathway that has been approved for second-line treatment of mCRC is ramucirumab which is a fully humanized monoclonal VEGFR2 targeting antibody. In combination with FOLFIRI in a second-line treatment setting addition of ramucirumab to the chemotherapy regimen resulted in a prolonged PFS and OS (Tabernero et al., 2015). Another approach to targeting VEGF is through a small molecule tyrosine kinase inhibitor regorafenib which showed no improvement of ORR in FOLFOX treated patients in a first line setting, but did show survival benefits in refractory mCRC (Argilés et al., 2015; Grothey et al., 2013). The advantage of regorafenib is that it can be taken as a tablet rather than administered intravenously as all of the previously mentioned drugs are.

Another signalling pathway targeting of which for mCRC is currently being investigated in clinical trials is the hepatocyte growth factor (HGF) and its receptor mesenchymal epithelial transition factor (c-MET) pathway. Upon HGF binding, activation of c-MET triggers a signalling cascade activating various downstream pathways such as MAPK/ERK, PI3K/AKT, and JAK/STAT ultimately promoting tumour growth and metastasis (Matsumoto et al., 2017). Patients with advanced CRC have elevated levels of serum HGF which decrease after tumour resection. Overexpression of HGF/c-MET mRNA and protein have been observed in CRC tumours, particularly in metastases (El-Deiry et al., 2015; Flavia Di Renzo et al., 1995; Kammula et al., 2007; Liu et al., 2012; Otte et al., 2000). Expression of HGF and c-MET have been correlated with poor prognosis in CRC (Gao et al., 2015; Liu et al., 2012). Due to its vital role in promoting tumour growth and progression the HGF/c-MET pathway has become an attractive therapeutic target and several different methods of blocking this pathway have emerged. Specifically in the context of mCRC two tyrosine kinase inhibitors that target the MET kinase domain have been evaluated in phase I and II clinical trials. A trial evaluating tivantinib (ARQ 197) in combination with irinotecan and cetuximab in patients with mCRC did not find a statistically significant difference in PFS although it was slightly longer in

the tivantinib treated group (Eng et al., 2016). A phase 2 trial evaluating savolitinib (AZD 6094), a selective MET inhibitor, in mCRC with amplified MET is currently ongoing (NCT03592641). Although targeted therapies have augmented chemotherapy treatments and shown some promise, resistance invariably occurs after several months of treatment. Additionally most KRAS mutations and mutations inactivating tumour suppressor genes remain untargetable thus new therapeutic approaches for mCRC are needed.

1.1.5.3 Immunotherapy

Another therapeutic approach is harnessing the immune system to treat tumours through immunotherapy. This rapidly growing class of drugs, particularly immune checkpoint inhibitors which will be described in more detail in section 1.6.1, have achieved remarkable responses in certain cancer types including late-stage cancers. Immune checkpoints are molecules expressed on immune cells that under normal conditions are responsible for regulation of immune responses and prevention of autoimmunity. However, tumours frequently exploit these checkpoints to avoid detection and destruction by the immune system by upregulating checkpoint ligands. Immune checkpoint inhibitors are monoclonal antibodies that interfere with these inhibitory signals and unleash antitumour immune responses. Checkpoint inhibitors have shown to be effective in many cancer types and have been approved for the treatment of melanoma, non-small cell lung cancer, renal cell carcinoma, and urothelial carcinoma among others. However, only patients with MSI CRC which make up only 5% of metastatic CRC have shown responses to checkpoint blockade (Le et al., 2017). Given the lack of response of MSS CRC to checkpoint immune blockade novel immunotherapeutic approaches are needed.

1.2 Immune system overview

1.2.1 The innate immune system

The human immune system is a complex network of cells, tissues, and organs that work together to protect the body from harmful pathogens. Protection against pathogens relies on several levels of defence, the first of which are anatomical and chemical barriers such as the skin and mucosal surfaces that prevent microbes from entering the body. However, those microorganisms that do manage to penetrate the epithelial surfaces of the body are then faced with the innate immune system. The innate immune system is comprised of cells that have differentiated from the common myeloid progenitor cells in the bone marrow and includes: neutrophils, monocytes, eosinophils, basophils, and mast cells. Although natural killer (NK) cells are of lymphoid origin, based on their function they are also categorised into the innate immune system. Innate immune cells rely on pattern recognition receptors (PRRs), such as Toll-like receptors (TLR), which detect regular patterns of molecular structures known as pathogen associated molecular patterns (PAMPs) such as bacterial lipopolysaccharides (LPS) and endotoxins which are exclusively expressed by microorganisms but not human cells (Janeway & Medzhitov, 2003) . Monocytes circulating in the blood migrate into tissues where they differentiate into macrophages which are resident in almost all tissues in the human body. During very early stages of infection macrophages secrete cytokines initiating recruitment of other immune cells such as neutrophils and dendritic cells. Once innate immune cells have recognised the presence of a pathogen they employ various mechanisms to eliminate it. For example, macrophages and neutrophils can engulf microbes and damaged cell debris through their phagocytic capabilities (Aderem & Underhill, 2003; Rosales & Uribe-Querol, 2017). Neutrophils can furthermore release antimicrobial substances such as reactive oxygen species, antimicrobial peptides, and enzymes that can kill or damage invading pathogens (Witko-Sarsat et al., 2000). Both neutrophils and macrophages also modulate the immune response by secreting inflammatory cytokines (small proteins involved in cell–cell communication and recruitment) such as IFN γ , TNF α , IL-1, IL-6, IL-12 (Duque & Descoteaux, 2014; Spees et al., 2014; Tecchio et al., 2014; Yin & Ferguson, 2009).

Dendritic cells are a heterogeneous immune cell population differing in their cell origin, function, and localisation (W. Heath & Carbone, 2009; Miller et al., 2012; Segura et al., 2010). In contrast to macrophages, whose main role is to engulf damaged cells or pathogenic microbes and promote tissue repair, the main function of dendritic cells is antigen presentation to T cells and thus initiation of the adaptive immune response. Immature dendritic cells residing in non lymphoid tissue (tissue-resident DCs) efficiently take up antigens from the environment and process them to present to T cells. The surfaces of DCs express a group of proteins known as the major histocompatibility complex (MHC). MHC are classified as either class I (human leukocyte antigen HLA-A, B and C) which are found on all nucleated cells, or class II (also termed HLA-DP, DQ and DR) which are found only on certain cells of the immune system, including macrophages, dendritic cells and B cells. Endogenous proteins are digested by the proteasome to small peptide fragments which are then transferred to the endoplasmic reticulum (ER) via the TAP transporter, where with the help of other proteins the peptides are loaded onto a class I MHC protein which is finally transport to the cell surface where it can be recognised by CD8 T cells of the adaptive immune system (Chaplin, 2010). Exogenous antigens are taken up by phagocytosis or endocytosis, digested by the action of lysosomal enzymes, and transported to the MHC II peptide loading compartment for loading into a class II protein. Exogenous antigens include proteins of extracellular pathogens such as most bacteria and parasites, and also virus particles that have been released from infected cells. While endogenous proteins under normal conditions present self-antigens thus preventing the immune system from attacking host's own cells, during a viral infection the immunoproteasome processes virus derived antigens allowing them to be presented on cell surface on MHC class I thus letting know the immune cells that the cell has been infected and needs to be destroyed. After encountering and phagocytising pathogens, dendritic cells migrate to the closest lymph node where they prime naïve T cells which are a key player in the adaptive immune response.

1.2.2 The adaptive immune system

The adaptive immune compartment is comprised of T cells and B cells which differentiate from lymphoid progenitor cells in the bone marrow. Although they start their differentiation in the bone marrow, T cells migrate to the thymus where they mature, while B cells remain within the bone marrow for the duration of their development. B and T cells express antigen-binding receptors on their membrane, known as the B cell receptor and T-cell receptor (TCR) respectively. The production of these antigen specific receptors results from a process of somatic recombination of multiple DNA fragments that code for the antigen binding sites of the receptor. These gene rearrangements lead to the production of a huge repertoire of antigen binding specificities ensuring that the immune system will be able to recognise a wide range of pathogens throughout the lifetime (Kranzel, 2009). Each T cell expresses a TCR of unique antigen specificity and has the capacity to rapidly proliferate and differentiate if it receives the appropriate signals. All T cells undergo positive and negative selection in the thymus to ensure that they are able to bind self-MHC molecules with sufficient affinity, but do not bind self-antigens. All T cells that fail either one of those selections undergo apoptosis. Fewer than 5% of the developing T cells survive positive and negative selection. If a developing T cell has adequate affinity for MHC class I protein they differentiate into CD8 T cells which are main cytotoxic T cells, but if the cell recognises MHC class II protein then it extinguishes its expression of CD8 and retains its expression of CD4 becoming T helper cells (Germain, 2002). Once a T cell has bound antigen presented on an MHC protein expressed by APC it also requires a second signal provided by co-stimulatory molecule CD28 binding to CD80 (B7.1) or CD86 (B7.2) on the APC. TCRs are associated with the CD3 complex on the surface of the cell. The CD3 chains contain immunoreceptor tyrosine-based activation motifs (ITAMs) in their cytoplasmic domains that can be phosphorylated to activate the intracellular signalling cascade leading to T cell activation, proliferation, and differentiation into the effector phenotype (Shah et al., 2021).

Interaction of peptide-MHC with the TCR without a co-stimulator can lead to an anergic state of prolonged T cell non-responsiveness or apoptosis (L. Chen & Flies, 2013; Schwartz, 2003; Schwartz et al., 1989).

Majority of T cells bear a TCR comprised of α and β heterodimers and is the subset referred to in this thesis. However, a small portion (0.5–5%) of T lymphocytes ($\gamma\delta$ T cells) expresses TCR γ and TCR δ isoforms (Allison et al., 2001). This subset of T cells is a unique population that is rare in secondary lymphoid organs but enriched in many peripheral tissues, such as the skin, intestines and lungs. In contrast to MHC-restricted $\alpha\beta$ T cells, $\gamma\delta$ T cells can directly recognise antigens in the form of intact proteins or non-peptide compounds. Following recognition of infected or transformed cells $\gamma\delta$ T cells have a broad range of function including target cell cytotoxicity, production of cytokines and chemokines, and even present antigens to conventional CD8 and CD4 T cells (Brandes et al., 2005, 2009; Lawand et al., 2017; Ribot et al., 2020). Effector CD8 T cells induce apoptosis in their target cell, for example a virus infected cell that presents a peptide antigen that can be recognised by the TCR on MHC class I, by secreting perforin which creates pores in the target cell surface and granzymes which are serine proteases that enter the cell and induce a signalling cascade leading to target cell apoptosis (Harty et al., 2003). Although some CD4 T cells have been shown to possess cytotoxic functions, their usual role is to modulate the immune response via specific cytokine secretion and to activate B cells. CD4 T-helper cells (Th cells) are functionally subdivided based on the cytokines they produce. Th1 cells produce IL-2, IFN γ , TNF α , which are cytokines that stimulate CD8 T cell proliferation and cytotoxicity. Whereas IL-4, IL-5, and IL-13 secreted by Th2 cells are involved in the development of immunoglobulin E (IgE) antibody-producing B cells, as well as the development and recruitment of mast cells and eosinophils that are essential for effective responses against many parasites such as helminths. In 2005 a new subset of CD4 T cells was identified, Th17 cells, which produce IL-17 and IL-22 and have a key role in defence against opportunistic pathogens such as

bacteria and fungi and has been implicated in inflammatory disorders (Harrington et al., 2006; Stockinger & Omenetti, 2017; X. Zhu & Zhu, 2020). A subset of the CD4 T cell, known as the regulatory T cell (T reg), limit and suppress immune responses thus maintaining homeostasis and preventing aberrant responses to self-antigens and the development of autoimmune disease. Tregs use several different mechanisms to exert its immunosuppressive effects. One of the mechanisms by which Tregs suppress immune responses is through the use of CTLA-4. CTLA-4, which is constitutively expressed on cell surface of Tregs, has a higher affinity for CD80/CD86 co-stimulatory molecules on APCs than the T cell co-stimulatory receptor CD28. Tregs engage with APCs and use CTLA-4 to outcompete CD28 for binding to CD80/CD86 thus limiting the co-stimulatory signal received by the effector T cell. Tregs also compete with effector T cells for extracellular IL-2 by expressing the high-affinity IL-2 receptor CD25 (IL-2 receptor α -chain) thus limiting effector T cell proliferation. Tregs express high levels of CD39 and CD73 ectonucleotidases which generate extracellular adenosine that binds to A2A receptors on effector T cells and suppress their proliferation and cytotoxicity. Tregs further inhibit effector T cells by secreting immunosuppressive cytokines such as IL-10 and TGF β (Sojka et al., 2008). In some instances, Tregs have been shown to directly induce apoptosis in CD8 T cells and NK (natural killer) cells via the perforin/granzyme mechanism (Cao et al., 2007). T reg cells also help in the resolution of immune responses once pathogens are eliminated. Another immune cell subset of the lymphoid lineage is the recently identified innate lymphoid cells (ILC) which are considered to be innate counterparts of helper T cells based on their cytokine secretion profiles. Unlike T cells, ILCs do not express a T cell receptor and thus do not respond in an antigen-specific manner. ILCs are abundant at the mucosal barriers, where they are exposed to allergens, commensal microbes, and pathogens. ILCs 1 secrete IFN γ , IL-12, IL-15, and IL-18, whereas ILCs 2, the innate counterparts of Th2, secrete type-2 cytokines such as IL-5, IL-9, IL-13, and amphiregulin. The third group of ILCs produce IL-22 and IL-17 thus mirroring Th17 cells (Panda & Colonna, 2019).

In contrast to the TCR on T cells, the B cell receptors (BCR) on B cells recognise their antigen in its native form without the need for presentation by another protein. Antigen recognised by the BCR is internalised, processed into short peptides that are loaded onto MHC class II and then presented on the surface where MHC class II-antigen complexes can be recognised by CD4 T cells. T cells provide co-stimulatory signals and produce cytokines which induce B cell activation as a result of which B cells undergo proliferation and differentiate into antibody-secreting plasma cells (Chaplin, 2010). Antibodies protect against pathogens via several different methods. Neutralisation occurs when an antibody binds a pathogen product such as a bacterial toxin or the microorganism itself preventing its interaction with the host cells. Coating of pathogens in antibodies, known as opsonisation, enables phagocytes such as macrophages and neutrophils to bind the Fc portion of the antibodies with their Fc receptors and ingest and destroy the pathogen (Marshall et al., 2018).

Another cell type derived from the lymphoid lineage is the NK cells. They develop in the bone marrow under the influence of IL-2, IL-15, and bone marrow stromal cells. Unlike B and T cells, NK cells do not carry polymorphic antigen receptors. One of the ways they contribute to immune responses is by recognising pathogens coated by antibodies via their Fc receptors and releasing cytotoxic granules, a process known as antibody-dependent cellular cytotoxicity (ADCC) (Mujal et al., 2021). Another pathway used by NK cells to kill target cells involves binding of TRAIL (tumour necrosis factor related apoptosis inducing ligand) to DR4 and DR5 expressed on many cell types resulting in activation of pro-enzyme caspase 8 ultimately leading to apoptosis (Perera Molligoda Arachchige, 2021). NK cells can also produce IFN γ , activating macrophages and enhancing their pathogen killing capacity early in the immune response, but also influence adaptive immunity by acting on dendritic cells, or on T cells, enhancing CD8 T cell cytotoxic responses or polarising Th cells into Th1 cells. The way an NK cell distinguishes between "self" and "non-self" is through a balance of signals by activating

and inhibitory receptors. The activating receptors recognise cell surface proteins that are induced on target cells by specific cellular events such as metabolic stress or DNA damage. Inhibitory receptors bind MHC I which are expressed by all nucleated cells but can be downregulated by viruses (such as herpesviruses) and other intracellular parasites(Mujal et al., 2021). Although the strategy of downregulating MHC class I expression potentially helps infected or transformed cells to evade CD8 T cell recognition and killing, it has the opposite effect on NK cells. If on interaction with a cell the inhibitory receptor is not bound by MHC class I, the NK cell triggers cytotoxic granule release and IFN γ secretion leading to target cell death.

In addition to specificity, another hallmark of adaptive immunity is the capacity for memory which enables the host to mount a more rapid and efficient immune response upon subsequent exposure to the pathogen. Upon resolution of infection, majority of effector T cells and plasma cells will die. However, some cells become long-lived memory cells which in the case of B cells results in rapid production of antigen-specific IgG, IgA, or IgE antibodies upon re-exposure to the same antigen. T cell memory cells can be categorized into two main types: central memory T cells (T_{cm}) and effector memory T cells(em). T_{cm} are primarily located in the lymph nodes and are responsible for the maintenance of immunological memory. They express high levels of CCR7 which allows them to migrate to secondary lymphoid organs and they can differentiate into effector T cells upon antigen re-exposure. T_{em} cells are found in the peripheral tissues and are responsible for immediate effector responses during a re-infection. T_{em} cells have an enhanced ability to produce cytokines and exert cytotoxic functions compared to T_{cm} or naïve T cells (Martin & Badovinac, 2018).

1.3 The role of the adaptive immune system in cancer

The foundation of immuno-oncology lies in the discovery that the immune system can mount spontaneous responses to tumours. The first clear evidence that the immune

system was involved in controlling tumour growth was provided by Boon and colleagues in 1977 when they demonstrated that cell clones that were derived from a teratocarcinoma cell line that was treated with a strong mutagen were incapable of forming progressive tumours when injected into syngeneic mice. Interestingly, these same clones were able to grow when injected into irradiated mice thus indicating the role of the immune system in rejection of tumours(Boon & Kellermann, 1977). Subsequently they showed that adoptive transfer of T cells that were collected from mice following the rejection of the tumour protected mice from growth of the same tumour variant in irradiated mice suggesting a direct role of T cells in tumour rejection. With the development in T cell in vitro culturing and single clone expansion, Maryanski and colleagues were able to obtain stable cytotoxic lymphocyte (CTL) clones that killed specific tumour variants but not other variants and not the parental tumour cells (Maryanski et al., 1983). The discovery of the nature of these antigens was aided by the discovery that antiviral CTLs recognized small peptides of eight to ten amino acids, which were derived from a viral protein and presented at the surface of infected cells in association with MHC class I molecules (Townsend et al., 1986). Further investigation revealed that these tumour antigens that triggered a T cell response were from ubiquitously expressed genes containing single point mutations that resulted in a change of a single acid in the peptide sequence (Lurquin et al., 1989; Sibille et al., 1990). Although these antigens were artificially induced by mutagen treatment, their identification led to the discovery that T cells can mount an immune response leading to a rejection of the tumour as a result of mutations in ubiquitously expressed genes. Another mechanism that produces tumour specific antigens is recognised by T cells was discovered when a gene encoding an antigenic peptide was found to be expressed by tumour cells and by spermatogonia and placental trophoblasts and not any other tissue (Van Den Eynde et al., 1991). This gene was not mutated but the reason its peptide was immunogenic was because it was only presented on the surface of tumour cells since the two other cell types expressing it do not express MHC class I molecules on their

surface and therefore cannot present the antigen to T cells. Lack of expression of this gene in any adult tissues prevented the establishment of immune tolerance and therefore led to T cell responses against this antigen presented on the surface of tumour cells. This established that in addition to point mutations in ubiquitously expressed genes activation of genes that are silent in normal tissues can result generation of tumour specific antigens and ultimately in spontaneous T cell responses leading to tumour rejection. In 1991, the first human gene that coded for a tumour-specific antigen recognized by T cells named MAGEA1 (melanoma antigen family A) was discovered. MAGE1A was expressed in tumours and male germline cells and trophoblastic cells exclusively, but as mentioned earlier these two cell types do not produce MHC molecules and therefore cannot present antigens to T cells. MAGE1A turned out to belong a large family of 25 cancer-germline genes which in addition to melanoma are also expressed in head and neck tumours, non small cell lung cancer, and bladder carcinomas (Boon et al., 1997). The phenomenon that unique tumour antigens could result from a single point mutation that was observed in mice was then confirmed in human tumour cells (Monach et al., 1995). Antitumour CTLs were shown to recognise peptides that were encoded by mutated genes encoding β -catenin and CDK4 (cyclin dependent kinase) (Robbins et al., 1996; Wölfel et al., 1995).

Three types of tumour antigens have the potential to elicit tumour specific immune responses: viral antigens, antigens that are encoded by cancer-germline genes (cancer testis antigens [CTA]), and antigens that result from a mutation in a ubiquitously expressed gene named “neoantigens”. Some cancers, such as cervical cancer, arise as a result of oncogenic viruses such as certain strains of the human papilloma virus (HPV) (van der Burg & Melief, 2011). Transformed cells express tumour-specific antigens of viral origin which are recognised and targeted by CTLs. However, majority of cancers are not caused by viruses, so the two main categories of tumour specific antigens are cancer-testis antigens and neoantigens. Following the discovery of the MAGE family of

proteins other germline gene families expressed in tumours were identified including BAGE, GAGE, SAGE, HAGE, SSX, SCP1, and NY-ESO-1 (Boël et al., 1995; Y. T. Chen et al., 1997; De Backer et al., 1999; Martelange et al., 2000; Türeci et al., 1998). These genes have been found to be expressed in a variety of cancers including melanoma, lung carcinoma, head and neck cancers, bladder carcinoma, breast carcinoma, sarcoma, and some colorectal carcinomas (Van der Bruggen et al., 2002). The mechanism that leads to the activation of these genes in tumour and germline cells is demethylation of the promoter which is methylated in all normal cells except the germline cells and results in inhibition of binding of transcription factors (De Smet et al., 1996; Weber et al., 1994).

Non-synonymous mutations which can result from a substitution of a single nucleotide (missense), a premature termination of protein synthesis through introduction of a stop codon into the mRNA sequence (non-sense), or an insertion or deletion of a nucleotide that disrupts the reading frame of the gene (frameshift) can all lead to the generation of immunogenic antigens recognised by T cells. Increased mutation rate is a well established feature of tumours. Abnormal activity in several different cellular pathways can increase the rate of somatic mutations in tumours. Defects in the DNA damage repair system can lead to accumulation of mutations caused by replicative errors. This abnormal activity can result from germline mutations as in Lynch syndrome or as de novo somatic mutations. Loss of function mutations in mismatch repair pathway genes are known to correlate with high tumour mutational burden (TMB) in tumours (Ah Cho 2021). The TMB is significantly higher in MSI CRC with a median TMB of 46.8 mutations/Mb compared to MSS CRC which have a median of only 3.6 mut/Mb (Fabrizio et al., 2018). Aberrant recognition and removal of errors during replication is another source of mutations in tumours. The exonuclease domains of POLD1 and POLE are responsible for proofreading during DNA replication and mutations in these domains are associated with hypermutation in colorectal cancer (Briggs & Tomlinson, 2013; Lange et

al., 2011). High mutation frequencies are also attributed to exposure to carcinogens such as ultraviolet radiation in the case of melanoma and smoking in case of lung cancers (Brash et al., 1991; Denissenko et al., 1996). Unsurprisingly melanoma and lung cancers have the highest tumour burden out of all tumour types excluding MSI and *POLE* mutated tumours (Alexandrov et al., 2013; Lawrence et al., 2013).

With technological advancements such as deep exome sequencing it has become possible to identify the mutations in the protein-encoding part of the genome of individual tumours which is essential for neoantigen prediction. Since the majority of mutations in human tumours is not shared between patients at meaningful enough frequencies the approach to neoantigen prediction and characterisation needs to be tumour or patient-specific. After the mutated genes have been identified by sequencing in silico prediction algorithms are used to determine the likelihood of target protein proteasomal processing, transport to ER, and affinity for the relevant MHC class I alleles. These neoantigen predictions can then be verified in vitro for their recognition by CD8 T cells in immunogenicity assays (Gubin et al., 2014; Van Rooij et al., 2013). However, this approach might not be clinically effective as it results in many predicted neoantigens, only a few of which prove to be immunogenic. An alternative method that directly assesses the repertoire of HLA-presented neoantigens is mass spectrometry immunopeptidomics. This approach led to a direct identification of multiple neoantigens and cancer testis antigens presented on a melanoma tumour with tumour reactive T cells with specificity for selected neoantigens detected in patient's tumour and blood (Bassani-Sternberg et al., 2016). However, this approach is more technically challenging and requires large amounts of starting material so for now most studies investigating neoantigens use the former method.

A study that predicted neoantigens based on whole exome sequencing of 619 colorectal tumours and subsequently used in silico methods to predict neoantigen loads has found a correlation between predicted neoantigen load and higher amounts of

tumour infiltrating lymphocytes (TILs) (Giannakis et al., 2016). Further supporting the notion that TMB predicts immunogenicity of tumours, consensus molecular subtyping of colorectal cancers revealed that CMS1 which encompasses majority of MSI tumours is characterised by high mutational count and an increased immune infiltrate mainly composed of Th1 and cytotoxic T cells (Guinney et al., 2015). Interestingly, the type, density and location of immune cells within tumours predicted survival in colorectal cancer better than the classical TNM pathological classification. Stratifying patients by a Th1 adaptive immunity signature comprised of genes such as *IFN γ* , *CD3*, *CD8*, *GZMB* (granzyme B) revealed an inverse correlation between the expression of these genes and tumour recurrence. Patients with higher densities of CD3+, CD8+, GZMB+, and CD45RO+ (memory T cells) cells in the tumour center (CT) and the invasive margin (IM) had longer OS. Shockingly patients with stage I-III tumours with low densities of CD3+ cells and CD45RO+ memory T cells in both tumour regions (CT and IM) had a very poor prognosis, similar to that of patients with distant metastasis (stage IV) (Galon et al., 2006). These findings show the important role of the immune system in cancer progression and in clinical prognosis of CRC.

1.4 Cancer immunoediting

Although the concept of immunosurveillance, the process by which the immune system recognises and eliminates tumour cells through continuous monitoring of tissues, was supported by many mouse studies, the question of how tumours develop and continue to grow despite a functioning immune system remained unanswered and a new model of immune-tumour interactions was proposed. The immunoediting theory proposes three phases, the three “Es”, of interaction between the immune system and cancer cells: elimination, equilibrium, and escape (Dunn et al., 2002). This theory suggests that the immune system not only protects the host by eliminating tumour cells, but also shapes

the tumour and therefore its progression. The elimination phase corresponds to immunosurveillance and during this phase the immune system recognises and kills immunogenic tumour cells. Then the tumour subclones that have survived the elimination phase progress into the equilibrium phase during which the immune system exerts selective pressure on the tumour cells that is enough to contain but not fully destroy the tumour. It is likely that equilibrium is the longest of the three phases and may occur over a period of many years. This immunological pressure selects for cancer cells with a non-immunogenic phenotype that are able to escape immune control through various mechanisms such as reduced immune recognition, resistance to cell death, and/or development of an immunosuppressive microenvironment. Escape from immune control is now recognised to be one of the hallmarks of cancer (Hanahan & Weinberg, 2011). Immune escape was observed well before the immunoediting model has emerged. In 1983 an interesting *in vivo* observation was made: chemically induced mutated clones were able to form tumours and grow initially, but then they almost completely regressed and then progressed again, which was then confirmed to be due to immunogenic antigen loss (Maryanski et al., 1983). This, along with further observations that cancers that originally arose in immunodeficient mice were often unsuccessful at initiating secondary tumours in immunocompetent hosts and that cancers in immunodeficient hosts were more immunogenic than the same tumours from immunocompetent mice supported the idea of immunological shaping or “editing” of the tumour (Engel et al., 1997; Shankaran et al., 2001; Svane et al., 1996). Tumours that first grew in immunodeficient mice had no selective pressure applied by the immune system which resulted in the development of a highly immunogenic tumour which was then successfully recognised and destroyed in the immunocompetent mice. Whereas tumours that arose in mice with fully functioning immune systems and were highly immunogenic underwent the elimination phase of immunoediting leaving behind non- or poorly immunogenic tumour cells. Tumour immunoediting has also been observed in humans. A melanoma patient whose tumour expressed antigens NY-ESO-1, MAGE-C1, and Melan-A was treated with a vaccine

against NY-ESO-1. This treatment initially resulted in tumour regression but ultimately lead to tumour progression caused by the outgrowth of a tumour that was NY-ESO-1 negative but positive for MAGE-C1, Melan-A, and MHC class I (von Boehmer et al., 2013). Cancer control and cancer escape in this patient were governed by NY-ESO-1-specific immunological pressure which provided evidence for the existence of immunoediting and immune escape.

1.5 The cancer-immunity cycle

For an anti-cancer immune response to lead to cancer cell killing, a series of stepwise events referred to as the cancer-immunity cycle must occur (Chen & Mellman, 2013) (Figure 1.2). The cycle begins with the release of cancer antigens (neoantigens and cancer-testis antigens) through immunogenic or necrotic cancer cell death. Dendritic cells can also capture antigens from apoptotic tumour cells, but for full maturation require signals from necrotic tumour cells such as TLR signalling (Cavassani et al., 2008; Sauter et al., 2000). Cancer treatment modalities such as chemotherapy and radiation therapy have been shown to induce immunogenic cancer cell death and enhance anti-tumour immune responses (Casares et al., 2005; Green et al., 2009). These antigens are captured and processed by dendritic cells which then present these antigens on MHC molecules to the T cells (step 2). As part of their maturation process into potent APCs, dendritic cells downregulate tissue specific chemokines and upregulate CCR7 which guides them from sites of antigen exposure (tumour) to the local lymph node (Sallusto & Lanzavecchia, 2000). The next step in the cycle is T cell priming and activation by the DCs. To generate an effective anti-tumour T cell response, this step must be accompanied by stimulatory immunological signals such as co-stimulatory molecules like CD80/CD86, CD137 (4-1BBL) and proinflammatory cytokines such as IL-1, TNF α , IFN γ , IFN α , IL-12, IL-2. In the next step of the cycle activated T cells migrate from the tumour

draining lymph node to the tumour. Chemokines CCL2, CCL3, CCL5, CXCL9, CXCL10, and CXCL11 secreted by the tumour or other immune cells present in the TME play a major role in T cell recruitment to the tumour (Franciszkievicz et al., 2012; Harlin et al., 2009). IFN γ induced CXCL9 and CXCL10 secreted by monocytes, dendritic cells, fibroblasts, endothelial cells, and cancer cells are considered to be major drivers of T cell infiltration in solid tumours (Chheda et al., 2016; Chow et al., 2019; Farber, 1997; Gorbachev et al., 2007; Tannenbaum et al., 1998; Tokunaga et al., 2018). CXCL9 and CXCL10 signal through CXCR3 which is rapidly induced on T cells following activation and remains highly expressed in Th1 CD4 T cells and effector CD8 T cells (Groom &

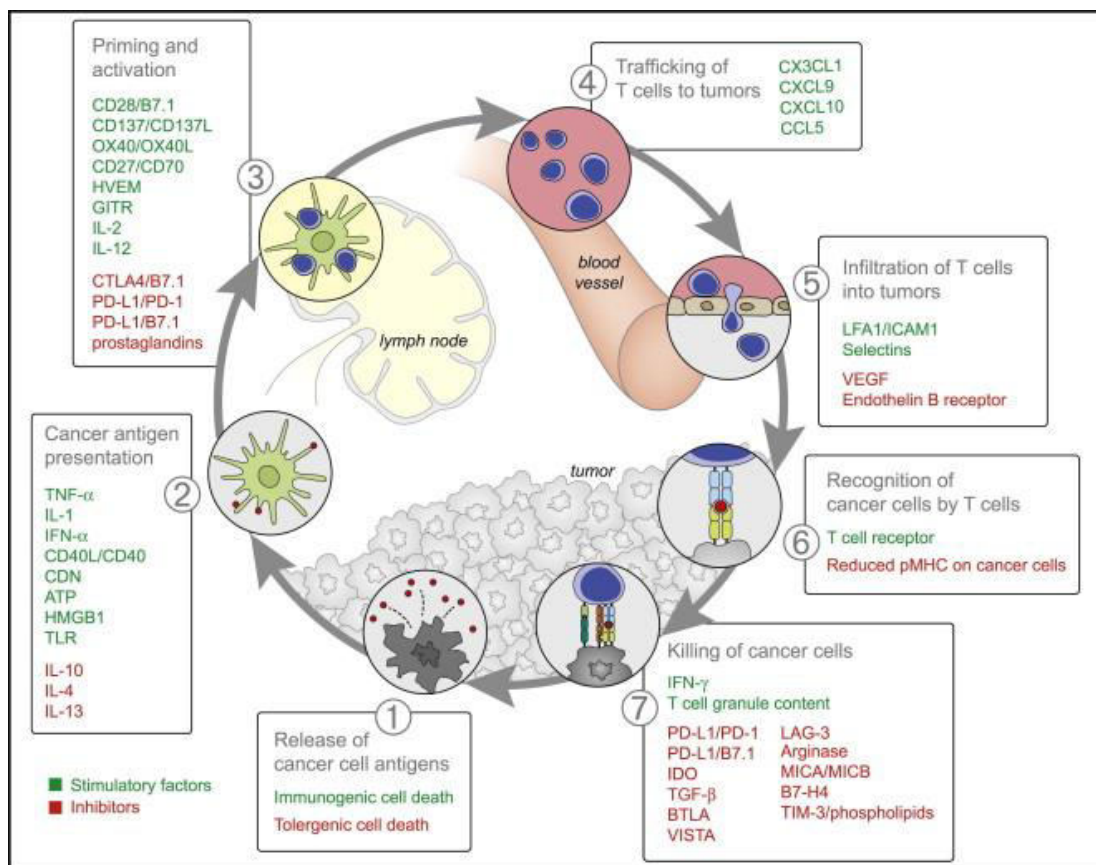


Figure 1.2 The cancer-immunity cycle. The generation of immunity to cancer is a cyclic process that can be self propagating, leading to an accumulation of immune-stimulatory factors that in principle should amplify and broaden T cell responses. The cycle is also characterized by inhibitory factors that lead to immune regulatory feedback mechanisms, which can halt the development or limit the immunity. This cycle can be divided into seven major steps, starting with the release of antigens from the cancer cell and ending with the killing of cancer cells. Each step is described above, with the primary cell types involved. Image taken from (Chen and Mellman, 2013).

Luster, 2011; Nakajima et al., 2002; Tokunaga et al., 2018). Expression of CXCR3 on circulating T cells or its chemokine ligands, CXCL9 and CXCL10, in tumour tissues is associated with increased intratumoral T-cell infiltration and with prolonged disease-free survival and overall survival in CRC (Mlecnik et al., 2010). Next T cells have to extravasate from the blood vessel via interaction of LFA-1 on their surface and ICAM1 expressed by endothelial cells and once they have reached the tumour they infiltrate into the tumour bed (step 5). Once in the tumour, T cells recognise and bind to cancer cells through the interaction of their TCR and its cognate antigen bound to MHC class I (step 6) and kill target cancer cells through the release of cytotoxic granules and secretion of cytokines such as IFN γ . Killing of the cancer cell releases more tumour antigens and the cancer-immunity cycle restarts.

1.5.1 Mechanisms of immune evasion

However, tumours utilise a number of mechanisms at each step of the cancer-immunity cycle to avoid immune attack thus disrupting the cycle and preventing an effective anti-tumour response. DCs are crucial for the induction of a potent immune response, however, tumour cells secrete several factors that lead to DC dysfunction. Immature dendritic cells have a high phagocytic capacity, but they have little or no expression of co-stimulatory molecules such as CD80/CD86 and they produce little or no IL-12 necessary for supporting T cell proliferation. However, once a DC matures it upregulates the expression of MHC molecules, co-stimulatory molecules, and increased production of IL-12 and can induce T cell activation. It has been demonstrated that tumours from cancer patients contain small numbers of DCs and those usually have the phenotype of immature DCs (Troy et al., 1998; Troy et al., 1998). DCs isolated from melanoma metastases showed a lack of CD86 expression (Enk et al., 1997). Similar observations were made about DCs isolated from basal cell carcinoma, with less than 1% of the intra-tumoral DCs and only ~10% of the peri-tumoral DCs expressing either CD80 or CD86

(Nestle et al., 1997). In addition to being considerably less potent inducers of T cell proliferation these DCs also induced T cell anergy which occurs when appropriate co-stimulatory signals are not provided (Harding et al., 1992). Tumour derived cytokines like VEGF and IL-10 inhibit maturation of DCs and therefore make T cells anergic thus preventing them from successfully killing tumour cells (Gabrilovich et al., 1996a; Steinbrink et al., 1997, 1999). Tumour cell intrinsic activation of an oncogenic pathway such as β -catenin can result in suppression of recruitment of DCs and therefore lead to T cell exclusion from the tumour (Spranger et al., 2015). STAT3 activity in tumour cells, which as described earlier can result from IL-6 secretion by cells in the TME, has been demonstrated to inhibit DC functional maturation (Wang et al., 2003) A direct negative effect of IL-6 on DCs was demonstrated in a multiple myeloma model where IL-6 suppressed the development of functional DCs (Ratta et al., 2002). Constitutive STAT3 activation in tumour infiltrating DCs resulted in reduced expression of MHC II, CD80, and CD86 and diminished ability to present antigen and activate antigen-specific CD4+ T cells (Kortylewski et al., 2005) Physical features of tumours such as hypoxia and increased production of lactic acid can also negatively regulate DC function and induce expression of immunosuppressive molecules such as indoleamine 2,3-dioxygenase (IDO)(Elia et al., 2008; Gottfried et al., 2006). Disruption of normal DC function is an essential component of tumour-mediated immune suppression that leads to tumour immune evasion.

Tumours have also developed a number of mechanisms to suppress the recruitment of T cells to the tumour site. Through releasing of chemokines that preferentially recruit certain immune cell types over others tumours are able to develop tumour microenvironments that are comprised of stromal and immune subsets that contribute to immunosuppression and promote tumour growth. For example, myeloid derived suppressor cells (MDSCs) recruited by tumour cells produce reactive nitrogen species which nitrosylate CCL2, an important chemokine for the recruitment of CTLs to

the tumour site, which abrogates CCL2's ability to attract tumour-specific CTLs, while maintaining its ability to attract more MDSCs to the tumour (Molon et al., 2011). Prostaglandin E2 (PGE2), a product of cyclooxygenases (COXs) which are overexpressed in many tumours including CRC, has been shown to inhibit IFN γ induced CXCL9 and CXCL10 expression in cancer cells (Bronger et al., 2012, 2016; Eberhart et al., 1994; Li et al., 2013; Roelofs et al., 2014; Wang & DuBois, 2018). Multiple studies have demonstrated that potent epigenetic silencing of genes encoding CXCL9 and CXCL10 in tumour cells results in poor trafficking of T cells into tumours thus leading to immunologically "cold" tumours (Nagarsheth et al., 2016; Peng et al., 2015). The expression levels of polycomb repressive complex 2 was shown to be inversely associated with *CXCL9/CXCL10* and *CD8* expression in human CRC tissue and patient overall survival (Nagarsheth et al., 2016). Proteolytic processing of CXCL11, one of the key chemokines responsible for T cell recruitment, by various cells in the tumour microenvironment such as macrophages, fibroblasts, and neutrophils, results in a truncated CXCL11 which has reduced binding, signalling, and chemotactic properties resulting in a reduced number of tumour-infiltrating lymphocytes (Proost et al., 2007). Evidence also indicates that the tumour vasculature establishes an active barrier that tumour-reactive T cells must cross in order to reach and eliminate their tumour targets. T cells must successfully extravasate through a direct interaction with endothelial cells to leave blood vessels and infiltrate the tumour. During a normal inflammatory response, TNF α upregulates adhesion molecules ICAM and VCAM on endothelial cells. While rolling, T cells bind to the adhesion molecules through LFA-1 and VLA-1 and then extravasate through the endothelium. However, in the tumour, tumour and stroma derived soluble factors like VEGF inhibit adhesion molecule expression on endothelial cells (Bouzin et al., 2007; Detmar et al., 1998; Dirx et al., 2003). Although TNF α is commonly present in the TME, in the presence of angiogenic growth factors such as VEGF it is unable to induce expression of ICAM-1 and VCAM-1 on endothelial cells (Bouzin et al., 2007). Additionally, angiogenesis resulting from VEGF signalling results

in growth of leaky and disorganised blood vessels and targeting VEGF has been shown to normalise vasculature and increase lymphocyte infiltration into tumours (Huang et al., 2012; Shrimali et al., 2010). Loss of *RGS5*, a gene responsible for abnormal tumour vascular morphology, resulted in vascular normalisation and an increased influx of effector immune cells into the tumour (Hamzah et al., 2008). Another molecule that has been implicated in preventing T cell adhesion to the endothelium is endothelin 1 (ET-1) which signals through the endothelin B receptor ETbR to prevent T cell adhesion and overexpression of this receptor was associated with the absence of TILs in ovarian cancer patients (Buckanovich et al., 2008). Endothelial cells can also negatively regulate T cell response independent of adhesive interactions by expression of immunosuppressive molecules including PD-L1, TIM3, IL-10, TGF β , and IDO (Huang et al., 2010; Mazanet & Hughes, 2002; Pirtskhalaishvili & Nelson, 2000; Riesenberber et al., 2007). Additionally, endothelial cells can directly kill CD8 effector cells via FasL expression which upon binding to its receptor Fas induces apoptosis. However, regulatory T cells which are an immunosuppressive and tumour promoting immune population, avoided killing mediated by FasL by highly expressing c-FLIP, an inhibitor of apoptosis, thereby establishing a CD8 to Treg T cell ratio that facilitates tumour growth (Mutz et al., 2014). These data demonstrate multiple ways in which tumour cells are able to inhibit T cell trafficking (step 4 of the cancer-immunity cycle) and infiltration into the tumour (step 5) and therefore prevent T cell mediated tumour cell killing.

Once the T cells have successfully crossed the endothelial barrier and infiltrated the tumour they are often met with an immunosuppressive TME created by the tumour through direct secretion of inhibitory cytokines such as TGF β and IL-10, expression of inhibitory molecules such as PD-L1, or active recruitment of immunosuppressive immune populations such as MDSCs and Tregs. All of these factors are usually associated with poor prognosis and synergise to suppress T cell function. An increased number of Tregs has been shown in a multitude of cancers including colorectal (Wolf et al., 2003). Tregs

are recruited to the tumour site by CCL22 expressed by tumour cells and macrophages which interacts with Treg CCR4 (Curiel et al., 2004; Ishida et al., 2006). Another chemokine axis through which the tumour recruits Tregs is CCL28-CCR10. Under hypoxic conditions tumour cells secrete CCL28 which attracts CCR10+ Treg cells to the tumour site establishing tumour tolerance (Facciabene et al., 2011). Once within the tumour, Tregs use various mechanisms to suppress T cell responses described earlier: deprivation of effector T cells of IL-2 through expression of high affinity IL-2ra (CD25), expression of CTLA-4 to interfere with T cell priming, generation of adenosine, down-regulating expression of co-stimulatory molecules on APCs, and secretion of immunosuppressive cytokines TGF β , IL-10, VEGF (Cederbom et al., 2000; Deaglio et al., 2007; Facciabene et al., 2011, 2012; Pandiyan et al., 2007). Hypoxia appears to enhance the immunosuppressive functions of Tregs such as inhibition of effector T cell proliferation through upregulation of Foxp3 expression, a transcriptional factor required for establishment and maintenance of Tregs and their suppressor functions (Ben-Shoshan et al., 2008). Tregs can also directly kill effector T cells through granzyme B mediated mechanisms or by expression of TRAIL (tumor necrosis factor-related apoptosis inducing ligand) (Gondek et al., 2005; Ren et al., 2007). In addition to natural Tregs (nTregs) which are derived from the thymus, Tregs can also be induced from naïve CD4 T cells in the periphery (iTregs) which exert suppressive functions similar to those observed in nTregs. Tumour cells directly convert CD4+CD25- T cells at the tumour site to Treg cells through production of high levels of TGF β (Chen et al., 2003; Liu et al., 2007). Furthermore, tumour cells can convert DCs into immature myeloid DCs capable of secreting TGF β which maintains nTregs and promotes generation of iTregs (Ghiringhelli et al., 2005). Depletion of Tregs in mouse models has demonstrated enhanced anti-tumour immunity and tumour rejection (Needham et al., 2006). Similar observations have also been made in humans; depletion of Tregs from peripheral blood mononuclear cells (PBMCs) of CRC patients unleashed an antigen specific CD4 T cell

response (Clarke et al., 2006). Based on this collective data it is clear that Tregs make an important contribution to tumour immune escape.

MDSCs are a heterogeneous population of cells of myeloid origin that comprises myeloid progenitor cells and immature macrophages, immature dendritic cells, and immature granulocytes (Almand et al., 2001). MDSCs are also found in large numbers within tumour sites and are also key contributors to T cell immunosuppression. A wide array of chemoattractants such as CCL2, CXCL12, CXCL5 released by both tumour and stromal cells recruit myeloid cells from the tumour vasculature into tumours (Murdoch et al., 2008). Additionally IL-6, commonly present in CRC, directly promotes the accumulation of MDSCs in tumours (Bunt et al., 2007). In addition to promoting tumour growth directly by promoting angiogenesis, MDSCs also employ a few different mechanisms to suppress anti-tumour immune responses (Shojaei et al., 2007; Yang et al., 2004). MDSCs mediate T cell suppression through the production of arginase I and reactive oxygen species (ROS) (Kusmartsev et al., 2004). Several tumour-derived factors, such as TGF β , IL-6, IL-10, and GM-CSF, can induce the production of ROS by MDSCs (Gabrilovich & Nagaraj, 2009). Arginase I leads to enhanced L-arginine catabolism depleting it from the TME. Shortage of L-arginine inhibits T cell proliferation through several different mechanisms including decreasing their expression of CD3 ζ (Rodriguez et al., 2002). MDSCs can also directly disrupt binding of TCR to peptide bound MHC complex by peroxynitrite production which leads to nitration of the TCR and CD8 preventing CD8 T cells from binding to MHC class I molecules and therefore inhibiting their ability to respond to specific peptides (Nagaraj 2007). A study showed that inhibition of NO synthase responsible for NO production decreased MDSCs inhibitory effect on T cells (Gabrilovich et al., 2001). MDSCs have been demonstrated to attenuate functional differentiation of tumour-specific CD4⁺ T cells into effector Th1 cells necessary for induction of CD8 T cell mediated anti-tumour activity through IL-6 production (Tsukamoto et al., 2013). Additionally MDSCs can induce Tregs from CD4 T cells and

expand Treg cells within the tumour site (Hoechst et al., 2008; Huang et al., 2006). However, due to their immature nature, MDSCs are highly plastic and have been shown to differentiate into other immune cell types under specific cytokine conditions. When exposed to Th2 cytokine IL-4 MDSCs were able to suppress CTL responses, whereas when they were cultured with IFN γ , TNF α , and IL-12 (Th1 cytokines) they converted into functional APCs able to stimulate T cell activity (Bronte et al., 2000). Similarly IL-12 and IFN γ mediated reprogramming of MDSCs was also observed in vivo (Kerkar et al., 2011). Both Tregs and MDSCs are enriched in MSS CRC which represent 95% of mCRC (Angelova et al., 2015). Other cell types in addition to Tregs and MDSCs are present in the TME, such as tumour associated macrophages (TAMs) which are described in Results Chapter 5.

If the T cells are able to overcome obstacles such as extravasation from vasculature and immunosuppressive TME they can then encounter further obstacles in the final steps of the cancer-immunity cycle, recognition (step 6) and killing of tumour cells (step 7), exerted directly by tumour cells. Tumour cells can induce T cell death directly through death receptor ligands such as FasL and TRAIL, while being protected from these pathways by expressing high levels of apoptosis inhibitors such as cFLIP and FAP-1 (Fas associated phosphatase) (Whiteside, 2002a). Tumour cells also frequently express PD-L1 which binds to PD-1 which is expressed on T cells following activation and this induces an inhibitory signal that attenuates activity of T cells (Francisco et al., 2010). In chronic infections the PD-L1/PD-1 axis is an important negative regulator that ensures immune homeostasis, but tumours exploit this negative feedback loop to evade immune attack. Tumours also secrete a number of soluble mediators, such as TGF β , IL-10, PGE2, adenosine, histamine, and hydrogen peroxide that directly inhibit T cell function and favour the development and maintenance of Tregs (Whiteside, 2002b). Tumour cells can also escape T cell attack by making themselves poor targets or “hiding” from the immune system. Tumours have been shown to frequently downregulate HLA

molecules and antigen processing machinery (APM) components (Seliger et al., 1996). APM was assessed in primary tumours and autologous lymph node metastases from patients with colorectal carcinoma. In comparison to autologous colorectal mucosa impaired TAP1, LMP2 and tapasin (all part of APM) expression was found in 42%, 42% and 63% respectively of primary adenocarcinomas of stage III disease and in 63%, 47% and 79% of the matched lymph node metastases (Atkins et al., 2004). To further support the idea that the immune system “edits” the tumour, it has been shown that HLA mutations occur at higher frequencies in tumours heavily infiltrated by CTLs (Castro et al., 2019; Shukla et al., 2015). The greatest number of mutations have been demonstrated to occur in the exon that codes for the TCR binding domain. Of the mutations found in the peptide binding domain of HLA, 46% mutations occurred in positions that come in direct contact with the peptide and would be expected to negatively affect peptide binding thus potentially resulting in ineffective presentation of the HLA:peptide complex to the immune system (Giannakis et al., 2016). These HLA and APM genes undergo a positive selection during an immune response and tumour cells with such mutations exhibit increased evolutionary fitness in the face of an immune attack because they are able to hide from T cells and continue to grow. All of the mechanisms described here create obstacles for an efficient anti-tumour immune response thus creating a need to therapeutically boost T cell responses and attenuate tumour-associated immune suppression through immunotherapy.

1.6 Cancer immunotherapy

The idea to use the immune system to treat cancer originated in 1891 when William Coley, now known as the “Father of Immunotherapy”, cured a patient with an inoperable cancer by injecting extracts of heat-inactivated *S. pyogenes* and *Serratia marcescens* (Coley’s Toxins) into the tumour and thus stimulating the immune system. However, lack of reproducibility and a known mechanism for his toxins in concert with the discovery of radiotherapy and chemotherapy prevented treatment with “Coley’s toxins” from

becoming standard practice (McCarthy, 2006). Later, the theory of immunosurveillance and evidence of T cell involvement in tumour regression caused the concept of immunotherapy to resurface. Earlier immunotherapy approaches such as high dose IL-2 showed limited responses and high toxicity, but some patients showed complete responses thus demonstrating that immune therapy for cancer can be effective in selected patients (Atkins et al., 1999; Fyfe et al., 1995; Rosenberg et al., 1994). Immunotherapy has come a long way since then and now a wide range of strategies that are used to enhance anti-tumour immunity including cancer vaccines, oncolytic viruses, adoptive cell transfer, CAR T cells, bispecific antibodies, and immune checkpoint targeting monoclonal antibodies.

1.6.1 Immune checkpoint blockade

Immune checkpoint inhibitors are the most successful type of immunotherapy to date. Immune checkpoints are usually ligand-receptor interactions that control the duration and amplitude of immune responses and are crucial for maintenance of self-tolerance and prevention of autoimmunity (Fife et al., 2009; Keir et al., 2006, 2007, 2008; Probst et al., 2005). Ultimately T cell activity is regulated by a balance of co-stimulatory and inhibitory immune checkpoints. The upregulation of checkpoints is highly controlled with naïve and resting T cells usually expressing co-stimulatory receptors such as CD28, but upon activation inhibitory receptors become upregulated such as CTLA-4, with both checkpoints sharing a common ligand such as CD80/CD86. Expression of CTLA-4 on the surface of T cells dampens the activation of T cells by outcompeting CD28 in binding CD80 and CD86 and also delivering inhibitory signals to the T cell (Chambers et al., 2001). The critical regulatory role of CTLA-4 is demonstrated by lethal systemic hyperactivation of lymphocytes and multiorgan destruction that develops in CTLA-4 knock out mice (Tivol et al., 1995; Waterhouse et al., 1995). In addition to its regulatory role in effector T cells, CTLA-4 is constitutively expressed by Tregs and its engagement

results in enhanced suppressor capability (Wing et al., 2008). Due to the ligand-receptor interaction type of checkpoints they can be readily blocked by monoclonal antibodies. Early mouse studies showed that CTLA-4 blocking as a monotherapy only enhanced anti-tumour immune responses in immunogenic tumours while poorly immunogenic tumours did not respond to anti-CTLA4 as a single agent but did respond when anti-CTLA4 was combined with a granulocyte–macrophage colony-stimulating factor (GM-CSF)-transduced cellular vaccine (Van Elsas et al., 1999). This study showed that an endogenous anti-tumour immune response was a prerequisite for anti-CTLA-4 antibody efficacy. Ipilimumab, an anti-CTLA-4 monoclonal antibody, showed survival benefit for patients with metastatic melanoma and was approved by the US Food and Drug Administration (FDA) for the treatment of advanced melanoma in 2010 (Hodi et al., 2010). CTLA-4 blockade induced long-lasting tumour regression, with 22% of patients with unresectable or metastatic melanoma who received ipilimumab surviving 3 years and some patients surviving as long as 10 years (Schadendorf et al., 2015).

While CTLA-4 checkpoint acts during early activation events, PD-L1/PD-1 axis works to control T cell responses in the periphery. After activation T cells upregulate PD-1 expression on their surface. Inflammatory signals such as IFN γ induce expression of PD-L1 by tumour cells as well as immune cells in the tumour microenvironment (Baumeister et al., 2016; Dong et al., 2002; Iwai et al., 2002; Kuang et al., 2009a; Liu et al., 2008). Once PD-1 engages with its ligand, its tyrosine in the cytoplasmic domain becomes phosphorylated and recruits tyrosine phosphatase SHP-2 which dephosphorylates signalling molecules downstream of the TCR involved in T cell activation thus dampening effector T cell activity (Freeman et al., 2000). Chronic antigen exposure which occurs during chronic viral infections and cancer leads to persistent PD-1 expression on T cells and reactive PD-L1 expression by target cells which induces an epigenetic program of T cell exhaustion (Sen et al., 2016). T cell exhaustion is a state of T cell dysfunction characterised by reduced cytokine secretion, impaired proliferation,

and reduced cytotoxicity (Ahmadzadeh et al., 2009). Exhaustion is partially reversible by PD-L1/PD-1 blockade (Barber et al., 2005). Mouse studies showed that PD-L1 expression on tumours prevents T cell mediated lysis and this formed the basis for PD-L1/PD-1 blockade as a therapeutic approach to treat cancer (Dong et al., 2002; Iwai et al., 2002). A study of melanoma demonstrated a strong correlation between cell surface PD-L1 expression on tumour cells and both lymphocytic infiltration and intratumoral IFN γ expression suggesting that PD-L1 upregulation is an adaptive immune resistance mechanism that occurs in response to anti-tumour immune response (Iwai et al., 2002; Taube et al., 2012). These findings provided rationale for antibody blockade of this pathway to enhance intratumoral immune responses. Treatment of advanced melanoma with pembrolizumab, anti-PD-1 monoclonal antibody, resulted in a 33% response rate compared to ipilimumab which only achieved 11.9%. Estimated 6-month PFS rates were 47.3% for pembrolizumab and 26.5% for ipilimumab (Robert et al., 2015). In addition to higher RR and PFS, anti-PD-1 therapy resulted in less immune related adverse events (irAEs) with approximately 10% of patients compared to 15-30% of patients treated with anti-CTLA-4 antibody (Baumeister et al., 2016). Currently, there are five anti-PD-1 or anti-PD-L1 antibodies approved by the FDA in 11 types of cancer: nivolumab (anti-PD-1), pembrolizumab (anti-PD-1), atezolizumab (anti-PD-L1), avelumab (anti-PD-L1), and durvalumab (anti-PD-L1) (Ribas & Wolchok, 2018). PD-L1 expression is the main biomarker used for selecting patients for immune checkpoint inhibitor (ICI) therapy (Patel & Kurzrock, 2015). However, due to the correlation of TMB and immunogenicity TMB has emerged as a predictive biomarker for response to ICI (Gandara et al., 2018; Hellmann et al., 2018; Meyers & Banerji, 2020). Tumours with high TMB such as melanoma and lung cancer showed 20-70% response rates to anti-PD-L1/PD-1 therapy (Ribas & Wolchok, 2018). This is attributed to higher lymphocyte infiltration of tumours which is associated with a better response to ICI (McGranahan et al., 2016; Tumei et al., 2014). As described earlier high TMB can arise as a result of mismatch repair deficiency in microsatellite instable tumours. Mismatch-repair status was shown to

predict clinical benefit of immune checkpoint blockade (Le et al., 2015, 2017). Objective radiographic responses were observed in 53% of patients with MSI-high tumours (Le et al., 2017). Efficacy of this therapy in colorectal cancer will be described in section 1.6.4.1.

Anti-CTLA-4 and anti-PD-1/PD-L1 antibodies target non-redundant co-inhibitory signals providing a rationale for combining these two therapies. In addition to using distinct molecular mechanisms of action, CTLA-4 and PD-1 regulate T cell activity through mechanisms that are separated spatially and temporally. Regarding the sites where these immune checkpoint molecules work it has been considered that CTLA-4 regulates T cell priming in the lymph node while PD-1 attenuates T cell activity in peripheral tissues. However, it has been demonstrated that anti-PD-1/PD-L1 therapy can also exert effects at regional lymph nodes. Analysis of tumour draining lymph nodes of patients with ovarian carcinoma revealed PD-L1 expression on monocyte-derived myeloid dendritic cells (MDCs) (CD11c⁺ and MHC-class II⁺) (Curiel et al., 2003). Blockade of the PD-1/PD-L1 interaction in xenograft ovarian tumour model enhanced dendritic cell-mediated T cell activation and significantly slowed tumour growth (Curiel et al., 2003). Another study showed that PD-L1 expression was significantly elevated in myeloid cells (CD11b⁺) in lymph nodes in a colon carcinoma mouse model. Anti-PD-1 therapy induced T cell activation and proliferation in tumour draining lymph nodes and resection of tumour draining lymph nodes strongly diminished anti-tumour immune responses induced by PD-1/PD-L1 blockade therapy (Fransen et al., 2018). Using multiple tumour mouse models including one of colon carcinoma, Dammeijer and colleagues have shown that tumour draining lymph nodes were enriched for tumour-specific PD-1⁺ T cells which closely associated with PD-L1⁺ cDCs. Tumour draining lymph node targeted PD-L1-blockade induced enhanced anti-tumour T cell immunity (Dammeijer et al., 2020). These data indicate that not only CTLA-4 but also PD-1/PD-L1 works as a negative regulator at tumour draining lymph nodes which are the main sites for anti-tumour T cell priming. Inhibitors of these two checkpoints act on

different T cell subpopulations with anti-PD-L1 inducing the expansion of exhausted-like CD8 T cells and anti-CTLA-4 inducing the expansion of a Th1-like CD4 effector subset (Wei et al., 2017). Patients with untreated melanoma that were given a combination treatment of ipilimumab and nivolumab demonstrated superior response, ORR of 61%, than those treated with ipilimumab alone, ORR of 11% (Postow et al., 2015). These results suggest that combination of anti-CTLA-4 and anti-PD-L1/PD-1 may better enhance anti-tumour immune responses than monotherapies and this combination has been approved for several cancer types (Marin-Acevedo et al., 2021).

The success of CTLA-4 and PD-L1/PD-1 targeting therapy has led to investigations of other immune checkpoints and several drugs are currently in clinical trials. LAG-3 (Lymphocyte Activation Gene-3) was discovered as a CD4 homolog in 1990, but its role as an immune checkpoint was not widely appreciated until 2004 when it was shown to have a role in enhancing the suppressive function of Tregs (C. T. Huang et al., 2004; Triebel et al., 1990). LAG-3 binds MHC class II which is expressed on tumour infiltrating macrophages, dendritic cells, and also on some epithelial cancers such as melanoma which upregulate it in response to IFN γ (Hemon et al., 2011). LAG-3 is expressed on activated CD8 and CD4 T cells, thymic and peripherally induced Tregs, NK cells, NKT cells, plasmacytoid dendritic cells, and B cells (Huard et al., 1994). LAG-3 and PD-1 are commonly co-expressed on exhausted T cells (Grosso et al., 2009). LAG-3 negatively regulates CD4 and CD8 T cell proliferation and function. LAG-3 has been shown to inhibit CD3/TCR signalling, decrease clonal expansion, decrease effector function, and restrict the size of the memory T cell pool (Grosso et al., 2007; Hannier et al., 1998; Workman et al., 2004; Workman & Vignali, 2005). Based on these data LAG-3 makes an attractive target for immunotherapy that can boost T cell activity and reduce the inhibitory effect of Tregs. Furthermore, mouse studies have shown a synergy between anti-LAG-3 and anti PD-L1/PD-1 therapy suggesting a promising combinatorial strategy for cancer treatment. Dual anti-LAG-3/anti-PD-1 antibody treatment cured most

mice of established tumours that were mostly resistant to single antibody treatment further supporting the non-redundancy of these checkpoints (Woo et al., 2012). Sixteen LAG-3 targeting therapies are currently being investigated in clinical trials with different targeting approaches being used: monoclonal antibodies, soluble LAG-3-immunoglobulin fusion proteins, and anti-LAG-3 bispecific antibodies. So far only two monoclonal antibodies targeting LAG-3, BMS-986016 (NCT05002569) and MK-4280 (NCT05064059) have reached phase III trials (Chocarro et al., 2022). Anti-PD-1 and anti-LAG3 combination treatments are also being investigated. A recent Phase II/III trial evaluating relatlimab (anti-LAG3 mAb) and nivolumab in previously untreated metastatic or unresectable melanoma showed that the inhibition of both immune checkpoints, LAG-3 and PD-1, provided a greater benefit with regard to PFS than inhibition of PD-1 alone. The median PFS was 10.1 months with relatlimab and nivolumab as compared with only 4.6 months with nivolumab alone (Tawbi et al., 2022). Other inhibitory checkpoints such as TIM-3, B7-H3, B7-H4, and TIGIT that have been shown to restrict anti-tumour immune responses in preclinical models are currently being evaluated in clinical trials (Andrews et al., 2019). Because tumour infiltrating lymphocytes express multiple inhibitory receptors there are opportunities through dual or triple blockade of immune checkpoints to enhance antitumour immunity.

1.6.2 Adoptive cell transfer/CAR T cell therapy

Another type of immunotherapy that utilises cellular components rather than monoclonal antibodies is adoptive cell transfer (ACT) therapy. In this type of therapy tumour infiltrating lymphocytes are extracted from resected tumours or biopsies, activated and expanded ex vivo, and then reinfused back into the patient. Following a preparative lymphodepletion, which is a temporary ablation of the immune system in a patient with cancer, achieved either with chemotherapy alone or in conjunction with total body irradiation, patients with metastatic melanoma were treated with the adoptive transfer of autologous tumour-infiltrating lymphocytes (TIL) along with IL-2. Fifty six percent of

patients achieved an OR, 22% achieved complete tumour rejection and those complete responders had a 93% 5 year survival rate (Rosenberg et al., 2011). An enhancement of this approach was identifying TCRs from antigen-specific TILs and virally transducing them into peripheral blood T-cells before reinfusing the expanded clonal antigen-specific T cell population back into the patient (Dudley et al., 2002; Zacharakis et al., 2018). However, as previously described due to high mutation rates melanoma tumours are particularly immunogenic and are heavily infiltrated by lymphocytes, but many other tumours lack lymphocyte infiltration which is a prerequisite for ACT. Therefore another therapeutic approach has been developed in which autologous T cells isolated from PBMCs through leukapheresis are harvested and genetically modified to target specific tumour antigens and expanded ex vivo and then reinfused into the patient. These CAR (chimeric antigen receptor) T cells contain an extracellular antigen binding scFv (single-chain fragment variable) derived from antibody, a hinge region, a transmembrane domain, and an intracellular signalling domain of TCR. Unlike TILs, CAR T are not MHC restricted and can bind proteins, glycolipids, and carbohydrates expressed on the tumour cell surface (Abbott et al., 2020). This is a major advantage over ACT which is dependent on antigen presentation on MHC molecules as tumours frequently downregulate MHC expression and alter APM. A patient with mCRC was treated with ACT but after initial metastases regression one lesion progressed due to loss of the chromosome 6 haplotype encoding the HLA-C*08:02 class I major histocompatibility complex (MHC) molecule thus directly driving immune evasion and resistance to ACT (Tran et al., 2016). The first generation CARs contained an scFv fused to elements from the CD3 complex such as CD3 ζ which led to poor proliferation and therefore lack of complete tumour clearance (Eshhar et al., 1993). Subsequent CAR T cell generations also incorporated signalling domains from co-stimulatory molecules with the third generation containing two co-stimulatory signalling domains (such as CD28, 4-1BB, OX40, and CD27) in tandem with the CD3 ζ chain. Upon CAR antigen engagement the T cell receives signal 1 and signal 2 for full activation bypassing the need for external co-stimulation by APCs.

Addition of co-stimulatory molecule domains to CAR T cells contributed to better expansion, prolonged antitumor activity, and enhanced cytokine secretion (Finney et al., 2004). CAR T cells mediate cytotoxicity through the same mechanisms as natural T cells: through secretion of perforin and granzyme granules, activation of death receptor signalling via Fas/Fas-ligand pathway, and cytokine secretion such as IFN γ (Yu et al., 2017). CAR T cells were further optimised and developed into TRUCKs (CAR T cells redirected for universal cytokine killing) which when activated produce and release a transgenic product such as IL-12 or IL-18 to activate innate immune responses against tumour cells which are invisible to CAR-T cells for example due to antigen loss (Avanzi et al., 2018; Chmielewski et al., 2011, 2014; Chmielewski & Abken, 2017, 2020; Glienke et al., 2022; Hu et al., 2017; Koneru et al., 2015). CAR T cell therapy targeting CD19 has achieved huge success in haematological cancers. CAR-T cell treatment (tisagenlecleucel) of children and young adults with B-cell lymphoblastic leukaemia achieved overall remission rate of 82% and a 90% and 76% OS rate at 6 months and 12 months respectively (Maude et al., 2018). Similarly promising results were seen in a trial evaluating CD19 targeting CAR T cells in adult patients with relapsed or refractory B-precursor acute lymphoblastic leukaemia. Seventy one percent of patients achieved overall complete remission or complete remission with incomplete haematological recovery (B. D. Shah et al., 2021). Since 2017 six CAR T cell therapies have been approved by the FDA: four targeting CD19 in patients with refractory or relapsed B cell acute lymphoblastic leukaemia (ALL), B cell non Hodgkin lymphoma (NHL), mantle cell lymphoma (MCL), and follicular lymphoma, and two targeting BCMA in relapsed or refractory multiple myeloma. However, CAR-T cells have not achieved the same success in solid tumours usually showing no responses, some patients achieving stable disease, and very rarely a few patients showing partial responses (Ahmed et al., 2015; Feng et al., 2016, 2018; Katz et al., 2015; Kershaw et al., 2006; Park et al., 2007). Lack of CAR T cell efficacy is attributed to inefficient trafficking to tumour site, limited persistence of

CAR T cells, target antigen loss, immunosuppressive TME, and suboptimal antigen recognition specificity (Li et al., 2018).

1.6.3 Bispecific antibodies

While CAR T cells have shown remarkable results in haematologic cancers and may be a promising therapy for solid tumours it is a highly personalised therapy as it relies on autologous T cells from each patient. This therapeutic approach is labour intensive, technically challenging, and highly expensive with tisagenlecleucel priced at \$475,000 per patient and that is not including costs associated with leukapheresis, lymphodepletion therapy, and the management of adverse effects of CAR-T immunotherapy (Hernandez et al., 2018). A more “off the shelf” therapeutic approach to promote T cell recognition of tumour cells are bispecific antibodies, particularly the bispecific T cell engagers (BiTEs). Unlike monoclonal antibodies that have specificity for a single antigen, BiTEs have dual-antigen specificity allowing them to bind two unique antigens at once and facilitate T cell and tumour cell interactions. These two single-chain variable fragments (scFvs) are connected by a linker the structure of which determines the flexibility of movement between the two scFvs and can be adjusted for optimal binding to both target cells. One arm of the bispecific binds to CD3 on T cells and the second arm binds the selected tumour antigen. As with CAR T cells, the best target antigen is one that is uniquely expressed on tumour cells with minimal expression in normal tissues in order to avoid on-target off-tumour responses. BiTE engagement of CD3 on a T cell and of the target antigen on tumour cell physically brings these two cells together and facilitates the formation of an immunological synapse which has been shown to be similar to those formed by cytotoxic T cells with target cells (Offner et al., 2006). BiTEs are also unique in their ability to activate T cells solely through the CD3 complex without the need for additional co-stimulation (Brischwein et al., 2007; Dreier et al., 2002; Lutterbuese et al., 2010). Following activation T cells secrete inflammatory cytokines, proliferate, and kill target cells via degranulation of granzyme and perforin

(Bacac et al., 2016; Osada et al., 2009). BiTEs are only able to trigger T cell activation when they have also bound tumour antigen which prevents non-specific T cell activation and makes this therapy tumour specific (Brischwein et al., 2007). One of the key advantages of this therapy is the ability of BiTEs to activate any CD3 expressing cell without the need for TCR-MHC interactions which is particularly important in tumours with low neoantigen numbers or those with antigen presentation defects.

BiTE treatments have so far only been approved for hematologic cancers: blinatumomab (CD3/CD19) for relapsed or refractory precursor B-cell acute lymphoblastic leukemia (ALL), mosunetuzumab (CD3/CD20) for relapsed or refractory follicular lymphoma, and teclistamab (CD3/BCMA) for relapsed or refractory multiple myeloma. However, some early phase clinical trials have been evaluating efficacy and safety of BiTEs in solid tumours. PMSA (prostate specific membrane antigen) targeted bispecific antibody for treatment of metastatic castration-resistant prostate cancer (mCRPC) achieved antitumour activity as measured by PSA (prostate specific antigen) serum decline in 63% of patients with reductions greater than or equal to 50% occurring in 60% of patients at the two highest dose levels (Tran et al., 2020). Another trial evaluating the efficacy and safety of tarlatamab, a bispecific T-cell engager binding CD3 and DLL3 (delta-like ligand 3) overexpressed in most small cell lung cancer, showed a 23% ORR including two complete responses with the median duration of response being 12.3 months (Paz-Ares et al., 2023). These early phase clinical investigations have shown that BiTE immunotherapy can be efficacious in solid tumours. There are currently tens of other early phase clinical trials evaluating efficacy and safety of BiTEs in solid tumours such as breast cancer, ovarian cancer, colorectal cancer, gastric cancer, and prostate cancer.

1.6.4 Immunotherapy in colorectal cancer

1.6.4.1 Immune checkpoint inhibitors

As described earlier immune checkpoint blockade has achieved remarkable responses in highly immunogenic tumours characterised by high mutational burden and expression of PD-L1 such as melanoma and non small cell lung cancer (Garon et al., 2015a; Larkin et al., 2015; Rizvi et al., 2015). Unsurprisingly, treatment of patients with MSI CRC, and therefore high TMB and neoantigen load, with pembrolizumab (anti-PD-1) resulted in 40% immune-related ORR and 78% immune-related PFS. However, disappointingly the same treatment achieved 0% immune related objective response in the MSS CRC group with a median PFS measuring a mere 2.2 months and OS 5 months thus demonstrating the lack of efficacy of this type of immunotherapy in this subgroup of patients which comprise 95% of metastatic CRC cases (Koopman et al., 2009; Le et al., 2015). Genomic analysis of both groups revealed a mean of 1782 somatic mutations per MSI tumour versus only 73 mutations per MSS cancer. Additionally computational algorithms predicted 578 mutation-associated neoantigens in MSI versus only 21 in MSS cancers (Le et al., 2015). However, computationally predicated neoantigens do not accurately represent the true neoantigen landscape in CRC. A study using MSS CRC patient derived organoids revealed that out of 196 non-silent mutations in expressed genes encoding for neoantigens as predicted by computational methods only 3 neoantigens were detected by mass spectrometry further highlighting the low abundance of neoantigens in MSS tumours and possibly explaining the low immunogenicity of these tumours (Newey et al., 2019).

Consensus molecular subtyping revealed the differential immune infiltration status of MSI and MSS tumours. MSI (CMS1) tumours are characterised by abundance of cytotoxic CD8 T cells, NK cells, Th1 cells and expression of immune checkpoints PD-L1, CTLA-4, LAG-3 (Becht et al., 2016; Guinney et al., 2015; Llosa et al., 2015). CMS2 and CMS3 tumours exhibit low immune and inflammatory signatures with very low numbers of CD8 T cells and also surprisingly low expression of MHC (Becht et al., 2016). CMS4 tumours exhibit a moderate amount of lymphocyte infiltration, many cells from myeloid and monocytic lineages and high amount of fibroblasts in concert with high expression of immunosuppressive cytokines and chemokines such as TGF β and CXCL12 (Becht et al., 2016). These findings fit well into the model categorizing the immune phenotype of tumours into four categories: immune cold (non inflamed), immune hot (inflamed), immune excluded, and immunosuppressed (Figure 1.3). Immune-hot tumours are characterised by high infiltration of CTLs, proinflammatory cytokines, and expression of immune checkpoints such as PD-L1 and clinical responses to PD-L1/PD-1 therapy occur most often in patients with this immune phenotype (Chen & Mellman,

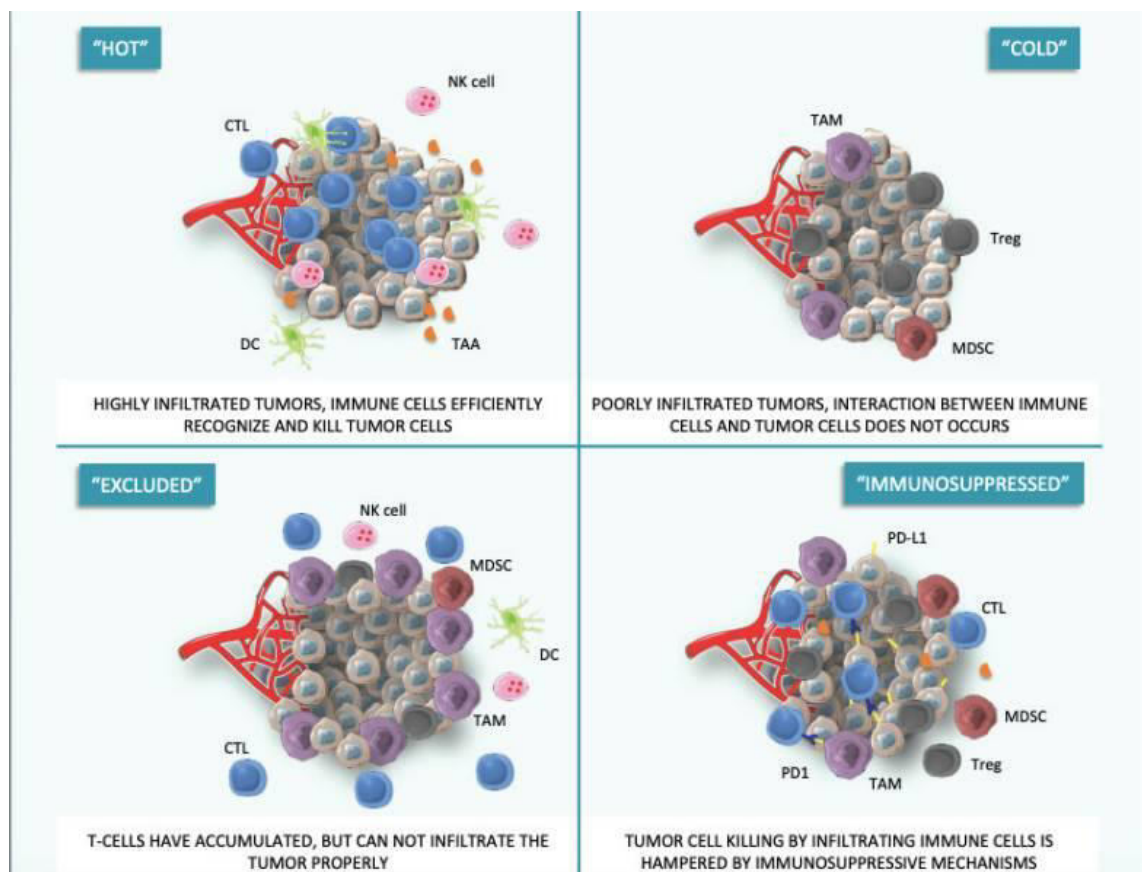


Figure 1.3 Four main phenotypes of anticancer immunity: hot, cold, excluded, and immunosuppressed. Immune-hot tumours are characterised by high infiltration of CTLs and expression of immune checkpoints such as PD-L1. Immune-cold tumours contain very few or no infiltrating lymphocytes. Immune-excluded tumours contain lymphocytes that are found at the edge of tumour sites (invasive margin) or retained in the stroma thus unable to infiltrate tumour parenchyma. Immunosuppressed tumours are infiltrated by lymphocytes but their activity is hampered by immunosuppressive immune cells such as Tregs, TAMs (tumour associated macrophages), and MDSCs, immunosuppressive cytokines (TGF β , VEGF, IL-10), and immune checkpoints (PD-L1, CTLA-4, TIM3, LAG3). Image taken from (Morganti and Curigliano, 2020).

2017; Galon & Bruni, 2019; Herbst et al., 2014; Topalian et al., 2012). Immune- cold or not inflamed phenotype contains very few or no infiltrating lymphocytes, no immune checkpoint expression, low mutational burden, and low expression of antigen presenting machinery such as MHC (Galon & Bruni, 2019). Immune excluded phenotype is characterised by T cell infiltration but the T cells are retained at edge of tumours commonly caught in the stroma suggesting the ability of the immune system to mount a response against these tumours but physical inability to reach the tumour bed. The final phenotype, immunosuppressed, contains a moderate lymphocyte infiltrate, immunosuppressive cytokines such as TGF β , IL-10, VEGF, immunosuppressive immune populations such as MDSCs and Tregs, and immune checkpoints such as PD-L1 and CTLA-4 (Galon & Bruni, 2019). Therefore, tumours with different immune phenotypes require different immunotherapy approaches. Combination therapy of heavily pre-treated patients with MSS CRC with botensilimab, a next-generation anti-CTLA-4 which in addition to preventing T cell inhibition promotes intratumoral regulatory T-cell (Treg) depletion via enhanced Fc-gamma receptor signalling, and balstilimab (anti-PD-1) showed promising results with 24% ORR, with patients with no history of liver metastases or post resection/ablation of liver metastases without recurrence achieving a higher ORR of 42% (Bullock et al., 2022). This combination therapy targeted multiple different parts of the cancer-immunity cycle such as T cell priming and activation with botensilimab, activity of activated T cells in the periphery with balstilimab, and

reprogrammed the TME by depleting Tregs with botensilimab showing that a multi-pronged approach might be more effective than monotherapeutic approaches.

1.6.4.2 Immune checkpoint inhibitors in combination with chemotherapy

Another approach to enhancing immunotherapy is using chemotherapy to induce immunogenic tumour cell death which is an essential part of the cancer-immunity cycle (Tesniere et al., 2009). Preclinical models have demonstrated that chemotherapy mediated immunogenic tumour cell death sensitises tumours to checkpoint blockade (Pfirschke et al., 2016). Following FOLFOX treatment of mCRC higher CD8 T cell infiltration and PD-L1 expression was observed (Wallin et al., 2016). As described earlier, in addition to its role in angiogenesis VEGF also exerts immunosuppressive effects promoting tumour immune evasion. Targeting VEGF with anti-angiogenic therapy leads to vasculature normalisation and enhanced infiltration of lymphocytes (Shrimali et al., 2010). Combined treatment of bevacizumab (anti-VEGF) plus ipilimumab (anti-CTLA-4) of patients with metastatic melanoma resulted in morphologic changes in intratumoral endothelia associated with increased trafficking of CD8 T cells into tumours ultimately leading to favourable clinical activity with combination treatment compared to ipilimumab alone (Hodi et al., 2014). Trials combining anti-VEGF agents and PD-L1/PD-1 immune checkpoint blockade for treatment of advanced MSS CRC have demonstrated mixed results with some trials achieving response rates of 22-33% while some showing much lower response rates of 0-7% possibly due to different dosing regimens (Barzi et al., 2022; M.Fakih et al., 2021; Fukuoka et al., 2020; Gomez-Roca et al., 2021; Saeed et al., 2022). Interestingly, the site of metastasis determined response to this combination therapy with 15% of patients with liver metastasis responding to treatment compared with 50% with lung metastasis (Fukuoka et al., 2020). In preclinical models liver metastasis are associated with more immunosuppressive TME compared to other metastatic sites such as lung. Preclinical studies in a melanoma model showed lower CD8/ Treg ratio and decreased percentage of activated PD-1+/CTLA-4+ CD8 cells

leading to lower response rate to PD-1 blockade (Lee et al., 2018). A clinical trial comparing FOLFOX6 plus bevacizumab (standard of care, SOC) and SOC plus nivolumab (anti-PD-1) in treatment of untreated and unresectable mCRC showed that addition of nivolumab achieved a higher response rate (60% vs 46%), higher PFS rates after 12 months, and enhanced durability of responses (12.9 months vs 9.3 months) (Lenz et al., 2022a). Other trials evaluating addition of anti-PD-L1/PD-1 immunotherapy to chemotherapy and bevacizumab have shown improvement in PFS (Antoniotti et al., 2022a; Mettu et al., 2022).

1.6.4.3 Immune checkpoint inhibitors in combination with anti-EGFR targeted therapy

Another rational treatment strategy for MSS mCRC is a combination of checkpoint inhibitors and anti-EGFR antibodies which can trigger immunogenic cell death and promote T-cell infiltration into tumours (Inoue et al., 2017; Woolston et al., 2019). Targeting multiple steps in the cancer-immunity cycle such as immunogenic cell death, T cell priming and activation, and T cell effector function for enhanced responses is supported by the results of a clinical trial evaluating the combination of ipilimumab (anti-CTLA-4), nivolumab (anti-PD-1), and panitumumab (anti-EGFR) in patients with KRAS/NRAS/BRAF WT MSS mCRC. The ORR was 35% which is an improvement upon the 22% achieved in a clinical trial evaluating panitumumab alone (Lee et al., 2021; Price et al., 2014).

1.6.4.4 Targeting LAG3 in colorectal cancer immunotherapy

As described earlier tumour infiltrating lymphocytes frequently express multiple actionable immune checkpoints therefore dual targeting of PD-L1/PD-1 and LAG3 has been taken as another approach to enhance anti-tumour immunity in MSS mCRC. However, the two clinical trials testing a combination of anti-PD-L1/PD-1 and anti-LAG3 showed modest response rates of 6.3 and 7.5%, but still achieving better responses than

anti-PD-L1/PD-1 therapy alone (Bendell et al., 2020; Garralda et al., 2021). Although these different strategies of combining immunotherapy with other treatment modalities have improved PFS and response rates compared with the complete lack of success of ICI alone in MSS mCRC, the improvements are very modest with only 1-2 months difference in the PFS. Therefore there is a need for other immunotherapeutic strategies, especially those increasing the presence of intratumoral lymphocytes which is an essential prerequisite for an effective anti-tumour immune response which is as described earlier lacking in majority of MSS CRC.

1.6.4.5 CAR T cell therapy

One approach to increasing T cell infiltration and tumour cell killing in immunologically cold tumours is the infusion of CAR T cells. To overcome limitations that have been observed with CAR T cells in solid tumours such as poor infiltration into tumours and weak cell expansion within tumours a novel CoupledCAR technology was developed which pairs CD19 targeting CAR T cells which have shown high efficacy in haematological cancers with CAR T cells targeting the enterocyte differentiation antigen guanylyl cyclase C (GUCY2C) which is expressed in the metastatic lesions of 70%-80% of patients with CRC. Activation of CD19 CAR T cells upon engagement with their target antigen on B cells causes release of cytokines that amplifies proliferation and activation of GCC targeting CAR-T cells (Cui et al., 2022). Treatment of mCRC patients GCC19CAR T cells resulted in combined overall response rate for both dose levels of 28.6%, with the higher dose achieving a higher response rate of 50% (Cui et al., 2022). Another antigen chosen as a target for CAR T cell therapy in CRC is CEA (carcinoembryonic antigen) which is a glycoprotein overexpressed in CRC and is an important CRC diagnostic and prognostic marker. CEA expression in healthy adult tissues is restricted to the apical surface of colon epithelium facing the lumen and thus remaining invisible to immune cells making it a strong candidate for CAR T cells which can frequently have on-target off-tumour effects (Nap et al., 1988). Treatment of mCRC

patients with CEA+ tumours with CEA targeting CAR T cells resulted in 20% of patients achieving response, 70% of patients who experienced progressive disease (PD) in previous treatments had stable disease with 29% of these remaining with stable disease for more than 30 weeks. Additionally, CAR T expansion was observed in peripheral blood and also tumour tissue in those patients receiving the higher dose of CAR-T therapy (Zhang et al., 2017). These are promising results showing that some patients with mCRC can achieve tumour regression with CAR T cell therapy.

1.6.4.6 T cell redirecting bispecific antibodies

Another immunotherapy approach to enhance T cell infiltration into CRC tumours is through BiTEs. A bispecific antibody targeting CEA on CRC cells and CD3 on T cells, cibisatamab or CEA-TCB, achieved tumour size reduction in 11% of patients with locally advanced and/or metastatic CEA+ CRC as monotherapy and in 50% of patients treated in combination with atezolizumab (anti PD-L1) (Tabernero et al., 2017). CEA-TCB belongs to the IgG-like bispecific antibody type that contains an Fc domain. One of the limitations of the earlier bispecific antibodies was the strong cytokine release resulting from CD3 clustering on T cells via the binding of Fc domain of the bispecific antibody to Fc receptors on other immune cell types. Catumaxomab, an anti CD3/EpCAM bispecific antibody induced high toxicity at low doses due to its binding to FcγR-positive Kupffer cells in the liver thus inducing off-target T cell activation thus limiting its clinical application to local peritoneal administration for the treatment of ascites (Borlak et al., 2016; Ruf et al., 2010). This limitation was overcome by the newer generation of BiTEs such as blinatumomab by removal of Fc domain and instead linking the anti-CD3 and anti-CD19 domains by a flexible linker. However, bispecific antibodies lacking Fc domains are no longer protected from catabolism by the neonatal Fc receptor (FcRn) thus resulting in a short plasma half life such as 1.25+/- 0.63 hours observed in blinatumomab treatment. As a consequence blinatumomab has to be continuously administered for multiple weeks thus severely limiting its clinical application (Klinger et

al., 2012). In order to prolong plasma half life but at the same time avoid FcR mediated toxicities CEA-TCB was designed with the introduction of P329G LALA mutations (Pro329Gly combined with Leu234Ala/Leu235Ala) which abrogate binding of the bispecific antibody to FcγRs but retains ability to bind to FcRn thus leading to slower drug clearance (Bacac et al., 2016). Another factor that has hampered bispecific antibody development for solid tumours is the expression of tumour associated antigens in normal tissues leading to on-target off-tumour toxicities (Fiedler et al., 2012). As described earlier CEA (CD66e, CEACAM5) is overexpressed in the majority of CRCs, but is also expressed at low levels on the apical surface of colonic epithelium. Its polarised expression pattern limits accessibility to therapeutic antibodies administered systemically thus protecting the colon from any bispecific antibody on-target off-tumour toxicities. Additionally CEA-TCB has been designed to bind two CEA molecules thus allowing this therapeutic approach to distinguish between high CEA expressing tumour and low CEA expressing normal colonic epithelium (Bacac et al., 2016). In order to further maximise tumour specificity CEA-TCB was designed to bind membrane proximal domain of CEA thus displaying preferential binding to membrane bound CEA rather than to shed CEA which is found at high concentrations in the serum of CRC patients. In vitro studies have demonstrated that there is a strong correlation between CEA expression level and CEA-TCB activity with only cancer cells containing >10,000 CEA binding sites being specifically lysed. Association tests were performed to find predictors of CEA-TCB response such as replication error status and common driver mutations in genes such as APC, TP53, KRAS, BRAF, and PIK3CA and no significant correlation was found thus leaving CEA expression as the strongest predictor of CEA-TCB activity (Bacac et al., 2016). Studies have shown that CD3 affinity of the bispecific antibody determines its distribution with higher CD3 affinity resulting in trapping of T cells in secondary lymphatic organs such as lymph nodes and spleen and lower CD3 affinity leading to a shift in distribution towards the tumour site (List & Neri, 2012; Mandikian et al., 2018). Therefore the CD3 binding arm of CEA-TCB was developed to have low affinity for CD3.

CEA-TCB is a very promising therapeutic approach for MSS CRC which are poorly immunogenic and frequently lack T cell infiltrate. However, clinical trial results indicate that most tumours are resistant to CEA-TCB treatment despite CEA expression on pre-treatment samples. CEA-TCB therapy skips the first three steps of the cancer-immunity cycle (release of cancer cell antigens, cancer antigen presentation, T cell priming and activation) thus suggesting that resistance mechanisms most likely arise from the remaining four steps which includes trafficking of T cells into tumours and infiltration into tumour beds and recognition of cancer cells by T cells followed by killing. Target antigen loss is one of the mechanisms used by tumours to escape immunotherapy such as CAR T cells and bispecific antibodies (Braig et al., 2017). A study from my lab using patient derived organoids (PDOs) showed CEA heterogeneity in CRC and demonstrated that CEA expression is highly plastic and allows CRC cells to switch between high and low CEA expression conferring resistance to CEA-TCB (Gonzalez-Exposito et al., 2019). Another resistance mechanism utilised by tumours is upregulation of checkpoints such as PD-L1 and preclinical studies of CEA-TCB have shown that CEA-TCB treatment increases PD-L1 expression in tumours (Bacac et al., 2016). Preclinical studies with other bispecifics demonstrated enhanced bispecific antibody mediated antitumour activity in combination with inhibition of the PD-1–PD-L1 axis (Junttila et al., 2014; Krupka et al., 2015; Osada et al., 2015). To further support these findings, data from a clinical trial evaluating efficacy of CEA-TCB showed that combination with atezolizumab enhanced clinical activity achieving tumour shrinkage in 50% of patients compared to only 11% in CEA-TCB only treated group (Tabernero et al., 2017). However, even with this combination treatment not all patients achieved tumour regression suggesting additional mechanisms of resistance such as immunosuppressive TME, that need to be investigated.

Currently preclinical models used for investigating bispecific antibodies rely predominantly on in vitro studies using cancer cell lines or mouse models. Preclinical

animal models investigating bispecific antibodies is complicated by the general lack of cross reactivity with mouse antigens and T cells. For example, CEA-TCB cross reacts with human CD3 and not mouse CD3. Additionally mice do not express *CEACAM5* therefore the mouse model that was used to investigate CEA-TCB activity in vivo was a human colon carcinoma xenograft model cografted subcutaneously with human PBMCs into immunodeficient NOG (NOD/Shi-scid/IL-2R γ -null) mice (Bacac et al., 2016). In order to assess ability of CEA-TCB to redirect T cells to the tumour site, the same human colon carcinoma cell line was injected subcutaneously into NOG mice followed by an intraperitoneal injection of human PBMCs once the tumours reached a certain size. Another approach to study human specific immunotherapy agents in mouse models is creating a human CD3 transgenic mouse in which all components of the CD3 complex are replaced by their human counterparts. However, in these immunocompetent models mouse tumour cell lines must be used which can be transduced with the human gene encoding the target antigen of the bispecific antibody (Ishiguro et al., 2017). Although mouse models allow for investigation of whole-body response to treatment, there are certain limitations in addition to those already described such as lack of TME, difficulty in controlling specific variables, high cost, and low throughput. Cancer cell lines which are the main in vitro models used to study bispecific antibodies poorly recapitulate tumour phenotypic and genotypic heterogeneity and may have lost certain molecular characteristics due to long term culture on plastic. Recently developed patient derived organoid (PDO) technologies have allowed long term propagation of cancer cells from CRC biopsies recapitulating the molecular features of the original tumour (Sato et al., 2011). To address the need for more patient-relevant preclinical models for studying novel immunotherapeutic agents such as CEA-TCB my lab has established a co-culture assay with multi-drug resistant mCRC PDOs and allogeneic T cells from healthy donors. Immunotherapy is most frequently used in a second or third line setting therefore making our PDO models highly clinically relevant as they have been generated from tumours resistant to chemotherapy. This initial study, which took place just as I had joined the lab

and has now been published, provided proof of concept that CEA-TCB efficacy can be evaluated in a PDO-T cell co-culture model (Gonzalez-Exposito et al., 2019).

1.7 PhD aims

The aims of my PhD thesis were:

- 1) To investigate factors regulating CEA expression using mCRC PDOs established by my host lab (Chapter 1)
- 2) To further validate and develop the PDO-T cell co-culture model established by my host lab (Chapter 2)
- 3) To perform a mini-screen in PDO-T cell co-cultures to investigate whether microenvironmental factors can confer resistance to CEA-TCB (Chapter 3)
- 4) To use the PDO-T cell co-culture model to develop therapeutic approaches to reverse resistance to CEA-TCB (Chapter 3)
- 5) To develop a 3D PDO-T cell coculture model to investigate how organoid architecture and size influences CEA-TCB responses

Chapter 2: Materials and methods

2.1 Materials

2.1.1 Tissue culture reagents

Reagent	Manufacturer	Catalogue No
ACK Lysing Buffer	Thermo Scientific	Fisher A1049201
Advanced DMEM:F12	Thermo Scientific	Fisher 12634028
Bovine Serum Albumin solution 7.5%	Sigma-Aldrich	A8412
Cell strainer (70µm)	Falcon	352350
Collagen I, High Concentration, Rat Tail	Corning	354249
Countess automated cell-counter slides	Thermo Scientific	Fisher C10283
Dimethyl sulfoxide (DMSO)	Sigma-Aldrich	D8418
DMEM (Dulbecco's Modified Eagle Medium)	Thermo Scientific	Fisher 11995073
DMEM:F12 (Dulbecco's Modified Eagle Medium/Nutrient Mixture F-12)	Thermo Scientific	Fisher 21331046
EDTA	In house	
Ficoll-Paque	Fisher Scientific	17-5442-02
Foetal Bovine Serum (FBS)	Thermo Scientific	Fisher 10270106
Foetal Bovine Serum (FBS) (T cells)	Labtech	FCS-SA/50
Glutamax	Thermo Scientific	Fisher 35050061
Insulin-Transferrin-Selenium (ITS) 100X	Thermo Scientific	Fisher 41400045
LS Columns	Miltenyi Biotec	130-122-729
Matrigel Growth Factor Reduced (GFR) Basement Membrane Matrix	Corning	356231
Matrigel Basement Membrane Matrix (for mouse injections)	Corning	354234
Minisart Syringe Filters 0.45µm	Sartorius	16533
Minisart Syringe Filters 0.22µm	Sartorius	16541
NaOH	In house	
OptiMEM	Thermo Scientific	Fisher 31985070

Paraformaldehyde	Sigma-Aldrich		15812-7
Penicillin-Streptomycin	Thermo Scientific	Fisher	15140122
Phosphate Buffered Saline (PBS)	In house		
Phosphate Buffered Saline (PBS) 10X	Sigma-Aldrich		D1408
Polybrene	Sigma-Aldrich		AL-118
RPMI 1640	Thermo Scientific	Fisher	31870074
TransIT 293 Transfection Reagent	Mirus		MIR 2700
Trypan Blue Stain	Thermo Scientific	Fisher	T10282
TrypLE Express	Thermo Scientific	Fisher	12605-010
Trypsin	In house		
Ultra filtered (UF) water	In house		

Table 2.1 Tissue culture reagents

2.1.2 Advanced media supplements

Supplement	Manufacturer	Catalogue No	Working Concentration
B27 50X	Thermo Scientific	Fisher 17504-044	1X
N2 100X	Thermo Scientific	Fisher 17502-048	1X
HEPES 1M	Thermo Scientific	Fisher 15630-056	10mM
NAC (N-Acetyl-L-cysteine)	Sigma-Aldrich	A9165	1mM
Nicotinamide	Sigma-Aldrich	N0636	10mM
EGF (human)	Peptotech	AF-100-15	50ng/mL
SB202190	Sigma-Aldrich	S7067	10µM
PGE2	R&D Systems	2296	10nM
Gastrin	Sigma-Aldrich	G9145	10nM
A-83-01	R&D Systems	2939/10	500nM
R-Spondin	Peptotech	120-38	1µg/mL
Noggin	Peptotech	250-38	100ng/mL
FGF10	Peptotech	100-26	100ng/mL
Wnt3a	R&D Systems	5036-WN	100ng/mL

Y27632	Sigma-Aldrich	Y0503	10µM
---------------	---------------	-------	------

Table 2.2 Advanced media supplements

2.1.3 Cytokines/Growth factors

Cytokine/Growth factor	Manufacturer	Catalogue No
IFNγ (human)	R&D Systems	285-IF-100/CF
IL-2 (human)	Roche	11011456001
IL-4 (human)	Peprotech	200-04
IL-10 (human)	Peprotech	200-10
IL-13 (human)	Peprotech	200-13
M-CSF (human)	Peprotech	300-25
sFas Ligand	Peprotech	310-03H
TGF-β1 (human)	R&D Systems	240-B-002
VEGF121 (human)	Peprotech	100-20A
VEGF165 (human)	Peprotech	100-20

Table 2.3 Cytokines/growth factors

2.1.4 Bispecific antibodies

Bispecific antibody	Manufacturer
DP47 TCB	Roche Glycart AG
CEA-TCB	Roche Glycart AG
DP47-4-1BBL	Roche Glycart AG
CEA-4-1BBL	Roche Glycart AG
FAP-IL2v	Roche Glycart AG

Table 2.4 Bispecific antibodies

2.1.5 Drugs

Drug	Target	Manufacturer
Compound 21	TNKS1/2	Provided by Professor Chris Lord (ICR)
Galunisertib	ALK4/ALK5 (TGF β RI)	Tocris

Table 2.5 Drugs

2.1.6 Flow cytometry

2.1.6.1 Antibodies

Antibody	Conjugate	Species	Manufacturer
CD8 (HIT8a)	PE	Mouse	BioLegend

CD8 (SK1)	Alexa Fluor 488	Mouse	SONY
CD4 (RPA-T4)	APC-Cy7	Mouse	BioLegend
CD68 (Y1/82A)	FITC	Mouse	BioLegend
CD206 (15-2)	PE	Mouse	BioLegend
CD95 (Fas) (DX2)	Alexa Fluor 700	Mouse	BioLegend
Granzyme B	Brilliant Violet 421	Rat	BioLegend
HLA-DR (L243)	APC-Cy7	Mouse	BioLegend
PD-L1 (29E.2A3)	Brilliant Violet 421	Mouse	BioLegend
Foxp3	Alexa Fluor 488	Mouse	Thermo Fisher Scientific
CEACAM5 (CH1A1A)	unconjugated	Human	Roche Glycart AG
CEACAM5 (487609)	unconjugated	Mouse	R&D Systems
AffiniPure F(ab')₂ Fragment Goat Anti-Human IgG, F(ab')₂ fragment specific	PE	Goat	Jackson Immuno Research
AffiniPure F(ab')₂ Fragment Goat Anti-Mouse IgG, Fcy Fragment Specific	PE	Goat	Jackson Immuno Research

Table 2.6 Flow cytometry antibodies

2.1.6.2 Viability dyes

Dye	Manufacturer	Catalog No
Zombie NIR Fixable Viability Kit	BioLegend	423105
Zombie Red Fixable Viability Kit	BioLegend	423109
DRAQ7	BioStatus	DR71000

Table 2.7 Viability dyes

2.1.6.3 Cell Proliferation assay

CellTrace Yellow Proliferation Kit, Thermo Fisher Scientific (C34573)

2.1.7 Blocking antibodies

Antibody	Manufacturer	Catalogue No
CD178 (Fas Ligand) Monoclonal Antibody (NOK-1) Functional Grade	Thermo Fisher Scientific	16-9919-81
Human IFNγ Monoclonal Antibody (25718)	R&D Systems	MAB285-100

Table 2.8 Blocking antibodies

2.1.8 Commercial Kits

Commercial Kit	Manufacturer	Catalogue No
Apo-ONE Homogeneous Caspase-3/7 Assay	Promega	G7790
CD14 MicroBeads	Miltenyi Biotec	130-050-201
CellTiter Blue Viability Assay	Promega	G8081
CellTiter Glo Viability Assay	Promega	G9242
Dynabeads FlowComp Human CD8	Thermo Fisher Scientific	11362D
Dynabeads Human T-Activator CD3/CD28	Thermo Fisher Scientific	11131D
Dynabeads Regulatory CD4+CD25+ T cell Kit	Thermo Fisher Scientific	11363D
eBioscience Foxp3 / Transcription Factor Staining Buffer Set	Thermo Fisher Scientific	00-5523-00
Human Tumour Dissociation Kit	Miltenyi Biotec	130-095-929
Mouse Cell Depletion Kit	Miltenyi Biotec	130-104-694
RNeasy Mini Plus Kit	Qiagen	74134
Qubit High Sensitivity RNA Quantification Kit	Invitrogen	Q32852

Table 2.9 Commercial kits

2.1.9 Real-time quantitative polymerase chain reaction (RTqPCR) primers

Gene	Identifier	Manufacturer
GAPDH	Hs02758991_g1	Thermo Fisher Scientific
CEACAM5	Hs00237075_m1	Thermo Fisher Scientific

Table 2.10 Real-time quantitative polymerase chain reaction (RTqPCR) primers

2.1.10 Immunohistochemistry reagents

Reagent	Manufacturer	Catalogue No
Antigen unmasking solution Citric acid based (pH6)	Vector Laboratories	H-3300
Antigen unmasking solution Tris based (pH9)	Vector Laboratories	H-3301
Cytoseal60	Thermo Fisher Scientific	8310-16
Ethanol absolute	VWR	20821.330

Harris Haematoxylin	Epredia	6765004
Hydrogen Peroxide (H₂O₂) solution 3%	Sigma-Aldrich	88597
Novolink Max DAB	Leica	RE7270-K
Protein block serum free	DAKO	X0909
SignalStain Boost IHC (HRP, mouse (yellow))	Cell Signalling Technology	8125S
T84.66 anti-CEACAM5 (primary antibody)	Roche Glycart AG	
TBS-T	In house	
Tween-20	Sigma-Aldrich	P9416
Xylene	Fisher Scientific	X/0250/17

Table 2.11 Immunohistochemistry reagents

2.2 Methods

2.2.1 Patient samples

Imaging-guided core biopsies from metastatic colorectal cancers that had been treated with at least two prior lines of chemotherapy were obtained from the Prospect C (clinical trials.gov number NCT02994888) and Prospect R (clinical trials.gov number NCT03010722) trials (Chief investigator: D. Cunningham, UK national ethics committee approval numbers: 12/LO/0914 and 14/LO/1812, respectively). One endoscopic biopsy from a treatment naïve primary colorectal cancer was obtained from the FORMAT trial (clinical trials.gov number NCT02112357, Chief investigator: N. Starling, UK national ethics committee approval number 13/LO/1274). Trials were run at the Royal Marsden Hospital and all patients provided written informed consent before trial inclusion.

2.2.2 Tissue culture

All cells were cultured at 37°C in a tissue culture incubator with humidified air, supplemented with CO₂ to 5%.

2.2.2.1 Generation of patient derived organoids (PDOs)

Direct cultures

PDO cultures from CRC-01, CRC-02 and CRC-06 were established directly from core biopsies by rough chopping followed by embedding in growth factor reduced Matrigel. The Matrigel was left to set at 37°C and then covered with supplemented Advanced DMEM:F12 media (from now referred to as Advanced media). List of supplements and the concentrations used are listed in Table 2.2.

Indirect cultures

Very small biopsy fragments were available from CRC-03, CRC-04, CRC-05, CRC-07 and CRC-08 and these were first grafted subcutaneously or under the kidney capsule of female CD1 nude mice by the Tumour Profiling Unit at the Institute of Cancer Research (Home office licence number PD498FF8D). Mice were culled once tumours had grown and tumours were removed and dissociated in a gentleMACS Octo dissociator using the Human Tumour Dissociation Kit. Mouse cells were magnetically removed using the Mouse Cell Depletion Kit, and purified human tumour cells were embedded into growth factor reduced Matrigel, left to set at 37°C and then covered with Advanced media.

2.2.2.2 Organoid passaging (3D configuration)

Once the organoids have been established, they were split every 1-2 weeks depending on growth rate. Media was changed 2-3 times a week. To passage, media was removed from the well, 1mL of PBS was added and using a 1mL pipette tip the Matrigel dome containing PDOs was mechanically disrupted. The 1mL of PBS was then transferred to a 15mL falcon tube containing 5mL of PBS and spun down at 300g for 5 minutes. Afterwards, PBS was aspirated and the Matrigel/cell pellet was resuspended in 1mL of TrypLE Express and incubated at 37°C for 20 minutes. TrypLE Express was neutralised with 5mL of DMEM:F12 media with 10% fetal bovine serum (FBS), 1X Glutamax, 100 units/mL penicillin/streptomycin and spun down at 300g for 5 minutes. After the supernatant was removed the cell pellet was resuspended in 150µL of growth factor

reduced Matrigel and placed in the center of a 12 well plate in a dome shape. The plate was incubated at 37°C for 30 minutes before adding 1mL of Advanced media.

2.2.2.3 Adaptation of organoids to different media and 2D growth

After at least 2 months of continuous growth in Matrigel domes and Advanced media, the PDOs were adapted to grow in DMEM/F12 (Sigma Aldrich) with 20% fetal bovine serum (FBS), 1X Glutamax, 100 units/mL penicillin/streptomycin (in the future referred to as 20% FBS DMEM:F12). After successful adaptation to DMEM:F12 20% FBS media, organoids were split as described above but instead of plating in 100% Matrigel domes, they were plated into 6 well plates in 20% FBS DMEM:F12 media containing 2% Matrigel. Once the cells have expanded they were cultured in T25 flasks.

2.2.2.4 Organoid passaging (2D configuration)

To split, media was aspirated from T25 flasks and then 5mL of PBS were added to wash away any remnants of media and aspirated after. Then, 2mL of TrypLE Express was added to the flask and the flask was put in an incubator at 37°C for 20 minutes. Afterwards, 5mL of 10% FBS DMEM:F12 media was added to neutralise TrypLE Express. All contents of the flask were transferred to a 15mL falcon tube and spun down at 300g for 5 minutes. If splitting rather than passaging, only a fraction of the cells were collected and spun down. After aspiration of supernatant, cells were resuspended in 1mL of 20% FBS DMEM:F12 media with 2% Matrigel and added to a new T25 flask containing 4mL of 20% FBS DMEM:F12 media with 2% Matrigel.

2.2.2.5 Organoid freezing

Organoids were split to single cells as described above, spun down at 300g for 5 minutes, and resuspended in 1mL of freezing media consisting of 10% DMSO in FBS and pipetted into a cryovial. Vials were then placed in polystyrene insulated boxes at -80°C for at least 24 hours before transfer to liquid nitrogen for long-term storage.

2.2.2.6 Organoid thawing

Cryovials were removed from liquid nitrogen on dry ice. Cryovials were thawed in a water bath at 37°C until fully liquid. Freezing media containing cells was transferred into a 15mL falcon tube and 8mL of 10% FBS DMEM:F12 media was slowly added on top. The cells were spun down at 300g for 5 minutes, supernatant was aspirated, and cells were resuspended either in Matrigel for 3D culture or in 20% FBS DMEM:F12 media for 2D culture.

2.2.2.7 Labelling PDOs with nuclear GFP

The nuclei of PDOs were labelled by introducing an eGFP tagged histone 2B construct (pLKO.1-LV-H2B-GFP) to enable visualisation by microscopy. HEK-293T cells were cultured in DMEM supplemented with 10% FBS, 1X Glutamax and 100units/mL penicillin/streptomycin. For virus generation HEK-293T cells were cultured in serum free media and 2×10^6 cells were plated in a 10cm petri dish and incubated at 37°C, 5% CO₂ overnight for transfection. Lentiviral particles were produced by overnight transfection with a plasmid mixture containing 9 µg of pLKO.1-LV-H2B-GFP (Addgene plasmid #25999), 2.25 µg of psPAX2 packaging plasmid (Addgene plasmid #12260) and 0.75 µg of pMD2.G envelope plasmid (Addgene plasmid # 12259) using TransIT-293 transfection reagent (Mirus). Media was subsequently changed and cells were incubated for 24 hours in DMEM supplemented with 10% FBS, 1X Glutamax and 100units/mL penicillin/streptomycin. Virus was harvested after 24 hours and passed through a 0.45µm filter before use. Virus was aliquoted into cryovials and stored at -80°C until use. For lentiviral transduction PDOs were harvested from the cultures and dissociated to single cells using TrypLE Express and spun down at 300g for 5 minutes. The pellets were resuspended in 250µL of virus containing media with 8µg/mL of polybrene (Sigma Aldrich) and Y27632 ROCK inhibitor (10nM) and centrifuged at 300g for 1 hour. Organoids were incubated for 6 hours at 37°C in the incubator. The tube was inverted every hour. Afterwards organoids were centrifuged at 300g for 5 minutes and virus

containing media was aspirated. The organoids were resuspended in 20% FBS DMEM:F12 media containing 2% Matrigel. Following recovery and expansion, highly eGFP positive cells were sorted by flow cytometry and further expanded before use.

2.2.2.8 PBMC isolation

Fresh blood

Fresh blood samples from healthy donors were obtained through Improving Outcomes in Cancer biobanking protocol at the Barts Cancer Institute (Chief investigator: T. Powles, UK national ethics committee approval number: 13/EM/0327) from individuals providing written informed consent. Blood samples from healthy donors were spun at 1600g for 10 minutes in EDTA tubes. After the spin plasma was aspirated. The remaining blood pellets were diluted with PBS and transferred to a 50mL falcon tube making up the volume to 35mL (3-4 EDTA tubes per gradient). This mixture was then carefully layered on top of 15mL of Ficoll and the falcon tubes spun at 400g for 30 minutes with centrifuge acceleration and deceleration breaks set to minimum. Afterwards, using a 5mL pipette PBMC layer was carefully harvested and transferred to a new falcon tube which was then topped up to 50mL with PBS and spun at 200g for 10 minutes. After the first wash, 5mL of ACK lysis buffer was added to the cell pellet for 5 minutes to deplete red blood cells. PBMCs were washed twice more and then cells were counted using a Countess automated cell counter system. The cells were spun down at 350g for 8 minutes and aliquoted for freezing in 10% DMSO in FBS freezing media. Vials were then placed in Mr. Frosty Freezing Container at -80°C for at least 24 hours before transfer to liquid nitrogen for long-term storage. Alternatively, the cells were used fresh for downstream applications.

Leukocyte reduction system (LRS) cones

LRS cones were obtained through the NHS Blood and Transplant service. Each LRS cone contained 8-10mL of concentrated blood. One LRS cone was split into 2 Ficoll gradients and prepared as described above (35mL of blood layered on top of 15mL of Ficoll). Gradients were centrifuged at 800g for 25 minutes with acceleration and deceleration breaks set to minimum. PBMC layer was collected using a 5mL pipette and diluted with PBS to 50mL. After the first wash, 5mL of ACK lysis buffer was added to the cell pellet for 5 minutes to deplete red blood cells. PBMCs were washed twice more and then cells were counted using a Countess automated cell counter system. The cells were spun down at 350g for 8 minutes and aliquoted for freezing in 10% DMSO in FBS freezing media. Vials were then placed in Mr. Frosty Freezing Container at -80°C for at least 24 hours before transfer to liquid nitrogen for long-term storage. Alternatively, the cells were used fresh for downstream applications.

2.2.2.9 T cell isolation from PBMCs

CD8 T cells were isolated from PBMCs with Human CD8 Dynabeads FlowComp kit according to manufacturer instructions. CD4+CD25- T cells were isolated from PBMCs with Dynabeads Regulatory CD4+/CD25+ T-Cell kit according to manufacturer instructions. The purity of CD8 and CD4 T cells was assessed by flow cytometry using Sony SH800 Cell Sorter and only populations with at least 90% purity were used either directly in experiments as freshly isolated T cells or first activated and expanded in vitro.

2.2.2.10 T cell activation and expansion

T cells were cultured in RPMI 1640 media supplemented with 10% FBS, 1X Glutamax, 100 units penicillin/streptomycin (from this point on referred to as T-cell media) and 30 U/mL IL-2. All FBS was batch tested. T cells were activated with CD3/CD28 Dynabeads Human T-Activator kit with a bead-to-cell ratio 1:1. T cells used in their pre-activated form were activated and expanded for 10-14 days prior addition to co-culture assay.

Expanded and activated T cells were also frozen for later use. First T cells were debeaded using DynaMag magnet, then they were spun down at 350g for 8 minutes, supernatant was aspirated and the cells were resuspended in T cell freezing media (10% DMSO in FBS). Cryovials were then placed in Mr. Frosty Freezing Container at -80°C for at least 24 hours before transfer to liquid nitrogen for long-term storage.

2.2.2.11 CAF culture

RC11 CAFs (gifted by Dr Fernando Calvo) were cultured in DMEM supplemented with 10% FBS, 1X Glutamax, 100 units penicillin/streptomycin, and 1X Insulin-transferrin-selenium (ITS) (referred to as CAF media).

2.2.2.12 Macrophage culture

Monocyte isolation from PBMCs

For monocyte isolation, PBMCs were thawed and spun down at 350g for 5 minutes. Cells were then filtered through a 30µm filter to remove any cell clumps that might block the column. Cells were resuspended in a buffer (0.5% BSA + 2mM EDTA in PBS) and mixed with CD14 microbeads at a specific ratio. The mix was incubated at 4°C for 15 minutes and afterwards washed with 1mL of buffer at 300g for 10 minutes. Cells were resuspended in 500µL of buffer and put into an LS Column that was pre-rinsed with 3mL of buffer and placed on a MACS Magnet. Unlabelled cells (non-monocyte fraction) were collected into a 15mL falcon, spun down and either used for further downstream applications or discarded. LS Column was removed from magnet and CD14+ cells were collected into a 15mL falcon tube and spun down at 300g for 8 minutes. Isolated monocytes were plated in 2mL of T cell media with the addition of 100ng/mL of M-CSF and seeded at $1-1.5 \times 10^6$ density into 6 well plates to be differentiated into macrophages.

Macrophage polarisation

After culturing CD14+ monocytes in T cell media + M-CSF for 5 days, 1mL of media was aspirated (all macrophages have attached by this point so no risk in aspirating them with media). Fresh T cell media with 100ng/mL of M-CSF was added (1mL). On day 7 of culture IL-4+IL-13+/-IL-10 or IL-10 alone were added at a concentration of 20ng/mL and macrophages were left to polarise for 48-72 hours after which the polarised macrophages were harvested for flow cytometry or 2D co-culture assays.

2.2.3 2D co-culture assay

PDOs growing in 2D were harvested with TrypLE Express and neutralised with 10% FBS DMEM/F12. Cells were filtered through a 70µm filter, counted and re-suspended in T cell media. Tumour cells were seeded at a density of 5000 tumour cells per well of a 96 well-plate (Corning Special Optics Microplate) in 50µL of T cell media and allowed to attach for 24 hours. On day 0, prior to any treatments the plates were imaged using Celigo Imaging Cytometer (Nexcelom Bioscience) to record the starting confluence of tumour cells. T cells (depending on experiment CD8 or CD4 T cells) were added on day 0 at the indicated effector to target (E:T) ratio in 25µL of T cell media with 20nM of CEA-TCB or 20nM of the untargeted control antibody DP47-TCB in 25µL T cell media (total well volume 100µL). Either pre-activated or freshly isolated T cells were used. Tumour cells without T cells and without bispecific antibodies were also included as controls. All conditions were plated in triplicates and T cells from multiple different healthy donors were tested. Outer wells of the plate were filled with 150µL of PBS to reduce evaporation.

2.2.3.1 Calculating tumour cell growth in 2D co-culture assay

The GFP confluence of PDOs was measured every 3-4 days over a 7-12 day period using the GFP confluence module on the Celigo Imaging Cytometer. For each 2D co-culture assay the growth of CEA-TCB treated PDOs over 7-12 days relative to DP47 treated PDOs was quantified. First the final confluence percentage was divided by the

initial confluence with 1 being subtracted to only consider growth post seeding. The growth for each treatment condition was calculated against the average growth of the untargeted control. In some cases the calculation was performed against tumour cell alone control where indicated.

2.2.3.2 2D co-culture assay with tankyrase inhibitor Compound 21

Two CEA-mixed PDOs CRC-06 and CRC-08 were treated with the combination of CEA-TCB and the tankyrase inhibitor Compound 21. PDOs were cultured over 7 days in the presence of CD8 T cells and 20 nM of CEA-TCB or the untargeted control antibody DP47. Co-cultures were either performed a) without tankyrase-inhibitor, b) following 48 hours of pre-treatment of tumour cells with tankyrase inhibitor which was removed when T cells were added, or c) following 48 hours pre-treatment with tankyrase inhibitor which was replenished at the time T cells were added for continuous tankyrase inhibitor exposure. Compound 21 was used at two doses 2 μ M and 10 μ M. All conditions were plated in triplicates. The confluence of the GFP labelled PDOs was tracked by microscopy for 7 days following addition of T cells and bispecific antibodies. Growth from the seeding density in the presence of DP47 to day 7 was defined as 100%.

2.2.3.3 2D co-culture assay: IFN γ and FasL blocking

A co-culture assay was set up according to the steps described earlier with either CD8 or CD4 T-cells. On the day of treatment (day 0), alongside CEA-TCB or the untargeted TCB DP47 either an IFN γ blocking antibody (5 μ g/mL) or a FasL blocking antibody (10 μ g/mL) were added to the co-culture assay. All conditions were plated in triplicates. PDO confluence was measured by microscopy as described earlier with the final timepoint being day 10.

2.2.3.4 TME soluble factors screen using 2D co-culture assay

Co-cultures were set up as described in 2.2.3, but prior to the addition to the assay the T cells were preincubated with IL-10 (20ng/mL and 100ng/mL), VEGF₁₂₁ (20ng/mL and

100ng/mL), VEGF₁₆₅ (20ng/mL and 100ng/mL), and TGFβ (10ng/mL) in T cell media for 72 hours. On day 0 of the assay T cells were collected, washed, counted, and added to the assay. Since PDOs were seeded in 50μL media, 25μL was aspirated and T cells, CEA-TCB/DP47, and cytokines (IL-10, VEGF, or TGFβ) were each added in 25μL of T cell media for a final volume of 100μL. All conditions were plated in triplicates. Co-cultures were grown for 12 days and quantified as described in 2.2.3.1.

2.2.3.5 Treatment of co-cultures with agents countering TGFβ induced immunosuppression

The experiments were set-up as described in 2.2.3 with T cells pre-incubated with TGFβ (10ng/mL) for 72 hours prior to addition to the co-culture. On day 0 of the assay after the starting confluence of the PDO was recorded, CD8 T cells and drug treatments were added. The following were combined with DP47 (20nM) or CEA-TCB (20nM) treatment: TGFβ (10ng/mL), galunisertib (5μM and 10μM), IL-2 (5U/mL and 10U/mL), FAP-IL2v (10nM and 100nM), DP47-41BBL (2nM), and CEA-41BBL (2nM). All conditions were plated in triplicates. Co-cultures were grown for 12 days and quantified as described in 2.2.3.1.

2.2.3.6 2D co-culture assay with the addition of macrophages

On day 0 of co-culture assay, macrophages were harvested on day 10 of culture (at the end of polarisation) by aspirating the media, washing the wells with 1mL of PBS, adding 5mM EDTA in PBS and incubating at 37°C for 30 minutes followed by gentle scraping. Collected cells were spun down at 350g for 8 minutes, resuspend in 500μL of T cell media, counted, and the chosen amount of macrophages spun down. T cells and macrophages were added to the assay in 25μL of T cell media at the same time. However, in this assay instead of treating the co-cultures on day 0, they were treated on day 1 (24 hours after the addition of macrophages and T cells) to allow macrophages to attach overnight. On day 1, co-cultures were treated with DP47 (20nM) or CEA-

TCB(20nM). All conditions were plated in triplicates. Growth was quantified as described in 2.2.3.1.

2.2.3.7 2D co-culture assay with the addition of CAF conditioned media

Assay was set up as described in 2.2.3. T cell media was conditioned by CAFs for 5 days and filtered through a 0.2µm filter. T cells were pre-treated with CAF CM (conditioned media) for 72 hours prior addition to the assay. On day 0 of assay fresh CAF CM was added to the co-culture assay in a 1:1 ratio with fresh T cell media along with T cells and DP47(20nM) or CEA-TCB (20nM). All conditions were plated in triplicates. Co-cultures were grown for 12 days and quantified as described in 2.2.3.1

2.2.3.8 2D co-culture assay with the addition of CAFs

Two different experimental set ups were used. In the first one, CAFs and PDO cancer cells were seeded at ratios of 1:1 and 0.5:1 in T cell media into a 96 well plate at the same time. After 24 hours, T cells were added in T cell media. The co-culture was left to incubate for 72 hours, after which DP47 (20nM) or CEA-TCB (20nM) were added. All conditions were plated in triplicates. Co-cultures were grown for 12 days and quantified as described in 2.2.3.1 In the second method, CAFs were first seeded in a 24 well in T cell media and left to attach for 24 hours. Then media was aspirated and T cells were added in 500µl of T cell media and left to incubate together with CAFs for 72 hours. PDO cancer cells were seeded into a 96 well plate 24 hours after T cell co-incubation with CAFs was started. After another 24 hours (48 hours into the CAF-T cell co-incubation) CAFs were seeded into the wells already containing cancer cells. After the 72 hours co-incubation of CAFs and T cells has finished, T cells were harvested, counted, and seeded into wells containing PDOs and CAFs. Subsequently DP47 (20nM) and CEA-TCB (20nM) were added to the assay. All conditions were plated in triplicates. Co-cultures were grown for 12 days and quantified as described in 2.2.3.1

2.2.3.9 2D co-culture assay under hypoxic conditions

Each PDO was seeded in four identical plates, one for each timepoint (day 0,4,7,10) and placed in a hypoxic chamber at 1% O₂ and one control plate was set up to run in parallel under normoxic conditions (21% O₂). The next day, plate 0 was scanned on the Celigo Imaging Cytometer to record the starting confluence prior to adding any T cells or treatment. Then pre-activated or non-activated CD8 T cells were added and co-cultured with the PDOs for a further 48 hours without any treatment. Afterwards, the co-culture was treated with either DP47 (20nM) or CEA-TCB (20nM). At each timepoint, the specified plate was removed from the hypoxic chamber and imaged using the Celigo Imaging Cytometer in parallel with the control plate. In all other experiments the same plate is imaged over the entire duration of the experiment, however, in this experiment I wanted to avoid oxygen fluctuations caused by removing the plate for imaging so I made a separate plate for each imaging timepoint. All conditions were plated in triplicates. Co-cultures were grown for 12 days and quantified as described in 2.2.3.1

2.2.4 Sensitivity of PDOs to IFN γ growth assay

PDOs were plated in 96 well plates in 6 replicates with 10,000 cells/well. After 24 hours the wells were treated with IFN γ at three different concentrations (1ng/mL, 10ng/mL, and 100ng/mL) and left to grow for 7 days. Cells were not seeded in outer wells, which were instead filled with 150 μ L of PBS to prevent incorrect reading due to excess evaporation. On day 0 a baseline Cell Titer Blue (CTB) reading of the reference plate was performed on Cytation3 (BioTek Instruments Inc.) at 590 nm following a 2 hour incubation at 37°C. On day 4 of experiment, 50 μ L from the total 100 μ L in the well was aspirated and replaced with 50 μ L containing fresh IFN γ . On day 7 a CTB assay was performed (2 hour incubation at 37°C). Data was then analysed by subtracting the mean value for the reference plate at day 0 of treatment to account for the initial cell number and the experimental wells normalised to the mean value for growth in control.

2.2.5 Validation of IFN γ blocking antibody

PDOs were plated in 96 well plates in 6 replicates with 10,000 cells/well. After 24 hours the wells were treated with IFN γ at three different concentrations (1ng/mL, 10ng/mL, and 100ng/mL) or in combination with an IFN γ blocking antibody (5 μ g/mL) and left to grow for 7 days. Cells were not seeded in outer wells, which were instead filled with 150 μ L of PBS to prevent incorrect reading due to excess evaporation. On day 0 a baseline Cell Titer Blue (CTB) reading of the reference plate was performed on Cytation3 at 590 nm following a 2 hour incubation at 37°C. On day 7 a CTB assay was performed (2 hour incubation at 37°C). Growth was assessed as a ratio compared to untreated control.

2.2.6 Validation of FasL blocking antibody

CRC-01 PDO were seeded in a 96 well plate at a density of 10,000 cells/well in 50 μ L of T cell media. After 24 hours, the media was carefully aspirated and cells were either treated with T cell media alone (control) or T cell media with IFN γ at a concentration of 10ng/mL for 48 hours. Afterwards, wells were treated with soluble Fas ligand (sFasL) at two concentrations (100ng/mL and 500ng/mL) +/- FasL blocking antibody NOK-1 at two concentrations (1 μ g/mL and 10 μ g/mL) or with staurosporine (1 μ M) as a control for apoptosis. After 24 hours Cell Titer Blue was added and a reading of cell viability recorded after a 2 hour incubation at 37°C using Cytation3. Afterwards The Apo-ONE Homogeneous Caspase-3/7 Assay kit was used according to manufacturer instructions. Plate was scanned on Cytation3 after 4 hours of incubation with Apo-ONE Reagent at room temperature and gentle shaking and fluorescence at 521nm was measured. Apo-ONE fluorescence was normalised to Cell Titer Blue fluorescence.

2.2.7 Flow cytometry

2.2.7.1 Surface CEA expression

PDOs were harvested as described in section 2.2.2.4 dissociating PDOs to single cells with TrypLE Express and spun down at 300g for 5 minutes following neutralisation with

10% FBS DMEM:F12 media. Cells were resuspended in FACS buffer (0.5% BSA in PBS), counted, and 2×10^5 cells were spun down in 1.5mL Eppendorf tubes at 300g for 5 minutes. Afterwards, cells were stained with 20nM of CH1A1A antibody (anti- human CEACAM5) or 10 μ g/mL anti-CEACAM5 antibody clone 487609 where specified in 50 μ L of FACS Buffer at 4°C for 30 minutes. Following primary antibody staining, cells were washed with 700 μ L of FACS Buffer 3 times, centrifuging at 300g for 5 minutes after each wash. After the third wash supernatant was taken off and cells were resuspended in 50 μ L FACS Buffer with R-Phycoerythrin conjugated secondary antibody AffiniPure F(ab')₂ Fragment Goat Anti-Human IgG, Fcy Fragment Specific or AffiniPure F(ab')₂ Fragment Goat Anti-Mouse IgG, Fcy Fragment Specific diluted 1:50. After a 30 minute incubation with secondary antibody at 4°C, cells were washed twice. Cells were resuspended in 200 μ L with DRAQ7 viability dye diluted 1:100 and incubated at 37°C for 10 minutes. CEA expression was analysed on Sony SH800 Cell Sorter. CEA negative gates were set using DRAQ7 stained but CEACAM5 unstained control. Data analysis was performed using FlowJo software. For all CEA expression experiments where 2D organoids were used they were cultured in 20% FBS DMEM:F12 media with 2% Matrigel unless specified in the Results section otherwise. Whenever experiments were performed with different supplements of Advanced media, the same concentrations were used as in Advanced media. For experiments testing the effect of IFN γ on CEA surface expression in PDOs tumour cells were seeded in 12 well plates at a density of 240,000 cells/well in 20% DMEM:F12 media with 2% Matrigel. After 24 hours, media was changed and PDOs were treated with two doses of IFN γ (10ng/mL and 100ng/mL) for 48 hours before they were harvested and analysed for CEA surface expression. For experiment one testing effect of density on CEA surface expression in PDOs tumour cells were seeded in 12 well plates at a density of 50,000 cells/well, 100,000 cells/well, and 200,000 cells/well in 20% FBS DMEM:F12 media with 2 % Matrigel. Cells were harvested and analysed by flow cytometry on day 10, when wells seeded with 200,000 cells have reached 90-100% confluence. For second experiment testing effect of density

on CEA surface expression of PDOs, tumour cells were seeded in 12 well plates at a density of 50,000 cells/well and 400,000 cells/well in 20% FBS DMEM:F12 media with 2% Matrigel. Cells were harvested for flow cytometry analysis on day 12 (4 days after the more densely seeded well has reached 100% confluency). For experiments testing effect of tankyrase inhibitor Compound 21 (C21) on CEA surface expression in PDOs, tumour cells were seeded in 12 well plates at a density of 100,000 cells/well in 20% FBS DMEM:F12 media with 2% Matrigel and treated either with DMSO (control), 2 μ M or 10 μ M of C21 for either 48 hours or 6 days (specified in the Results chapter).

2.2.7.2 Flow cytometry analysis of T cells recovered from 2D co-culture assay

For T cell flow cytometry staining the 2D co-culture assay was scaled up to either a 24-well plate (30,000 PDO cells, 60,000 T cells, E:T 2:1) or 12-well plate (60,000 PDO cells, 120,000 T cells, E:T 2:1). For TGF β experiments, prior to adding the T cells to the co-culture they were pre-incubated with TGF β (10ng/mL) for 72hrs and on the day of seeding were labelled with CellTrace Yellow proliferation dye (10 μ M) for proliferation tracking. For CellTrace Yellow staining cells were incubated with 10 μ M CellTrace Yellow in PBS at 37°C for 20 minutes, inverting the tube every 5 minutes to prevent cells from settling on the bottom of the tube. Then 5mL of T cells media was added and the cells were left to stand at room temperature for 5 minutes before being spun down at 350g for 8 minutes. T cells from 2D co-culture assays were harvested by collecting the media from the wells, and subsequently washing the wells with PBS multiple times. Collected cells were put into a round bottom 96 well plate, separate well for each condition, and spun down at 300g for 5 minutes. Cells were resuspended in 50 μ L PBS with Zombie NIR Fixable Viability Dye diluted 1:500 and left to incubate at room temperature for 30 minutes in the dark. Afterward cells were washed twice by adding 200 μ L FACS Buffer (0.5% BSA in PBS) and centrifuging at 300g for 5 minutes. Afterwards cells were stained with directly conjugated antibodies for extracellular markers CD8 and CD4 at a dilution 1:20 at 4°C for 30 minutes. To remove unbound antibody cells were washed with 200 μ L FACS

Buffer per well, three times, centrifuged at 300g for 5 minutes. Cells were fixed with Fixation Buffer from eBioscience Foxp3 / Transcription Factor Staining Buffer Set at 4°C for 30 minutes. The cells were washed twice with Permeabilisation Buffer from eBioscience Foxp3 / Transcription Factor Staining Buffer Set after diluting it according to manufacturer instruction. Afterwards cells were stained with directly conjugated antibodies for intracellular markers Granzyme B and Foxp3 at a dilution 1:20 in 50µL of Permeabilisation Buffer at 4°C for 30 minutes. Then cells were washed twice more with Permeabilisation Buffer and once with FACS buffer. Finally, cells were resuspended in 400µL of FACS Buffer and analysed on BD LSRII flow cytometer. For proliferation dye control, T cells were labelled with CellTrace Yellow (10µM) on the day of the flow cytometry experiment to represent the undivided cells control. Flow cytometry data analysis was performed using FlowJo. Gates were set using appropriate fluorescence minus one (FMO) controls.

2.2.7.3 Surface Fas expression in PDOs

PDOs were seeded in 12 well plates at a density of 100,000 cells/well in 20% FBS DMEM:F12 media with 2% Matrigel. Some wells were treated with IFN γ at two concentrations (10ng/mL and 100ng/mL) for 72 hours. Cells were harvested as described in 2.2.2.4 and 2×10^5 cells were stained with an anti-Fas antibody diluted 1:20 in FACS Buffer (0.5% BSA in PBS) for 30 minutes at 4°C. Cells were washed 3 times with FACS Buffer and centrifugation at 300g for 5 minutes. For viability cells were stained with DRAQ7 viability dye diluted 1:100 in FACS Buffer at 37°C for 10 minutes. Cells were analysed for Fas surface expression using Sony SH800 Cell Sorter. Flow cytometry analysis was performed using FlowJo software.

2.2.7.4 Analysis of M2 macrophage markers

After 7 days culture in T cell media with M-CSF (100ng/mL) and 72 hours of polarisation towards the M2 phenotype with IL-4/IL-13/IL-10 (20ng/mL) macrophages were harvested

from 6 well plates with 5mM EDTA in PBS incubating at 37°C for 30 minutes followed by gentle scraping. Cells were first stained with Zombie Red viability dye diluted 1:100 in PBS at 4°C for 30 minutes in the dark. Cells were washed twice with FACS Buffer (0.5% BSA in PBS). Cells were resuspended in 80µL of FACS Buffer and 20µL of Miltenyi FcR Blocking Reagent was added, mixed well, and incubated at 4°C for then minutes and then the cells were washed with FACS Buffer. Following that, cells were stained with directly conjugated antibodies against extracellular markers: CD206, HLA-DR, PD-L1. All antibodies were diluted 1:20 in FACS Buffer and cells were incubated at 4°C for 30 minutes. Afterwards, unbound antibody was removed by washing the cells three times with FACS Buffer and centrifugation at 300g for 5 minutes. Cells were fixed with Fixation Buffer from eBioscience Foxp3 / Transcription Factor Staining Buffer Set at 4°C for 30 minutes. The cells were washed twice with Permeabilisation Buffer from eBioscience Foxp3 / Transcription Factor Staining Buffer Set after diluting it according to manufacturer instruction. Afterwards cells were stained with directly conjugated antibodies for intracellular marker CD68 at a dilution 1:20 in Permeabilisation Buffer at 4°C for 30 minutes. Then cells were washed twice more with Permeabilisation Buffer and once with FACS buffer. Finally, cells were resuspended in 400µL of FACS Buffer and analysed on BD LSRII flow cytometer. Flow cytometry analysis was performed using FlowJo software.

2.2.8 3D PDO-T cell co-culture assay

PDOs were grown for 10-12 days (or for up to 21 days for the experiment using different organoid sizes) in Matrigel domes overlayed with 20% FBS DMEM:F12 media. To harvest the organoids, the domes were mechanically disrupted and the pieces of broken up Matrigel containing PDOs were resuspended in cold PBS for 20 minutes with inversion of the falcon tube every 5 minutes followed by moderate pipetting. Afterwards PDOs were spun down at 300g for 5 minutes, supernatant aspirated, and the organoids were resuspended in 75-100µL of T cell media depending on the amount of organoids.

For the immune cell component of the assay, pre-activated T cells were either thawed the day before and cultured in T cell media with IL-2 (30U/mL) for 24 hours or if they were used directly after activation and expansion they were debeaded prior to use in the assay. T cells were labelled with CellTrace Yellow (4 μ M) in PBS for 20 minutes at 37°C in the dark, inverting the tube every 5 minutes to prevent cells from settling and to ensure homogenous staining. Afterwards T cells were spun down at 350g for 8 minutes and counted. In parallel, the ECM matrix was prepared on ice with pre-cooled pipette tips. Rat tail collagen I was prepared according to the manufacturer instructions. To calculate the volume of collagen to be added the following equation was used: final volume needed x final collagen concentration (6mg/mL)/Stock concentration of collagen (lot specific). Then the concentrated collagen stock was mixed with a mix of 10X PBS (10% of final volume), 1 N NaOH (volume of collagen to be added x 0.023), dH₂O (final volume-volume of concentrated collagen -volume of 10x PBS -volume of 1 N NaOH). Collagen was then thoroughly mixed and then combined with an equal volume Matrigel to create an ECM with 3mg/mL collagen concentration. This ECM was used to coat the bottom of the plate (12 μ L). This coating procedure was done on ice and afterwards the plate was put into an incubator at 37°C for 1 hour. CellTrace labelled T cells (45,000/condition) in T cell media were mixed with the Matrigel/collagen matrix in a 0.5:1 ratio reducing the collagen concentration to 2mg/mL. At this point DP47 or CEA-TCB bispecific antibodies were added to the gel. Then this T cell containing gel was mixed with 10 μ L of PDOs in T cell media and 50 μ L of the final mix were added to the 96 well plate on top of the polymerised base matrix layer. During this procedure the plate was not kept on ice to not re-liquify the base matrix, but the ECM containing T cells and PDOs were kept on ice to keep the gel in liquid form for pipetting. Afterwards the plate was placed in the incubator at 37°C for 1 hour to allow the gel to polymerise. Following that 100 μ L of T cell media containing DP47/CEA-TCB (both 20nM) and DRAQ7 (final dilution 1:100) was added on top of the ECM containing PDOs and T cells. The plate was then placed in a chamber of a live imaging spinning disk microscope where the temperature was maintained at 37°C and

CO₂ level was 5%. Three lasers were used: 488 nm for organoids, 561 nm for T cells, and 640 nm for DRAQ7. In each well (each condition), 3-6 fields of view were selected to be imaged. The imaging was performed as a 3D timelapse so for each field of view a Z-stack was taken with 5µm steps between slices. The co-culture was continuously imaged over 72 hours; for some experiments images were taken every 2 hour and for some every 6. Max and sum projections and subtraction of background signal were performed in Slidebook 6.0 software. Image analysis was performed in Cell Profiler software where a special pipeline was created to address the necessary questions. Afterward, the data was processed using an R script which was created by me under the guidance of Dr. Andrew Woolston, a bioinformatician in my lab, specifically for this assay and project. Final graphs were created in GraphPad Prism software.

2.2.9 Real-time quantitative polymerase chain reaction (RTqPCR)

mRNA was extracted using Qiagen RNeasy Mini Plus kit according to manufacturer protocol. Cells were lysed with 350µL of RLT Plus buffer directly in the 6 well. Scrapers were used to collect the cells. Following that cells were collected into RNase-free Eppendorfs and syringed through a 20 gauge syringe 5 times before putting the lysate into the gDNA eliminator column and proceeding with the rest of the protocol. RNA was eluted in 30µL of RNase-free H₂O and quantified using Qubit RNA High Sensitivity kit according to manufacturer instructions. RNA (1µg) was converted to cDNA using the SuperScript II Reverse Transcriptase protocol. RT-PCR reactions were set up using 2µL of cDNA, 1µL of Taqman Gene Expression Assay probe, 10µL of Taqman Universal Master Mix II with UNG and 7µL of H₂O per reaction. Relative quantification was performed on QuantStudio6-Flex sequence detection and all reactions were performed in triplicate. Gene expression was normalised to endogenous control GAPDH and analysed using the delta-delta CT method.

For experiments comparing the effect of Advanced media versus 20% FBS DMEM:F12 media on CEA expression in PDOs 100,000 tumour cells were seeded in a 6 well with

both media containing 2% Matrigel. RNA was collected on day 12. For experiments comparing the effect of SB202190 and nicotinamide on CEA expression in PDOs 100,000 tumour cells were seeded in a 6 well with both media containing 2% Matrigel. RNA was collected on day 12. For tankyrase inhibitor Compound 21 treatment, 150,000 cells were seeded in a 6 well in 20% FBS DMEM:F12 media and treated either with DMSO (1/1000 dilution), C21 2 μ M (1/5000 dilution), or C21 10 μ M (1/1000 dilution) for 6 days prior to RNA collection.

2.2.10 RNA sequencing

PDOs were seeded at 50,000 cells/well in 6 well plates in DMEM:F12 20% FBS media with 2% Matrigel with or without the addition of SB202190 (10 μ M) and nicotinamide (10mM). RNA was collected on day 12. RC11 CAFs were seeded in 10cm dishes with 750,000 cells/dish in CAF media (DMEM 10% FBS + ITS 1X) or T cell media (RPMI 1640 10% FBS) and RNA was harvested after 72 hours. RNA was extracted according to Qiagen RNeasy Mini Plus kit protocol. RNA was eluted into 30 μ L of RNase-free water. RNA was quantified using Qubit RNA High Sensitivity Kit. RNA (250ng) was prepared for sequencing using Lexogen QuantSeq 3' mRNA-Seq Library Prep Kit FWD for Illumina using the manufacturer's recommended protocol. qPCR was performed on all libraries to deduce optimal cycles of PCR amplification. Final libraries were quantified using Agilent TapeStation High Sensitivity D1000 ScreenTape to facilitate equimolar pooling. The final pool was sequenced with single read 100 cycles and 12 nt unique dual indices on an Illumina NovaSeq 6000 SP flowcell to a median 9M reads per sample. The resulting demultiplexed fastq were analysed with the Lexogen in-house Data Analysis pipeline comprising: alignment to the Homo sapiens GRCh38 ensembl release 107 (ERCC/SIRV); fastqc and STAR quality control; and generation of raw read counts. Differential gene expression analysis was performed on the raw read counts using the DESeq2 R package.

2.2.11 Immunohistochemistry: CEA staining of FFPE tissue sections

2.2.11.1 CRC xenografts

PDOs were grown in 2D in 20% FBS DMEM:F12 media in T75 flasks. PDOs were harvested with TrypLE Express as described in 2.2.2.4. For each PDO line, 1×10^6 cells were injected in 50 μ L (25 μ L cold 20% DMEM:F12 media and 25 μ L Matrigel) subcutaneously into NSG mice. For each PDO, 2 mice were used and for each one there were 2 (left and right) flank injections totalling 4 injections per PDO. Mice were culled and tumours harvested when they reached tumour volume of 1000mm³. Some tumours were harvested earlier due to ulceration. Tumours were processed and embedded by Breast Cancer Now (BCN) Histopathology Core Facility.

2.2.11.2 PDO preparation for FFPE slides

PDOs were plated in 150 μ L of Matrigel in 12 well plate as single cells and cultured in DMEM:F12 20% FBS media for 13 days. To harvest the organoids media was aspirated, wells washed with PBS, and cold 4% PFA was added on top (500 μ L/well) and incubated for 30 minutes at room temperature. Then Matrigel was disrupted by pipetting and organoids were washed twice with PBS with centrifugation at 300g for 5 minutes. Samples were stored overnight at 4°C with a small amount of PBS on top of the organoid pellet. Samples were then embedded by Breast Cancer Now (BCN) Histopathology Core Facility.

2.2.11.3 CEA immunohistochemical staining of FFPE slides

FFPE slides were deparaffinised by placing them in an oven at 63°C and then incubated in xylene for 8 minutes twice and subsequently rehydrated with graded ethanols (100%, 95%, 70%, 50%). After washing the slides in DI water, slides were submerged into antigen unmasking pH solution and microwaved for 1.5 minutes at 1000 watts and then microwaved at 100 watts for 15 minutes. After letting them cool at room temperature the slides were washed with DI water 3 times 3 minutes each and then with TBS-T 3 times

3 minutes each. To block endogenous peroxidase slides were treated with hydrogen peroxidase 3% for 10 minutes. After washing the slides with TBS-T 3 times 3 minutes each the slides were treated with serum-free protein block for 1 hour at room temperature. After tapping off the excess serum-free block, 150µL of T84.66 anti-CEACAM5 diluted antibody (1/400) was added to the slide for 1 hour at room temperature. Following that slides were washed with TBS-T 3 times for 3 minutes each and then treated with HRP conjugated secondary antibody for 1 hour. Then slides were washed with TBS-T 3 times 3 minutes each. DAB (3,3'-Diaminobenzidine) solution was prepared as per manufacturer instructions by mixing DAB chromogen to DAB substrate in the ratio of 1:20. DAB solution was pipetted onto the slide and left for 10 minutes in the dark. Subsequently slides were washed with DI water and counterstained with haematoxylin for 2 minutes. Slides were then washed with DI water and dehydrated with ethanol solutions (50%, 70%, 95%, 100%). After submerging the slides in xylene twice for 2 minutes they were mounted with coverslips with Cytoseal 60. Slides were then allowed to dry at room temperature overnight. Slides were scanned on the Hamamatsu microscope with a NanoZoomer XR camera.

2.2.12 Measuring patient tumour nest size

15 RAS mutant Metastatic Colorectal Cancer, ProspectR, pre-treatment biopsies were processed and H&E stained. Regions of highest density of viable tumour cell infiltration were imaged at 20x on Microscope mounted 3.1mp Amscope MU300 digital camera. Pixel measurements calibrated to microscope Vernier scale. Tumour nests were measured across largest diameter; including largest and smallest nest per image field and three intermediate sized tumour nests. Annotation was performed using Amscope software version 3.7.13522.20181209.

2.2.13 Statistics

Pearson correlation analysis and the unpaired t-tests were performed with the GraphPad Prism software. All error bars represent standard deviation. T-tests rather than ANOVA were performed because only 2 sets of data were compared. However, in most cases a one-way ANOVA followed by multiple testing should have been used when multiple groups within an experiment were compared. Gene set enrichment analysis was performed with the GSEA software and the Hallmarks and KEGG gene set collections (Subramanian et al., 2005).

Acknowledgements

The following people are credited for their work presented in this thesis. Dr Louise Barber performed all RNA library preparations for Lexogen sequencing. Beatrice Griffiths established PDO culturing methods. In vivo experiment was performed by Jian Ning from Cancer Biology: Development and Cancer laboratory. Tumour embedding was performed by Breast Cancer Now Histopathology Unit. Immunohistochemistry was performed by Nanna Sivamanoharan. Dr Ben Challoner performed patient tumour nest size analysis.

Chapter 3: Investigating factors regulating CEA expression in CRC patient derived organoids

3.1 Introduction

The aim of my project was to develop 2D and 3D immunocompetent CRC models which would be used to investigate the determinants of CEA-TCB sensitivity and resistance in vitro. The majority of preclinical immunological research has been performed in mouse models due to the advantage of having a full intact immune system which is difficult to simulate in vitro. However, widely available syngeneic mouse models of CRC have mutation loads and hence antigenicities that far surpass those of MSS CRCs (CT26: 56 mutations/megabase, MC38: 75 mutations/megabase compared with 5 mutations per megabase in human MSS CRCs) (Zhong et al., 2020). A more specific limitation of mouse models in studying CEA-TCB is the lack of CEA expression in mice, therefore highlighting the need for immunocompetent in vitro pre-clinical models. Cell lines are the most frequently used in vitro cancer models to date and many of these can be grown either in 2 dimensions as adherent cells or in a form of artificially generated 3 dimensional spheroids. However, cell lines may have lost important molecular features of the original tumours over long periods of culture on plastic. Therefore, new methods enabling long term in vitro propagation of cancer cells from tumour biopsies in the form of patient derived organoids (PDOs) provide a unique opportunity to create more biologically representative pre-clinical models. In addition to the preserved tumour features, PDO generation is more rapid than in vivo studies and also come with established disease stage and treatment history of the patient. My host lab has previously shown that CRC PDOs can be co-cultured with allogeneic CD8 T cells to dissect determinants of response and resistance to the T cell redirecting antibody CEA-TCB (Gonzalez-Exposito et al., 2019). The CRC PDOs, the co-culture models and the results from this study were critical

materials for my PhD and I will briefly summarise the pertinent findings and characteristics.

3.2 CEA expression in Patient Derived Organoids (PDOs) grown in 2D

My lab previously has established PDOs from three CRC clinical trials: PROSPECT-C, PROSPECT-R, and Format. In my project I used eight of the best growing PDOs: seven from multi-drug resistant metastatic CRCs (CRC-01-07) and one from a treatment naïve primary CRC (CRC-08). After establishment, PDOs had been adapted to different growth conditions. The group had shown that all eight PDOs were able to grow in both, a 3D matrix (100% Matrigel domes) and in 2D either as monolayers of cells or as spheroid-like structures sitting directly on the plastic surface of cell culture dishes or plates (2% Matrigel added to the media) (Figure 3.1). Matrigel is an ECM hydrogel mimicking basal lamina comprised of laminin, collagen IV, entactin, and heparan sulfate proteoglycans. During establishment PDOs were grown in Advanced DMEM:F12 media (from this point on referred to as advanced media) which contains multiple growth factors and supplements (Table 2.2). This was formulated by Hans Clever's group to promote stem cell proliferation and maintain proliferative potential long term (Sato et al., 2011). PDOs that showed long term viability (>6 months in culture) had also been switched into DMEM:F12 media with 20% FCS without impairing long term propagation.

The key result that had been generated in my lab previously was that CEA cell surface expression is usually heterogeneous within individual PDO lines and that there is a high degree of expression plasticity which has not been described to our knowledge in CRC cell lines. Thus, tumour cells can up- or downregulate CEA expression. CEA is widely used as a diagnostic and prognostic tumour marker for gastrointestinal cancers, but how CEA expression is regulated has not been well characterised (Arnaud et al., 1980; Lee & Lee, 2017). Therefore my aim was to confirm the findings in 2D growing organoids and extend the characterisation of CEA expression in PDOs to those grown in the 3D configuration as well as investigating which factors, particularly those relevant

to in vitro culture and therefore the PDO-T cell co-culture assay, influence CEA expression.

PDOs grown in 2D format were dissociated into single cells and CEA cell surface expression was analysed by flow cytometry using the CH1A1A antibody which has identical CEA antigen binding sites as the CEA-TCB bispecific antibody. Gating on live single cells and using an unstained sample as a CEA- gate control I confirmed that 20nM was the appropriate concentration by performing a titration on two PDOs (CRC-01 and CRC-02) which showed that there was a maximum of 2% increase in the proportion of

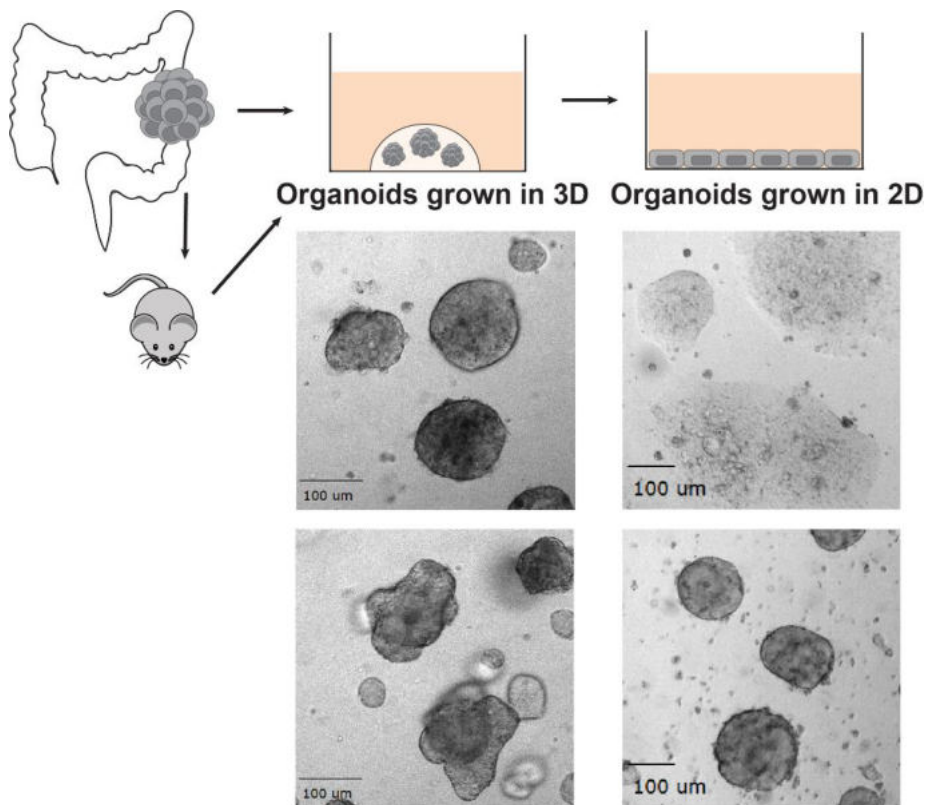


Figure 3.1 Patient derived organoid (PDO) growth in 2D and 3D. Schematic showing 2D and 3D growth of PDOs in vitro along with brightfield images of PDOs grown in 2D and 3D configurations. Some PDO cultures were established directly from core biopsies. For some tumours very small biopsy fragments were available and were first grafted subcutaneously or under the kidney capsule of female CD1 nude mice before in vitro culture.

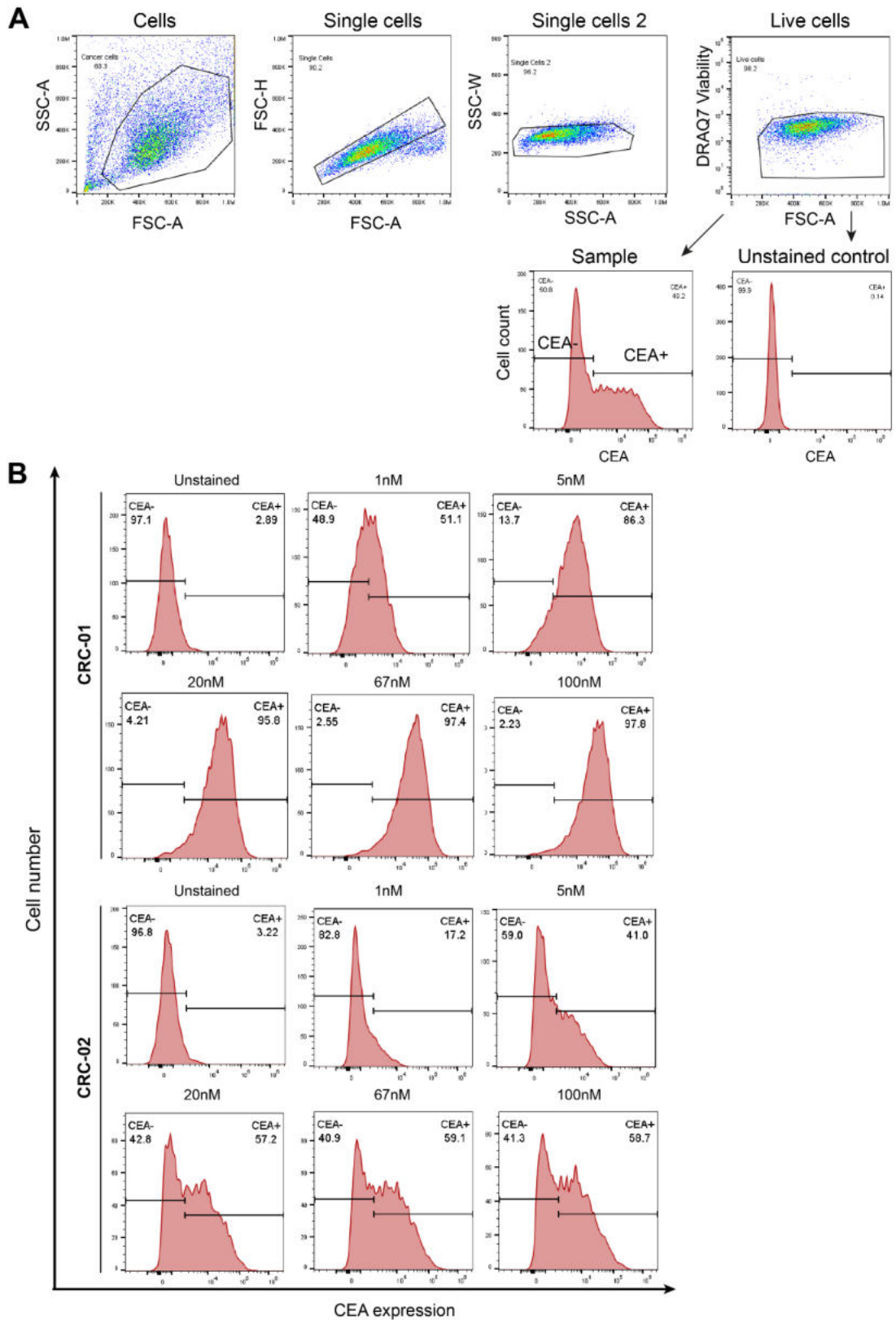
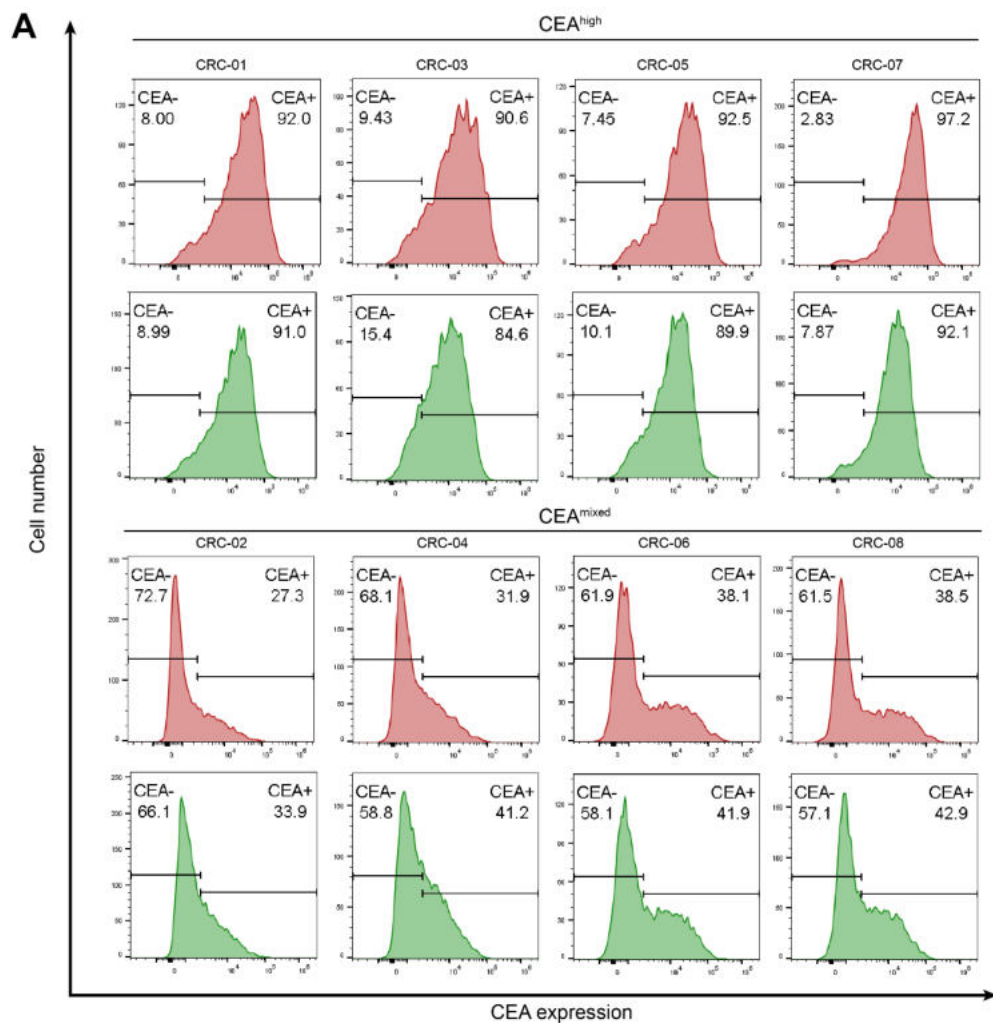


Figure 3.2 CEA antibody titration. (A) Gating strategy for cell surface CEA expression analysis in PDOs using flow cytometry. **(B)** Histograms of CEA expression in two PDO lines CRC-01 and CRC-02 with various concentrations of CH1A1A antibody (1nM, 5 nM, 20 nM, 67 nM, 100 nM). Gates were set using the unstained control. Experiment performed once.

CEA+ cells when the antibody concentration was increased to 100nM. All further CEA analysis was performed using 20nM concentration (Figure 3.2). Measuring CEA expression in 2D PDOs grown in DMEM:F12 20% FCS media showed two patterns of expression: predominantly CEA positive (CRC-01, CRC-03, CRC-05, CRC-07) and lines containing a mixture of CEA positive and CEA negative cells (CRC-02, CRC-04, CRC-06, CRC-08) (Figure 3.3A). This expression profile was confirmed using another antibody that binds a different CEA epitope (Figure 3.3A).



B

		CEA+ cells (%)	CEA- cells (%)	Total MFI	MFI CEA+	MFI CEA-
CEA-high	CRC-01	92.0	8.0	35215	36805	1264
	CRC-05	92.5	7.5	24345	25934	1333
	CRC-07	97.2	7.9	35861	38182	1215
	CRC-03	90.6	9.4	17577	22949	1111
CEA-mixed	CRC-02	27.3	72.7	10311	16621	1000
	CRC-04	31.9	68.1	8488	10966	1372
	CRC-06	38.1	61.9	11526	27866	722
	CRC-08	38.5	61.5	12269	24005	923

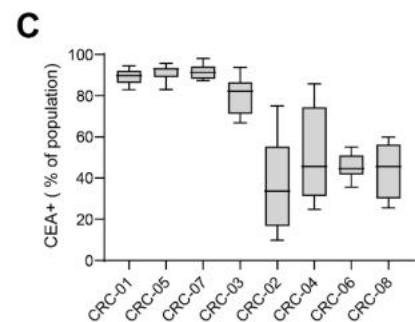


Figure 3.3 CEA expression in PDOs grown in 2D. (A) Flow cytometry analysis of CEA surface expression in 8 PDO lines (CRC-01, CRC-02, CRC-03, CRC-04, CRC-05, CRC-06, CRC-07, CRC-08) grown in 2D in DMEM:F12 20% FCS media. PDOs were grouped into CEA-high and CEA-mixed CEA expression profiles. Experiments were performed with two different CEA binding antibodies: CH1A1A (red histograms) and CEACAM5 clone 487609 (green histograms). **(B)** Table showing analysis of data displayed in (A). Percent of CEA+ and CEA- cells, total CEA MFI, and CEA+ and CEA- population CEA MFI was calculated for each of the 8 PDO lines. **(C)** Box and whisker plot of 10 flow cytometry experiments combined to show the variability in CEA cell surface expression in 8 PDO lines. MFI: mean fluorescent intensity

In two of the CEA-mixed PDOs CRC-06 and CRC-08, the mean fluorescent intensity (MFI) of expression of CEA per cell was similar to one of the CEA-high expressing PDOs (CRC-05) (Figure 3.3B). The other two CEA-mixed PDOs, CRC-02 and CRC-04, showed much lower levels of CEA expression on CEA+ cells. Next it was important to determine the stability of these CEA expression profiles as all of my experiments, some of which over prolonged periods of time, were going to be performed with these PDO models. When my colleague analysed the CEA expression of these 8 PDO lines she identified 3 CEA expression profiles: CEA-high, CEA-mixed, and CEA-low. At the time CRC-06 exhibited lower levels of CEA expression being only 33% CEA+. Additionally, she found that CRC-02 was 68% CEA+ and CRC-04 was 74% CEA+, whereas I had found that those were 27% and 32% respectively CEA+. After continuously culturing the PDOs for up to 3 months and performing regular CEA expression checks every 7-10 days with flow cytometry I demonstrated that three CEA-high PDOs CRC-01, CRC-05, and CRC-07 had very little variability in their CEA levels while the CEA-mixed PDOs showed more variability during constant culturing conditions (Figure 3.3C). PDOs CRC-02 and CRC-04 exhibited the greatest fluctuations in CEA expression ranging from 10-75% and 25-86% of CEA+ cells respectively. The rise of CEA expression did not correlate with time in culture.

3.3 CEA expression in PDOs grown in 3D

Since one of the models I was developing used organoids in their 3D form, it was important to also characterise the CEA expression profiles of the same PDO lines in 3D (Figure 3.4A). CEA expression levels after 10 days of culture were highly similar between 2D and 3D forms of the same PDO lines and correlation analysis showed a strong and significant correlation ($r=0.957$, 95% CI 0.732 to 0.994, $p=0.001$) (Figure 3.4B). However, with longer time in culture and therefore increased size of the individual organoid spheres, the CEA positive population increased in all CEA-mixed 3D PDOs with no change in the already CEA-high lines (Figure 3.4C). Taking CRC-08 as an example, when CEA levels were tested on day 5 since last split to single cell 29% of cells were CEA+, however on day 15 the CEA+ population increased to 44%, and on day 21 to 88% (Figure 3.4C). Epithelial cells in the colon crypt regularly shed CEA, however, CH1A1A is specific for the membrane-anchored CEA protein rather than shed CEA (Bacac et al., 2016). Therefore, the increase in CEA cannot be explained by the accumulation of shed CEA in culture but is a result of increased CEA surface expression. This gradual increase in the proportion of CEA+ cells should be considered when evaluating CEA-TCB sensitivity of 3D PDOs.

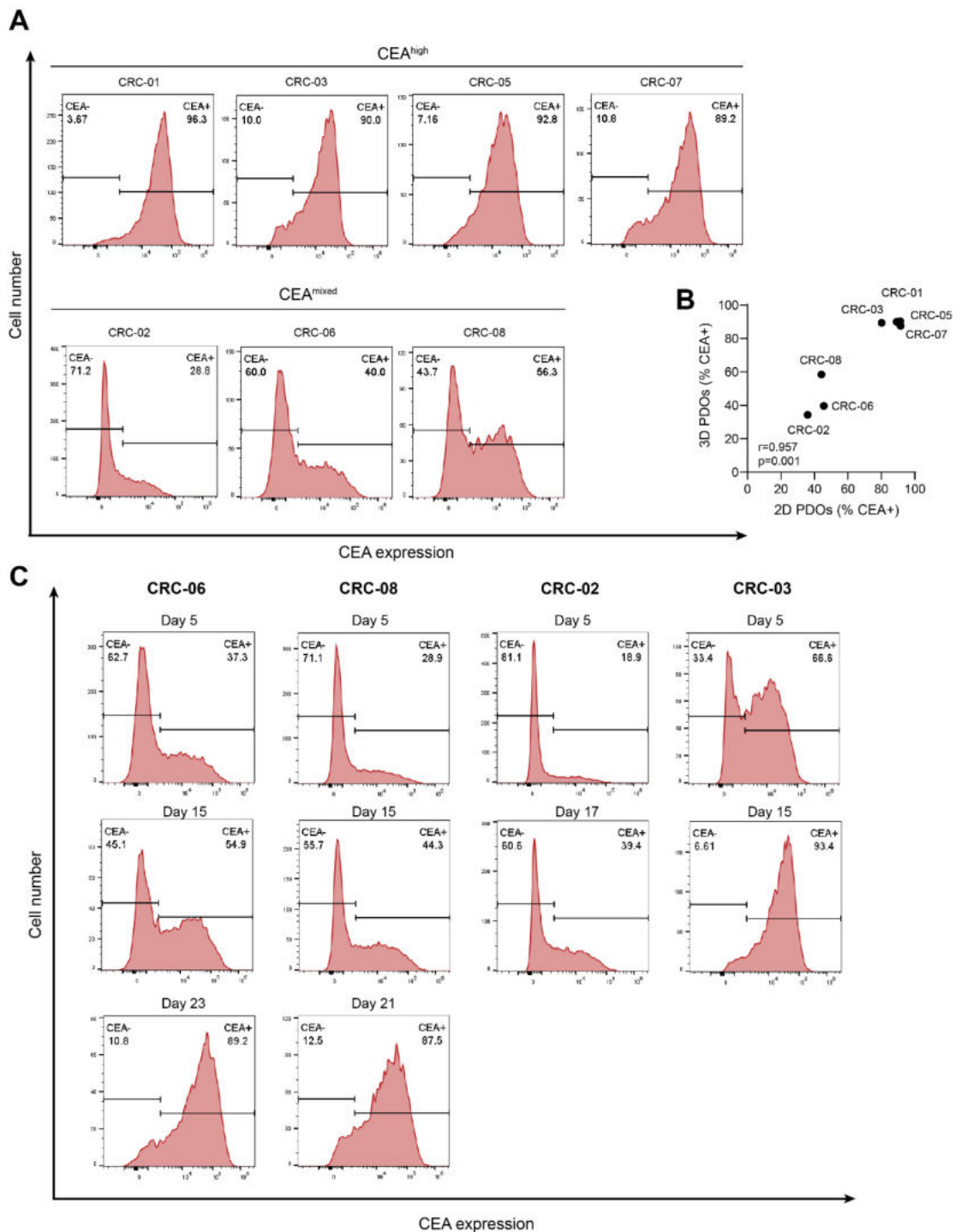


Figure 3.4 CEA expression in PDOs grown in 3D. (A) Flow cytometry analysis of CEA surface expression in 7 PDO lines (CRC-01, CRC-02, CRC-03, CRC-05, CRC-06, CRC-07, CRC-08) grown in 3D in DMEM:F12 20% FCS media. PDOs are grouped into CEA-high and CEA-mixed CEA expression profiles. **(B)** Scatter plot showing correlation between percent of CEA+ cells in 2D PDOs vs the same line 3D PDOs. For 2D PDOs a mean of 10 experiments was plotted and 3 experiments for 3D. PDOs were grown between 10-15 days for these experiments. Pearson correlation test was performed ($r=0.957$, $p=0.001$). **(C)** Flow cytometry analysis of CEA expression in 4 PDO lines (CRC-02, CRC-03, CRC-06, CRC-08) grown in 3D for various periods of time (5 days, 15-17 days, and 21-23 days). Data are representative of 2 repeats.

3.4 Immunohistochemical analysis of CEA expression in PDOs and tumour tissue

In order to further dissect CEA expression in our PDOs, FFPE slides of PDOs and corresponding xenograft tumour tissue were immunohistochemically stained for CEA. As can be observed in Figure 3.5, CEA expression in PDOs matched the flow cytometry data with PDOs CRC-05 and CRC-07 that were CEA-high on flow cytometry analysis harbouring only cells with strong CEA staining whereas the PDOs CRC-04, CRC-06, and CRC-08 that were CEA-mixed by flow displayed CEA expression heterogeneity, predominantly between different organoids but also within organoids. Furthermore xenografts had a similar CEA expression profile to their corresponding PDO. CEA-mixed tumours showed areas of CEA-high expressing cells and areas with minimal or completely absent CEA expression, while tumours corresponding to CEA-high PDOs were uniformly highly CEA positive. This analysis revealed spatial patterns of heterogeneity in PDOs and confirmed that these expression patterns are maintained in xenografts thus indicating that it is not an in vitro artefact.

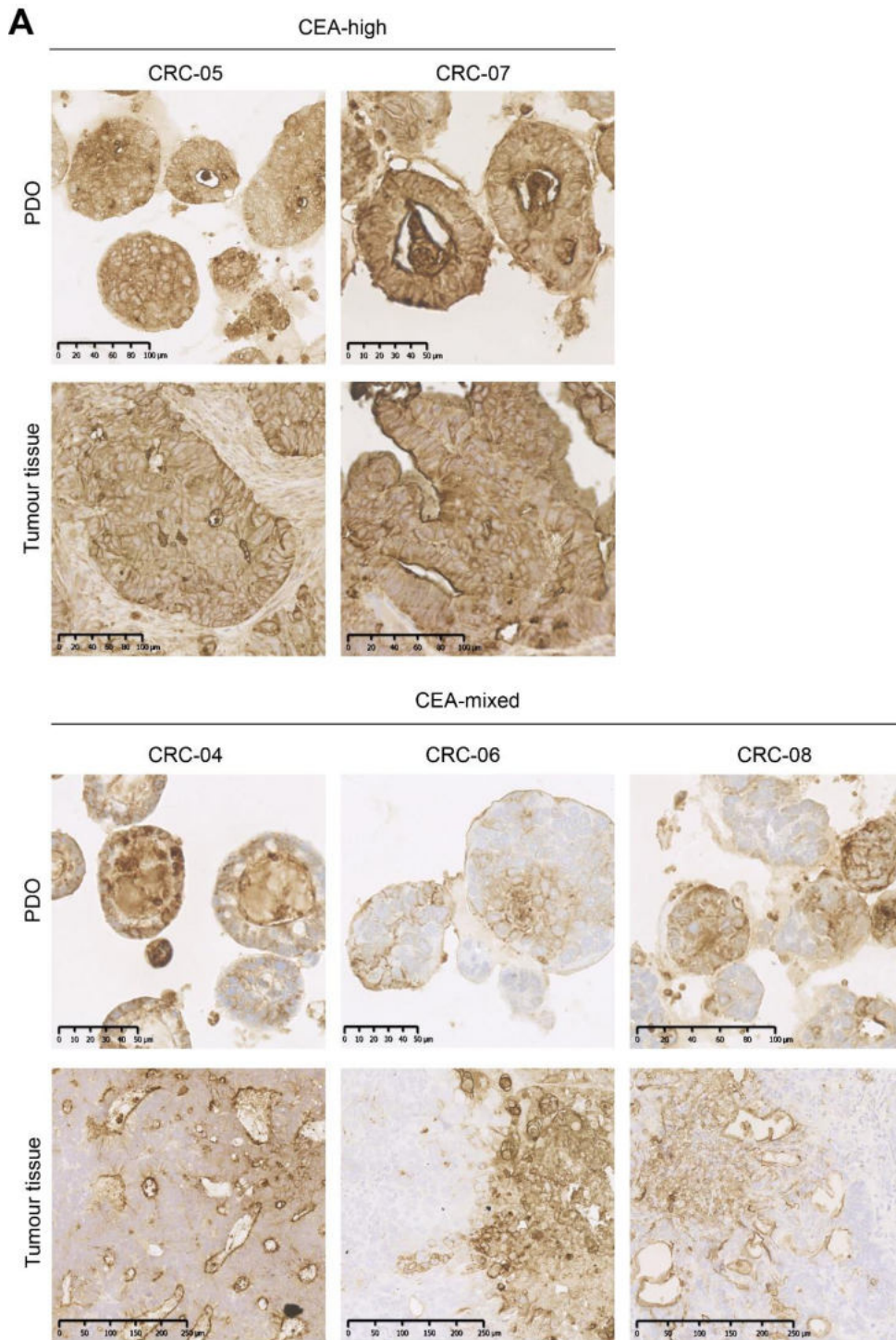


Figure 3.5 Immunohistochemistry (IHC) analysis of CEA expression in PDOs and tumour tissue. For each PDO line a representative image is shown for CEA stained organoid and corresponding xenograft tumour tissue. For PDOs only 1 FFPE slide was stained and imaged, and representative images of PDOs were selected. For tumour tissue, 2-3 slides were stained and imaged and representative areas chosen.

3.5 Effect of PDO-T cell co-culturing conditions on CEA expression in 2D PDO

In order to create optimal conditions for T cells, the PDO-T cell co-culture assay was set up using T cell media rather than the 20% FCS DMEM:F12 media used to culture PDOs. Therefore I checked whether the CEA expression of two CEA-high PDOs (CRC-01 and CRC-05) and two CEA-mixed PDOs (CRC-06 and CRC-08) changed when PDOs were grown in T cell media (10% FCS RPMI) versus their usual culture media (20% FCS DMEM:F12). When cultured in T cell media the PDOs did not change their CEA expression compared to their usual culture media (Figure 3.6A). The PDOs were also usually cultured with 2% Matrigel added to the media, however, in order to prevent anything hindering the contact between tumour and immune cells the assay was set up without the addition of Matrigel to the media. CEA has been implicated in adhesion of tumour cells, therefore it was important for me to ensure that the exclusion of Matrigel from the assay would not alter their CEA expression (Benchimol et al., 1989; Öbrink, 1997; Zhou et al., 1993). Three CEA-mixed PDOs (CRC-04, CRC-06, and CRC-08) were cultured in DMEM:F12 with 20% FCS with or without the addition of 2% Matrigel. When seeded without Matrigel these PDOs showed an increase in CEA expression with an average increase by 29% on day 2. However, with time the CEA expression gradually decreased until it reached the same CEA expression profile as with 2% Matrigel on day 6 (Figure 3.6B). Based on these experiments all 2D co-culture assays were seeded in T cell media with no addition of Matrigel.

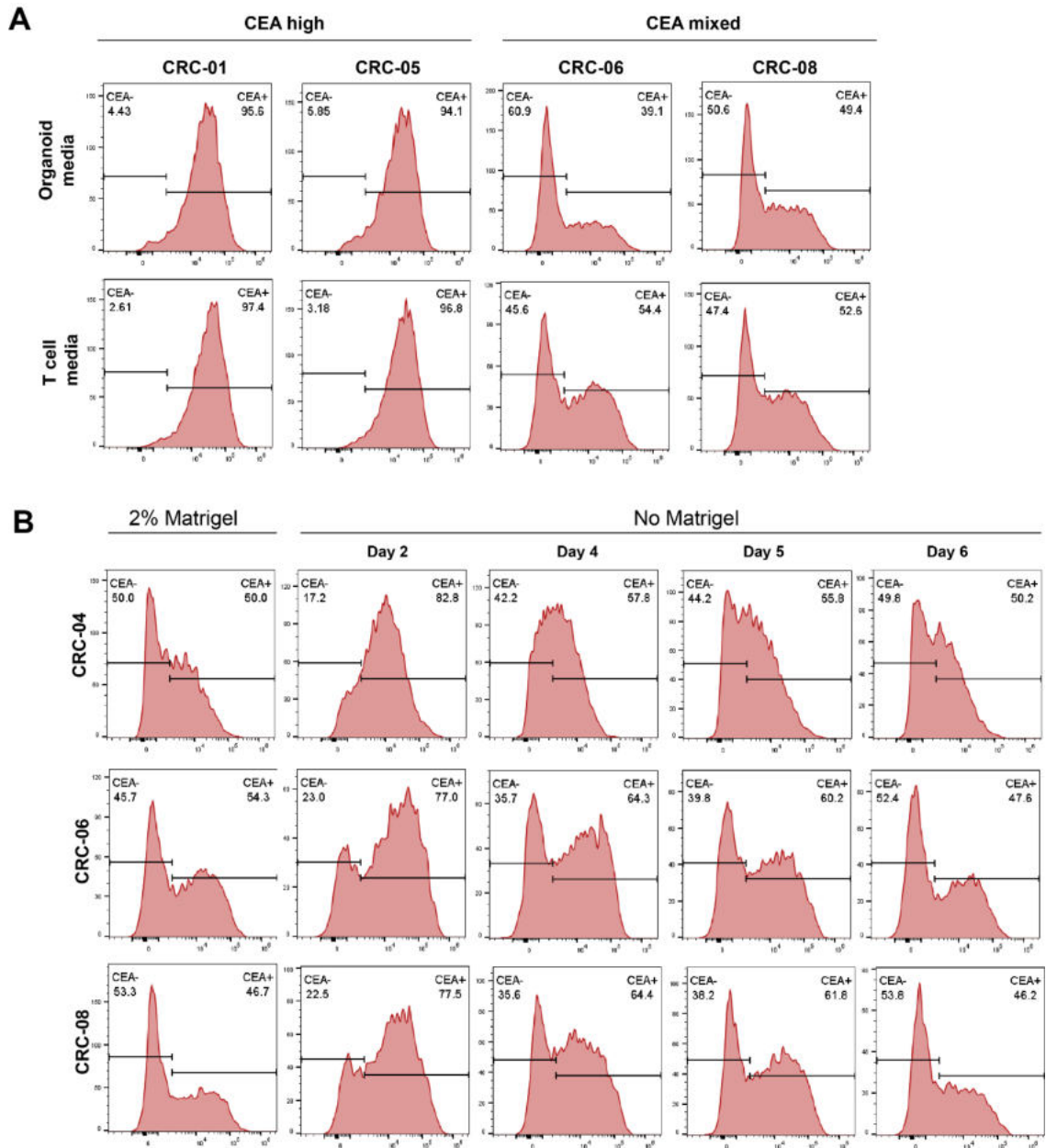


Figure 3.6 Effect of PDO-T cell co-culture conditions on CEA expression of 2D PDOs
(A) Flow cytometry histograms showing CEA expression of two CEA-high PDOs CRC-01 and CRC-05 and two CEA-mixed PDOs CRC-06 and CRC-08 grown in either organoid (DMEM:F12 20% FCS) or T cell media. **(B)** Flow cytometry histograms showing CEA expression of three CEA-mixed PDOs CRC-04, CRC-06, and CRC-08 which had been cultured either in the presence of 2% Matrigel in the media (DMEM:F12 20% FCS) or without. Both experiments were performed once.

3.6 Effect of cell growth density on CEA expression

Another factor that was important to consider is the effect of cell density on CEA expression. Two CEA-mixed PDOs were seeded at different densities: 50,000 cells/well, 100,000 cells/well, and 200,000 cells/well. Cells were harvested once the most densely seeded well reached a confluence of 90-100% and CEA surface expression was analysed by flow cytometry. Despite the different cell densities, both PDOs showed minimal change in their proportion of CEA expressing cells, with CRC-06 showing a 13% and CRC-08 a 5% increase in CEA+ proportion of cells at the highest density (Figure 3.7A). However, when cells were left as a confluent monolayer for 4 days after they had

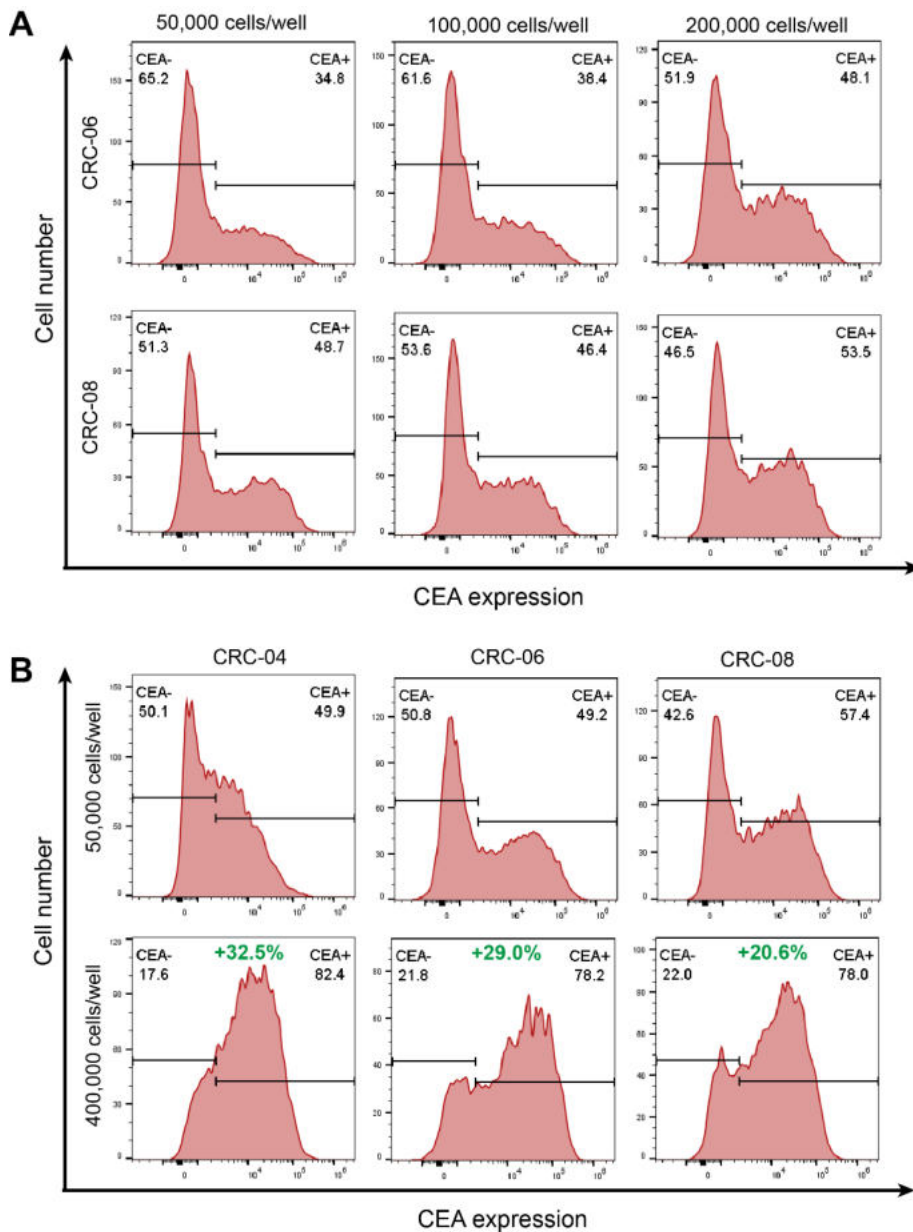


Figure 3.7 Effect of cell density on CEA expression in PDOs. (A) Flow cytometry histograms showing CEA expression in two CEA-mixed PDOs (CRC-06 and CRC-08) seeded at different densities and harvested when the most dense condition (200,000 cells/well) reached 90-100% confluence on day 10. **(B)** Flow cytometry histograms showing CEA expression in three CEA-mixed PDOs (CRC-04, CRC-06, CRC-08) which were seeded at two densities (50,000 cells/well and 400,000 cells/well) and harvested for CEA analysis on day 12, 4 days after the more dense condition has reached 100% confluence. Both experiments were performed once.

reached full confluence the proportion of CEA+ cells increased by 20% or more (Figure 3.7B). Out of the three CEA-mixed PDOs tested CRC-08 showed the lowest increase in proportion of CEA+ cells which may be due to its 3D-like growth pattern even in 2D which meant that this PDO did not grow as a monolayer and therefore did not reach the same level of confluency as the two other PDOs. These observations of CEA expression increasing with higher cell density are in line with what has been shown previously in colorectal cancer cell lines (Kitadai et al., 1996).

3.7 IFN γ increases CEA expression in CEA-mixed PDOs

IFN γ is one of the main cytokines secreted by tumour infiltrating lymphocytes as part of an anti-tumour response and has been shown to be secreted by T cells activated by CEA-TCB (Bacac et al., 2016). IFN γ has also been previously shown to enhance cell surface expression of tumour associated antigens including CEA in cell lines therefore it was important to investigate the effect of IFN γ on CEA expression in our PDO models. Two doses of IFN γ (10ng/mL and 100ng/mL) were tested in three CEA-mixed lines (CRC-02, CRC-06, CRC-08) and one CEA-high PDO (CRC-05). In two of the CEA-mixed PDOs, CRC-06 and CRC-08, after 48 hours of treatment both doses of IFN γ resulted in a significant increase of the CEA+ population, with both PDOs being 83% and 84% respectively CEA+ at the higher dose of IFN γ (Figure 3.8). The other CEA-mixed PDO, CRC-02, started at a higher level of CEA expression than the other two CEA-mixed PDOs and only showed a very modest increase from 75% CEA+ to 83%.

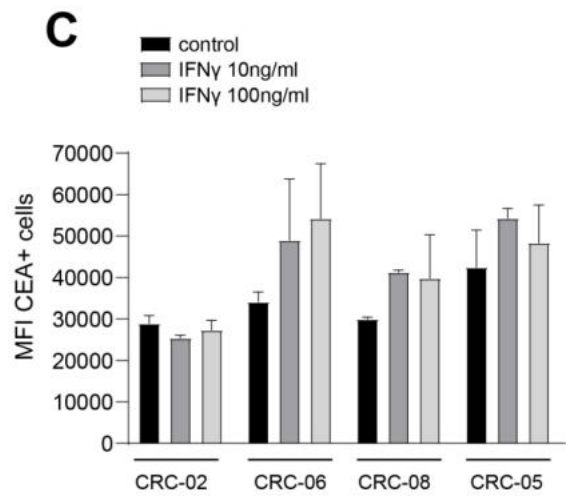
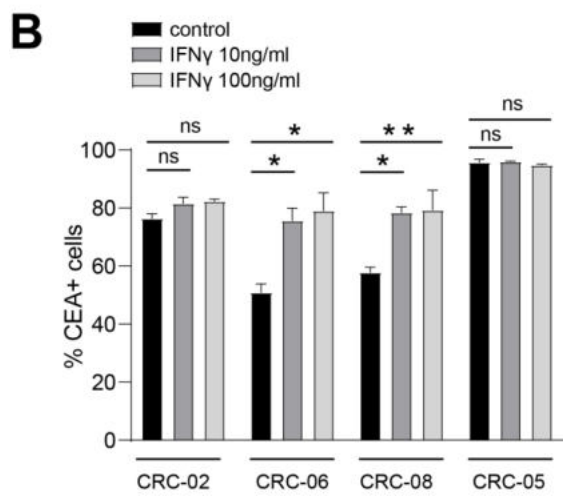
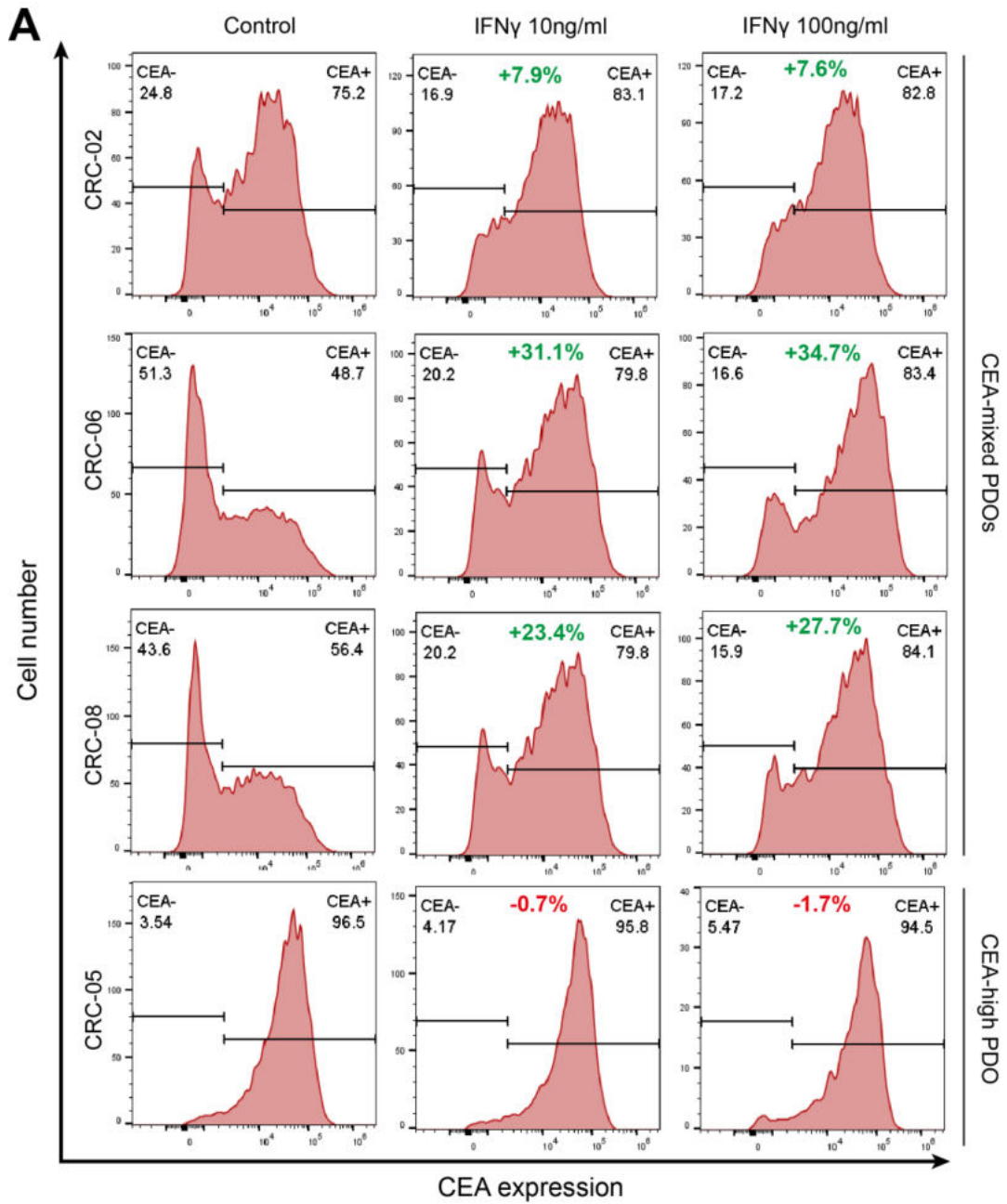
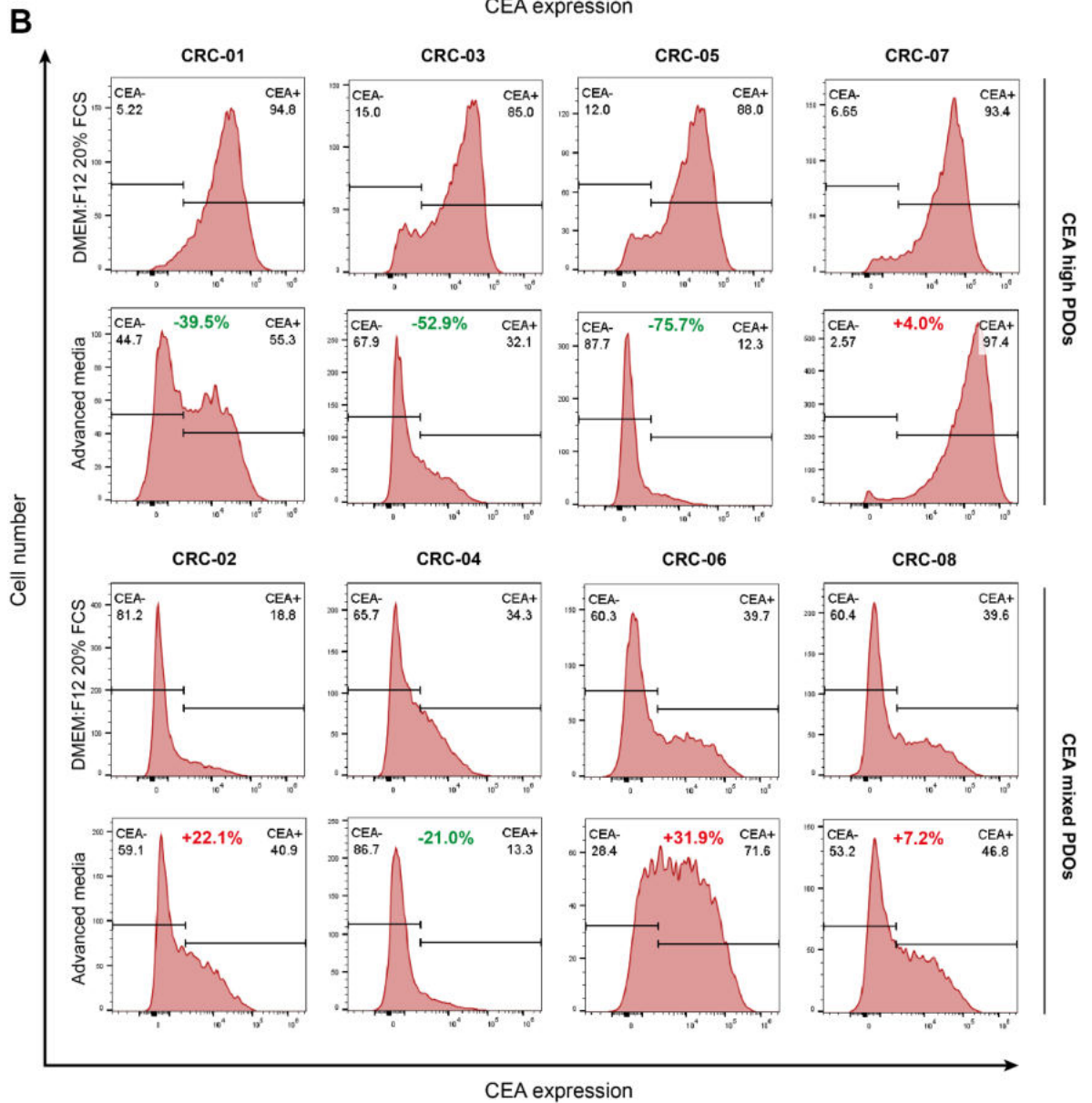
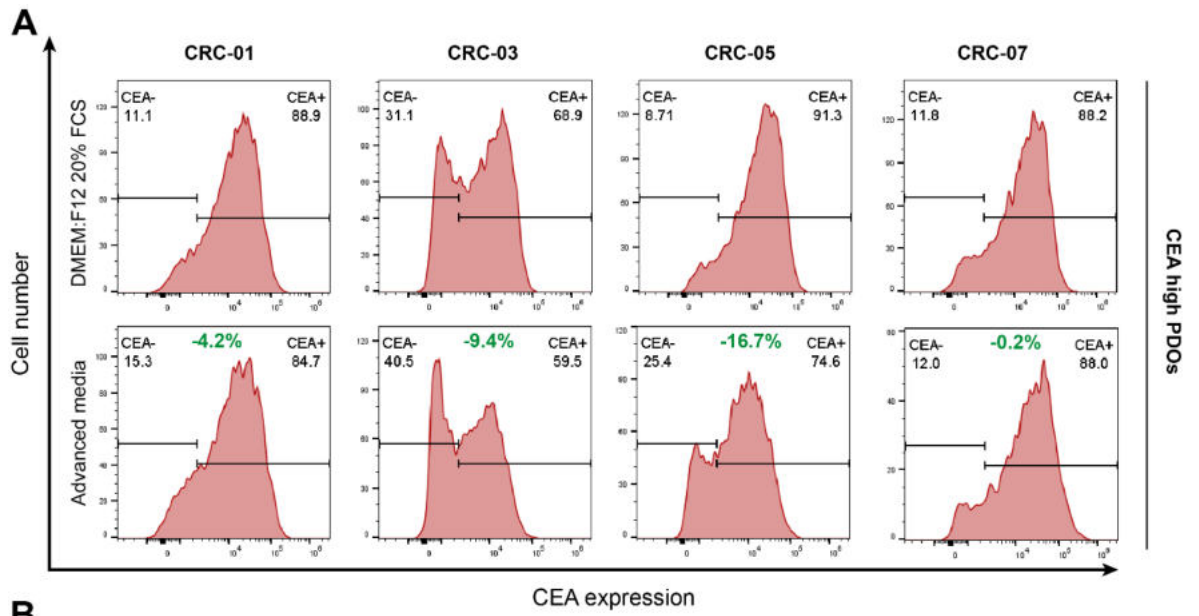


Figure 3.8 Effect of IFN γ on CEA expression in PDOs. (A) Flow cytometry histograms showing CEA expression in four PDOs (CRC-02, CRC-06, CRC-08, and CRC-05) in control condition and with IFN γ treatment at two different doses (10ng/mL and 100ng/mL). Percent in green or red font on each plot indicates change (green=increase, red=decrease) in % CEA $^{+}$ cells compared to control. Data are representative of 2 repeats. **(B)** Bar graph showing proportion of CEA $^{+}$ cells in each PDO at two IFN γ concentrations (10ng/mL and 100ng/mL) and under control conditions. Experiment was performed twice, error bars indicate SD. Unpaired t-test was performed. P values are as follows: > 0.05 is ns, < 0.05 is *, < 0.01 is **, <0.001 is ***, <0.0001 is ****. **(C)** Bar graph showing MFI of CEA of CEA $^{+}$ cells in four PDOs. Experiment was performed twice, error bars

Interestingly, all of the CEA-mixed lines only increased up to a maximum of 84% CEA $^{+}$ cells at the higher dose of IFN γ regardless of their starting CEA expression level; CRC-02 only showed an 8% increase, CRC-06 35%, and CRC-08 28%. The proportion of CEA $^{+}$ cells in the CEA-high PDO CRC-05 did not increase any further. Also the expression of CEA on a per cell level increased in all PDO lines tested except for CRC-02 which maintained the same level of CEA expression per cell at both IFN γ doses (Figure 3.8C). The ability of IFN γ to increase CEA expression has been previously shown in colorectal cell lines and has now been confirmed in PDOs (Dansky-Ullmann et al., 1995; Fahlgren et al., 2003; Guadagni et al., 1990). This is an important finding because upon activation with CEA-TCB, T cells secrete IFN γ which may increase the number of CEA expressing cells within the organoid, further enhancing the effect of the treatment.

3.8 Advanced media downregulates CEA expression in CEA-high PDOs

When organoids are first being established from tumour biopsies or xenografts they are cultured in advanced organoid media which was formulated by Clever's lab to support long-term human intestinal epithelial cell culture. The combination of supplements and growth factors added to the media promotes proliferation of colonic stem cells leading to long term propagation of primary cells. In a healthy colonic crypt the stem cells are located at the bottom and their daughter cells become transit-amplifying cells that proliferate and differentiate as they migrate up towards the top of the crypt.



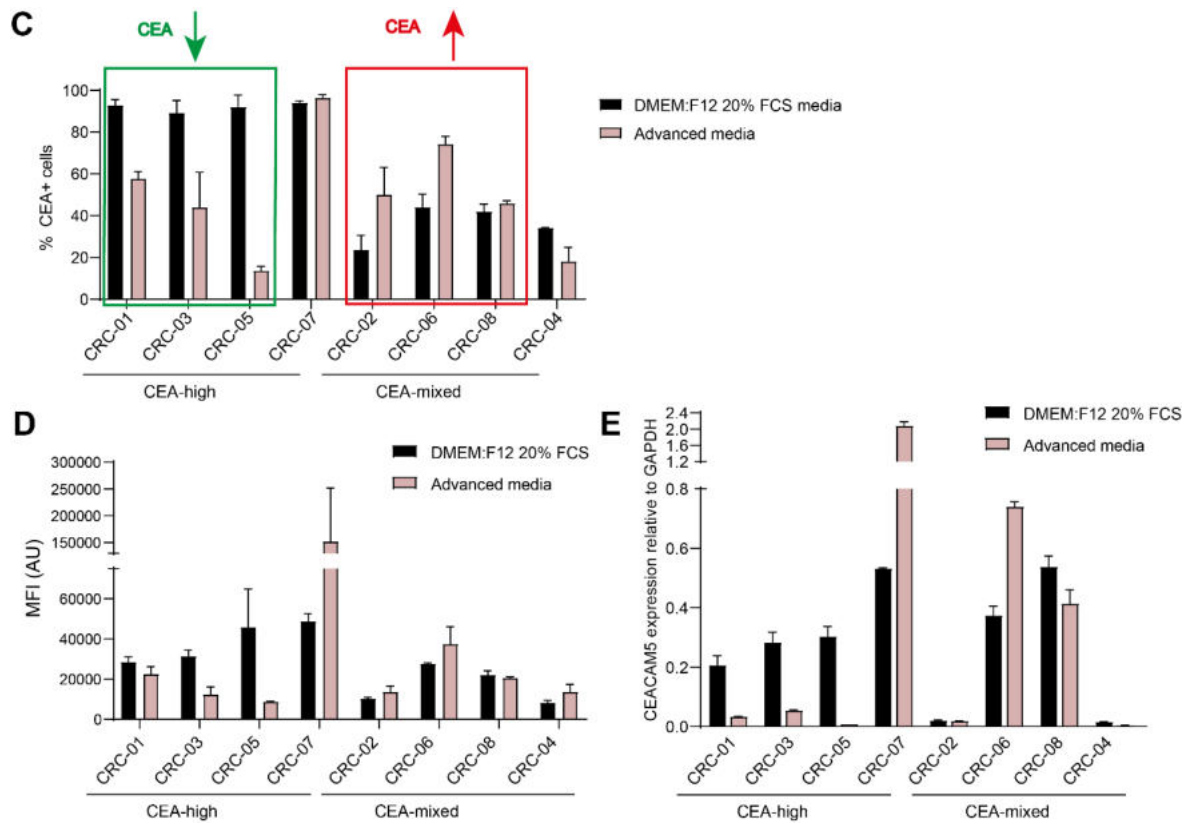


Figure 3.9 Effect of advanced media on CEA expression in 2D PDOs. (A) Flow cytometry histograms showing surface CEA expression of 4 CEA-high PDOs (CRC-01, CRC-03, CRC-05, CRC-07) after being cultured for 4 days either in DMEM:F12 20% FCS media or advanced media. On histograms percent change indicates a decrease (green) in CEA surface expression compared to PDOs grown in DMEM:F12 20% FCS media. Experiment performed once. (B) Flow cytometry histograms show surface CEA expression on 8 PDOs divided into CEA-high and CEA-mixed groups. All PDOs were grown in either advanced media or DMEM:F12 20% FCS media for 11 days. On histograms percent change indicates a decrease (green) or increase (red) in CEA surface expression compared to PDOs grown in DMEM:F12 20% FCS media. Data are representative of 2 repeats. (C) Bar graph comparing percent of CEA+ cells in PDOs grown in advanced media vs. DMEM F12 20% FCS media. Green box groups CEA-high expressing PDOs that showed a decrease in CEA expression in response to advanced media treatment and red box grouping CEA-mixed PDOs that showed an increase in CEA expression after advanced media treatment. (D) Bar graph showing mean fluorescence intensity (MFI) values of CEA expression in the CEA+ population for each PDO line and both media conditions. (E) *CEACAM5* expression relative to *GAPDH* in all PDOs determined by qPCR after culture in 20% FCS DMEM:F12 medium vs advanced organoid media for 11 days. Error bars indicate the standard deviation of triplicate measurements.

CEA expression is tightly regulated in healthy colonic crypts where expression is absent at the crypt bottom and gradually increases in epithelial cells as they become more differentiated towards the top of the crypt (Jothy et al., 1993; Kuhnert et al., 2004; Vermeulen et al., 2010). Therefore I hypothesized that media promoting stemness may downregulate CEA expression. In order to test this hypothesis I transitioned all of the PDO lines to advanced media. After 4 days of culture in advanced media CEA-high PDOs CRC-03 and CRC-05 showed a modest decrease in the proportion of CEA+ cells, while CRC-01 and CRC-07 showed no change (Figure 3.9A). However, when culture time was increased to 11 days CRC-03 and CRC-05 showed a dramatic decrease in proportion of the CEA+ population, CRC-01 showed a moderate decrease, and CRC-07 remained strongly CEA+. Upon treatment with advanced media CRC-01 CEA+ population decreased from 95% to 55%, CRC-03 decreased from 85% to 32%, and CRC-05 showed the most dramatic decrease from 88% to 12% (Figure 3.9B&C). In addition to the decrease in the proportion of CEA+ cells, advanced media caused less CEA expression per cell as can be observed in the decrease in the MFI of CEA+ cells (Figure 3.9D). The response to transition into advanced media in the CEA-mixed group was different. CRC-04 showed a decrease in CEA+ cells, similar to that seen in three of the four CEA-high PDOs. CRC-08 showed a minor increase in CEA+ cells and CRC-02 and CRC-06 a moderate increase (Figure 3.9B&C). Downregulation of the CEA in CEA-high PDOs at 11 days after transition into advanced media was regulated at the transcriptional level as confirmed with a CEACAM5 qPCR probe. However, *CEACAM5* expression in CEA-mixed PDOs did not match up to the cell surface expression as neatly, with only CRC-04 and CRC-06 showing a similar trend to flow cytometry results. A possible explanation for the discrepancy between flow cytometry results and qPCR is that flow cytometry analysis shows multiple changes in a complex population expression structure and qPCR just shows total RNA. Overall, this shows that transition from media with 20% FCS to advanced media suppresses CEA expression in most PDOs that had

high CEA levels before transition and that those showing mixed CEA profiles are less sensitive to this environmental change.

3.9 Identifying advanced media components responsible for CEA downregulation in CEA-high PDOs

Next I investigated whether the addition of FCS is responsible for the high CEA expression observed in CEA-high PDOs when cultured in DMEM:F12 with 20% FCS. Addition of 20% FCS to advanced media only very modestly increased percentage of CEA+ cells suggesting that it is not the key factor that is responsible for the different CEA expression profiles of CEA-high PDOs cultured in these two medias.

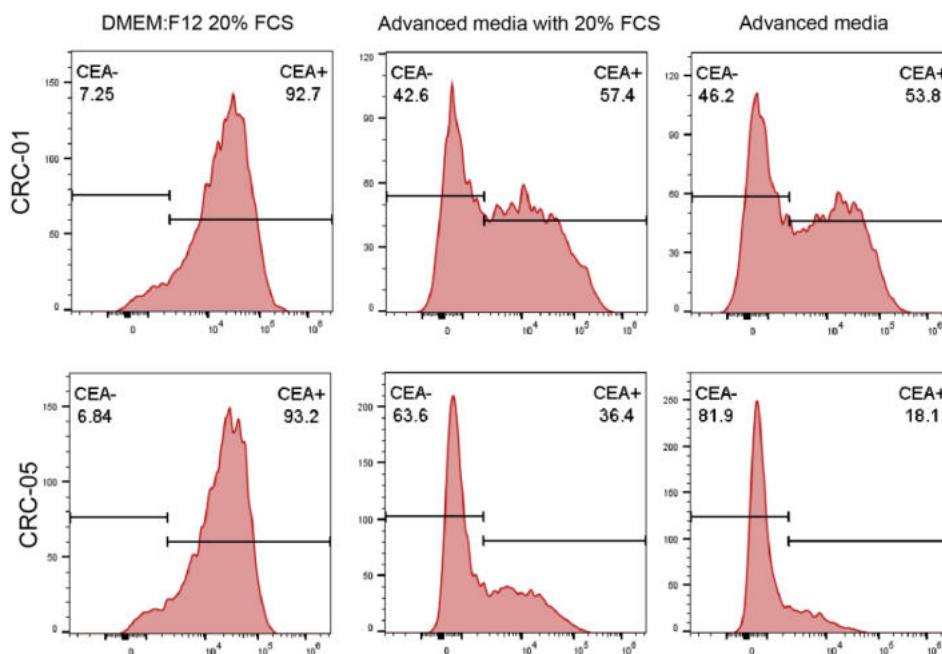
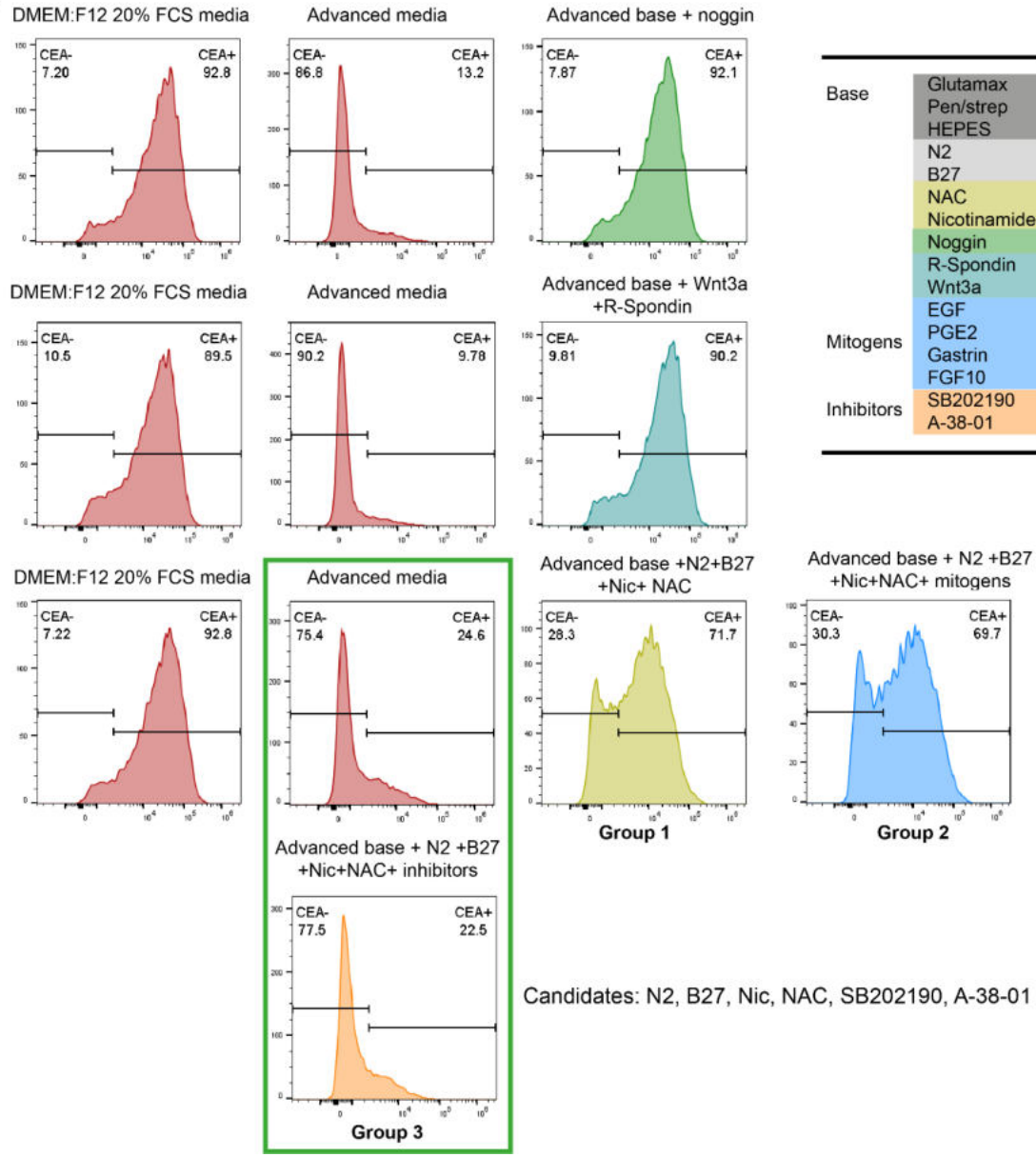


Figure 3.10 Effect of FCS on CEA surface expression in CEA-high PDOs. Flow cytometry histograms showing surface CEA expression in CRC-01 and CRC-05 which had been cultured either in DMEM:F12 20% FCS media, advanced media with 20% FCS, or advanced media for 10 days. Experiment performed once.

In order to determine which specific factors in the advanced medium were responsible for CEA downregulation in CEA-high PDOs I first tested the supplements organised into groups based on molecular function such as “inhibitors” or “mitogens”. Advanced media

base contained advanced DMEM:F12 with glutamax, pen/strep, and HEPES. The selected growth factors and inhibitors were added to the base media. CRC-05 was chosen for these tests as it showed the biggest decrease in the proportion of CEA expressing cells out of the CEA-high PDO group when treated with advanced media. CRC-05 showed no change in CEA when cultured in media supplemented with noggin, Wnt3a, or R-Spondin (Figure 3.11A). The three treatment conditions under which CEA expression was decreased were advanced base media + N2 + B27 + nicotinamide + NAC (group 1), advanced base media + N2 + B27 + nicotinamide + NAC + EGF + PGE2 + gastrin + FGF10 (group 2), and advanced base media + N2 + B27 + nicotinamide + SB202190 + A-38-01 (group 3) (Figure 3.11A). Treatment group 1 and group 2 both showed a partial downregulation of CEA expression with 70-72% CEA+ cells compared to fully supplemented advanced media condition with 25% CEA+ cells. Since both groups showed the same CEA expression profile it was concluded that mitogens (EGF, PGE2, gastrin, FGF10) did not affect CEA expression. When CRC-05 was treated with group 3 supplements the CEA expression profile (23% CEA+) matched that of PDO treated with fully supplemented advanced media (25% CEA+). Therefore this combination of supplements contained the factors responsible for CEA downregulation. Based on this data the possible candidates were N2, B27, nicotinamide, NAC, SB202190, and A-38-01. In order to identify which factors in group 3 were downregulating CEA expression CRC-05 was cultured in advanced media base with the addition of individual supplements: N2, B27, nicotinamide, NAC, SB202190, or A-38-01. Out of the candidate factors the p38 inhibitor SB202190 and nicotinamide, a precursor of oxidised nicotinamide adenine dinucleotide, were the only two factors that decreased CEA expression (Figure 3.11B).

A



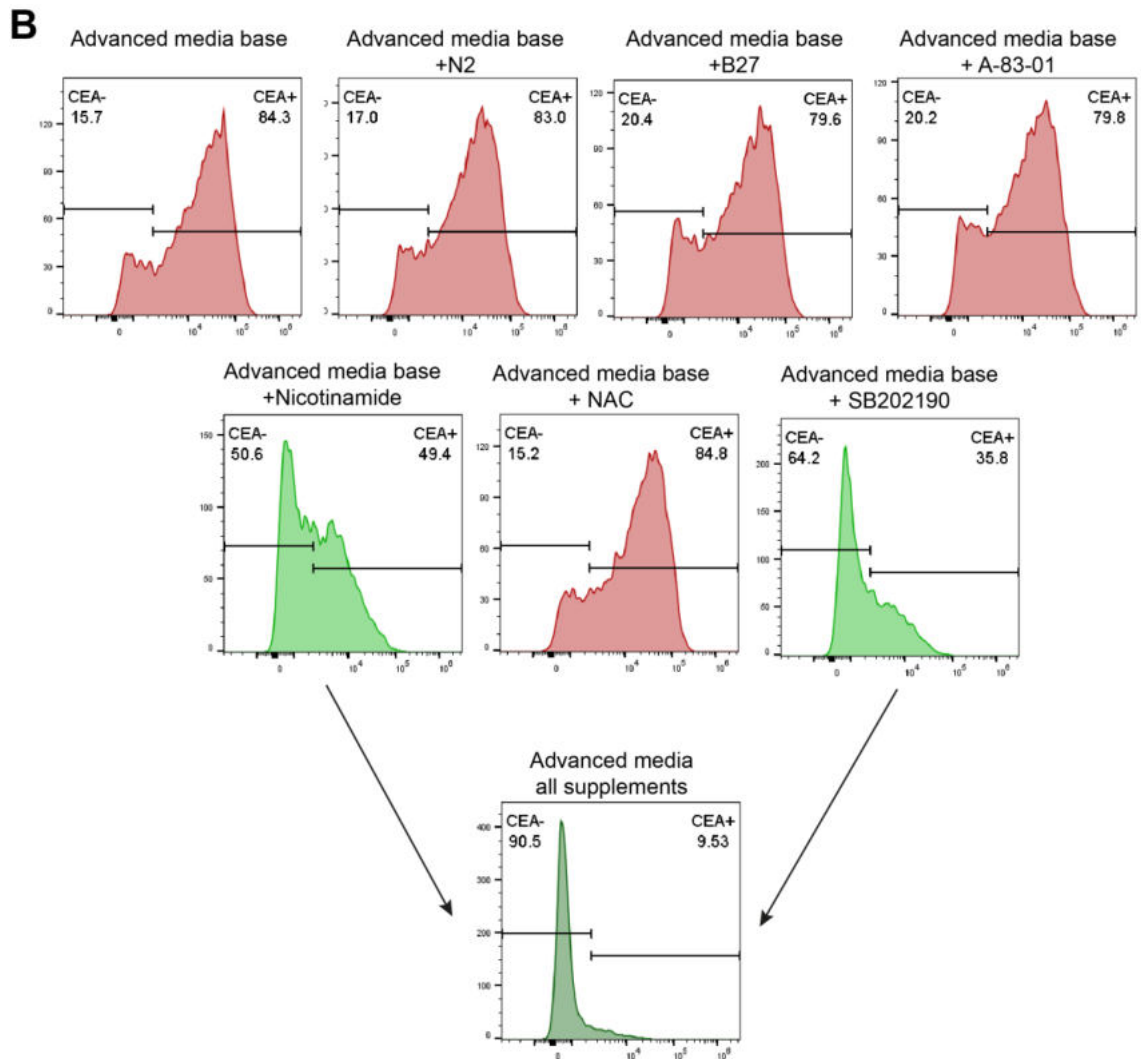
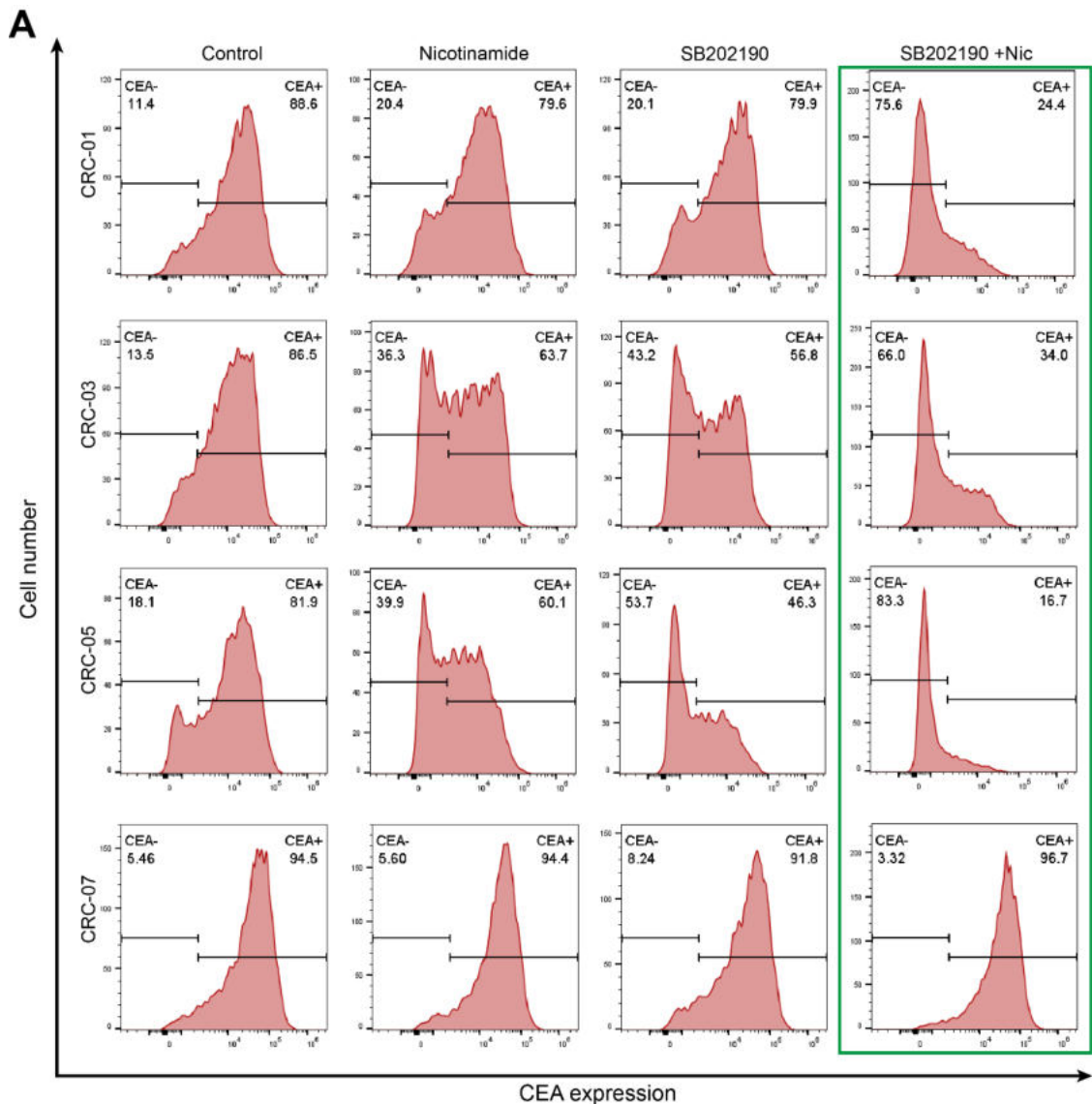


Figure 3.11 Effect of different advanced media components on CEA expression in CEA-high PDO. (A) Flow cytometry histograms showing CEA expression of CRC-05 when cultured in media containing different growth factors and supplements for 12 days. Supplements/growth factors are listed on top of the corresponding histogram. The concentrations of supplements/growth factors is the same as in advanced media and are listed in Table 2.2. Histograms have been colour coded and the list of all supplements/growth factors used is listed on the right. **(B)** Flow cytometry histograms showing CEA expression of CRC-05 which has been cultured in advanced media base (Advanced DMEM:F12 media supplemented with glutamax, pen/strep, and HEPES) with individually added supplements (N2, B27, A-83-01, nicotinamide, NAC, SB202190) or in fully supplemented advanced media for 12 days.

To further validate the finding that SB202190 and nicotinamide decrease CEA expression all CEA-high PDOs (CRC-01, CRC-03, CRC-05, CRC-07) were treated with DMEM:F12 20% FCS media alone (control) or with the addition of nicotinamide and SB202190 separately and combined. Individually each of these chemicals only partially reduced CEA expression, however, combining them achieved the same strong reduction which had been observed with complete advanced media (Figure 3.12A&B, Figure 3.9B). In addition to reducing the proportion of CEA+ cells, combined treatment of nicotinamide and SB202190 also decreased CEA surface expression on a per cell basis (Figure 3.12C). For example, MFI of CEA in CEA+ cells in CRC-05 control condition was 34,744,



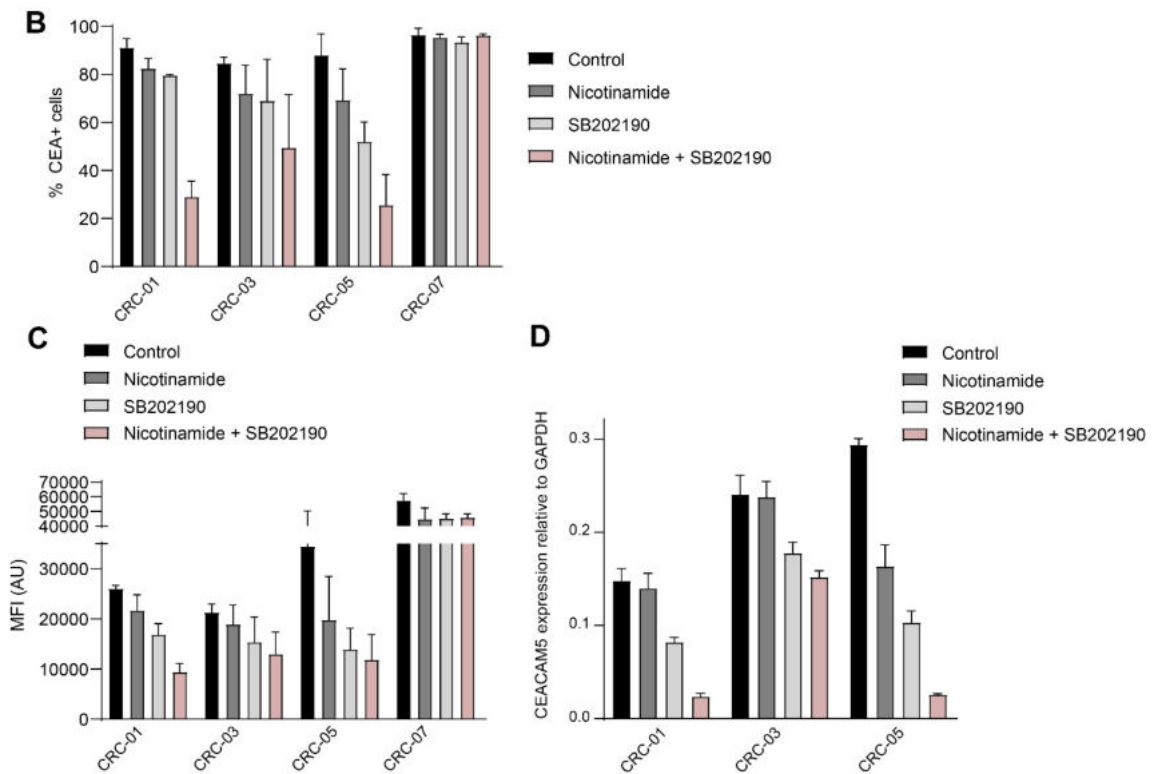


Figure 3.12 Effect of nicotinamide and p38 MAP kinase inhibitor SB202190 on CEA expression in 2D PDOs. (A) Flow cytometry histograms showing surface CEA expression on 4 CEA-high PDOs (CRC-01, CRC-03, CRC-5, CRC-07). PDOs were cultured in DMEM:F12 20% FCS media with the addition of nicotinamide and/or SB202190 for 12 days. Data are representative of 2 repeats. (B) Bar graph showing percent CEA+ cells in PDOs grown in DMEM:F12 20% FCS media with or without the addition of nicotinamide and/or SB202190. Experiment was performed twice, error bars indicate SD. (C) Bar graph showing mean fluorescence intensity (MFI) values of CEA expression in the CEA+ population for each PDO line in different treatment conditions. (D) *CEACAM5* expression relative to *GAPDH* in CEA-high PDOs determined by qPCR after culture in 20% FCS DMEM:F12 media with the addition of nicotinamide and/or SB202190 for 12 days .

which was reduced to 11,847 with combined nicotinamide and SB202190 treatment. Just as with advanced media, CRC-07 showed no CEA downregulation in response to combined nicotinamide and SB202190 treatment (Figure 3.12A&B). Gene expression analysis by qPCR confirmed that CEA downregulation occurred at the transcriptional level (Figure 3.12D).

This CEA downregulation effect remained stable even after 8 weeks of continuous treatment with either advanced media or DMEM:F12 20% FCS media with the addition

of nicotinamide and SB202190 (Figure 3.13A). The decrease in CEA surface expression induced by culture in advanced media was gradual over 10 days, with minimal downregulation observed on day 4 of culture. However, the transition back to the CEA expression profile seen in DMEM:F12 20% FCS media occurred more quickly with CEA levels returning almost completely back to normal within 5 days in CRC-01 and more than halfway in CRC-05 after removal of SB202190 and nicotinamide (Figure 3.13B).

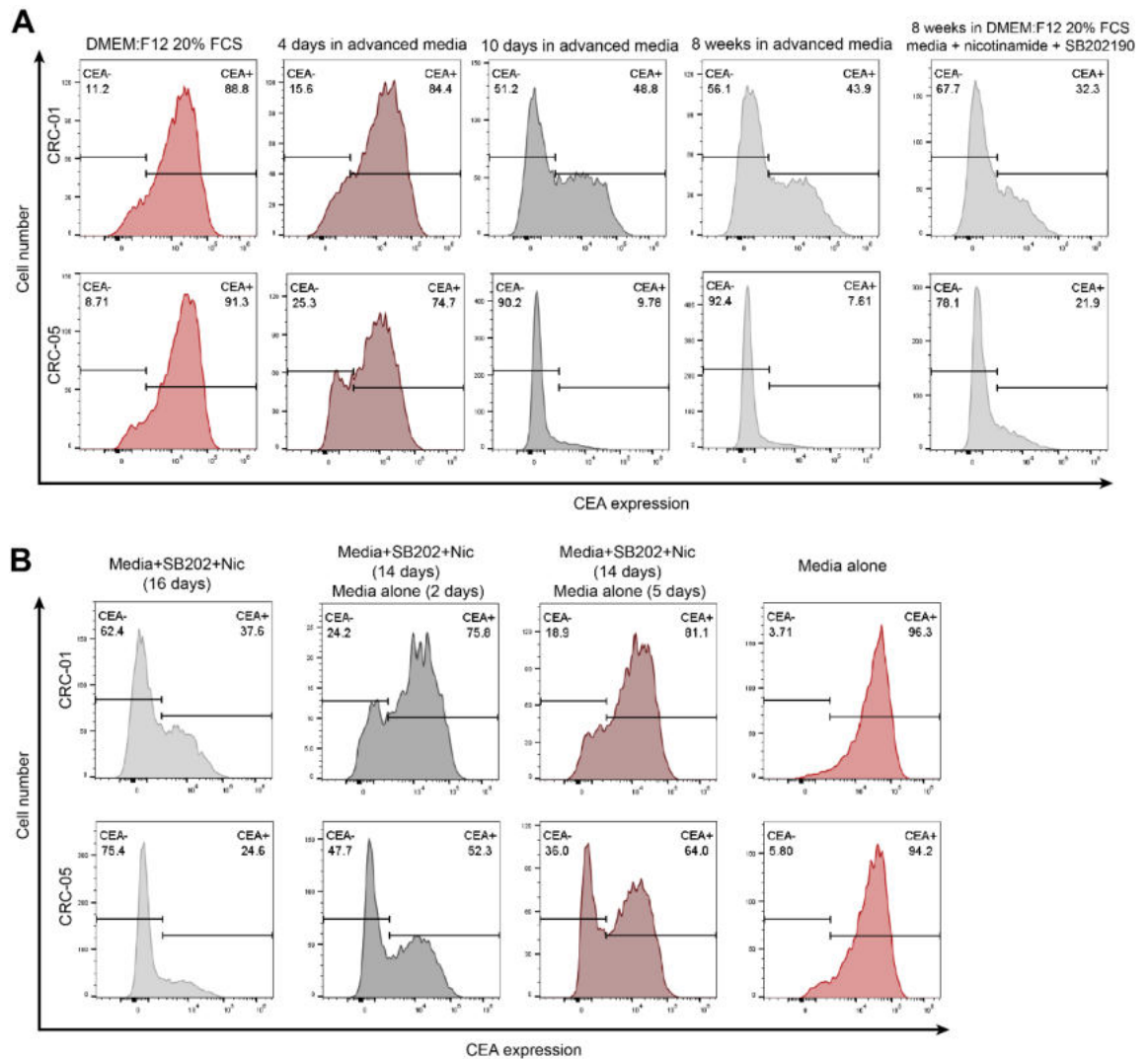
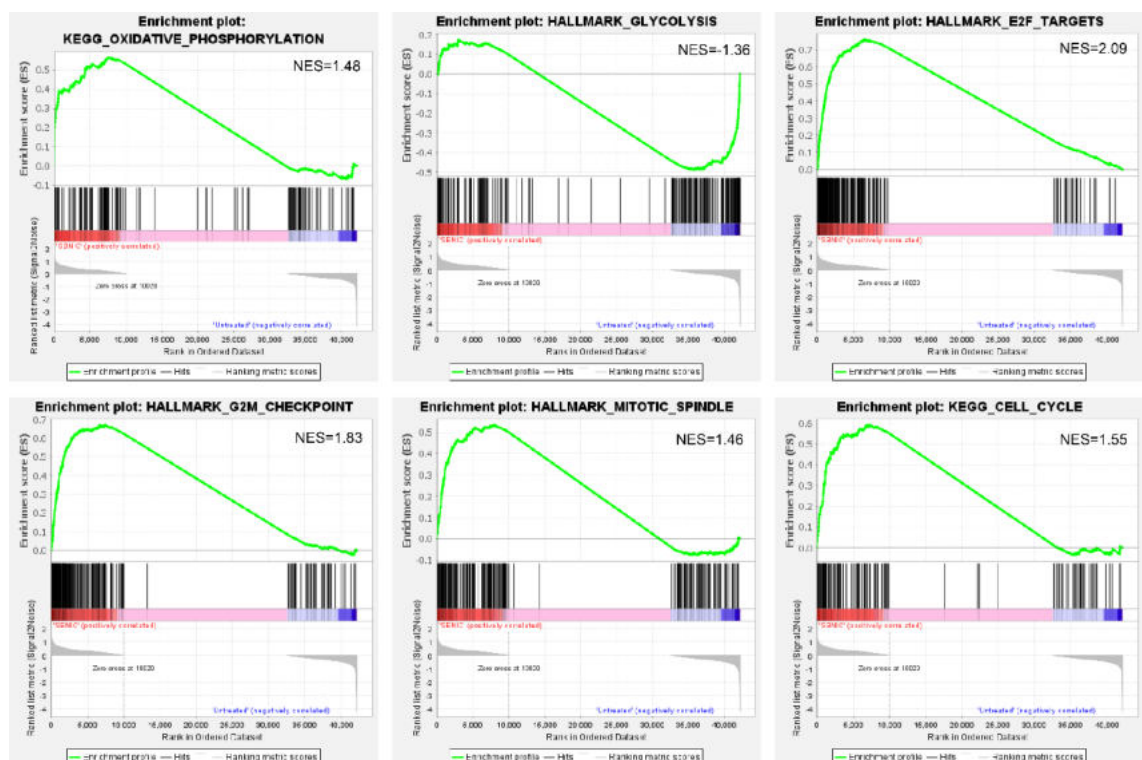


Figure 3.13 Temporal regulation of CEA surface expression. (A) Flow cytometry histograms showing CEA expression of two CEA-high PDOs CRC-01 and CRC-05 cultured in advanced media or in DMEM:F12 20% FCS media with the addition of nicotinamide and SB202190 harvested at different timepoints (4 days, 10 days, 8 weeks). **(B)** Flow cytometry histograms showing CEA expression on two CEA-high PDOs CRC-01 and CRC-05 in transition from DMEM:F12 20% FCS media containing nicotinamide and SB202190 into DMEM:F12 20% FCS media alone. Both experiments performed once.

3.10 Gene set enrichment analysis (GSEA) reveals pathways enriched in p38 inhibitor and nicotinamide treated PDOs

In the RNA-seq data comparing SB202190 and nicotinamide treated CEA-high PDOs versus untreated CEA-high PDOs, a KEGG pathway analysis by GSEA revealed enrichment of oxidative phosphorylation and cell cycle signatures in the treated group (Figure 3.14). Glycolysis signature was significantly enriched in the untreated PDOs. Additionally, GSEA Hallmark signature analysis revealed that E2F targets, G2M checkpoint, and mitotic spindle signatures were enriched in the PDOs treated with SB202190 and nicotinamide (Figure 3.14). The genes in these enriched signatures are involved in cell cycle progression and DNA replication.



3.14 GSEA of SB202190 and nicotinamide treated CEA-high PDOs. Significantly enriched signatures (FDR<25%): Oxidative phosphorylation enrichment plot (KEGG gene set), Glycolysis enrichment plot (HALLMARK gene set), E2F Targets enrichment plot (HALLMARK gene set), G2M checkpoint enrichment plot (HALLMARK gene set), Mitotic spindle enrichment plot (HALLMARK gene set), Cell cycle enrichment plot (KEGG gene set). NES, normalised enrichment score.

3.11 Discussion

Since the focus of my project was on investigating the determinants of CEA-TCB sensitivity and resistance using in vitro PDO-T cell co-culture models it was important to characterise CEA expression in PDOs under different in vitro conditions as CEA expression level is the strongest predictor of CEA-TCB activity (Bacac et al., 2016). Using PDOs grown in 2D in DMEM:F12 20% FCS media containing 2% Matrigel I validated the previous finding from my lab that CEA has a heterogeneous expression in CRC PDOs. Based on surface CEA expression PDOs could be categorised into CEA-high, those that are predominantly CEA+, and CEA-mixed which contain both CEA-/low cells and CEA+ cells. Regular CEA expression checks during prolonged culture showed that 3/4 CEA-high PDOs showed little variability in CEA expression always being 80-95% CEA+, while CEA-mixed PDOs demonstrated great variability in CEA expression with 2 CEA mixed PDOs showing as much as a 60-65% difference in CEA expression between different flow cytometry experiments despite constant culturing conditions and with no correlation to the time in culture. Furthermore, PDOs grown in 3D in Matrigel domes showed very similar CEA expression profiles when harvested around day 10, but with increased time in culture and therefore size CEA expression increased in CEA-mixed PDOs. Immunohistochemical staining of FFPE slides of PDOs matched the flow cytometry CEA expression profiles with CEA-high PDOs being strongly CEA+ and CEA-mixed PDOs displaying CEA expression heterogeneity between organoids as well as within organoids. PDOs were xenografted into NSG mice, harvested once they have reached a certain size (1000mm³), and processed into FFPE slides which were subsequently stained for CEA expression by IHC. Tumour CEA expression pattern matched that of corresponding PDO with CEA-high PDOs resulting in strongly CEA+ tumours and CEA-mixed PDOs resulting in tumours that displayed CEA expression heterogeneity with some CEA+ areas and some areas in which CEA expression was low or absent entirely. These findings indicate that these CEA expression patterns are not an artefact of in vitro cultures but are maintained in vivo. Importantly, the heterogeneous

CEA expression profiles of these PDOs is reminiscent of the CEA expression heterogeneity which has been described in CRC samples from patients (Gonzalez-Exposito et al., 2019; Yan et al., 2016). To my knowledge CEA heterogeneity has not been described in cell lines therefore these findings support the notion that PDOs better represent the molecular heterogeneity of colorectal cancers than established cell lines and are therefore more clinically relevant models for investigating CEA-TCB activity.

Next I investigated factors that may influence CEA expression in co-culture model such as T cell media, absence of Matrigel, cell density, and IFN γ . In T cell media PDOs maintained their CEA expression patterns thus making the PDO-T cell co-culture which is cultured in T cell media a valid model of CEA expression. Density only increased CEA expression in CEA-mixed PDOs once the cells have been 100% confluent for multiple days, thus indicating that density would not have an impact on CEA expression in co-culture model as the cells would not reach such densities. Importantly IFN γ , a cytokine secreted by T cells upon activation with CEA-TCB, increased CEA expression in CEA-mixed PDOs which is favourable as this would lead to higher CEA-TCB sensitivity. Therefore CEA-TCB may potentially show good activity even against CEA-mixed tumours because T cells activated by CEA expressing cells would secrete IFN γ causing an increase in CEA expression in CEA-/low cells and making them sensitive to CEA-TCB. One way to test this would be to treat CEA-mixed PDOs with media from co-cultures and see if it causes an increase in CEA expression. Additionally, these findings showed that IFN γ does not alter CEA expression on already CEA-high PDOs thus ensuring that target antigen would not be downregulated in response to IFN γ upon T cell activation by CEA-TCB allowing identification of resistance mechanisms to CEA-TCB using CEA-high PDOs as models.

When organoids are first established they are cultured in advanced media containing multiple growth factors and supplements that was formulated by Clever's group to promote stem cell proliferation and maintain proliferative potential long term.

Since in healthy colonic crypts epithelial cells at the crypt bottom that harbours intestinal stem cells express low levels of CEA which gradually increases in epithelial cells as they become more differentiated towards the top of the crypt, I hypothesized that advanced media may decrease CEA expression. Culture of CEA-high PDOs in advanced media resulted in a dramatic decrease in two PDOs, a moderate decrease in one PDO, and had no effect on CEA expression in one PDO. Investigation of individual components of advanced media revealed that nicotinamide in combination with a p38 MAPK inhibitor SB202190 strongly decreases CEA expression in 3/4 CEA-high PDOs. Gene expression analysis by qPCR confirmed that CEA downregulation occurred at the transcriptional level. RNA sequencing of PDOs treated with the combination of nicotinamide and p38 MAPK inhibitor followed by gene set enrichment analysis revealed that oxidative phosphorylation signature was enriched in the treated PDOs while genes in a glycolysis signature was enriched in the untreated PDOs. These findings match the findings by my colleagues which showed that oxidative phosphorylation signature was enriched in CEA-low cells which were sorted from CEA-mixed PDOs. This might suggest that regulation of CEA expression might be similar in CRC PDOs and healthy colon epithelial cells as it has been demonstrated that intestinal stem cells at the crypt bottom are more dependent on oxidative phosphorylation than their more differentiated progeny towards the top of the crypt (Rodríguez-Colman et al., 2017). Additionally, they have demonstrated that inhibition of p38 activity reduced differentiation and crypt formation. Similar observations were made about human colon and small intestinal organoids which showed a lack of enterocyte differentiation when cultured in medium containing nicotinamide and p38 inhibitor SB202190 (Sato et al., 2011). Both compounds prolonged the culture period by preventing differentiation and maintaining proliferative potential. Several studies have shown a positive correlation between degree of differentiation of colorectal cell lines and CEA expression with well differentiated cancer cell lines having a higher content of CEA than less well differentiated ones (Guadagni et al., 1990; Shi et al., 1983). The same correlation has been found in colorectal tumours, with less differentiated tumours

expressing low levels of CEA while well differentiated tumours were strongly CEA+ (Denk et al., 1972; Yan et al., 2016). Therefore, treatment of CEA-high PDOs with nicotinamide and p38 inhibitor may have altered their differentiation status resulting in a strong decrease in CEA expression. However, when comparing CEA+ and CEA-/low cells my colleagues found that specific genes which have frequently been associated with stemness in cells of the colon (*CD133*, *CD44*, *LGR5*) in CRC were not upregulated in CEA-/low cells suggesting that potentially there is a severance of the mechanisms that regulate differentiation processes including CEA expression and stemness in PDOs from CRC tumours (Gonzalez-Exposito et al., 2019). Furthermore, multiple gene signatures relating to cell cycle progression were enriched in the SB202190 and nicotinamide treated PDOs. These findings were not surprising as p38 has been shown to inhibit cell cycle progression through induction of G1/S and G2/M checkpoints (Bulavin et al., 2002; Mikhailov et al., 2004; Molnár et al., 1997; Takenaka et al., 1998; Yee et al., 2004). As the RNA sequencing data was one of the final experiments before the submission of this thesis I have not had the opportunity to investigate the role of cell cycle in CEA regulation. However, in the future cell cycle analysis of SB202190 and nicotinamide treated PDOs or CEA-low sorted cells can be conducted. One study has found that culturing human colon carcinoma cells in serum-free medium inhibited cell replication and stimulated the production of CEA. To determine whether CEA expression was inversely correlated with cell division, a colon carcinoma cell line was treated with mitomycin-C, a chemotherapeutic agent, to arrest cell division. This treatment resulted in a complete inhibition of cell division and induced higher CEA expression suggesting that CEA production may be related to decline in cell proliferation (Kitadai et al., 1996). Overall, results from this chapter show that CEA expression is highly plastic therefore in vitro culturing conditions should be tested for their effect on CEA expression especially when evaluating immunotherapeutic agents targeting CEA such as bispecific antibodies and CAR T cells.

Chapter 4: Developing and validating a robust and versatile T cell and CRC PDO co-culture platform for pre-clinical CEA-TCB research

4.1 Introduction

Preclinical immunological research has been predominantly performed in mouse models due to the advantage of having a full intact immune system which is difficult to simulate in vitro. The limitation of syngeneic subcutaneous graft mouse models is the lack of natural tumour microenvironment which can play a crucial role in shaping an anti-cancer immune response. It has been shown that response to immune checkpoint blockade is different in tumours subcutaneously injected versus orthotopic implantation (Ho et al., 2021; B. Lehmann et al., 2017). While orthotopic mouse models address this caveat of syngeneic subcutaneous grafts, they pose a different problem. The surgical procedure that is required for orthotopic implantation, besides being more time consuming and technically challenging, causes post-procedural inflammation which can impact the tumour and its microenvironment in a non-physiological way thus making this model potentially unsuitable for immunotherapy studies. For CEA-TCB, pre-clinical modelling in mice is also further complicated by the fact that they lack the gene encoding CEA (*CEACAM5*) and that CEA-TCB binds human but not murine CD3. A mouse model that has been used to study activity of CEA-TCB in vivo was a subcutaneous implantation of a human colorectal cell line co-grafted together with human PBMCs into an immunodeficient NOG mouse (Bacac et al., 2016). The tumour microenvironment in these models is poorly defined. It is furthermore difficult to dissect the individual processes that may hinder immune response in an in vivo model where a large number of factors are influencing immune responses simultaneously. Lastly, in addition to high cost and the long length of time required for in vivo experiments, there are differences in human and mouse biology resulting in limited translation into the clinic (Mestas &

Hughes, 2004). Therefore there is a need for pre-clinical in vitro models to study tumour cell and immune cell interactions and evaluate the efficacy of and resistance to immunotherapy. In vitro models allow precise control of conditions, for example through the addition of specific molecules at defined concentrations or specific immune cell populations and are amenable to a broad range of readouts. While in vitro assays using cancer cell and T cell lines are simple in their technical aspect, they have caveats. Cancer cell lines are clonal and do not represent the heterogeneity of tumours and due to their long term, sometimes decades long, culture on plastic they may have undergone molecular changes. T cell lines available such as Jurkat E6.1 and HuT78 both come from T cell malignancies and it has been shown that they differ from primary T cells in the expression and function of costimulatory receptors and in the range of cytokines and chemokines released upon activation (Bartelt et al., 2009). In vitro immune checkpoint blockade studies are limited by the need for autologous immune and tumour cell systems and it is challenging to acquire matched patient tumour/immune cell samples. The advantage of studying CD3-binding bispecific antibodies in vitro is that they are not restricted by TCR specificity meaning that they can direct any CD3+T cell to the tumour where it can perform its cytotoxic function. After the importance of the immune response in cancer progression and treatment has been discovered, there has been a big effort in the development of co-culture systems modelling tumour-immune interactions. For example, there are ex vivo tumour slice models which conserve cellular and microenvironmental heterogeneity and thus are able to recapitulate the complexity of the original tumour in vitro (Majumder et al., 2015). However this methodology is challenging, time consuming, costly and is limited by the short timing for which these tumour slices remain viable ex vivo. To address this need for simpler yet robust in vitro assays my lab established a co-culture comprised of PDOs grown in 2D and allogeneic CD8 T cells that can be used for investigating determinants of sensitivity and resistance to T cell redirecting antibodies. I further developed and validated this model as will be described in this chapter.

4.2 Optimisation and validation of PDO-T cell co-culture model

4.2.1 Co-culture model experimental set-up

As described in the previous chapter, the PDOs have been established from multi-drug resistant metastatic colorectal cancers and adapted to 2D culture. The PDOs were labelled with a GFP nuclear marker to enable visualisation with microscopy. Peripheral Blood Mononuclear Cells (PBMCs) were isolated from leukocyte reduction system (LRS) cones obtained from a blood bank or whole blood from healthy donors. CD8⁺ T cells were subsequently isolated using CD8 antibody coated magnetic beads. The isolated T cells were tested for purity using flow cytometry, with only populations with at least 90% purity used in assays. The extraction kit was highly specific and generated purities exceeding 90% in all samples. The isolated T cells were activated and expanded using anti CD3/CD28 beads and IL-2 for 10-14 days prior to addition to the co-culture. GFP labelled PDO cells were seeded into a 96 well plate in T cell media and allowed to attach for 24 hours and the following day T cells along with bispecific antibodies were added to the assay (Figure 4.1A). All conditions were plated in triplicate. All experiments had appropriate controls: PDOs alone, PDOs with T cells, PDOs with T cells and the untargeted bispecific DP47 (a control TCB that binds to T cells, but does not bind to any tumour antigen and thus cannot activate T cells), and PDOs with T cells and CEA-TCB. Since I was using allogeneic T cells in this assay it was important to have a control for alloreactivity. Alloreactivity was detected when there was tumour growth inhibition in the presence of T cells alone compared to the condition with only PDOs (Figure 4.1B). Experiments where alloreactivity was detected were discarded and T cells from this donor were not used for any future experiments. However, this was an extremely rare occurrence with only 1 donor out of 18 healthy donor blood or LRS cone samples that were used showing alloreactivity. The tumour growth was measured by imaging the co-culture every 3-4 days for 7-12 days on an automated plate imaging microscope. For each well the percent confluence of tumour cells was calculated and used as a surrogate

for the assessment of cancer cell growth. The growth of PDOs in the presence of T cells and CEA-TCB was calculated against the average growth of PDOs cultured with T cells and the untargeted control antibody DP47. I was unable to use the method of measuring the total GFP intensity because the GFP expression was heterogenous despite sorting only GFP high cells post GFP tagging. I was also unable to use methods like Cell Titre Blue assay which measures viability because of the presence of T cells in the wells in addition to the tumour cells. CEA-TCB induces proliferation of T cells and therefore the number of T cells between control and experimental conditions would be different thus rejecting this as a viable method and making imaging the best option. The advantage of the imaging approach is that I could track the PDO growth at various timepoints throughout the assay giving me a better understanding of the dynamics of CEA-TCB mediated tumour cell growth inhibition.

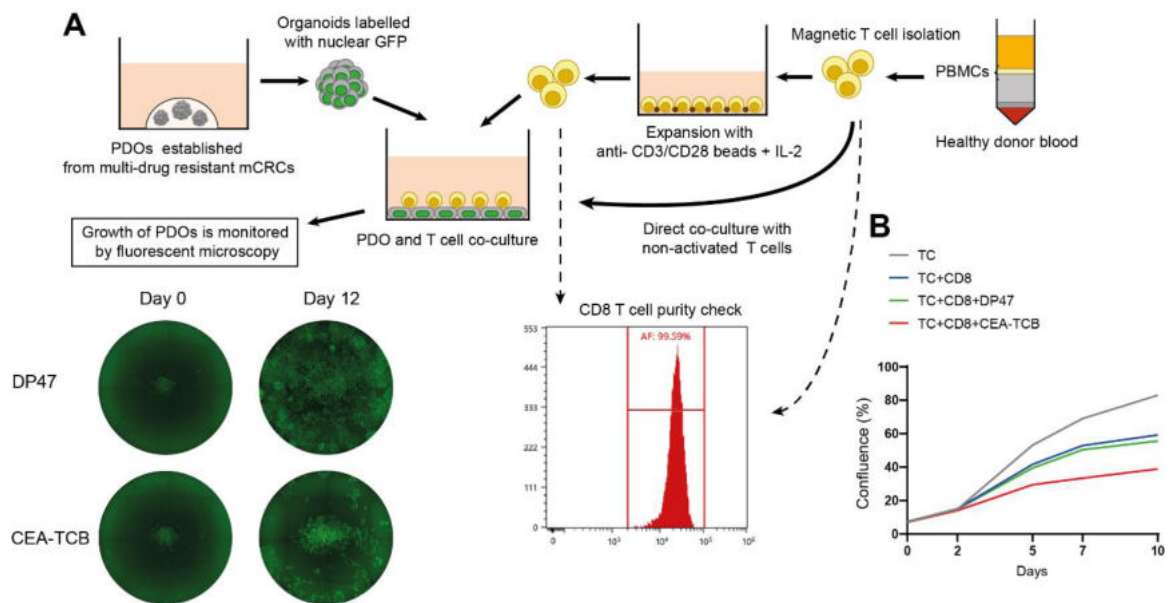


Figure 4.1 PDO-T cell co-culture experimental set up. (A) Diagram showing PDO and allogeneic T cell co-culture model. Flow cytometry histogram shows percent of CD8+ T cells after their isolation from PBMCs. Circle images show growth of GFP tagged CRC-01 on days 0 and 12 treated with either control TCB DP47 or CEA-TCB. **(B)** Example of alloreactivity within the assay as shown by the growth curves of four different conditions in the assay. Grey line is tumour cells alone, blue line is tumour cells with CD8 T cells, green line is tumour cells with CD8 T cells and the untargeted TCB DP47 (20nM), red line is tumour cells with CD8 T cells and CEA-TCB (20nM). Growth is measured on days 0,2,5,7, and 10.

4.2.2 CEA-TCB activity against PDOs with different CEA expression profiles

I conducted a screen of 7 PDOs (CRC-03 had very poor GFP unsuitable for imaging) treated with CD8 T cells from two healthy donors at an effector: target (E:T) ratio of 2:1 and either DP47 (20nM) or CEATCB (20nM) for 10 days imaging the assay on days 0, 2, 5, 7, and 10. The drug concentration was recommended by Roche who had extensively tested CEA-TCB in 110 colorectal cell lines. The three CEA-high PDOs, CRC-01, CRC-05, and CRC-07, showed the biggest response to CEA-TCB treatment with 90, 77, and 130% growth reduction when calculated against DP47 condition on day 10. However, the growth rate of the three PDOs greatly varied with CRC-01 reaching >90% confluence by day 10, CRC-05 reaching ~60%, and CRC-07 showing the slowest growth and reaching only 40% confluence. All CEA-mixed PDOs except for CRC-08 grew at a much slower rate reaching 20-30% confluence by day 10. CRC-06 and CRC-08, the CEA-mixed PDOs showing consistently large CEA-low population, showed the worst response to CEA-TCB with 52% and 51% growth reduction respectively. This difference in response with PDOs CRC-01, CRC-05, and CRC-07 showing an average of 99% reduction and CRC-06 and CRC-08 52% can be explained by their differences in their CEA levels. CEA-high PDOs express CEA between 83% and 98% as shown in the previous chapter, while CRC-06 and CRC-08 were only 45% CEA+ on average which is half of the expression of CEA in CEA-high PDOs. There is also a correlation between CEA expression per cell and the CEA-TCB response in CEA-high PDOs. CRC-07 showed the highest CEA expression per cell as evidenced by the highest MFI of CEA+ population at 38182 (Figure 3.3B) compared to 36805 in CRC-01 and 25934 in CRC-05. In this screen CRC-07 showed the greatest response to CEA-TCB and CRC-05 showed the worst out of the three CEA-high PDOs. However, the correlation between CEA expression and response to CEA-TCB is not perfect, because CRC-02 and CRC-04 showed 69% and 77% growth reduction in response to CEA-TCB while being only 36% and 50% CEA+ on average. However, as mentioned in the previous chapter those two

PDOs showed the greatest variability in their CEA expression ranging from 10-75% and 25-86% CEA+. Since I have not investigated the reason behind these fluctuations and these fluctuations in CEA expression occurred independently of culture conditions as they were constant and time in culture, their CEA expression could have been towards the higher end of their range and subsequently they showed a greater response to CEA-TCB compared to CRC-06 and CRC-08. However, there might be other factors that make them more sensitive to CEA-TCB treatment which requires further investigation.

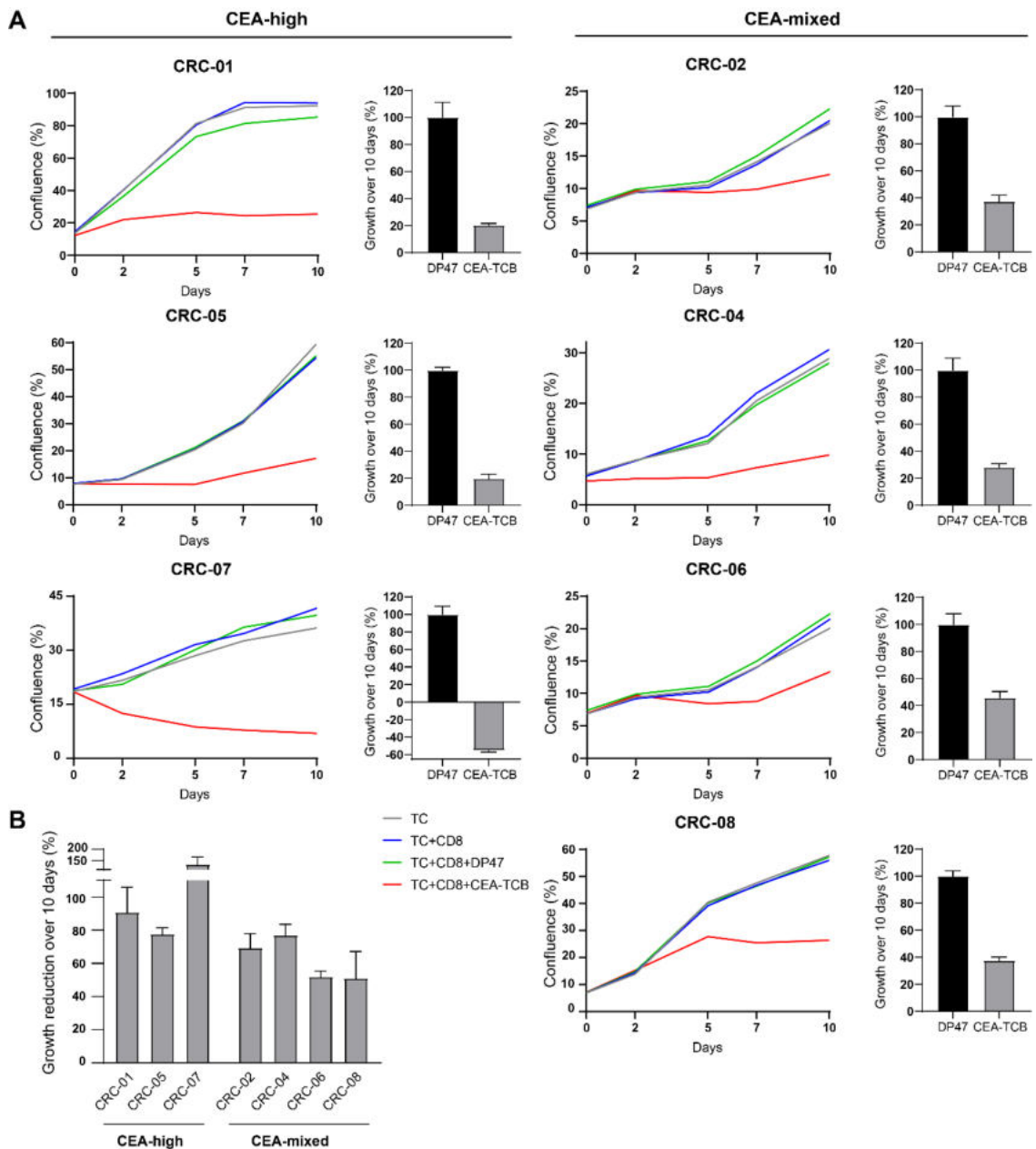


Figure 4.2 Assessment of CEA-TCB efficacy in CEA-high and CEA-mixed PDOs
(A) Growth curves of 7 PDOs divided into CEA-high and CEA-mixed groups based on their CEA expression. PDOs were cultured with pre-activated CD8 T cells at an effector:target ratio of 2:1 in and treated with either the untargeted TCB DP47 (20nM) and CEA-TCB (20nM). All conditions were seeded in triplicate and the averages plotted. Confluence was measured on days 0,2,5,7 and 10. Next to the growth curves are bar charts showing growth quantification of CEA-TCB treated PDOs over 10 days relative to DP47 treated PDOs. Data are representative of 2 repeats. **(B)** Bar chart showing growth reduction percent (%) over 10 days of co-culture of 7 tested PDOs. Each PDO was cultured with T cells from two different allogeneic donors. Error bars represent SD.

4.2.3 Inter- and intra-donor variability as a caveat of co-culture assay

When using primary cells from different donors there is inherent variability in T cell activity which is an important contributing factor to the outcome of the co-culture assay. Even when CEA levels are consistently high as they are in the three CEA-high PDOs, the response to CEA-TCB treatment was not always the same due to the inherent donor variability. At the beginning of my project I was able to use fresh whole blood for CD8 T cell isolation, however this supply was not consistent and due to cell numbers required for experiments not feasible long term. Therefore I had to switch to Leukocyte Reduction System (LRS) cones purchased from the NHS Blood and Transplant Service. The cell numbers were much higher compared to a blood draw from a healthy donor. From a single blood draw I was able to isolate between $2.5-4.5 \times 10^7$ PBMCs while from LRS cones I would isolate $4-11 \times 10^8$ (7.8×10^8 on average) PBMCs. While the cell numbers is an advantage of this method, the disadvantage is the often poor viability and subsequent poor proliferation and killing activity. Potentially the LRS cone system puts a stress on the cells resulting in lower viability. Additionally the time difference between collection and processing of the sample which could have ranged from a few hours to 1-2 days as the NHS service could not guarantee same day delivery could have contributed to poor viability and activity. NHS Blood and Transplant Service did not provide the time of

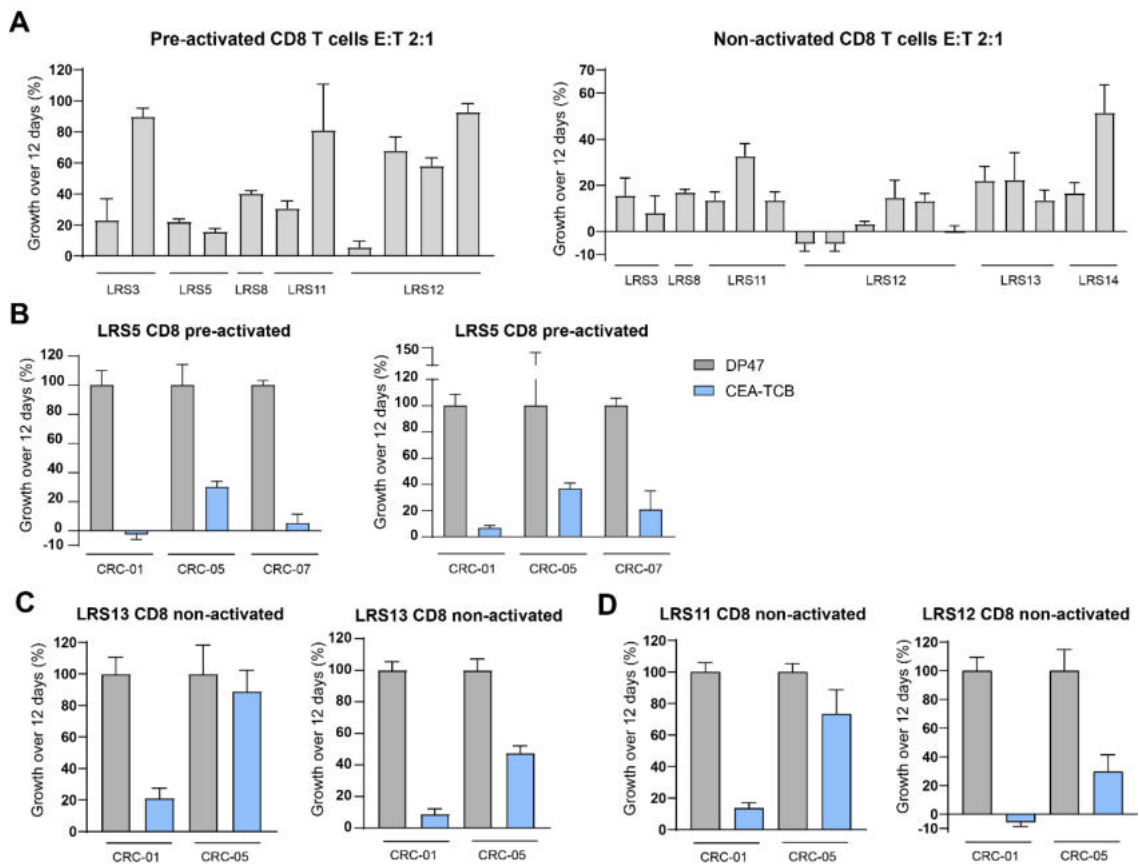


Figure 4.3 Donor variability in ability to inhibit PDO growth (A) Bar graphs showing growth of CRC-01 co-cultured with CD8 T cells from different donors (LRS) and treated with CEA-TCB compared to growth in the DP47 control condition (100%) on day 12 (only CEA-TCB bars are shown). Some donors were used for multiple experiments and individual growth percentages are shown on the graphs for inter-experiment comparison. The graph on the left shows growth of CRC-01 when treated with pre-activated CD8 T cells (pre-activated with anti- CD3/CD28 beads for 10-12 days), while the graph on the right is with non-activated CD8 T cells (freshly isolated CD8 T cells). All experiments shown in these graphs were performed with an E:T ratio of 2:1. **(B)** Two bar graphs showing the growth quantification from two different experiments but with the same PDOs (CRC-01, CRC-05, CRC-07) and the same donor (LRS5). **(C)** Two bar graphs showing the growth quantification from two different experiments but with the same PDOs (CRC-01, CRC-05) and the same donor (LRS13). **(D)** Two bar graphs showing the growth quantification from the same experiment, with the same PDOs (CRC-01, CRC-05) but two different donors (LRS11 and LRS12). Error bars represent standard deviation calculated from three replicates.

collection information which made it impossible for me to draw a correlation between viability/killing ability to the time between LRS5 collection and processing. In order to show the great variability I encountered when using different donors I have included data from

multiple experiments some of which have used pre-activated CD8 T cells and some were conducted with non-activated CD8 T cells (cells that were freshly isolated from PBMCs and used directly in the co-culture without prior activation in vitro). In figure 4.3A each bar shows growth of CRC-01 (as this was the most frequently used PDO) when treated with CD8 T cells at an E:T ratio 2:1 and CEA-TCB compared with the control treatment with the untargeted TCB DP47 on day 12 (as this was the most frequently used end timepoint). Each bar represents a separate experiment and some of the donors are shown multiple times in order to show that not only is there inter-donor variability, but there is also intra-donor variability. Non-activated T cells were always used fresh, isolated on the day of experiment, while pre-activated cells were expanded and frozen for future use. This potentially explains the consistently better performance of LRS12 non-activated T cells compared to the pre-activated cells which were all used from frozen stocks except for the very first experiment which was performed right after expansion in vitro. Some donors were more reproducible than others; Figure 4.3B shows two different experiments performed with the same PDOs (CRC-01, CRC-05, and CRC-07) and CD8 T cells from the same donor (LRS5). This level of reproducibility was extremely rare in my model system. Because of the inter- and intra-donor variability it is more important to look at the trend rather than the absolute values. Figure 4.3C shows two experiments performed with the same PDOs (CRC-01 and CRC-05) and the same donor (LRS13). While the absolute values of growth are very different, with CRC-05 showing 89% growth in experiment 1 and 47% in the other, the trend remains the same with CRC-01 showing a much better response to CEA-TCB treatment than CRC-05. However, the variability of response might not only be dependant on the donor but on the specific PDO-donor interaction. Figure 4.3D shows the growth of two PDOs (CRC-01 and CRC-05) from the same experiment performed with two different donors (LRS11 and LRS12). CRC-01 shows good response with both donors (14% and -6% growth), while CRC-05 shows a poor response with LRS11 (74% growth) and a good response with LRS12 (29% growth). Donor variability in in vitro studies of bispecific antibodies have been shown

previously and while this variability in donors is a caveat of a model system that uses primary T cells, it does not make this system unusable (Dreier et al., 2002). With correct controls in place and repeats with different donors this model system can be used to address important experimental questions relevant to immuno-oncology and provide insights of great translational value.

4.2.4 Comparing PDO growth inhibition efficacy of in vitro pre-activated and non-activated CD8 T cells

I investigated whether the same response to CEA-TCB will be achieved with naïve (non-activated) T cells as with T cells that have been pre-activated with CD3/CD28 beads and IL-2. In previous experiments T cells were activated and expanded in vitro, however, it is more clinically relevant to use non-activated T cells. Two CEA-high PDOs (CRC-01 and CRC-05) and two CEA-mixed PDOs (CRC-06 and CRC-08) were treated with either a control bispecific antibody or CEA-TCB in the presence of either pre-activated CD8 T cells or naïve CD8 T cells that have been freshly isolated from PBMCs and used directly in the 2D co-culture assay (Figure 4.4). To clarify, the naïve T cell group was not analysed for true naïve T cell markers such as CD45RA, therefore this peripheral T cell population most likely consists of a mix of truly naïve CD8 T cells and other subsets such as memory cytotoxic T cells which have been shown to be preferentially activated by BiTEs (Bargou et al., 2008; Dreier et al., 2002; Renner et al., 1997; Topp et al., 2011). During an assay that was cultured for 10 days, by day 7 for three out of the four PDOs tested, activated and non-activated CD8 T cells were able to achieve the same amount of tumour growth reduction and in CRC-01 they performed slightly worse than their pre-activated counterparts. However, by day 10, non-activated CD8 T cells outperformed pre-activated CD8 T cells in all PDOs and achieved significantly more killing in three out of the four PDOs tested (Figure 4.4). This difference between day 7 and day 10 can potentially be explained by the extra time the non-activated T cells require for activation

and production of granzyme/perforin cytotoxic granules and effector cytokines such as IFN γ .

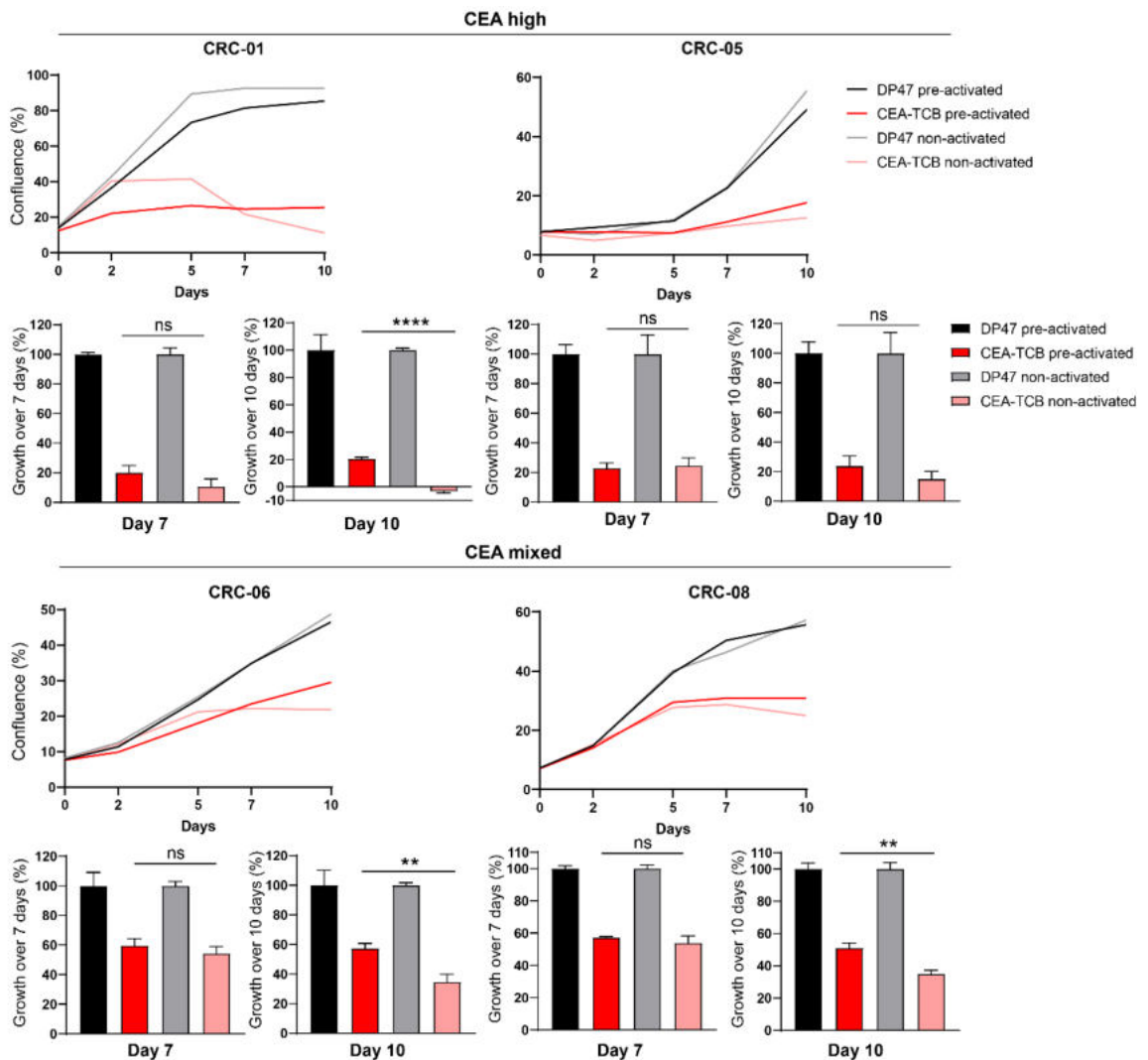


Figure 4.4 Comparison of pre-activated and non-activated CD8 T cell PDO growth control. PDO growth curves over 10 days of co-culture with CD8 T cells treated with DP47 (20nM) or CEA-TCB (20nM). Tumour cell growth quantification on day 7 and 10 for two CEA-high lines (CRC-01 and CRC-05) and CEA-mixed lines (CRC-06 and CRC-08) treated with DP47 or CEA-TCB and either pre-activated or non-activated CD8 T cells. Error bars represent one standard deviation calculated from three replicates. Statistical analysis was performed using an unpaired t-test. For all growth analysis P values are as follows: > 0.05 is ns, < 0.05 is *, < 0.01 is **, <0.001 is ***, <0.0001 is **** and ns = not significant.

These experiments showed that CEA-TCB is able to induce enough activation for tumour growth control without the requirement for signal 2 which is usually required under normal priming and activation conditions. One of the reasons bispecific antibody mediated T cell activation does not require costimulatory signals is the highly effective formation of immunological synapses that occurs when the bispecific engages CD3 on T cells and the target tumour antigen (Dreier et al., 2002; Kamakura et al., 2021; Wolf et al., 2005). When bispecifics engage TAs on tumour cells it forms many CD3/TCR complexes on the T cells and this clustering leads to formation of a tight immunological synapse and T cell activation in the absence of a costimulatory signal. These experiments also demonstrate that activating the T cells twice (once for in vitro culturing with anti-CD3/CD28 beads and once with CEA-TCB) does not dampen their cytotoxic response. Although if these assays were to be extended to longer time periods, pre-activated T cells may reach exhaustion sooner than non-activated T cells and start showing diminished killing activity, however the question of T cell exhaustion in response to CEA-TCB is outside the scope of this research project.

4.3 Investigating whether Wnt/ β -catenin inhibition increases CEA expression and sensitivity to CEA-TCB therapy

4.3.1 Treatment of CEA-mixed PDOs with tankyrase inhibitor increases CEA expression

My lab sorted CEA-high and CEA-low cells from three CEA-mixed PDOs, RNA sequenced them and performed gene set enrichment analysis (GSEA). This analysis revealed a negative correlation between CEA expression and Wnt/ β -catenin pathway activity (Gonzalez-Exposito et al., 2019). Tankyrase 1 and 2 are proteins that promote Wnt signalling by stimulating degradation of Axin which is a key protein constituting the β -catenin destruction complex. Tankyrases destabilise β -catenin destruction complex

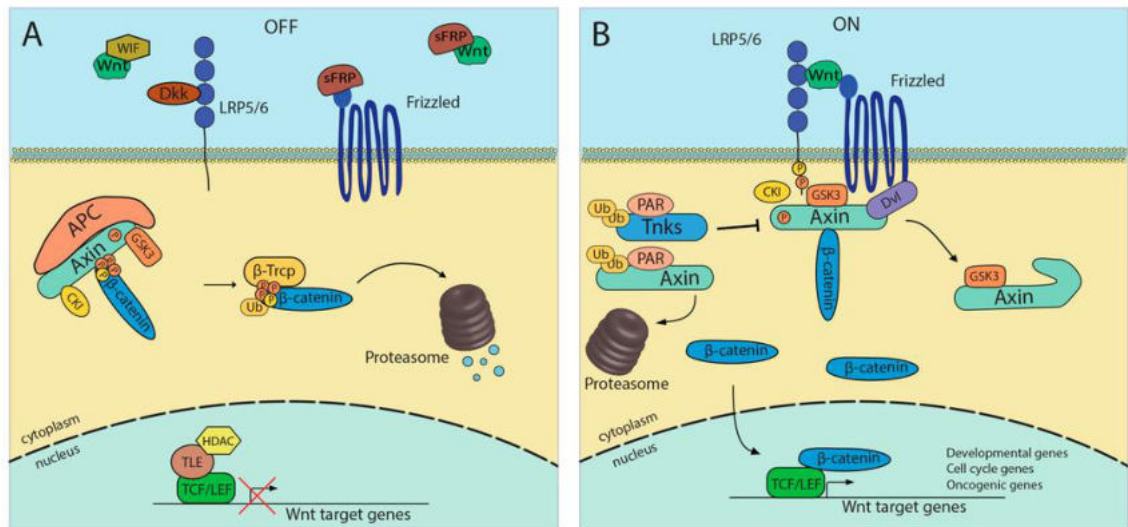


Figure 4.5 Wnt/ β -catenin signalling pathway. (A) In the absence of Wnt the β -catenin destruction complex composed of APC, Axin1, GSK-3 β , and CK1 phosphorylates serine residues in β -catenin leading to its ubiquitination by β -Trcp and degradation by the proteasome. In the absence of nuclear β -catenin a repressive complex containing TCF/LEF and TLE/Groucho recruits HDACs to repress target genes. **(B)** During canonical Wnt signalling, binding of Wnt ligand to Frizzled and LRP5/6 receptor complex causes recruitment of the members of the destruction complex to the membrane which ultimately stabilises β -catenin and results in its translocation to the nucleus where it forms an active complex with LEF and TCF proteins to induce expression of target genes. Regulation of Axin is the rate limiting step in the assembly and function of the β -catenin destruction complex. Through PARsylation tankyrase proteins mark Axin for proteosomal degradation, inhibiting β -catenin destruction complex formation resulting in β -catenin accumulation in the nucleus. APC, Adenomatous polyposis coli; GSK-3 β , Glycogen synthase kinase 3- β ; CK1, casein kinase 1; β -Trcp, F box/WD repeat containing protein 1A; TCF, T cell factor; LEF, lymphoid enhancer factor 1; HDAC, histone deacetylase; LRP5/6, low-density lipoprotein-related protein 5/6. Image taken from (Amado et al., 2014).

resulting in stabilisation and accumulation of β -catenin which then translocates into the nucleus where it binds Tcf/Lef and promotes the transcription of Wnt target genes (Figure 4.5). Therefore inhibition of tankyrases may be a promising method to reduce Wnt signalling (Huang et al., 2009; Mariotti et al., 2017).

I investigated in our PDO models whether tankyrase inhibitors can increase CEA expression and make these tumour cells more susceptible to CEA-TCB. CEA-mixed PDOs CRC-04, CRC-06, CRC-08 were treated with a tankyrase inhibitor Compound 21(C21) at two different concentrations (2 μ M and 10 μ M) (Elliott et al., 2015).

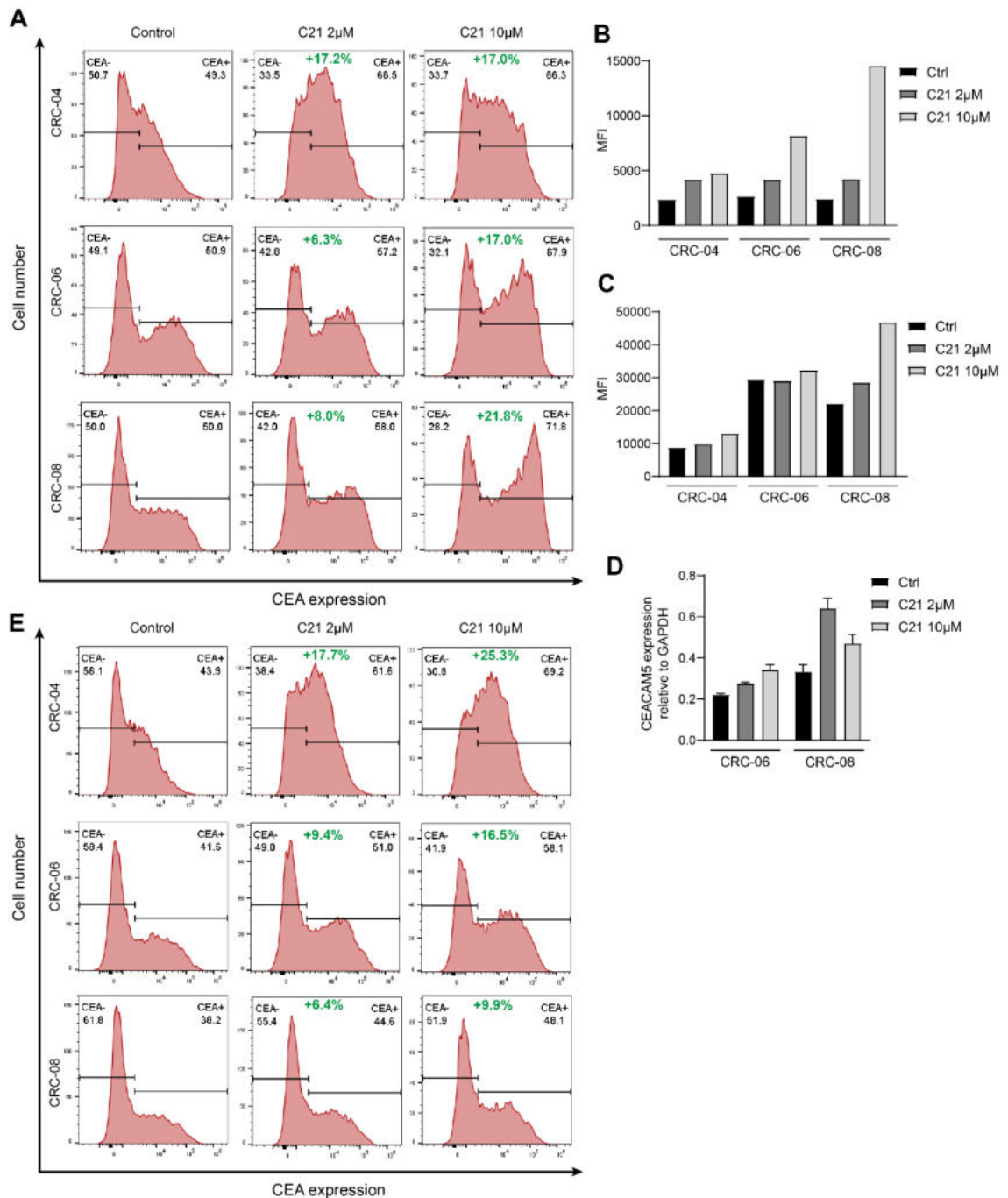


Figure 4.6 Effect of tankyrase inhibition on CEA expression in CEA-mixed PDOs. (A) Flow cytometry histograms showing CEA expression in three CEA-mixed PDOs CRC-04, CRC-06, CRC-08 +/- tankyrase inhibitor Compound 21 treatment at either 2µM or 10µM concentration for 6 days. Data are representative of 2 repeats. (B) Total MFI measurements for CEA expression for flow cytometry experiment in A. (C) MFI of CEA of CEA+ cells from flow experiment A. (D) *CEACAM5* expression relative to *GAPDH* determined by qPCR after treatment with Compound 21 tankyrase inhibitor (2µM and 10µM concentrations) for 6 days. Error bars represent SD from three replicates. (E) Flow cytometry histograms showing CEA expression in three CEA-mixed PDOs CRC-04, CRC-06, CRC-08 +/- Compound 21 at either 2µM or 10µM concentration for 48 hours and then grown under control conditions for 4 days. Experiment performed once.

Tankyrase inhibition led to an increase in the CEA⁺ proportion of the population (Figure 4.6A&B). The CEA increase with the 2 μ M dose was small in CRC-06 and CRC-08 with a 6.3% and 8.0% increase. CRC-04 appeared to be more sensitive to tankyrase inhibition and exhibited an increase of 17% in CEA expression at both doses (Figure 4.6A). The amount of CEA expressed per cell only showed a minimal increase in CRC-04 and CRC-06 at 10 μ M of Compound 21, while CRC-08 exhibited a dose dependant increase with the MFI of CEA⁺ cells doubling at the 10 μ M dose (Figure 4.6C). qPCR results showed that with C21 treatment CEA expression level increased indicating that CEA expression is regulated at the gene expression level (Figure 4.6D). These results were consistent with RNA sequencing results from sorted CEA-low and CEA-high subpopulations that showed regulation at the RNA level. I furthermore investigated how stable CEA upregulation through C21 is. I treated PDOs with the two different doses of Compound 21 for 48 hours and afterwards continued to grow these PDOs for 4 days without any further treatment. Even at the lower dose the CEA expression profile was preserved after 4 days without treatment. While CRC-04 and CRC-06 retained the increased CEA expression at the level of or higher than seen with continuous Compound 21 treatment, CRC-08 showed a reduced CEA expression at only 10% increase compared to 22% observed with continuous treatment with the 10 μ M dose (Figure 4.6E). These results confirmed the role of Wnt/ β -catenin signalling as a regulator of CEA expression in CRC PDOs and demonstrated that it is possible to pharmacologically alter CEA expression.

4.3.2 Tankyrase inhibition sensitises CEA-mixed PDOs to CEA-TCB treatment

My next question was whether treatment of CEA-mixed PDOs with C21 would sensitise them to CEA-TCB treatment as a result of the increase in CEA expression. CRC-08 and CRC-06 were cultured for 7 days in the presence of CD8 T cells and 20nM of the non-targeted bispecific antibody or with 20nM of CEA-TCB. Co-cultures were either performed a) without tankyrase-inhibitor, b) following 48 hours of pre-treatment with tankyrase-inhibitor which was removed when T cells were added, or c) following 48 hours

pre-treatment with tankyrase inhibitor which was replenished at the time T cells were added for continuous tankyrase inhibitor exposure. At the 10 μ M dose only conditions a and b were evaluated since continuous treatment was toxic to the tumour cells and resulted in poor growth even in the control wells (Figure 4.7B). CRC-06 also showed a modest decrease in growth when continuously grown in 2 μ M and when pre-treated with 10 μ M. However, the decrease was only 22% and 48% respectively which still allowed me to perform the experiment because CEA-TCB mediated tumour cell growth inhibition is always measured against the DP47 control condition which would also show the Compound 21 induced growth inhibition effect (Figure 4.7B). Due to the intra- and inter-donor variability described earlier these experiments were repeated multiple times with the same donor and also with a different donor. Pre-treatment of PDOs with 2 μ M of C21 for 48 hours prior to the addition of T cells showed a modest increase in growth reduction only reaching significance in one of the three experiments shown (Figure 4.7A). However, continuous treatment with this dose showed a significant or near significant increase in the growth reduction percent averaging 20% difference compared to control. Pre-treatment with the higher dose of 10 μ M showed the biggest increase in growth reduction averaging 30% (CRC-06 31.3% and CRC-08 28.6%)(Figure 4.7A). The better response to CEA-TCB treatment seen at the higher dose of the tankyrase inhibitor can be explained with the dose dependant increase in CEA expression shown in 4.3.1. These data demonstrates proof of principle that it is possible to pharmacologically sensitise colorectal cancer cells to CEA-TCB treatment. Based on these data, the combination of a Wnt signalling inhibitor and CEA-TCB has been patented by our collaborator Roche Glycart.

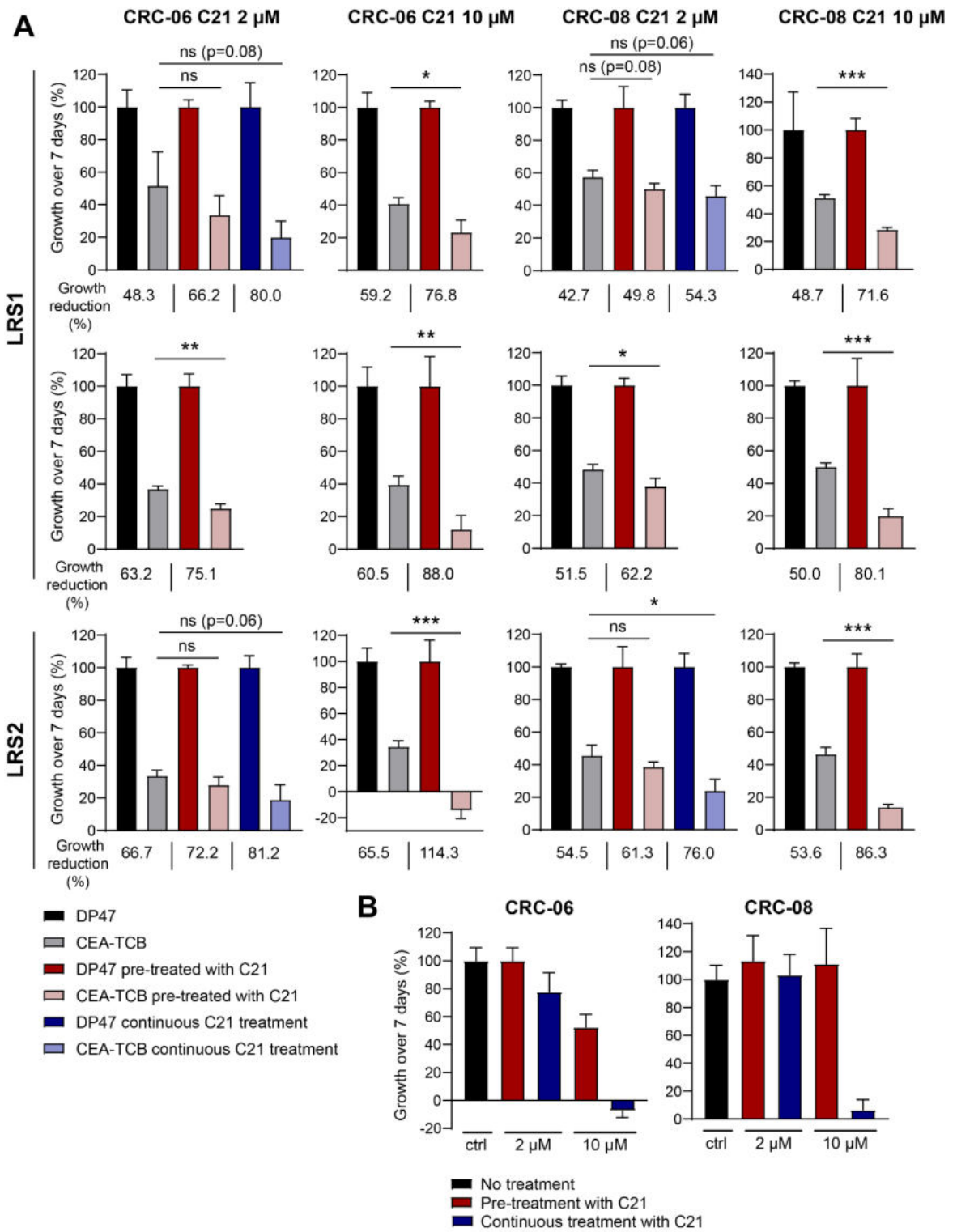


Figure 4.7 Effect of tankyrase inhibitor Compound 21 on sensitivity of PDOs to CEA-TCB treatment. (A) Growth quantification of CEA-TCB treated PDOs (CRC-06 and CRC-08) over 7 days relative to untargeted TCB treated PDOs in the presence or absence of Compound 21 at 2 doses (2 μ M and 10 μ M). PDOs were either pre-treated with C21 for 48hrs prior to the addition of pre-activated CD8 T cells with C21 removed on the day T cells and DP47/CEATCB were added or they were continuously treated with C21 for the entire duration of the experiment. Three different experiments are shown; two repeats with the same donor LRS1 and one experiment with donor LRS2. **(B)** Bar graphs showing growth of tumour cells from 2 PDOs (CRC-06 and CRC-08) cultured either under control, pre-treatment, or continuous treatment conditions with two doses of C21. Error bars represent one standard deviation calculated from three replicates. Statistical analysis was performed using an unpaired t-test. For all growth analysis P values are as follows: > 0.05 is ns, < 0.05 is *, < 0.01 is **, <0.001 is ***, <0.0001 is **** and ns = not significant.

4.3 Assessing the contribution of CD8 and CD4 T cells to CEA-TCB mediated tumour cell growth control

CEA-TCB binds CD3 which is expressed on both CD8 and CD4 T cells therefore it was important to assess the contribution of each of these subsets to tumour control mediated by this T cell redirecting bispecific antibody. CD4 T cells are traditionally considered to be helper cells that support the development and maintenance of CD8 T cells and B cell responses. Contrastingly CD8 T cells are considered to be the main immune cell subset responsible for cytotoxic responses in viral infections and anti-tumour responses. Therefore immunotherapy development has been primarily focused on conventional cytotoxic CD8 T cell-mediated responses. However, it has been shown that in addition to their helper role, CD4 T cells can acquire a cytotoxic phenotype that is capable of inducing tumour cell death via granzyme B and perforin secretion. Cytotoxic T cells have been observed in chronic viral infections such as cytomegalovirus and Epstein-Barr, acute infections such as influenza virus, and also in several tumour types (Appay et al., 2002; Brien et al., 2008; Brown et al., 2012; Hildemann et al., 2013; Hua et al., 2013; Kitano et al., 2013; Mattoo et al., 2016; Oh et al., 2020; Quezada et al., 2010; Śledzińska et al.,

2020; Xie et al., 2010; Zaunders et al., 2004; Zheng et al., 2017). Both, CD8 and CD4 T cells have been shown to contribute to T cell redirecting bispecific antibody mediated tumour cell killing. Some models demonstrated CD8 to be more efficacious than CD4 T cells (Dreier et al., 2002; Ishiguro et al., 2017b; S. Lehmann et al., 2016; J. Li et al., 2017). Van Hall and colleagues showed that CD8+ and CD4+ T cells had equal tumour cell killing capacity and in fact showed that CD4 T cells could replace CD8 T cells in their mouse melanoma model treated with 2C11xTA99 bispecific antibody targeting CD3 and the surface melanocyte differentiation protein TRP1 (Benonisson et al., 2019). Whereas Li and colleagues demonstrated that CD4 T cells were dispensable for anti-HER2/CD3 TDB efficacy because after depleting CD4 T cells in their mouse breast cancer model the anti-tumour response achieved was comparable with that when both T cell subsets were present (Li et al., 2018) .

In my 2D co-culture model I compared tumour growth inhibition mediated by CD8 and CD4 T cells from three different donors using the three CEA-high PDOs CRC-01, CRC-05, and CRC-07. All T cells have been pre-activated and expanded prior to addition to the assay. The CD4 T cell population consisted of activated and expanded CD4+CD25- T cells thus removing the Treg population. With donor LRS5 CRC-01 actually showed that CD4 T cells achieved better tumour growth control than CD8 T cells. CRC-05 showed a small difference of 13% in the favour of CD8 T cells, and CRC-07 showed the biggest difference between CD8 and CD4 mediated killing with 70% difference in tumour growth reduction in favour of CD8 T cells (Figure 4.8A). However, with the two other donors, LRS3 and LRS8, CD4 T cells performed worse than CD8 T cells in all three PDO lines with an average growth reduction difference of 36% in CRC-01, 44% in CRC-05, and 37% in CRC-07 (Figure 4.8A). Thus, CD4 T-cells can contribute to CEA-TCB mediated tumour control, yet the effect of CD8 T cells is stronger.

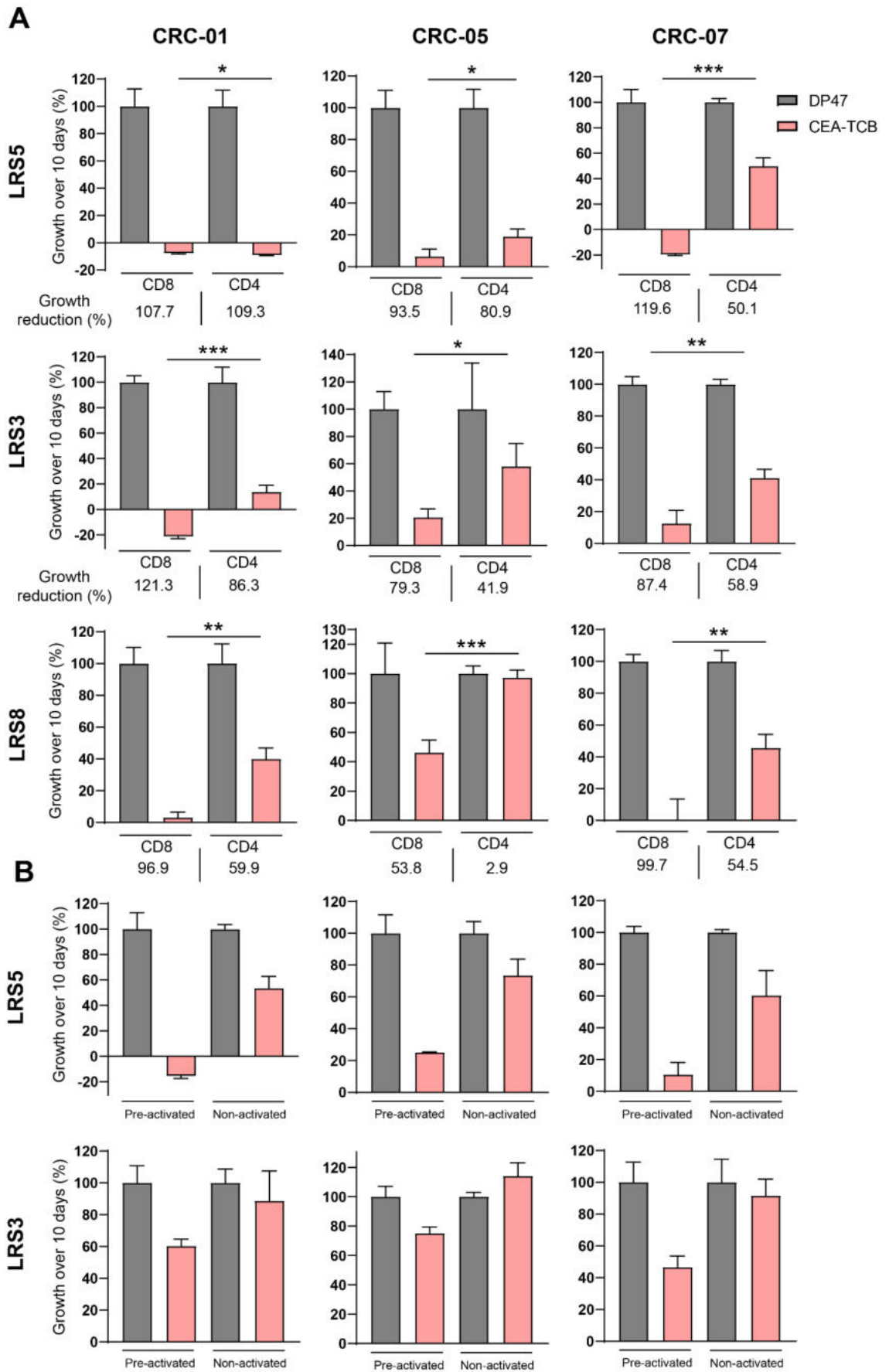


Figure 4.8 Comparing CD8 and CD4 T cell mediated PDO growth inhibition (A) Growth quantification of CEA-TCB treated CEA-high PDOs (CRC-01, CRC-05, CRC-07) over 10 days relative to untargeted TCB DP47 treated PDOs. Experiments were performed with pre-activated CD8 or CD4 T cells from 3 donors (LRS3,5,8). Two repeats were performed with each donor, only one shown. **(B)** Growth quantification of CEA-TCB treated CEA-high PDOs (CRC-01, CRC-05, CRC-07) over 10 days relative to untargeted TCB DP47 treated PDOs. Experiments were performed with pre-activated or non-activated CD4 T cells from 2 donors (LRS 3,5). Error bars represent one standard deviation calculated from three replicates. Statistical analysis was performed using an unpaired t-test. For all growth analysis P values are as follows: > 0.05 is ns, < 0.05 is *, < 0.01 is **, <0.001 is ***, <0.0001 is **** and ns = not significant.

Additionally I investigated the difference in tumour growth inhibition between non-activated and pre-activated CD4 T cells. Non-activated T cells from donor LRS5 achieved less tumour growth inhibition than their pre-activated counterparts, but nonetheless there was still an average of 38% tumour growth reduction. However, non-activated CD4 T cells from donor LRS3 achieved virtually no tumour growth control (Figure 4.8B). Both donors showed that non-activated CD4 T cells are less effective at CEA-TCB mediated tumour growth inhibition compared to pre-activated CD4 T cells which is different to what was found with CD8 T cells where non-activated T cells were either equal to or better than pre-activated T cells at tumour cell growth inhibition.

4.4 Investigating effector mechanisms of CD8 versus CD4 T cells

There are several T cell effector mechanisms: release of lytic granules containing pore-forming protein perforin and serine proteases called granzymes that activate an enzyme cascade ultimately inducing programmed cell death, apoptosis induction through binding of FAS ligand (FAS-L) expressed on T cells to the FAS death receptor on target cells, IFN γ secretion by T cells which triggers cell cycle arrest and apoptosis in target cells, and TNF α and TRAIL (TNF-related apoptosis-inducing ligand) induced apoptosis in

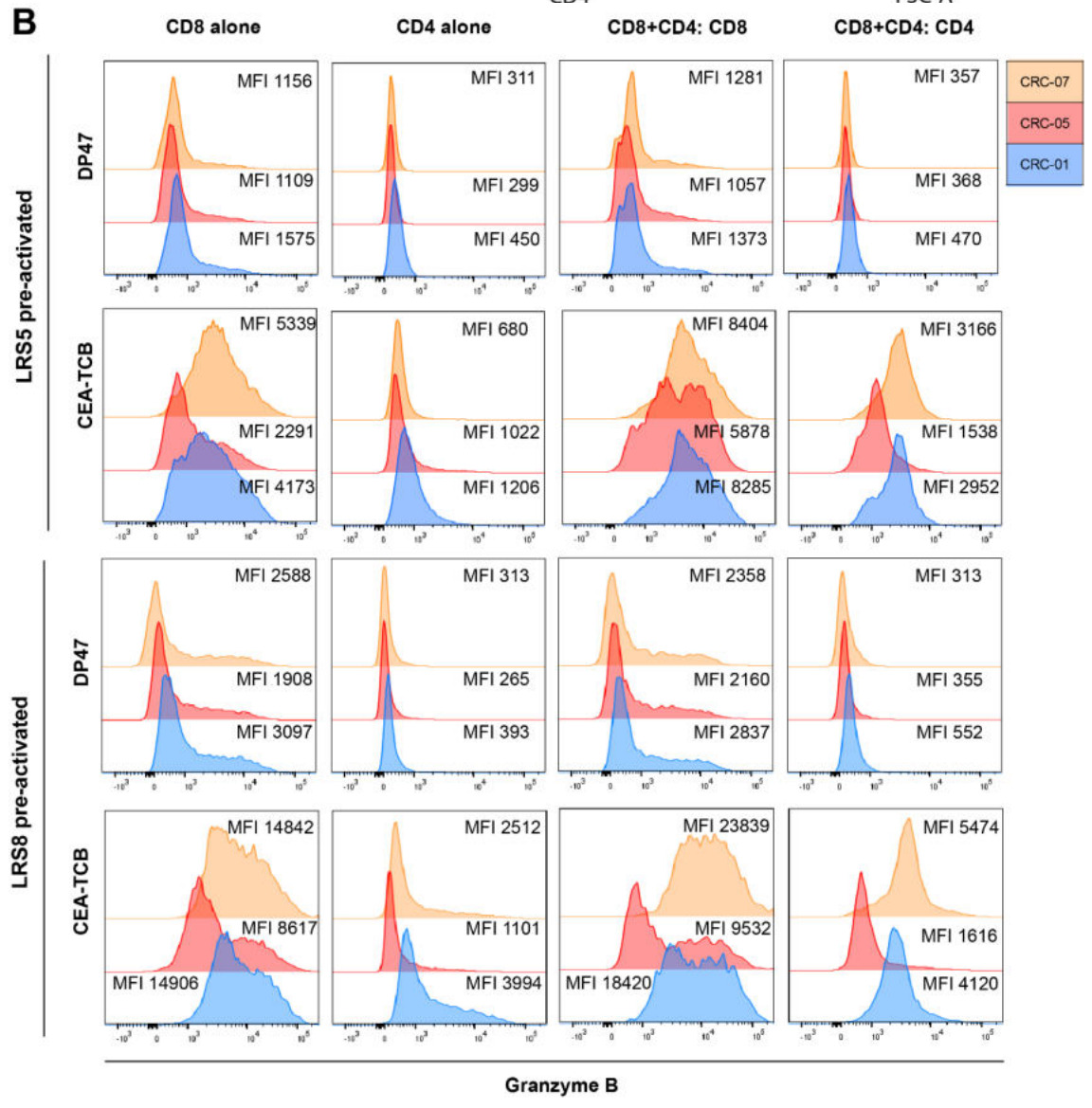
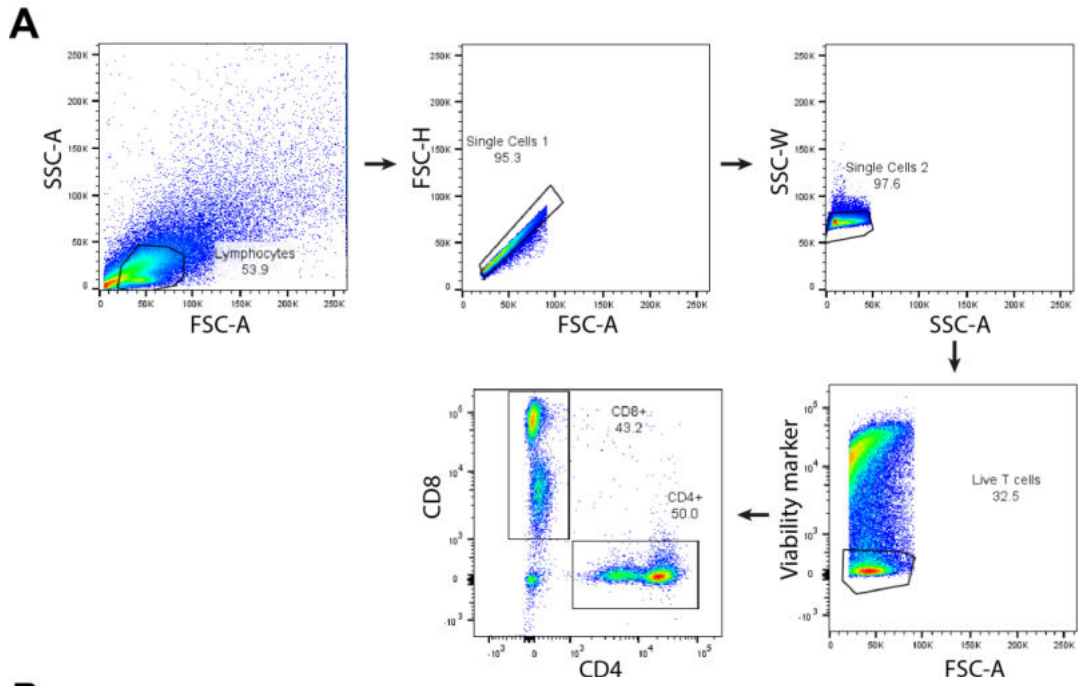
target cell (Russell & Ley, 2002). However, it has not been investigated in the context of CEA-TCB, which mechanism or combination of results in cancer cell killing.

4.4.1 Granzyme B expression in CD8 and CD4 T cells activated by CEA-TCB

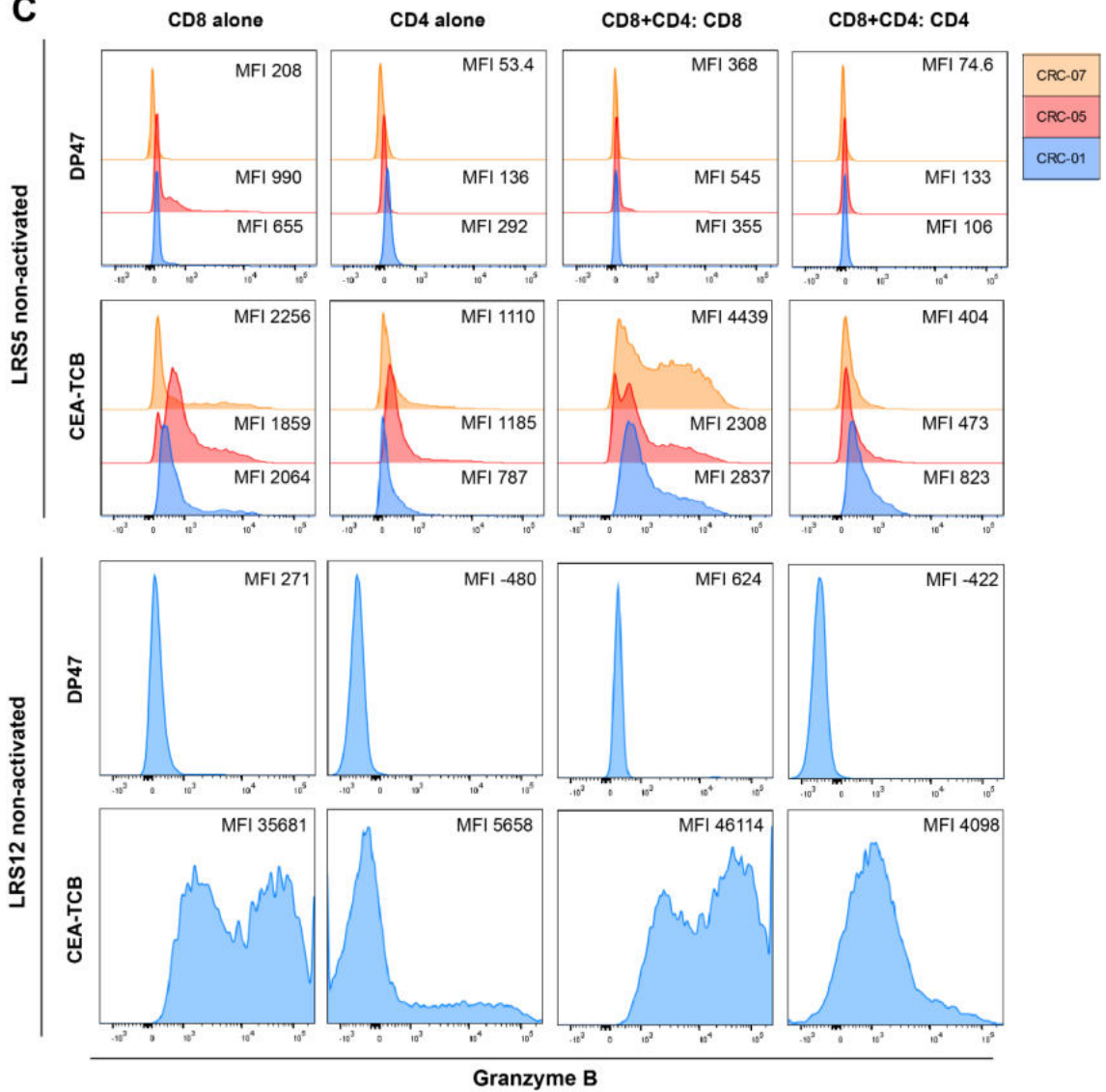
To examine granzyme production I upscaled the 2D co-culture assay to a 24-well plate format in order to be able to harvest enough T cells for flow cytometry experiments. There was a total of six conditions per PDO with two different donors (2 separate experiments): CD8, CD4, and CD8+CD4 T-cells treated with DP47 and the same set treated with CEA-TCB. After 8 days of co-culture the T cells were harvested from the assay, stained with live/dead dye, fixed, and stained with anti-CD8, CD4, and granzyme B antibodies. The gating strategy used is shown in Figure 4.9A. Flow cytometry analysis showed a dramatically stronger upregulation of granzyme B in CD8 compared to CD4 T cells when treated with CEA-TCB with all three PDOs (Figure 4.9B). Granzyme expression is higher in CD8 compared to CD4 even with DP47 treatment and since DP47 does not induce activation the granzyme levels in this condition reflect the granzyme expression level that was induced during the pre-activation. With donor LRS5 both CD8 and CD4 T cells in the CEA-TCB condition are majority granzyme B positive, ranging between 80-100%, whereas with donor LRS8 all CD8 T cells are granzyme B positive (94-100%) while on average only 39% of CD4 T cells are granzyme B positive (Figure 4.9E). However, the proportion of granzyme expressing CD4 T cells increases to 97% with CRC-01 and CRC-07, and only to 42% (from 18% in alone condition) with CRC-05 when both T cell subsets were combined. In addition to having the smallest population of granzyme+ cells, T cells co-cultured with CRC-05 also have the lowest granzyme expression in both CD8 and CD4 T cells with both donors which may be a result of lower CEA expression compared to the other two CEA-high PDOs as demonstrated in the previous chapter. CD4 T cells co-cultured with CRC-01 show the highest granzyme expression. These results correspond to the growth reduction data from co-culture assays discussed in 4.3, where with 3/3 donors CRC-05 showed the poorest growth reduction with CD8 T cells, and with

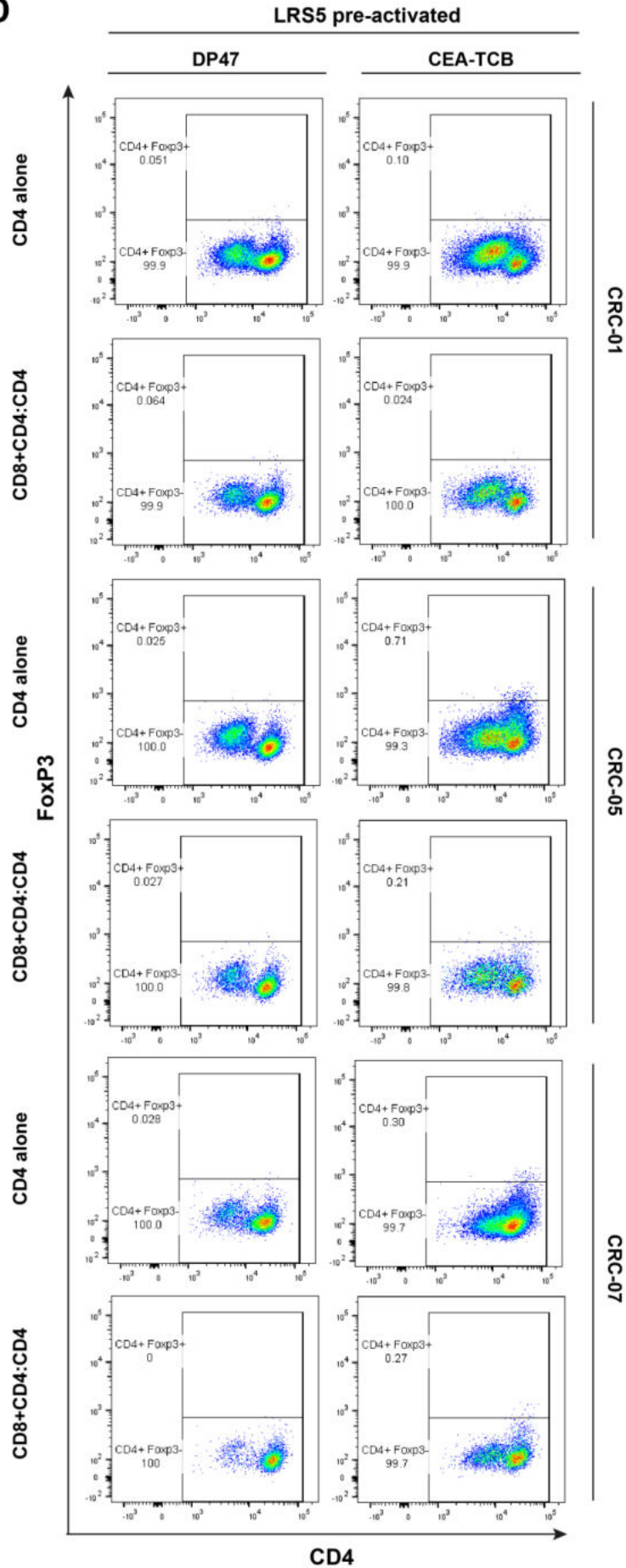
2/3 donors for CD4 T cells. CRC-01 exhibited the greatest growth reduction with both T cell subsets and both donors except for LRS5 where CRC-07 has the biggest growth reduction. This agrees with granzyme expression data showing that LRS5 CD8 T cells express the highest amount of granzyme when co-cultured with CRC-07. Including both T cell subsets in the co-culture appears to be enhancing the granzyme expression of both CD8 and CD4 T cells, increasing it 1.3-2.9 fold (Figure 4.9B). When comparing the MFI granzyme B values for CD4 T cells alone versus when they were combined with CD8 T cells, the change isn't that big (2.9 fold for LRS5 and 1.6 fold for LRS8), but if I compare the mode, the increase in granzyme B expression becomes more clear. For LRS5, the mode (averaged across all PDOs) for granzyme expression for CD4 T cells alone treated with CEA-TCB is 504 and it increases to 2,268 when co-cultured with CD8 T cells. For LRS8 we see a similar change from 419 to 2,285. Only a very small proportion of granzyme B+ CD4 T cells (alone condition) express high levels of granzyme B which increases the MFI value, but leaves the mode relatively low. Whereas when CD4 T cells are combined with CD8, there are less very high granzyme+ cells, but the majority of the population expresses moderate levels of granzyme which results in a small MFI change and a major change in mode.

When the same experiments were performed with non-activated T cells, the trends were similar. CD4 T cells expressed less granzyme B in comparison to CD8 T cells (Figure 4.9C). The changes in the proportion of CD4 granzyme+ cells were similar to those seen in LRS8 pre-activated experiment. When only CD4 T cells were present, an average of 47% of the population expressed granzyme which increased to an average of 97% when CD4 T cells were co-cultured together with CD8 T cells (Figure 4.9E). When two subsets were combined there was an increase in granzyme expression in both populations, except for LRS5 CD4 T cells that actually expressed lower levels of granzyme B than when alone. LRS12 CD4 T cells showed the same trend as was seen



C



D

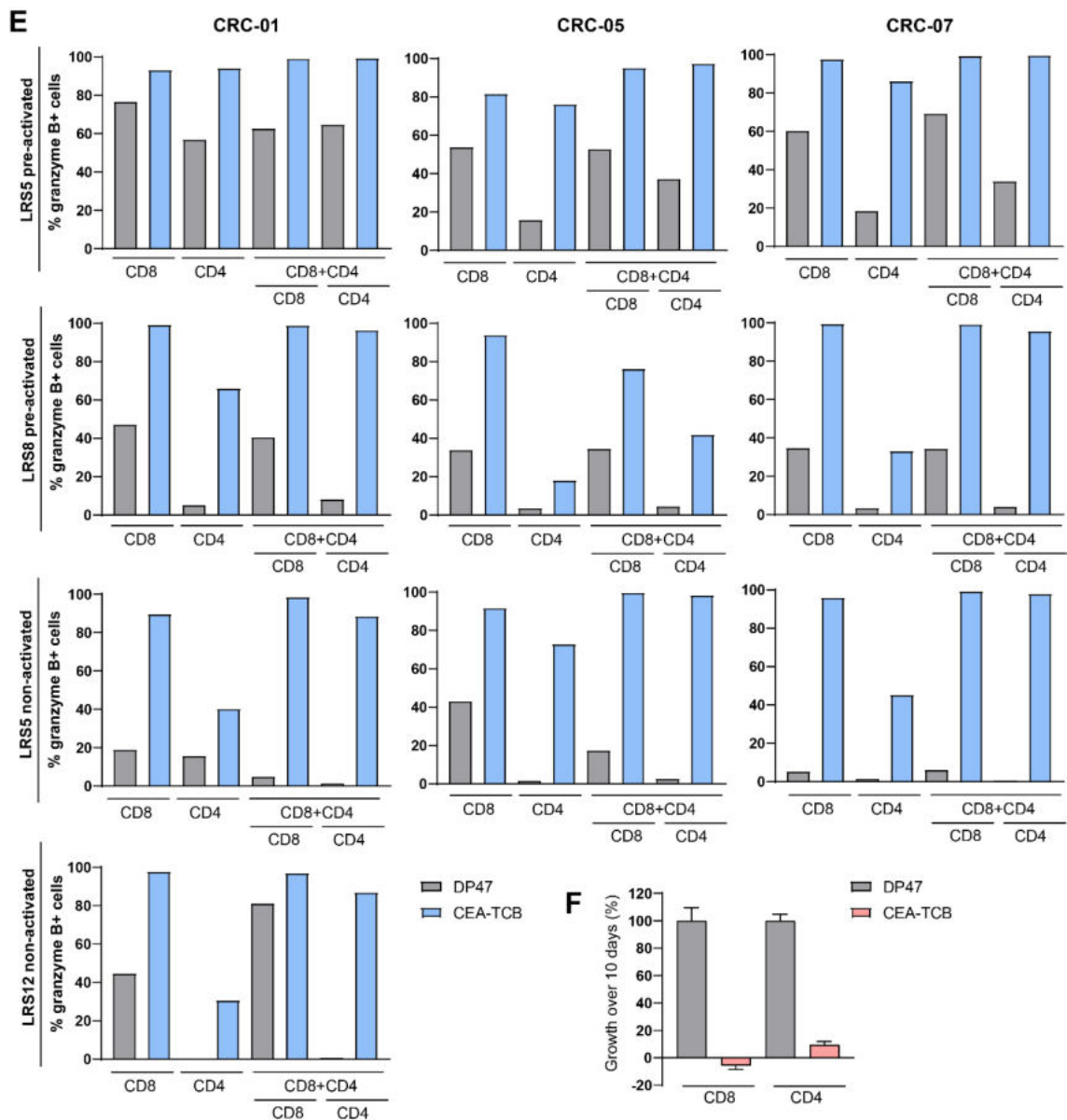


Figure 4.9 Granzyme B expression in CD8 and CD4 T cells treated with CEA-TCB. (A) Representative FACS plots of the gating strategy used to identify live CD8 and CD4 T cells harvested from 2D killing assay. (B) Histograms showing granzyme B expression assessed by flow cytometry in pre-activated CD8 and CD4 T-cells from two donors (LRS5 and LRS8) harvested from co-culture with three CEA-high PDOs (CRC-01, CRC-05, CRC-07) and CEA-TCB (20 nM) or untargeted TCB DP47 (20 nM). Mean Fluorescence Intensity (MFI) values are shown. (C) Histograms showing granzyme B expression assessed by flow cytometry in non-activated CD8 and CD4 T-cells from two donors (LRS5 and LRS12) harvested from co-culture with PDOs and CEA-TCB (20 nM) or untargeted TCB (20 nM). Mean Fluorescence Intensity (MFI) values are shown. For LRS12 only CRC-01 was tested. (D) FACS plots of Foxp3 and CD4 expression in CD4 T cells harvested from 2D co-culture assay in (A). (E) Bar graphs showing percentage of granzyme B positive CD8 or CD4 T cells in different treatment conditions. Continued on next page.

(F) Growth quantification of CEA-TCB treated CRC-01 over 10 days relative to untargeted TCB DP47 treated PDOs in the presence of non-activated CD8 or CD4 T cells from LRS12 donor. Error bars represent one standard deviation calculated from three replicates.

in pre-activated experiments. When CD4 T cells were used alone, the majority of granzyme expressing cells showed a modest granzyme expression with a small proportion of the population expressing very high levels. However, when they were combined with CD8 T, expression increased from low to moderate in most cells. LRS12 non-activated CD4 T cells expressed the highest amount of granzyme B compared with all other donors used in these experiments so I tested whether their killing ability would be better than that of LRS5 non-activated CD4s which showed a relatively poor growth reduction (37% growth reduction averaged across all PDOs) (Figure 4.8B). Indeed LRS12 CD4 non-activated T cells showed a much more dramatic growth reduction of 91% which was almost equivalent to the killing achieved by their CD8 counterparts which achieved 106% growth reduction (Figure 4.9F). Through these experiments I have demonstrated that CEA-TCB induces granzyme B expression in both pre-activated and non-activated CD4 T cells thus showing that this bispecific antibody is capable of inducing cytotoxic phenotype in CD4 T cells. But as expected, CD8 T cells, which are considered to represent the main cytotoxic lymphocyte in anti-tumour immune responses and have also shown, expressed much higher granzyme B levels potentially explaining the superior tumour cell killing capacity observed in my model. None of the CD4 T cells were converted into the Treg phenotype as assessed by their lack of Foxp3 expression which was expected as induced Tregs require a specific cytokine milieu including TGF β which is either not expressed or expressed at very low levels in our PDOs as assessed by RNA sequencing (Figure 4.9D). Additionally I have demonstrated that co-culture of CD8 and CD4 T cells together enhances their granzyme B expression in response to CEA-TCB treatment which could mean that combined presence and activation of CD8 and CD4 T cells would lead to better responses in patients.

4.4.2 Role of Fas/FasL axis in CD8 and CD4 T cell mediated PDO growth control

The second mechanism employed by T cells to kill their target cells relies on the interaction of the Fas ligand (FasL) that is upregulated during T cell activation with the apoptosis-inducing Fas receptor on the target cell. FasL drives Fas clustering and binding of Fas to FADD which recruits pro-caspase 8 and 10 followed by processing of the pro-enzyme into active forms. These active caspases then propagate the death signal through proteolysis of effector caspases such as caspase 3, 6 and 7 ultimately leading to eventual cell death (Russell & Ley, 2002; Yamada et al., 2017). Although the FasL/Fas pathway has been mostly studied in the context of immunological tolerance and autoimmune diseases that arise as a result of dysregulation of this pathway, it has been shown to play a role in CD8 and also CD4 mediated cytotoxicity (Hanabuchi et al., 1994; Ju et al., 1994; Kägi et al., 1996; Lowin et al., 1994; Stalder et al., 1994). Several studies have shown the contribution of this pathway to an anti-tumour immune response (Afshar-Sterle et al., 2014; Morales-Kastresana et al., 2013; Seki et al., 2002). The importance of the Fas/FasL pathway in immunotherapy has been highlighted by multiple studies investigating activity and resistance to CAR-T cell therapy which showed that impaired death receptor signalling in tumour cells causes reduced CAR-T cell cytotoxicity and that this pathway can mediate off-target “bystander” killing of antigen-negative tumour cells (Singh et al., 2020; Upadhyay et al., 2021). Fas expression in tumours has also been shown to be a predictor of survival in response to CAR-T cells therapy with patients expressing high tumoral levels of Fas showing significantly prolonged survival relative to those with lower expression (Upadhyay et al., 2021). However the role of this pathway has not been fully explored in the context of bispecific antibody mediated killing and may depend on the target cells used in the experimental model. In their model of Hodgkin’s lymphoma, Renner and colleagues have shown that while T cells activated by a bispecific antibody expressed FasL and their chosen target cells expressed Fas, this mechanism did not contribute to target cell killing and all of the T cell mediated

cytotoxicity was attributed to the granzyme/perforin pathway (Renner et al., 1997). Contrastingly, an ALL cell line showed resistance to bispecific antibody treatment when Fas was knocked out (Liu et al., 2021). Therefore it was important to evaluate the contribution of this pathway in my model system.

First I measured the level of Fas expression on cell surface of the three CEA-high PDOs; CRC-01 expressed it at the highest level and CRC-07 didn't express it at all. Fas has been shown to be upregulated by IFN γ signalling which I confirmed with CRC-01 (Figure 4.10A). Since I wanted to block FasL signalling in my co-culture model system to see if the tumour cell growth reduction mediated by CEA-TCB treated T cells would be affected, I first needed to confirm that the Fas/FasL axis was functional in PDOs and that the chosen FasL blocking antibody NOK-1 would successfully inhibit FasL/Fas interactions. Previous studies have shown that NOK-1 effectively blocks for FasL-induced apoptosis in a 1-10 μ g/ml concentration range (Bertram et al., 2006; Hombach et al., 2006; Jodo, Hohlbaum, et al., 2000; Jodo, Strehlow, et al., 2000; Kim et al., 2008; Lin et al., 2007; Nobuhiko Kayagaki et al., 1995; Todaro et al., 2006). Soluble FasL (sFasL) has been shown to induce cytotoxicity in Jurkat cells, which are known to have a high Fas expression on the cell surface and therefore are particularly sensitive to FasL, with an ED50 of 10ng/ml. When CRC-01 was treated with 100 and 500ng/mL of sFasL no apoptosis was detected as assessed by Apo-one assay that measures apoptosis by measuring caspase 3 and 7 activity. However, after treatment with IFN γ both doses of sFasL induced apoptosis in a dose dependant fashion comparable to the apoptosis induced by staurosporine used as an apoptosis control (Figure 4.10B). Addition of NOK-1 prevented induction of apoptosis with the higher dose 10 μ g/mL showing a slightly better effect thus confirming the blocking functionality of this FasL binding antibody. NOK-1 was added to the culture alongside either the control bispecific antibody or CEA-TCB and either CD8 or CD4 T cells. There was no difference in tumour growth between control and NOK-1 treated conditions thus indicating that in this model system the

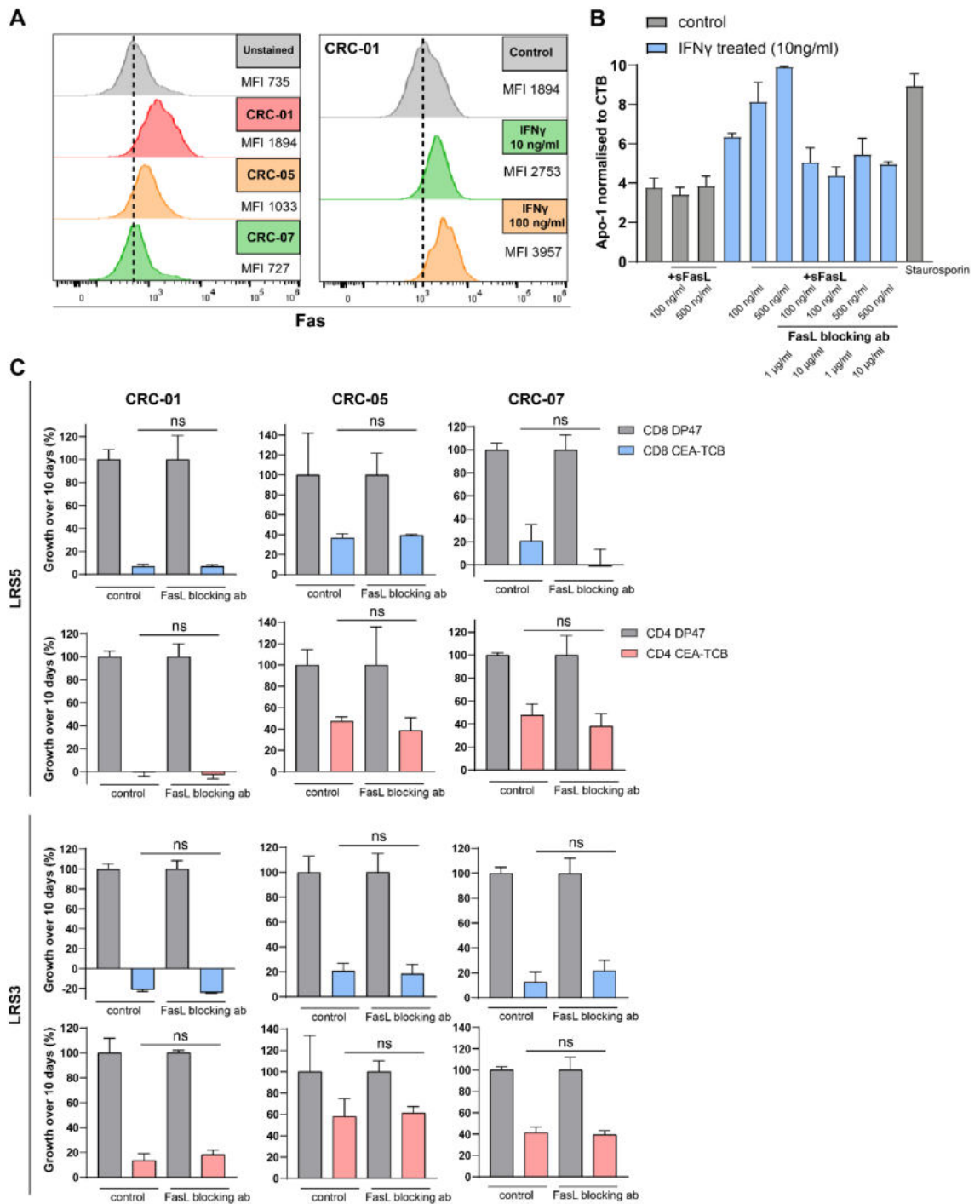


Figure 4.10 Role of Fas/FasL pathway in CEA-TCB mediated killing of PDOs. (A) Flow cytometry histograms showing Fas expression in three CEA-high PDOs (CRC-01, CRC-05, CRC-07) as compared to an unstained control (left). The histogram overlays on the right show Fas expression in CRC-01 with IFN γ treatment (10ng/mL and 100ng/mL). Each experiment performed once. **(B)** Bar graphs showing Apo-one fluorescence signal normalised to CellTitre Blue signal showing apoptosis normalised to cell number in CRC-01 in response to sFasL treatment (100ng/mL and 500ng/mL) and staurosporine (1 μ M). Blue bars show CRC-01 pre-treated with IFN γ (10ng/mL). FasL blocking antibody NOK-1 was used at two concentrations (1 μ g/mL and 10 μ g/mL). Error bars represent standard deviation calculated from three replicates. **(C)** Continued on next page.

(C) Bar graphs showing growth quantification of CEA-TCB treated PDOs over 10 days relative to untargeted TCB treated PDOs in the presence or absence of a FasL blocking antibody NOK1 (10µg/mL) and pre-activated CD8 or CD4 T cells from 2 donors (LRS5 and LRS3). Error bars represent one standard deviation calculated from three replicates. Statistical analysis was performed using an unpaired t-test. Ns=not significant.

Fas/FasL pathway does not contribute to CD8 and CD4 mediated cytotoxicity (Figure 4.10C).

4.4.3 Role of IFN γ in CD8 and CD4 T cell mediated PDO growth control

IFN γ orchestrates a big range of immune responses such as CD4 T cell differentiation to Th1 lineage, upregulation of MHC class I expression, direct antiviral effects, potent chemoattractant directing immune cells to sites of inflammation through induction of CXCL9/CXCL10 expression, B cell isotype switching, and regulation of local leukocyte-endothelial interactions (Boehm et al., 1997; Schroder et al., 2004). However, the IFN γ receptor is expressed ubiquitously on all nucleated cells thus exerting its effect on a wide range of cells including those not part of the immune system. Although IFN γ has many indirect antitumour effects such as stimulation of M1 macrophage polarisation, inhibition of angiogenesis, increased efficacy of immune checkpoint blockade by PD-L1 induction, and enhanced cytotoxic T cell response, IFN γ also has a direct effect on tumour cell growth (Jorgovanovic et al., 2020). IFN γ has been shown to inhibit tumour cell growth and induce apoptosis via activation of caspase 3 and 7 by the classical JAK-STAT pathway (Chin et al., 1997a; Hao & Tang, 2018; Ni et al., 2013; Rubin et al., 1983; Song et al., 2019).

In order to test PDO sensitivity to IFN γ , all 8 PDOs were treated with three different doses of IFN γ (1ng/mL, 10ng/mL, and 100ng/mL) for 7 days and growth was measured by Cell Titre Blue assay. Three PDOs CRC-01, CRC-05, and CRC-04 showed high sensitivity to IFN γ showing significantly inhibited tumour growth even at the lowest IFN γ concentration (Figure 4.11A). These results are further supported by the increase

in caspase 3 and 7 signalling seen in CRC-01 treated with 10ng/ml of IFN γ (Figure 4.10B). Contrastingly, CRC-07 showed either no or very minor growth inhibition in response to IFN γ treatment (Figure 4.11A). An IFN γ blocking antibody was added to the PDO culture treated with various concentrations of IFN γ and growth was assessed on day 7 by CTB assay. In IFN γ neutralising assays this IFN γ blocking antibody has been used in a range of concentrations from 50ng/ml to 5 μ g/ml (Chang et al., 2009, 2010; Ebert & Mehta, 2006; Filén et al., 2010; Ranzani et al., 2015; Schilbach et al., 2020; Szabo et al., 2019; Wolk et al., 2002; Yang et al., 2018, 2021; Zhang et al., 2018). For my experiments I decided to use the highest dose in that range (5 μ g/ml). The blocking antibody was able to rescue the growth of all three IFN γ sensitive PDOs treated with 1ng/mL IFN γ , however, at higher concentrations CRC-01 and CRC-04 still exhibited

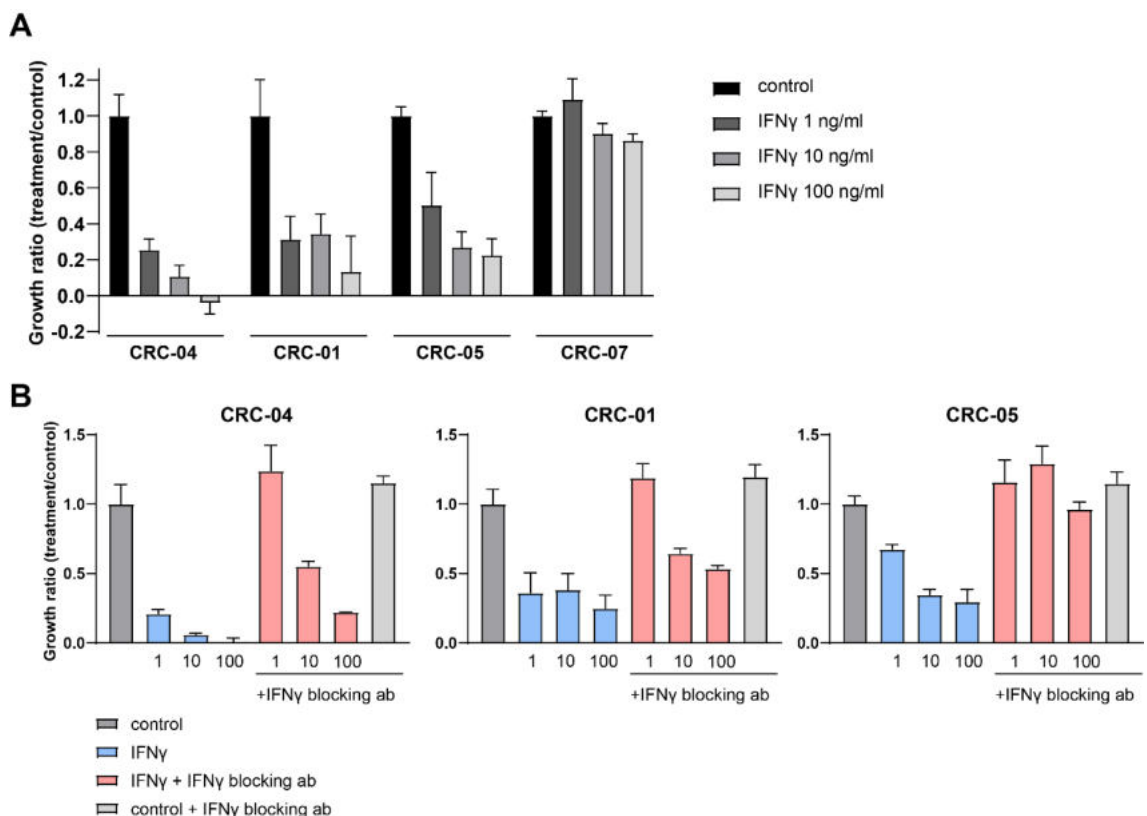


Figure 4.11 Sensitivity of PDOs to IFN γ (A) Bar graph showing growth of IFN γ treated PDOs compared to control. Three different doses of IFN γ were used (1ng/mL, 10ng/mL, 100ng/mL) and the assay was performed for 7 days. (B) Three IFN γ sensitive PDOs were treated with IFN γ (1ng/mL, 10ng/mL, and 100ng/mL) +/- an IFN γ blocking antibody (5 μ g/mL) for 7 days. Growth was assessed as a ratio compared to untreated control. Error bars represent one standard deviation calculated from six replicates.

reduced growth compared to control. CRC-04 appeared to be the most sensitive to IFN γ showing strong growth reduction at 10ng/mL and 100ng/mL IFN γ treatment even in the presence of the IFN γ blocking antibody. In the same conditions, CRC-01 showed less than 50% growth inhibition and CRC-05 no IFN γ induced growth inhibition in the presence of the IFN γ blocking antibody making it the least IFN γ sensitive PDO out of the three. Next the IFN γ blocking antibody was added to the co-culture assay alongside DP47 or CEA-TCB treatment in order to assess the contribution of IFN γ to the anti-tumour response. Unfortunately CRC-04 showed alloreactivity and therefore was excluded from further analysis so only the data from the three CEA-high PDOs was analysed and included. IFN γ blocking strongly reduced CD4 efficacy, but had a more modest effect on CD8 mediated killing (Figure 4.12). The two IFN γ sensitive PDOs CRC-01 and CRC-05 showed an average of 36% growth reduction difference between control and IFN γ blocking antibody treated condition with donor LRS5 CD8 T cells (36.4% and 35.5% respectively) and 27% with donor LRS3 (34.6% and 20.1% respectively). Whereas when treated with CD4 T cells and the IFN γ blocking antibody the growth reduction difference compared to control was 54% (60.6% for CRC-01 and 48.2% for CRC-05) for donor LRS5 and 55% for donor LRS3 (42.9% and 67.8% respectively). With both donors CRC-05 showed complete abrogation of killing with CD4 T cells in the presence of the IFN γ blocking antibody while CRC-01 still showed some CD4 mediated tumour growth control. This may be explained by two factors: 1) CRC-05 is less sensitive to IFN γ than CRC-01 thus the IFN γ blocking antibody was able to fully rescue its tumour cell growth and only partially for CRC-01 and 2) CRC-05 induced less granzyme expression in CD4 than CRC-01. IFN γ blocking antibody did not significantly alter killing efficacy of CD8 and CD4 T cells co-cultured with CRC-07 which aligns with the IFN γ insensitivity shown earlier (Figure 4.11A). IFN γ has been reported to affect cytolytic ability of T cells independently of direct IFN γ mediated cytotoxicity (Bhat et al., 2017; Mckisic et al., 1993; Ravichandran et al., 2019). It is possible that by blocking IFN γ , I

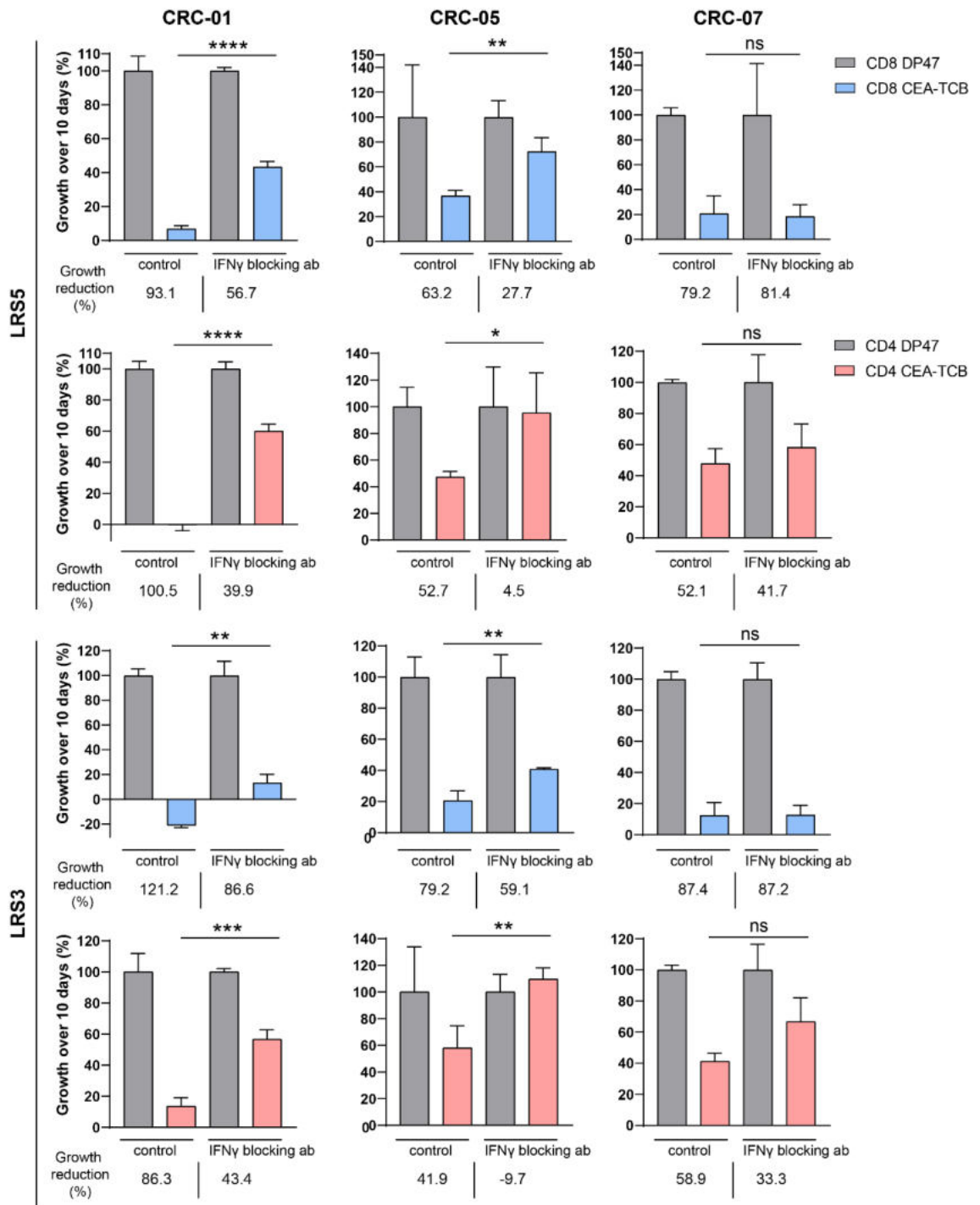


Figure 4.12 IFN γ blocking in PDO-T cell co-culture assay. Bar graphs showing growth quantification of CEA-TCB treated PDOs over 10 days relative to untargeted TCB treated PDOs in the presence or absence of an IFN γ blocking antibody (5 μ g/mL). Assays were performed with pre-activated CD8 and CD4 T cells from two donors (LRS5 and LRS3). Error bars represent one standard deviation calculated from three replicates. Statistical analysis was performed using an unpaired t-test. For all growth analysis P values are as follows: > 0.05 is ns, < 0.05 is *, < 0.01 is **, < 0.001 is ***, < 0.0001 is **** and ns = not significant.

also decreased granzyme B production which resulted in less tumour cell killing. This could be investigated further by measuring the proportion of granzyme B expressing T cells and the level of granzyme expression in those cells after treatment with CEA-TCB and IFN γ blocking antibody.

4.5 Discussion

Immunotherapy is rapidly evolving as one of the major options for cancer treatment. However, relevant pre-clinical models to study immune-tumour interactions and understand determinants of sensitivity and resistance are still lacking. Due to a full intact immune system a lot of pre-clinical immunological research has been performed in mouse models. And although these models have generated a plethora of important knowledge, the insights derived from mouse modeling are not always translatable to patients and therefore often fail to predict outcomes in clinical trials due to inherent differences in between human and mouse immune systems (Mestas & Hughes, 2004b). Additionally mouse models are slow, expensive, not available for all tumor types, or are incompatible with human-specific reagents. Immune responses are highly complex and in mouse models it is often difficult to assess the contribution of individual factors or cell types. Xenograft models improve the human relevance factor, but they are only suitable for immunotherapy studies with the transplantation of human hematopoietic stem cells (HSC) in order to establish an intact human immune system since xenografts require hosts to be immunocompromised in order to avoid rejection of human tumour tissue by the mouse immune system. These procedures are costly, technically challenging, and also require matched HSC cells from cancer patient which are difficult to obtain. Cell lines are the most commonly used model in cancer research due to high throughput, cheap cost, handling ease, and direct comparability. However cell lines fail to capture tumour heterogeneity which plays an important role in response and resistance to therapeutic agents. In the past decade the technology that allows long-term propagation of tumour cells from patient tumours as patient derived organoids (PDOs) has

transformed in vitro cancer studies. Sato et al established a methodology that allows PDO generation from CRC biopsies (Sato et al., 2011). PDO models have been suggested to better recapitulate patient tumours by maintaining heterogeneity and molecular characteristics that have been lost in cell lines. Additionally these models have the advantage of having patient treatment history and disease stage information. However, in vitro immunotherapy studies are often limited by the requirement of autologous cells which are frequently difficult to obtain. Fortunately bispecific antibody immunotherapy bypasses the need for autologous cells due to its ability to bind and activate any T cell irrespective of neoantigen presentation and TCR specificity.

While CEA-TCB showed high efficacy with CRC cell lines, clinical trial data showed a response rate of 11% (4/36) as monotherapy and 50% (5/10) in combination with anti-PD-L1 in patients pre-selected based on CEA expression (Tabernero et al., 2017). Therefore there is a need to evaluate this therapeutic agent in a more clinically relevant in vitro model. To address this need my lab has developed a 2D co-culture comprising of PDOs established from multi-drug resistant metastatic colorectal cancers and adapted to 2D growth and allogeneic T cells isolated from healthy donor PBMCs. PDO cells were labelled with nuclear GFP via lentiviral transfection to allow for confluence tracking by microscopic imaging which served as a readout for tumour cell growth. One of the caveats of this in vitro assay is alloreactivity due to the use to allogeneic rather than autologous T cells. However, this was addressed by always including a control condition with PDOs alone and PDOs in combination with T cells and the control bispecific antibody DP47. If any tumour killing activity was detected in the control condition this experiment was discarded and this PBMC donor was not used in further experiments. Another caveat of this system is the inherent donor variability that arises with the use of primary cells. PBMCs were isolated from Leukocyte Reduction System (LRS) cones which were provided by the NHS Blood and Transplant service. The information regarding collection time was not provided thus making it a possibility

that there was a 1-2 day time gap between sample collection and processing possibly explaining the differences in viability and cytotoxic capacity between donors. In order to address this issue all experiments were performed with multiple donors. Performing 2D co-culture experiments with seven PDOs showed a correlation between CEA expression and CEA-TCB mediated tumour growth reduction. CEA-high lines showed 80-100% growth reduction and CEA-mixed lines CRC-06 and CRC-08 that showed a highly consistent expression of CEA in the 50% range (Chapter 3) showed an average of 52% growth reduction.

My lab has performed Gene Set Enrichment Analysis (GSEA) on sorted CEA-high and CEA-low cells from CEA-mixed PDOs and found that the Wnt/ β -catenin pathway is negatively correlated with CEA expression. This CEA-Wnt axis is mirrored in colonic crypts where cells at the bottom of the crypt express low levels of CEA but high Wnt signalling and cells at the top of the crypt express high levels of CEA and low Wnt signalling thus potentially highlighting the similarity of CEA-low cells to intestinal stem cells at the crypt bottom. Based on these findings I hypothesized that an inhibitor of tankyrase which destabilises the β -catenin destruction complex and thus promotes Wnt/ β -catenin signalling would increase CEA expression. Tankyrase inhibitor Compound 21 (C21) did increase the proportion of CEA expressing cells in three CEA-mixed PDOs and this increase was regulated at the gene expression level. In order to test whether this increase in CEA expression would translate to improved sensitivity to CEA-TCB I either pre-treated or continuously treated PDO cells with C21 in combination with CEA-TCB treatment. Co-treatment resulted in greater growth reduction in the two CEA-mixed PDOs tested thus providing proof of concept that CEA can be pharmacologically enhanced leading to greater sensitivity to CEA-TCB suggesting opportunities for combination therapies. However, the full potential of Wnt targeting agents may be limited by intestinal toxicity associated with inhibition of Wnt/ β -catenin signalling due to the essential role of Wnt signalling in the healthy gut tissues (Kahn, 2014).

In this chapter I also examined the contribution of both CD3 bearing T cell subsets CD8 and CD4 to a CEA-TCB mediated immune response using three CEA-high PDOs that showed good sensitivity to CEA-TCB treatment (CRC-01, CRC-05, and CRC-07). While CD4 T cells did achieve tumour growth reduction, CD8 T cells performed significantly better with three different donors and in all three PDOs. When CD8 T cells that have not been pre-activated in vitro prior to the addition to the assay were used they killed tumour cells with the same efficacy as pre-activated ones and even overtook them when the assay was extended from 7 to 10 days. This may be explained by the longer time needed by non-activated T cells to activate and produce cytokines and lytic granules. However, PDOs treated with non-activated CD4 T cells showed much poorer growth reduction than when treated with pre-activated CD4 T cells. IL-2 has been shown both in vitro and in vivo to be vital to the induction of the granzyme secreting cytotoxic CD4 phenotype and its sequestration by Tregs restricted their differentiation (Brown, 2010; Śledzińska et al., 2020). When T cells were pre-activated with anti-CD3/CD28 beads they were also treated with exogenous IL2 (30U/ml) which may explain why pre-activated CD4 T cells performed better than non-activated CD4 T cells. Perhaps the non-activated CD4 T cells do not produce enough IL-2 upon activation with CEA-TCB for autocrine and paracrine signalling that would differentiate them into the cytotoxic phenotype.

Next I evaluated the contribution of the three main T cell effector mechanisms – granzyme/perforin lytic granule pathway, Fas/FasL pathway, and IFN γ secretion – to the CEA-TCB mediated response in both CD8 and CD4 T cells. CEA-TCB induced much higher expression of granzyme B in CD8 T cells compared to CD4 T cells, but nonetheless some CD4 T cells acquired the cytotoxic phenotype and expressed granzyme B. However, granzyme B expression was dramatically enhanced when the two T cell subsets were added to the co-culture together. More CD4 T cells expressed granzyme (90-100%) and granzyme expression on a per cell basis also increased. CRC-

05 induced the lowest expression of granzyme in both CD8 and CD4 T cells which correlates with the killing assay data that showed that CRC-05 showed less growth reduction than CRC-01 and CRC-07 with both CD8 and CD4 (except for one donor where CRC-05 showed a slightly better response than CRC-07 with CD4s). In contrast, CD4 T cells showed a much greater reliance on IFN γ mediated cytotoxicity. When co-cultures were treated with an IFN γ blocking antibody PDOs treated with CD8 T cells showed an average of 32% increase in growth compared to CEA-TCB treatment alone, whereas those treated with CD4 T cells showed a greater difference in growth reduction averaging 55%. However, the IFN γ insensitive PDO CRC-07 showed no significant difference in both CD8 and CD4 mediated tumour growth control. Tumours frequently acquire resistance to checkpoint inhibitors through inactivation of the IFN γ pathway, but it appears that IFN γ mediated cytotoxicity is not the main mechanism employed by CD8 T cells activated with CEA-TCB therefore this therapeutic agent can still have efficacy in tumours with dysfunctional IFN γ signalling. But tumour responsiveness to IFN γ sensitises them to killing by T cells activated with CEA-TCB therefore making IFN γ sensitivity a predictor of response to this therapy. Additionally, patients with tumours expressing heterogenous levels of CEA and showing sensitivity to IFN γ may benefit from bystander killing by T cells that have been activated by the target antigen expressing cells and are secreting IFN γ , particularly when effector to target ratios are low. This could be further investigated in my model system because the methodology for CEA expression and IFN γ sensitivity assessment have been established. Blockade of Fas-L/Fas interaction with a monoclonal antibody had no impact on the efficacy of CEA-TCB treatment in both CD8 and CD4 T cells suggesting that it is not a cytotoxicity mechanism used by CEA-TCB activated T cells and that they mostly rely on granzyme expression and IFN γ secretion. However, there are other pathways whose contribution to a CEA-TCB mediated immune response need to be investigated such as TNF α and TRAIL. It is feasible to examine both of these factors using my co-culture assay methodology.

Overall I have demonstrated that an in vitro co-culture killing assay comprised of PDOs and allogeneic T cells can be a novel tool to investigate efficacy and determinants of response to CEA-TCB therapy. I extended my analysis beyond CD8 T cells which have been the primary focus of immunotherapy due to their role as the main cytotoxic immune cell subset, and have shown that CD4 T cells can also contribute to CEA-TCB mediated anti-tumour immune response. CEA-TCB proved capable of differentiating CD4 T cells into the granzyme producing cytotoxic cells which was particularly enhanced when they were co-cultured together with CD8s. Since CEA-TCB binds all CD3 bearing T cells, in patients it is likely to recruit and activate both CD8 and CD4 T cells thus resulting in a better response than if only CD8 T cells were targeted. This model could be used to further dissect individual steps of a bispecific-mediated immune response including more detailed studies of the effector mechanisms employed by for example blocking the granzyme/perforin pathway.

Chapter 5: Investigating effect of microenvironmental factors commonly found in CRC on CEA-TCB activity

5.1 Introduction

In the past decade, immunotherapy with monoclonal antibodies that block the immune checkpoint molecules CTLA-4 or PD-L1/PD-1 has proven to be an effective therapeutic approach in several cancer types. However, only a subset of patients show durable responses while the majority experience minimal or no clinical benefit. For example, a meta-analysis of the efficacy of PD-1 and PD-L1 inhibitors in clinical trials has found that the mean objective response rate to PD-L1/PD-1 inhibitors was on average 20% across multiple different cancer types (Chen et al., 2021). Cancer immune landscapes have been categorised into four main phenotypes (Galon & Bruni, 2019). The first phenotype is the inflamed or immunologically “hot” tumours which are highly infiltrated by cytotoxic T cells, but also by other immune cell subtypes such as Tregs, tumour associated macrophages, and MDSCs. These tumours also exhibit immune checkpoint upregulation expressed by tumour cells and other immune cells present in the microenvironment (Fehrenbacher et al., 2016; Herbst et al., 2014; Powles et al., 2014; Taube et al., 2014). As a result, clinical responses to anti-PD-L1/PD-1 therapy occur most often in patients with T cell inflamed tumours (Herbst et al., 2014; Garon et al., 2015; Rosenberg et al., 2016). The immune-desert phenotype occurs as a result of immunological ignorance likely due to low neoantigen expression and a subsequent failure by the immune system to recognise the tumour and mount an immune response. This phenotype is characterised by lack of T cell infiltrates and therefore such tumours rarely respond to anti-PD-L1/PD-1 therapy (Herbst et al., 2014). The third phenotype is the immune-excluded which is characterised by an abundant presence of immune cells, however they are unable to penetrate into the tumour core and are trapped in the tumour margin or stroma. T cell infiltration into the tumour bed is therefore the rate limiting step in the

cancer-immunity cycle for this phenotype. Tumours employ different mechanisms to escape immune surveillance by reprogramming the TME to an immunosuppressive and tumour promoting phenotype. It has been reported that despite the presence of antigen specific cytotoxic lymphocytes and no antigen loss tumour progression occurs thus supporting the notion that there are mechanisms hindering the anti-tumour immune response (Rosenberg et al., 2005). Many different cytokines, signalling pathways, and immune cell subtypes have been implicated in inhibiting cytotoxic T cell activity leading to immune escape and tumour progression. Therefore the fourth phenotype identified is “immunosuppressed” and is characterised by poor but not absent infiltration by T cells, presence of soluble inhibitory mediators (TGF β , VEGF, IL-10), and presence of immune and stromal suppressive cells (MDSCs, Tregs, CAFs). The finding that the type, density, and location of immune cells within tumours can predict survival in CRC better than the classical TNM system led to the development of the Immunoscore which is a robust and standardised scoring system based on the quantification of CD3 and CD8 expressing lymphocytes in the tumour centre and the invasive margin of CRCs (Angell & Galon, 2013; Galon et al., 2006, 2013). The Immunoscore ranges from 0 (I0, where densities of both cell types are low in both regions) to 4 (I4, which has high densities of both cell populations in both regions). The four immune phenotypes correspond to Immunoscores with the inflamed tumours having a high Immunoscore, the immune-desert tumours have a low Immunoscore, while “altered” tumours which have been further subdivided into immune-excluded and immunosuppressed have intermediate Immunoscores (Galon & Bruni, 2019). An international validation study of the consensus Immunoscore for the classification of colon cancer found that 22% of patients had a low Immunoscore, 51% of patients had an intermediate Immunoscore, and 27% patients had a high Immunoscore (Pagès et al., 2018). A high Immunoscore was observed in 21% of patients with MSS tumours indicating that majority of MSS tumours have intermediate or low Immunoscore (Pagès et al., 2018). Combination treatment with CEA-TCB and atezolizumab (anti-PD-L1) increased the response rate in patients with mCRC from 11%

to 50% suggesting that one mechanism of resistance to CEA-TCB is upregulation of PD-L1 (Tabernero et al., 2017). However, even with the combination therapy approach 50% of patients did not show a response indicating that there are other factors suppressing the anti-tumour response mediated by CEA-TCB. Thus there is a need to investigate tumour microenvironment factors that confer resistance to CEA-TCB. The advantage of my model system is that it allows for careful dissection of resistance mechanisms through evaluation of the effect of individual microenvironmental factors on bispecific antibody activity. Using three CEA-high expressing PDOs with good sensitivity to CEA-TCB I investigated the role of the most frequently cited immunosuppressive factors found in the TME in resistance to CEA-TCB therapy.

5.2 Investigating effect of IL-10 on CEA-TCB activity using PDO-T cell co-culture model

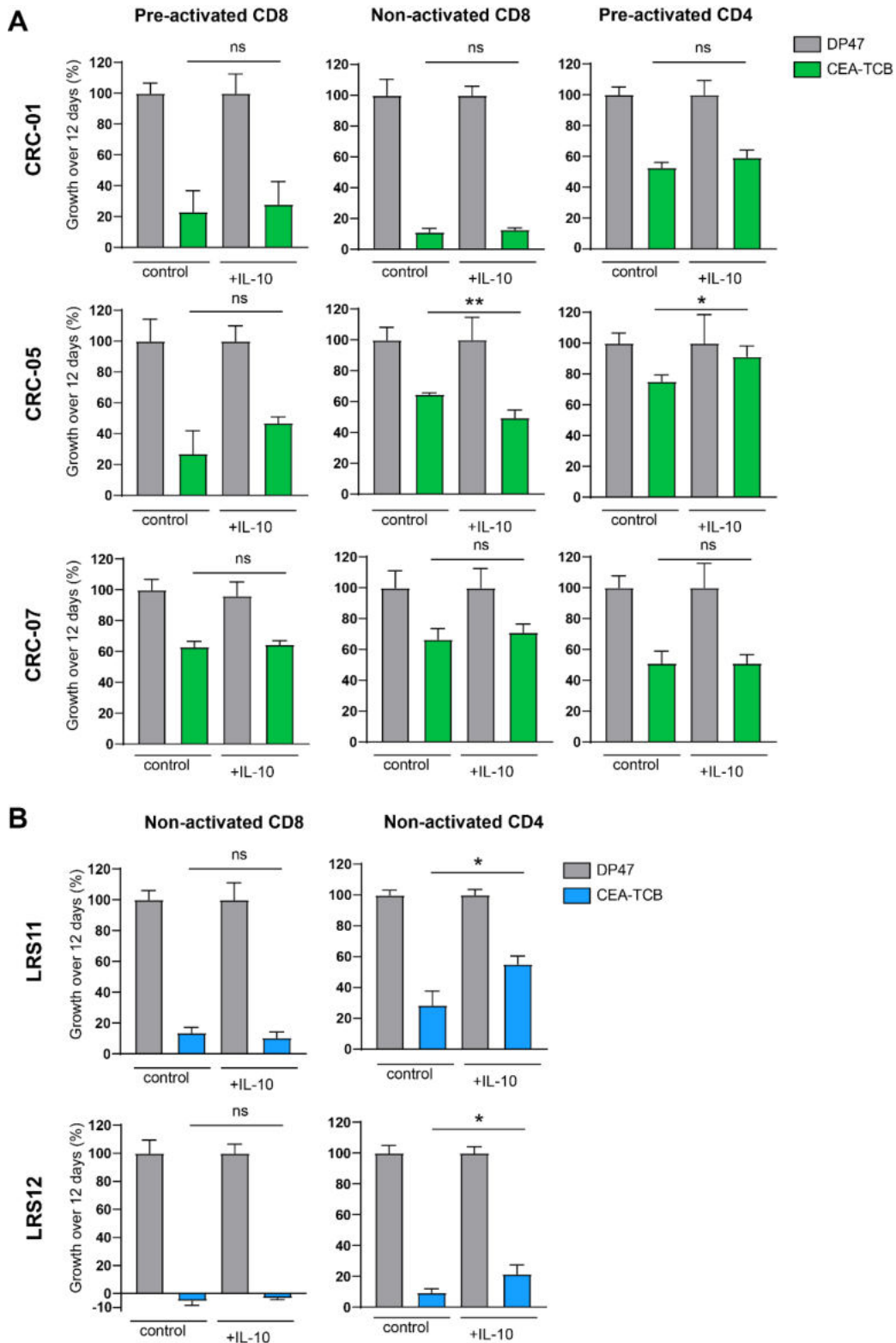
Interleukin-10 (IL-10) is a multifunctional cytokine with diverse effects on many immune cell types. Initially IL-10 was considered to be an immunosuppressive cytokine. In monocytes and macrophages IL-10 has been shown to suppress production of inflammatory cytokines such as IL-1, IL-6, IL-8, and TNF α , inhibit co-stimulatory activity by decreasing B7 expression, and reduce antigen-presenting capacity by downregulating class II MHC (Armstrong et al., 1996; Bogdan et al., 1991; Ding et al., 1993; Thomassen et al., 1996; Waal Malefyt et al., 1991). While indirect suppressive effects of IL-10 on T cell activity mediated by macrophages and dendritic cells have been well characterised, there have been fewer studies investigating direct effects of IL-10 on T cells and they showed controversial results. Early studies suggested that IL-10 was a product of Th2 cells that decreases IL-2 and IFN γ production in Th1 cells (Fiorentino et al., 1991). Due to the polyfunctionality of this cytokine its effects have been shown to be context specific. For example, it has been reported to induce anergic states in CD8 and CD4 T cells when added concomitantly with antigen in the presence of APCs, whereas when cultured with CD8 T cells alone it promoted proliferation and increased cytotoxicity

but only in combination with IL-2 (Groux et al., 1996, 1998; Santin et al., 2000; Steinbrink et al., 2002). There have been multiple studies showing conflicting results regarding effect of IL-10 on proliferation and cytotoxicity of CD8 T cells in vitro most likely explained by the different activation and culture conditions (Chen & Zlotnik, 1991; Rowbottom et al., 1999; Taga et al., 1993). For example, IL-10 blocked PHA induced activation and proliferation of CD8 T cells but in contrast IL-10 enhanced IL-2 induced proliferation and cytotoxicity (Ebert, 2001). Another direct effect demonstrated to be mediated by IL-10 on CD8 T cells is reduction to antigen sensitivity (Smith et al., 2018). However, the role of IL-10 in cancer and particularly in anti-tumour immune responses remains unclear because of its stimulatory and inhibitory functions. Mice deficient in IL-10 developed spontaneous tumours and inflammatory bowel disease (Berg et al., 1996). IL-10 serum levels increase overtime in CRC progression and high levels correlates with more advanced stage, worse survival, and higher recurrence rate (Li et al., 2019; Stanilov et al., 2010; Zhao et al., 2015). TME contains high amounts of IL-10 because many different cell types are capable of secreting it including tumour cells, macrophages, Tregs, and CD8/CD4 T cells. Some mouse models of various tumour types have challenged the previously assumed immunosuppressive function of IL-10 and have demonstrated that IL-10 actually enhances anti-tumour immune responses by eliciting strong cytotoxic lymphocyte activity (Berman et al., 1996; Emmerich et al., 2012; Giovarelli et al., 1995; Mumm et al., 2011). Treatment of cancer patients with PEGylated IL-10 (Pegilodecakin) induced systemic and intratumoral CD8⁺ T cell proliferation and activation marked by elevation of interferon- γ and Granzyme B and upregulation of immune checkpoints (Naing et al., 2018). Contrastingly some studies have reported opposite effects and showed that blockade of IL-10 inhibited tumour growth, potentially through regulation of dendritic cell and MDSC compartments (Rossowska et al., 2015, 2018). Using organotypic slice cultures from human colorectal cancer liver metastasis Sullivan and colleagues demonstrated that IL-10 blockade dramatically enhanced anti-tumour function of both endogenous T cells and CEA targeting CAR-T cells (Sullivan et al., 2019;

Sullivan et al., 2023). Due to the controversial role of IL-10 in anti-tumour immune responses and modulation of immunotherapy it was necessary to evaluate the effect of IL-10 on CEA-TCB activity mediated by CD8 and CD4 T cells.

Santin and colleagues used 1-20ng/mL of IL-10 in their studies of IL-10 effect on proliferation and cytotoxicity of CD8 T cells and observed differences in both with concentrations as low as 1 or 5ng/mL (Santin et al., 2000). In my experiment I decided to go with the higher concentration and pre-treated CD8 and CD4 T cells with 20ng/mL of IL-10 for 72 hours prior to adding them to the co-culture killing assay. After the pre-treatment, the T cells were seeded with three of the CEA-high PDOs (CRC-01, CRC-05, and CRC-07) that showed good CEA-TCB sensitivity and the co-culture was treated with DP47 or CEA-TCB in the presence or absence of IL-10. The assay was cultured for 12 days and then the PDO growth was assessed and compared between the different conditions. In CRC-01 and CRC-07 IL-10 had no effect on CEA-TCB activity in both CD8s (pre-activated and non-activated) and CD4s (Figure 5.1A). Only pre-activated CD4 T cells were used as non-activated CD4 T cells showed very poor killing ability from this particular donor. CRC-05 showed mixed results showing a slightly worse tumour growth inhibition with pre-activated CD8 and CD4 T cells, and contrastingly a small enhancement of tumour growth control in non-activated CD8 T cells (Figure 5.1A). When non-activated CD8 and CD4 T cells from two donors were evaluated in a co-culture with CRC-01, IL-10 had no effect of CD8 T cell mediated tumour cell killing while it inhibited CD4 T cell mediated tumour growth control (Figure 5.1B). However, when a higher dose of 100ng/mL employed by Ebert and colleagues when investigating effect of IL-10 on proliferation and cytotoxicity of human intestinal lymphocytes was used, IL-10 appeared to have a stimulatory effect rather than an expected inhibitory one (Ebert, 2001). The pre-activated CD8 T cells from both donors exhibited poor tumour growth reduction reaching only 20.5% and 24.9%, but with IL-10 treatment they achieved a much greater tumour growth reduction of 68% (Figure 5.1C). The IL-10 (100ng/mL) mediated

increased CEA-TCB activity was observed in all T cells: CD8 (pre-activated and non-activated) and CD4 (pre-activated and non-activated). In this CRC PDO co-culture



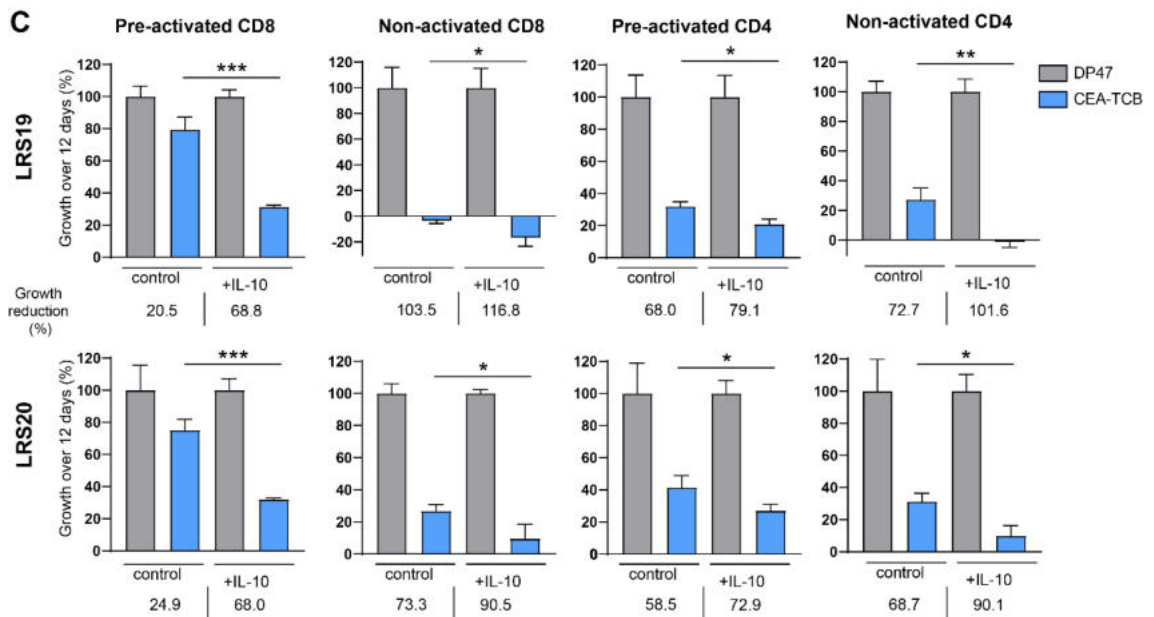


Figure 5.1 Effect of IL-10 on CEA-TCB activity. (A) Growth quantification of CEA-TCB treated PDOs (CRC-01, CRC-05, CRC-07) over 12 days relative to untargeted TCB (DP47) treated PDOs in the presence or absence of IL-10 (20ng/mL). T-cells +/- IL-10 were pre-incubated together for 72 hours prior to the addition of CEA-TCB or DP47. Pre-activated and non-activated CD8 and pre-activated CD4 T cells from the same donor were used. (B) Growth quantification of CEA-TCB treated PDO CRC-01 over 12 days relative to untargeted TCB (DP47) treated PDOs in the presence or absence of IL-10 (20ng/mL). T-cells +/- IL-10 were pre-incubated together for 72 hours prior to the addition of CEA-TCB or DP47. Non-activated CD8 and CD4 T cells from 2 different donors were used. (C) Growth quantification of CEA-TCB treated PDO CRC-01 over 12 days relative to untargeted TCB (DP47) treated PDOs in the presence or absence of IL-10 (100ng/mL). CD8 T-cells +/- IL-10 were pre-incubated together for 72 hours prior to the addition of CEA-TCB or DP47. Pre-activated and non-activated CD8 and CD4 T cells from 2 different donors were used. Error bars represent one standard deviation calculated from three replicates. Statistical analysis was performed using an unpaired t-test. For all growth analysis P values are as follows: > 0.05 is ns, < 0.05 is *, < 0.01 is **, <0.001 is ***, <0.0001 is **** and ns = not significant.

model, IL-10 has no effect on CD8 T cells and an inhibitory effect on non-activated CD4 T cells at a lower concentration (20ng/mL), but it appeared to enhance CEA-TCB efficacy in both CD8 and CD4 at a higher concentration (100ng/mL). However, although the direct effect of IL-10 on cytotoxic lymphocytes is stimulatory in the context of CEA-TCB activity, IL-10 can also regulate T cell activity through indirect means such as PD-L1 upregulation on tumour infiltrating dendritic cells (Lamichhane et al., 2017).

5.3 Investigating effect of VEGF on CEA-TCB activity using PDO-T cell co-culture model

Vascular endothelial growth factor (VEGF) in cancer has been well characterised in the context of angiogenesis, however it has also been shown to be an immunosuppressive modulator of the tumour microenvironment. VEGF has been reported to hinder the differentiation and activation of dendritic cells, increase accumulation of myeloid-derived suppressor cells (MDSCs) and Tregs, and to interfere with extravasation of cytotoxic CD8 T cells into tumours (Gabilovich et al., 1996; Ko et al., 2009; Mimura et al., 2007; Schmittnaegel et al., 2017; Wada et al., 2009). Zhang et al, showed correlation between increased levels of VEGF expression in the tumour and absence of intratumoral T cells in advanced-stage ovarian carcinomas (Zhang et al., 2003). VEGF has also been shown to reduce proliferation and cytotoxic activity of T cells mediated through VEGFR-2 signalling (Gavalas et al., 2012; Ziogas et al., 2012). Additionally VEGF has been demonstrated to drive T cell exhaustion by upregulating immune checkpoint inhibitory receptors such as PD-1, TIM3, LAG3, and CTLA-4 on T cells (Kim et al., 2019; Ozao-Choy et al., 2009; Voron et al., 2015). Several studies evaluating combination treatment with bevacizumab, a monoclonal antibody targeting VEGF, and anti-PD-1/PD-L1 agents have shown synergy between these two therapies and enhancement of anti-PD-1 response (Kim et al., 2019; Meder et al., 2018; Voron et al., 2015). Due to its potent immunosuppressive properties and high expression in CRC TME, VEGF was an important growth factor to examine in the context of CEA-TCB therapy. While its effect on dendritic cells is not relevant in this model as T cell priming is circumvented by direct activation of T cells, its antiproliferative and cytotoxicity hampering effects on T cells made it a strong potential candidate for resistance to CEA-TCB.

Previous studies investigating the effects of VEGF on T cell proliferation and function have used a range of concentrations from 1-500ng/mL. Ziogas and colleagues observed inhibition of proliferation at concentrations as low as 1ng/mL, however a

moderate anti-proliferative effect was seen at 20ng/mL with no further enhancement at the highest concentration of 500ng/mL (Ziogas et al., 2012). A statistically significant reduction of cytotoxic activity was seen at 5ng/mL. Kim and colleagues also observed

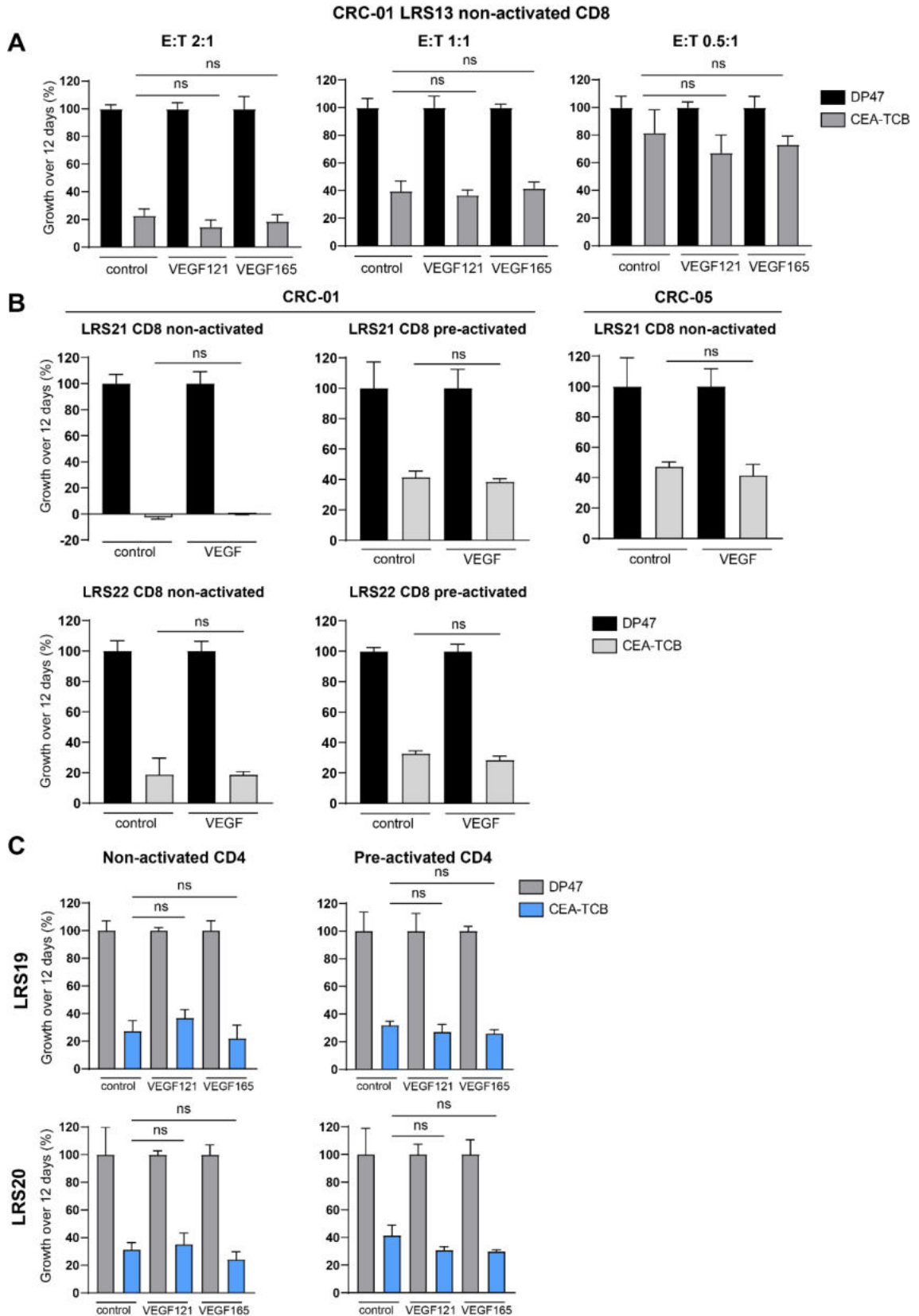


Figure 5.2 Effect of VEGF on CEA-TCB activity. (A) Growth quantification of CEA-TCB treated PDO CRC-01 over 12 days relative to untargeted TCB (DP47) treated PDOs in the presence or absence of VEGF121 or VEGF165 (20ng/mL). CD8 T-cells +/- VEGF were pre-incubated together for 72 hours prior to the addition of CEA-TCB or DP47. Non-activated CD8 T cells were used at three different E:T ratios (2:1, 1:1, 0.5:1). **(B)** Growth quantification of CEA-TCB treated PDOs CRC-01 and CRC-05 over 12 days relative to untargeted TCB (DP47) treated PDOs in the presence or absence of VEGF165 (100ng/mL). Non-activated and pre-activated CD8 T cells from 2 different donors were used at an E:T 2:1. **(C)** Growth quantification of CEA-TCB treated PDO CRC-01 over 12 days relative to untargeted TCB (DP47) treated PDO CRC-01 in the presence or absence of VEGF121 and VEGF165 (100ng/mL). CD4 T-cells +/- VEGF were pre-incubated together for 72 hours prior to the addition of CEA-TCB or DP47. Pre-activated and non-activated CD4 T cells from 2 different donors were used. Error bars represent one standard deviation calculated from three replicates. Statistical analysis was performed using an unpaired t-test. Ns = not significant.

reduced proliferation at 5 and 20ng/mL and a strong reduction in the percent of IFN γ and TNF α positive T cells at 20ng/mL (Kim et al., 2019). VEGF has been reported to mediate its effects on T cells through VEGFR2 receptor which binds multiple different isoforms of VEGF. I tested effects of VEGF121 and VEGF165 in my co-culture assays. As with IL-10, T cells were pre-incubated with 20ng/mL VEGF and then added to co-culture assay which was also treated with VEGF. Initial test with CRC-01 and CD8 T cells showed that neither isoform of VEGF has an impact of CEA-TCB efficacy (Figure 5.2A). For the next experiments I decided to increase the concentration to 100ng/mL as Kim and colleagues showed that increase in exhaustion markers such as PD-1, TIM-3, LAG-3, and TIGIT only strongly increased at 50 and 100ng/mL VEGF treatment. Multiple different donors were tested with both non- and pre-activated CD8 T cells. VEGF did not inhibit T cell mediated tumour growth inhibition of neither CRC-01 or CRC-05 (Figure 5.2B). As CD4 and CD8 T cells have differential biology it was also important to evaluate effect of VEGF on CD4 T cells since they also contribute to CEA-TCB mediated tumour cell growth inhibition. Both VEGF isoforms at a concentration of 100ng/mL were tested on both non-activated and pre-activated CD4 T cells from two different donors, but even at this higher concentration VEGF did not have any effect on CEA-TCB efficacy. Therefore VEGF

does not directly inhibit T cell activity induced by CEA-TCB in this in vitro co-culture model.

5.4 Investigating effect of hypoxia on CEA-TCB activity using PDO-T cell co-culture model

Hypoxia is a major feature of the tumour microenvironment in solid tumours. Tissue hypoxia, measured by the activation of a transcriptional hypoxia response signature, occurs in over one third of colorectal cancers and is associated with poor outcomes in CRC (Qi et al., 2020; Vaupel, 2004). Hypoxia is particularly prevalent in metastases of CRC. A study found that hypoxia as determined by pimonidazole staining was present in all biopsies of the liver metastases of all patients with the hypoxic fraction being 15% on average (Van Laarhoven et al., 2006). Immune cells experience a broad range of oxygen tension even at physiological conditions, but also in disease where they face inflammation. Secondary lymphoid organs have been shown to have hypoxic microenvironments with <5% oxygen levels and robust T cell responses occur at highly hypoxic inflammatory sites (Caldwell et al., 2001; Ohta et al., 2011). Therefore this would suggest that immune cells are capable of functioning under hypoxic conditions, however studies have presented conflicting results. Hypoxia can lead to accumulation of adenosine which attenuates proliferation, cytotoxicity, and cytokine production of T cells thus suppressing their function (Hatfield et al., 2014; Ohta et al., 2009). Hypoxia affects many different immune cell types. For example, hypoxia promotes immunosuppressive function of MDSCs through HIF-1 α , main transcriptional mediator in hypoxia response, dependant increase in nitric oxide production and arginase activity (Corzo et al., 2010). Macrophages expressing HIF1 α have been shown to suppress T cell function, potentially through increased levels of VEGF expression (Doedens et al., 2010; Lewis et al., 2000). Similarly, hypoxia also inhibits T cell activating capacity of DCs (Noman et al., 2015). However, when direct effects of hypoxia on CD8 T cells were examined some studies point to hypoxia driven enhancement of effector function and some suggest

immunosuppressive role of hypoxia. Multiple studies demonstrated increased lytic ability of hypoxic CD8 T cells, with one of the studies showing a 7 fold higher killing potential compared to atmospheric oxygen conditions (20% O₂) (Caldwell et al., 2001; Doedens et al., 2013; Gropper et al., 2017; Nakagawa et al., 2015). Effect of hypoxia on T cell cytokine secretion such as IFN γ has been less clear with studies showing mixed results with some showing increased production in hypoxic conditions and some suggesting a reduction in cytokine production (Guo et al., 2009; Lukashev et al., 2006; Naldini et al., 1997; Roman et al., 2010). Proliferation of T cells appears to be negatively affected under low oxygen conditions (1-5%)(Atkuri et al., 2005; Larbi et al., 2010; Naldini et al., 1997). In one study, T cell activation, as indicated by CD69 and CD40L upregulation, positively correlated with oxygen concentration in the atmosphere (Ohta et al., 2011). Hypoxia may also affect different T cell subsets differently as one study showed that while naïve and central memory T cells are suppressed in hypoxia, effector memory T cells show elevated proliferation, survival, and cytotoxic activity(Xu et al., 2016). Additionally, hypoxia has been shown to protect activated T cells from activation-induced death (AICD) (Makino et al., 2003). However, a more recent study demonstrated that hypoxia (1% O₂) caused CAR-T cell impairment in vitro. CAR-T cells showed reduced proliferation, cytokine production, and granzyme B release (Berahovich et al., 2019). Due to hypoxia being a common feature of CRC and some evidence suggesting a suppressive direct effect on T cells it was important to investigate whether hypoxia would impair CEA-TCB efficacy because how hypoxia affects response to T-cell redirecting immunotherapies is currently unknown.

Oxygen level in hypoxic tumour tissues is on average between 1%–2% O₂ and below(Muz et al., 2015). PDOs and T cells were cultured together in 1% O₂ for 48 hours before addition of DP47 or CEA-TCB treatment to allow for hypoxia induced transcriptional changes. A control plate that was set up at the same time was cultured in parallel under normoxic conditions of 21% O₂ (atmospheric O₂ level). Hypoxia increased

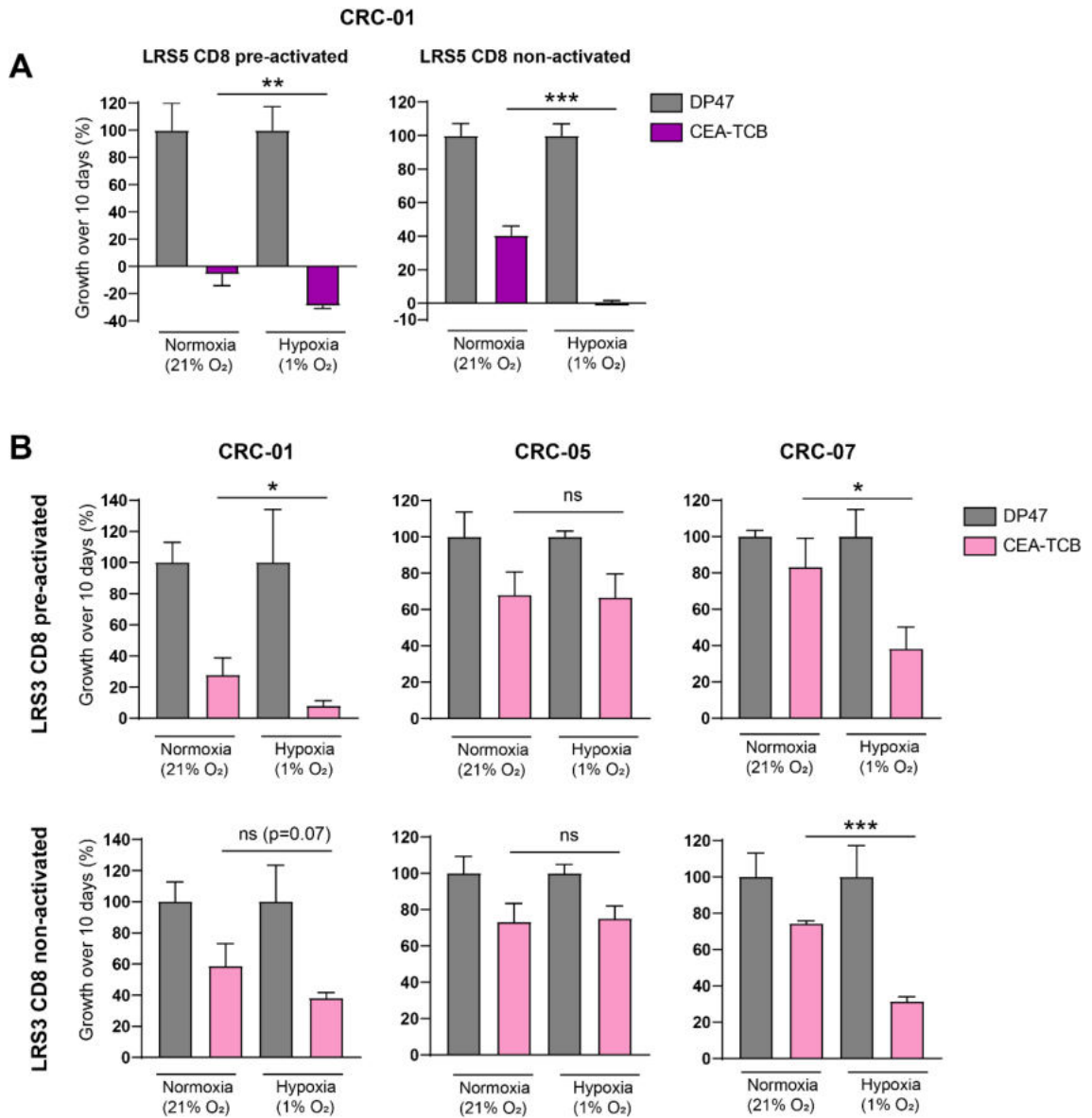


Figure 5.3 Effect of hypoxia on CEA-TCB activity. (A) Growth quantification of CEA-TCB treated PDO CRC-01 over 12 days relative to untargeted TCB (DP47) treated PDOs under normoxic (21% O₂) or hypoxic (1% O₂) conditions. T cells and PDOs were incubated under normoxic/hypoxic conditions for 48 hours prior to adding DP47 or CEA-TCB treatment. Pre-activated and non-activated CD8 T cells were used at E:T 2:1. **(B)** Growth quantification of CEA-TCB treated PDOs (CRC-01, CRC-05, CRC-07) over 12 days relative to untargeted TCB (DP47) treated PDOs under normoxic (21% O₂) or hypoxic (1% O₂) conditions. T cells and PDOs were incubated under normoxic/hypoxic conditions for 48 hours prior to adding DP47 or CEA-TCB treatment. Pre-activated and non-activated CD8 T cells were used. Error bars represent one standard deviation calculated from three replicates. Statistical analysis was performed using an unpaired t-test. For all growth analysis P values are as follows: > 0.05 is ns, < 0.05 is *, < 0.01 is **, < 0.001 is ***, < 0.0001 is **** and ns = not significant.

CD8 mediated significantly tumour growth control with both pre-activated and non-activated T cells. The assay using pre-activated CD8 T cells showed that the tumour growth reduction increased from 106% in control to 129% under hypoxic conditions (Figure 5.3A). The effect was even greater with non-activated CD8 T cells with 59% growth reduction observed under control condition and 99.9% under hypoxic condition (Figure 5.3A). When the experiment was expanded to all three CEA-high PDOs (CRC-01, CRC-5, and CRC-07) the results showed a similar trend as in the first experiment in CRC-01 and CRC-07 (Figure 5.3B). In the co-cultures with those two PDOs, T cell mediated tumour cell growth inhibition was enhanced under hypoxic conditions. Tumour growth reduction was quite poor in this experiment under both conditions in CRC-05 and CRC-07. This could be potentially due to the skewed E:T ratio that resulted from the 48 hour pre-incubation of T cells and PDOs without any treatment allowing continued proliferation of tumour cells during that time. Previous results have shown that good CRC-01 killing is achieved even under low E:T ratios (0.5:1), whereas almost no tumour growth reduction was seen in CRC-05 with E:T 0.5:1. However, under hypoxic conditions the tumour growth reduction in CRC-07 increased from 16.8% and 25.6% to 61.7% and 68.6% (with pre-activated and non-activated CD8 T cells respectively)(Figure 5.3B). Interestingly, there was no difference between control and hypoxia in CRC-05 with both pre-activated and non-activated CD8 T cells. Therefore hypoxia appears to favourably impact CEA-TCB efficacy in 2/3 PDOs tested, increasing the T cell mediated tumour growth control. However, as with all the factors discussed in this chapter, hypoxia is part of a highly complex tumour microenvironment with many different immune and stromal cells therefore it might have a positive direct effect on T cell function in the context of CEA-TCB therapy, but it could have indirect negative effects through other cell types such as macrophages and MDSCs.

5.5 Investigating effect of TGF β on CEA-TCB activity using PDO-T cell co-culture model

TGF β is a pleiotropic cytokine produced in large amounts in the tumour microenvironment by many different cell types including tumour cells, stromal cells, and immune cells. In addition to its direct effect on tumour progression through promotion of tumour cell migration and stimulation of epithelial to mesenchymal transition, TGF β plays a crucial role in immune evasion (Colak & Dijke, 2017; Massagué, 2008). TGF β affects many immune processes such as T cell proliferation, differentiation, and T cell apoptosis and is a key regulator of immune homeostasis and self-tolerance. Studies of TGF β deficient mice have shown that lack of TGF β expression results in severe multifocal and fatal inflammatory response thus highlighting its important role in immune regulation (Shull, 1992; Kulkarni 1993, Yaswen 1996, Diebold 1995). In addition to negatively affecting antigen presenting cells and therefore the mounting of an adequate immune response, TGF β affects T cell activation and function directly. Early studies have demonstrated TGF β 's ability to inhibit CD8 T cell IL-2 production, IL2 receptor expression, IL-2 mediated proliferation as well as blocking their differentiation into CTLs (Brabletz et al., 1993; Das & Levine, 2008; Fox et al., 1992; Kehrl et al., 1986; Letterio & Roberts, 1998; Ranges et al., 1987; Thomas & Massagué, 2005). The antiproliferative effect is mediated by SMAD3, one of the transcription factors downstream of TGF β R, as T cells from SMAD3^{-/-} mice were resistant to antiproliferative effect of TGF β (McKarns et al., 2004; Yang et al., 1999). In addition to modulating T cell proliferation TGF β also inhibits differentiation of CD8 T cells into CTLs and downregulates cytolytic activity of already converted T cell effectors by downregulating expression of granzyme and perforin which are essential proteins for inducing target cell apoptosis (Inge et al., 1992; Smyth et al., 1991; Thomas & Massagué, 2005). TGF β also prevents differentiation of naïve CD4 T cells into Th1 and Th2 subtypes through inhibition of transcription factors T-bet and GATA3 respectively (Bright & Sriram, 1998; Giroux et al., 2010; Gorelik &

Flavell, 2000, 2002; V. L. Heath et al., 2000; Sad & Mosmann, 1994; Schmitt et al., 1994). TGF β effects can outlive its presence as has been demonstrated by Ludviksson in their study in which they showed that if CD4 naïve cells are primed in the presence of TGF β they have reduced antigen specific responses even after TGF β is no longer present (Ludvíksson et al., 2000). Using a mouse model expressing of a dominant-negative form of TGF β receptor type II (dnTGF β RII) Gorelik and colleagues were able to show that absence of TGF β signalling in CD8 and CD4 T cells resulted in spontaneous activation and differentiation into cytokine producing effector cells (Gorelik & Flavell, 2000). An indirect pathway through which TGF β can dampen CTL mediated responses is through induction of differentiation of naïve CD4 T cells into Tregs through direct action of SMAD3 on Foxp3 promoter (Chen et al., 2003; Fantini et al., 2004; Marie et al., 2005; Tone et al., 2007). However, the immunosuppressive effect of TGF β is not only mediated through Treg induction as transfer of wild-type Treg cells into a mice model in which peripheral CD8 and CD4 T cells lacked surface TGF- β RII expression did not alleviate the lethal inflammation and effector T cells retained their active phenotype therefore further supporting the notion that TGF β affects CD8 and CD4 effector functions directly (Li, Sanjabi, et al., 2006). Inhibition of TGF β signalling through TGF β receptor, induction of overexpression of a dominant negative TGF β R, or knocking out the TRG β R have shown to enhance T cell mediated tumour elimination in many different models (Chen et al., 2018; Foster et al., 2008; Gorelik & Flavell, 2001; Holmgaard et al., 2018; Sow et al., 2019). Therefore TGF β blockade has become of particular interest as a way to increase the benefit of cancer immunotherapy. Using quadruple-mutant mice tumour models which recapitulated key features of human microsatellite-stable colorectal cancers Tauriello and colleagues showed that inhibition of TGF β with galunisertib increased CD8 CTL and CD4 Th1 recruitment into tumour and metastases thus converting the immunologically cold tumour into immune hot tumours susceptible to check-point blockade therapy (Tauriello et al., 2018). Combination treatment with galunisertib and PD-L1 further boosted the immune anti-tumour response by increasing granzyme B

production in CTLs and T-bet and IFN γ levels in CD4⁺ Th cells, completely eradicating metastases (Tauriello et al., 2018). In a CAR-T cell model TGF β repressed target cell lysis, reduced cytokine (IL-2 and IFN γ) secretion, decreased expression of cytotoxicity related genes (GZMA, GZMB, GRZB, GRZK), and upregulated exhaustion markers (PD1, TIM3, LAG3, and CTLA4) while also inducing conversion of CD4 T cells into Tregs by upregulation of Foxp3. All of these immunosuppressive effects were abrogated with a TGF β R2 knock out in CAR-T cells (Tang et al., 2020). An anti-TGF β /PD-L1 bispecific antibody was shown to increase T cell infiltration into tumours, increased number of activated and proliferating CD8 T cells, and induced a higher proportion of granzyme B⁺ and perforin⁺ CD8 T cells extending mouse survival more effectively than anti-PD-L1 alone (Yi et al., 2022). Given that high TGF β activity has been described in the majority of metastatic CRCs and a plethora of strong evidence indicating suppression of T cell function by TGF β it was highly relevant to evaluate the effect of TGF β on CEA-TCB activity (Calon et al., 2012).

5.5.1 TGF β confers resistance to CEA-TCB

TGF β exists in one of the three isoforms TGF- β 1, TGF- β 2, or TGF- β 3, with TGF- β 1 being the most abundant and ubiquitously expressed isoform and is the predominant isoform expressed in the immune system (Li et al., 2006). TGF β is secreted in a biologically inactive form, composed of a homodimer of TGF- β non-covalently associated with the latency-associated protein (LAP). This complex is either secreted or associated with another protein, latent-TGF- β -binding protein (LTBP), that directs TGF- β to the extracellular matrix. In order for TGF β to become functionally active it must be released from the LAP and LTBP complex which is usually achieved through interaction with integrins or proteolysis by matrix metalloproteases (MMPs) in the extracellular matrix (Travis & Sheppard, 2014). Although tumour cells themselves can secrete TGF β , other immune (Tregs) and stromal cells (CAFs) in the TME greatly contribute to TGF β secretion. Since I was culturing tumour cells and T cells without the addition of these

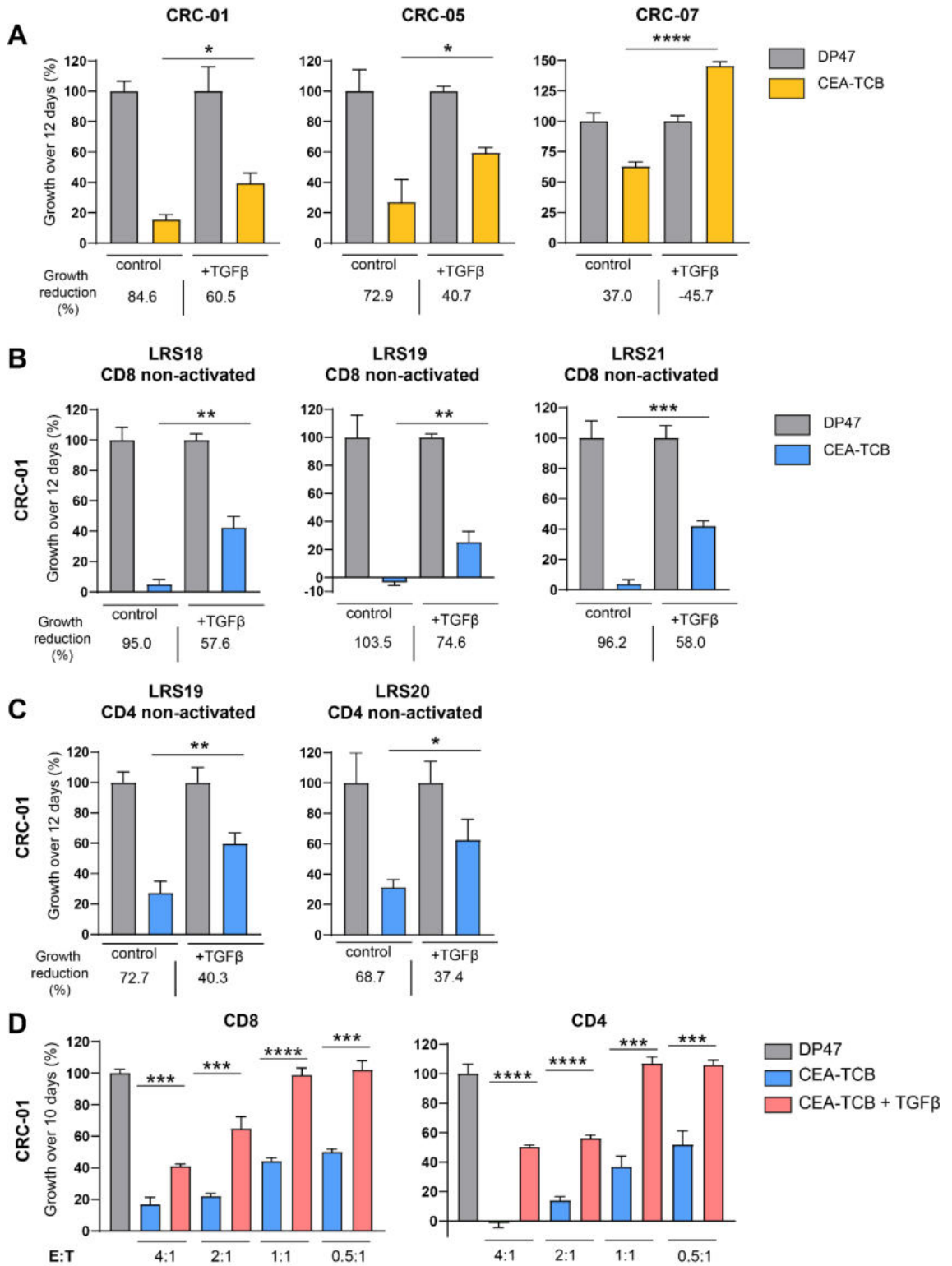


Figure 5.4 Effect of TGF β on CEA-TCB activity. **(A)** Growth quantification of PDOs (CRC-01, CRC-05, CRC-07) treated with pre-activated CD8 T cells and CEA-TCB over 12 days relative to untargeted TCB treated PDOs in the presence or absence of TGF β (10ng/mL). CD8 T cells and PDOs +/- TGF β were pre-incubated together for 72 hours prior to the addition of CEA-TCB or untargeted TCB. Experiments were performed with pre-activated CD8 T cells. **(B)** Growth quantification of PDO CRC-01 treated with CD8 T cells and CEA-TCB over 12 days relative to untargeted TCB (DP47) treated PDOs in the presence or absence of TGF β (10ng/ml). CD8 T cells +/- TGF β were pre-incubated together for 72 hours prior to the addition of CEA-TCB or untargeted TCB. Experiments were performed with non-activated CD8 T cells from three different donors. **(C)** Growth quantification of PDO CRC-01 treated with CD4 T-cells and CEA-TCB over 12 days relative to untargeted TCB (DP47) treated PDOs in the presence or absence of TGF β (10ng/mL). CD4 T-cells +/- TGF β were pre-incubated together for 72 hours prior to the addition of CEA-TCB or untargeted TCB. Experiments were performed with non-activated CD4 T cells from two different donors. **(D)** Growth quantification of CEA-TCB treated PDO CRC-01 over 10 days relative to untargeted TCB treated PDOs in the presence or absence of TGF β (10ng/mL). Experiments were performed at various effector:target ratios (4:1, 2:1, 1:1, 0.5:1) with pre-activated CD8 or CD4 T cells. T cells +/- TGF β were pre-incubated together for 72 hours prior to the addition of CEA-TCB or untargeted TCB. Error bars represent one standard deviation calculated from three replicates. Statistical analysis was performed using an unpaired t-test. For all growth analysis P values are as follows: > 0.05 is ns, < 0.05 is *, < 0.01 is **, <0.001 is ***, <0.0001 is **** and ns = not significant.

other TGF β producing subsets to evaluate the effect of TGF β on CEA-TCB efficacy in my in vitro model I needed to treat the co-cultures with exogenous TGF β . Previous in vitro studies of TGF β effect on T cell function used a range of TGF β concentrations from 1-10ng/mL (Cottrez & Groux, 2001; Di Bari et al., 2009; Kim et al., 2005; McKarns et al., 2004; Nguyen et al., 2016; Ranges et al., 1987; Sanjabi et al., 2009; Smyth et al., 1991; Tang et al., 2020). These experiments revealed reduction in proliferation and inhibition of cytotoxic activity at 10ng/mL therefore I chose this dose for my experiments (Holmgaard et al., 2018; Kim et al., 2005). Pre-activated T cells were pre-treated with 10ng/mL TGF β for 72 hours prior to being added to the killing assays. Three CEA-high PDOs (CRC-01, CRC-05, CRC-07) were combined with control or TGF β treated CD8 T cells and treated with DP47 or CEA-TCB in the presence or absence of TGF β for 12 days. TGF β significantly inhibited tumour growth reduction in all three PDOs on average

decreasing growth reduction by 46% (Figure 5.4A). Next, non-activated CD8 T cells from three different donors were tested in the same experimental set-up but only using CRC-01. The results were similar to those observed with pre-activated CD8 T cells. Non-activated T cells from all three donors showed significantly inhibited tumour growth control with an average growth reduction of 35% (Figure 5.4B). TGF β affected non-activated CD4 T cells similarly, decreasing the tumour cell growth reduction by 32% (Figure 5.4C). Anti-tumour activity of CEA-TCB redirected CD8 and also of CD4 T-cells was examined across a range of effector to target (E:T) ratios of 4:1 to 0.5:1. Complete loss of cancer control through TGF β was observed at E:T ratios of 1:1 and 0.5:1 (Figure 5.4D). These low E:T ranges are perhaps clinically most relevant as cancer cells usually outnumber T cells in metastatic CRC (Elomaa 2022).

5.5.2 TGF β inhibits CD8 T cell proliferation and reduces granzyme expression

TGF β has been shown to reduce cytotoxic gene expression and proliferation of T cells therefore I assessed these two parameters in my model system. Flow cytometry analysis of CD8 T cells that were co-cultured for 8 days with CRC-01 and CRC-05 confirmed that TGF β strongly decreased granzyme B expression (Figure 5.5A). CD8 T cells co-cultured with CRC-01 showed a 5.6-fold reduction in granzyme B MFI, while those co-culture with CRC-05 showed a 4.5 fold reduction. TGF β also reduced CEA-TCB induced proliferation of T cells (Figure 5.5B). The proliferation mode of T cells co-cultured with CRC-01 under control conditions was the third division peak while in the TGF β treatment group it was the second. In the TGF β treated group, 16.6% of T cells did not divide compared to 8.4% in the absence of TGF β (Figure 5.5B). T cells co-cultured with CRC-05 did not exhibit as much proliferation but the proportion of proliferating cells reduced from 52.4% to 34.7%. Thus, TGF β suppresses CEA-TCB mediated tumour cell growth control by blocking proliferation and effector functions.

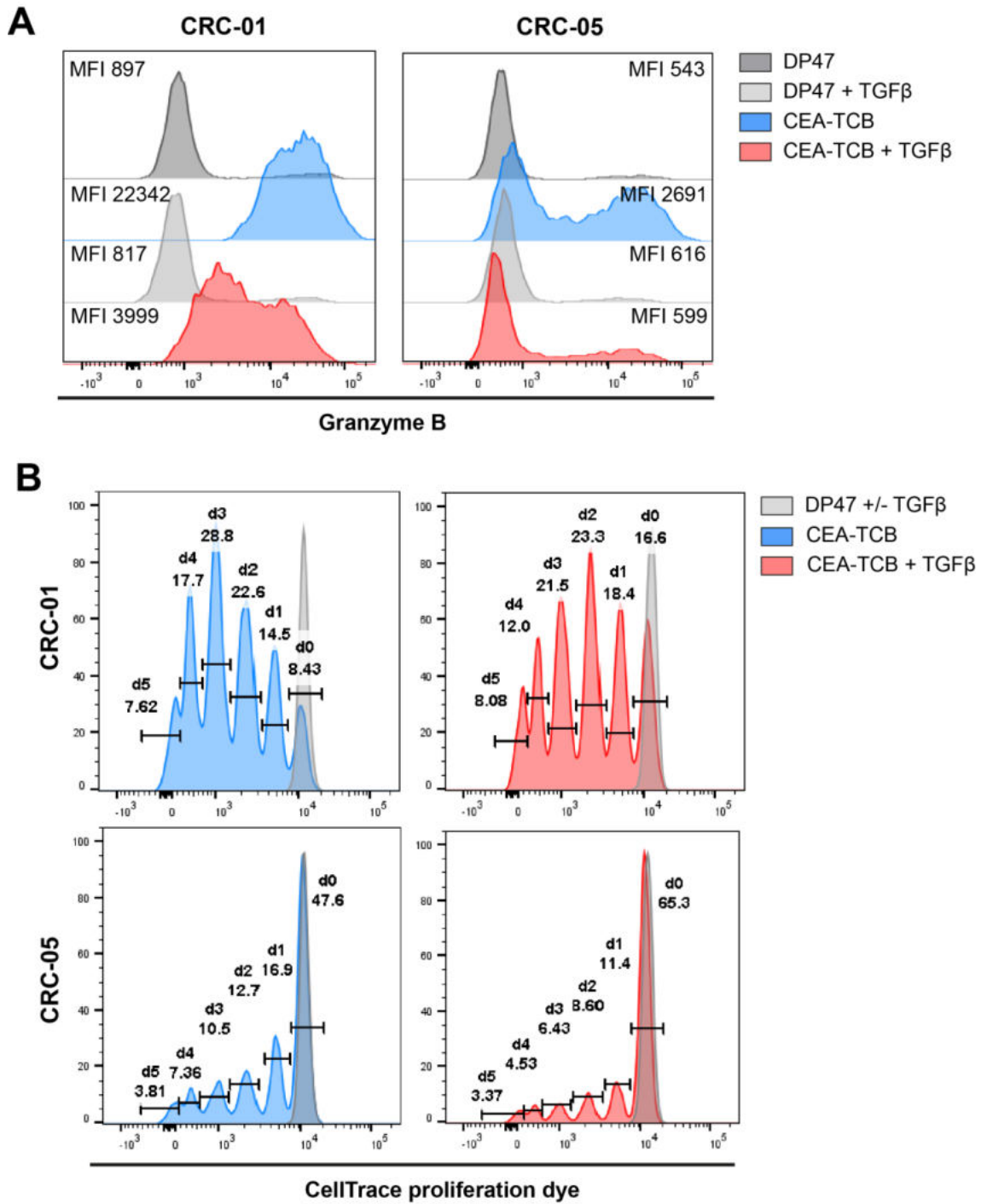


Figure 5.5 TGFβ decreases granzyme expression and inhibits proliferation of CD8 T cells. (A) Granzyme B expression assessed by flow cytometry in CD8 T cells that were harvested from co-culture assays with CRC-01 and CRC-05 on day 8. Mean fluorescence intensity (MFI) values are shown next to each condition. **(B)** Proliferation assessed by flow cytometry using CellTrace proliferation dye in CD8 T cells harvested from co-culture assays with CRC-01 or CRC-05 on day 8. Left: proliferation of CD8 T-cells harvested from CEA-TCB treated PDOs. Right: CD8 T cells harvested from CEA-TCB + TGFβ (10ng/mL) treated PDOs. Percent of cells within each generation are listed above each peak.

5.6 TGF β blockade and IL-2 overcome TGF β mediated CEA-TCB resistance

My next aim was to identify combination therapy strategies that reverse the inhibitory effect of TGF β on CEA-TCB treatment. I first assessed galunisertib, a small molecule inhibitor of the TGF β receptor I. Holmgaard and colleagues demonstrated a dose dependant rescue of proliferation in TGF β treated T cells with a full rescue observed at 1 μ M and enhanced proliferation at higher doses of 3 μ M and 10 μ M of galunisertib (Holmgaard et al., 2018). Therefore I tested three galunisertib doses 1, 5, and 10 μ M in my co-culture assays treated with TGF β . I observed a dose dependent reversal of TGF β inhibitory effect on CEA-TCB activity, with a complete reversal seen at 10 μ M (Figure 5.6A). Thomas and Massague have reported that IL-2 restores TGF β suppressed T cell proliferation and cytotoxic gene expression (Thomas & Massagué, 2005). In their study T cells were activated in the presence of TGF β and subsequently washed and re-cultured in media containing IL-2 without a further addition of TGF β . However, in my experiment I decided to concomitantly treat with TGF β and IL-2 since this is more clinically relevant because the TGF β would still be continuously secreted in the TME. They did not specify the concentration of IL-2 used so I chose a range (1-10U/mL) that was below the concentration used during activation of T cells in vitro (30U/mL). The results observed with IL-2 treatment was similar to those seen with galunisertib. T cell mediated tumour growth control increased in a dose dependant fashion with almost a full rescue with 5U/mL and an enhanced response with 10U/ml (Figure 5.6A). These two agents were used with CRC-01 with two different CD8 E:T ratios (1:1 and 0.5:1) because as discussed earlier TGF β inhibitory effect is greater at lower E:T ratios. Only one E:T ratio was used with CRC-05, as this PDO showed barely any response to CEA-TCB at ratios below 1:1. Galunisertib showed a significant reversal of inhibitory effects of TGF β at both concentrations (5 μ M and 10 μ M) in CRC-01 E:T 1:1, but failed to rescue T cell mediated tumour growth control in CRC-05 only showing a modest increase in tumour cell growth reduction compared to TGF β treated condition (Figure 5.6B). Galunisertib also failed to

reverse TGFβ effects in CRC-01 at the lower E:T ratio (0.5:1) showing a negligible increase in tumour cell growth reduction. However, IL-2 was a more potent stimulator of T cell activity and led to a significant decrease of tumour cell growth even at the lower concentration (5U/ml) at both E:T ratios in CRC-01 (Figure 5.6C). CRC-05 showed almost no difference in tumour growth between TGFβ and TGFβ plus IL-2 5 U/ml conditions, but it did show decreased growth to a near significant level (p=0.055) with

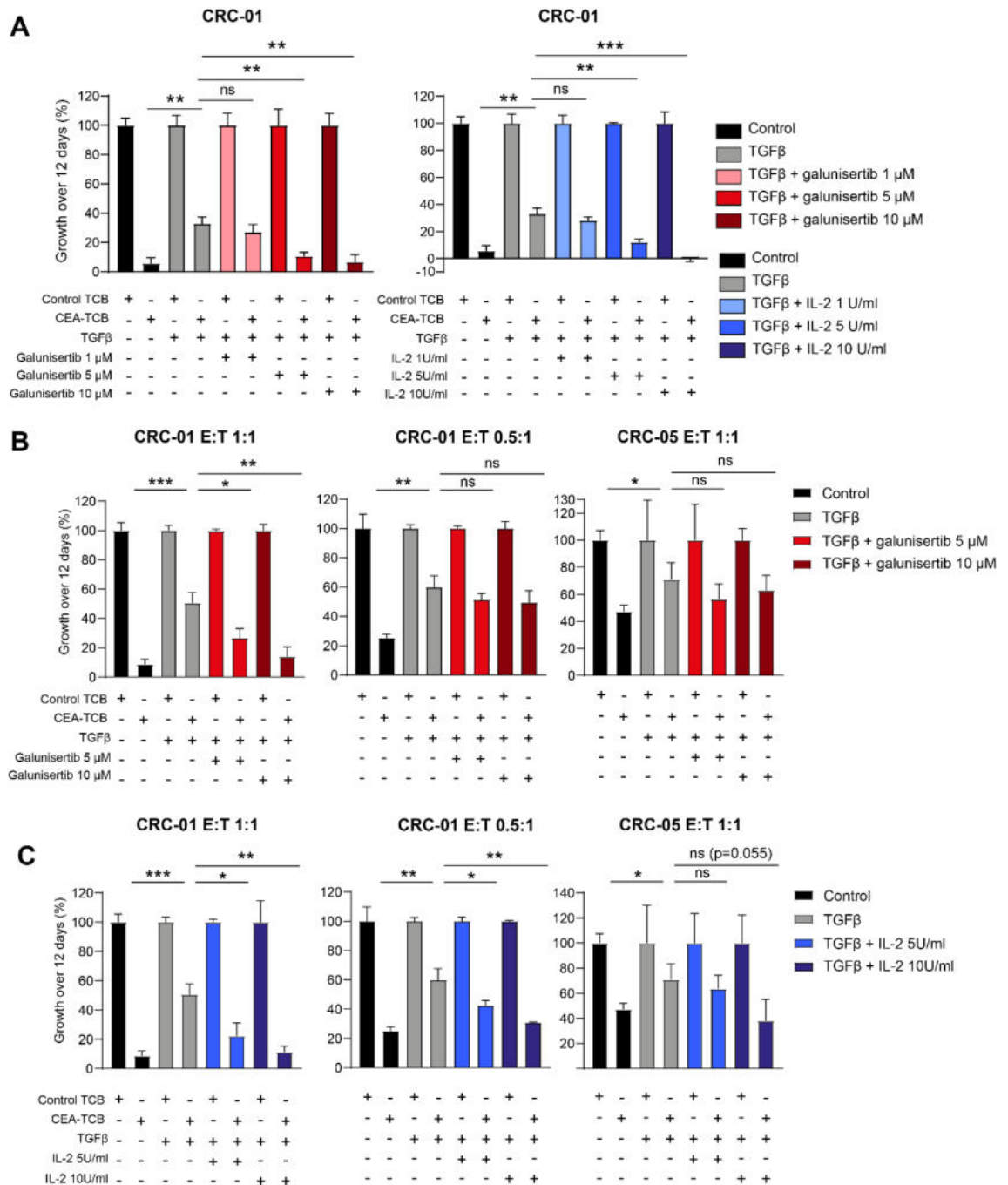


Figure 5.6 Galunisertib and IL-2 reverse immunosuppressive effects of TGF β . (A) Growth quantification of PDO CRC-01 treated with CEA-TCB and pre-activated CD8 T cells (E:T 1:1) over 12 days relative to PDOs treated with untargeted TCB (DP47) and CD8 T cells in the presence or absence of TGF β (10ng/mL) as well as galunisertib (1 μ M, 5 μ M and 10 μ M) or IL-2 (1 U/mL, 5 U/mL, and 10 U/mL). (B) Growth quantification of PDO CRC-01 and CRC-05 treated with CEA-TCB and non-activated CD8 T cells over 12 days relative to PDOs treated with untargeted TCB (DP47) and CD8 T-cells in the presence or absence of TGF β (10ng/mL) as well as galunisertib (5 μ M and 10 μ M). Two different E:T were used with CRC-01 (1:1 and 0.5:1) but only one with CRC-05 (1:1). (C) Growth quantification of PDO CRC-01 and CRC-05 treated with CEA-TCB and non-activated CD8 T cells over 12 days relative to PDOs treated with untargeted TCB (DP47) and CD8 T-cells in the presence or absence of TGF β (10ng/mL) as well as IL-2 (5 U/mL and 10 U/mL). Two different E:T were used with CRC-01 (1:1 and 0.5:1) but only one with CRC-05 (1:1). Error bars represent one standard deviation calculated from three replicates. Statistical analysis was performed using an unpaired t-test. For all growth analysis P values are as follows: > 0.05 is ns, < 0.05 is *, < 0.01 is **, <0.001 is ***, <0.0001 is **** and ns = not significant.

IL-2 10U/ml treatment which contrasts with galunisertib treatment which did not achieve any significant increase in tumour growth reduction (Figure 5.6C).

5.7 Novel stroma-targeted IL2v and tumour-targeted 4-1BBL bispecific antibody reverse TGF β induced immunosuppression

Even though IL-2 provided proof of concept that TGF β inhibition of CEA-TCB efficacy can be reversed with a T cell stimulating cytokine, IL-2 has considerable toxicity in patients (Dutcher et al., 2014). Therefore I wanted to assess more novel agents that have been developed to avoid systemic toxicities. 4-1BB (also known as CD137) is a surface glycoprotein that belongs to the tumour necrosis factor (TNF)-receptor family and is expressed on activated T cells where it serves as a co-stimulatory molecule. 4-1BB co-stimulation of T cells enhances proliferation, cytotoxicity, Th1 polarization and cytokine secretion, and counteracts exhaustion (Hernandez-Chacon et al., 2011; Shuford et al., 1997; Wilcox et al., 2004). This T cell stimulatory pathway has been

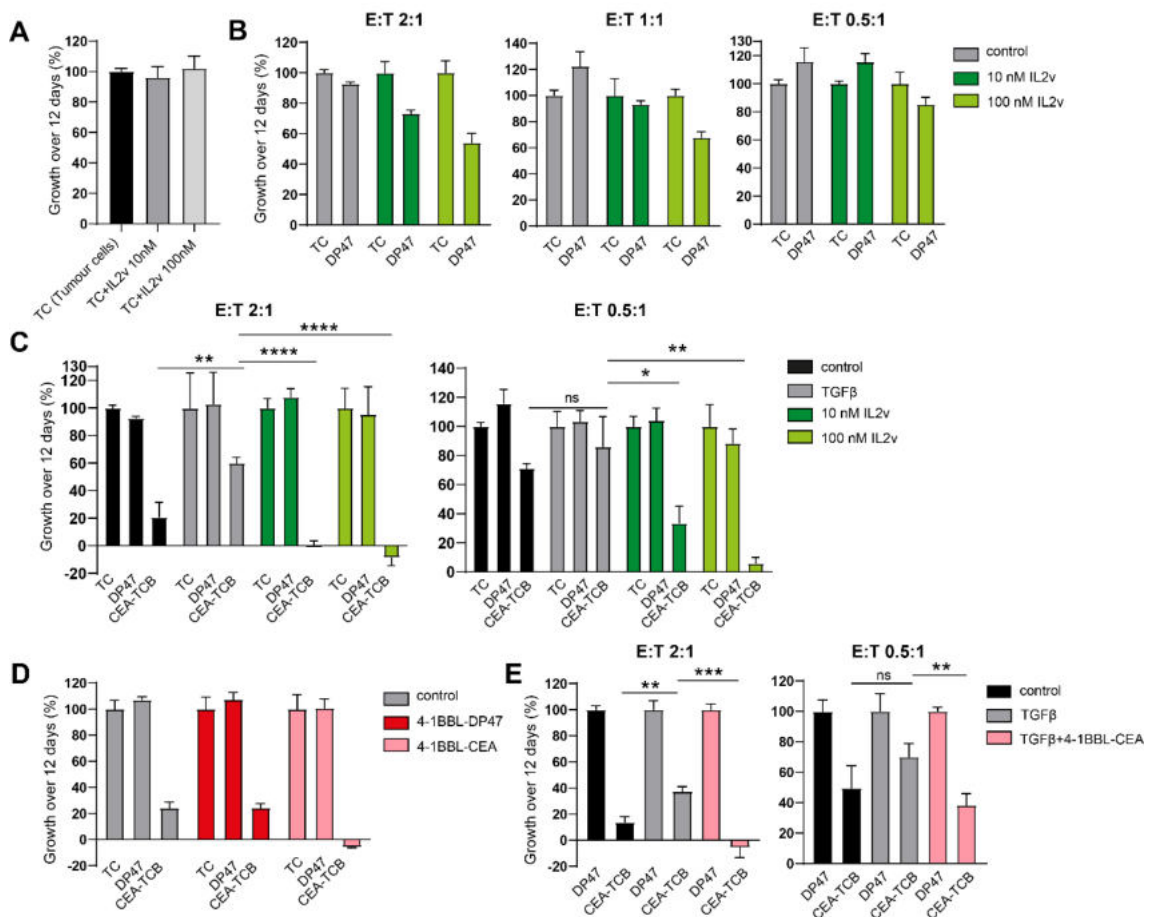


Figure 5.7 Effect of FAP-IL2v and 4-1BBL-CEA on CEA-TCB activity. (A) Tumour cells of CRC-01 were treated with 2 different doses of FAP-IL2v (10 nM and 100 nM) for 12 days and growth quantification was calculated against untreated tumour cells. (B) Growth quantification of PDO CRC-01 treated with DP47 and non-activated CD8 T cells over 12 days relative to tumour cells in the presence of FAP-IL2v (10 nM and 100 nM). (C) Growth quantification of PDO CRC-01 treated with CEA-TCB or DP47 and non-activated CD8 T cells over 12 days relative to tumour cells alone and in the presence or absence of TGFβ (10ng/mL) and FAP-IL2v (10 nM and 100 nM). (D) Growth quantification of PDO CRC-01 treated with CEA-TCB or DP47 and non-activated CD8 T cells over 12 days relative to tumour cells alone in the presence of 4-1BBL-DP47 or 4-1BBL-CEA. (E) Growth quantification of PDO CRC-01 treated with CEA-TCB and non-activated CD8 T cells over 12 days relative to PDOs treated with untargeted TCB (DP47) and CD8 T-cells in the presence or absence of TGFβ (10ng/mL) and 4-1BBL-CEA (2 nM). Error bars represent one standard deviation calculated from three replicates. Statistical analysis was performed using an unpaired t-test. For all growth analysis P values are as follows: > 0.05 is ns, < 0.05 is *, < 0.01 is **, <0.001 is ***, <0.0001 is **** and ns = not significant.

utilised for immunotherapy with the development of agonistic anti-4-1BB antibodies such as urelumab and utomilumab. Although they have been shown to be effective pre-clinically they have not advanced to phase 3 trials because of Fcγ receptor-mediated

hyperclustering and hepatotoxicity (Ascierto et al., 2010; Chester et al., 2018; Segal et al., 2017). The second approach of 4-1BB agonism is second-/third-generation 4-1BB/CD3 ζ chimeric antigen receptor (CAR) T cells (Kawalekar et al., 2016). Although approved and very effective in relapsed/refractory patients with B cell malignancies, CAR T cells have not yet been successful for treatment of solid tumours. To overcome these issues, Roche Glycart engineered proteins simultaneously targeting 4-1BB on T cells and CEA on tumour cells. Their bispecific antibodies have been engineered with a mutation in the Fc region abrogating cross-linking by Fc γ receptors (Fc γ R_s) and therefore avoiding liver toxicities during systemic administration (Claus et al., 2019). 4-11BBL-CEA can only induce 4-1BB activation when cross-linked via CEA-expressing cells and this bispecific antibody can be combined with CEA-TCB as it binds a different CEA epitope and therefore does not compete. A similar approach has been taken in the development of a bispecific antibody targeting IL-2 variant (IL2v) to tumour stroma. FAP-IL2v (simlukafusp alfa) is a FAP-targeted IL-2R $\beta\gamma$ biased immunocytokine that targets an IL-2 variant (IL2v), which binds IL2R $\beta\gamma$ but not the high affinity IL2 α receptor to avoid regulatory T-cell expansion, to FAP which is expressed on cancer associated fibroblasts (CAFs) (Waldhauer et al., 2021). Since at this stage CAFs had not been incorporated into my co-culture model I used FAP-IL2v just as a modified cytokine as FAP-IL2v is still active even if it is not crosslinked via FAP. While on its own IL2v did not affect tumour cell growth, when it was combined with T cells and DP47 it activated the T cells and partially inhibited tumour cell growth in a dose dependant fashion even without CEA-TCB treatment (Figure 5.7A&B). However, this effect was abrogated at a lower E:T ratio (0.5:1). When CRC-01 was treated with CEA-TCB in the presence or absence of TGF β (10ng/mL) and FAP-IL2v protein (10nM) the inhibitory effect of TGF β was reversed with an even enhanced tumour growth inhibition compared to control condition (Figure 5.7C). This rescue effect was observed at both E:T ratios. When treating the PDO-T cell co-culture with 4-1BBL-DP47 in addition to CEA-TCB, there was no difference with CEA-TCB only condition as expected because without binding a target tumour antigen (CEA)

the bispecific antibody (4-1BBL-DP47) would not induce clustering and therefore would not stimulate the T cells (Figure 5.7D). Treating tumour cells in the presence of T cells with 4-1BBL-CEA also did not induce tumour cell killing as expected because without CEA-TCB T cells would not be activated and would also not express 4-1BB. However, when CEA-TCB and 4-1BBL-CEA treatments were combined the tumour growth control was enhanced as expected (Figure 5.7D). Concomitant treatment with CEA-TCB and 4-1BBL in the presence of TGF β caused a similar level of rescue as was observed with IL2v, however, at the lower E:T ratio 4-1BBL-CEA treatment only fully rescued tumour cell killing but did not enhance it further as was seen with IL2v (Figure 5.7E). These results were further confirmed with the other two CEA-high PDOs CRC-05 and CRC-07. Treatments with 4-1BBL-CEA and IL2v significantly reversed TGF β inhibitory effect on CD8 mediated tumour growth control in all PDOs except for 4-1BBL-CEA condition in CRC-07 which only saw a minor improvement in tumour growth control and did not reach statistical significance (Figure 5.8A&B). When the E:T ratio was reduced to 0.25:1 there was no tumour growth inhibition under control conditions, however, IL2v induced some T cell mediated killing leading to a 40% tumour cell growth decrease while 4-1BBL-CEA treatment had no effect suggesting that IL2v is a more potent stimulator of T cell activity than 4-1BBL (Figure 5.8C). Combining these two treatments resulted in big decrease in tumour growth and even led to a reversal of inhibitory TGF β effects at this very low E:T ratio. When the E:T ratio was reduced even lower to 0.1:1, the combination treatment (CEA-TCB+4-1BBL-CEA+IL2v) could not overcome the inhibitory effects of TGF β , but could still induce T cell mediated tumour cell killing.

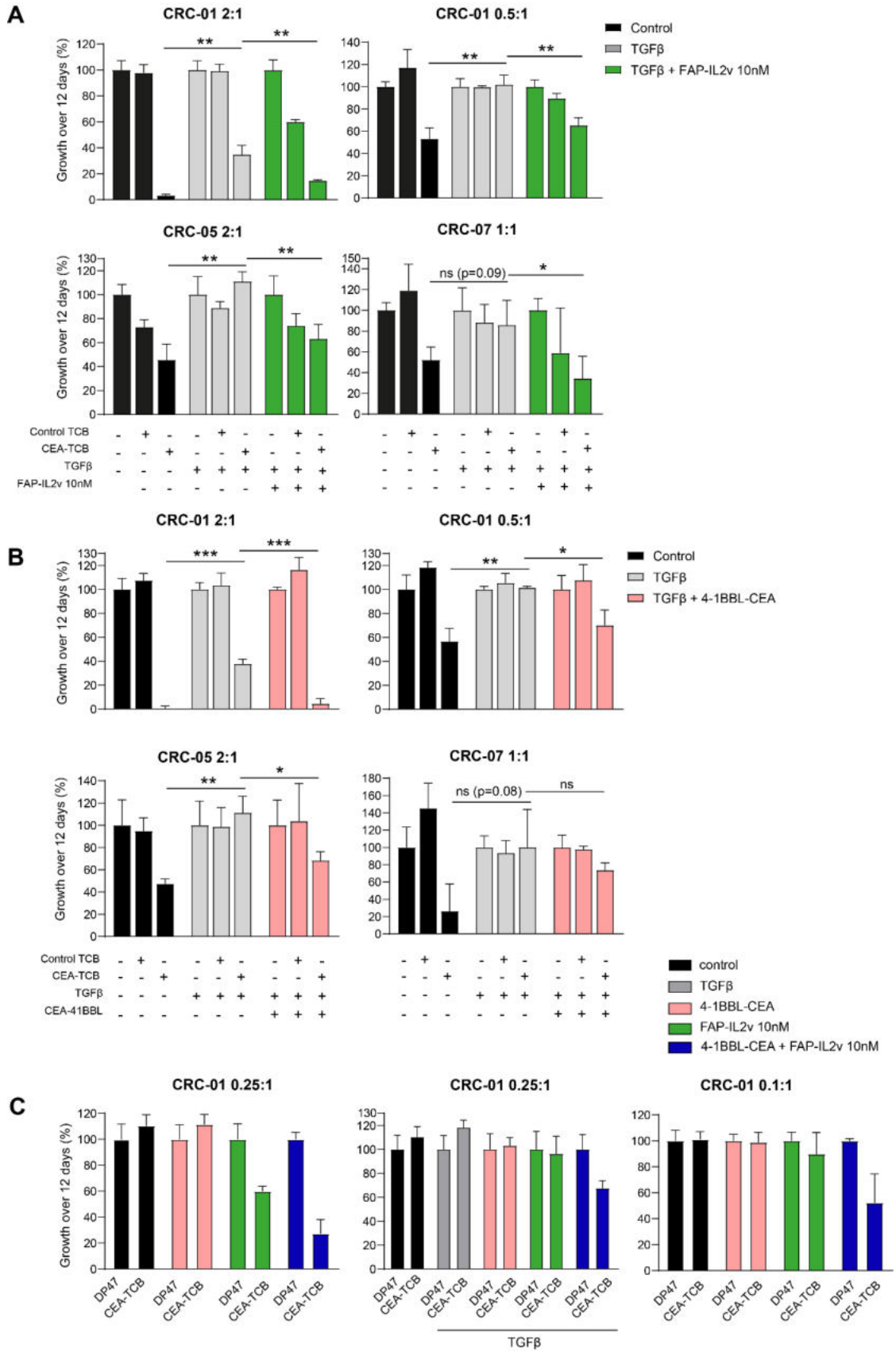


Figure 5.8 FAP-IL2v and 4-1BBL-CEA in combination with CEA-TCB reverse immunosuppressive TGF β effect. **(A)** Growth quantification of CEA-TCB treated PDOs (CRC-01, CRC-05, CRC-07) over 12 days relative to untargeted TCB treated PDOs in the presence or absence of TGF β (10ng/mL) and FAP-IL2v bispecific antibody (10nM). **(B)** Growth quantification of CEA-TCB treated PDOs over 12 days relative to untargeted TCB treated PDOs in the presence or absence of TGF β (10ng/mL) and CEA-41BBL bispecific antibody (2nM). **(C)** Growth quantification of PDO CRC-01 treated with CEA-TCB and CD8 T-cells over 12 days relative to PDOs treated with untargeted TCB (DP47) and CD8 T-cells in the presence or absence of TGF β (10ng/mL) and FAP-IL2v (10nM) or 4-1BBL-CEA (2nM) at E:T ratios 0.25:1 and 0.1:1. Error bars represent one standard deviation calculated from three replicates. Statistical analysis was performed using an unpaired t-test. For all growth analysis P values are as follows: > 0.05 is ns, < 0.05 is *, < 0.01 is **, <0.001 is ***, <0.0001 is **** and ns = not significant.

Next I investigated how these two agents rescue T-cell function suppressed by TGF β . FACS analysis of CD8 T cells extracted after 8 days from a killing assay showed that FAP-IL2v enhanced granzyme B expression and increased T cell proliferation to a level beyond that seen with CEA-TCB alone (Figure 5.9). In all other treatment conditions proportion of T cells that have divided 5+ times was 2% or less whereas with IL2v treatment that proportion was 19%. In contrast, CEA-4-1BBL had a lower impact on proliferation but led to far higher granzyme B levels (Figure 5.9A&C). Both agents increased the proportion of granzymeB+ T cells from 68% in the control condition and 16% in TGF β treated group to 95% or higher (Figure 5.9C). However, T cells treated with 4-1BBL-CEA expressed more than double the amount of granzyme B observed in the IL2v condition. Thus, both agents reverse TGF β effects with a predominant proliferative effect through FAP-IL2v and stronger granzyme B boosting effect of CEA-4-1BBL.

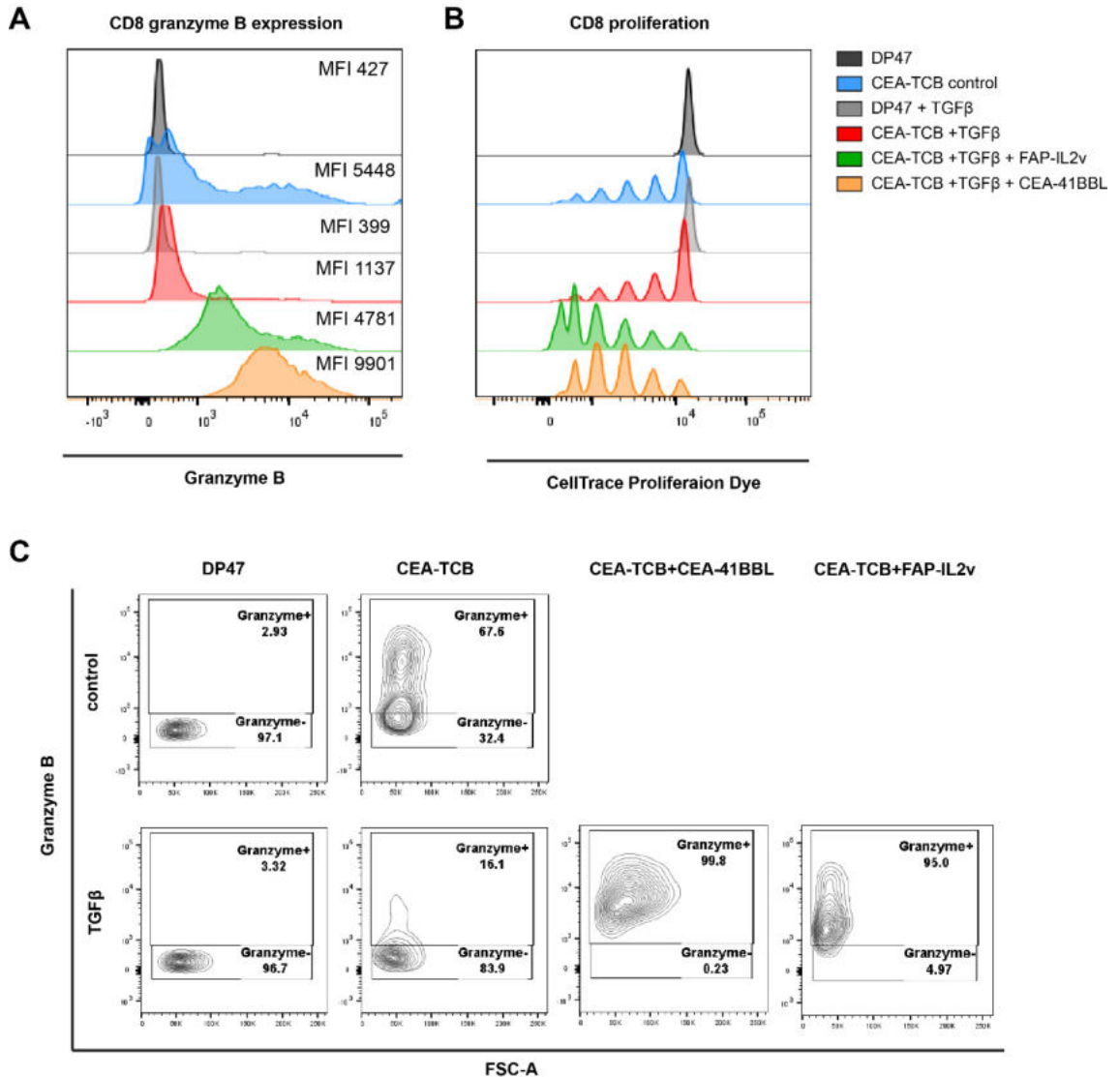


Figure 5.9 FAP-IL2v and 4-1BBL-CEA differentially increase TGFβ inhibited proliferation and granzyme B expression. (A) Histogram of granzyme B expression assessed by flow cytometry in CD8 T cells harvested on day 8 from co-culture assay with CRC-01 and the indicated drug additions. MFI values are next to the corresponding histograms. (B) As in (A), CD8 T cells were harvested on day 8 of co-culture assays with the indicated drug additions and proliferation was assessed by flow cytometry. (C) FACS plots from the same experiment as in (A) showing granzyme B expression in CD8 T cells harvested from a co-culture assay on day 8 from different treatment conditions indicated. All experiments were performed with non-activated CD8 T cells. Experiment was attempted multiple times but completed successfully only once due to poor T cell killing activity with other donors.

5.8 Incorporation of macrophages into the PDO-T cell co-culture model

Macrophages are key players in innate immunity and are one of the most prominent leukocyte populations in tumours. Macrophages promote multiple aspects of tumorigenesis through a variety of mechanisms including promotion of angiogenesis and metastasis, and most importantly through modulating the anti-tumour immune responses (Murdoch et al., 2008; Pollard, 2004; Ruffell & Coussens, 2015). Macrophages are highly plastic cells that polarise and acquire different functional properties in response to different environmental signals. Classically activated macrophages referred to as M1 macrophages are polarised to this phenotype by IFN γ alone or in concert with microbial products such as lipopolysaccharide (LPS) or cytokines such as TNF α . M1 macrophages are characterised by production of inflammatory cytokines such as IL-12, IL-23, IL-1, TNF α and therefore induction of a Th1 response, T cell recruiting chemokines CXCL9, CXCL10, and CXCL11, expression of inducible nitric oxide synthase (iNOS; also known as NOS2) and nitric oxide (NO) production, and high capacity for antigen presentation. Alternatively activated macrophages, or M2 macrophages, are induced by exposure to IL-4 and IL-13 or IL-10. M2 macrophages are known for immune suppression and tissue remodelling and are defined by expression of scavenger receptors, mannose receptor (CD206), secretion of IL-10 and TGF β , and high expression of arginase 1 (ARG1) (Biswas & Mantovani, 2010; Mantovani et al., 2004). Tumour associated macrophages (TAMs) are usually polarised towards the M2 phenotype and are therefore known as tumour promoting or anti-inflammatory. The presence of TAMs is generally associated with poor prognosis in solid tumours, however, in colorectal cancer high density of TAMs is surprisingly associated with better survival (Forssell et al., 2007; Roxburgh & McMillan, 2012; Zhang et al., 2012). However, most of these studies do not distinguish between M1 and M2 macrophages and rely on CD68 which is expressed by both populations as it is a general macrophage marker. One study did compare M1 macrophages, defined by NOS2 expression, and M2 macrophages, identified by CD163 expression, in relation

to survival in colorectal cancer and has found that an increase in M1 macrophages was accompanied by a concomitant increase in M2 macrophages and that both subtypes correlated to significantly improved prognosis (Edin et al., 2012). The good prognosis correlated to the presence of M2 macrophages in colorectal cancer may be due to the fact that there is also an M1 population present that may counteract or balance out the effects of M2 macrophages. TAMs can modulate anti-tumour responses through indirect methods such as increasing the degree of fibrosis and therefore causing T cell exclusion from tumours and promoting Treg recruitment via CCL2 (Curiel et al., 2004b; Quaranta et al., 2018). Equally and potentially more importantly, TAMs can directly inhibit cytotoxic T cell responses through several different mechanisms. One is through production of inhibitory cytokines such as IL-10 and TGF β . One study demonstrated that in addition to secretion of TGF β macrophages are also able to activate TGF β from its latent form through expression of integrin α v β 8 and matrix metalloproteinase 14 (MMP14) (Kelly et al., 2018). Macrophages are able to suppress T cell proliferation and are able to do so with low ratios to T cells under hypoxic conditions (Doedens et al., 2010; Movahedi et al., 2010). Kusmartsev and colleagues reported that TAMs induced T cell apoptosis through increased production of NO and high arginase activity (Kusmartsev & Gabrilovich, 2005). Through expression of B7-H4 TAMs inhibit T cell proliferation, decrease IFN γ and IL-2 production, reduce cytotoxicity, and induce T cell exhaustion (Kryczek et al., 2006; Li, Lee, et al., 2018). Decreased cytotoxic activity has also been observed as a result of interaction between CD45 on T cell surface and CD206 (mannose receptor) on TAM surface (Schuette et al., 2016). Macrophages can also inhibit T cell activity by expressing PD-L1 and its expression on macrophages and dendritic cells predict clinical efficacy of PD-1/PD-L1 blockade in some cancers (Kuang et al., 2009; Lin et al., 2018). Due to their tumour promoting and immunosuppressive functions macrophages have become an attractive target for immunotherapy. CSF1/CSF1R blockade either alone or in combination with other immunotherapy agents have shown efficacy in various tumour models and also in clinical trials (Mok et al., 2014; Zhu et al.,

2014). However, the role of this immune population in responses to T cell redirecting bispecific antibodies has not been evaluated.

5.8.1 Macrophage polarisation towards the M2 phenotype

CD14⁺ monocytes were isolated from PBMCs and were seeded in T cell media with the addition of M-CSF (100ng/mL) to induce macrophage differentiation. After 7 days, they were then polarised to the M2 phenotype with IL-4 and IL13 or IL-10 or left in M-CSF alone as “M0” macrophages (Figure 5.10A). Harvesting the macrophages proved particularly difficult due to their highly adhesive property. Different methods were tested: enzyme free dissociation buffer, EDTA in PBS at 37°C/RT/4°C, and scrapping. The best method was incubation with 5mM EDTA in PBS at 37°C followed by gentle scrapping. After the macrophages were harvested they were assessed by flow cytometry for M2 markers CD206 and CD163 in order to confirm their M2 phenotype (Mantovani et al., 2002). Although PD-L1 is not exclusively an M2 macrophage marker, it was important to evaluate its expression as PD-L1 may attenuate T cell activity in co-culture (Cai et al., 2021). All macrophages expressed high levels of CD68 confirming their macrophage differentiation. None of the macrophages were positive for CD163 despite several different attempts with different antibody clones. M2 polarised macrophages expressed high levels of CD206, higher than in the M0 population (Figure 5.10B). Some studies have suggested that M-CSF induces macrophage differentiation already leaning towards the M2 phenotype and GM-CSF pre-orientes them to the M1 subtype thus potentially explaining CD206 expression even on the M0 macrophages. There was no difference in CD206 expression between IL-4 and IL-4+IL-13 polarisation methods, but macrophages polarised with IL-4+IL-10 showed the highest CD206 expression. PD-L1 expression was only present on the M2 macrophages with the highest levels observed in the IL-4/IL-10 polarised population (Figure 5.10B). I also investigated whether culturing the monocytes in PDO conditioned media (CM) would also induce macrophage differentiation and polarise them towards the M2 phenotype. Macrophages grown in conditioned media all

expressed high levels of CD68, but their levels of CD206 expression were lower, particularly in the macrophages grown in CRC-07 CM. Unlike the cytokine polarised

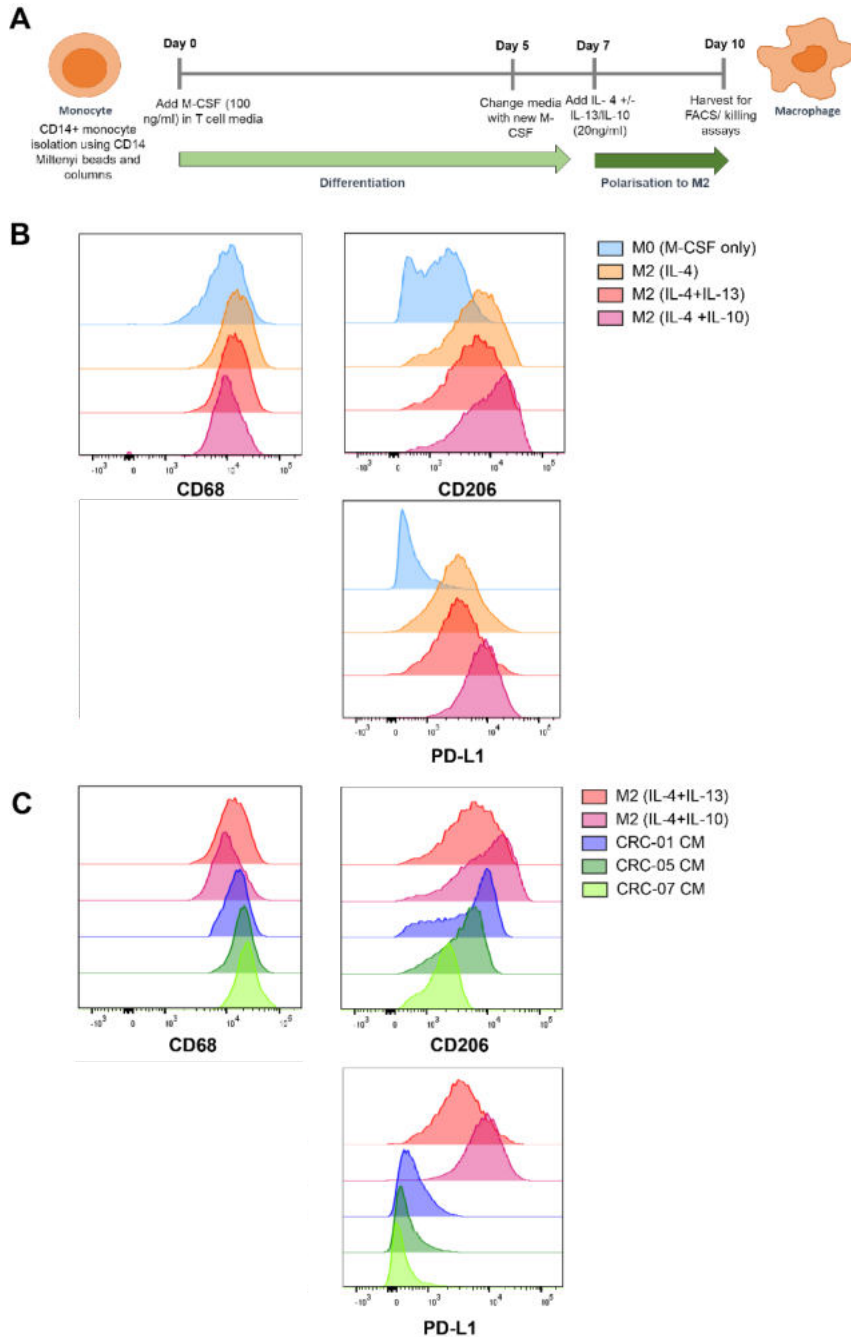


Figure 5.10 Macrophage polarisation to M2 phenotype. (A) Schematic showing the workflow for differentiation and polarisation of CD14+ monocytes into M2 macrophages. **(B)** Flow cytometry histograms of M2 macrophage marker (CD68, CD206, PD-L1) expression on macrophages polarised by different cytokine combinations indicated. Data is representative of 3 experiments. **(C)** Expression of markers as in (B) in macrophages polarised by PDO conditioned media in comparison to the cytokine polarised macrophages. Experiment performed once.

macrophages, those grown in CM showed no or minimal PD-L1 expression (Figure 5.10C).

5.8.2 Effect of M2 macrophages on CEA-TCB activity

Next, I wanted to investigate the effect of M2 macrophages on CEA-TCB efficacy in my co-culture model. The macrophages were polarised as described before and added to the co-culture assay at the same time as T cells from the same donor and allowed to attach for 24 hours before the addition of DP47 or CEA-TCB. I tested two different E:T ratios 2:1 and 1:1 with always double the amount of macrophages compared to T cells as macrophages outnumber T cells in tumours (Frohwitter et al., 2022). Co-culturing macrophages with tumour cells alone or with CD8 T cells and DP47 did not affect tumour cell growth (Figure 5.11A). When the cultures were treated with CEA-TCB, macrophages enhanced tumour cell killing. Macrophages increased tumour growth inhibition mediated by both pre-activated and non-activated CD8 T cells from one donor, but only non-activated T cells from the second donor (Figure 5.11B). In one of the conditions where the tumour growth inhibition was poor in control conditions (pre-activated T cells donor LRS8), macrophages increased the growth reduction from a mere 18.9% to 110.7% (IL-4+IL-13 polarised macrophages) and 89.7%(IL-4+IL-10 polarised macrophages). Therefore in my model, M2 macrophages appear to have a stimulatory role rather than an immunosuppressive one. However, as described earlier macrophages are highly plastic and the two subtype classification system has been criticised as too simplistic and it has been suggested that it is more of a spectrum and the two subtypes are their extremes. It has been shown that IFN γ can induce switching from the M2 phenotype towards the pro-inflammatory tumour suppressor M1 phenotype (Duluc et al., 2009). Therefore it is possible that due to IFN γ secretion induced by CEA-TCB activation of T cells the and in the absence of IL-4/IL-13/IL-10 macrophages underwent a phenotype switch which resulted in an enhanced tumour cell growth inhibition.

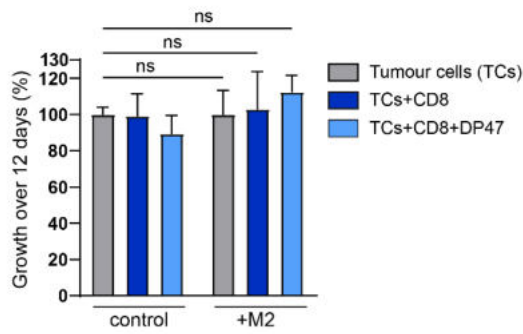
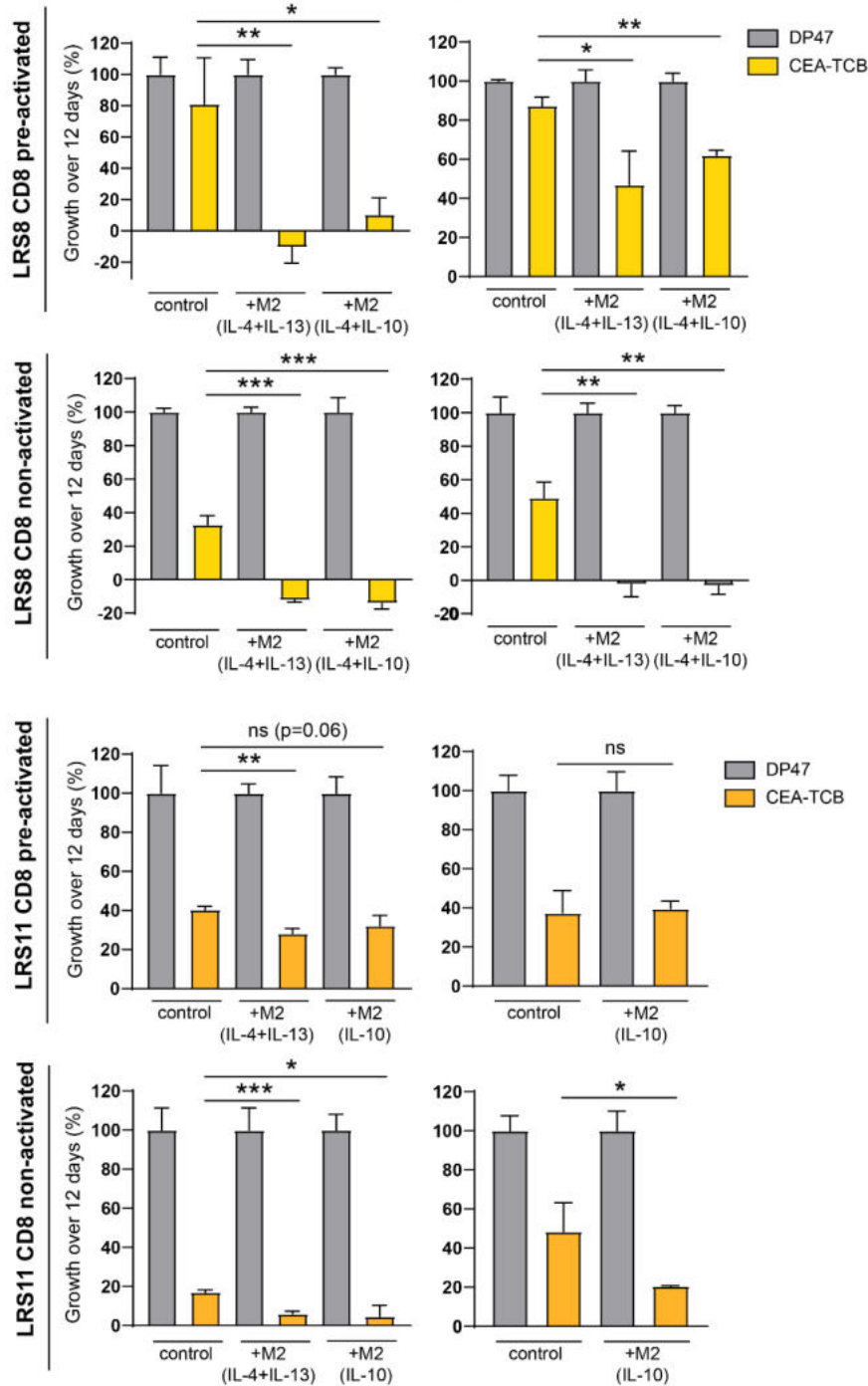
A**Macrophage: T cell: Tumour cell (4:2:1)****B****Macrophage: T cell: Tumour cell (4:2:1) Macrophage: T cell: Tumour cell (2:1:1)**

Figure 5.11 Macrophages enhance CEA-TCB mediated PDO growth inhibition by T cells.

(A) Growth of PDO CRC-01 growth in the presence of M2 macrophages relative to tumour cell growth alone over 12 days. **(B)** Growth quantification of PDO CRC-01 treated with CEA-TCB and CD8 T cells over 12 days relative to PDOs treated with untargeted TCB (DP47) and CD8 T cells in the presence or absence differentially polarised macrophages. Experiments were performed at different E:T ratios (2:1 and 1:1) with the macrophage to T cell ratio always being 2:1. Experiments were performed with pre-activated and non-activated CD8 T cells from two different donors. Error bars represent one standard deviation calculated from three replicates. Statistical analysis was performed using an unpaired t-test. For all growth analysis P values are as follows: > 0.05 is ns, < 0.05 is *, < 0.01 is **, <0.001 is ***, <0.0001 is **** and ns = not significant.

It would have been useful to assess their phenotype by flow cytometry after they have been in the co-culture assay, however, there were multiple technical difficulties that prevented me from carrying out this experiment. The first is the cell number as the assay needs to be scaled up for flow cytometry and after all the differentiation/polarisation/harvesting steps I would only have about 20% of the monocyte number isolated from PBMCs. Secondly, as mentioned earlier, macrophages are highly adhesive and it would have been difficult to harvest them from the co-culture in large enough numbers for flow cytometry assessment. These experiments can be performed with continuous treatment with IL-4/IL-13/IL-10 to ensure that the macrophages retain their M2 phenotype. Appropriate controls would need to be in place in order to know if the cytokines alone have an effect on T cells. Additionally cytokine arrays can be performed to determine what soluble factors polarised macrophages are secreting.

5.9 Incorporation of CAFs into the PDO-T cell co-culture model

Fibroblasts are non-vascular, non-epithelial, and non-immune cells of mesenchymal origin residing in connective tissues. One of the main functions of fibroblasts under normal physiological conditions is the deposition and maintenance of extracellular matrix

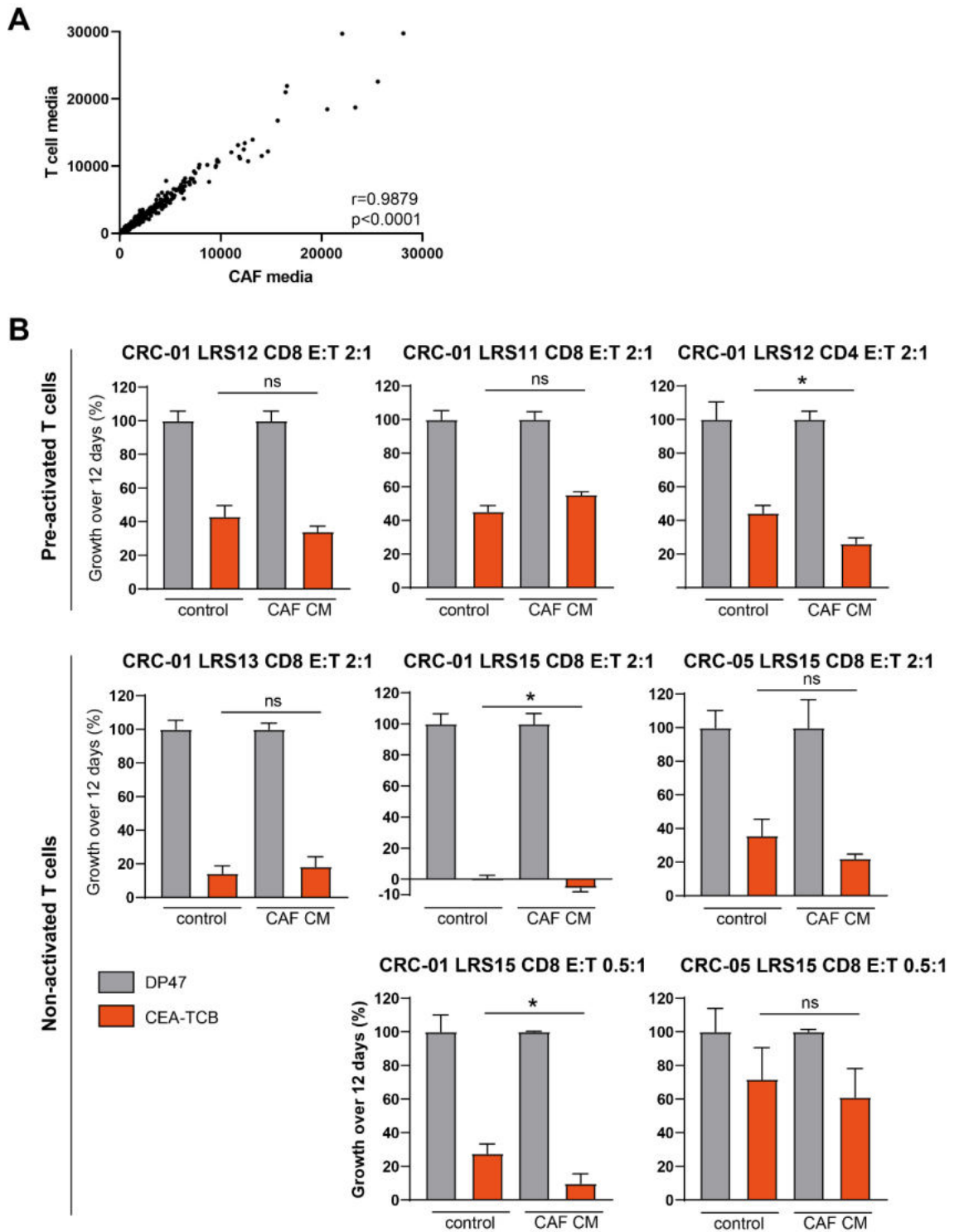
(ECM). Fibroblasts are usually quiescent but can become activated during wound healing responses. This activated phenotype is characterised by increased proliferation and metabolic activity, enhanced secretion of ECM components such as type I, III, IV, V collagen, fibronectin, and tenascin C, expression of ECM remodelling enzymes such as matrix metalloproteinases (MMPs), acquisition of migratory properties and contractile activity, and secretion of cytokines, chemokines, and growth factors. However, when the wound healing process is complete CAFs are either reprogrammed back to their non-activate state or undergo apoptosis. But in some pathological conditions such as chronic inflammation, fibrosis, and cancer the fibroblasts remain constitutively active. Activated fibroblasts that are present in many solid tumours are known as cancer associated fibroblasts (CAFs) and comprise a key cellular component of the tumour microenvironment. CAFs engage in cross talk with tumour cells and have been implicated in tumour growth and progression by promoting angiogenesis, metastasis, epithelial-mesenchymal transition (EMT), cancer cell stemness, and even drug resistance (Dimanche-Boitrel et al., 1994; Elenbaas & Weinberg, 2001; Kalluri & Zeisberg, 2006; Orimo et al., 2005; Paraiso & Smalley, 2013). However, in addition to their direct tumour promoting functions, CAFs have been assigned an immunomodulatory role and been shown to promote the development of an immunosuppressive tumour microenvironment. Due to their polyfunctionality, CAFs are able to regulate many different immune cell types through direct and indirect mechanisms. Through their IL-6 secretion CAFs drive monocyte precursors towards an MDSC phenotype and also inhibit DC maturation and therefore their ability to activate T cells (Mace et al., 2013). CAFs also promote the recruitment of monocytes to the TME and their differentiation towards the immunosuppressive M2 phenotype by secreting M-CSF, IL-6, CCL2, SDF1 (Kuen et al., 2017; Takahashi et al., 2017; Zhang et al., 2019). Additionally, CAFs interfere with NK cell functions by decreasing their cytotoxicity and cytokine production (Balsamo et al., 2009; Inoue et al., 2016). Eliminating CAFs in a murine breast cancer model shifted the immune response from Th2 to Th1 and reduced

the recruitment of immune suppressor cells such as Tregs, MDSCs, and TAMs (Liao et al., 2009). CAFs are able to suppress T cell proliferation and effector function by secreting VEGF and TGF β and also by expressing PD-L1 (Pinchuk et al., 2008; Ziani et al., 2018). CAFs also modulate T cell activity by regulating metabolic pathways. For example, through secretion of IDO1 CAFs deplete tryptophan and increase the accumulation of immunosuppressive tryptophan catabolites (Ziani et al., 2018). Similarly, CAF production of arginase 2 leads to deprivation of arginine which is important for T cell proliferation and function (Ziani et al., 2018). It has also been reported that CAFs express CD73 leading to accumulation of adenosine which suppresses T cell functions through the A2A receptor (Yu et al., 2020). Another important finding was that CAFs can directly kill T cells via PD-L2 and FasL engagement (Lakins et al., 2018). CAFs are also the major source of the chemokine CXCL12, which has been shown to mediate T cell exclusion in solid tumours (Feig et al., 2013). By remodelling ECM CAFs can also contribute to creation of hypoxic zones because tumours with high levels of fibrosis are often poorly oxygenated and as described earlier hypoxia can reprogram the immune TME. Due to their pleiotropic effects on both innate and adaptive immune cells within the TME, CAFs can contribute to resistance to immunotherapy agents. For example, in a model of multiple myeloma, CAFs inhibited CAR T-cell antitumour activity (Sakemura et al., 2022). Targeting CAFs has emerged as a novel approach to enhance anti-tumour immune responses and augment other immunotherapy agents such as inhibitors of the PD-1/PD-L1 pathway (De Sostoa et al., 2019; Feig et al., 2013).

To investigate the effect of CAF secreted factors on CEA-TCB activity in the co-culture assay I used CAF conditioned T cell media (CAF CM). RNA sequencing of CAFs grown in their own media versus T cell media was performed and showed that gene expression is highly similar in both medias (Figure 5.12A). T cell media was conditioned by CAFs for 5 days and CD8 T cells were pre-treated with CAF CM for 72 hours prior addition to the assay. Fresh CAF CM was added to the co-culture assay in a 1:1 ratio

with fresh T cell media. CAF CM either had no significant effect on CD8 T cell mediated tumour growth control or enhanced it (Figure 5.12B). Next, CAFs were added to the co-culture assay. CAFs were seeded at a 1:1 or 0.5:1 ratio with PDO tumour cells at the same time, after 24 hours CD8 T cells were added, the co-culture was incubated for 72 hours before addition of DP47 or CEA-TCB. Due to the extra 4 days post seeding of cancer cells prior to addition of bispecific antibodies the E:T between cancer cells and CD8 T cells was skewed resulting in poorer tumour growth inhibition particularly with pre-activated CD8 T cells. However, addition of CAFs actually increased tumour growth reduction from 32.1% to 95.9% with pre-activated CD8 T cells (Figure 5.12C). Tumour growth reduction was also increased with the addition of CAFs to non-activated CD8 T cells, however the reduction was further increased only by 14.3% because tumour cell growth reduction was already substantial under control conditions (85.2%). In order to avoid skewing of E:T, in the next experiments T cells were pre-incubated with CAFs for 72 hours prior to the addition to the co-culture. While T cells were pre-incubating with CAFs separately, CAFs and PDO cancer cells were seeded. On day 0 of the assay, T cells were harvested from co-culture with CAFs and added to the co-culture already containing CAFs and cancer cells. On the same day the assay was treated with bispecific antibodies. When this co-culture method was used CAFs did not enhance tumour cell growth reduction as there was no significant difference between control wells and those containing CAFs (Figure 5.12D). These results were surprising as CAFs expressed genes for TGF β , CXCL12, CD73, VEGFA which are all considered to be immunosuppressive and reduce T cell proliferation and effector function. However, RNA sequencing also showed that CAFs expressed small amounts IL-15 which is a stimulatory cytokine for T cells. Additionally, using T cells and fibroblasts isolated from human non-small cell lung cancers (NSCLC) a study showed that tumour associated fibroblasts elicited a contact-dependent enhancement of tumour associated T cell activation even in the presence of TGF β (Nazareth et al., 2007). However, these are

preliminary findings and further experiments would be required to investigate this unexpected finding. The RNA sequencing of CAFs was performed when CAFs were



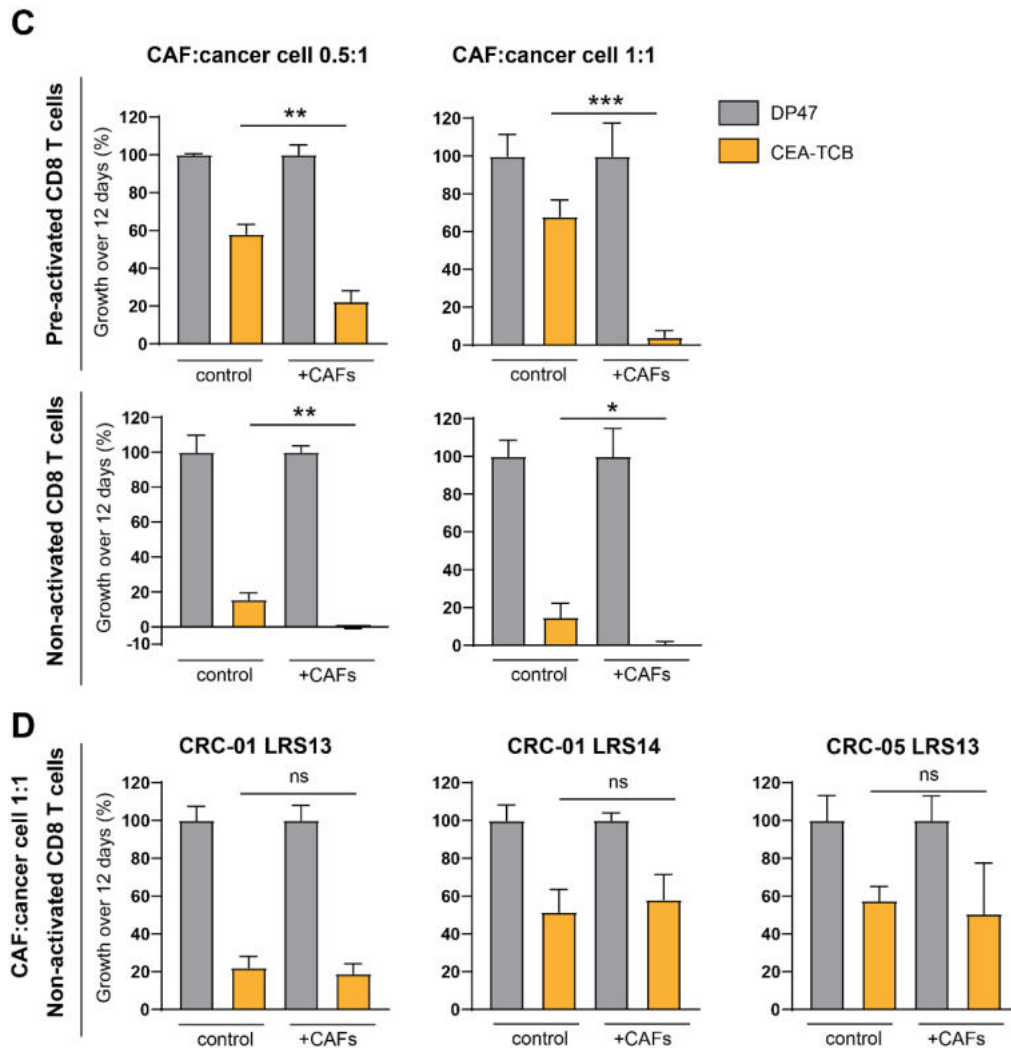


Figure 5.12 Effect of CAF conditioned media and CAFs on CEA-TCB activity. (A) Gene expression (normalised counts) of CAFs cultured in CAF media (DMEM with 10% FCS and ITS (insulin-transferrin-selenium) or in T cell media (RPMI 1640 with 10% FCS). Pearson correlation coefficient and p value of the significance test are shown. **(B)** Growth quantification of PDO CRC-01 and CRC-05 treated with CEA-TCB (20nM) and CD8 T-cells over 12 days relative to PDOs treated with untargeted TCB (DP47, 20nM) and CD8 T-cells in the presence or absence of CAF conditioned media. Experiments were performed with pre-activated and non-activated CD8 T cells from two different donors. **(C)** Growth quantification of PDO CRC-01 treated with CEA-TCB and CD8 T-cells over 12 days relative to PDOs treated with untargeted TCB (DP47) and CD8 T-cells in the presence or absence of CAFs. Experiments were performed at different CAF to cancer cell ratios (1:1, 0.5:1). Experiments were performed with pre-activated and non-activated CD8 T cells from the same donor. For this assay, cancer cells and CAFs were seeded together and left to attach for 24 hours. Following that CD8 T cells were added and the co-culture was incubated together for 72 hours prior to the addition of DP47 (20nM) or CEA-TCB (20nM). Continued on next page.

(D) Growth quantification of PDO CRC-01 and CRC-05 treated with CEA-TCB and CD8 T-cells over 12 days relative to PDOs treated with untargeted TCB (DP47) and CD8 T-cells in the presence or absence of CAFs. Experiments were performed at a CAF to cancer cell ratio of 1:1. Experiments were performed with non-activated CD8 T cells from 2 different donors. For this experiment, T cells were pre-incubated with CAFs for 72 hours prior to addition to the co-culture containing cancer cells and CAFs. Error bars represent one standard deviation calculated from three replicates. Statistical analysis was performed using an unpaired t-test. For all growth analysis P values are as follows: > 0.05 is ns, < 0.05 is *, < 0.01 is **, <0.001 is ***, <0.0001 is **** and ns = not significant.

cultured alone, therefore it is possible that in the co-culture they secrete different soluble factors due to communication with both PDOs and T cells. Post co-culture transcriptomic data along with cytokine arrays would provide data that may be able to explain this result.

5.10 Discussion

The idea that T cells can recognise neoantigens generated by mutations in cancer originated in the 1980s with the work of Thierry Boon who first identified tumour neoantigen specific T cells in mice. Over the past several decades it has become well recognised that the immune system plays a key role in cancer development and progression. However, tumours evolve mechanisms to escape immune control which is supported by the findings that there is a subgroup of patients that either don't respond at all, or show initial response but eventually develop disease progression indicating acquired resistance. It has become widely appreciated that tumours establish immunosuppressive environments that support their growth and promote immune evasion through secretion of immunosuppressive cytokines, and recruitment and cross-talk with immune and stromal cells found in the TME. Studies in mice have shown that CEA-TCB increases T cell infiltration into tumours and increases tumour PD-L1 expression, yet phase Ia and Ib clinical trials reported that only 11% of patients showed response to CEA-TCB as monotherapy and 50% when it was combined with atezolizumab indicating that there are additional immunosuppressive mechanisms

occurring in the TME that must be overcome for effective therapy (Tabernero et al., 2017).

The advantage of using an in vitro model as the one I have established is the opportunity to evaluate individual factors or their combinations in relation to their effect on immunotherapy agents, in my case CEA-TCB. Using three CEA-high PDOs with a good response to CEA-TCB a screen of some cytokines and immune cell types that have been shown to exhibit immunosuppressive functions in the TME was performed. IL-10 at lower concentration had no effect on CD8 T cells and partially inhibited non-activated CD4 T cells. However, when the concentration was increased to 100ng/mL IL-10 had a stimulatory effect on both populations and increased T cell mediated tumour growth control. Studies investigating IL-10 in the context of anti-tumour immune responses have reported mixed results, some supporting the original notion that IL-10 is immunosuppressive and promotes tumour immune evasion and some providing evidence that IL-10 actually enhances activity of cytotoxic lymphocytes within tumours. These opposing results may be due to the different models used in different studies as cytokine signalling in immune cells is highly context specific. IL-10 has been consistently shown to negatively affect the macrophage population by suppression of inflammatory cytokine secretion, downregulation of co-stimulatory molecules, inhibition of NO production, and decreasing antigen presentation capacity (Bogdan et al., 1991; Ding et al., 1993; Thomassen et al., 1996; Waal Malefyt et al., 1991). Timing appears to be of high importance in IL-10 regulation of immune responses. It has been demonstrated that IL-10 may interfere with DC mediated T cell priming, but is necessary for maintenance of CTL effector function post clonal expansion (Fu et al., 2015; Fujii et al., 2001). My findings align with reported stimulatory effect of IL-10 on CD8 T cells such as increase in cytotoxic enzymes and cytolytic activity, IFN γ secretion, and enhanced tumour cell killing (Berman et al., 1996; Chen & Zlotnik, 1991; Emmerich et al., 2012; Giovarelli et al., 1995; Mumm et al., 2011; Naing et al., 2018; Oft, 2014; Santin et al., 2000). Although

indirect effects of IL-10 on CD8 T cell activity and function such as inhibited priming by APCs is not relevant in the context of CEA-TCB because the activation occurs through hyperclustering of CD3 rather than interaction with the TCR, there are indirect effects of IL-10 that may negatively impact CEA-TCB efficacy such as polarisation of TAM towards the M2 anti-inflammatory and tumour promoting phenotype and need to be investigated further.

VEGF was another candidate factor for my screen as it has been described as potent immunosuppressor in addition to its angiogenesis promoting function. However, its direct effect on T cells has not been well characterised. In my model I found that VEGF did not inhibit CEA-TCB induced T cell activity even at a high dose of 100ng/mL. However, as described earlier, VEGF signalling occurs in many different cell types in the TME therefore it can exert immunosuppression also through indirect mechanisms such as Treg and MDSC recruitment. VEGF may also contribute to a poor anti-tumour immune response by controlling T cell trafficking into the tumour and leading to T cell exclusion. Angiogenic inhibitors targeting VEGF and its receptor have been shown to induce vascular normalisation leading to an increase in TILs and improvement in the efficacy of adoptive cell transfer (ACT) immunotherapy in preclinical models (Schmittnaegel et al., 2017; Shrimali et al., 2010). Additionally VEGF, IL-10, and prostaglandin E induced FasL expression on endothelial cells within the tumour resulting CD8 T cell killing and accumulation of Tregs due to their resistance to FasL induced apoptosis through high expression of c-FLIP (Mutz et al., 2014). However, these indirect effects on T cell ability to traffic to the tumour can not be modelled using my co-culture, but can be evaluated in mouse models or in in vitro angiogenesis models.

Hypoxia, being a major feature in solid tumours was a highly relevant factor that needed to be investigated in the context of CEA-TCB activity. Hypoxia at a relevant level for solid tumours (1% O₂) did not hinder the activity of CEA-TCB redirected T cells but improved growth control in 2 of 3 PDO lines. However, validation of hypoxic status by

measurement of HIF1 α or pimonidazole staining was not performed and should be done in the future to assure that the tumour cells and T cells are truly hypoxic. It would also be valuable to investigate the effect of hypoxia on CD4 T cells as its effect appears to be differential to CD8 T cells. Hypoxia increases Foxp3 expression in CD4s through direct binding of HIF-1a to the Foxp3 promoter region inducing Treg differentiation (Clambey et al., 2012). Westendorf et al, showed that hypoxia caused a reduced differentiation of CD4 effector T cells and enhanced number and activity of Tregs (Westendorf et al., 2017). Considering the contribution of CD4 T cells to CEA-TCB mediated tumour cell killing it would be important to investigate whether hypoxia would favour the differentiation of Tregs over induction of the cytotoxic phenotype they acquired under normoxic conditions described in the previous chapter. These findings showing that hypoxia enhances CEA-TCB mediated T cell activity in vitro does not exclude the possibility that hypoxia impairs immunotherapy through other mechanisms such as limited perfusion and T cell infiltration into hypoxic tumour regions and as with VEGF need to be evaluated in other models.

Majority of metastatic CRCs are characterised by high TGF β activity which is predictive of adverse outcomes. Immunosuppressive effects of TGF β on T cell proliferation and effector function have been extensively characterised. TGF β inhibition in a metastatic CRC model unleashed a potent cytotoxic T-cell response leading to tumour regression and rendered tumours susceptible to anti-PD-1–PD-L1 therapy (Tauriello et al., 2018). It has also been demonstrated that CAR-T cells, which have shown poor activity in solid tumours at least in part due to immunosuppressive TME, were inhibited by TGF β with a marked decrease in IFN γ and IL-2 secretion, decrease in cytotoxic gene expression, and increased exhaustion characterised by upregulation of PD-1, CTLA-4, TIM3, and LAG3 (Tang et al., 2020). Knocking out of TGFBR2 abrogated these negative effects and led to improved tumour elimination efficacy. Although some CRC secrete TGF β themselves, majority of the TGF β in the TME is produced by CAFs

(Calon et al., 2015). Therefore in my model, I treated T cell and PDO co-cultures with exogenous TGF β . TGF β impaired CEA-TCB activity, with this inhibitory effect more pronounced at lower E:T ratios which was similarly observed by Tang and colleagues. Mechanistically, TGF β reduced CD8 T cell proliferation and granzyme B expression. Treating the co-cultures with galunisertib, a TGF β RI small molecule inhibitor, resulted in reversal of TGF β inhibitory effects, however this therapeutic approach was only effective at 2:1 E:T and failed to rescue T cell function at lower E:T 0.5:1. IL-2 appeared to more potently reverse TGF β mediated resistance to CEA-TCB therapy as it fully rescued T cell mediated tumour growth control in two PDO models and two different E:T ratios. However, the clinical development of wildtype IL-2 has been hampered by severe toxicities when administered systemically therefore I investigated the effect of a more novel agent FAP-IL2v which is a fusion protein that was engineered to bind IL2R γ β but not the high affinity IL2 α receptor in order to avoid regulatory T cell expansion, and target FAP expressing CAFs in the TME. IL2v cytokine remains active even when it's not cross-linked via FAP which allowed me to use it in my model as a modified cytokine without the incorporation of CAFs into the co-culture. 4-1BBL stimulation has been demonstrated to enhance T cell cytotoxicity, proliferation and alleviate exhaustion therefore it was chosen as the second candidate for reversing TGF β resistance to CEA-TCB. Instead of using anti 4-1BB monoclonal antibodies which are associated with high liver toxicities in patients, I used a novel bispecific antibody that binds 4-1BB and CEA, which has been engineered to avoid cross-linking by Fc γ receptors (Fc γ Rs) and therefore reduce liver toxicity. Both agents reversed TGF β mediated resistance and restored T cell proliferation and granzyme B expression. Currently clinical trials evaluating combination of galunisertib with other immunotherapy agents are being conducted (NCT02734160 and NCT02423343) making it a potential agent for combination treatment with CEA-TCB immunotherapy. Based on my work the combination of CEA-TCB with a TGF β signalling inhibitor has been patented by Roche Glycart. The high prevalence of TGF β activity in metastatic CRCs warrants testing whether CEA-TCB combined with IL2v

immunocytokines or tumour/stroma targeted 4-1BB agonists improve outcomes in clinical trials. FAP-4-1BBL is currently being tested in a Phase 1b clinical trial in combination with CEA-TCB (NCT04826003).

Chapter 6: Establishing a 3D PDO-T cell co-culture model to investigate T cell infiltration and killing of organoids in response to CEA-TCB

6.1 Introduction

The majority of preclinical in vitro cancer research uses cancer cell lines grown as a two-dimensional monolayer. However, over the past couple of decades three-dimensional culture techniques have been developed in order to more closely reflect the characteristics of in vivo tumours. Growing cancer cell lines in a 3D configuration as spheroids has demonstrated key biological differences when compared to traditional 2D cultures. Three dimensional cancer cell line spheroids exhibit different gene expression profiles, altered metabolic profiles, decreased proliferation capacity, decreased sensitivity to cytokines such as interferons, decreased sensitivity to chemotherapy agents and irradiation, and increased resistance to apoptosis (Dangles et al., 2002; Faute et al., 2002; Feder-Mengus et al., 2007; Ghosh et al., 2005; Görlach et al., 1994; Kim et al., 2012; Myungjin Lee et al., 2013; Santini et al., 2004; Weaver et al., 2002). Although 3D cancer cell line culturing more closely mimics tumours than traditional 2D culture, these spheroids still lack morphology patterns observed in tumours. Additionally, due to the long term culture, cancer cell lines may no longer represent the phenotype of their original tumours. These limitations have been addressed by the development of patient derived organoid technologies which allows in vitro propagation of cancer cells from tumour biopsies in 3D conserving the molecular and morphological features of the original tumour (Clevers, 2016). PDOs have been used as a platform for evaluating sensitivity and response to chemotherapy and radiation (K. Ganesh et al., 2019; Pasch et al., 2019; Tiriach et al., 2018). Data from studies comparing PDO and patient responses suggested that PDOs can recapitulate patient responses in the clinic (Vlachogiannis et al., 2018).

The rapid growth of the immunotherapy field has created a need for preclinical in vitro models that allow investigation of tumour-immune cell interactions and thus require the integration of the immune component into existing in vitro models. Although most in vitro models that are used for evaluation of efficacy of immunotherapy agents such as immune checkpoint inhibitors, CAR T cells, and bispecific antibodies are 2D co-cultures of cancer cell lines with immune cells, 3D co-cultures have shown differential response and sensitivity to immune cells thus suggesting that data generated from 2D coculture models might be less clinically relevant. 3D spheroid co-culture studies have shown that changes in structure from two to three dimensional resulted in a dramatic decrease in tumour cells' capacity to activate autologous T cells (Dangles-Marie et al., 2003). Tumour infiltrating lymphocytes that were capable of killing autologous bladder tumour cells in 2D failed to recognise and kill the same tumour cells grown in 3D (Dangles, Validire, et al., 2002). In a melanoma model, functions of tumour associated antigen specific CTLs were impaired when target cells were cultured in a 3D spheroid configuration. CTLs displayed decreased granzyme B, perforin, and FasL expression and reduced IFN γ secretion (Feder-Mengus et al., 2007). It was shown that multiple mechanisms underlie this defective recognition of melanoma cells by antigen specific CTLs including downregulation of TAA expression, downregulation of HLA class I molecules, and increased lactic acid production. Impaired immunorecognition of target cells grown in 3D by T cells has been confirmed by other groups (Ghosh, et al., 2005). In another study, glioma cells grown in 3D upregulated HLA-E expression in comparison to 2D culture which conferred resistance to NK cell cytotoxicity (He et al., 2014). Although these spheroid-immune models more closely resemble the complexity of tumours than 2D cultures, they come with a number of caveats. Most of these spheroid models are generated through ultra-low adhesion U-bottom plates, hanging drop method, or spinner flask cultures forcing the cells to grow in a 3D configuration. However, the resulting spheroids lack organised tissue architecture and polarity and instead form homogenous aggregates of cells which do not recapitulate the tissue architecture of tumours which in

CRC frequently have a glandular morphology with lumen. Additionally these models lack an ECM component adding the immune cells in media thus bringing them into close contact with the cancer cell spheroid (Dangles, Va et al., 2002; Dangles-Marie et al., 2003; Feder-Mengus et al., 2007; Ghosh, Rosenthal, et al., 2005; Thakur et al., 2012, 2013). In vitro systems to analyse tumour-immune interactions have predominantly focused on melanoma, but a few colorectal models have been established. A heterotypic spheroid model comprised of colorectal cancer cell line and fibroblast spheroids generated through hanging drop method and PBMCs added on top was established for the evaluation of immune cell infiltration and assessment of the activity of bispecific antibodies including CEA-TCB (Herter et al., 2017). A similar approach was taken by Courau and colleagues, except they used low adhesion round bottom plates instead of the hanging drop method and they did not incorporate fibroblasts (Courau et al., 2019). Both of these models showed T cell infiltration into the spheroids, but these models did not incorporate an ECM component that the T cells would need to migrate through to infiltrate the spheroid. Recently PDO and immune cell co-cultures have been established. Different culturing approaches have been used. In two organoid-T cell models, pancreatic and rectal cancer, organoids were cultured under normal conditions in 3D embedded in 100% Matrigel domes and T cells were added on top in media. In both of these models T cells collected around the Matrigel dome and some T cells were able to infiltrate organoids at the edge of the dome, but failed to infiltrate more deeply embedded organoids (Kong et al., 2018; Tsai et al., 2018). A study investigating CAR NK cell activity in CRC PDOs experimented with different co-culture methods and found that CAR NK cells were only able to migrate and induce organoid lysis when the organoids were seeded on a thin layer of Matrigel and CAR NK cells were added on top in media, but CAR NK cells failed to infiltrate organoids embedded in Matrigel domes (Schnalzger et al., 2019). Studies of bispecific antibody activity in 3D co-culture using PDOs to my knowledge have not been established therefore my aim was to establish a 3D PDO-T cell co-culture model incorporating an ECM component for investigating T cell

migration and infiltration into different PDO lines. Additionally I wanted to investigate whether organoid size or specific morphology would preclude T cells from infiltrating and successfully killing the organoids when treated with CEA-TCB.

6.2 Establishment of a 3D PDO-T cell co-culture model

My model aimed to combine allogeneic CD8 T cells and PDOs in an extracellular matrix that permits T cell migration and maintains organoid growth. T cells and PDOs needed to be identifiable through distinct fluorescent labels and the assay needed to be stable

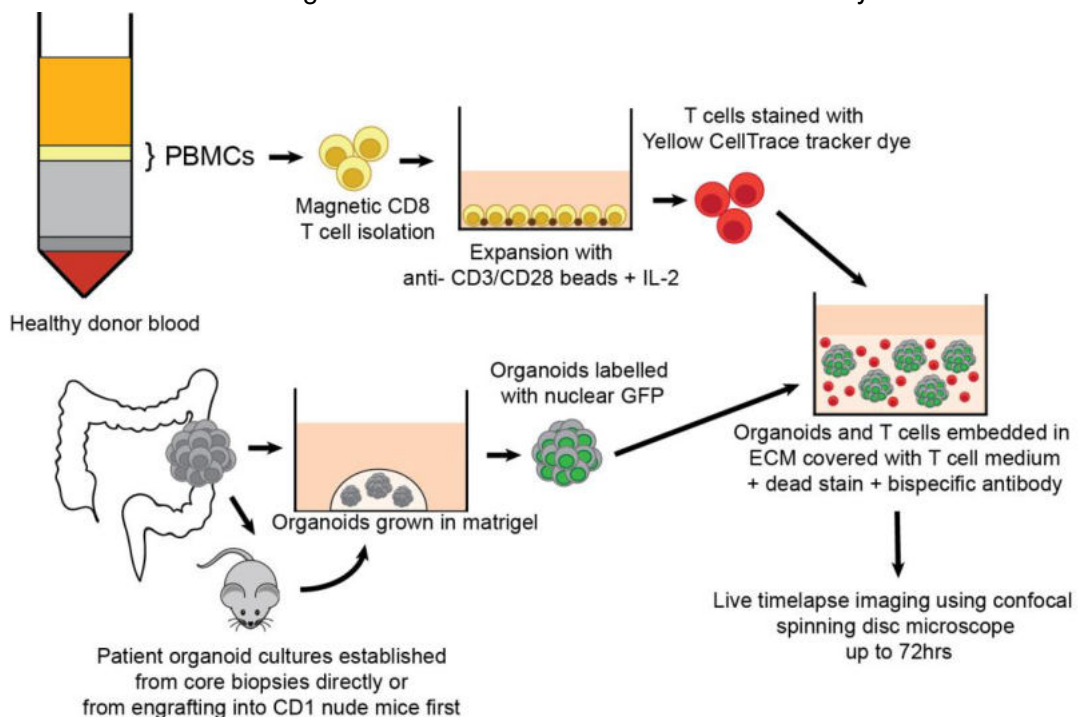


Figure 6.1 Experimental workflow of setting up a 3D CRC PDO and T cell co-culture model. PBMCs were isolated from healthy donor blood from which CD8 T cells were isolated using magnetic beads and were activated and expanded in vitro with anti-CD3/CD28 beads and IL-2. Tumour organoids were established either directly from core biopsies or first undergoing engraftment into CD1 nude and grown in vitro embedded in Matrigel. PDOs had been lentivirally labelled with a GFP tagged histone 2B construct in order to enable visualisation with microscopy. The tumour organoids were carefully harvested for the assay preserving their 3D structure. Prior to the assay the T cells were labelled with a Yellow CellTrace tracker dye. Then the PDOs and T cells were embedded in a Matrigel-collagen extracellular matrix and media containing a DNA binding viability dye (Draq7) and either a control or a CEA binding bispecific antibody was added on top after the gel has polymerised. Multiple conditions were set up in a 96 well plate and were imaged for 72 hours with a spinning disc microscope.

for at least 72 hours of live confocal imaging. In vitro pre-activated CD8 T cells labelled with CellTrace proliferation dye were to be co-cultured with GFP labelled PDOs in a Matrigel-collagen matrix in a 96 well plate overlaid with T cell media with bispecific antibodies and a viability dye. After developing the 3D co-culture methodology my next aim was to develop methods for quantitative analysis of organoid growth, T cell migration/infiltration, and cancer cell killing.

6.2.1 Optimisation of organoid harvesting

First the method for PDO harvesting was optimised in order to assure that intact organoids were seeded into the 3D co-culture assay. PDO stock cultures were grown in 100% Matrigel domes covered by DMEM:F12 20% FCS media. For maintenance passaging the domes were disrupted with a P1000 tip and resuspended in Tryple Express dissociating reagent for 20 minutes at 37°C followed by vigorous pipetting to break up the organoids into single cells. However, for the assay the goal was to preserve organoid structure and remove some of the Matrigel so the PDOs can be resuspended in the 3D co-culture assay matrix. Therefore, I decreased the Tryple Express incubation

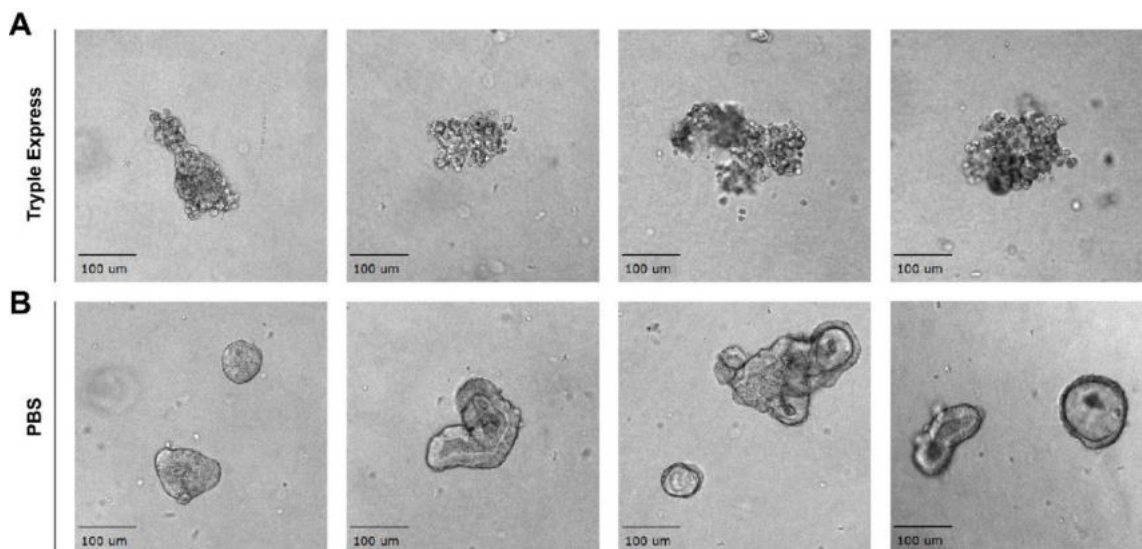


Figure 6.2 Different methods of organoid harvesting. (A) Brightfield images of PDOs that have been harvested with Tryple Express dissociating reagent for 5 min. (B) Brightfield images of PDOs that have been harvested with cold PBS. Brightfield images were acquired with a 10x objective. Scale bars are 100µm.

time down to 5 and 10 minutes, however, in both conditions the organoid structure was disrupted as evidenced by the rough edges and disorganised structure (Figure 6.2A). Matrigel becomes a viscous liquid at 4°C, therefore I investigated whether harvesting with cold PBS would preserve organoid structure while removing the old Matrigel. The domes were mechanically disrupted and the pieces of broken up Matrigel containing PDOs were resuspended in cold PBS for 20 minutes with inversion of the falcon tube every 5 minutes followed by moderate pipetting. Afterwards the organoids were spun down. Although this method failed to remove all of the old Matrigel, it removed enough for the purposes of this procedure and more importantly resulted in preservation of the 3D structure of organoids which is indicated by the clear smooth border and evidence of lumen (Figure 6.2B).

6.2.2 Matrix selection

First I confirmed the findings of previous studies that showed that T cells do not readily infiltrate into PDO containing Matrigel domes. In my model, CD8 T cells showed no migration when either added on top of Matrigel containing PDOs or mixed in together with PDOs in Matrigel in a 96 well plate. After T cells have trafficked to the tumour site they must successfully extravasate from blood vessels penetrating the subendothelial basal lamina. Afterwards they must navigate through the extracellular matrix composed of glycosaminoglycans (GAGs), proteoglycans (PGs), glycoproteins, and collagens, particularly being rich in collagen type I. Collagens form fibre networks that provide a lattice for T cell migration. Based on T cell migration studies collagen type I concentration 2mg/mL was chosen to allow T cell migration within the matrix (Wolf 2003, Kuczek 2019, Friedl 2006, Friedl 1995, Weigelin 2010). Matrigel and collagen were mixed in a 1:1 ratio and then diluted with T cell medium to achieve a matrix that is 33% Matrigel and with a collagen concentration of 2mg/mL. Although the matrix was left to polymerise at 37°C for 1 hour before addition of media on top and start of the timelapse I observed that the

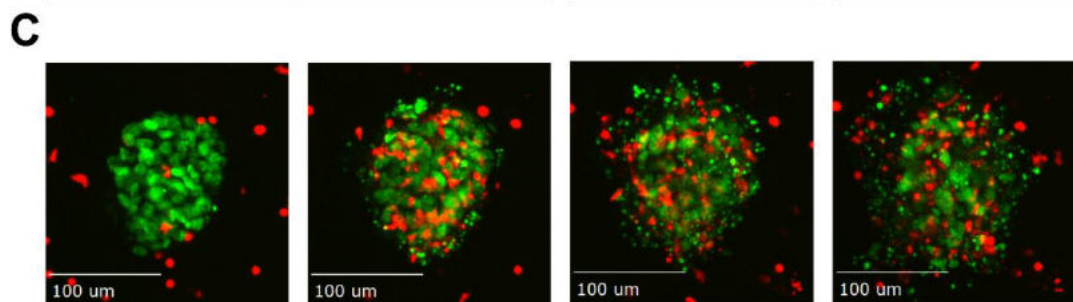
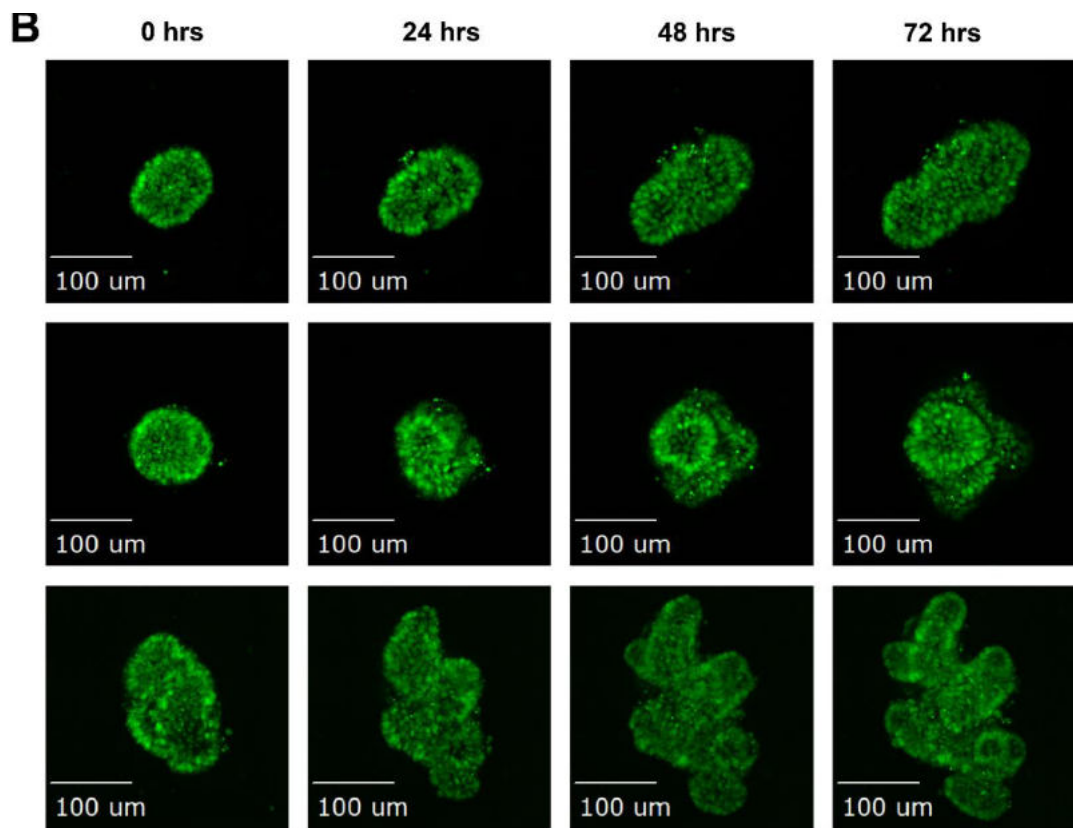
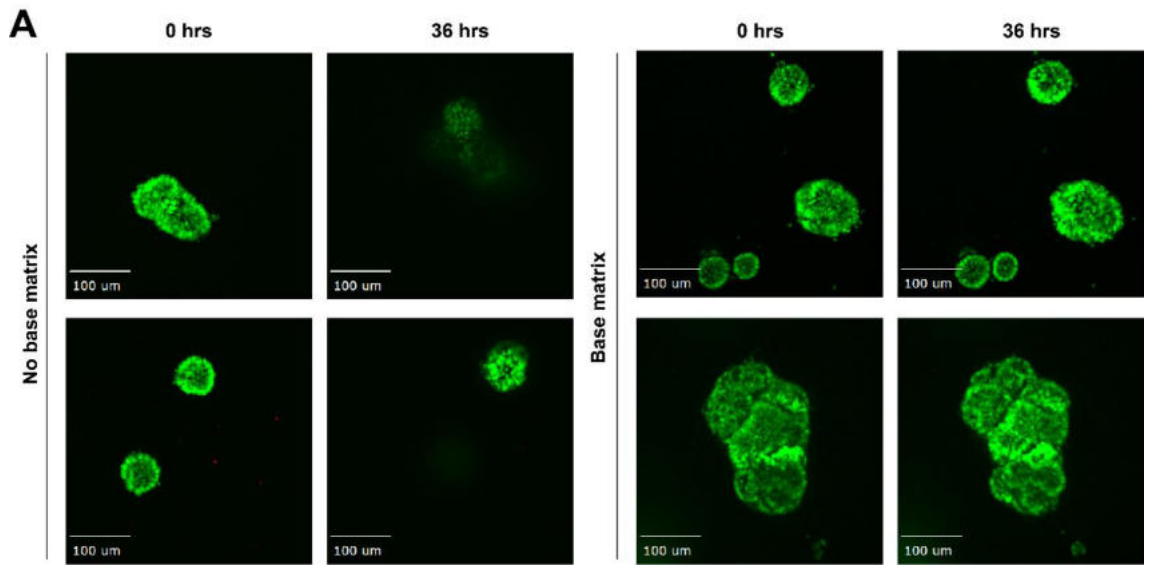


Figure 6.3 Collagen-Matrigel matrix supports PDO growth and T cell migration. (A) Images of PDOs at timepoints 0 hrs and 36 hours of timelapse either plated with or without a base matrix. **(B)** Representative images of PDO growth at timepoints 0 hrs, 24 hrs, 48 hrs, and 72 hrs of timelapse. **(C)** Representative images of T cell (red) infiltration of PDO (green) at timepoints 0 hrs, 24 hrs, 48 hrs, and 72 hrs of timelapse.

PDOs would shift throughout the timelapse with some of them leaving the field of view thus making image analysis impossible. Therefore, I added a new step to the 3D co-culture protocol of coating the bottom of the well with a Matrigel-collagen matrix (without the addition of T cell media) which successfully prevented the PDO shift issue with PDOs remaining in the exact same location throughout the duration of the timelapse (Figure 6.3A). This matrix was able to support PDO growth and T cell migration over 72 hours of live confocal imaging (Figure 6.3B&C).

6.2.3 T cell infiltration analysis

Next my aim was to investigate T cell migration and infiltration into tumours by tracking individual T cell movements. However, with images taken every 30 minutes T cell movement between two timepoints was too great for the software to track because for individual cell tracking analysis to be feasible, migrating cells need to move less than half of the distance between other migrating cells in each time frame. T cells took 24 hours or more to migrate to and infiltrate PDOs followed by another 24-48 hours of PDO killing thus sufficiently short time intervals were not possible due to large data size of 1 TB for a single experiment with 30 minute intervals for 72 hours. A study investigating T cell migration in collagen matrices found that T cells move at an average step length of 7 μ m/min and imaged T cells every 1 min to track individual cells. In addition to the limitation of large data size, imaging this frequently over a span of 72 hours would probably result in high phototoxicity. Therefore, I focused on evaluating the T cell infiltration into PDOs as a first step. In order to estimate the amount of T cells that have

migrated from one timepoint to another I created an image analysis approach that overlaid images taken at various timepoints with the image taken at timepoint 0. This allowed me to count the number of T cells which remained in the exact same position and those that have moved thus estimating the fraction of T cells that have migrated. By 6 hours 66% and 48% from experiment 1 and 2 respectively CD8 T cells co-cultured together with PDOs migrated from their original position at the start of the timelapse (Figure 6.4). CD8 T cells that were seeded alone in the matrix also migrated, but to a lesser extent. By 6 hours 47% and 29% in experiments 1 and 2 respectively of CD8 T cells migrated from their original position. Interestingly, CD8 T cells alone mostly stopped migrating between 36 and 72 hours with an average of 10% migrating between 36 and 72 hours and 2% migrating between 60 and 72 hours (Figure 6.4). Contrastingly, CD8 T cells co-cultured with PDOs continued to migrate throughout the entire duration of the experiment thus suggesting that the PDOs were stimulating T cells to migrate. These findings are in line with a previous study that showed that only 20-50% of T cells developed spontaneous migration in a collagen matrix with the rest of the cells only showing temporary migration or remaining in a spherical non-migratory state (Friedl & Brocker, 2000).

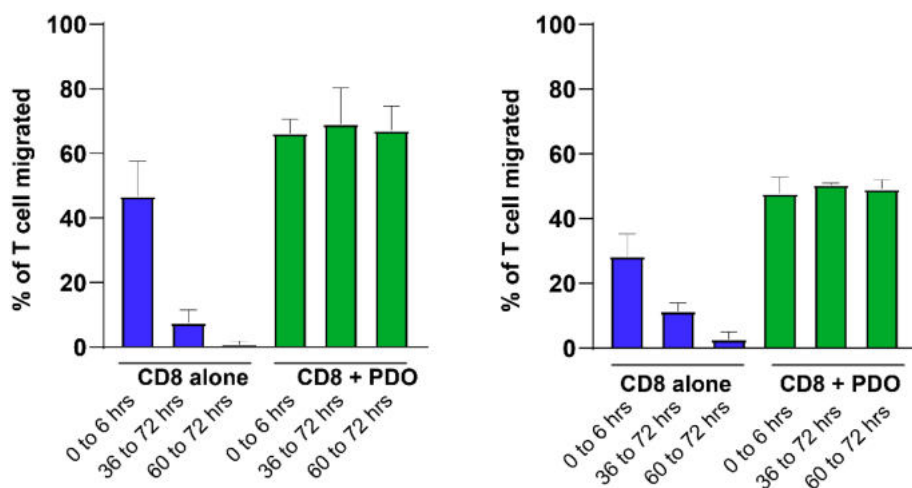


Figure 6.4 T cell migration analysis. Bar graphs showing percent of T cell migration from one time point to another (specified on graph) either alone (blue) or in a co-culture with PDOs (green). Data from two experiments. Error bars represent standard deviation.

To quantitatively assess T cell infiltration into PDOs over time I created a custom pipeline in Cell Profiler software to analyse my timelapse data. Three dimensional timelapses were max projected to create 2D timelapses. For a maximum intensity projection for each XY coordinate, only the pixel with the highest intensity value within the Z-stack is represented so that in a single bidimensional image all structures in a given volume are observed. Organoids were segmented using GFP intensity and organoids close together were separated by shape. After organoids have been segmented (Figure 6.5A1) they were assigned a unique ID (Figure 6.5A2). The module used for that was originally designed for cell tracking, but I used it to give organoids a unique ID because I needed to measure growth and T cell infiltration over time. Since the organoids did not move during the timelapse they retained their unique IDs from time frame to time frame. At the

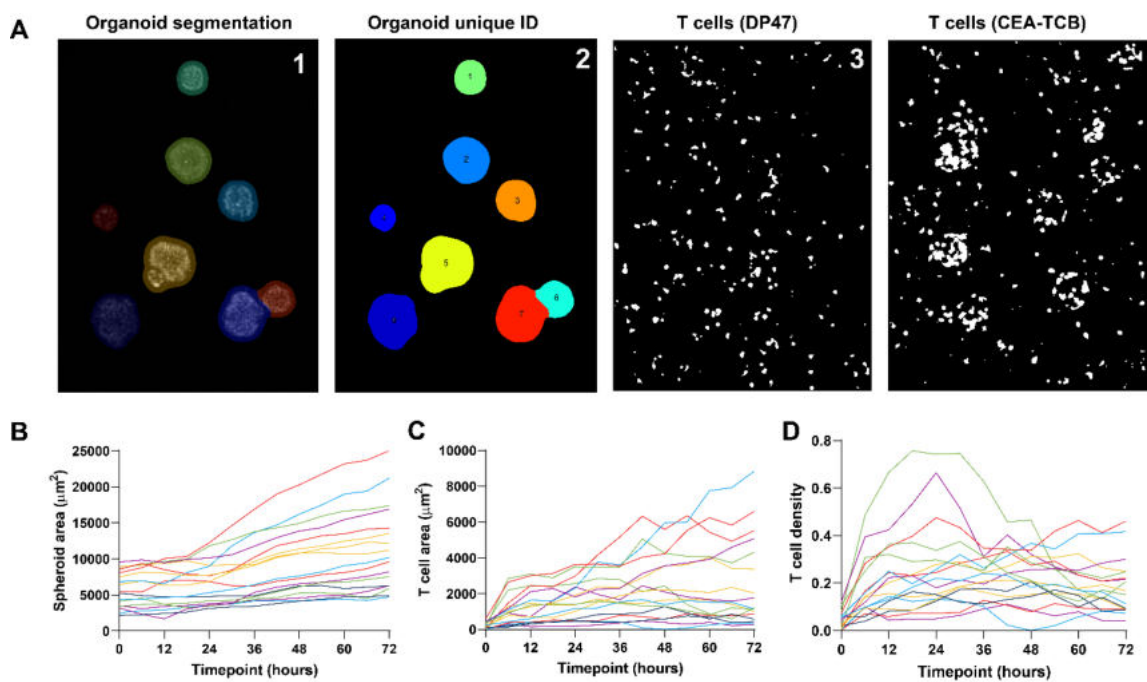


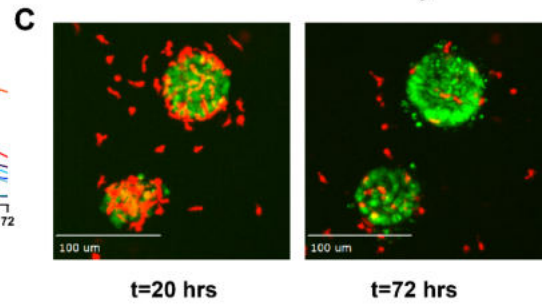
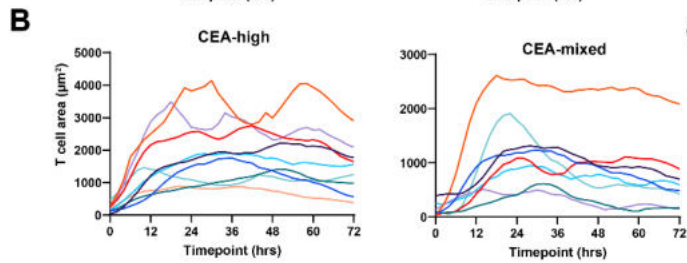
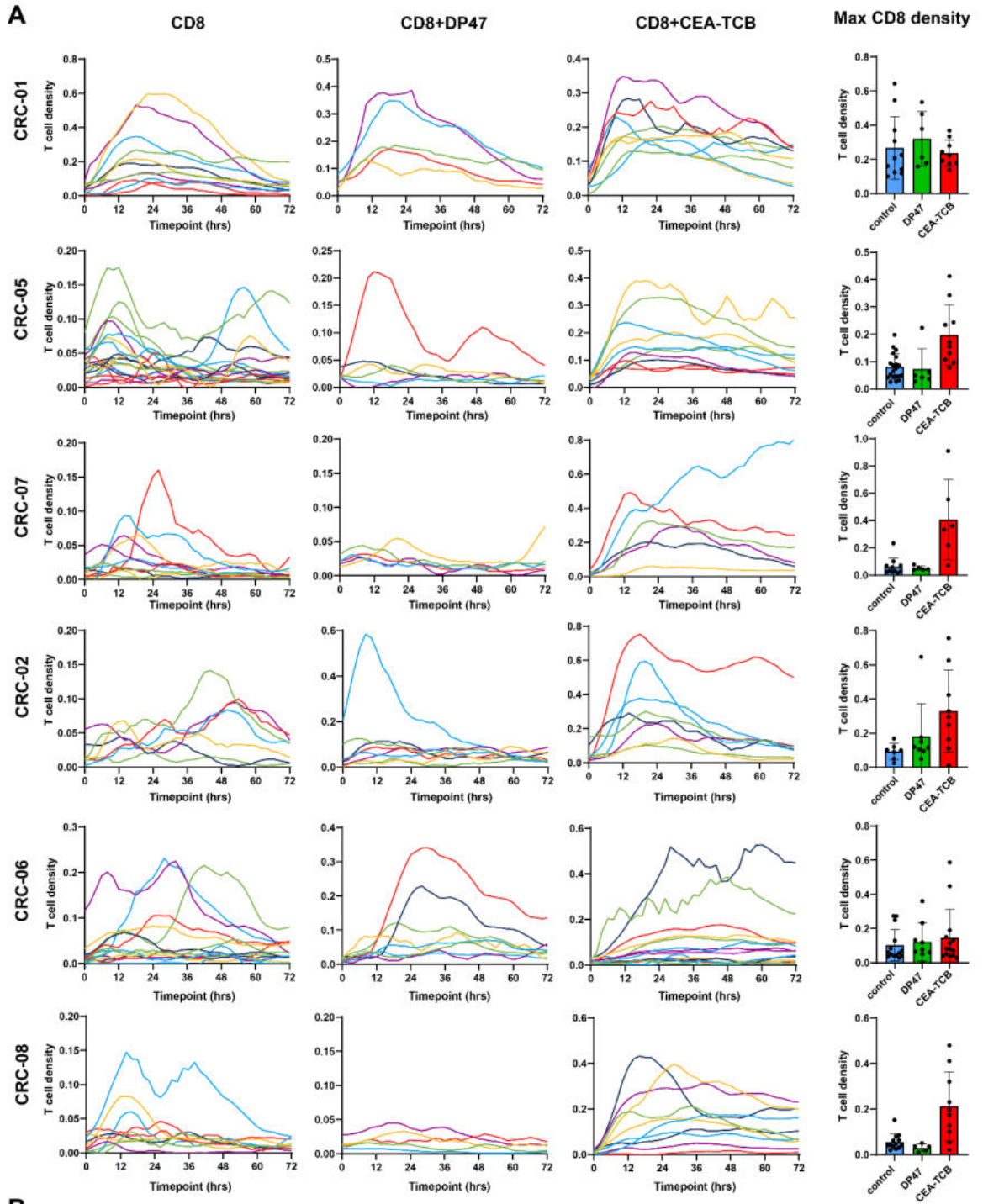
Figure 6.5 T cell infiltration analysis. (A1) Image showing an example of organoid segmentation by Cell Profiler. (A2) Image showing assignment of unique organoid IDs for the duration of the timelapse. (A3) Images showing T cell segmentation by Cell Profiler. An example of DP47 and CEA-TCB conditions are shown. (B) Spheroid growth (spheroid area in μm^2) over 72 hours. Each line represents a single organoid. (C) T cell area inside each organoid over 72 hours. (D) T cell area normalised to organoid area thus showing T cell density. Each line represents T cell density within a single organoid.

same time T cells were segmented based on Cell Trace fluorescence. Because Cell Trace is a proliferation dye its intensity halves every time a T cell divides therefore instead of using total intensity I used T cell area as a surrogate for calculating T cell infiltration (Figure 6.5C). Total T cell area inside each organoid was measured and normalised to organoid area as a proxy for size (Figure 6.5D). Figure 6.5 A3 shows an example of T cell segmentation from a DP47 condition where the T cells are relatively evenly distributed throughout the image, whereas in the CEA-TCB condition T cells are more dense in the organoid areas indicating infiltration.

6.3 Investigating T cell infiltration into PDOs using 3D co-culture model

Firstly I investigated whether PDOs differed in their ability to attract T cells, be infiltrated by them, and the effect of CEA-TCB on both. Six PDO lines were selected: three CEA-high (CRC-01, CRC-05, CRC-07) and three CEA-mixed lines (CRC-02, CRC-06, CRC-08). Each PDO line was set up with three conditions: PDO with CD8 T cells, PDO with CD8 T cells and DP47 (20nM), and PDO with CD8 T cells and CEA-TCB (20nM). Timelapse images were acquired using a spinning disk microscope every 2 hours for 72 hours and were analysed using the analysis method described in 6.2.3. Organoids with CD8 T cells with or without DP47 treatment showed similar low infiltration rates across all PDO lines except for CRC-01. Some organoids in each PDO line exhibited increased infiltration. T cells infiltrated these organoids without killing them as shown in Figure 6.6C, therefore suggesting that these organoids trigger a response that leads to T cell attraction and infiltration. However, in the case of CRC-01 the increase in T cell infiltration in the control and DP47 treated conditions can most likely be attributed to alloreactivity because small amounts of GFP nuclear debris can be observed Figure 6.7B. However, T cell mediated killing caused by alloreactivity did not kill the organoids fully as compared to CEA-TCB treated organoids which were destroyed either nearly or to full completion as indicated by the cloud of GFP debris and lack of intact nuclei at the final timepoint of

the timelapse (Figure 6.7A). Except for CRC-01 which exhibited similarly high levels of CD8 T cell infiltration when treated with CEA-TCB compared to T cells alone or treatment with DP47 and CRC-06 which showed similarly low levels of T cell infiltration under all three conditions, CEA-TCB increased T cell infiltration in all PDOs, both CEA-high and CEA-mixed. An interesting observation is the heterogeneity in T cell infiltrates between organoids within the same PDO line suggesting that even in the presence of CEA-TCB organoids have different ability to attract T cells. Taking CRC-02 as an example, 3 organoids had T cell density below 0.2, 3 had T cell density between 0.2-0.4, and 3 between 0.4-0.8 (Total T cell area in μm^2 /Organoid area in μm^2) (Figure 6.6A). Most organoids also appear to exhibit a decline in T cell density after peak infiltration is reached, which in most cases occurred by 36 hours. In case the reason for the observed decline was due to the organoid growth rate becoming greater than the infiltration rate, absolute T cell area within each organoid was considered. As can be seen in Figure 6.6B, total T cell area within organoids also declined after reaching the peak. This occurred regardless of whether or not the organoids were killed. Images of CRC-02 in Figure 6.6C show peak infiltration at 20 hours and a marked decrease in infiltration by 72 hours, even though the organoids were not killed as they show minimal GFP debris. When a median is taken across all organoids within each PDO line at each timepoint of the timelapse, CRC-02 and CRC-06 show the greatest infiltration with CD8 T cells and DP47 treatment (disregarding CRC-01 which exhibits high infiltration potentially due to alloreactivity) (Figure 6.6D). However, when PDOs and CD8 T cells were treated with CEA-TCB, CRC-02 and CRC-07 showed the greatest infiltration, CRC-01, CRC-05, and CRC-08 showed medium infiltration, and CRC-06 showed the least infiltration (Figure 6.6D). Based on this data, CEA expression status does not appear to determine level of CD8 T cell infiltration and other factors such as chemokine profiles may play a role.



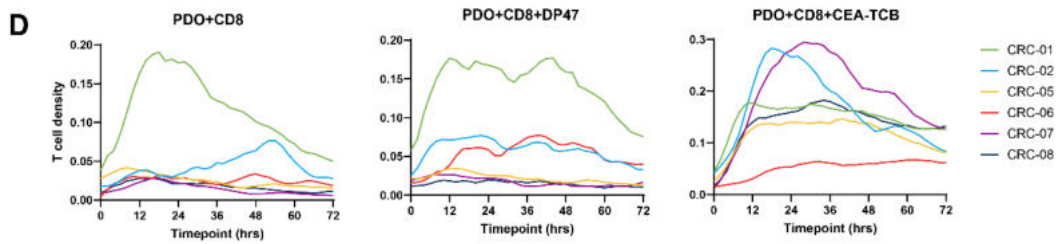


Figure 6.6 CD8 T cell infiltration into PDOs quantification. (A) T cell density curves calculated for individual organoids in six PDOs (CRC-01, CRC-02, CRC-05, CRC-06, CRC-07, CRC-08). Data is organised by columns with each of the three columns representing different treatment conditions: PDO+CD8 T cells, PDO+CD8 T cells+DP47, PDO+CD8 T cells+CEA-TCB. Graphs have been smoothed for ease of visualisation. Bar graphs in column four show maximum T cell density during timelapse with each data point representing a single organoid. Data is also organised by the three treatment conditions. Experiment was performed twice, but only one is shown. **(B)** T cell area (μm^2) calculated for individual organoids in a CEA-high PDO and CEA-mixed PDO over 72 hours. **(C)** Images of CD8 T cell infiltration of CRC-02 treated with CEA-TCB at timepoints 20 hours and 72 hours (final timepoint). Organoids are in green and CD8 T cells in red. The scale bar is $100\mu\text{m}$. **(D)** A median of T cell density was taken across all organoids within each PDO line. Each line represents a PDO line. Graphs have been smoothed for ease of visualisation. Three treatment conditions are presented: PDO and CD8 T cells with no treatment, PDO and CD8 T cells treated with DP47, and PDO and CD8 T cells treated with CEA-TCB.

After developing the T cell infiltration readouts my aim was to assess how tumour cell death can be assessed in this assay. Analysis of area of organoids cultured with or without CEA-TCB was performed in order to assess whether GFP positive organoid area could be used as a surrogate for tumour cell death as it decreases in size with progressive T cell mediated killing. However, the high density of strongly GFP positive nuclear debris prevented accurate measurement of the remaining viable organoid area therefore a different quantitative approach needed to be established (Figure 6.7D). However, even in the absence of a quantitative cancer cell death readout a couple observations can be made based on visual assessment of the images. CEA-high PDOs showed either complete or near complete death when treated with CEA-TCB as evidenced by the large area of nuclear debris and few or none intact nuclei remaining. Whereas CEA-mixed PDOs showed a range of organoid destruction, some showed no killing despite high infiltration, some showed partial death with some nuclear debris but

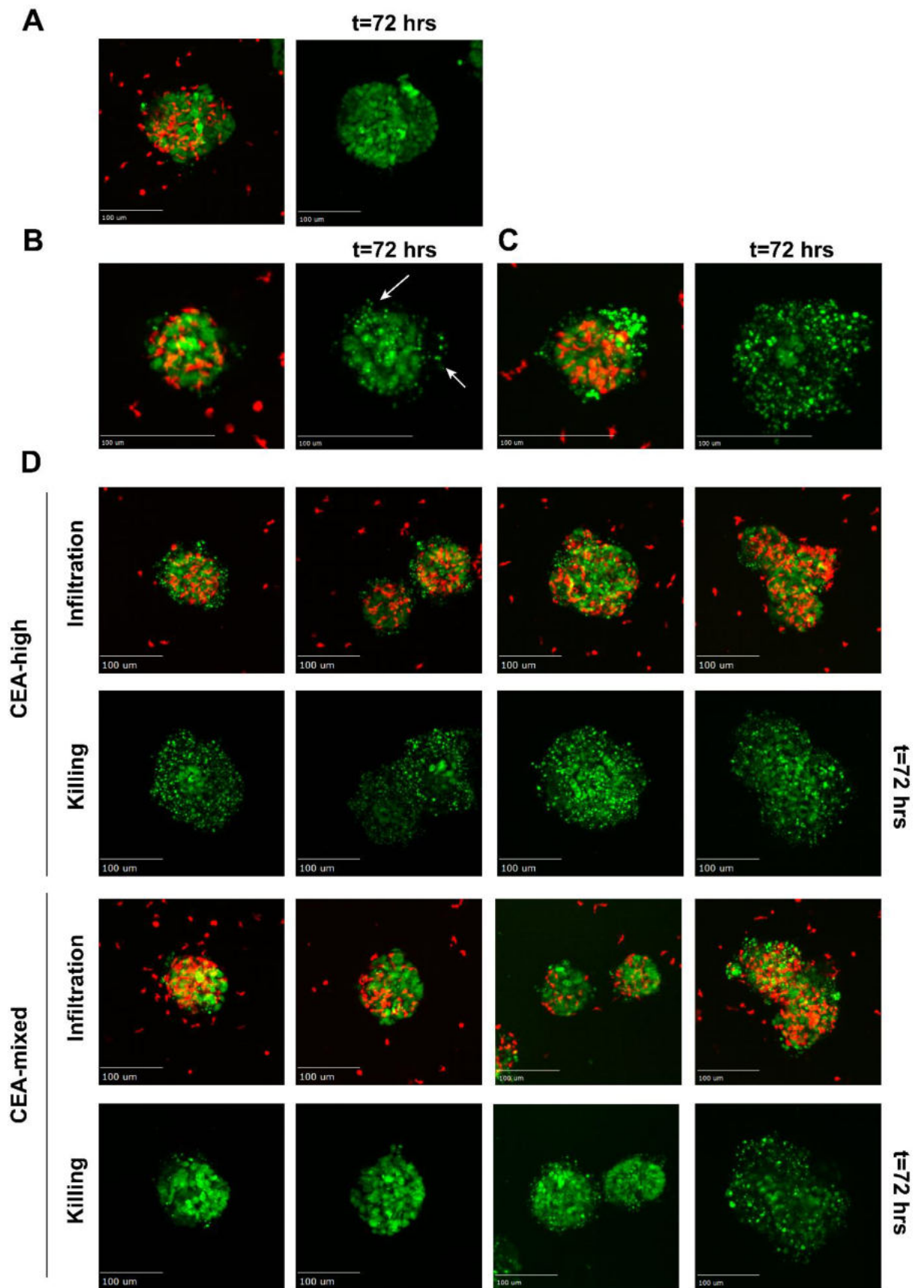


Figure 6.7 Images of T cell infiltration into PDOs and T cell mediated tumour cell death. (A) Images of CRC-06 organoid co-cultured with CD8 T cells and no bispecific antibody treatment. First image shows T cell infiltration into the organoid. In the second image the T cell fluorescence channel was removed to be able to clearly see the full organoid at the final timepoint of 72 hours. (B) Images of CRC-01 organoids co-cultured with CD8 T cells with no bispecific antibody treatment. First image shows T cell infiltration while the second image shows organoid at the final timepoint of 72 hours. In the second image the T cell fluorescence channel was removed to be able to clearly see nuclear debris indicating tumour cell death and the remaining intact nuclei. (C) Images of CRC-01 organoids co-cultured with CD8 T cells treated with CEA-TCB. First image shows T cell infiltration while the second image shows organoid at the final timepoint of 72 hours. In the second image the T cell fluorescence channel was removed to be able to clearly see nuclear debris indicating tumour cell death and the remaining intact nuclei. (D) Images showing T cell infiltration (different timepoints, images were chosen based on peak infiltration levels) and organoids at 72 hours (final timepoint was chosen to show maximal tumour cell death if any was present). Images were grouped by CEA expression profiles with 2 groups: CEA-high and CEA-mixed. All images have a scale bar of 100µm.

still many remaining intact nuclei, and some showed complete or near death with large amounts of debris and few or none intact nuclei remaining (Figure 6.7D). Most CRC-06 organoids showed no killing despite high infiltration whereas CRC-08 showed a wide range of responses with either no death, partial death, or complete death. Both of these PDOs have similar CEA expression levels (Chapter 1) therefore some CEA-TCB resistance might be at play. To investigate this further, organoids need to be harvested post killing assay and stained for CEA expression to determine if all of the remaining cells are CEA low or negative, or if some CEA-high expressing cells were able to evade CEA-TCB facilitated T cell mediated killing.

6.4 Establishment of cancer cell death readout

In order to be able to quantify cancer cell death, DRAQ7 which is a membrane impermeable dye that stains double stranded DNA of dead cells, was added to the media of the 3D co-culture model. However, this stain does not distinguish between cancer cell death and T cell death that may occur as a result of activation-induced cell death (AICD).

Two CEA-high PDOs, CRC-01 and CRC-07, were chosen to test the new method of measuring cancer cell death. This time a different PBMC donor was used and neither PDO line showed alloreactivity. As seen in the previous assay, CEA-TCB increased CD8 T cell infiltration into the organoids compared with the level of T cell infiltration observed in control conditions (PDO+CD8 and PDO+CD8+DP47). Both PDOs showed a similar level of organoid infiltration when treated with CEA-TCB (Figure 6.8A). However, CRC-01 organoids were more infiltrated under control conditions when compared with CRC-07. A median was taken across all organoids within the same condition of each PDO to show the general trend of infiltration in each condition. Both PDOs achieved a median peak T cell density of 0.25. Whereas under control conditions T cell density in CRC-07 was below 0.05, while that of CRC-01 was between 0.05 and 1 (Figure 6.8A). The average maximum T cell density was 0.14 in PDO plus T cell condition and 0.22 in DP47 treated condition in CRC-01, while in CRC-07 those values were 0.04 and 0.06 respectively (Figure 6.8B). The average maximum T cell density for CEA-TCB treated condition was similar between both PDOs at 0.32 for CRC-01 and 0.37 for CRC-07.

In order to measure cancer cell death within each organoid, DRAQ7 median fluorescence intensity was measured within the organoid area. Under control conditions organoids exhibited either no or low levels of cancer cell death. It should be noted that organoids exhibit some spontaneous cell death even when cultured alone without T cells. With CEA-TCB treatment, both PDOs showed an increase in cancer cell death which correlates with what can be observed visually. Images in Figure 6.8D show organoids for both CRC-01 and CRC-07 at timepoint 0 (start of the timelapse) and the final timepoint of the timelapse at 72 hours. Both PDOs were effectively killed by T cells as indicated by the lack of intact nuclei remaining and the presence of nuclear debris. The third image in each row shows DRAQ7 fluorescence at 72 hours confirming extensive cell death.

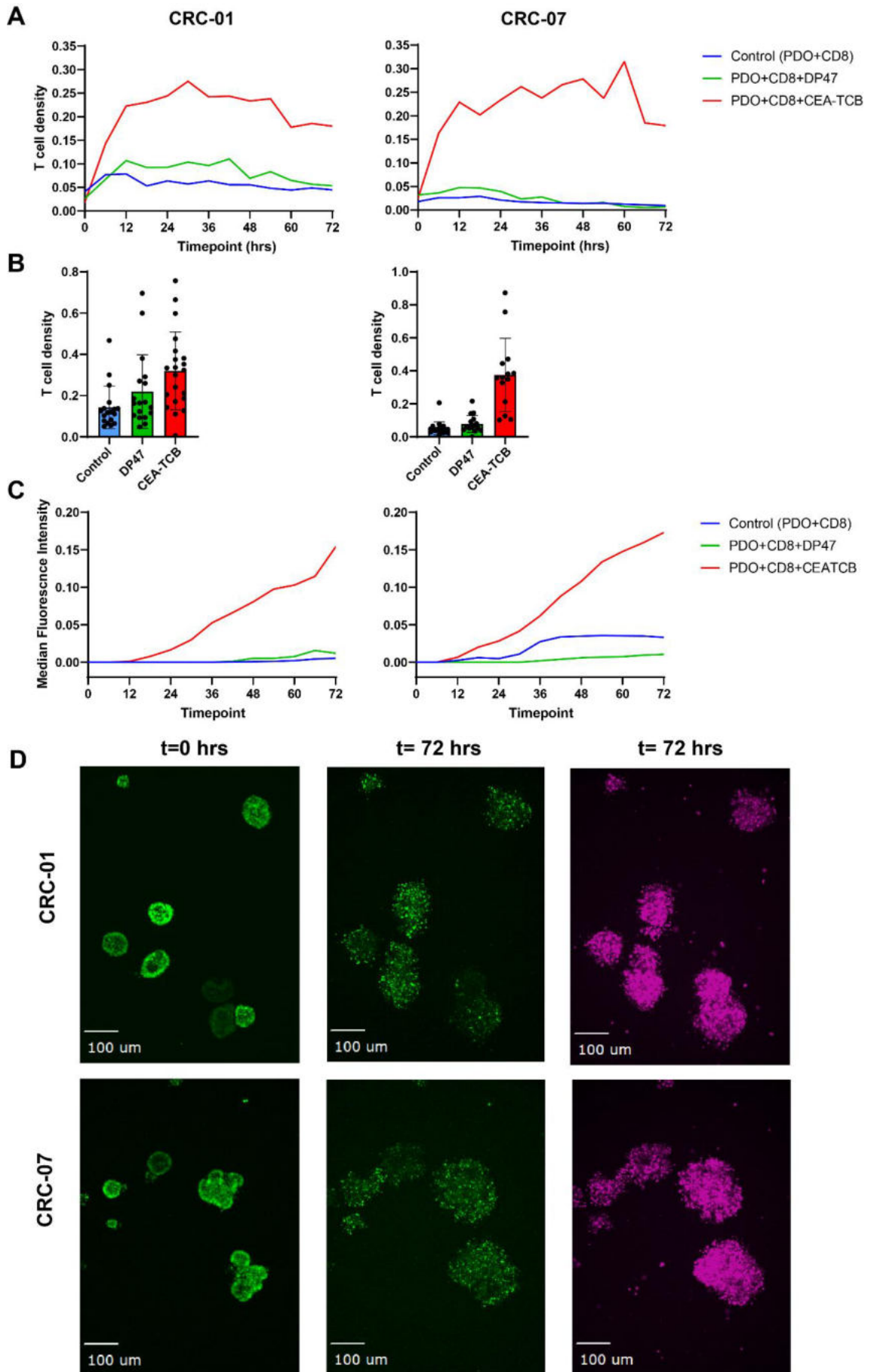


Figure 6.8 Quantifying cancer cell death in 3D co-culture assay. (A) Graphs of CEA-high PDO, CRC-01 and CRC-07, CD8 T cell infiltration over 72 hours of 3D co-culture assay. Median values of T cell density of all organoids within each condition and each PDO is plotted. Three treatment conditions are shown: PDO+CD8 (blue), PDO+CD8+DP47(green), PDO+CD8+CEA-TCB (red). **(B)** Bar graphs showing maximal T cell density of individual organoids within each condition and PDO. Each point represents a single organoid. Graph shows mean maximum T cell density with SD. **(C)** Graphs showing median fluorescence intensity of DRAQ7 with a median taken across all organoids within each of the three treatment conditions and each PDO line. **(D)** Images showing CRC-01 and CRC-07 treated with CD8 T cells and CEA-TCB at timepoints 0 and 72 hours. For all images T cell fluorescence channel has been removed to focus on cancer cell death. First two images show GFP signal from organoids and the third image shows DRAQ7 fluorescence signal at the final timepoint of 72 hours. All scale bars are 100µm.

6.5 Effect of organoid size and morphology on T cell infiltration

Cancer cell agglomerates in actual tumours can be large, requiring T-cells to deeply penetrate for effective tumour control. There, T cells encounter harsh conditions including nutrient depletion and high concentrations of metabolites such as lactate which can promote T-cell dysfunction (Fischer et al., 2007; Lanitis et al., 2017). Colon cancers can furthermore show different growth morphologies, from well differentiated tumours that retain gland-like structures to poorly differentiated ones growing as densely packed cancer cell nodules (Figure 6.10A&B) (Fleming et al., 2012). Whether large size or specific morphologies represent barriers to T cells penetration or function during CEA-TCB treatment is unknown. Six PDO lines were categorised based on morphology; CRC-01, CRC-04, and CRC-05 show well differentiated gland like structure with lumen (hollow), CRC-05 and CRC-06 grow as poorly differentiated solid masses (compact), and CRC-02 exhibits a unique growth pattern of gland like structures with lumen that are filled with densely packed nuclei (Figure 6.9A). Imaging of the central slice of organoids revealed that all growth patterns were infiltrated by CEA-TCB redirected T cells, which were present on the inside and outside of walls of well differentiated organoids growing as glands or spheres and throughout the compact spheroid mass of poorly differentiated organoids (Figure 6.9B).

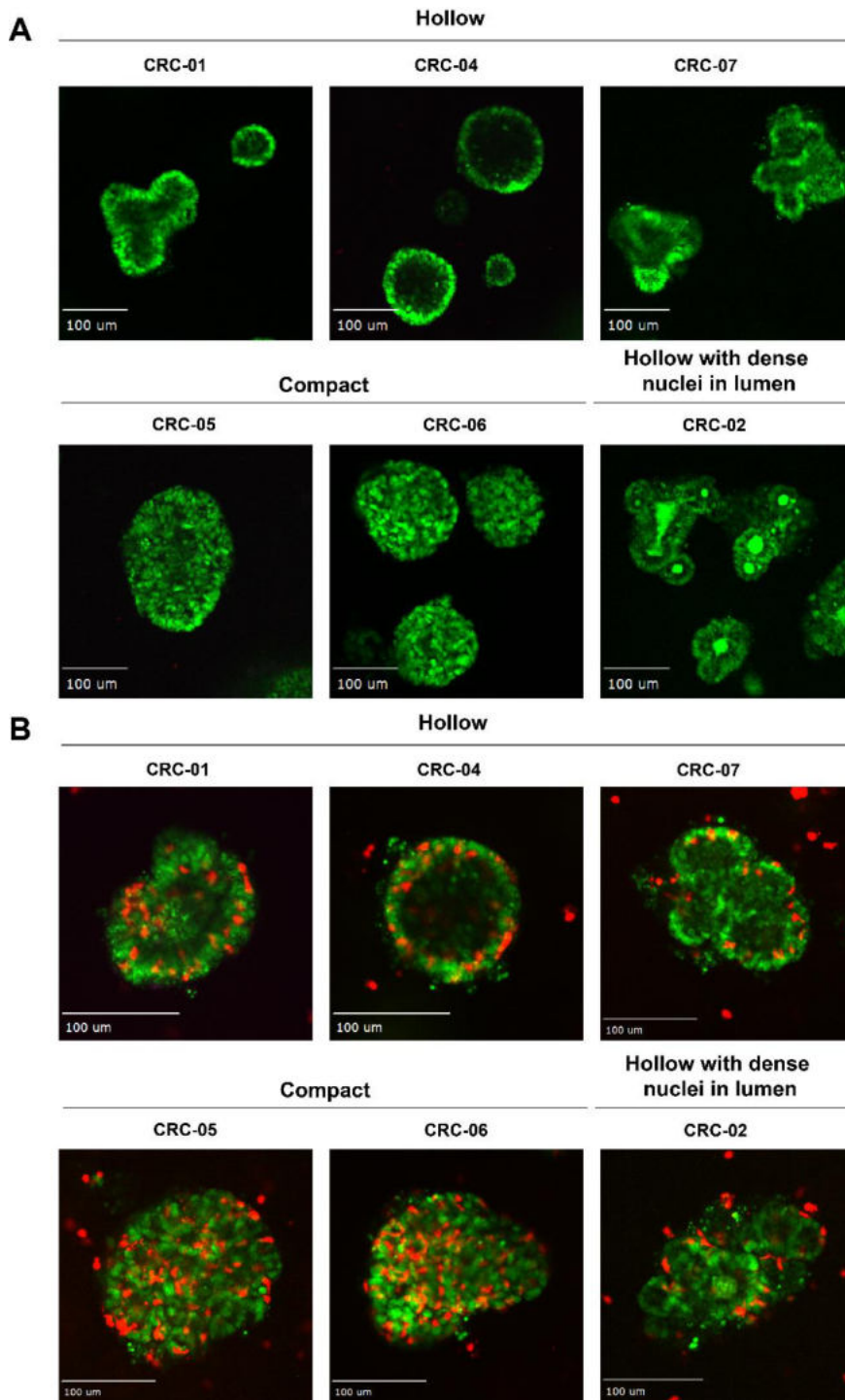


Figure 6.9 Effect of organoid morphology on T cell infiltration. All images are slices from 3D z-stacks showing the middle of the organoid. Organoids are in green and where applicable CD8 T cells are in red. All scale bars are 100 μ m. **(A)** Images showing morphology of six PDOs CRC-01, CRC-02, CRC-04, CRC-05, CRC-06, CRC-07, organised by morphology type. **(B)** Images of T cell infiltration from CEA-TCB treated PDO and CD8 T cell co-cultures organised by different morphologies.

In order to address the effect of organoid size on T cell infiltration and killing organoids were grown for different amounts of time and combined together for the 3D organoid-T cell co-culture assay. Smaller organoids were grown for 11 days while larger ones were cultured for 21 days prior to seeding for the assay. For analysis organoids were classified by size into small organoids (organoid area at 0 hours $6000\mu\text{m}^2$ or less), medium organoids (organoid area at 0 hours greater than $6000\mu\text{m}^2$ or less than or equal to $12,000\mu\text{m}^2$), and large organoids (organoid area greater than $12,000\mu\text{m}^2$ at 0 hours). Median diameter was $67\mu\text{m}$ for small organoids, $102\mu\text{m}$ for medium, and $147\mu\text{m}$ for large. These diameters are similar to the size of cancer cell nodules or glands histologically observed in patient tumours (Figure 6.10C). Images of central slice of organoids showed that T cells redirected by CEA-TCB were able to infiltrate into small

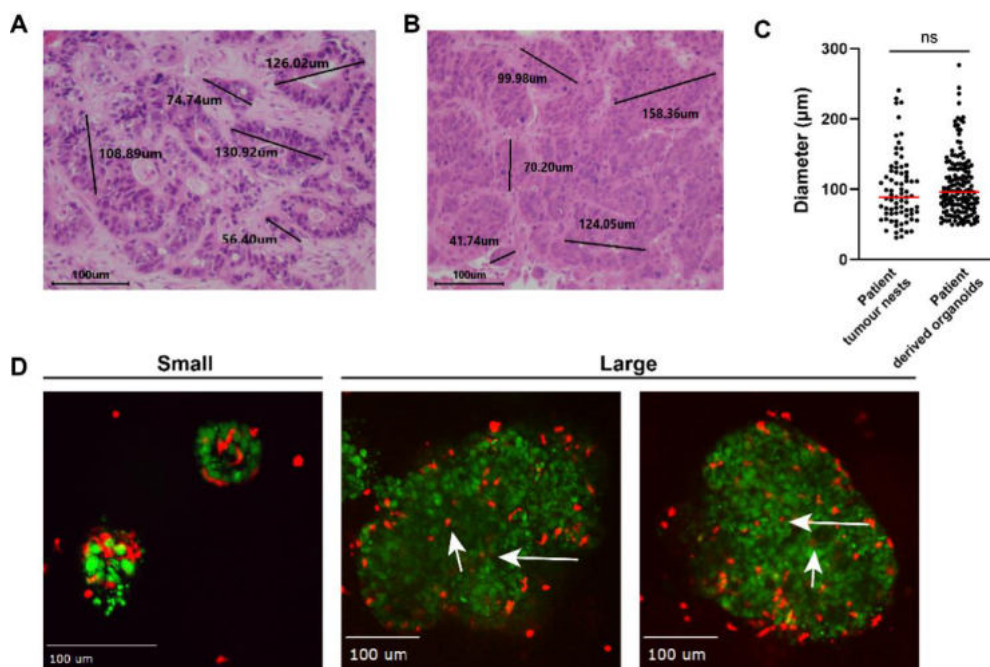


Figure 6.10 Comparison of patient tumour nest and PDO size. (A) Example image of tumour nest measurements on H&E stained well differentiated CRC. (B) Example image of tumour nest measurements on H&E stained poorly differentiated CRC. Both images were taken and analysed by Dr Ben Challoner in my lab. (C) Size comparison between tumour nest in 15 CRCs (5 measurements per tumour) and all PDOs from experiment comparing different organoid sizes. (D) Images of T cell infiltration from CEA-TCB treated PDOs (CRC-01, -05, -06) and CD8 T cell co-cultures organised by size (small and large). All images are slices from 3D z-stacks showing the middle of the organoid. Organoids are in green and CD8 T cells are in red. All scale bars are $100\mu\text{m}$. White arrows pointing to T cells in the centre of large organoids.

organoids as well as into the centre of large compact organoids measuring up to 355µm in diameter (Figure 6.10D).

6.5.1 T cell infiltration into organoids of different sizes

Under control conditions, more T cells infiltrated large organoids from CEA-mixed PDOs (CRC-02, CRC-04, CRC-06) than organoids from CEA-high PDOs (CRC-01, CRC-05, CRC-07) (Figure 6.11C). T cell infiltration quantification showed that T cell densities were similar regardless of organoid size in CEA-TCB treated organoids except for CRC-06 which showed a correlation between organoid size and T cell density with the smallest organoids being most infiltrated and large organoids being the least infiltrated (Figure 6.11A). CEA-TCB significantly or near significantly increased T cell infiltration in all PDOs and all organoid sizes (Figure 6.11B). Despite being CEA-high, CRC-05 and CRC-07 were the least infiltrated in both treatment conditions and organoid sizes, the difference being most dramatic in large CEA-TCB treated organoids (Figure 6.11C). Interestingly, CRC-02 and CRC-06 which have a mixed CEA expression profile, showed the greatest infiltration in both small and large organoids when co-cultures were treated with CEA-TCB (Figure 6.11C). T cell infiltration analysis of this experiment showed that neither the distinct PDO architecture, nor the size of individual organoids negatively affected T cell infiltration into PDOs.

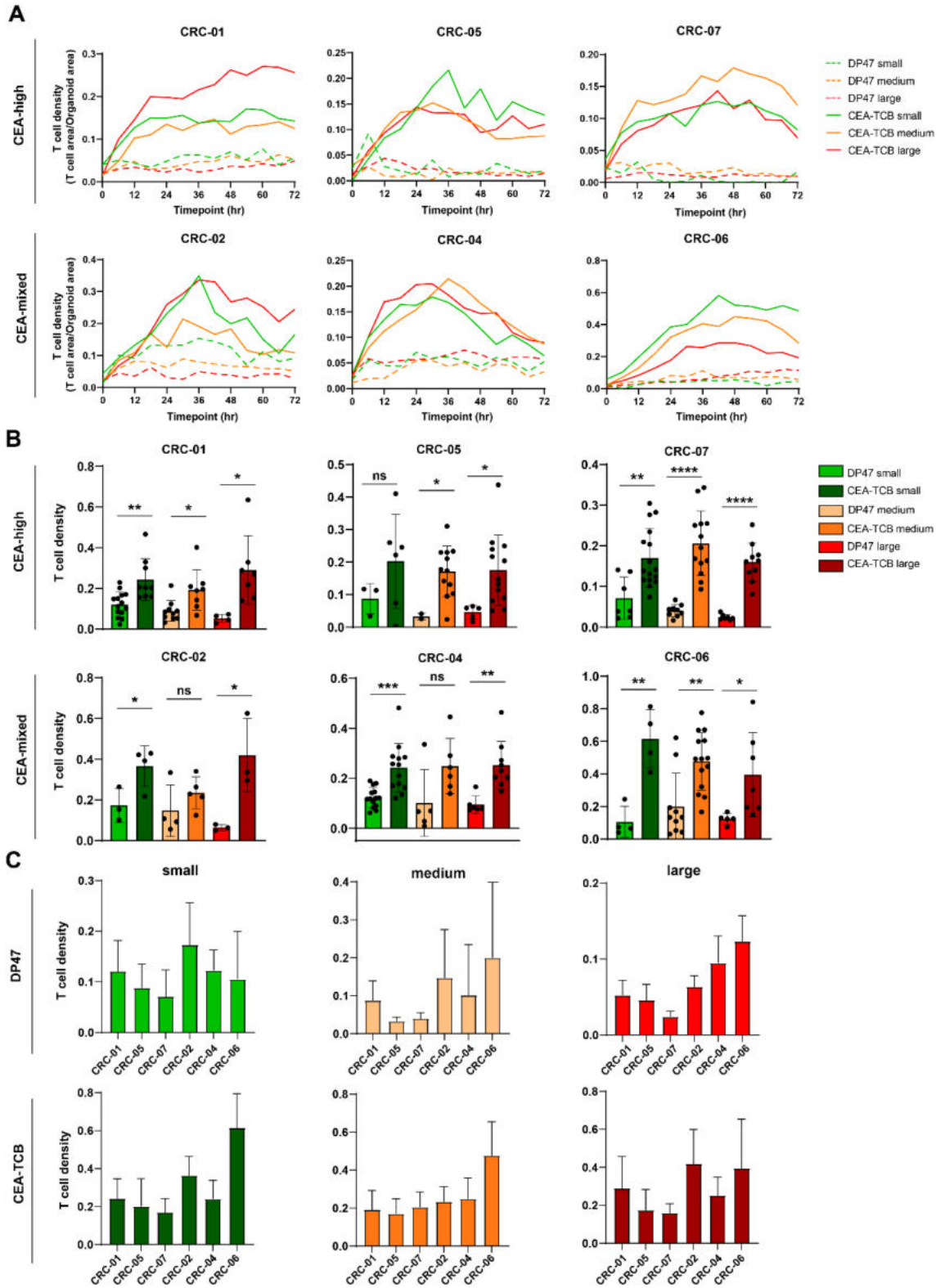


Figure 6.11 Quantification of T cell infiltration into organoids of different sizes. (A) Graphs of T cell density in organoids over 72 hours. Median values of T cell density of all organoids within each condition and each PDO is plotted. Data is organised by CEA expression status, treatment conditions (DP47 and CEA-TCB), and three organoid sizes (small, medium, large). (B) Maximum T cell density within each organoid during the 72 hour co-culture assay (same data as in B but organised by organoid size rather than PDO). Each point represents an individual organoid. Data is organised by CEA expression status, treatment conditions (DP47 and CEA-TCB), and three organoid sizes (small, medium, large). Statistical analysis was performed using an unpaired t-test. For all growth analysis P values are as follows: > 0.05 is ns, < 0.05 is *, < 0.01 is **, <0.001 is ***, <0.0001 is **** and ns = not significant. (C) Graphs of maximum T cell density in organoids. Data is organised by treatment (DP47 and CEA-TCB), organoid size (small, medium, large) and PDO line.

6.5.2 Effect of organoid size on T cell mediated killing of tumour cells

In order to investigate if organoids of different sizes are as effectively killed by CD8 T cells in the presence of CEA-TCB, DRAQ7 median fluorescence intensity was quantified. All organoids exhibited low levels of cancer cell death even in the control condition (treated with DP47). But large organoids in the control condition in particular showed the highest level of cancer cell death. Figure 6.12B shows an example of dead cancer cells accumulating in the lumen of an organoid grown without T cells over the span of 72 hours. When treated with CEA-TCB all three size groups exhibited cancer cell death. (Figure 6.12A). Interestingly, in CEA-high organoids CRC-01 and CRC-05 smaller organoids exhibited more resistance to killing compared to larger ones, while CRC-07 small organoids got killed more efficiently than medium and larger organoids (Figure 6.12A). The timing of cancer cell death also varied between different PDOs. In most PDOs cancer cell death occurred gradually, whereas CRC-06 showed no cancer cell death until 48 hours and after that timepoint experienced rapidly increasing cancer cell death. This was despite the same time of peak T cell infiltration in CRC-06 and CRC-07 (Figure 6.11A). High CEA expression and adequate T cell infiltration may not be the only

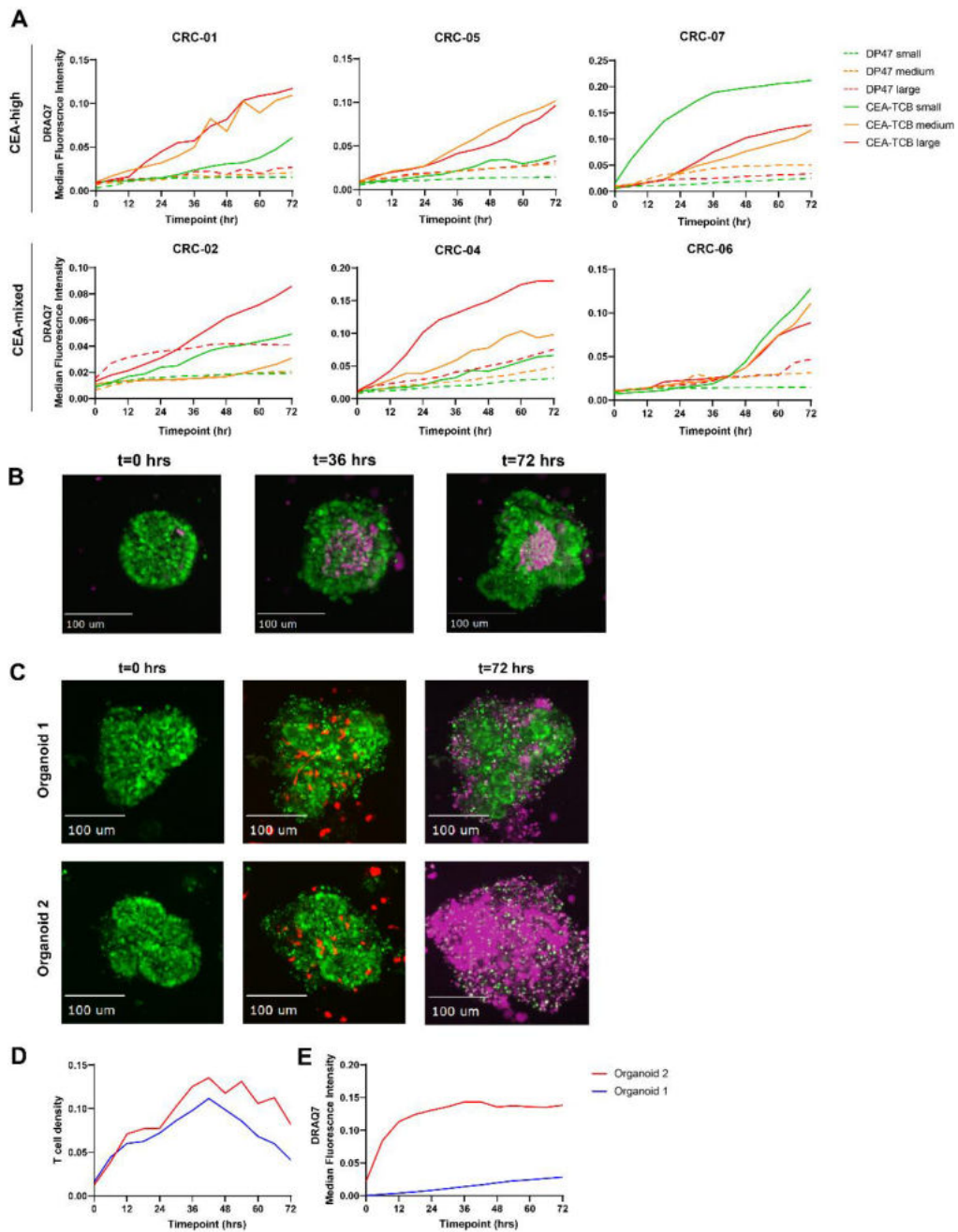


Figure 6.12 Tumour cell killing by CD8 T cells. (A) Graphs of DRAQ7 median fluorescence intensity in organoids over 72 hours. Median values of DRAQ7 MFI of all organoids within each condition and each PDO is plotted. Data is organised by CEA expression status, treatment conditions (DP47 and CEA-TCB), and three organoid sizes (small, medium, large). Data is from a single experiment in which data from individual organoids were pooled. (B) Image of an organoid (green) grown alone without co-culture with T cells and DRAQ7 (purple) at three timepoints: 0, 36, 72 hours. Scale bar is 100 μ m. (C) Images of two CRC-07 organoids co-culture with CD8 T cells and treated with CEA-TCB. Left images show organoid at the beginning of timelapse (0 hrs). Middle images are representative images of CD8 T cell (red) infiltration into organoids (green). Right images show organoid (green) and DRAQ7 (purple) at 72 hours, the final timepoint of timelapse. All scale bars are 100 μ m. Continued on next page.

(D) Graph showing T cell density quantification in organoid 1 and 2 from (C). (E) Graph showing DRAQ7 median fluorescence intensity in organoids 1 and 2 from (C).

factors affecting CEA-TCB activity. Two similarly sized CRC-07 organoids were compared in their T cell infiltration and cancer cell death. Both had similar levels of T cell infiltration, but organoid 1 exhibited minimal death, while organoid 2 was completely destroyed as evidenced by the strong DRAQ7 fluorescence and GFP positive nuclear debris therefore suggesting CEA-TCB resistance (Figure 6.12C-E). To investigate the mechanisms driving resistance to CEA-TCB a method of individual organoid harvesting post 3D killing assay needs to be developed. These organoids could be single cell RNA sequenced to determine drivers of resistance. However, due to the complexity of this potential methodology and COVID related restrictions I have not had the opportunity to develop this technique.

6.6 Increasing complexity of 3D co-culture model by adding a stromal component

Successful infiltration of T cells into the tumour is a prerequisite for T cell mediated killing of cancer cells. However, frequently tumours exhibit an immune excluded phenotype, with T cells being restricted to the invasive margins or the stromal regions of the tumour. Multiple studies have reported reduced CTL infiltration in CAF (cancer associated fibroblast) rich tumours compared to CAF low tumours (Ford et al., 2020; Jiang et al., 2018; Kato et al., 2018). CAFs have been shown to prevent T cell infiltration into tumours by several different mechanisms. CAFs secrete soluble factors such as CXCL12 and TGF β that have been demonstrated to lead to T cell exclusion (Ene-Obong et al., 2013; Feig et al., 2013; Mariathasan et al., 2018). A hallmark of activated CAFs is their ability to aberrantly deposit and remodel extracellular matrix (ECM) leading to dense networks of collagen, fibronectin, and other ECM proteins around tumour islets. A study using live

cell imaging of viable slices of human lung tumours revealed that T cells preferentially accumulated in the stromal regions and were rarely found in tumour cell regions (Salmon et al., 2012). Tumour islets were encapsulated by dense networks of parallel ECM fibres that prevented successful T cell migration and infiltration into tumours. They showed that T cell counts were negatively correlated with ECM density and that fibronectin rich regions, such as areas immediately surrounding tumour islets, inhibited T cell motility. Matrix loosening through collagenase treatment led to an increased infiltration of CD8 T cells into tumour islets, with a twofold increase in the number of T cells in contact with tumour cells (Salmon et al., 2012). Another study supported these findings by showing that T cell migration was inhibited in dense collagen matrices compared to active migration observed in low density collagen matrices (Hartmann et al., 2014). Due to their immunomodulatory functions and their role in T cell exclusion, CAFs have been incorporated into in vitro models studying tumour-immune interactions and evaluating activity of immunotherapeutic agents (Herter et al., 2017; Tsai et al., 2018). However, modelling tumour stroma in a physiologically relevant way is difficult. In a colon heterotypic spheroid model fibroblasts and tumour cells were co-cultured together prior to addition of immune cells. Tumour cells formed an external peripheral layer surrounding the central core of fibroblasts while in patient tumours the fibroblasts usually surround tumours, thus better models incorporating CAFs are needed (Herter et al., 2017).

RNA sequencing of RC11 CAFs which are human fibroblasts from rectal carcinoma (provided by Dr.Fernando Calvo) showed that they express high levels of CXCL12 and TGF β 1 compared to no or minimal levels of expression by PDOs (Figure 6.13A). Next, RC11 were grown in different matrices and a viability assay using CellTiter Glo was performed. When cultured in Matrigel alone CAFs remained round and after 4 days of culture the viable cell number was reduced by 57% compared to viability after 24 hours (Figure 6.13B). Culturing CAFs in the matrix used in the 3D co-culture model reduced the number of viable cells by 40%, which was an improvement over Matrigel

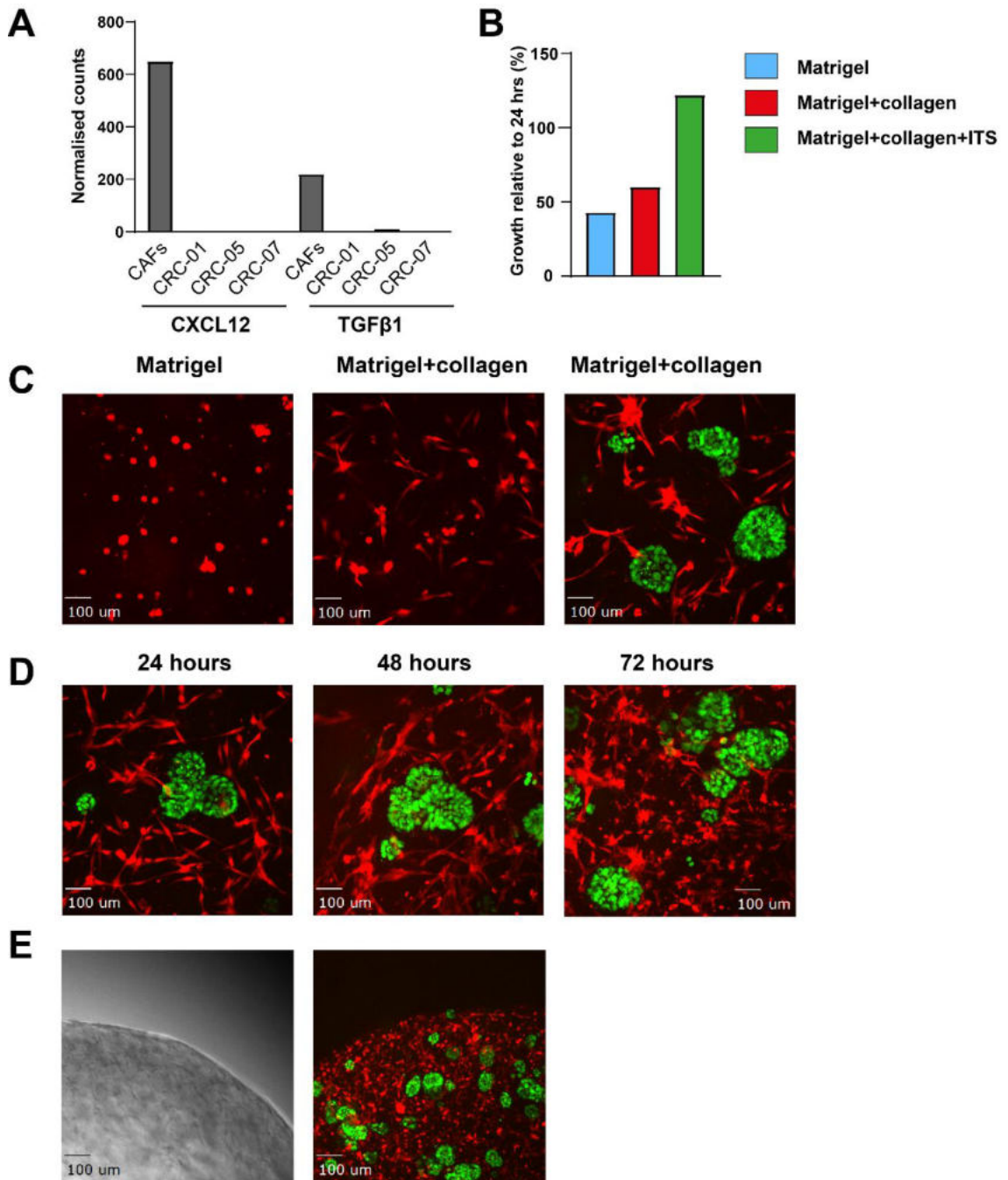


Figure 6.13 Incorporation of CAFs to 3D PDO-T cell co-culture. (A) Graph showing gene expression data for CXCL12 and TGFβ1 for CAFs and 3 PDOs: CRC-01, CRC-05, CRC-07 as determined by RNA sequencing (normalised counts). (B) CAFs were grown in different matrices for 5 days and cell viability was determined using CellTiter Glo. Percent growth was calculated against a baseline viability readout 24 hours after seeding. Experiment performed once. (C) Images of CAFs cultured in Matrigel (alone) and 3D co-culture assay Matrigel-collagen matrix alone or together with PDOs (CRC-01). (D) Images of CAFs co-cultured with PDOs in a Matrigel-collagen matrix for 72 hours with images taken at 24, 48, and 72 hours. (E) Images (brightfield and fluorescence) showing Matrigel-collagen gel contraction caused by CAFs.

only culture. Addition of ITS (insulin-transferrin-selenium) which is a supplement added to CAF media, improved cell viability and even resulted in CAF proliferation compared to the 24 hour baseline (Figure 6.13B). CAFs cultured in Matrigel-collagen-T cell media matrix with the addition of ITS showed typical elongated shape (Figure 6.13C). CAFs were able to maintain this shape throughout the 72 hour timelapse forming links with each other and surrounding PDOs (Figure 6.13D). However, due to being highly contractile cells and their ability to remodel ECM, CAFs caused a severe contraction of the ECM matrix containing PDOs thus shifting all of the PDOs from their imaging positions. Figure 6.13D shows the border of the gel in brightfield and fluorescent imaging which is usually not visible as the gel sits against the walls of the 96 well plate well. As the organoids need to remain in the same position throughout the timelapse for quantification of T cell infiltration and cancer cell death, addition of CAFs proved problematic. Due to COVID restrictions and limited access to tissue culture and microscopes, I was unable to optimise this triple co-culture further. One approach would be to image organoids at specific timepoints rather than continuously imaging them throughout 72 hours. As the organoids would shift from one timepoint to the next, I would find the same organoids at different timepoints. If the same organoids can not be found after the shift, imaging any organoids would provide some valuable information. Although I would not be able to observe the dynamics of the infiltration, I would still be able to quantify T cell infiltration into organoids at different timepoints and see if the presence of CAFs impedes T cell infiltration into organoids.

6.7 Discussion

Since the introduction of multicellular tumour spheroids (MCTS) in 1971 by Sutherland and colleagues, 3D in vitro models have emerged as a powerful tool to investigate tumour biology (Sutherland et al., 1971). Three dimensional spheroids more closely mimic in vivo tumours than traditional two-dimensional cell cultures recapitulating key

features such as chemical, nutrient, and oxygen gradients, cell-cell interactions, and growth kinetics more closely resembling *in vivo* tumours. The closer a cell is to the core of the spheroid the less oxygen and nutrients is available, and the higher the accumulation of metabolic waste. Tumour cells cultured in 3D have different metabolic profiles compared to 2D cultured counterparts exhibiting increased glycolysis and high lactic acid production (Feder-Mengus et al., 2007; Santini et al., 2004). Although in Chapter 5 I have demonstrated that hypoxia does not impair T cell function in the context of CEA-TCB, I have not tested the effect of lactic acid on T cells in my model and it has been reported to suppress T cell proliferation and cytokine production and to reduce cytotoxic activity (Fischer et al., 2007). Therefore nutrient depletion and accumulation of metabolic waste may be factors that impair CEA-TCB efficacy. Importantly, gene expression profiles of cells cultured in 3D differ from those grown as monolayers, with upregulation of genes encoding chemokines and cytokines (Fischbach et al., 2007; Ghosh, Spagnoli, et al., 2005). Another study found that culturing tumour cells in a spheroid configuration resulted in upregulation of genes related to immune response, lymphocyte stimulation, and response to cytokine stimulation (Kim et al., 2012). To further increase clinical relevance of 3D models, methods for culturing patient derived organoids have been developed. In addition to recapitulating molecular features, patient derived organoids better model tumour architecture than spheroids being able to form well differentiated gland like structures that match the morphology of the original tumour.

Multiple models and studies have shown that tumour cells cultured in 3D exhibited defective immune recognition by CTLs (Dangles, Validire, et al., 2002; Feder-Mengus et al., 2007; Ghosh, Rosenthal, et al., 2005). However, very few models have been adapted to study T cell migration and infiltration which are essential steps for an antitumour immune response to occur and for immunotherapies such as checkpoint inhibitors, CAR-T cells, and bispecific antibodies to work as T cells need to be in close proximity to the tumour cells. One of the most common co-culture methods used to

evaluate tumour-immune interactions and lymphocyte infiltration into tumour spheroids involves generation of MCTS through various techniques such as liquid overlay technique or hanging drop method and addition of lymphocytes on top in culture medium (Courau et al., 2019; Fischer et al., 2007; Giannattasio et al., 2015; Herter et al., 2017; Hoffmann et al., 2009; Koeck et al., 2017). Afterwards the spheroids are harvested and lymphocyte infiltration is determined by flow cytometry or immunohistochemistry. However, due to lack of an extracellular matrix component these models are not suitable for evaluation of T cell migration through the extracellular matrix which T cells are met with after extravasation from blood vessels at the tumour site. Tumours employ various strategies to prevent T cell trafficking and infiltration such as deregulation of chemokine expression and development of aberrant vasculature. Another important mechanism responsible for preventing T cells from reaching the tumour is the remodelling of extracellular matrix by both tumour and stromal cells. Although tumours also contribute, stromal cells such as CAFs are the main producers of various ECM components such as collagens, fibronectin, and laminins. Using matrix metalloproteinases (MMP) CAFs degrade and remodel the ECM. Additionally they use lysyl oxidase (LOX) which covalently cross-links collagen fibres forming dense collagen networks (Brauchle et al., 2018). Resulting collagen dense matrix found in many solid tumours including CRC is much stiffer than the submucosal collagen-rich layer of healthy colonic tissues (Brauchle et al., 2018; Li et al., 2020; Liu et al., 2020). In vivo stiffness measurements of tumour ECM showed a positive correlation with ECM crosslinking and a negative correlation with T cell migration (Nicolas-Boluda et al., 2021). Using ex vivo fresh tumour slices of lung and ovarian tumours, Bougherara and colleagues identified the extracellular matrix as a major stromal component in influencing T cell migration (Bougherara et al., 2015). This and other studies have found that T cell migration is inhibited in collagen dense regions and that T cells preferentially localise in less collagen dense regions of the stroma, far from tumour islets which are frequently surrounded by dense ECM which limits T cells

access to tumour cells (Bougherara et al., 2015; Hartmann et al., 2014; Salmon et al., 2012).

Due to the important role the ECM plays in T cell migration and infiltration into tumours some in vitro models have added an ECM component. Some studies have developed 2.5D models in which spheroids or organoids are plated on a layer of matrix (usually Matrigel) and immune cells are added on top in media (Schnalzger et al., 2019; Thakur et al., 2012, 2013). However, T cell motility on 2D surfaces and within 3D matrices significantly differ. T cell migration on 2D surfaces (haptokinetic T cell migration) involves integrin mediated binding to surface, while migration of T cell in 3D matrices is integrin independent and is an amoeboid-like migration characterised by crawling along collagen fibrils (contact guidance) and squeezing through pre-existing matrix gaps by vigorous shape change (Friedl et al., 1998; Friedl & Brocker, 2000; Ivanoff et al., 2005; Lämmermann et al., 2008; Wolf et al., 2003). One in vitro model incorporated the T cell migration through ECM step by establishing a “sandwich assay” where target cells were plated as a monolayer at the bottom of the culture plate and an overlaying collagen gel layer containing CTLs (Weigelin & Friedl, 2010). However, this specific model lacked three dimensional tumour structure that resembles in vivo tumours.

Therefore, my aim was to combine all of these different aspects of T cell migration and infiltration into tumours and develop a 3D co-culture assay that would allow investigation of tumour-immune interactions and CEA-TCB activity. My model was comprised of PDOs, T cells, and an extracellular matrix component permitting organoid growth and T cell migration. The main aims were to determine whether organoids could be infiltrated by CD8 T cells in the presence or absence of CEA-TCB, and whether organoid size or morphology would preclude T cell infiltration and CEA-TCB facilitated cancer cell killing. My experiments showed that under control conditions, PDO and CD8 co-culture alone or treated with DP47, majority of organoids exhibited low levels of T cell infiltration. However, some organoids within different PDO lines became heavily

infiltrated with no subsequent killing of cancer cells thus eliminating the possibility that this was a result of an alloreactivity reaction. This suggests that organoids differ in their propensity to acquire T cell infiltrates potentially due to differential secretion of T cell attracting chemokines. Treatment of PDO-T cell co-cultures with CEA-TCB overall increased T cell infiltration into all PDOs, irrespective of their CEA expression status. Organoid infiltration heterogeneity was observed within PDO lines meaning that even in the presence of CEA-TCB organoids differed in their ability to attract and be infiltrated by CD8 T cells. Next, I investigated whether different organoid morphologies affected T cell infiltration. Some PDOs grow in a gland-like structure containing lumen or hollow spheroids mimicking more differentiated CRC tumours whereas others grow as dense compact masses of cells reminiscent of poorly differentiated CRCs. Conveniently CEA expression profile did not correlate with a specific morphology, with CRC-01 and CRC-07 (CEA-high) growing as hollow structures, while CRC-05 (CEA-high) grows as compact spheres. Vice versa CRC-04 and CRC-06 (CEA-mixed) grew as hollow spheres and compact spheres respectively. This allowed me to evaluate the effect of morphology on CEA-TCB driven T cell infiltration regardless of CEA expression status. All morphologies were permissive of T cell infiltration, with T cells localised in the walls of gland-like organoids and throughout the dense cellular mass of compact organoids. Similarly, the size of the organoids did not affect T cell infiltration with small (median diameter 67 μ m), medium (median diameter 102 μ m), and large (median diameter 147 μ m) organoids infiltrated to similar T cell densities. Even particularly large compact organoids measuring more than 300 μ m in diameter were infiltrated by T cells throughout thus showing that cancer cells themselves do not act as a physical barrier and are not the mediators T cell exclusion frequently observed in solid tumours.

T cells are frequently localised in the stroma of solid tumours which is composed of non-cancer and non-immune components of the TME such as the extracellular matrix and stromal cells such as CAFs. Therefore, in order to investigate

whether CAFs can act as a barrier to successful T cell infiltration into the organoids RC11 CAFs from a human rectal carcinoma were incorporated into the 3D co-culture model. However due to their highly contractile nature and ECM remodelling abilities CAFs strongly contracted the matrix gel containing PDOs, moving them out of their imaging positions and thus making the current method of T cell and cancer cell death quantification not suitable as it relies on the organoids remaining in the same positions throughout the 72 hour duration of the timelapse. Unfortunately, due to COVID I was unable to further optimise this model. However, in the future several different approaches can be taken. Potentially a smaller amount of CAFs can be added to the co-culture. However, if that does not resolve the matrix contraction issue then a different analysis approach should be developed. Perhaps rather than measuring T cell infiltration and cancer cell death of individual organoids throughout the duration of the assay, I could measure both at specific timepoints analysing different organoids and getting an overall picture of whether or not the presence of CAFs affects T cell migration, infiltration, and cancer cell killing.

Another feature of this model that can be further adjusted to more closely mimic in vivo tumours is the density of the matrix. It has been well established that increased tissue stiffness is a classic characteristic of solid tumours. One of the major contributing factors is increased density of collagen fibres in the ECM (Cox & Eler, 2011; Lu et al., 2012; Nissen et al., 2019; Pankova et al., 2016). A study measuring the elastic modulus (EM), resistance of material to elastic deformation or how soft or stiff a material is, of tumour and normal tissues showed that stroma adjacent to tumour had an EM of 918 ± 269 Pa while collagen at a concentration of 2mg/mL had an EM of only 328 ± 87 Pa thus being significantly less stiff. Increasing the collagen density to 4mg/mL increased EM to 1589 ± 380 Pa (Paszek et al., 2005). Furthermore, a study investigating effect of matrix stiffness on T cell activity showed that culturing T cells in a high density matrix (collagen 4mg/mL) versus low density matrix (collagen 1mg/mL) showed reduced

proliferation, downregulation of cytotoxic activity markers such as granzyme, perforin, and IFN γ , and reduced cytotoxic activity against target melanoma cells (Kuczek et al., 2019). It would be important to investigate whether CEA-TCB activated T cells in the 3D co-culture assay would exhibit similar responses and decrease CEA-TCB efficacy. Overall I have developed a relevant model for studying tumour-immune interactions and evaluating activity of immunotherapeutic agents within a 3D microenvironment which can be further developed to incorporate other cell types relevant for cancer progression and response to immunotherapy.

Chapter 7: Final discussion and future perspectives

First line metastatic cancer treatment typically involves a fluoropyrimidine-based chemotherapy regimen, combining fluorouracil (5-FU) and leucovorin with oxaliplatin (FOLFOX) or irinotecan (FOLFIRI) achieving in median duration of survival of 18-21 months (de Gramont et al., 2000; Douillard et al., 2000; Tournigand et al., 2004). Further advances in treatment of mCRC have been made with the introduction of targeted therapies. Drugs targeting EGFR and VEGF in combination with chemotherapy improves progression free survival, response rates, with some clinical trials reporting median overall survival to be 24 months (Bokemeyer et al., 2012; Cunningham et al., 2004; Cutsem et al., 2011; Douillard et al., 2010; Van Cutsem et al., 2012). Advances in molecular profiling of patients and identification of resistance driving mutations has allowed for better selection of patient subsets. For the 50% of patients with KRAS/NRAS/BRAF wild-type metastatic CRC, median survival with chemotherapy and targeted therapy combination treatment is approximately 30 months (Cremolini et al., 2015; Venook et al., 2017). However, despite improvements in survival, after several months of treatment resistance invariably occurs through genetic and epigenetic mechanisms and microenvironmental influences thus creating a need for novel therapeutic approaches. Immunotherapy with Immune checkpoint blockade has shown remarkable responses in MSI CRC, however fewer than 5% of mCRC are MSI. Low mutation and neoantigen loads and consequently low lymphocyte infiltration as these tumours are poorly immunogenic are considered to be the main reason for lack of immunotherapy responses. In the past several years different therapeutic approaches have been taken to improve responses to immunotherapy in MSS CRCs. One approach has been combining chemotherapy or anti-EGFR monoclonal antibodies with immune checkpoint inhibitors following the rationale that chemotherapy and anti-EGFR drugs can induce immunogenic cell death leading to release of tumour antigens ultimately leading to T cell infiltration and activation (Inoue & Tani, 2014; Woolston et al., 2019). However,

clinical trials have shown that response rates, PFS, and OS were not significant making this therapeutic approach largely unsuccessful (Antoniotti et al., 2022; Lenz et al., 2022; Mettu et al., 2022; Stein et al., 2020). For a successful anti-tumour immune response to occur T cells need to be present within the tumour. One approach to increase T cell infiltration into CRC tumours is through bispecific antibodies which redirect CD3 expressing T cells to tumour antigens. CEA-TCB, a bispecific antibody targeting CEA on tumour cells, is a promising approach to treat poorly immunogenic MSS CRC tumours because bispecific antibodies mediate cancer cell recognition by T cells independently of neoantigen load. However, an early clinical trial has shown that despite selecting patients with CEA positive tumours, not all patients respond to this therapy. While efficacy of CEA-TCB was improved in combination with a PD-L1, 50% of patients still do not show clinical benefit (Tabernero et al., 2017).

In order to investigate determinants of CEA-TCB activity and resistance, clinically relevant models need to be developed. The advantage of studying bispecific antibodies in vitro is the use of allogeneic T cells since CEA-TCB mediated T cell activation occurs independently of TCR specificity. Patient derived organoid models have the potential to generate clinically relevant insights into determinants of immunotherapy activity and resistance due to their preserved molecular features of tumours and previous treatment experience. My lab has established PDOs from multidrug-resistant metastatic CRCs thus making it a highly clinically relevant model as most immunotherapy agents are tested in second and third line settings after patients have become resistant to chemotherapy and/or targeted therapy. When I started my PhD, my lab was in the midst of characterising CEA expression profiles of PDOs. They have shown that in contrast to cell lines, CEA expression is frequently heterogeneous within PDO populations reminiscent of the CEA expression heterogeneity which has been described in CRC samples from patients (Gonzalez-Exposito et al., 2019; Yan et al., 2016). Furthermore my colleagues have demonstrated high plasticity of CEA expression by FACS-sorting

CEA-high and CEA-low cells from PDOs with mixed CEA expression, allowing these cultures to expand, and measuring CEA expression in the resulting population. CEA-low cells were able to re-establish CEA-high subpopulations and similarly CEA-high cells were able to re-establish a CEA-low populations, but with different conversion rates. I further confirmed the two CEA expression patterns in PDOs: CEA-high and CEA-mixed groups. While three CEA-high expressing PDOs showed very little variability in their CEA levels over prolonged culture, the CEA-mixed PDOs showed much more variability with some PDOs ranging from 10% to 75% in their proportion of CEA high cells despite constant culturing conditions. CEA expression profiles were highly similar between 2D and 3D forms of the same PDO lines. Importantly these CEA expression profiles were maintained in xenografts which was confirmed by immunohistochemistry. These xenografts showed similar spatial patterns of heterogeneity as what has been found in PDOs and patient samples thus indicating that these expression profiles are not an artefact of in vitro culture and that they accurately represent CEA expression in tumours.

Growing PDOs in advanced organoid media, which incorporates a combination of essential growth factors and small molecule inhibitors developed to maintain long term proliferative potential of organoids, resulted in a dramatic decrease in CEA expression in three CEA-high expressing PDOs. The factors responsible for CEA downregulation was a combination of p38 MAPK inhibitor SB202190 and nicotinamide. The downregulation was not only at surface level expression as assessed by flow cytometry, but also at gene expression level. P38 has been implicated in differentiation of enterocytes, and its inhibition has been shown to reduce differentiation (Rodríguez-Colman et al., 2017; Sato et al., 2011). CEA is a marker of differentiation in the colonic crypt cells, therefore treating PDOs with p38 inhibitor may have resulted in their dedifferentiation and generation of a more crypt progenitor like phenotype with reduced CEA expression. This is further supported by the finding that treated PDOs expressing low levels of CEA were more reliant on oxidative phosphorylation while untreated PDOs

used glycolysis as was determined by GSEA. It has been demonstrated that intestinal stem cells at the crypt bottom are more dependent on oxidative phosphorylation than their more differentiated progeny towards the top of the crypt (Rodríguez-Colman et al., 2017). Additionally, treated PDOs had multiple enriched signatures associated with cell cycle progression and proliferation thus further supporting the notion that the treated cells acquire the less differentiated phenotype usually present at the bottom of the crypt where progenitor populations are actively proliferating. Interestingly, one of the CEA-high expressing PDOs was insensitive to this treatment and maintained high expression of CEA. Therefore investigating transcriptional and signalling differences between CEA-high treatment sensitive PDOs and the CEA-high insensitive PDO may generate mechanistic insights into how CEA is regulated. Antigen loss is a common resistance mechanism in therapies like bispecific antibodies and CAR T cells, therefore dissecting the mechanisms of CEA regulation can inform combination treatments that would prevent antigen loss and therefore enhance efficacy of CEA targeting therapies.

Through RNA sequencing followed by GSEA of CEA-high and CEA-low cells my colleagues demonstrated a negative correlation between CEA expression and Wnt/ β -catenin pathway activity. To investigate whether CEA expression can be increased through pharmacological perturbation of this pathway, I treated CEA-mixed PDOs with a tankyrase inhibitor which stabilises β -catenin destruction complex and therefore inhibits the downstream Wnt/ β -catenin pathway signalling. In response to tankyrase inhibition proportion of CEA+ cells in CEA-mixed PDOs increased validating the hypothesis that Wnt/ β -catenin signalling represses CEA expression. These findings further suggest a similarity in CEA regulation between healthy colon epithelial cells and tumours because CEA expression is absent at the colonic crypt bottom where Wnt/ β -catenin signalling is high, and it gradually increases in epithelial cells as they become more differentiated towards the top of the crypt where Wnt/ β -catenin signalling is low (Barker, 2013; Jothy et al., 1993; Mariadason et al., 2001; Naishiro et al., 2001). Loss-of-function mutations

in *APC* are the initiating event in the onset of the majority of colorectal tumours and are present in 80-90% of sporadic CRCs leading to a defective β -catenin degradation complex and subsequent nuclear accumulation of β -catenin (Korinek et al., 1997; Morin et al., 1997; Muzny et al., 2012; Powell et al., 1992). However, immunohistochemical studies have revealed that colon carcinomas harbouring *APC* mutations do not contain nuclear β -catenin homogeneously and exhibit heterogeneous intracellular distributions β -catenin within primary tumours as well as their metastases (Brabletz et al., 2001; Fodde & Brabletz, 2007; Hlubek et al., 2007; Vermeulen et al., 2010). In well-differentiated cancer cells located at the centre of the tumour β -catenin was localised in the membrane and cytoplasm which is an expression pattern comparable to normal colon epithelium, whereas nuclear β -catenin was found in dedifferentiated mesenchyme-like tumour cells at the invasive front (Brabletz et al., 2001). These studies demonstrate that despite *APC* mutations β -catenin signalling remains regulated in CRC cells. My finding that tankyrase inhibition resulted in upregulation of CEA expression are in line with these observations as all three CEA-mixed PDOs harboured *APC* mutations. The fact that this pathway remains regulated and can be perturbed pharmacologically is favourable for CEA targeting therapeutic agents including CEA-TCB. Using the PDO-T cell co-culture model I demonstrated that co-treatment with CEA-TCB and a tankyrase inhibitor resulted in greater sensitivity to CEA-TCB in two CEA-mixed PDOs. My findings were used as a basis for patenting a combination of CEA-TCB and a Wnt signalling inhibitor for cancer treatment by Roche Glycart. An additional benefit of inhibiting Wnt/ β -catenin signalling may be enhanced T cell infiltration into tumours as Wnt/ β -catenin signalling in cancer cells has been correlated with immune exclusion (Luke et al., 2019). Initially it was demonstrated that tumour-intrinsic active β -catenin signalling in a mouse melanoma model prevented the early steps of T cell priming against tumour-associated antigens, which is not relevant in the context of CEA-TCB as no priming is required (Spranger et al., 2015). However, later they demonstrated that β -catenin signalling in tumours results in failed trafficking of adoptively transferred tumour-specific effector T

cells into tumours (Spranger et al., 2017). Another study has shown that β -catenin inhibition in tumour cells enhanced T cell infiltration into tumours and improved response to immune checkpoint inhibition in murine models of melanoma, mammary carcinoma, neuroblastoma, and renal adenocarcinoma (Ganesh et al., 2018). T cell trafficking to the tumour is highly relevant for bispecific antibody immunotherapy, therefore in addition to increasing expression of target antigens Wnt/ β -catenin pathway inhibition may also enhance T cell infiltration. Additionally, tankyrase inhibitors have shown to reduce proliferation of APC-mutated colorectal cell lines and CRC xenografts (Huang et al., 2009; Lau et al., 2013; Okada-Iwasaki et al., 2016; Waaler et al., 2012). Therefore tankyrase inhibition may increase tumour growth control in addition to sensitising cells to CEA-TCB treatment. Since CEA-TCB therapy is T cell mediated it is important to also examine the effect of tankyrase/Wnt/ β inhibition on T cell function. It has been reported that Wnt signalling arrests differentiation of naïve CD8 T cells into effector T cell subtype (Gattinoni et al., 2009). Wnt/ β -catenin signalling also regulates the differentiation of CD4⁺ helper T cells. TCF-1 and β -catenin support Th2 polarisation through activation of the expression of the Th2 master transcription factor GATA binding protein 3 (GATA3) (Yu et al., 2009). Therefore, tankyrase inhibition and subsequent inhibition of Wnt/ β -catenin signalling should favour development of Th1 cells important for anti-tumour responses and should not impair differentiation of CD8 naïve cells into CD8 effector T cells. However, targeting the Wnt pathway might be challenging as it has an essential role in many normal tissues and therefore its targeting results in toxicities (Kahn, 2014). As better understanding of Wnt regulation in cancer cells develops and enables design of molecules resulting in lower toxicity, combination therapy with CEA-TCB and Wnt inhibitors should be investigated in clinical trials.

To investigate activity and resistance mechanisms to CEA-TCB colleagues from my lab established a 2D co-culture assay with PDOs and pre-activated allogeneic T cells that provided proof of concept that CEA-TCB efficacy can be evaluated in a clinically

relevant in vitro model. Demonstrating that CEA expression in CEA-high PDOs remains stable over prolonged time in culture has allowed me to use these three PDO models to dissect determinants of sensitivity and resistance to CEA-TCB. While originally this model was set-up using T cells pre-activated in vitro, it was important to investigate whether T cells freshly isolated from PBMCs would achieve the same level of tumour cell growth control because T cells redirected by CEA-TCB are most likely recruited from the periphery. Freshly isolated CD8 T cells as effectively controlled tumour cell growth as pre-activated ones thus further supporting that this is a clinically relevant model to study CEA-TCB activity. Using three CEA-high PDOs showing good sensitivity to CEA-TCB I demonstrated that CD4 T cells can control tumour growth, but less than their CD8 expressing counterparts. These findings were similar to those described in other T cell redirecting antibody in vitro models which demonstrated that although both populations contributed to T cell mediated cytotoxicity, CD4 T cells induced lower levels of specific tumour cell lysis (Dreier et al., 2002; Ishiguro et al., 2017; Li et al., 2017).

The key mechanisms through which T cells mediated cytotoxicity are granzyme and perforin lytic granule secretion, Fas/FasL pathway, and IFN γ production. I investigated whether effector mechanisms differed between CD8 and CD4 T cells especially due to their difference in ability to control tumour cell growth thus suggesting potentially different mechanisms of control. Fas-FasL axis appeared to not play a role in either CD8 or CD4 T cell mediated tumour growth control. Flow cytometry studies demonstrated a 2.2-7.8 fold higher expression of granzyme B in CD8 compared to CD4 T cells. The increase in the granzyme $^{+}$ proportion of cells was much less in CD4 T cells than in CD8 T cells of which 90-100% of cells were granzyme $^{+}$ in response to CEA-TCB treatment. Nonetheless a subpopulation of CD4 T cells expressed granzyme B potentially pointing to their ability to become cytotoxic T cells which have been previously described in chronic viral infections and some tumour types (Appay et al., 2002; Brien et al., 2008; Brown, 2010; Hildemann et al., 2013; Hua et al., 2013; Kitano et al., 2013;

Mattoo et al., 2016; Oh et al., 2020; Quezada et al., 2010; Śledzińska et al., 2020; Xie et al., 2010; Zaunders et al., 2004; Zheng et al., 2017). However, the direct role of granzyme in CD4 tumour growth inhibition needs to be investigated further through granzyme inhibition. Interestingly, CEA-high PDO that has the lowest CEA expression per cell elicited smaller levels of granzyme than the other two CEA-high expressing PDOs suggesting that amount of CEA bindings sites might regulate the extent of T cell activation during CEA-TCB treatment. However, this was only observed in one PDO therefore further investigation is required with additional PDOs displaying similar levels of CEA. When CD8 and CD4 T cells were added to the co-culture together both T cell subsets exhibited an increase in granzyme expression compared to when each subset was cultured alone; on average CD8 granzyme expression increased by 1.8 fold and by 2.5 fold in CD4 T cells. Given that CEA-TCB activates both subsets the mutual enhancement of granzyme expression may translate into better tumour growth control. However, it is important to investigate the effect of Tregs on CD4 mediated tumour growth inhibition because IL-2 was shown to be central to the acquisition of the cytotoxic program and driver of granzyme B expression in CD4 T cells and one of the key mechanisms used by Tregs to suppress T cell immune responses is through IL-2 deprivation (Śledzińska et al., 2020).

In addition to regulating different aspects of immune responses IFN γ can also directly inhibit tumour cell growth and induce apoptosis therefore contribution of IFN γ secretion by CD8 and CD4 T cells to tumour cell growth inhibition was examined (Bromberg et al., 1996; Chin et al., 1997b; Detjen et al., 2001). IFN γ blocking strongly reduced CD4 efficacy (51% decrease in growth inhibition in IFN γ sensitive PDOs), but had a more modest effect on CD8 mediated growth inhibition (32% decrease in growth inhibition in IFN γ sensitive PDOs) further showing that these two subsets both rely on the same effector mechanisms but to different degrees. One CEA-high PDO showed complete abrogation of killing with CD4 T cells in the presence of an IFN γ blocking

antibody. This PDO induced lower levels of granzyme expression and exhibited less sensitivity to IFN γ out of the IFN γ sensitive PDOs. Therefore the main mechanism used by CD4 T cells to control the growth of this PDO was through IFN γ secretion and once that was blocked CD4 T cells could no longer inhibit growth. IFN γ blocking antibody did not significantly alter killing efficacy of CD8 and CD4 T cells co-cultured with a PDO exhibiting no sensitivity to IFN γ . Although these findings suggest that activation of IFN γ signalling in cancer cells is not a prerequisite for CEA-TCB mediated CD8 T cell efficacy as they were still effective against IFN γ sensitive PDOs with IFN γ blockade and against an IFN γ insensitive PDO, a reduction in tumour cell inhibition was observed with IFN γ blockade therefore patients with intact IFN γ signalling in tumours may benefit more. Inactivation of IFN γ signalling by tumour cells through loss of function genetic mutations to JAK1/2, kinases downstream of IFN γ receptor, as well as through epigenetic silencing of JAK1 gene expression is a mechanism of immune evasion (Dunn et al., 2005; Kaplan et al., 1998; Mazzolini et al., 2003). Loss-of-function mutations in JAK1/2 can lead to primary and acquired resistance to checkpoint immunotherapy as demonstrated in mouse models and patients (Gao et al., 2016; Shin et al., 2017; Zaretsky et al., 2016). However, CD4 T cells predominantly rely on IFN γ mediated tumour growth inhibition and since CEA-TCB activates both T cell subsets it should be investigated in clinical trials whether intact IFN γ signalling in cancer cells improves CEA-TCB response rates. Additionally, patients with tumours expressing heterogenous levels of CEA and showing sensitivity to IFN γ may benefit from bystander killing by T cells that have been activated by CEA expressing cells. This co-culture model can be used to address these questions in addition to being suitable for further investigation of cytotoxic CD T cell function as it is not yet a well characterised cell subset.

Tumours employ different mechanisms such as secretion of cytokines and recruitment of immunosuppressive immune cell populations to reprogram the TME into an immunosuppressive phenotype. This allows for evasion of T cell responses and limits

the immune system's ability to restrain tumour growth and the effectiveness of immunotherapies. The TME is highly complex with many different immune populations and multiple stimulatory and suppressive factors acting simultaneously thus making the dissection of causative resistance mechanisms in patient or murine tumour samples difficult. The ability to precisely control variables of interest is a key advantage of in vitro models such as the co-culture model described in this thesis. Using three CEA-high PDOs showing good sensitivity to CEA-TCB a screen of immunosuppressive factors and cell populations commonly present in the CRC TME was performed. In this in vitro model IL-10 and VEGF has no negative effect on CEA-TCB efficacy. Importantly, hypoxia did not impair CEA-TCB activity and in fact improved CD8 T cell mediated tumour growth inhibition in two out of the three models tested. Therefore CEA-TCB can be effective in hypoxic tumours. Although the impact of sparse vessel network on ability to deliver CEA-TCB and T cells were not tested. Additionally, very low levels of O₂ (<1%) which can be found in some tumours were not tested and should be investigated in the future as it might affect T cell function differently (Hammond et al., 2014; McKeown, 2014). Furthermore this screen identified TGFβ as factor conferring resistance to CEA-TCB. This is an important finding as high TGFβ activity has been described in majority of metastatic CRCs (Calon et al., 2012). I found that TGFβ dampens CEA-TCB activity through suppression of T cell cytolytic and proliferative abilities. Similar findings have been made in the context of CAR-T cell therapy where TGFβ caused impaired function through reduction in cytolytic activity, cytokine production and proliferation (Stüber et al., 2020; Tang et al., 2020). TGFβ induced resistance to CEA-TCB was reversed with administration of a small molecule inhibitor of TGFβ receptor, galunisertib. Reversal of resistance with galunisertib validates that immunosuppression mediated by TGFβ is through its cognate receptor TGFβRI. Galunisertib is a clinically applicable compound that has been investigated in clinical trials in combination with other immunotherapy agents such as immune checkpoint inhibitors (NCT02734160 and NCT02423343) making it a potential agent for combination treatment with CEA-TCB immunotherapy.

Based on these findings the combination of CEA-TCB and a TGF β signalling inhibitor has been patented by Roche Glycart.

IL-2, a cytokine driving survival and proliferation in T cells, has been shown to restore TGF β suppressed T cell proliferation and cytotoxic gene expression (Thomas & Massagué, 2005). Therefore I investigated whether IL-2 would reverse TGF β mediated resistance to CEA-TCB. IL-2 was able to rescue CD8 function and reverse TGF β driven resistance to CEA-TCB suggesting that T cell stimulating agents may overcome this resistance mechanism. However, IL-2 is toxic in patients and also leads to an increase in Tregs, which is an immunosuppressive population that has been correlated with worse prognosis and resistance to immunotherapy with immune checkpoint blockade (Ahmadzadeh & Rosenberg, 2006; Berntsen et al., 2010; Betts et al., 2012; Curiel et al., 2004; Marshall et al., 2020; Saleh & Elkord, 2019; Tang et al., 2014). In order to more selectively deliver IL-2 to the tumour, immunocytokine conjugates consisting of IL-2 molecularly linked to antibodies directed against common tumour associated antigens have been developed and although this design results in improved pharmacokinetics these immunocytokines have shown poor responses and increases in Treg frequencies similar to IL-2 (Connor et al., 2013; King et al., 2004; Weide et al., 2014). Therefore I evaluated a more novel agent, FAP-IL2v, which is an immunocytokine comprising an antibody against fibroblast activation protein α (FAP) and an IL-2 variant with abolished binding to CD25 which is a subunit of IL-2 receptor which is constitutively expressed on Tregs (Waldhauer et al., 2021). It has been previously evaluated in cancer cell lines but to my knowledge it is the first study of this agent being tested in PDOs. FAP-IL2v was able to reverse TGF β induced immunosuppression by increasing granzyme B expression and proliferation in CD8 T cells even to levels beyond those observed with CEA-TCB treatment under control conditions.

4-1BB, a co-stimulatory molecule expressed on activated T cells, signalling enhances proliferation, cytotoxicity, and cytokine secretion, and counteracts exhaustion

(Hernandez-Chacon et al., 2011; Shuford et al., 1997; Wilcox et al., 2004). CAR T cells that have a 4-1BB co-stimulatory receptor have shown enhanced proliferation, cytotoxic ability, longer persistence, and more potent tumour cell eradication in comparison to CD28-expressing CAR T cells (Dai et al., 2020; Philipson et al., 2020; Zhao et al., 2020). It has also been shown that 4-1BB co-stimulation reverses TGF- β -mediated suppression through reducing Smad2 phosphorylation induced by TGF- β (Kim et al., 2005). Therefore 4-1BB was another candidate for countering TGF β driven resistance to CEA-TCB. Unlike early 4-1BB agonists which have been hampered by Fc γ receptor-mediated hyperclustering and hepatotoxicity, 4-11BBL-CEA is targeted to CEA expressing tumour cells and has been engineered to provide potent T cell co-stimulation only when bound to target tumour antigen thus avoiding systemic toxicities (Claus et al., 2019). 4-11BBL-CEA was able to rescue CD8 T cell function dampened by TGF β through increase of granzyme B expression and proliferation. It induced higher levels of granzyme expression than FAP-IL2v while increasing proliferation to a lesser degree than FAP-IL2v. These findings show that FAP-IL2v and CEA-4-1BBL are rational combination therapies with CEA-TCB for tumours with high TGF β activity. Currently FAP targeted 4-11BBL fusion protein is being evaluated in a Phase 1b clinical trial in combination with CEA-TCB for the treatment of patients with previously treated metastatic MSS CRC with high CEA expression (NCT04826003). My findings are likely to have broad relevance for the design of more effective immunotherapy combinations for tumour types with high TGF β activity. Overcoming TGF β induced immunosuppression may improve response rates to checkpoint inhibitors, T cell re-directing antibodies, and CAR T cells. Furthermore this study demonstrated that this in vitro model enables the identification of combination therapies that address resistance and can inform subsequent clinical testing.

In addition to causing T cell dysfunction high TGF β signalling in stroma has been demonstrated to lead to T cell exclusion (Mariathasan et al., 2018; Tauriello et al., 2018).

This excluded phenotype was reversed with TGF β signalling blockade and anti-PD-L1 treatment increasing lymphocyte infiltration into the tumour centre. Therefore FAP-IL2v and 4-11BBL-CEA should be evaluated for their ability to overcome T cell exclusion commonly accompanying high TGF β expression. Many preclinical studies have shown that TGF β blockade augments anti-PD-L1 therapy (Greco et al., 2020; Holmgaard et al., 2018; Lan et al., 2018; Mariathasan et al., 2018; Principe et al., 2019; Sow et al., 2019; Tauriello et al., 2018; Yi et al., 2021). Given the encouraging anti-tumour effects of combined TGF β and immune checkpoint inhibition in preclinical testing, these approaches are beginning to emerge in clinical trials. Combination treatment with vactosertib, a potent and selective TGF β receptor I kinase inhibitor, and pembrolizumab in patients with MSS mCRC achieved a response rate of 15.2% (Kim et al., 2021). This modest response rate may be due to low lymphocyte infiltration associated with poor immunogenicity of MSS tumours. Combination therapy with CEA-TCB and anti-PD-L1 therapy resulted in a response in 50% of patients addressing the lack of tumour infiltrating lymphocytes by redirecting CD3 T cells to the tumour. Addition of TGF β signalling inhibitor or tumour/stroma-targeted co-stimulatory molecules on top of bispecific antibody and anti-PD-L1 agent may therefore enhance response to this therapy even further.

For CEA-TCB to work T cells and tumour cells must be in proximity, therefore the ability of T cells to infiltrate tumours is an important factor controlling effect of this immunotherapy. In addition to recapitulating key molecular features PDOs also mimic growth patterns of tumours. In order to investigate whether different organoid morphology or size would pose a barrier to T cell infiltration I established a 3D model incorporating PDOs, allogeneic T cells, and extracellular matrix that could be monitored through live timelapse microscopy. Through development of image analysis pipelines that allowed for segmentation of organoids and for measuring T cell area inside the organoids over time I was able to quantify T cell infiltration into organoids and cell death

in response to CEA-TCB treatment. Neither morphology nor size of the organoid precluded T cells from infiltrating. CD8 T cells were able to penetrate into the centre of large organoids with a dense compact structure. This indicates that other components of the TME such as the ECM, TGF β expression, stromal cell types such as fibroblasts, suppressive immune cell types, or vascular characteristics are main drivers of lymphocyte exclusion commonly observed in CRC. ECM composition and density can be altered to more closely resemble the stiff and dense ECM observed in tumours, especially considering that it has been shown to regulate T cell motility and function (Bougherara et al., 2015; Hartmann et al., 2014; Kuczek et al., 2019; Salmon et al., 2012). Given the observation that T cells are frequently found in the stroma rather than the tumour, I incorporated CAFs into my 3D model in an effort to investigate whether CAFs would act as a physical barrier to successful T cell infiltration into organoids or through chemokine-related mechanisms such as through secretion of CXCL12 which has been demonstrated to lead to T cell exclusion (Ene-Obong et al., 2013; Feig et al., 2013). This is currently a work in progress and as described in Chapter 6 adjustments to the analysis methods need to be made to be able to draw useful insights from this triple component 3D model.

Given that TME is a highly complex dynamic network of soluble factors, cytokines, chemokines, ECM, and stromal and immune cell types efforts have been made to characterise and understand the TME and its effect on tumour progression and also in response to immunotherapeutic agents. In a first of its kind study of TME in high-grade serous ovarian cancer (HGSOC) analysed gene expression, matrix proteomics, cytokine/chemokine expression, ECM organization, and biomechanical properties of metastatic biopsies. This study provided valuable insights into molecular, cellular, and mechanical regulation of the TME and can be used as a resource for developing more complex TME models incorporating different cell subsets (Pearce et al., 2018). Addressing the poor performance of CAR T cells in solid tumours, a 3D co-culture model

of HGSOC cell lines, primary fibroblasts, and CAR-T cells embedded in collagen showed that targeting ECM in conjunction with CAR T cell therapy might improve efficacy of CAR T cells in solid tumours thus further demonstrating that multicellular 3D models are essential for generating insights that can not be obtained through 2D co-cultures (Joy et al., 2022). One ex vivo approach for studying lymphocyte-tumour interactions and TME components is through fresh tissue slices which are made by embedding in agarose a piece of a tumour rapidly obtained after tumour resection and then slicing it with a vibratome creating thin sheets of tumour tissue. Methods have been developed where these fresh tissue slices are stained with conjugated antibodies and imaged through confocal and two-photon microscopy allowing visualisation and tracking of different immune cell types as well as ECM proteins and tumour cells (Bougherara et al., 2015; Laforêts et al., 2023; Peranzoni et al., 2018; Salmon et al., 2012). These studies have identified ECM as a major stromal component influencing T cell migration and showed that in the tumour stroma, macrophages mediate lymphocyte trapping by forming long lasting interactions with CD8 T cells. Although these models accurately depict the TME, their major drawback is the very limited time these slices remain viable (less than 24 hours) thus not being suitable for drug testing. Additionally many laboratories do not have access to tumour resections and these models can not be easily modified to include or exclude certain variables. Therefore findings from these models need to be further tested and validated in other in vitro models where variables can be controlled or in mouse models as was done by Peranzoni and colleagues who after having observed that macrophage prevent T cell infiltration into tumours used a mouse tumour model to demonstrate that macrophage depletion through inhibition of colony-stimulating factor-1 receptor (CSF-1R) resulted in enhanced CD8 T cell migration and infiltration into tumour islets (Peranzoni et al., 2018).

To conclude, using a novel co-culture model comprised of PDOs and allogeneic T cells I have demonstrated in this thesis that both CD8 and CD4 T cells can contribute

to CEA-TCB mediated tumour growth inhibition, however, CD8 T cells were more consistently active across PDOs. Furthermore I have found a differential reliance of these two cell subsets on multiple effector mechanisms. Importantly IFN γ sensitivity was found not to be essential for CD8 T cell mediated tumour growth control as CD8 T cells effectively inhibited growth of an IFN γ insensitive PDO. However, patients with IFN γ sensitive tumours may respond better to CEA-TCB treatment as CD4 T cells predominantly rely on IFN γ secretion as a method of cytotoxicity. Furthermore, I modified this co-culture model into a screening platform for investigating potential resistance mechanisms to bispecific antibody therapy. Through this screen of various tumour microenvironment factors I identified TGF β as a driver of resistance to CEA-TCB through direct effect on CD8 T cell proliferation and cytolytic function. TGF β -induced CEA-TCB resistance was reversed by TGF β inhibition, treatment with IL-2, and T-cell co-stimulation with stroma targeted FAP-IL2v or tumour targeted CEA-4-1BBL fusion proteins, which both restored CD8 T-cell proliferation and granzyme expression. Thus, bispecific T-cell redirecting antibodies combined with FAP-IL2v or CEA-4-1BBL may be rational combination partners for tumours exhibiting TGF β immunosuppression. Additionally, I developed a 3D co-culture model that is suitable for studying T cell migration and infiltration into organoids. This model can be further developed to include more stromal and immune cell types to more closely recapitulate the complex tumour microenvironment and thus more accurately model responses to bispecific antibodies. I was able to pharmacologically increase CEA expression in organoids through targeting of the Wnt/ β -catenin pathway which translated into greater sensitivity to CEA-TCB and can be further investigated in clinical trials. I additionally demonstrated that the combination of a p38 MAPK inhibitor and nicotinamide can strongly downregulate CEA expression. RNA sequencing revealed differential metabolic and proliferation related signatures of untreated organoids and organoids treated with this combination. Further investigation of these pathways may provide insight into CEA regulation in tumours and

inform strategies to enhance CEA expression in tumours leading to better responses to CEA targeting therapies.

Chapter 8: References

- Abbott, R. C., Cross, R. S., & Jenkins, M. R. (2020). Finding the Keys to the CAR: Identifying Novel Target Antigens for T Cell Redirection Immunotherapies. *International Journal of Molecular Sciences* 2020, Vol. 21, Page 515, 21(2), 515. <https://doi.org/10.3390/IJMS21020515>
- Afshar-Sterle, S., Zotos, D., Bernard, N. J., Scherger, A. K., Rödling, L., Alsop, A. E., Walker, J., Masson, F., Belz, G. T., Corcoran, L. M., O'reilly, L. A., Strasser, A., Smyth, M. J., Johnstone, R., Tarlinton, D. M., Nutt, S. L., & Kallies, A. (2014). Fas ligand-mediated immune surveillance by T cells is essential for the control of spontaneous B cell lymphomas. *Nature Medicine* 2014 20:3, 20(3), 283–290. <https://doi.org/10.1038/nm.3442>
- Ahmadzadeh, M., Johnson, L. A., Heemskerk, B., Wunderlich, J. R., Dudley, M. E., White, D. E., & Rosenberg, S. A. (2009). Tumor antigen-specific CD8 T cells infiltrating the tumor express high levels of PD-1 and are functionally impaired. *Blood*, 114(8), 1537–1544. <https://doi.org/10.1182/BLOOD-2008-12-195792>
- Ahmadzadeh, M., & Rosenberg, S. A. (2006). IL-2 administration increases CD4+CD25hi Foxp3+ regulatory T cells in cancer patients. *Blood*, 107(6), 2409–2414. <https://doi.org/10.1182/BLOOD-2005-06-2399>
- Ahmed, N., Brawley, V. S., Hegde, M., Robertson, C., Ghazi, A., Gerken, C., Liu, E., Dakhova, O., Ashoori, A., Corder, A., Gray, T., Wu, M. F., Liu, H., Hicks, J., Rainusso, N., Dotti, G., Mei, Z., Grilley, B., Gee, A., ... Gottschalk, S. (2015). Human epidermal growth factor receptor 2 (HER2) - Specific chimeric antigen receptor - Modified T cells for the immunotherapy of HER2-positive sarcoma. *Journal of Clinical Oncology*, 33(15), 1688–1696. <https://doi.org/10.1200/JCO.2014.58.0225>
- Alexandrov, L. B., Nik-Zainal, S., Wedge, D. C., Aparicio, S. A. J. R., Behjati, S., Biankin, A. V., Bignell, G. R., Bolli, N., Borg, A., Børresen-Dale, A. L., Boyault, S., Burkhardt, B., Butler, A. P., Caldas, C., Davies, H. R., Desmedt, C., Eils, R., Eyfjörd, J. E., Foekens, J. A., ... Stratton, M. R. (2013). Signatures of mutational processes in human cancer. *Nature* 2013 500:7463, 500(7463), 415–421. <https://doi.org/10.1038/nature12477>
- Allison, T. J., Winter, C. C., Fournié, J. J., Bonneville, M., & Garboczi, D. N. (2001). Structure of a human $\gamma\delta$ T-cell antigen receptor. *Nature* 2001 411:6839, 411(6839), 820–824. <https://doi.org/10.1038/35081115>
- Almand, B., Clark, J. I., Nikitina, E., van Beynen, J., English, N. R., Knight, S. C., Carbone, D. P., & Gaborilovich, D. I. (2001). Increased Production of Immature Myeloid Cells in Cancer Patients: A Mechanism of Immunosuppression in Cancer. *The Journal of Immunology*, 166(1), 678–689. <https://doi.org/10.4049/JIMMUNOL.166.1.678>
- Amado, R. G., Wolf, M., Peeters, M., Van Cutsem, E., Siena, S., Freeman, D. J., Juan, T., Sikorski, R., Suggs, S., Radinsky, R., Patterson, S. D., & Chang, D. D. (2015). Wild-type KRAS is required for panitumumab efficacy in patients with metastatic colorectal cancer. *JOURNAL OF CLINICAL ONCOLOGY*, 26(10), 1626–1634. <https://doi.org/10.1200/JCO.2007.14.7116>

- Andrews, L. P., Yano, H., & Vignali, D. A. A. (2019). Inhibitory receptors and ligands beyond PD-1, PD-L1 and CTLA-4: breakthroughs or backups. *Nature Immunology* 2019 20:11, 20(11), 1425–1434. <https://doi.org/10.1038/s41590-019-0512-0>
- Angell, H., & Galon, J. (2013). From the immune contexture to the Immunoscore: the role of prognostic and predictive immune markers in cancer. *Current Opinion in Immunology*, 25(2), 261–267. <https://doi.org/10.1016/J.COI.2013.03.004>
- Angelova, M., Charoentong, P., Hackl, H., Fischer, M. L., Snajder, R., Krogsdam, A. M., Waldner, M. J., Bindea, G., Mlecnik, B., Galon, J., & Trajanoski, Z. (2015). Characterization of the immunophenotypes and antigenomes of colorectal cancers reveals distinct tumor escape mechanisms and novel targets for immunotherapy. *Genome Biology*, 16(1), 1–17. <https://doi.org/10.1186/S13059-015-0620-6/FIGURES/4>
- Antoniotti, C., Rossini, D., Pietrantonio, F., Catteau, A., Salvatore, L., Lonardi, S., Boquet, I., Tamberi, S., Marmorino, F., Moretto, R., Ambrosini, M., Tamburini, E., Tortora, G., Passardi, A., Bergamo, F., Kassambara, A., Sbarato, T., Morano, F., Ritorto, G., ... Cremolini, C. (2022a). Upfront FOLFOXIRI plus bevacizumab with or without atezolizumab in the treatment of patients with metastatic colorectal cancer (AtezoTRIBE): a multicentre, open-label, randomised, controlled, phase 2 trial. *The Lancet Oncology*, 23(7), 876–887. [https://doi.org/10.1016/S1470-2045\(22\)00274-1](https://doi.org/10.1016/S1470-2045(22)00274-1)
- Antoniotti, C., Rossini, D., Pietrantonio, F., Catteau, A., Salvatore, L., Lonardi, S., Boquet, I., Tamberi, S., Marmorino, F., Moretto, R., Ambrosini, M., Tamburini, E., Tortora, G., Passardi, A., Bergamo, F., Kassambara, A., Sbarato, T., Morano, F., Ritorto, G., ... Cremolini, C. (2022b). Upfront FOLFOXIRI plus bevacizumab with or without atezolizumab in the treatment of patients with metastatic colorectal cancer (AtezoTRIBE): a multicentre, open-label, randomised, controlled, phase 2 trial. *The Lancet Oncology*, 23(7), 876–887. [https://doi.org/10.1016/S1470-2045\(22\)00274-1](https://doi.org/10.1016/S1470-2045(22)00274-1)
- Appay, V., Zaunders, J. J., Papagno, L., Sutton, J., Jaramillo, A., Waters, A., Easterbrook, P., Grey, P., Smith, D., McMichael, A. J., Cooper, D. A., Rowland-Jones, S. L., & Kelleher, A. D. (2002). Characterization of CD4+ CTLs Ex Vivo. *The Journal of Immunology*, 168(11), 5954–5958. <https://doi.org/10.4049/JIMMUNOL.168.11.5954>
- Arango, D., Wilson, A. J., Shi, Q., Corner, G. A., Arañes, M. J., Nicholas, C., Lesser, M., Mariadason, J. M., & Augenlicht, L. H. (2004). Molecular mechanisms of action and prediction of response to oxaliplatin in colorectal cancer cells. *British Journal of Cancer* 2004 91:11, 91(11), 1931–1946. <https://doi.org/10.1038/sj.bjc.6602215>
- Argilés, G., Saunders, M. P., Rivera, F., Sobrero, A., Benson, A., Guillén Ponce, C., Cascinu, S., Van Cutsem, E., MacPherson, I. R., Strumberg, D., Köhne, C. H., Zalberg, J., Wagner, A., Luigi Garosi, V., Grunert, J., Tabernero, J., & Ciardiello, F. (2015). Regorafenib plus modified FOLFOX6 as first-line treatment of metastatic colorectal cancer: A phase II trial. *European Journal of Cancer*, 51(8), 942–949. <https://doi.org/10.1016/J.EJCA.2015.02.013>
- Armstrong, L., Jordan, N., & Millar, A. (1996). Interleukin 10 (IL-10) regulation of tumour necrosis factor alpha (TNF-alpha) from human alveolar macrophages and

peripheral blood monocytes. *Thorax*, 51(2), 143–149.
<https://doi.org/10.1136/THX.51.2.143>

- Arnaud, J. P., Koehl, C., & Adloff, M. (1980). Carcinoembryonic antigen (CEA) in diagnosis and prognosis of colorectal carcinoma. *Diseases of the Colon and Rectum*, 23(3), 141–144. <https://doi.org/10.1007/bf02587615>
- Ascierto, P. A., Simeone, E., Sznol, M., Fu, Y. X., & Melero, I. (2010). Clinical Experiences With Anti-CD137 and Anti-PD1 Therapeutic Antibodies. *Seminars in Oncology*, 37(5), 508–516. <https://doi.org/10.1053/J.SEMINONCOL.2010.09.008>
- Atkins, D., Breuckmann, A., Schmahl, G. E., Binner, P., Ferrone, S., Krummenauer, F., Störkel, S., & Seliger, B. (2004). MHC class I antigen processing pathway defects, ras mutations and disease stage in colorectal carcinoma. *International Journal of Cancer*, 109(2), 265–273. <https://doi.org/10.1002/IJC.11681>
- Atkins, M. B., Lotze, M. T., Dutcher, J. P., Fisher, R. I., Weiss, G., Margolin, K., Abrams, J., Sznol, M., Parkinson, D., Hawkins, M., Paradise, C., Kunkel, L., & Rosenberg, S. A. (1999). High-dose recombinant interleukin 2 therapy for patients with metastatic melanoma: Analysis of 270 patients treated between 1985 and 1993. *Journal of Clinical Oncology*, 17(7), 2105–2116.
<https://doi.org/10.1200/jco.1999.17.7.2105>
- Atkuri, K. R., Herzenberg, L. A., & Herzenberg, L. A. (2005). Culturing at atmospheric oxygen levels impacts lymphocyte function. *Proceedings of the National Academy of Sciences of the United States of America*, 102(10), 3756–3759.
<https://doi.org/10.1073/PNAS.0409910102/ASSET/D4527287-3816-4B77-8E77-C22C1878619C/ASSETS/GRAPHIC/ZPQ0080574490002.JPEG>
- Bacac, M., Fauti, T., Sam, J., Colombetti, S., Weinzierl, T., Oualet, D., Bodmer, W., Lehmann, S., Hofer, T., Hosse, R. J., Moessner, E., Ast, O., Bruenker, P., Grau-Richards, S., Schaller, T., Seidl, A., Gerdes, C., Perro, M., Nicolini, V., ... Umaña, P. (2016). A novel carcinoembryonic antigen T-cell bispecific antibody (CEA TCB) for the treatment of solid tumors. *Clinical Cancer Research*, 22(13), 3286–3297.
<https://doi.org/10.1158/1078-0432.CCR-15-1696/268428/AM/A-NOVEL-CARCINOEMBRYONIC-ANTIGEN-T-CELL-BISPECIFIC>
- Baker, S. J., Fearon, E. R., Nigro, J. M., Hamilton, S. R., Preisinger, A. C., Jessup, J. M., Vantuinen, P., Ledbetter, D. H., Barker, D. F., Nakamura, Y., White, R., & Vogelstein, B. (1989). Chromosome 17 Deletions and p53 Gene Mutations in Colorectal Carcinomas. *Science*, 244(4901), 217–221.
<https://doi.org/10.1126/SCIENCE.2649981>
- Baker, S. J., Markowitz, S., Fearon, E. R., Willson, J. K. V., & Vogelstein, B. (1990). Suppression of Human Colorectal Carcinoma Cell Growth by Wild-Type p53. *Science*, 249(4971), 912–915. <https://doi.org/10.1126/SCIENCE.2144057>
- Balsamo, M., Scordamaglia, F., Pietra, G., Manzini, C., Cantoni, C., Boitano, M., Queirolo, P., Vermi, W., Facchetti, F., Moretta, A., Moretta, L., Mingari, M. C., & Vitale, M. (2009). Melanoma-associated fibroblasts modulate NK cell phenotype and antitumor cytotoxicity. *Proceedings of the National Academy of Sciences of the United States of America*, 106(49), 20847–20852.
https://doi.org/10.1073/PNAS.0906481106/SUPPL_FILE/0906481106SI.PDF

- Barber, D. L., Wherry, E. J., Masopust, D., Zhu, B., Allison, J. P., Sharpe, A. H., Freeman, G. J., & Ahmed, R. (2005). Restoring function in exhausted CD8 T cells during chronic viral infection. *Nature* 2005 439:7077, 439(7077), 682–687. <https://doi.org/10.1038/nature04444>
- Bargou, R., Leo, E., Zugmaier, G., Klinger, M., Goebeler, M., Knop, S., Noppeney, R., Viardot, A., Hess, G., Schuler, M., Einsele, H., Brandl, C., Wolf, A., Kirchinger, P., Klappers, P., Schmidt, M., Riethmüller, G., Reinhardt, C., Baeuerle, P. A., & Kufer, P. (2008). Tumor regression in cancer patients by very low doses of a T cell-engaging antibody. *Science*, 321(5891), 974–977. https://doi.org/10.1126/SCIENCE.1158545/SUPPL_FILE/BARGOU.SOM.PDF
- Barker, N. (2013). Adult intestinal stem cells: critical drivers of epithelial homeostasis and regeneration. *Nature Reviews Molecular Cell Biology* 2013 15:1, 15(1), 19–33. <https://doi.org/10.1038/nrm3721>
- Bartelt, R. R., Cruz-Orcutt, N., Collins, M., & Houtman, J. C. D. (2009). Comparison of T Cell Receptor-Induced Proximal Signaling and Downstream Functions in Immortalized and Primary T Cells. *PLOS ONE*, 4(5), e5430. <https://doi.org/10.1371/JOURNAL.PONE.0005430>
- Barzi, A., Azad, N. S., Yang, Y., Tsao-Wei, D., Rehman, R., Fakhri, M., Iqbal, S., El-Khoueiry, A. B., Millstein, J., Jayachandran, P., Zhang, W., & Lenz, H.-J. (2022). Phase I/II study of regorafenib (rego) and pembrolizumab (pembro) in refractory microsatellite stable colorectal cancer (MSSCRC). *Journal of Clinical Oncology*, 40(4_suppl), 15–15. https://doi.org/10.1200/JCO.2022.40.4_SUPPL.015
- Bassani-Sternberg, M., Bräunlein, E., Klar, R., Engleitner, T., Sinitcyn, P., Audehm, S., Straub, M., Weber, J., Slotta-Huspenina, J., Specht, K., Martignoni, M. E., Werner, A., Hein, R., Busch, D. H., Peschel, C., Rad, R., Cox, J., Mann, M., & Krackhardt, A. M. (2016). Direct identification of clinically relevant neoepitopes presented on native human melanoma tissue by mass spectrometry. *Nature Communications* 2016 7:1, 7(1), 1–16. <https://doi.org/10.1038/ncomms13404>
- Baumeister, S. H., Freeman, G. J., Dranoff, G., & Sharpe, A. H. (2016). Coinhibitory Pathways in Immunotherapy for Cancer. *Annual Review of Immunology*, 34, 539–573. <https://doi.org/10.1146/ANNUREV-IMMUNOL-032414-112049>
- Becht, E., De Reyniès, A., Giraldo, N. A., Pilati, C., Buttard, B., Lacroix, L., Selves, J., Sautès-Fridman, C., Laurent-Puig, P., & Fridman, W. H. (2016). Immune and stromal classification of Colorectal cancer is associated with molecular subtypes and relevant for precision immunotherapy. *Clinical Cancer Research*, 22(16), 4057–4066. <https://doi.org/10.1158/1078-0432.CCR-15-2879/274376/AM/IMMUNE-AND-STROMAL-CLASSIFICATION-OF-COLORECTAL>
- Becker, C., Fantini, M. C., Schramm, C., Lehr, H. A., Wirtz, S., Nikolaev, A., Burg, J., Strand, S., Kiesslich, R., Huber, S., Ito, H., Nishimoto, N., Yoshizaki, K., Kishimoto, T., Galle, P. R., Blessing, M., Rose-John, S., & Neurath, M. F. (2004). TGF- β Suppresses Tumor Progression in Colon Cancer by Inhibition of IL-6 trans-Signaling. *Immunity*, 21(4), 491–501. <https://doi.org/10.1016/J.IMMUNI.2004.07.020>

- Benchimol, S., Fuks, A., Jothy, S., Beauchemin, N., Shirota, K., & Stanners, C. P. (1989). Carcinoembryonic antigen, a human tumor marker, functions as an intercellular adhesion molecule. *Cell*, *57*(2), 327–334. [https://doi.org/10.1016/0092-8674\(89\)90970-7](https://doi.org/10.1016/0092-8674(89)90970-7)
- Bendell, J., Ulahannan, S. V., Chu, Q., Patel, M., George, B., Auguste, A., Leo-Kress, T., Stadermann, K. B., Kraemer, N., Elgadi, M., & Johnson, M. (2020). Abstract 779: A phase I study of BI 754111, an anti-LAG-3 monoclonal antibody (mAb), in combination with BI 754091, an anti-PD-1 mAb: Biomarker analyses from the microsatellite stable metastatic colorectal cancer (MSS mCRC) cohort. *Cancer Research*, *80*(16_Supplement), 779–779. <https://doi.org/10.1158/1538-7445.AM2020-779>
- Benonisson, H., Altıntaş, I., Sluijter, M., Verploegen, S., Labrijn, A. F., Schuurhuis, D. H., Houtkamp, M. A., Sijf Verbeek, J., Schuurman, J., & van Hall, T. (2019). CD3-bispecific antibody therapy turns solid tumors into inflammatory sites but does not install protective memory. *Molecular Cancer Therapeutics*, *18*(2), 312–322. <https://doi.org/10.1158/1535-7163.MCT-18-0679/87728/AM/CD3-BISPECIFIC-ANTIBODY-THERAPY-TURNS-SOLID-TUMORS>
- Ben-Shoshan, J., Maysel-Auslender, S., Mor, A., Keren, G., & George, J. (2008). Hypoxia controls CD4+CD25+ regulatory T-cell homeostasis via hypoxia-inducible factor-1 α . *European Journal of Immunology*, *38*(9), 2412–2418. <https://doi.org/10.1002/EJI.200838318>
- Benvenuti, S., Sartore-Bianchi, A., Di Nicolantonio, F., Zanon, C., Moroni, M., Veronese, S., Siena, S., & Bardelli, A. (2007). Oncogenic Activation of the RAS/RAF Signaling Pathway Impairs the Response of Metastatic Colorectal Cancers to Anti-Epidermal Growth Factor Receptor Antibody Therapies. *Cancer Research*, *67*(6), 2643–2648. <https://doi.org/10.1158/0008-5472.CAN-06-4158>
- Berahovich, R., Liu, X., Zhou, H., Tsadik, E., Xu, S., Golubovskaya, V., & Wu, L. (2019). Hypoxia Selectively Impairs CAR-T Cells In Vitro. *Cancers 2019, Vol. 11, Page 602*, *11*(5), 602. <https://doi.org/10.3390/CANCERS11050602>
- Berg, D. J., Davidson, N., Kühn, R., Müller, W., Menon, S., Holland, G., Thompson-Snipes, L., Leach, M. W., & Rennick, D. (1996). Enterocolitis and colon cancer in interleukin-10-deficient mice are associated with aberrant cytokine production and CD4(+) TH1-like responses. *The Journal of Clinical Investigation*, *98*(4), 1010–1020. <https://doi.org/10.1172/JCI118861>
- Berman, R. M., Suzuki, T., Tahara, H., Robbins, P. D., Narula, S. K., & Lotze, M. T. (1996). Systemic administration of cellular IL-10 induces an effective, specific, and long-lived immune response against established tumors in mice. *The Journal of Immunology*, *157*(1), 231–238. <https://doi.org/10.4049/JIMMUNOL.157.1.231>
- Berntsen, A., Brimnes, M. K., Straten, P. T., & Svane, I. M. (2010). Increase of circulating CD4+CD25highFoxp3+ Regulatory T cells in patients with metastatic renal cell carcinoma during treatment with dendritic cell vaccination and low-dose interleukin-2. *Journal of Immunotherapy*, *33*(4), 425–434. <https://doi.org/10.1097/CJI.0B013E3181CD870F>
- Bertram, J., Peacock, J. W., Tan, C., Mui, A. L. F., Chung, S. W., Gleave, M. E., Dedhar, S., Cox, M. E., & Ong, C. J. (2006). Inhibition of the Phosphatidylinositol

3'-Kinase Pathway Promotes Autocrine Fas-Induced Death of Phosphatase and Tensin Homologue-Deficient Prostate Cancer Cells. *Cancer Research*, 66(9), 4781–4788. <https://doi.org/10.1158/0008-5472.CAN-05-3173>

- Betts, G., Jones, E., Junaid, S., El-Shanawany, T., Scurr, M., Mizen, P., Kumar, M., Jones, S., Rees, B., Williams, G., Gallimore, A., & Godkin, A. (2012). Suppression of tumour-specific CD4+ T cells by regulatory T cells is associated with progression of human colorectal cancer. *Gut*, 61(8), 1163–1171. <https://doi.org/10.1136/GUTJNL-2011-300970>
- Bhat, P., Leggatt, G., Waterhouse, N., & Frazer, I. H. (2017). Interferon- γ derived from cytotoxic lymphocytes directly enhances their motility and cytotoxicity. *Cell Death & Disease* 2017 8:6, 8(6), e2836–e2836. <https://doi.org/10.1038/cddis.2017.67>
- Biswas, S. K., & Mantovani, A. (2010). Macrophage plasticity and interaction with lymphocyte subsets: cancer as a paradigm. *Nature Immunology* 2010 11:10, 11(10), 889–896. <https://doi.org/10.1038/ni.1937>
- Boehm, U., Klamp, T., Groot, M., & Howard, J. C. (1997). CELLULAR RESPONSES TO INTERFERON- γ . *Annual Review of Immunology*, 15, 749–795. <https://doi.org/10.1146/ANNUREV.IMMUNOL.15.1.749>
- Boël, P., Wildmann, C., Sensi, M. L., Brasseur, R., Renaud, J. C., Coulie, P., Boon, T., & van der Bruggen, P. (1995). BAGE: a new gene encoding an antigen recognized on human melanomas by cytolytic T lymphocytes. *Immunity*, 2(2), 167–175. [https://doi.org/10.1016/S1074-7613\(95\)80053-0](https://doi.org/10.1016/S1074-7613(95)80053-0)
- Bogdan, C., Vodovotz, Y., & Nathan, C. (1991). Macrophage deactivation by interleukin 10. *Journal of Experimental Medicine*, 174(6), 1549–1555. <https://doi.org/10.1084/JEM.174.6.1549>
- Bokemeyer, C., Cutsem, E. Van, Rougier, P., Ciardiello, F., Heeger, S., Schlichting, M., Celik, I., & Köhne, C. H. (2012). Addition of cetuximab to chemotherapy as first-line treatment for KRAS wild-type metastatic colorectal cancer: Pooled analysis of the CRYSTAL and OPUS randomised clinical trials. *European Journal of Cancer*, 48(10), 1466–1475. <https://doi.org/10.1016/J.EJCA.2012.02.057>
- Boon, T., Coulie, P. G., & Van Den Eynde, B. (1997). Tumor antigens recognized by T cells. *Immunology Today*, 18(6), 267–268. [https://doi.org/10.1016/S0167-5699\(97\)80020-5](https://doi.org/10.1016/S0167-5699(97)80020-5)
- Boon, T., & Kellermann, O. (1977). Rejection by syngeneic mice of cell variants obtained by mutagenesis of a malignant teratocarcinoma cell line. *Proceedings of the National Academy of Sciences*, 74(1), 272–275. <https://doi.org/10.1073/PNAS.74.1.272>
- Borlak, J., Länger, F., Spänel, R., Schöndorfer, G., & Dittrich, C. (2016). Immune-mediated liver injury of the cancer therapeutic antibody catumaxomab targeting EpCAM, CD3 and Fc γ receptors. *Oncotarget*, 7(19), 28059. <https://doi.org/10.18632/ONCOTARGET.8574>
- Bougherara, H., Mansuet-Lupo, A., Alifano, M., Ngô, C., Damotte, D., Le Frère-Belda, M. A., Donnadieu, E., & Peranzoni, E. (2015). Real-time imaging of resident T cells in human lung and ovarian carcinomas reveals how different tumor

- microenvironments control T lymphocyte migration. *Frontiers in Immunology*, 6(OCT), 500. <https://doi.org/10.3389/FIMMU.2015.00500/BIBTEX>
- Bouzin, C., Brouet, A., De Vriese, J., DeWever, J., & Feron, O. (2007). Effects of Vascular Endothelial Growth Factor on the Lymphocyte-Endothelium Interactions: Identification of Caveolin-1 and Nitric Oxide as Control Points of Endothelial Cell Energy. *The Journal of Immunology*, 178(3), 1505–1511. <https://doi.org/10.4049/JIMMUNOL.178.3.1505>
- Brabletz, T., Jung, A., Reu, S., Porzner, M., Hlubek, F., Kunz-Schughart, L. A., Knuechel, R., & Kirchner, T. (2001). Variable β -catenin expression in colorectal cancers indicates tumor progression driven by the tumor environment. *Proceedings of the National Academy of Sciences of the United States of America*, 98(18), 10356–10361. <https://doi.org/10.1073/PNAS.171610498/ASSET/01EAA5E9-0913-4AF7-942E-10A5B771806F/ASSETS/GRAPHIC/PQ1716104005.JPEG>
- Brabletz, T., Pfeuffer, I., Schorr, E., Siebelt, F., Wirth, T., & Serfling, E. (1993). Transforming Growth Factor β and Cyclosporin A Inhibit the Inducible Activity of the Interleukin-2 Gene in T Cells Through a Noncanonical Octamer-Binding Site. *Molecular and Cellular Biology*, 13(2), 1155–1162. <https://doi.org/10.1128/MCB.13.2.1155-1162.1993>
- Braig, F., Brandt, A., Goebeler, M., Tony, H. P., Kurze, A. K., Nollau, P., Bumm, T., Böttcher, S., Bargou, R. C., & Binder, M. (2017). Resistance to anti-CD19/CD3 BiTE in acute lymphoblastic leukemia may be mediated by disrupted CD19 membrane trafficking. *Blood*, 129(1), 100–104. <https://doi.org/10.1182/BLOOD-2016-05-718395>
- Brandes, M., Willmann, K., Bioley, G., Lévy, N., Eberl, M., Luo, M., Tampé, R., Lévy, F., Romero, P., & Moser, B. (2009). Cross-presenting human $\gamma\delta$ T cells induce robust CD8+ $\alpha\beta$ T cell responses. *Proceedings of the National Academy of Sciences of the United States of America*, 106(7), 2307–2312. https://doi.org/10.1073/PNAS.0810059106/SUPPL_FILE/0810059106SI.PDF
- Brandes, M., Willmann, K., & Moser, B. (2005). Immunology: Professional antigen-presentation function by human $\gamma\delta$ cells. *Science*, 309(5732), 264–268. https://doi.org/10.1126/SCIENCE.1110267/SUPPL_FILE/BRANDES.SOM.PDF
- Brash, D. E., Rudolph, J. A., Simon, J. A., Lin, A., Mckenna, G. J., Baden, H. P., Halperin, A. J., & Pontén, J. (1991). A role for sunlight in skin cancer: UV-induced p53 mutations in squamous cell carcinoma. *Proceedings of the National Academy of Sciences*, 88(22), 10124–10128. <https://doi.org/10.1073/PNAS.88.22.10124>
- Brauchle, E., Kasper, J., Daum, R., Schierbaum, N., Falch, C., Kirschniak, A., Schäffer, T. E., & Schenke-Layland, K. (2018). Biomechanical and biomolecular characterization of extracellular matrix structures in human colon carcinomas. *Matrix Biology*, 68–69, 180–193. <https://doi.org/10.1016/J.MATBIO.2018.03.016>
- Bray, F., Ferlay, J., Soerjomataram, I., Siegel, R. L., Torre, L. A., & Jemal, A. (2018). Global cancer statistics 2018: GLOBOCAN estimates of incidence and mortality worldwide for 36 cancers in 185 countries. *CA: A Cancer Journal for Clinicians*, 68(6), 394–424. <https://doi.org/10.3322/CAAC.21492>

- Brien, J. D., Uhrlaub, J. L., & Nikolich-Žugich, J. (2008). West Nile Virus-Specific CD4 T Cells Exhibit Direct Antiviral Cytokine Secretion and Cytotoxicity and Are Sufficient for Antiviral Protection. *The Journal of Immunology*, *181*(12), 8568–8575. <https://doi.org/10.4049/JIMMUNOL.181.12.8568>
- Briggs, S., & Tomlinson, I. (2013). Germline and somatic polymerase ϵ and δ mutations define a new class of hypermutated colorectal and endometrial cancers. *The Journal of Pathology*, *230*(2), 148–153. <https://doi.org/10.1002/PATH.4185>
- Bright, J. J., & Sriram, S. (1998). TGF- β Inhibits IL-12-Induced Activation of Jak-STAT Pathway in T Lymphocytes. *The Journal of Immunology*, *161*(4), 1772–1777. <https://doi.org/10.4049/JIMMUNOL.161.4.1772>
- Brischwein, K., Parr, L., Pflanz, S., Volkland, J., Lumsden, J., Klinger, M., Locher, M., Hammond, S. A., Kiener, P., Kufer, P., Schlereth, B., & Baeuerle, P. A. (2007). Strictly target cell-dependent activation of T cells by bispecific single-chain antibody constructs of the BiTE class. *Journal of Immunotherapy*, *30*(8), 798–807. <https://doi.org/10.1097/CJI.0B013E318156750C>
- Bromberg, J. F., Horvath, C. M., Wen, Z., Schreiber, R. D., & Darnell, J. E. (1996). Transcriptionally active Stat1 is required for the antiproliferative effects of both interferon alpha and interferon gamma. *Proceedings of the National Academy of Sciences*, *93*(15), 7673–7678. <https://doi.org/10.1073/PNAS.93.15.7673>
- Bronger, H., Kraeft, S., Schwarz-Boeger, U., Cerny, C., Stöckel, A., Avril, S., Kiechle, M., & Schmitt, M. (2012). Modulation of CXCR3 ligand secretion by prostaglandin E 2 and cyclooxygenase inhibitors in human breast cancer. *Breast Cancer Research*, *14*(1), 1–14. <https://doi.org/10.1186/BCR3115/FIGURES/7>
- Bronger, H., Singer, J., Windmüller, C., Reuning, U., Zech, D., Delbridge, C., Dorn, J., Kiechle, M., Schmalfeldt, B., Schmitt, M., & Avril, S. (2016). CXCL9 and CXCL10 predict survival and are regulated by cyclooxygenase inhibition in advanced serous ovarian cancer. *British Journal of Cancer* *2016 115:5*, *115*(5), 553–563. <https://doi.org/10.1038/bjc.2016.172>
- Bronte, V., Apolloni, E., Cabrelle, A., Ronca, R., Serafini, P., Zamboni, P., Restifo, N. P., & Zanovello, P. (2000). Identification of a CD11b⁺/Gr-1⁺/CD31⁺ myeloid progenitor capable of activating or suppressing CD8⁺T cells. *Blood*, *96*(12), 3838–3846. <https://doi.org/10.1182/BLOOD.V96.12.3838>
- Brown, D. M. (2010). Cytolytic CD4 cells: Direct mediators in infectious disease and malignancy. *Cellular Immunology*, *262*(2), 89–95. <https://doi.org/10.1016/J.CELLIMM.2010.02.008>
- Brown, D. M., Lee, S., Garcia-Hernandez, M. de la L., & Swain, S. L. (2012). Multifunctional CD4 Cells Expressing Gamma Interferon and Perforin Mediate Protection against Lethal Influenza Virus Infection. *Journal of Virology*, *86*(12), 6792. <https://doi.org/10.1128/JVI.07172-11>
- Buckanovich, R. J., Facciabene, A., Kim, S., Benencia, F., Sasaroli, D., Balint, K., Katsaros, D., O'Brien-Jenkins, A., Gimotty, P. A., & Coukos, G. (2008). Endothelin B receptor mediates the endothelial barrier to T cell homing to tumors and disables immune therapy. *Nature Medicine* *2008 14:1*, *14*(1), 28–36. <https://doi.org/10.1038/nm1699>

- Bulavin, D. V., Amundson, S. A., & Fornace, A. J. (2002). p38 and Chk1 kinases: different conductors for the G2/M checkpoint symphony. *Current Opinion in Genetics & Development*, *12*(1), 92–97. [https://doi.org/10.1016/S0959-437X\(01\)00270-2](https://doi.org/10.1016/S0959-437X(01)00270-2)
- Bullock, A., Grossman, J., Fakih, M., Lenz, H., Gordon, M., Margolin, K., Wilky, B., Mahadevan, D., Trent, J., Bockorny, B., Moser, J., Balmanoukian, A., Schlechter, B., Ortuzar Feliu, W., Rosenthal, K., Bullock, B., Stebbing, J., Godwin, J., O'Day, S., ... El-Khoueiry, A. (2022). LBA O-9 Botensilimab, a novel innate/adaptive immune activator, plus balstilimab (anti-PD-1) for metastatic heavily pretreated microsatellite stable colorectal cancer. *Annals of Oncology*, *33*, S376. <https://doi.org/10.1016/j.annonc.2022.04.453>
- Bunt, S. K., Yang, L., Sinha, P., Clements, V. K., Leips, J., & Ostrand-Rosenberg, S. (2007). Reduced Inflammation in the Tumor Microenvironment Delays the Accumulation of Myeloid-Derived Suppressor Cells and Limits Tumor Progression. *Cancer Research*, *67*(20), 10019–10026. <https://doi.org/10.1158/0008-5472.CAN-07-2354>
- Cai, H., Zhang, Y., Wang, J., & Gu, J. (2021). Defects in Macrophage Reprogramming in Cancer Therapy: The Negative Impact of PD-L1/PD-1. *Frontiers in Immunology*, *12*, 690869. <https://doi.org/10.3389/FIMMU.2021.690869/BIBTEX>
- Caldwell, C. C., Kojima, H., Lukashev, D., Armstrong, J., Farber, M., Apasov, S. G., & Sitkovsky, M. V. (2001). Differential Effects of Physiologically Relevant Hypoxic Conditions on T Lymphocyte Development and Effector Functions. *The Journal of Immunology*, *167*(11), 6140–6149. <https://doi.org/10.4049/JIMMUNOL.167.11.6140>
- Calon, A., Espinet, E., Palomo-Ponce, S., Tauriello, D. V. F., Iglesias, M., Céspedes, M. V., Sevillano, M., Nadal, C., Jung, P., Zhang, X. H. F., Byrom, D., Riera, A., Rossell, D., Mangués, R., Massagué, J., Sancho, E., & Batlle, E. (2012). Dependency of Colorectal Cancer on a TGF- β -Driven Program in Stromal Cells for Metastasis Initiation. *Cancer Cell*, *22*(5), 571–584. <https://doi.org/10.1016/J.CCR.2012.08.013>
- Calon, A., Lonardo, E., Berenguer-Llargo, A., Espinet, E., Hernando-Momblona, X., Iglesias, M., Sevillano, M., Palomo-Ponce, S., Tauriello, D. V. F., Byrom, D., Cortina, C., Morral, C., Barceló, C., Tosi, S., Riera, A., Attolini, C. S. O., Rossell, D., Sancho, E., & Batlle, E. (2015). Stromal gene expression defines poor-prognosis subtypes in colorectal cancer. *Nature Genetics* *2015* *47*:4, *47*(4), 320–329. <https://doi.org/10.1038/ng.3225>
- Cao, X., Cai, S. F., Fehniger, T. A., Song, J., Collins, L. I., Piwnica-Worms, D. R., & Ley, T. J. (2007). Granzyme B and Perforin Are Important for Regulatory T Cell-Mediated Suppression of Tumor Clearance. *Immunity*, *27*(4), 635–646. <https://doi.org/10.1016/J.IMMUNI.2007.08.014>
- Casares, N., Pequignot, M. O., Tesniere, A., Ghiringhelli, F., Roux, S., Chaput, N., Schmitt, E., Hamai, A., Hervas-Stubbs, S., Obeid, M., Coutant, F., Métivier, D., Pichard, E., Aucouturier, P., Pierron, G., Garrido, C., Zitvogel, L., & Kroemer, G. (2005). Caspase-dependent immunogenicity of doxorubicin-induced tumor cell death. *Journal of Experimental Medicine*, *202*(12), 1691–1701. <https://doi.org/10.1084/JEM.20050915>

- Castro, A., Ozturk, K., Pyke, R. M., Xian, S., Zanetti, M., & Carter, H. (2019). Elevated neoantigen levels in tumors with somatic mutations in the HLA-A, HLA-B, HLA-C and B2M genes. *BMC Medical Genomics*, *12*(6), 1–13. <https://doi.org/10.1186/S12920-019-0544-1/FIGURES/5>
- Cavassani, K. A., Ishii, M., Wen, H., Schaller, M. A., Lincoln, P. M., Lukacs, N. W., Hogaboam, C. M., & Kunkel, S. L. (2008). TLR3 is an endogenous sensor of tissue necrosis during acute inflammatory events. *Journal of Experimental Medicine*, *205*(11), 2609–2621. <https://doi.org/10.1084/JEM.20081370>
- Cederbom, L., Hall, H., & Ivars, F. (2000). CD4+CD25+ regulatory T cells down-regulate co-stimulatory molecules on antigen-presenting cells. *European Journal of Immunology*, *30*(6), 1538–1543. <https://pubmed.ncbi.nlm.nih.gov/10898488/>
- Chambers, C. A., Kuhns, M. S., Egen, J. G., & Allison, J. P. (2001). CTLA-4-Mediated Inhibition in Regulation of T Cell Responses: Mechanisms and Manipulation in Tumor Immunotherapy. *Annual Review of Immunology*, *19*, 565–594. <https://doi.org/10.1146/ANNUREV.IMMUNOL.19.1.565>
- Chang, H. C., Han, L., Goswami, R., Nguyen, E. T., Pelloso, D., Robertson, M. J., & Kaplan, M. H. (2009). Impaired development of human Th1 cells in patients with deficient expression of STAT4. *Blood*, *113*(23), 5887–5890. <https://doi.org/10.1182/BLOOD-2008-09-179820>
- Chang, H. C., Sehra, S., Goswami, R., Yao, W., Yu, Q., Stritesky, G. L., Jabeen, R., McKinley, C., Ahyi, A. N., Han, L., Nguyen, E. T., Robertson, M. J., Perumal, N. B., Tepper, R. S., Nutt, S. L., & Kaplan, M. H. (2010). The transcription factor PU.1 is required for the development of IL-9-producing T cells and allergic inflammation. *Nature Immunology* *2010 11:6*, *11*(6), 527–534. <https://doi.org/10.1038/ni.1867>
- Chang, Q., Bournazou, E., Sansone, P., Berishaj, M., Gao, S. P., Daly, L., Wels, J., Theilen, T., Granitto, S., Zhang, X., Cotari, J., Alpaugh, M. L., de Stanchina, E., Manova, K., Li, M., Bonafe, M., Ceccarelli, C., Taffurelli, M., Santini, D., ... Bromberg, J. (2013). The IL-6/JAK/Stat3 Feed-Forward Loop Drives Tumorigenesis and Metastasis. *Neoplasia*, *15*(7), 848-IN45. <https://doi.org/10.1593/NEO.13706>
- Chaplin, D. D. (2010). Overview of the immune response. *Journal of Allergy and Clinical Immunology*, *125*(2), S3–S23. <https://doi.org/10.1016/J.JACI.2009.12.980>
- Chen, D. S., & Mellman, I. (2013). Oncology Meets Immunology: The Cancer-Immunity Cycle. *Immunity*, *39*(1), 1–10. <https://doi.org/10.1016/J.IMMUNI.2013.07.012>
- Chen, D. S., & Mellman, I. (2017). Elements of cancer immunity and the cancer-immune set point. *Nature* *2017 541:7637*, *541*(7637), 321–330. <https://doi.org/10.1038/nature21349>
- Chen, L., & Flies, D. B. (2013). Molecular mechanisms of T cell co-stimulation and co-inhibition. *Nature Reviews Immunology* *2013 13:4*, *13*(4), 227–242. <https://doi.org/10.1038/nri3405>
- Chen, S., Zhang, Z., Zheng, X., Tao, H., Zhang, S., Ma, J., Liu, Z., Wang, J., Qian, Y., Cui, P., Huang, D., Huang, Z., Wu, Z., & Hu, Y. (2021). Response Efficacy of PD-1 and PD-L1 Inhibitors in Clinical Trials: A Systematic Review and Meta-Analysis.

Frontiers in Oncology, 11, 562315.
<https://doi.org/10.3389/FONC.2021.562315/FULL>

- Chen, W. F., & Zlotnik, A. (1991). IL-10: a novel cytotoxic T cell differentiation factor. *The Journal of Immunology*, 147(2), 528–534.
<https://doi.org/10.4049/JIMMUNOL.147.2.528>
- Chen, W. J., Jin, W., Hardegen, N., Lei, K. J., Li, L., Marinos, N., McGrady, G., & Wahl, S. M. (2003a). Conversion of peripheral CD4+CD25- naive T cells to CD4+CD25+ regulatory T cells by TGF-beta induction of transcription factor Foxp3. *The Journal of Experimental Medicine*, 198(12), 1875–1886.
<https://doi.org/10.1084/JEM.20030152>
- Chen, W. J., Jin, W., Hardegen, N., Lei, K. J., Li, L., Marinos, N., McGrady, G., & Wahl, S. M. (2003b). Conversion of Peripheral CD4+CD25- Naive T Cells to CD4+CD25+ Regulatory T Cells by TGF-β Induction of Transcription Factor Foxp3. *Journal of Experimental Medicine*, 198(12), 1875–1886.
<https://doi.org/10.1084/JEM.20030152>
- Chen, X., Wang, L., Li, P., Song, M., Qin, G., Gao, Q., Zhang, Z., Yue, D., Wang, D., Nan, S., Qi, Y., Li, F., Yang, L., Huang, L., Zhang, M., Zhang, B., Gao, Y., & Zhang, Y. (2018). Dual TGF-β and PD-1 blockade synergistically enhances MAGE-A3-specific CD8+ T cell response in esophageal squamous cell carcinoma. *International Journal of Cancer*, 143(10), 2561–2574.
<https://doi.org/10.1002/IJC.31730>
- Chen, Y. T., Scanlan, M. J., Sahin, U., Türeci, Ö., Gure, A. O., Tsang, S., Williamson, B., Stockert, E., Pfreundschuh, M., & Old, L. J. (1997). A testicular antigen aberrantly expressed in human cancers detected by autologous antibody screening. *Proceedings of the National Academy of Sciences of the United States of America*, 94(5), 1914–1918.
<https://doi.org/10.1073/PNAS.94.5.1914/ASSET/2D4CC202-5DC3-4D28-8BDE-C2DF13E82A4F/ASSETS/GRAPHIC/PQ0573801004.JPEG>
- Chester, C., Sanmamed, M. F., Wang, J., & Melero, I. (2018). Immunotherapy targeting 4-1BB: mechanistic rationale, clinical results, and future strategies. *Blood*, 131(1), 49–57. <https://doi.org/10.1182/BLOOD-2017-06-741041>
- Chheda, Z. S., Sharma, R. K., Jala, V. R., Luster, A. D., & Haribabu, B. (2016). Chemoattractant Receptors BLT1 and CXCR3 Regulate Antitumor Immunity by Facilitating CD8+ T Cell Migration into Tumors. *The Journal of Immunology*, 197(5), 2016–2026. <https://doi.org/10.4049/JIMMUNOL.1502376>
- Chin, Y. E., Kitagawa, M., Kuida, K., Flavell, R. A., & Fu, X.-Y. (1997a). Activation of the STAT signaling pathway can cause expression of caspase 1 and apoptosis. *Molecular and Cellular Biology*, 17(9), 5328–5337.
<https://doi.org/10.1128/MCB.17.9.5328>
- Chin, Y. E., Kitagawa, M., Kuida, K., Flavell, R. A., & Fu, X.-Y. (1997b). Activation of the STAT signaling pathway can cause expression of caspase 1 and apoptosis. *Molecular and Cellular Biology*, 17(9), 5328–5337.
<https://doi.org/10.1128/MCB.17.9.5328>
- Chmielewski, M., Hombach, A. A., & Abken, H. (2014). Of CARs and TRUCKs: chimeric antigen receptor (CAR) T cells engineered with an inducible cytokine to

- modulate the tumor stroma. *Immunological Reviews*, 257(1), 83–90.
<https://doi.org/10.1111/IMR.12125>
- Chocarro, L., Blanco, E., Arasanz, H., Fernández-Rubio, L., Bocanegra, A., Echaide, M., Garnica, M., Ramos, P., Fernández-Hinojal, G., Vera, R., Kochan, G., & Escors, D. (2022). Clinical landscape of LAG-3-targeted therapy. *Immuno-Oncology Technology*, 14, 100079.
<https://doi.org/10.1016/J.IOTECH.2022.100079>
- Chung, Y. C., & Chang, Y. F. (2003). Serum interleukin-6 levels reflect the disease status of colorectal cancer. *Journal of Surgical Oncology*, 83(4), 222–226.
<https://doi.org/10.1002/JSO.10269>
- Clambey, E. T., McNamee, E. N., Westrich, J. A., Glover, L. E., Campbell, E. L., Jedlicka, P., De Zoeten, E. F., Cambier, J. C., Stenmark, K. R., Colgan, S. P., & Eltzschig, H. K. (2012). Hypoxia-inducible factor-1 alpha-dependent induction of FoxP3 drives regulatory T-cell abundance and function during inflammatory hypoxia of the mucosa. *Proceedings of the National Academy of Sciences of the United States of America*, 109(41), E2784–E2793.
https://doi.org/10.1073/PNAS.1202366109/SUPPL_FILE/PNAS.201202366SI.PDF
- Clarke, S. L., Betts, G. J., Plant, A., Wright, K. L., El-Shanawany, T. M., Harrop, R., Torkington, J., Rees, B. I., Williams, G. T., Gallimore, A. M., & Godkin, A. J. (2006). CD4+CD25+FOXP3+ Regulatory T Cells Suppress Anti-Tumor Immune Responses in Patients with Colorectal Cancer. *PLOS ONE*, 1(1), e129.
<https://doi.org/10.1371/JOURNAL.PONE.0000129>
- Claus, C., Ferrara, C., Xu, W., Sam, J., Lang, S., Uhlenbrock, F., Albrecht, R., Herter, S., Schlenker, R., Hösser, T., Diggelmann, S., Challier, J., Mössner, E., Hosse, R. J., Hofer, T., Brönker, P., Joseph, C., Benz, J., Ringler, P., ... Umaña, P. (2019). Tumor-Targeted 4-1BB agonists for combination with T cell bispecific antibodies as off-The-shelf therapy. *Science Translational Medicine*, 11(496), 5989.
https://doi.org/10.1126/SCITRANSLMED.AAV5989/SUPPL_FILE/AAV5989_SM.PDF
- Clevers, H. (2016). Modeling Development and Disease with Organoids. *Cell*, 165(7), 1586–1597. <https://doi.org/10.1016/J.CELL.2016.05.082>
- Colak, S., & ten Dijke, P. (2017). Targeting TGF- β Signaling in Cancer. *Trends in Cancer*, 3(1), 56–71. <https://doi.org/10.1016/J.TRECAN.2016.11.008>
- Compton, C. C., Frederick, J., & Greene, L. (2004). The Staging of Colorectal Cancer: 2004 and Beyond. *CA: A Cancer Journal for Clinicians*, 54(6), 295–308.
<https://doi.org/10.3322/CANJCLIN.54.6.295>
- Connor, J. P., Cristea, M. C., Lewis, N. L., Lewis, L. D., Komarnitsky, P. B., Mattiacci, M. R., Felder, M., Stewart, S., Harter, J., Henslee-Downey, J., Kramer, D., Neugebauer, R., & Stupp, R. (2013). A phase 1b study of humanized KS-interleukin-2 (huKS-IL2) immunocytokine with cyclophosphamide in patients with EpCAM-positive advanced solid tumors. *BMC Cancer*, 13(1), 1–12.
<https://doi.org/10.1186/1471-2407-13-20/TABLES/5>
- Corcoran, R. B., Ebi, H., Turke, A. B., Coffee, E. M., Nishino, M., Cogdill, A. P., Brown, R. D., Pelle, P. Della, Dias-Santagata, D., Hung, K. E., Flaherty, K. T., Piris, A.,

- Wargo, J. A., Settleman, J., Mino-Kenudson, M., & Engelman, J. A. (2012). EGFR-mediated reactivation of MAPK signaling contributes to insensitivity of BRAF-mutant colorectal cancers to RAF inhibition with vemurafenib. *Cancer Discovery*, *2*(3), 227–235. <https://doi.org/10.1158/2159-8290.CD-11-0341/42083/AM/EGFR-MEDIATED-RE-ACTIVATION-OF-MAPK-SIGNALING>
- Corzo, C. A., Condamine, T., Lu, L., Cotter, M. J., Youn, J. I., Cheng, P., Cho, H. II, Celis, E., Quiceno, D. G., Padhya, T., McCaffrey, T. V., McCaffrey, J. C., & Gabilovich, D. I. (2010). HIF-1 α regulates function and differentiation of myeloid-derived suppressor cells in the tumor microenvironment. *Journal of Experimental Medicine*, *207*(11), 2439–2453. <https://doi.org/10.1084/JEM.20100587>
- Cottrez, F., & Groux, H. (2001). Regulation of TGF- β Response During T Cell Activation Is Modulated by IL-10. *The Journal of Immunology*, *167*(2), 773–778. <https://doi.org/10.4049/JIMMUNOL.167.2.773>
- Courau, T., Bonnereau, J., Chicoteau, J., Bottois, H., Remark, R., Assante Miranda, L., Toubert, A., Blery, M., Aparicio, T., Allez, M., & Le Bourhis, L. (2019). Cocultures of human colorectal tumor spheroids with immune cells reveal the therapeutic potential of MICA/B and NKG2A targeting for cancer treatment. *Journal for ImmunoTherapy of Cancer* *2019 7:1*, *7*(1), 1–14. <https://doi.org/10.1186/S40425-019-0553-9>
- Cox, T. R., & Epler, J. T. (2011). Remodeling and homeostasis of the extracellular matrix: implications for fibrotic diseases and cancer. *Disease Models & Mechanisms*, *4*(2), 165–178. <https://doi.org/10.1242/DMM.004077>
- Cremolini, C., Loupakis, F., Antoniotti, C., Lupi, C., Sensi, E., Lonardi, S., Mezi, S., Tomasello, G., Ronzoni, M., Zaniboni, A., Tonini, G., Carlomagno, C., Allegrini, G., Chiara, S., D'Amico, M., Granetto, C., Cazzaniga, M., Boni, L., Fontanini, G., & Falcone, A. (2015). FOLFOXIRI plus bevacizumab versus FOLFIRI plus bevacizumab as first-line treatment of patients with metastatic colorectal cancer: updated overall survival and molecular subgroup analyses of the open-label, phase 3 TRIBE study. *The Lancet Oncology*, *16*(13), 1306–1315. [https://doi.org/10.1016/S1470-2045\(15\)00122-9](https://doi.org/10.1016/S1470-2045(15)00122-9)
- Cui, J., Chen, N., Pu, C., Zhao, L., Li, N., Wang, C., Huang, Y., Luo, S., Li, X., Yang, Z., Bie, J., Zhu, R., Huang, X., Tang, H., Liang, T., Wang, Y., Kennedy, E. P., Wu, Z., Song, Y., ... University, T. F. B. H. of J. (2022). A phase 1 dose-escalation study of GCC19 CART a novel coupled CAR therapy for subjects with metastatic colorectal cancer. *Journal of Clinical Oncology*, *40*(16_suppl), 3582–3582. https://doi.org/10.1200/JCO.2022.40.16_SUPPL.3582
- Cunningham, D., Atkin, W., Lenz, H. J., Lynch, H. T., Minsky, B., Nordlinger, B., & Starling, N. (2010). Colorectal cancer. *The Lancet*, *375*(9719), 1030–1047. [https://doi.org/10.1016/S0140-6736\(10\)60353-4](https://doi.org/10.1016/S0140-6736(10)60353-4)
- Cunningham, D., Humblet, Y., Siena, S., Khayat, D., Bleiberg, H., Santoro, A., Bets, D., Mueser, M., Harstrick, A., Verslype, C., Chau, I., Van Cutsem, E., Bordet, J., & Clini-co Humanitas, I. (2004). Cetuximab Monotherapy and Cetuximab plus Irinotecan in Irinotecan-Refractory Metastatic Colorectal Cancer. *The New England Journal of Medicine*, *351*(4), 337–345. <https://doi.org/10.1056/NEJMOA033025>

- Curiel, T. J., Coukos, G., Zou, L., Alvarez, X., Cheng, P., Mottram, P., Evdemon-Hogan, M., Conejo-Garcia, J. R., Zhang, L., Burow, M., Zhu, Y., Wei, S., Kryczek, I., Daniel, B., Gordon, A., Myers, L., Lackner, A., Disis, M. L., Knutson, K. L., ... Zou, W. (2004a). Specific recruitment of regulatory T cells in ovarian carcinoma fosters immune privilege and predicts reduced survival. *Nature Medicine* 2004 10:9, 10(9), 942–949. <https://doi.org/10.1038/nm1093>
- Curiel, T. J., Coukos, G., Zou, L., Alvarez, X., Cheng, P., Mottram, P., Evdemon-Hogan, M., Conejo-Garcia, J. R., Zhang, L., Burow, M., Zhu, Y., Wei, S., Kryczek, I., Daniel, B., Gordon, A., Myers, L., Lackner, A., Disis, M. L., Knutson, K. L., ... Zou, W. (2004b). Specific recruitment of regulatory T cells in ovarian carcinoma fosters immune privilege and predicts reduced survival. *Nature Medicine* 2004 10:9, 10(9), 942–949. <https://doi.org/10.1038/nm1093>
- Curiel, T. J., Wei, S., Dong, H., Alvarez, X., Cheng, P., Mottram, P., Krzysiek, R., Knutson, K. L., Daniel, B., Zimmermann, M. C., David, O., Burow, M., Gordon, A., Dhurandhar, N., Myers, L., Berggren, R., Hemminki, A., Alvarez, R. D., Emilie, D., ... Zou, W. (2003). Blockade of B7-H1 improves myeloid dendritic cell-mediated antitumor immunity. *Nature Medicine* 2003 9:5, 9(5), 562–567. <https://doi.org/10.1038/nm863>
- Cutsem, E. Van, Köhne, C.-H., Láng, I., Folprecht, G., Nowacki, M. P., Cascinu, S., Shchepotin, I., Maurel, J., Cunningham, D., Tejpar, S., Schlichting, M., Zube, A., Celik, I., Rougier, P., & Ciardiello, F. (2011). Cetuximab Plus Irinotecan, Fluorouracil, and Leucovorin As First-Line Treatment for Metastatic Colorectal Cancer: Updated Analysis of Overall Survival According to Tumor KRAS and BRAF Mutation Status. *J Clin Oncol*, 29. <https://doi.org/10.1200/JCO.2010.33.5091>
- Dai, Q., Han, P., Qi, X., Li, F., Li, M., Fan, L., Zhang, H., Zhang, X., & Yang, X. (2020). 4-1BB Signaling Boosts the Anti-Tumor Activity of CD28-Incorporated 2nd Generation Chimeric Antigen Receptor-Modified T Cells. *Frontiers in Immunology*, 11, 2931. <https://doi.org/10.3389/FIMMU.2020.539654/BIBTEX>
- Dammeijer, F., van Gulijk, M., Mulder, E. E., Lukkes, M., Klaase, L., van den Bosch, T., van Nimwegen, M., Lau, S. P., Latupeirissa, K., Schetters, S., van Kooyk, Y., Boon, L., Moyaart, A., Mueller, Y. M., Katsikis, P. D., Eggermont, A. M., Vroman, H., Stadhouders, R., Hendriks, R. W., ... Aerts, J. G. (2020). The PD-1/PD-L1-Checkpoint Restrains T cell Immunity in Tumor-Draining Lymph Nodes. *Cancer Cell*, 38(5), 685-700.e8. <https://doi.org/10.1016/J.CCELL.2020.09.001>
- Dangles, V., Lazar, V., Validire, P., Richon, S., Wertheimer, M., Laville, V., Janneau, J. L., Barrois, M., Bovin, C., Poynard, T., Vallancien, G., & Bellet, D. (2002). Gene expression profiles of bladder cancers: evidence for a striking effect of in vitro cell models on gene patterns. *British Journal of Cancer* 2002 86:8, 86(8), 1283–1289. <https://doi.org/10.1038/sj.bjc.6600239>
- Dangles, V., Validire, P., Wertheimer, M., Richon, S., Bovin, C., Zeliszewski, D., Vallancien, G., & Bellet, D. (2002). Impact of human bladder cancer cell architecture on autologous T-lymphocyte activation. *International Journal of Cancer*, 98(1), 51–56. <https://doi.org/10.1002/IJC.10140>
- Dangles-Marie, V., Richon, S., Behi, M. El, Echchakir, H., Dorothée, G., Thiery, J., Validire, P., Vergnon, I., Menez, J., Ladjimi, M., Chouaib, S., Bellet, D., & Mami-

- Chouaib, F. (2003). A Three-Dimensional Tumor Cell Defect in Activating Autologous CTLs Is Associated with Inefficient Antigen Presentation Correlated with Heat Shock Protein-70 Down-Regulation 1. *CANCER RESEARCH*, 63, 3682–3687. <http://aacrjournals.org/cancerres/article-pdf/63/13/3682/2505208/ch1303003682.pdf>
- Dansky-Ullmann, C., Salgaller, M., Adams, S., Schlom, J., & Greiner, J. W. (1995). Synergistic Effects of IL-6 and IFN- γ on Carcinoembryonic Antigen (CEA) and HLA Expression by Human Colorectal Carcinoma Cells: Role for Endogenous IFN- β . *Cytokine*, 7(2), 118–129. <https://doi.org/10.1006/cyto.1995.1016>
- Das, L., & Levine, A. D. (2008). TGF- β Inhibits IL-2 Production and Promotes Cell Cycle Arrest in TCR-Activated Effector/Memory T Cells in the Presence of Sustained TCR Signal Transduction. *The Journal of Immunology*, 180(3), 1490–1498. <https://doi.org/10.4049/jimmunol.180.3.1490>
- De Backer, O., Arden, K. C., Boretti, M., Vantomme, V., De Smet, C., Czekay, S., Viars, C. S., De Plaen, E., Brasseur, F., Chomez, P., Benoit Van Den Eynde, B., Boon, T., & Van Der Bruggen, P. (1999). Characterization of the GAGE Genes That Are Expressed in Various Human Cancers and in Normal Testis 1. *CANCER RESEARCH*, 59, 3157–3165. <http://aacrjournals.org/cancerres/article-pdf/59/13/3157/3244786/ch139903157p.pdf>
- de Gramont, A., Figer, A., Seymour, M., Homerin, M., Hmissi, A., Cassidy, J., Boni, C., Cortes-Funes, H., Cervantes, A., Freyer, G., Papamichael, D., Le Bail, N., Louvet, C., Hendler, D., De Braud, F., Wilson, C., Morvan, F., & Bonetti, A. (2000). Leucovorin and fluorouracil with or without oxaliplatin as first-line treatment in advanced colorectal cancer. *Journal of Clinical Oncology*, 18(16), 2938–2947. <https://doi.org/10.1200/JCO.2000.18.16.2938>
- De Smet, C., De Backer, O., Faraoni, I., Lurquin, C., Brasseur, F., & Boon, T. (1996). The activation of human gene MAGE-1 in tumor cells is correlated with genome-wide demethylation. *Proceedings of the National Academy of Sciences*, 93(14), 7149–7153. <https://doi.org/10.1073/PNAS.93.14.7149>
- De Sostoa, J., Fajardo, C. A., Moreno, R., Ramos, M. D., Farrera-Sal, M., & Alemany, R. (2019). Targeting the tumor stroma with an oncolytic adenovirus secreting a fibroblast activation protein-targeted bispecific T-cell engager. *Journal for ImmunoTherapy of Cancer*, 7(1), 1–15. <https://doi.org/10.1186/S40425-019-0505-4/FIGURES/6>
- Deaglio, S., Dwyer, K. M., Gao, W., Friedman, D., Usheva, A., Erat, A., Chen, J. F., Enjyoji, K., Linden, J., Oukka, M., Kuchroo, V. K., Strom, T. B., & Robson, S. C. (2007). Adenosine generation catalyzed by CD39 and CD73 expressed on regulatory T cells mediates immune suppression. *Journal of Experimental Medicine*, 204(6), 1257–1265. <https://doi.org/10.1084/JEM.20062512>
- Denissenko, M. F., Pao, A., Tang, M. S., & Pfeifer, G. P. (1996). Preferential Formation of Benzo[a]pyrene Adducts at Lung Cancer Mutational Hotspots in P53. *Science*, 274(5286), 430–432. <https://doi.org/10.1126/SCIENCE.274.5286.430>
- Denk, H., Tappeiner, G., Eckerstorfer, R., & Holzner, J. H. (1972). Carcinoembryonic antigen (CEA) in gastrointestinal and extragastrointestinal tumors and its

- relationship to tumor-cell differentiation. *International Journal of Cancer*, 10(2), 262–272. <https://doi.org/10.1002/IJC.2910100206>
- Detjen, K. M., Farwig, K., Welzel, M., Wiedenmann, B., & Rosewicz, S. (2001). Interferon γ inhibits growth of human pancreatic carcinoma cells via caspase-1 dependent induction of apoptosis. *Gut*, 49(2), 251–262. <https://doi.org/10.1136/GUT.49.2.251>
- Detmar, M., Brown, L. F., Schön, M. P., Elicker, B. M., Velasco, P., Richard, L., Fukumura, D., Monsky, W., Claffey, K. P., & Jain, R. K. (1998). Increased Microvascular Density and Enhanced Leukocyte Rolling and Adhesion in the Skin of VEGF Transgenic Mice. *Journal of Investigative Dermatology*, 111(1), 1–6. <https://doi.org/10.1046/J.1523-1747.1998.00262.X>
- Di Bari, M. G., Lutsiak, M. E. C., Takai, S., Mostböck, S., Farsaci, B., Tolouei Semnani, R., Wakefield, L. M., Schlom, J., & Sabzevari, H. (2009). TGF- β modulates the functionality of tumor-infiltrating CD8 + T cells through effects on TCR signaling and Spred1 expression. *Cancer Immunology, Immunotherapy*, 58(11), 1811–1820. <https://doi.org/10.1007/s00262-009-0692-9>
- Di Nicolantonio, F., Martini, M., Molinari, F., Sartore-Bianchi, A., Arena, S., Saletti, P., De Dosso, S., Mazzucchelli, L., Frattini, M., Siena, S., & Bardelli, A. (2008). Wild-type BRAF is required for response to panitumumab or cetuximab in metastatic colorectal cancer. *Journal of Clinical Oncology*, 26(35), 5705–5712. <https://doi.org/10.1200/JCO.2008.18.0786>
- Dienstmann, R., Mason, M. J., Sinicrope, F. A., Phipps, A. I., Tejpar, S., Nesbakken, A., Danielsen, S. A., Sveen, A., Buchanan, D. D., Clendenning, M., Rosty, C., Bot, B., Alberts, S. R., Milburn Jessup, J., Lothe, R. A., Delorenzi, M., Newcomb, P. A., Sargent, D., & Guinney, J. (2017). Prediction of overall survival in stage II and III colon cancer beyond TNM system: a retrospective, pooled biomarker study. *Annals of Oncology*, 28(5), 1023–1031. <https://doi.org/10.1093/ANNONC/MDX052>
- Dimanche-Boitrel, M. T., Vakaet, L., Pujuguet, P., Chauffert, B., Martin, M. S., Hammann, A., Van Roy, F., Mareel, M., & Martin, F. (1994). In vivo and in vitro invasiveness of a rat colon-cancer cell line maintaining E-cadherin expression: An enhancing role of tumor-associated myofibroblasts. *International Journal of Cancer*, 56(4), 512–521. <https://doi.org/10.1002/IJC.2910560410>
- Ding, L., Linsley, P. S., Huang, L.-Y., Germain, R. N., & Shevach, E. M. (1993). IL-10 inhibits macrophage costimulatory activity by selectively inhibiting the up-regulation of B7 expression. *The Journal of Immunology*, 151(3), 1224–1234. <https://doi.org/10.4049/JIMMUNOL.151.3.1224>
- Dirkx, A. E. M., Oude Egbrink, G. A., Kuijpers, M. J. E., Van Der Niet, S. T., Heijnen, V. V. T., Bouma-Ter Steege, J. C. A., Wagstaff, J., & Griffioen, A. W. (2003). Tumor Angiogenesis Modulates Leukocyte-Vessel Wall Interactions in Vivo by Reducing Endothelial Adhesion Molecule Expression 1. *CANCER RESEARCH*, 63, 2322–2329. <http://aacrjournals.org/cancerres/article-pdf/63/9/2322/2513583/ch0903002322.pdf>
- DIVELLA, R., DANIELE, A., DE LUCA, R., SIMONE, M., NAGLIERI, E., SAVINO, E., ABBATE, I., GADALETA, C. D., & RANIERI, G. (2017). Circulating Levels of

VEGF and CXCL1 Are Predictive of Metastatic Organotropism in Patients with Colorectal Cancer. *Anticancer Research*, 37(9).

- Doedens, A. L., Phan, A. T., Stradner, M. H., Fujimoto, J. K., Nguyen, J. V., Yang, E., Johnson, R. S., & Goldrath, A. W. (2013). Hypoxia-inducible factors enhance the effector responses of CD8+ T cells to persistent antigen. *Nature Immunology* 2013 14:11, 14(11), 1173–1182. <https://doi.org/10.1038/ni.2714>
- Doedens, A. L., Stockmann, C., Rubinstein, M. P., Liao, D., Zhang, N., DeNardo, D. G., Coussens, L. M., Karin, M., Goldrath, A. W., & Johnson, R. S. (2010). Macrophage expression of hypoxia-inducible factor-1 α suppresses T-cell function and promotes tumor progression. *Cancer Research*, 70(19), 7465–7475. <https://doi.org/10.1158/0008-5472.CAN-10-1439/656430/P/MACROPHAGE-EXPRESSION-OF-HYPOXIA-INDUCIBLE-FACTOR>
- Dong, H., Strome, S. E., Salomao, D. R., Tamura, H., Hirano, F., Flies, D. B., Roche, P. C., Lu, J., Zhu, G., Tamada, K., Lennon, V. A., Cells, E., & Chen, L. (2002). Tumor-associated B7-H1 promotes T-cell apoptosis: A potential mechanism of immune evasion. *Nature Medicine* 2002 8:8, 8(8), 793–800. <https://doi.org/10.1038/nm730>
- Douillard, J. Y., Cunningham, D., Roth, A. D., Navarro, M., James, R. D., Karasek, P., Jandik, P., Iveson, T., Carmichael, J., Alakl, M., Gruia, G., Awad, L., & Rougier, P. (2000). Irinotecan combined with fluorouracil compared with fluorouracil alone as first-line treatment for metastatic colorectal cancer: a multicentre randomised trial. *The Lancet*, 355(9209), 1041–1047. [https://doi.org/10.1016/S0140-6736\(00\)02034-1](https://doi.org/10.1016/S0140-6736(00)02034-1)
- Douillard, J. Y., Siena, S., Cassidy, J., Tabernero, J., Burkes, R., Barugel, M., Humblet, Y., Bodoky, G., Cunningham, D., Jassem, J., Rivera, F., Kocákova, I., Ruff, P., Błasińska-Morawiec, M., Šmakal, M., Canon, J. L., Rother, M., Oliner, K. S., Tian, Y., ... Sidhu, R. (2014). Final results from PRIME: randomized phase III study of panitumumab with FOLFOX4 for first-line treatment of metastatic colorectal cancer. *Annals of Oncology*, 25(7), 1346–1355. <https://doi.org/10.1093/ANNONC/MDU141>
- Douillard, J. Y., Siena, S., Cassidy, J., Tabernero, J., Burkes, R., Barugel, M., Humblet, Y., Bodoky, G., Cunningham, D., Jassem, J., Rivera, F., Kocákova, I., Ruff, P., Błasińska-Morawiec, M., Šmakal, M., Canon, J. L., Rother, M., Oliner, K. S., Wolf, M., & Gansert, J. (2010). Randomized, Phase III trial of panitumumab with infusional fluorouracil, leucovorin, and oxaliplatin (FOLFOX4) Versus FOLFOX4 alone as first-line treatment in patients with previously untreated metastatic colorectal cancer: The PRIME study. *Journal of Clinical Oncology*, 28(31), 4697–4705. <https://doi.org/10.1200/JCO.2009.27.4860>
- Downward, J. (1998). Ras signalling and apoptosis. *Current Opinion in Genetics & Development*, 8(1), 49–54. [https://doi.org/10.1016/S0959-437X\(98\)80061-0](https://doi.org/10.1016/S0959-437X(98)80061-0)
- Dreier, T., Lorenczewski, G., Brandl, C., Hoffmann, P., Syring, U., Hanakam, F., Kufer, P., Riethmuller, G., Bargou, R., & Baeuerle, P. A. (2002). Extremely potent, rapid and costimulation-independent cytotoxic T-cell response against lymphoma cells catalyzed by a single-chain bispecific antibody. *International Journal of Cancer*, 100(6), 690–697. <https://doi.org/10.1002/IJC.10557>

- Dudley, M. E., Wunderlich, J. R., Robbins, P. F., Yang, J. C., Hwu, P., Schwartzentruber, D. J., Topalian, S. L., Sherry, R., Restifo, N. P., Hubicki, A. M., Robinson, M. R., Raffeld, M., Duray, P., Seipp, C. A., Rogers-Freezer, L., Morton, K. E., Mavroukakis, S. A., White, D. E., & Rosenberg, S. A. (2002). Cancer regression and autoimmunity in patients after clonal repopulation with antitumor lymphocytes. *Science*, *298*(5594), 850–854. https://doi.org/10.1126/SCIENCE.1076514/SUPPL_FILE/DUDLEY.SOM.PDF
- Duluc, D., Corvaisier, M., Blanchard, S., Catala, L., Descamps, P., Gamelin, E., Ponsoda, S., Delneste, Y., Hebbar, M., & Jeannin, P. (2009). Interferon- γ reverses the immunosuppressive and protumoral properties and prevents the generation of human tumor-associated macrophages. *International Journal of Cancer*, *125*(2), 367–373. <https://doi.org/10.1002/IJC.24401>
- Dunn, G. P., Bruce, A. T., Ikeda, H., Old, L. J., & Schreiber, R. D. (2002). Cancer immunoediting: from immunosurveillance to tumor escape. *Nature Immunology* *2002 3:11*, *3*(11), 991–998. <https://doi.org/10.1038/ni1102-991>
- Dunn, G. P., Sheehan, K. C. F., Old, L. J., & Schreiber, R. D. (2005). IFN Unresponsiveness in LNCaP Cells Due to the Lack of JAK1 Gene Expression. *Cancer Research*, *65*(8), 3447–3453. <https://doi.org/10.1158/0008-5472.CAN-04-4316>
- Duque, G. A., & Descoteaux, A. (2014). Macrophage Cytokines: Involvement in Immunity and Infectious Diseases. *Frontiers in Immunology*, *5*(OCT). <https://doi.org/10.3389/FIMMU.2014.00491>
- Dutcher, J. P., Schwartzentruber, D. J., Kaufman, H. L., Agarwala, S. S., Tarhini, A. A., Lowder, J. N., & Atkins, M. B. (2014). High dose interleukin-2 (Aldesleukin) - expert consensus on best management practices-2014. *Journal for ImmunoTherapy of Cancer*, *2*(1), 26. <https://doi.org/10.1186/S40425-014-0026-0>
- Eberhart, C. E., Coffey, R. J., Radhika, A., Giardiello, F. M., Ferrenbach, S., & Dubois, R. N. (1994). Up-regulation of cyclooxygenase 2 gene expression in human colorectal adenomas and adenocarcinomas. *Gastroenterology*, *107*(4), 1183–1188. [https://doi.org/10.1016/0016-5085\(94\)90246-1](https://doi.org/10.1016/0016-5085(94)90246-1)
- Ebert, E. C. (2001). IL-10 enhances IL-2-induced proliferation and cytotoxicity by human intestinal lymphocytes. *Clinical and Experimental Immunology*, *119*(3), 426–432. <https://doi.org/10.1046/J.1365-2249.2000.01147.X>
- Ebert, E. C., & Mehta, V. (2006). Human intestinal intraepithelial lymphocytes keep TNF α levels low by cell uptake and feedback inhibition of transcription. *Cellular Immunology*, *241*(1), 7–13. <https://doi.org/10.1016/J.CELLIMM.2006.07.005>
- Edin, S., Wikberg, M. L., Dahlin, A. M., Rutegård, J., Öberg, Å., Oldenberg, P. A., & Palmqvist, R. (2012). The Distribution of Macrophages with a M1 or M2 Phenotype in Relation to Prognosis and the Molecular Characteristics of Colorectal Cancer. *PLOS ONE*, *7*(10), e47045. <https://doi.org/10.1371/JOURNAL.PONE.0047045>
- El-Deiry, W. S., Vijayvergia, N., Xiu, J., Scicchitano, A., Lim, B., Yee, N. S., Harvey, H. A., Gatalica, Z., & Reddy, S. (2015). Molecular profiling of 6,892 colorectal cancer samples suggests different possible treatment options specific to metastatic sites. *Cancer Biology and Therapy*, *16*(12), 1726–1737.

https://doi.org/10.1080/15384047.2015.1113356/SUPPL_FILE/KCBT_A_1113356_SM4959.DOCX

- Elenbaas, B., & Weinberg, R. A. (2001). Heterotypic Signaling between Epithelial Tumor Cells and Fibroblasts in Carcinoma Formation. *Experimental Cell Research, 264*(1), 169–184. <https://doi.org/10.1006/EXCR.2000.5133>
- Elia, A. R., Cappello, P., Puppo, M., Fraone, T., Vanni, C., Eva, A., Musso, T., Novelli, F., Varesio, L., & Giovarelli, M. (2008). Human dendritic cells differentiated in hypoxia down-modulate antigen uptake and change their chemokine expression profile. *Journal of Leukocyte Biology, 84*(6), 1472–1482. <https://doi.org/10.1189/JLB.0208082>
- Elliott, R. J. R., Jarvis, A., Rajasekaran, M. B., Menon, M., Bowers, L., Boffey, R., Bayford, M., Firth-Clark, S., Key, R., Aqil, R., Kirton, S. B., Niculescu-Duvaz, D., Fish, L., Lopes, F., McLeary, R., Trindade, I., Vendrell, E., Munkonge, F., Porter, R., ... Lord, C. J. (2015). Design and discovery of 3-aryl-5-substituted-isoquinolin-1-ones as potent tankyrase inhibitors. *MedChemComm, 6*(9), 1687–1692. <https://doi.org/10.1039/C5MD00210A>
- Emmerich, J., Mumm, J. B., Chan, I. H., LaFace, D., Truong, H., McClanahan, T., Gorman, D. M., & Oft, M. (2012). IL-10 directly activates and expands tumor-resident CD8+ T cells without De Novo infiltration from secondary lymphoid organs. *Cancer Research, 72*(14), 3570–3581. <https://doi.org/10.1158/0008-5472.CAN-12-0721/650452/AM/IL-10-DIRECTLY-ACTIVATES-AND-EXPANDS-TUMOR>
- Ene-Obong, A., Clear, A. J., Watt, J., Wang, J., Fatah, R., Riches, J. C., Marshall, J. F., Chin-Aleong, J., Chelala, C., Gribben, J. G., Ramsay, A. G., & Kocher, H. M. (2013). Activated Pancreatic Stellate Cells Sequester CD8+ T Cells to Reduce Their Infiltration of the Juxtatumoral Compartment of Pancreatic Ductal Adenocarcinoma. *Gastroenterology, 145*(5), 1121–1132. <https://doi.org/10.1053/J.GASTRO.2013.07.025>
- Eng, C., Bessudo, A., Hart, L. L., Severtsev, A., Gladkov, O., Müller, L., Kopp, M. V., Vladimirov, V., Langdon, R., Kotiv, B., Barni, S., Hsu, C., Bolotin, E., Von Roemeling, R., Schwartz, B., & Bendell, J. C. (2016). A randomized, placebo-controlled, phase 1/2 study of tivantinib (ARQ 197) in combination with irinotecan and cetuximab in patients with metastatic colorectal cancer with wild-type KRAS who have received first-line systemic therapy. *International Journal of Cancer, 139*(1), 177–186. <https://doi.org/10.1002/IJC.30049>
- Engel, A. M., Svane, I. M., Rygaard, J., & Werdelin, O. (1997). MCA Sarcomas Induced in scid Mice are More Immunogenic than MCA Sarcomas Induced in Congenic, Immunocompetent Mice. *Scandinavian Journal of Immunology, 45*(4), 463–470. <https://doi.org/10.1046/J.1365-3083.1997.D01-419.X>
- Enk, A. H., Jonuleit, H., Saloga, J., & Knop, J. (1997). DENDRITIC CELLS AS MEDIATORS OF TUMOR-INDUCED TOLERANCE IN METASTATIC MELANOMA. *J. Cancer, 73*, 309–316. [https://doi.org/10.1002/\(SICI\)1097-0215\(19971104\)73:3](https://doi.org/10.1002/(SICI)1097-0215(19971104)73:3)
- Eshhar, Z., Waks, T., Gross, G., & Schindler, D. G. (1993). Specific activation and targeting of cytotoxic lymphocytes through chimeric single chains consisting of

antibody-binding domains and the gamma or zeta subunits of the immunoglobulin and T-cell receptors. *Proceedings of the National Academy of Sciences*, 90(2), 720–724. <https://doi.org/10.1073/PNAS.90.2.720>

- Fabrizio, D. A., George, T. J., Dunne, R. F., Frampton, G., Sun, J., Gowen, K., Kennedy, M., Greenbowe, J., Schrock, A. B., Hezel, A. F., Ross, J. S., Stephens, P. J., Ali, S. M., Miller, V. A., Fakih, M., & Klempner, S. J. (2018). Beyond microsatellite testing: assessment of tumor mutational burden identifies subsets of colorectal cancer who may respond to immune checkpoint inhibition. *Journal of Gastrointestinal Oncology*, 9(4), 610. <https://doi.org/10.21037/JGO.2018.05.06>
- Facciabene, A., Motz, G. T., & Coukos, G. (2012). T-Regulatory Cells: Key Players in Tumor Immune Escape and Angiogenesis. *Cancer Research*, 72(9), 2162–2171. <https://doi.org/10.1158/0008-5472.CAN-11-3687>
- Facciabene, A., Peng, X., Hagemann, I. S., Balint, K., Barchetti, A., Wang, L. P., Gimotty, P. A., Gilks, C. B., Lal, P., Zhang, L., & Coukos, G. (2011). Tumour hypoxia promotes tolerance and angiogenesis via CCL28 and Treg cells. *Nature* 2011 475:7355, 475(7355), 226–230. <https://doi.org/10.1038/nature10169>
- Fahlgren, A., Baranov, V., Frangsmyr, L., Zoubir, F., Hammarstrom, M.-L., & Hammarstrom, S. (2003). Interferon-gamma Tempers the Expression of Carcinoembryonic Antigen Family Molecules in Human Colon Cells: a Possible Role in Innate Mucosal Defence. *Scandinavian Journal of Immunology*, 58(6), 628–641. <https://doi.org/10.1111/j.1365-3083.2003.01342.x>
- Fakih, M. G., Kopetz, S., Kuboki, Y., Kim, T. W., Munster, P. N., Krauss, J. C., Falchook, G. S., Han, S. W., Heinemann, V., Muro, K., Strickler, J. H., Hong, D. S., Denlinger, C. S., Girotto, G., Lee, M. A., Henary, H., Tran, Q., Park, J. K., Ngarmchamnanrith, G., ... Price, T. J. (2022). Sotorasib for previously treated colorectal cancers with KRASG12C mutation (CodeBreak100): a prespecified analysis of a single-arm, phase 2 trial. *The Lancet Oncology*, 23(1), 115–124. [https://doi.org/10.1016/S1470-2045\(21\)00605-7](https://doi.org/10.1016/S1470-2045(21)00605-7)
- Fakih, M., Raghav, K. P. S., Chang, D. Z., Bendell, J. C., Larson, T., Cohn, A. L., Huyck, T. K., Cosgrove, D., Fiorillo, J. A., Garbo, L. E., Ravimohan, S., Potter, V., D'Adamo, D., Sharma, N., Wang, Y. A., Coppieters, S., Herpers, M., Oliveira, C. S. V. de, & Paulson, A. S. (2021). Single-arm, phase 2 study of regorafenib plus nivolumab in patients with mismatch repair-proficient (pMMR)/microsatellite stable (MSS) colorectal cancer (CRC). *Journal of Clinical Oncology*, 39(15_suppl), 3560–3560. https://doi.org/10.1200/JCO.2021.39.15_SUPPL.3560
- Fantini, M. C., Becker, C., Monteleone, G., Pallone, F., Galle, P. R., & Neurath, M. F. (2004). Cutting Edge: TGF- β Induces a Regulatory Phenotype in CD4+CD25- T Cells through Foxp3 Induction and Down-Regulation of Smad7. *The Journal of Immunology*, 172(9), 5149–5153. <https://doi.org/10.4049/JIMMUNOL.172.9.5149>
- Farber, J. M. (1997). Mig and IP-10: CXC chemokines that target lymphocytes. *Journal of Leukocyte Biology*, 61(3), 246–257. <https://doi.org/10.1002/JLB.61.3.246>
- Faute, M. A. D., Laurent, L., Ploton, D., Poupon, M. F., Jardillier, J. C., & Bobichon, H. (2002). Distinctive alterations of invasiveness, drug resistance and cell-cell organization in 3D-cultures of MCF-7, a human breast cancer cell line, and its

- multidrug resistant variant. *Clinical and Experimental Metastasis*, 19(2), 161–167. <https://doi.org/10.1023/A:1014594825502/METRICS>
- Fearon, E. R., & Vogelstein, B. (1990). A genetic model for colorectal tumorigenesis. *Cell*, 61(5), 759–767. [https://doi.org/10.1016/0092-8674\(90\)90186-l](https://doi.org/10.1016/0092-8674(90)90186-l)
- Feder-Mengus, C., Ghosh, S., Weber, W. P., Wyler, S., Zajac, P., Terracciano, L., Oertli, D., Heberer, M., Martin, I., Spagnoli, G. C., & Reschner, A. (2007). Multiple mechanisms underlie defective recognition of melanoma cells cultured in three-dimensional architectures by antigen-specific cytotoxic T lymphocytes. *British Journal of Cancer* 2007 96:7, 96(7), 1072–1082. <https://doi.org/10.1038/sj.bjc.6603664>
- Fehrenbacher, L., Spira, A., Ballinger, M., Kowanetz, M., Vansteenkiste, J., Mazieres, J., Park, K., Smith, D., Artal-Cortes, A., Lewanski, C., Braiteh, F., Waterkamp, D., He, P., Zou, W., Chen, D. S., Yi, J., Sandler, A., & Rittmeyer, A. (2016). Atezolizumab versus docetaxel for patients with previously treated non-small-cell lung cancer (POPLAR): A multicentre, open-label, phase 2 randomised controlled trial. *The Lancet*, 387(10030), 1837–1846. [https://doi.org/10.1016/S0140-6736\(16\)00587-0](https://doi.org/10.1016/S0140-6736(16)00587-0)
- Feig, C., Jones, J. O., Kraman, M., Wells, R. J. B., Deonarine, A., Chan, D. S., Connell, C. M., Roberts, E. W., Zhao, Q., Caballero, O. L., Teichmann, S. A., Janowitz, T., Jodrell, D. I., Tuveson, D. A., & Fearon, D. T. (2013). Targeting CXCL12 from FAP-expressing carcinoma-associated fibroblasts synergizes with anti-PD-L1 immunotherapy in pancreatic cancer. *Proceedings of the National Academy of Sciences of the United States of America*, 110(50), 20212–20217. https://doi.org/10.1073/PNAS.1320318110/SUPPL_FILE/SAPP.PDF
- Feng, K., Guo, Y., Dai, H., Wang, Y., Li, X., Jia, H., & Han, W. (2016). Chimeric antigen receptor-modified T cells for the immunotherapy of patients with EGFR-expressing advanced relapsed/refractory non-small cell lung cancer. *Science China Life Sciences*, 59(5), 468–479. <https://doi.org/10.1007/S11427-016-5023-8/METRICS>
- Feng, K., Liu, Y., Guo, Y., Qiu, J., Wu, Z., Dai, H., Yang, Q., Wang, Y., & Han, W. (2018). Phase I study of chimeric antigen receptor modified T cells in treating HER2-positive advanced biliary tract cancers and pancreatic cancers. *Protein & Cell*, 9(10), 838–847. <https://doi.org/10.1007/S13238-017-0440-4>
- Ferlay, J., Soerjomataram, I., Dikshit, R., Eser, S., Mathers, C., Rebelo, M., Parkin, D. M., Forman, D., & Bray, F. (2015). Cancer incidence and mortality worldwide: Sources, methods and major patterns in GLOBOCAN 2012. *International Journal of Cancer*, 136(5), E359–E386. <https://doi.org/10.1002/IJC.29210>
- Ferrara, N., Hillan, K. J., Gerber, H. P., & Novotny, W. (2004). Discovery and development of bevacizumab, an anti-VEGF antibody for treating cancer. *Nature Reviews Drug Discovery* 2004 3:5, 3(5), 391–400. <https://doi.org/10.1038/nrd1381>
- Fiedler, W. M., Wolf, M., Kebenko, M., Goebeler, M.-E., Ritter, B., Quaas, A., Vieser, E., Hijazi, Y., Patzak, I., Friedrich, M., Kufer, P., Frankel, S., Seggewiss-Bernhardt, R., & Kaubitzsch, S. (2012). A phase I study of EpCAM/CD3-bispecific antibody (MT110) in patients with advanced solid tumors. *Journal of Clinical Oncology*, 30(15_suppl), 2504–2504. https://doi.org/10.1200/JCO.2012.30.15_SUPPL.2504

- Fife, B. T., Pauken, K. E., Eagar, T. N., Obu, T., Wu, J., Tang, Q., Azuma, M., Krummel, M. F., & Bluestone, J. A. (2009). Interactions between PD-1 and PD-L1 promote tolerance by blocking the TCR-induced stop signal. *Nature Immunology* 2009 10:11, 10(11), 1185–1192. <https://doi.org/10.1038/ni.1790>
- Filén, S., Ylikoski, E., Tripathi, S., West, A., Björkman, M., Nyström, J., Ahlfors, H., Coffey, E., Rao, K. V. S., Rasool, O., & Lahesmaa, R. (2010). Activating Transcription Factor 3 Is a Positive Regulator of Human IFNG Gene Expression. *The Journal of Immunology*, 184(9), 4990–4999. <https://doi.org/10.4049/JIMMUNOL.0903106>
- Finney, H. M., Akbar, A. N., & Lawson, A. D. G. (2004). Activation of Resting Human Primary T Cells with Chimeric Receptors: Costimulation from CD28, Inducible Costimulator, CD134, and CD137 in Series with Signals from the TCR ζ Chain. *The Journal of Immunology*, 172(1), 104–113. <https://doi.org/10.4049/JIMMUNOL.172.1.104>
- Fiorentino, D. F., Zlotnik, A., Vieira, P., Mosmann, T. R., Howard, M., Moore, K. W., & O'garra, A. (1991). IL-10 acts on the antigen-presenting cell to inhibit cytokine production by Th1 cells. *The Journal of Immunology*, 146(10), 3444–3451. <https://doi.org/10.4049/JIMMUNOL.146.10.3444>
- Fischbach, C., Chen, R., Matsumoto, T., Schmelzle, T., Brugge, J. S., Polverini, P. J., & Mooney, D. J. (2007). Engineering tumors with 3D scaffolds. *Nature Methods* 2007 4:10, 4(10), 855–860. <https://doi.org/10.1038/nmeth1085>
- Fischer, K., Hoffmann, P., Voelkl, S., Meidenbauer, N., Ammer, J., Edinger, M., Gottfried, E., Schwarz, S., Rothe, G., Hoves, S., Renner, K., Timischl, B., Mackensen, A., Kunz-Schughart, L., Andreesen, R., Krause, S. W., & Kreutz, M. (2007). Inhibitory effect of tumor cell-derived lactic acid on human T cells. *Blood*, 109(9), 3812–3819. <https://doi.org/10.1182/BLOOD-2006-07-035972>
- Flavia Di Renzo, M., Olivero, M., Giacomini, A., Porte, H., Chastre, E., Mirossay, L., Nordlinger, B., Bretti, S., Bottardi, S., Giordano, S., Plebani, M., Gespach, C., & Comoglio, P. M. (1995). Overexpression and Amplification of the Met/HER2 Receptor Gene during the Progression of Colorectal Cancer. *Clinical Cancer Research*. <http://aacrjournals.org/clincancerres/article-pdf/1/2/147/1950193/147.pdf>
- Fleming, M., Ravula, S., Tatishchev, S. F., & Wang, H. L. (2012). Colorectal carcinoma: Pathologic aspects. *Journal of Gastrointestinal Oncology*, 3(3), 153. <https://doi.org/10.3978/J.ISSN.2078-6891.2012.030>
- Fodde, R., & Brabletz, T. (2007). Wnt/ β -catenin signaling in cancer stemness and malignant behavior. *Current Opinion in Cell Biology*, 19(2), 150–158. <https://doi.org/10.1016/J.CEB.2007.02.007>
- Folprecht, G., Pericay, C., Saunders, M. P., Thomas, A., Lopez Lopez, R., Roh, J. K., Chistyakov, V., Höhler, T., Kim, J. S., Hofheinz, R. D., Ackland, S. P., Swinson, D., Kopp, M., Udovitsa, D., Hall, M., Iveson, T., Vogel, A., & Zalberg, J. R. (2016). Oxaliplatin and 5-FU/folinic acid (modified FOLFOX6) with or without aflibercept in first-line treatment of patients with metastatic colorectal cancer: the AFFIRM study. *Annals of Oncology*, 27(7), 1273–1279. <https://doi.org/10.1093/ANNONC/MDW176>

- Ford, K., Hanley, C. J., Mellone, M., Szyndralewicz, C., Heitz, F., Wiesel, P., Wood, O., Machado, M., Lopez, M. A., Ganesan, A. P., Wang, C., Chakravarthy, A., Fenton, T. R., King, E. V., Vijayanand, P., Ottensmeier, C. H., Al-Shamkhani, A., Savelyeva, N., & Thomas, G. J. (2020). NOX4 inhibition potentiates immunotherapy by overcoming cancer-associated fibroblast-mediated CD8 T-cell exclusion from tumors. *Cancer Research*, *80*(9), 1846–1860. <https://doi.org/10.1158/0008-5472.CAN-19-3158/653979/AM/NOX4-INHIBITION-POTENTIATES-IMMUNOTHERAPY-BY>
- Forssell, J., Öberg, Å., Henriksson, M. L., Stenling, R., Jung, A., & Palmqvist, R. (2007). High Macrophage Infiltration along the Tumor Front Correlates with Improved Survival in Colon Cancer. *Clinical Cancer Research*, *13*(5), 1472–1479. <https://doi.org/10.1158/1078-0432.CCR-06-2073>
- Foster, A. E., Dotti, G., Lu, A., Khalil, M., Brenner, M. K., Heslop, H. E., Rooney, C. M., & Bollard, C. M. (2008). Antitumor activity of EBV-specific T lymphocytes transduced with a dominant negative TGF- β receptor. *Journal of Immunotherapy*, *31*(5), 500–505. <https://doi.org/10.1097/CJI.0B013E318177092B>
- Fox, F. E., Capocasale, R. J., Ford, H. C., Lamb, R. J., Moore, J. S., & Nowell, P. C. (1992). Transforming growth factor-beta inhibits human T-cell proliferation through multiple targets. *Lymphokine and Cytokine Research*, *11*(6), 299–305. <https://europepmc.org/article/med/1477183>
- Francisco, L. M., Sage, P. T., & Sharpe, A. H. (2010). The PD-1 pathway in tolerance and autoimmunity. *Immunological Reviews*, *236*(1), 219–242. <https://doi.org/10.1111/J.1600-065X.2010.00923.X>
- Franciszkiwicz, K., Boissonnas, A., Boutet, M., Combadière, C., & Mami-Chouaib, F. (2012). Role of chemokines and chemokine receptors in shaping the effector phase of the antitumor immune response. *Cancer Research*, *72*(24), 6325–6332. <https://doi.org/10.1158/0008-5472.CAN-12-2027/658415/P/ROLE-OF-CHEMOKINES-AND-CHEMOKINE-RECEPTORS-IN>
- Fransen, M. F., Schoonderwoerd, M., Knopf, P., Camps, M. G., Hawinkels, L. J., Kneilling, M., van Hall, T., & Ossendorp, F. (2018). Tumor-draining lymph nodes are pivotal in PD-1/PD-L1 checkpoint therapy. *JCI Insight*, *3*(23). <https://doi.org/10.1172/JCI.INSIGHT.124507>
- Freeman, G. J., Long, A. J., Iwai, Y., Bourque, K., Chernova, T., Nishimura, H., Fitz, L. J., Malenkovich, N., Okazaki, T., Byrne, M. C., Horton, H. F., Fouser, L., Carter, L., Ling, V., Bowman, M. R., Carreno, B. M., Collins, M., Wood, C. R., & Honjo, T. (2000). Engagement of the Pd-1 Immunoinhibitory Receptor by a Novel B7 Family Member Leads to Negative Regulation of Lymphocyte Activation. *Journal of Experimental Medicine*, *192*(7), 1027–1034. <https://doi.org/10.1084/JEM.192.7.1027>
- Friedl, P., & Brocker, E. B. (2000). T Cell Migration in Three-dimensional Extracellular Matrix: Guidance by Polarity and Sensations. *Developmental Immunology*, *7*(2–4), 249. <https://doi.org/10.1155/2000/56473>
- Friedl, P., Entschladen, F., Conrad, C., Niggemann, B., & Zänker, K. S. (1998). CD4 + T lymphocytes migrating in three-dimensional collagen lattices lack focal adhesions and utilize beta1 integrin-independent strategies for polarization,

- interaction with collagen fibers and locomotion. *European Journal of Immunology*, 28(8). [https://doi.org/10.1002/\(SICI\)1521-4141\(199808\)28:08](https://doi.org/10.1002/(SICI)1521-4141(199808)28:08)
- Frohwitter, G., Kerta, M., Vogl, C., Geppert, C. I., Werry, J. E., Ries, J., Kesting, M., & Weber, M. (2022). Macrophage and T-Cell Infiltration and Topographic Immune Cell Distribution in Non-Melanoma Skin Cancer of the Head and Neck. *Frontiers in Oncology*, 12, 947. <https://doi.org/10.3389/FONC.2022.809687/BIBTEX>
- Fu, C., Liang, X., Cui, W., Ober-Blöbaum, J. L., Vazzana, J., Shrikant, P. A., Lee, K. P., Clausen, B. E., Mellman, I., & Jiang, A. (2015). β -Catenin in dendritic cells exerts opposite functions in cross-priming and maintenance of CD8⁺ T cells through regulation of IL-10. *Proceedings of the National Academy of Sciences of the United States of America*, 112(9), 2823–2828. https://doi.org/10.1073/PNAS.1414167112/SUPPL_FILE/PNAS.201414167SI.PDF
- Fujii, S. I., Shimizu, K., Shimizu, T., & Lotze, M. T. (2001). Interleukin-10 promotes the maintenance of antitumor CD8⁺ T-cell effector function in situ. *Blood*, 98(7), 2143–2151. <https://doi.org/10.1182/BLOOD.V98.7.2143>
- Fujita, K. I., Kubota, Y., Ishida, H., & Sasaki, Y. (2015). Irinotecan, a key chemotherapeutic drug for metastatic colorectal cancer. *World Journal of Gastroenterology*, 21(43), 12234. <https://doi.org/10.3748/WJG.V21.I43.12234>
- Fukuoka, S., Hara, H., Takahashi, N., Kojima, T., Kawazoe, A., Asayama, M., Yoshii, T., Kotani, D., Tamura, H., Yuichi Mikamoto, Bp., Hirano, N., Wakabayashi, M., Nomura, S., Sato, A., Kuwata, T., Togashi, Y., Nishikawa, H., & Shitara, K. (2020). Regorafenib plus Nivolumab in Patients with Advanced Gastric or Colorectal Cancer: An Open-Label, Dose-Escalation, and Dose-Expansion Phase Ib Trial (REGONIVO, EPOC1603). *Journal of Clinical Oncology*, 38(18), 2053–2061. <https://doi.org/10.1200/JCO.19.03296>
- Fyfe, G., Fisher, R. I., Rosenberg, S. A., Sznol, M., Parkinson, D. R., & Louie, A. C. (1995). Results of treatment of 255 patients with metastatic renal cell carcinoma who received high-dose recombinant interleukin-2 therapy. *Journal of Clinical Oncology*, 13(3), 688–696. <https://doi.org/10.1200/JCO.1995.13.3.688>
- Gabrilovich, D. I., Chen, H. L., Girgis, K. R., Cunningham, H. T., Meny, G. M., Nadaf, S., Kavanaugh, D., & Carbone, D. P. (1996a). Production of vascular endothelial growth factor by human tumors inhibits the functional maturation of dendritic cells. *Nature Medicine* 1996 2:10, 2(10), 1096–1103. <https://doi.org/10.1038/nm1096-1096>
- Gabrilovich, D. I., Chen, H. L., Girgis, K. R., Cunningham, H. T., Meny, G. M., Nadaf, S., Kavanaugh, D., & Carbone, D. P. (1996b). Production of vascular endothelial growth factor by human tumors inhibits the functional maturation of dendritic cells. *Nature Medicine* 1996 2:10, 2(10), 1096–1103. <https://doi.org/10.1038/nm1096-1096>
- Gabrilovich, D. I., & Nagaraj, S. (2009). Myeloid-derived suppressor cells as regulators of the immune system. *Nature Reviews Immunology* 2009 9:3, 9(3), 162–174. <https://doi.org/10.1038/nri2506>
- Gabrilovich, D. I., Velders, M. P., Sotomayor, E. M., & Kast, W. M. (2001). Mechanism of Immune Dysfunction in Cancer Mediated by Immature Gr-1⁺ Myeloid Cells. *The*

Journal of Immunology, 166(9), 5398–5406.
<https://doi.org/10.4049/JIMMUNOL.166.9.5398>

- Galizia, G., Orditura, M., Romano, C., Lieto, E., Castellano, P., Pelosio, L., Imperatore, V., Catalano, G., Pignatelli, C., & De Vita, F. (2002). Prognostic Significance of Circulating IL-10 and IL-6 Serum Levels in Colon Cancer Patients Undergoing Surgery. *Clinical Immunology*, 102(2), 169–178.
<https://doi.org/10.1006/CLIM.2001.5163>
- Galon, J., Angell, H. K., Bedognetti, D., & Marincola, F. M. (2013). The Continuum of Cancer Immunosurveillance: Prognostic, Predictive, and Mechanistic Signatures. *Immunity*, 39(1), 11–26. <https://doi.org/10.1016/J.IMMUNI.2013.07.008>
- Galon, J., & Bruni, D. (2019). Approaches to treat immune hot, altered and cold tumours with combination immunotherapies. *Nature Reviews Drug Discovery* 2018 18:3, 18(3), 197–218. <https://doi.org/10.1038/s41573-018-0007-y>
- Galon, J., Costes, A., Sanchez-Cabo, F., Kirilovsky, A., Mlecnik, B., Lagorce-Pagès, C., Tosolini, M., Camus, M., Berger, A., Wind, P., Zinzindohoué, F., Bruneval, P., Cugnenc, P. H., Trajanoski, Z., Fridman, W. H., & Pagès, F. (2006). Type, density, and location of immune cells within human colorectal tumors predict clinical outcome. *Science*, 313(5795), 1960–1964.
https://doi.org/10.1126/SCIENCE.1129139/SUPPL_FILE/GALON.SOM.PDF
- Gandara, D. R., Paul, S. M., Kowanetz, M., Schleifman, E., Zou, W., Li, Y., Rittmeyer, A., Fehrenbacher, L., Otto, G., Malboeuf, C., Lieber, D. S., Lipson, D., Silterra, J., Amler, L., Riehl, T., Cummings, C. A., Hegde, P. S., Sandler, A., Ballinger, M., ... Shames, D. S. (2018). Blood-based tumor mutational burden as a predictor of clinical benefit in non-small-cell lung cancer patients treated with atezolizumab. *Nature Medicine* 2018 24:9, 24(9), 1441–1448. <https://doi.org/10.1038/s41591-018-0134-3>
- Ganesh, K., Wu, C., O'Rourke, K. P., Szeglin, B. C., Zheng, Y., Sauvé, C. E. G., Adileh, M., Wasserman, I., Marco, M. R., Kim, A. S., Shady, M., Sanchez-Vega, F., Karthaus, W. R., Won, H. H., Choi, S. H., Pelossof, R., Barlas, A., Ntiamoah, P., Pappou, E., ... Smith, J. J. (2019). A rectal cancer organoid platform to study individual responses to chemoradiation. *Nature Medicine* 2019 25:10, 25(10), 1607–1614. <https://doi.org/10.1038/s41591-019-0584-2>
- Ganesh, S., Shui, X., Craig, K. P., Park, J., Wang, W., Brown, B. D., & Abrams, M. T. (2018). RNAi-Mediated β -Catenin Inhibition Promotes T Cell Infiltration and Antitumor Activity in Combination with Immune Checkpoint Blockade. *Molecular Therapy*, 26(11), 2567–2579. <https://doi.org/10.1016/j.ymthe.2018.09.005>
- Gao, H. L., Guan, M., Sun, Z., & Bai, C. M. (2015). High c-Met expression is a negative prognostic marker for colorectal cancer: a meta-analysis. *Tumor Biology*, 36(2), 515–520. <https://doi.org/10.1007/S13277-014-2659-5/FIGURES/6>
- Gao, J., Shi, L. Z., Zhao, H., Chen, J., Xiong, L., He, Q., Chen, T., Roszik, J., Bernatchez, C., Woodman, S. E., Chen, P. L., Hwu, P., Allison, J. P., Futreal, A., Wargo, J. A., & Sharma, P. (2016). Loss of IFN- γ Pathway Genes in Tumor Cells as a Mechanism of Resistance to Anti-CTLA-4 Therapy. *Cell*, 167(2), 397-404.e9.
<https://doi.org/10.1016/J.CELL.2016.08.069>

- Garon, E. B., Rizvi, N. A., Hui, R., Leighl, N., Balmanoukian, A. S., Eder, J. P., Patnaik, A., Aggarwal, C., Gubens, M., Horn, L., Carcereny, E., Ahn, M.-J., Felip, E., Lee, J.-S., Hellmann, M. D., Hamid, O., Goldman, J. W., Soria, J.-C., Dolled-Filhart, M., ... Gandhi, L. (2015a). Pembrolizumab for the Treatment of Non–Small-Cell Lung Cancer. *New England Journal of Medicine*, *372*(21), 2018–2028. https://doi.org/10.1056/NEJMOA1501824/SUPPL_FILE/NEJMOA1501824_DISCLOSURES.PDF
- Garon, E. B., Rizvi, N. A., Hui, R., Leighl, N., Balmanoukian, A. S., Eder, J. P., Patnaik, A., Aggarwal, C., Gubens, M., Horn, L., Carcereny, E., Ahn, M.-J., Felip, E., Lee, J.-S., Hellmann, M. D., Hamid, O., Goldman, J. W., Soria, J.-C., Dolled-Filhart, M., ... Gandhi, L. (2015b). Pembrolizumab for the Treatment of Non–Small-Cell Lung Cancer. *New England Journal of Medicine*, *372*(21), 2018–2028. https://doi.org/10.1056/NEJMOA1501824/SUPPL_FILE/NEJMOA1501824_DISCLOSURES.PDF
- Garralda, E., Sukari, A., Lakhani, N. J., Patnaik, A., Lou, Y., Im, S.-A., Golan, T., Geva, R., Wermke, M., Miguel, M. De, Palcza, J., Jha, S., Chaney, M. F., Healy, J. A., & Falchook, G. S. (2021). A phase 1 first-in-human study of the anti-LAG-3 antibody MK4280 (favezelimab) plus pembrolizumab in previously treated, advanced microsatellite stable colorectal cancer. *Journal of Clinical Oncology*, *39*(15_suppl), 3584–3584. https://doi.org/10.1200/JCO.2021.39.15_SUPPL.3584
- Gattinoni, L., Zhong, X. S., Palmer, D. C., Ji, Y., Hinrichs, C. S., Yu, Z., Wrzesinski, C., Boni, A., Cassard, L., Garvin, L. M., Paulos, C. M., Muranski, P., & Restifo, N. P. (2009). Wnt signaling arrests effector T cell differentiation and generates CD8+ memory stem cells. *Nature Medicine* *2009* *15*:7, *15*(7), 808–813. <https://doi.org/10.1038/nm.1982>
- Gavalas, N. G., Tsiatas, M., Tsitsilonis, O., Politi, E., Ioannou, K., Ziogas, A. C., Rodolakis, A., Vlahos, G., Thomakos, N., Haidopoulos, D., Terpos, E., Antsaklis, A., Dimopoulos, M. A., & Bamias, A. (2012). VEGF directly suppresses activation of T cells from ascites secondary to ovarian cancer via VEGF receptor type 2. *British Journal of Cancer* *2012* *107*:11, *107*(11), 1869–1875. <https://doi.org/10.1038/bjc.2012.468>
- Germain, R. N. (2002). T-cell development and the CD4–CD8 lineage decision. *Nature Reviews Immunology* *2002* *2*:5, *2*(5), 309–322. <https://doi.org/10.1038/nri798>
- Ghiringhelli, F., Puig, P. E., Roux, S., Parcellier, A., Schmitt, E., Solary, E., Kroemer, G., Martin, F., Chauffert, B., & Zitvogel, L. (2005). Tumor cells convert immature myeloid dendritic cells into TGF- β -secreting cells inducing CD4+CD25+ regulatory T cell proliferation. *Journal of Experimental Medicine*, *202*(7), 919–929. <https://doi.org/10.1084/JEM.20050463>
- Ghosh, S., Rosenthal, R., Zajac, P., Weber, W. P., Oertli, D., Heberer, M., Martin, I., Spagnoli, G. C., Reschner, A., & Eggermont. (2005). Culture of melanoma cells in 3-dimensional architectures results in impaired immunorecognition by cytotoxic T lymphocytes specific for Melan-A/MART-1 tumor-associated antigen. *Annals of Surgery*, *242*(6), 851–858. <https://doi.org/10.1097/01.SLA.0000189571.84213.B0>
- Ghosh, S., Spagnoli, G. C., Martin, I., Ploegert, S., Demougin, P., Heberer, M., & Reschner, A. (2005). Three-dimensional culture of melanoma cells profoundly

affects gene expression profile: A high density oligonucleotide array study. *Journal of Cellular Physiology*, 204(2), 522–531. <https://doi.org/10.1002/JCP.20320>

- Giannakis, M., Mu, X. J., Shukla, S. A., Qian, Z. R., Cohen, O., Nishihara, R., Bahl, S., Cao, Y., Amin-Mansour, A., Yamauchi, M., Sukawa, Y., Stewart, C., Rosenberg, M., Mima, K., Inamura, K., Noshō, K., Nowak, J. A., Lawrence, M. S., Giovannucci, E. L., ... Garraway, L. A. (2016). Genomic Correlates of Immune-Cell Infiltrates in Colorectal Carcinoma. *Cell Reports*, 15(4), 857–865. <https://doi.org/10.1016/J.CELREP.2016.03.075>
- Giannattasio, A., Weil, S., Kloess, S., Ansari, N., Stelzer, E. H. K., Cerwenka, A., Steinle, A., Koehl, U., & Koch, J. (2015). Cytotoxicity and infiltration of human NK cells in in vivo-like tumor spheroids. *BMC Cancer*, 15(1), 1–13. <https://doi.org/10.1186/S12885-015-1321-Y/FIGURES/4>
- Giovarelli, M., Musiani, P., Modesti, A., Dellabona, P., Casorati, G., Allione, A., Consalvo, M., Cavallo, F., di Pierro, F., & De Giovanni, C. (1995). Local release of IL-10 by transfected mouse mammary adenocarcinoma cells does not suppress but enhances antitumor reaction and elicits a strong cytotoxic lymphocyte and antibody-dependent immune memory. *The Journal of Immunology*, 155(6).
- Giroux, M., Delisle, J.-S., O'Brien, A., Hébert, M.-J., & Perreault, C. (2010). T Cell Activation Leads to Protein Kinase C θ -Dependent Inhibition of TGF- β Signaling. *The Journal of Immunology*, 185(3), 1568–1576. <https://doi.org/10.4049/JIMMUNOL.1000137>
- Gomez-Roca, C., Yanez, E., Im, S.-A., Alvarez, E. C., Senellart, H., Doherty, M., García-Corbacho, J., Lopez, J. S., Basu, B., Maurice-Dror, C., Gill, S. S., Ghori, R., Kubiak, P., Jin, F., Norwood, K. G., & Chung, H. C. (2021). LEAP-005: A phase II multicohort study of lenvatinib plus pembrolizumab in patients with previously treated selected solid tumors—Results from the colorectal cancer cohort. *https://Doi.Org/10.1200/JCO.2021.39.3_suppl.94*, 39(3_suppl), 94–94. https://doi.org/10.1200/JCO.2021.39.3_SUPPL.94
- Gondek, D. C., Lu, L.-F., Quezada, S. A., Sakaguchi, S., & Noelle, R. J. (2005). Cutting Edge: Contact-Mediated Suppression by CD4+CD25+ Regulatory Cells Involves a Granzyme B-Dependent, Perforin-Independent Mechanism. *The Journal of Immunology*, 174(4), 1783–1786. <https://doi.org/10.4049/JIMMUNOL.174.4.1783>
- Gonzalez-Exposito, R., Semiannikova, M., Griffiths, B., Khan, K., Barber, L. J., Woolston, A., Spain, G., Von Loga, K., Challoner, B., Patel, R., Ranes, M., Swain, A., Thomas, J., Bryant, A., Saffery, C., Fotiadis, N., Guettler, S., Mansfield, D., Melcher, A., ... Gerlinger, M. (2019). CEA expression heterogeneity and plasticity confer resistance to the CEA-targeting bispecific immunotherapy antibody cibusatamab (CEA-TCB) in patient-derived colorectal cancer organoids. *Journal for ImmunoTherapy of Cancer*, 7(1). <https://doi.org/10.1186/s40425-019-0575-3>
- Gorbachev, A. V., Kobayashi, H., Kudo, D., Tannenbaum, C. S., Finke, J. H., Shu, S., Farber, J. M., & Fairchild, R. L. (2007). CXC Chemokine Ligand 9/Monokine Induced by IFN- γ Production by Tumor Cells Is Critical for T Cell-Mediated Suppression of Cutaneous Tumors. *The Journal of Immunology*, 178(4), 2278–2286. <https://doi.org/10.4049/JIMMUNOL.178.4.2278>

- Gorelik, L., & Flavell, R. A. (2000). Abrogation of TGF β Signaling in T Cells Leads to Spontaneous T Cell Differentiation and Autoimmune Disease. *Immunity*, *12*(2), 171–181. [https://doi.org/10.1016/S1074-7613\(00\)80170-3](https://doi.org/10.1016/S1074-7613(00)80170-3)
- Gorelik, L., & Flavell, R. A. (2001). Immune-mediated eradication of tumors through the blockade of transforming growth factor- β signaling in T cells. *Nature Medicine*, *7*(10), 1118–1122. <https://doi.org/10.1038/nm1001-1118>
- Gorelik, L., & Flavell, R. A. (2002). Transforming growth factor- β in T-cell biology. *Nature Reviews Immunology* *2002 2:1*, *2*(1), 46–53. <https://doi.org/10.1038/nri704>
- Görlach, A., Herter, P., Hentschel, H., Frosch, P. J., & Acker, H. (1994). Effects of nIFN β and rIFN γ on growth and morphology of two human melanoma cell lines: Comparison between two- and three-dimensional culture. *International Journal of Cancer*, *56*(2), 249–254. <https://doi.org/10.1002/IJC.2910560218>
- Gottfried, E., Kunz-Schughart, L. A., Ebner, S., Mueller-Klieser, W., Hoves, S., Andreesen, R., Mackensen, A., & Kreutz, M. (2006). Tumor-derived lactic acid modulates dendritic cell activation and antigen expression. *Blood*, *107*(5), 2013–2021. <https://doi.org/10.1182/BLOOD-2005-05-1795>
- Grady, W. M., & Markowitz, S. D. (2003). GENETIC AND EPIGENETIC ALTERATIONS IN COLON CANCER. *Annual Review of Genomics and Human Genetics*, *3*, 101–128. <https://doi.org/10.1146/ANNUREV.GENOM.3.022502.103043>
- Greco, R., Qu, H., Qu, H., Theilhaber, J., Shapiro, G., Gregory, R., Winter, C., Malkova, N., Sun, F., Jaworski, J., Best, A., Pao, L., Hebert, A., Levit, M., Protopopov, A., Pollard, J., Bahjat, K., Wiederschain, D., & Sharma, S. (2020). Pan-TGF β inhibition by SAR439459 relieves immunosuppression and improves antitumor efficacy of PD-1 blockade. *Oncotarget*, *9*(1). https://doi.org/10.1080/2162402X.2020.1811605/SUPPL_FILE/KONI_A_1811605_SM8142.DOCX
- Green, D. R., Ferguson, T., Zitvogel, L., & Kroemer, G. (2009). Immunogenic and tolerogenic cell death. *Nature Reviews Immunology* *2009 9:5*, *9*(5), 353–363. <https://doi.org/10.1038/nri2545>
- Grivnennikov, S., Karin, E., Terzic, J., Mucida, D., Yu, G. Y., Vallabhapurapu, S., Scheller, J., Rose-John, S., Cheroutre, H., Eckmann, L., & Karin, M. (2009). IL-6 and Stat3 Are Required for Survival of Intestinal Epithelial Cells and Development of Colitis-Associated Cancer. *Cancer Cell*, *15*(2), 103–113. <https://doi.org/10.1016/J.CCR.2009.01.001>
- Groom, J. R., & Luster, A. D. (2011). CXCR3 in T cell function. *Experimental Cell Research*, *317*(5), 620–631. <https://doi.org/10.1016/J.YEXCR.2010.12.017>
- Gropper, Y., Feferman, T., Shalit, T., Salame, T. M., Porat, Z., & Shakhar, G. (2017). Culturing CTLs under Hypoxic Conditions Enhances Their Cytotoxicity and Improves Their Anti-tumor Function. *Cell Reports*, *20*(11), 2547–2555. <https://doi.org/10.1016/J.CELREP.2017.08.071>
- Grosso, J. F., Goldberg, M. V., Getnet, D., Bruno, T. C., Yen, H.-R., Pyle, K. J., Hipkiss, E., Vignali, D. A. A., Pardoll, D. M., & Drake, C. G. (2009). Functionally Distinct LAG-3 and PD-1 Subsets on Activated and Chronically Stimulated CD8 T

Cells. *The Journal of Immunology*, 182(11), 6659–6669.
<https://doi.org/10.4049/JIMMUNOL.0804211>

- Grosso, J. F., Kelleher, C. C., Harris, T. J., Maris, C. H., Hipkiss, E. L., De Marzo, A., Anders, R., Netto, G., Getnet, D., Bruno, T. C., Goldberg, M. V., Pardoll, D. M., & Drake, C. G. (2007). LAG-3 regulates CD8⁺ T cell accumulation and effector function in murine self- and tumor-tolerance systems. *The Journal of Clinical Investigation*, 117(11), 3383–3392. <https://doi.org/10.1172/JCI31184>
- Grothey, A., Van Cutsem, E., Sobrero, A., Siena, S., Falcone, A., Ychou, M., Humblet, Y., Bouché, O., Mineur, L., Barone, C., Adenis, A., Tabernero, J., Yoshino, T., Lenz, H. J., Goldberg, R. M., Sargent, D. J., Cihon, F., Cupit, L., Wagner, A., & Laurent, D. (2013). Regorafenib monotherapy for previously treated metastatic colorectal cancer (CORRECT): an international, multicentre, randomised, placebo-controlled, phase 3 trial. *The Lancet*, 381(9863), 303–312.
[https://doi.org/10.1016/S0140-6736\(12\)61900-X](https://doi.org/10.1016/S0140-6736(12)61900-X)
- Groux, H., Bigler, M., De Vries, J. E., & Roncarolo, M. G. (1996). Interleukin-10 induces a long-term antigen-specific anergic state in human CD4⁺ T cells. *Journal of Experimental Medicine*, 184(1), 19–29. <https://doi.org/10.1084/JEM.184.1.19>
- Groux, H., Bigler, M., de Vries, J. E., & Roncarolo, M.-G. (1998). Inhibitory and Stimulatory Effects of IL-10 on Human CD8⁺ T Cells. *The Journal of Immunology*, 160(7), 3188–3193. <https://doi.org/10.4049/JIMMUNOL.160.7.3188>
- Guadagni, F., Witt, P. L., Robbins, P. F., Schlom, J., & Greiner, J. W. (1990). Regulation of carcinoembryonic antigen expression in different human colorectal tumor cells by interferon-gamma. *Cancer Research*, 50(19), 6248–6255.
<http://www.ncbi.nlm.nih.gov/pubmed/2119252>
- Gubin, M. M., Zhang, X., Schuster, H., Caron, E., Ward, J. P., Noguchi, T., Ivanova, Y., Hundal, J., Arthur, C. D., Krebber, W. J., Mulder, G. E., Toebes, M., Vesely, M. D., Lam, S. S. K., Korman, A. J., Allison, J. P., Freeman, G. J., Sharpe, A. H., Pearce, E. L., ... Schreiber, R. D. (2014). Checkpoint blockade cancer immunotherapy targets tumour-specific mutant antigens. *Nature* 2014 515:7528, 515(7528), 577–581. <https://doi.org/10.1038/nature13988>
- Guinney, J., Dienstmann, R., Wang, X., De Reyniès, A., Schlicker, A., Soneson, C., Marisa, L., Roepman, P., Nyamundanda, G., Angelino, P., Bot, B. M., Morris, J. S., Simon, I. M., Gerster, S., Fessler, E., De Sousa .E Melo, F., Missiaglia, E., Ramay, H., Barras, D., ... Tejpar, S. (2015). The consensus molecular subtypes of colorectal cancer. *Nature Medicine* 2015 21:11, 21(11), 1350–1356.
<https://doi.org/10.1038/nm.3967>
- Guo, J., Lu, W., Shimoda, L. A., Semenza, G. L., & Georas, S. N. (2009). Enhanced Interferon- γ Gene Expression in T Cells and Reduced Ovalbumin-Dependent Lung Eosinophilia in Hypoxia-Inducible Factor-1- α -Deficient Mice. *International Archives of Allergy and Immunology*, 149(2), 98–102.
<https://doi.org/10.1159/000189191>
- Hammond, E. M., Asselin, M.-C., Forster, D., O'connor, J. P. B., Senra, J. M., & Williams, K. J. (2014). The Meaning, Measurement and Modification of Hypoxia in the Laboratory and the Clinic . *Clinical Oncology*, 26, 277–288.
<https://doi.org/10.1016/j.clon.2014.02.002>

- Hamzah, J., Jugold, M., Kiessling, F., Rigby, P., Manzur, M., Marti, H. H., Rabie, T., Kaden, S., Gröne, H. J., Hämmerling, G. J., Arnold, B., & Ganss, R. (2008). Vascular normalization in Rgs5-deficient tumours promotes immune destruction. *Nature* 2008 453:7193, 453(7193), 410–414. <https://doi.org/10.1038/nature06868>
- Hanabuchi, S., Koyanagi, M., Kawasaki, A., Shinohara, N., Matsuzawa, A., Nishimura, Y., Kobayashi, Y., Yonehara, S., Yagita, H., & Okumura, K. (1994). Fas and its ligand in a general mechanism of T-cell-mediated cytotoxicity. *Proceedings of the National Academy of Sciences*, 91(11), 4930–4934. <https://doi.org/10.1073/PNAS.91.11.4930>
- Hanahan, D., & Weinberg, R. A. (2011). Hallmarks of cancer: The next generation. *Cell*, 144(5), 646–674. <https://doi.org/10.1016/J.CELL.2011.02.013/ATTACHMENT/3F528E16-8B3C-4D8D-8DE5-43E0C98D8475/MMC1.PDF>
- Hannier, S., Tournier, M., Bismuth, G., & Triebel, F. (1998). CD3/TCR Complex-Associated Lymphocyte Activation Gene-3 Molecules Inhibit CD3/TCR Signaling. *The Journal of Immunology*, 161(8), 4058–4065. <https://doi.org/10.4049/JIMMUNOL.161.8.4058>
- Hao, Q., & Tang, H. (2018). Interferon- γ and Smac mimetics synergize to induce apoptosis of lung cancer cells in a TNF α -independent manner. *Cancer Cell International*, 18(1), 1–12. <https://doi.org/10.1186/S12935-018-0579-Y/FIGURES/7>
- Harding, F. A., McArthur, J. G., Gross, J. A., Raulet, D. H., & Allison, J. P. (1992). CD28-mediated signalling co-stimulates murine T cells and prevents induction of anergy in T-cell clones. *Nature* 1992 356:6370, 356(6370), 607–609. <https://doi.org/10.1038/356607a0>
- Harlin, H., Meng, Y., Peterson, A. C., Zha, Y., Tretiakova, M., Slingluff, C., McKee, M., & Gajewski, T. F. (2009). Chemokine expression in melanoma metastases associated with CD8 + T-Cell recruitment. *Cancer Research*, 69(7), 3077–3085. <https://doi.org/10.1158/0008-5472.CAN-08-2281/654525/P/CHEMOKINE-EXPRESSION-IN-MELANOMA-METASTASES>
- Harrington, L. E., Mangan, P. R., & Weaver, C. T. (2006). Expanding the effector CD4 T-cell repertoire: the Th17 lineage. *Current Opinion in Immunology*, 18(3), 349–356. <https://doi.org/10.1016/J.COI.2006.03.017>
- Hartmann, N., Giese, N. A., Giese, T., Poschke, I., Offringa, R., Werner, J., & Ryschich, E. (2014). Prevailing role of contact guidance in intrastromal T-cell trapping in human pancreatic cancer. *Clinical Cancer Research*, 20(13), 3422–3433. <https://doi.org/10.1158/1078-0432.CCR-13-2972/86295/AM/PREVAILING-ROLE-OF-CONTACT-GUIDANCE-IN>
- Harty, J. T., Tvinnereim, A. R., & White, D. W. (2003). CD8+ T Cell Effector Mechanisms in Resistance to Infection. *Annual Review of Immunology*, 18, 275–308. <https://doi.org/10.1146/ANNUREV.IMMUNOL.18.1.275>
- Hatfield, S. M., Kjaergaard, J., Lukashev, D., Belikoff, B., Schreiber, T. H., Sethumadhavan, S., Abbott, R., Philbrook, P., Thayer, M., Shujia, D., Rodig, S., Kutok, J. L., Ren, J., Ohta, A., Podack, E. R., Karger, B., Jackson, E. K., & Sitkovsky, M. (2014). Systemic oxygenation weakens the hypoxia and hypoxia

inducible factor 1 α -dependent and extracellular adenosine-mediated tumor protection. *Journal of Molecular Medicine*, 92(12), 1283–1292.
<https://doi.org/10.1007/S00109-014-1189-3/FIGURES/5>

- He, W., He, W., Kuang, Y., Xing, X., Simpson, R. J., Huang, H., Yang, T., Chen, J., Yang, L., Liu, E., & Gu, J. (2014). Proteomic comparison of 3D and 2D glioma models reveals increased HLA-E expression in 3D models is associated with resistance to NK cell-mediated cytotoxicity. *Journal of Proteome Research*, 13(5), 2272–2281.
https://doi.org/10.1021/PR500064M/SUPPL_FILE/PR500064M_SI_005.XLSX
- Heath, V. L., Murphy, E. E., Crain, C., Tomlinson, M. G., & O'garra, A. (2000). TGF beta down-regulates Th2 development and results in decreased IL-4-induced STAT6 activation and GATA-3 expression. *European Journal of Immunology*, 30(9), 2639–2649. <https://doi.org/10.1002/1521-4141>
- Heath, W. R., & Carbone, F. R. (2009). Dendritic cell subsets in primary and secondary T cell responses at body surfaces. *Nature Immunology* 2009 10:12, 10(12), 1237–1244. <https://doi.org/10.1038/ni.1822>
- Hellmann, M. D., Callahan, M. K., Awad, M. M., Calvo, E., Ascierto, P. A., Atmaca, A., Rizvi, N. A., Hirsch, F. R., Selvaggi, G., Szustakowski, J. D., Sasson, A., Golhar, R., Vitazka, P., Chang, H., Geese, W. J., & Antonia, S. J. (2018). Tumor Mutational Burden and Efficacy of Nivolumab Monotherapy and in Combination with Ipilimumab in Small-Cell Lung Cancer. *Cancer Cell*, 33(5), 853-861.e4. <https://doi.org/10.1016/J.CCELL.2018.04.001>
- Hemon, P., Jean-Louis, F., Ramgolam, K., Brignone, C., Viguier, M., Bachelez, H., Triebel, F., Charron, D., Aoudjit, F., Al-Daccak, R., & Michel, L. (2011). MHC Class II Engagement by Its Ligand LAG-3 (CD223) Contributes to Melanoma Resistance to Apoptosis. *The Journal of Immunology*, 186(9), 5173–5183. <https://doi.org/10.4049/JIMMUNOL.1002050>
- Herbst, R. S., Soria, J. C., Kowanetz, M., Fine, G. D., Hamid, O., Gordon, M. S., Sosman, J. A., McDermott, D. F., Powderly, J. D., Gettinger, S. N., Kohrt, H. E. K., Horn, L., Lawrence, D. P., Rost, S., Leabman, M., Xiao, Y., Mokatrin, A., Koeppen, H., Hegde, P. S., ... Hodi, F. S. (2014a). Predictive correlates of response to the anti-PD-L1 antibody MPDL3280A in cancer patients. *Nature* 2014 515:7528, 515(7528), 563–567. <https://doi.org/10.1038/nature14011>
- Herbst, R. S., Soria, J. C., Kowanetz, M., Fine, G. D., Hamid, O., Gordon, M. S., Sosman, J. A., McDermott, D. F., Powderly, J. D., Gettinger, S. N., Kohrt, H. E. K., Horn, L., Lawrence, D. P., Rost, S., Leabman, M., Xiao, Y., Mokatrin, A., Koeppen, H., Hegde, P. S., ... Hodi, F. S. (2014b). Predictive correlates of response to the anti-PD-L1 antibody MPDL3280A in cancer patients. *Nature* 2014 515:7528, 515(7528), 563–567. <https://doi.org/10.1038/nature14011>
- Hernandez, I., Prasad, V., & Gellad, W. F. (2018). Total Costs of Chimeric Antigen Receptor T-Cell Immunotherapy. *JAMA Oncology*, 4(7), 994. <https://doi.org/10.1001/JAMAONCOL.2018.0977>
- Hernandez-Chacon, J. A., Li, Y., Wu, R. C., Bernatchez, C., Wang, Y., Weber, J., Hwu, P., & Radvanyi, L. (2011). Co-stimulation through the CD137/4-1BB pathway protects human melanoma tumor-infiltrating lymphocytes from activation-induced

cell death and enhances anti-tumor effector function. *Journal of Immunotherapy (Hagerstown, Md. : 1997)*, 34(3), 236.
<https://doi.org/10.1097/CJI.0B013E318209E7EC>

- Herter, S., Morra, L., Schlenker, R., Sulcova, J., Fahrni, L., Waldhauer, I., Lehmann, S., Reisländer, T., Agarkova, I., Kelm, J. M., Klein, C., Umana, P., & Bacac, M. (2017). A novel three-dimensional heterotypic spheroid model for the assessment of the activity of cancer immunotherapy agents. *Cancer Immunology, Immunotherapy*, 66(1), 129–140. <https://doi.org/10.1007/S00262-016-1927-1/FIGURES/6>
- Hildemann, S. K., Eberlein, J., Davenport, B., Nguyen, T. T., Victorino, F., & Homann, D. (2013). High Efficiency of Antiviral CD4+ Killer T Cells. *PLOS ONE*, 8(4), e60420. <https://doi.org/10.1371/JOURNAL.PONE.0060420>
- Hlubek, F., Brabletz, T., Budczies, J., Pfeiffer, S., Jung, A., & Kirchner, T. (2007). Heterogeneous expression of Wnt/ β -catenin target genes within colorectal cancer. *International Journal of Cancer*, 121(9), 1941–1948. <https://doi.org/10.1002/IJC.22916>
- Ho, W. W., Gomes-Santos, I. L., Aoki, S., Datta, M., Kawaguchi, K., Talele, N. P., Roberge, S., Ren, J., Liu, H., Chen, I. X., Andersson, P., Chatterjee, S., Kumar, A. S., Amoozgar, Z., Zhang, Q., Huang, P., Ng, M. R., Chauhan, V. P., Xu, L., ... Jain, R. K. (2021). Dendritic cell paucity in mismatch repair-proficient colorectal cancer liver metastases limits immune checkpoint blockade efficacy. *Proceedings of the National Academy of Sciences of the United States of America*, 118(45), e2105323118. https://doi.org/10.1073/PNAS.2105323118/SUPPL_FILE/PNAS.2105323118.SD02.XLSX
- Hodi, F. S., Lawrence, D., Lezcano, C., Wu, X., Zhou, J., Sasada, T., Zeng, W., Giobbie-Hurder, A., Atkins, M. B., Ibrahim, N., Friedlander, P., Flaherty, K. T., Murphy, G. F., Rodig, S., Velazquez, E. F., Mihm, M. C., Russell, S., Di Piro, P. J., Yap, J. T., ... McDermott, D. (2014). Bevacizumab plus Ipilimumab in Patients with Metastatic Melanoma. *Cancer Immunology Research*, 2(7), 632–642. <https://doi.org/10.1158/2326-6066.CIR-14-0053/470348/AM/BEVACIZUMAB-PLUS-IPILIMUMAB-IN-PATIENTS-WITH>
- Hodi, F. S., O'Day, S. J., McDermott, D. F., Weber, R. W., Sosman, J. A., Haanen, J. B., Gonzalez, R., Robert, C., Schadendorf, D., Hassel, J. C., Akerley, W., van den Eertwegh, A. J. M., Lutzky, J., Lorigan, P., Vaubel, J. M., Linette, G. P., Hogg, D., Ottensmeier, C. H., Lebbé, C., ... Urban, W. J. (2010). Improved Survival with Ipilimumab in Patients with Metastatic Melanoma. *New England Journal of Medicine*, 363(8), 711–723. https://doi.org/10.1056/NEJMOA1003466/SUPPL_FILE/NEJMOA1003466_DISCLOSURES.PDF
- Hoechst, B., Ormandy, L. A., Ballmaier, M., Lehner, F., Krüger, C., Manns, M. P., Greten, T. F., & Korangy, F. (2008). A New Population of Myeloid-Derived Suppressor Cells in Hepatocellular Carcinoma Patients Induces CD4+CD25+Foxp3+ T Cells. *Gastroenterology*, 135(1), 234–243. <https://doi.org/10.1053/J.GASTRO.2008.03.020>

- Hoffmann, T. K., Schirlau, K., Sonkoly, E., Brandau, S., Lang, S., Pivarcsi, A., Balz, V., Müller, A., Homey, B., Boelke, E., Reichert, T., Friebe-Hoffmann, U., Greve, J., Schuler, P., Scheckenbach, K., Schipper, J., Bas, M., Whiteside, T. L., & Bier, H. (2009). A novel mechanism for anti-EGFR antibody action involves chemokine-mediated leukocyte infiltration. *International Journal of Cancer*, *124*(11), 2589–2596. <https://doi.org/10.1002/IJC.24269>
- Holash, J., Davis, S., Papadopoulos, N., Croll, S. D., Ho, L., Russell, M., Boland, P., Leidich, R., Hylton, D., Burova, E., Ioffe, E., Huang, T., Radziejewski, C., Bailey, K., Fandl, J. P., Daly, T., Wiegand, S. J., Yancopoulos, G. D., & Rudge, J. S. (2002). VEGF-Trap: A VEGF blocker with potent antitumor effects. *Proceedings of the National Academy of Sciences of the United States of America*, *99*(17), 11393–11398. https://doi.org/10.1073/PNAS.172398299/SUPPL_FILE/3982SUPPTXT.HTML
- Holmgaard, R. B., Schaer, D. A., Li, Y., Castaneda, S. P., Murphy, M. Y., Xu, X., Inigo, I., Dobkin, J., Manro, J. R., Iversen, P. W., Surguladze, D., Hall, G. E., Novosiadly, R. D., Benhadji, K. A., Plowman, G. D., Kalos, M., & Driscoll, K. E. (2018). Targeting the TGF β pathway with galunisertib, a TGF β RI small molecule inhibitor, promotes anti-tumor immunity leading to durable, complete responses, as monotherapy and in combination with checkpoint blockade. *Journal for ImmunoTherapy of Cancer*, *6*(1), 1–15. <https://doi.org/10.1186/S40425-018-0356-4/FIGURES/6>
- Hombach, A., Köhler, H., Rappl, G., & Abken, H. (2006). Human CD4⁺ T Cells Lyse Target Cells via Granzyme/Perforin upon Circumvention of MHC Class II Restriction by an Antibody-Like Immunoreceptor. *The Journal of Immunology*, *177*(8), 5668–5675. <https://doi.org/10.4049/JIMMUNOL.177.8.5668>
- Hong, D. S., Morris, V. K., El Osta, B., Sorokin, A. V., Janku, F., Fu, S., Overman, M. J., Piha-Paul, S., Subbiah, V., Kee, B., Tsimberidou, A. M., Fogelman, D., Bellido, J., Shureiqi, I., Huang, H., Atkins, J., Tarcic, G., Sommer, N., Lanman, R., ... Kopetz, S. (2016). Phase IB study of vemurafenib in combination with irinotecan and cetuximab in patients with metastatic colorectal cancer with BRAFV600E mutation. *Cancer Discovery*, *6*(12), 1352–1365. <https://doi.org/10.1158/2159-8290.CD-16-0050/42521/AM/PHASE-1B-STUDY-OF-VEMURAFENIB-IN-COMBINATION-WITH>
- Hua, L., Yao, S., Pham, D., Jiang, L., Wright, J., Sawant, D., Dent, A. L., Braciale, T. J., Kaplan, M. H., & Sun, J. (2013). Cytokine-Dependent Induction of CD4⁺ T cells with Cytotoxic Potential during Influenza Virus Infection. *Journal of Virology*, *87*(21), 11884–11893. <https://doi.org/10.1128/JVI.01461-13/ASSET/D441880B-1787-4862-AB4D-FAEC6AE023F7/ASSETS/GRAPHIC/ZJV9990982410007.JPEG>
- Huang, B., Pan, P. Y., Li, Q., Sato, A. I., Levy, D. E., Bromberg, J., Divino, C. M., & Chen, S. H. (2006). Gr-1⁺CD115⁺ Immature Myeloid Suppressor Cells Mediate the Development of Tumor-Induced T Regulatory Cells and T-Cell Anergy in Tumor-Bearing Host. *Cancer Research*, *66*(2), 1123–1131. <https://doi.org/10.1158/0008-5472.CAN-05-1299>
- Huang, C. T., Workman, C. J., Flies, D., Pan, X., Marson, A. L., Zhou, G., Hipkiss, E. L., Ravi, S., Kowalski, J., Levitsky, H. I., Powell, J. D., Pardoll, D. M., Drake, C. G.,

- & Vignali, D. A. A. (2004). Role of LAG-3 in Regulatory T Cells. *Immunity*, 21(4), 503–513. <https://doi.org/10.1016/J.IMMUNI.2004.08.010>
- Huang, S. M. A., Mishina, Y. M., Liu, S., Cheung, A., Stegmeier, F., Michaud, G. A., Charlat, O., Wiellette, E., Zhang, Y., Wiessner, S., Hild, M., Shi, X., Wilson, C. J., Mickanin, C., Myer, V., Fazal, A., Tomlinson, R., Serluca, F., Shao, W., ... Cong, F. (2009). Tankyrase inhibition stabilizes axin and antagonizes Wnt signalling. *Nature* 2009 461:7264, 461(7264), 614–620. <https://doi.org/10.1038/nature08356>
- Huang, S.-M. A., Mishina, Y. M., Liu, S., Cheung, A., Stegmeier, F., Michaud, G. A., Charlat, O., Wiellette, E., Zhang, Y., Wiessner, S., Hild, M., Shi, X., Wilson, C. J., Mickanin, C., Myer, V., Fazal, A., Tomlinson, R., Serluca, F., Shao, W., ... Cong, F. (2009). Tankyrase inhibition stabilizes axin and antagonizes Wnt signalling. *Nature*, 461(7264), 614–620. <https://doi.org/10.1038/nature08356>
- Huang, X., Bai, X., Cao, Y., Wu, J., Huang, M., Tang, D., Tao, S., Zhu, T., Liu, Y., Yang, Y., Zhou, X., Zhao, Y., Wu, M., Wei, J., Wang, D., Xu, G., Wang, S., Ma, D., & Zhou, J. (2010). Lymphoma endothelium preferentially expresses Tim-3 and facilitates the progression of lymphoma by mediating immune evasion. *Journal of Experimental Medicine*, 207(3), 505–520. <https://doi.org/10.1084/JEM.20090397>
- Huang, Y., Yuan, J., Righi, E., Kamoun, W. S., Ancukiewicz, M., Nezivar, J., Santosuosso, M., Martin, J. D., Martin, M. R., Vianello, F., Leblanc, P., Munn, L. L., Huang, P., Duda, D. G., Fukumura, D., Jain, R. K., & Poznansky, M. C. (2012). Vascular normalizing doses of antiangiogenic treatment reprogram the immunosuppressive tumor microenvironment and enhance immunotherapy. *Proceedings of the National Academy of Sciences of the United States of America*, 109(43), 17561–17566. https://doi.org/10.1073/PNAS.1215397109/SUPPL_FILE/PNAS.201215397SI.PDF
- Huard, B., Gaulard, P., Faure, F., Hercend, T., & Triebel, F. (1994). Cellular expression and tissue distribution of the human LAG-3-encoded protein, an MHC class II ligand. *Immunogenetics*, 39(3), 213–217. <https://doi.org/10.1007/BF00241263/METRICS>
- Hurwitz, H., Fehrenbacher, L., Novotny, W., Cartwright, T., Hainsworth, J., Heim, W., Berlin, J., Baron, A., Griffing, S., Holmgren, E., Ferrara, N., Fyfe, G., Rogers, B., Ross, R., & Kabbinavar, F. (2004). Bevacizumab plus Irinotecan, Fluorouracil, and Leucovorin for Metastatic Colorectal Cancer. *The New England Journal of Medicine*, 350(23), 2335–2342. <https://doi.org/10.1056/NEJMOA032691>
- Ikenoue, T., Hikiba, Y., Kanai, F., Tanaka, Y., Imamura, J., Imamura, T., Ohta, M., Ijichi, H., Tateishi, K., Kawakami, T., Aragaki, J., Matsumura, M., Kawabe, T., & Omata, M. (2003). Functional Analysis of Mutations within the Kinase Activation Segment of B-Raf in Human Colorectal Tumors. *CANCER RESEARCH*, 63, 8132–8137. <http://aacrjournals.org/cancerres/article-pdf/63/23/8132/2510904/zch02303008132.pdf>
- Inge, T. H., Hoover, S. K., Susskind, B. M., Barrett, S. K., & Bear2, H. D. (1992). Inhibition of Tumor-specific Cytotoxic T-Lymphocyte Responses by Transforming Growth Factor 0,1. *CANCER RESEARCH*, 52, 1386–1392. <http://aacrjournals.org/cancerres/article-pdf/52/6/1386/2449948/cr0520061386.pdf>

- Inoue, H., & Tani, K. (2014). Multimodal immunogenic cancer cell death as a consequence of anticancer cytotoxic treatments. *Cell Death & Differentiation*, *21*(1), 39–49. <https://doi.org/10.1038/cdd.2013.84>
- Inoue, T., Adachi, K., Kawana, K., Taguchi, A., Nagamatsu, T., Fujimoto, A., Tomio, K., Yamashita, A., Eguchi, S., Nishida, H., Nakamura, H., Sato, M., Yoshida, M., Arimoto, T., Wada-Hiraike, O., Oda, K., Osuga, Y., & Fujii, T. (2016). Cancer-associated fibroblast suppresses killing activity of natural killer cells through downregulation of poliovirus receptor (PVR/CD155), a ligand of activating NK receptor. *International Journal of Oncology*, *49*(4), 1297–1304. <https://doi.org/10.3892/IJO.2016.3631/HTML>
- Inoue, Y., Hazama, S., Suzuki, N., Tokumitsu, Y., Kanekiyo, S., Tomochika, S., Tsunedomi, R., Tokuhisa, Y., Iida, M., Sakamoto, K., Takeda, S., Ueno, T., Yoshino, S., & Nagano, H. (2017). Cetuximab strongly enhances immune cell infiltration into liver metastatic sites in colorectal cancer. *Cancer Science*, *108*(3), 455–460. <https://doi.org/10.1111/CAS.13162>
- Ishida, T., Ishii, T., Inagaki, A., Yano, H., Komatsu, H., Iida, S., Inagaki, H., & Ueda, R. (2006). Specific Recruitment of CC Chemokine Receptor 4–Positive Regulatory T Cells in Hodgkin Lymphoma Fosters Immune Privilege. *Cancer Research*, *66*(11), 5716–5722. <https://doi.org/10.1158/0008-5472.CAN-06-0261>
- Ishiguro, T., Sano, Y., Komatsu, S. I., Kamata-Sakurai, M., Kaneko, A., Kinoshita, Y., Shiraiwa, H., Azuma, Y., Tsunenari, T., Kayukawa, Y., Sonobe, Y., Ono, N., Sakata, K., Fujii, T., Miyazaki, Y., Noguchi, M., Endo, M., Harada, A., Frings, W., ... Nezu, J. (2017a). An anti-glypican 3/CD3 bispecific T cell-redirecting antibody for treatment of solid tumors. *Science Translational Medicine*, *9*(410). https://doi.org/10.1126/SCITRANSLMED.AAL4291/SUPPL_FILE/AAL4291_TABLE_S10.ZIP
- Ishiguro, T., Sano, Y., Komatsu, S. I., Kamata-Sakurai, M., Kaneko, A., Kinoshita, Y., Shiraiwa, H., Azuma, Y., Tsunenari, T., Kayukawa, Y., Sonobe, Y., Ono, N., Sakata, K., Fujii, T., Miyazaki, Y., Noguchi, M., Endo, M., Harada, A., Frings, W., ... Nezu, J. (2017b). An anti-glypican 3/CD3 bispecific T cell-redirecting antibody for treatment of solid tumors. *Science Translational Medicine*, *9*(410). https://doi.org/10.1126/SCITRANSLMED.AAL4291/SUPPL_FILE/AAL4291_TABLE_S10.ZIP
- Ivanoff, J., Talme, T., & Sundqvist, K. G. (2005). The role of chemokines and extracellular matrix components in the migration of T lymphocytes into three-dimensional substrata. *Immunology*, *114*(1), 53. <https://doi.org/10.1111/J.1365-2567.2004.02005.X>
- Iwai, Y., Ishida, M., Tanaka, Y., Okazaki, T., Honjo, T., & Minato, N. (2002). Involvement of PD-L1 on tumor cells in the escape from host immune system and tumor immunotherapy by PD-L1 blockade. *Proceedings of the National Academy of Sciences of the United States of America*, *99*(19), 12293–12297. <https://doi.org/10.1073/PNAS.192461099/ASSET/0E18DCD1-4D55-4829-AD15-01D16A1FBDD7/ASSETS/GRAPHIC/PQ1924610004.JPEG>
- Jain, R. K. (2001). Normalizing tumor vasculature with anti-angiogenic therapy: A new paradigm for combination therapy. *Nature Medicine* *2001* 7:9, *7*(9), 987–989. <https://doi.org/10.1038/nm0901-987>

- Janeway, C. A., & Medzhitov, R. (2003). Innate Immune Recognition. *Annual Review of Immunology*, 20, 197–216.
<https://doi.org/10.1146/ANNUREV.IMMUNOL.20.083001.084359>
- Jiang, P., Gu, S., Pan, D., Fu, J., Sahu, A., Hu, X., Li, Z., Traugh, N., Bu, X., Li, B., Liu, J., Freeman, G. J., Brown, M. A., Wucherpfennig, K. W., & Liu, X. S. (2018). Signatures of T cell dysfunction and exclusion predict cancer immunotherapy response. *Nature Medicine* 2018 24:10, 24(10), 1550–1558.
<https://doi.org/10.1038/s41591-018-0136-1>
- Jodo, S., Hohlbaum, A. M., Xiao, S., Chan, D., Strehlow, D., Sherr, D. H., Marshak-Rothstein, A., & Ju, S.-T. (2000). CD95 (Fas) Ligand-Expressing Vesicles Display Antibody-Mediated, FcR-Dependent Enhancement of Cytotoxicity. *The Journal of Immunology*, 165(10), 5487–5494.
<https://doi.org/10.4049/JIMMUNOL.165.10.5487>
- Jodo, S., Strehlow, D., & Ju, S.-T. (2000). Bioactivities of Fas Ligand-Expressing Retroviral Particles. *The Journal of Immunology*, 164(10), 5062–5069.
<https://doi.org/10.4049/JIMMUNOL.164.10.5062>
- Jorgovanovic, D., Song, M., Wang, L., & Zhang, Y. (2020). Roles of IFN- γ in tumor progression and regression: a review. *Biomarker Research* 2020 8:1, 8(1), 1–16.
<https://doi.org/10.1186/S40364-020-00228-X>
- Jothy, S., Yuan, S. Y., & Shirota, K. (1993). Transcription of carcinoembryonic antigen in normal colon and colon carcinoma. In situ hybridization study and implication for a new in vivo functional model. *The American Journal of Pathology*, 143(1), 250–257. <http://www.ncbi.nlm.nih.gov/pubmed/8317550>
- Joy, J. D., Malacrida, B., Laforêts, F., Kotantaki, P., Maniati, E., Hopkins, S., Calleja, I., Brett, S., Athanasopoulos, T., Ali, S., Emery-Billcliff, P., Ricciardelli, I., Kay, C., Colebrook, J., Ali, M., Strong, K., & Balkwill, F. (2022). Abstract 693: TGF β -mediated targeting of the extracellular matrix enhances the migration and cytotoxicity of CAR-T cells in 3D models of ovarian cancer. *Cancer Research*, 82(12_Supplement), 693–693. <https://doi.org/10.1158/1538-7445.AM2022-693>
- Ju, S. Te, Cui, H., Panka, D. J., Ettinger, R., & Marshak-Rothstein, A. (1994). Participation of target Fas protein in apoptosis pathway induced by CD4⁺ Th1 and CD8⁺ cytotoxic T cells. *Proceedings of the National Academy of Sciences of the United States of America*, 91(10), 4185–4189.
<https://doi.org/10.1073/PNAS.91.10.4185>
- Junttila, T. T., Li, J., Johnston, J., Hristopoulos, M., Clark, R., Ellerman, D., Wang, B. E., Li, Y., Mathieu, M., Li, G., Young, J., Luis, E., Phillips, G. L., Stefanich, E., Spiess, C., Polson, A., Irving, B., Scheer, J. M., Junttila, M. R., ... Ebens, A. (2014). Antitumor efficacy of a bispecific antibody that targets HER2 and activates T cells. *Cancer Research*, 74(19), 5561–5571. <https://doi.org/10.1158/0008-5472.CAN-13-3622-T/659395/P/ANTITUMOR-EFFICACY-OF-A-BISPECIFIC-ANTIBODY-THAT>
- Kägi, D., Ledermann, B., Bürki, K., Zinkernagel, R. M., & Hengartner, H. (1996). Molecular mechanisms of lymphocyte-mediated cytotoxicity and their role in immunological protection and pathogenesis in vivo. *Annual Review of Immunology*, 14, 207–232. <https://doi.org/10.1146/ANNUREV.IMMUNOL.14.1.207>

- Kahn, M. (2014). Can we safely target the WNT pathway? *Nature Reviews Drug Discovery* 2014 13:7, 13(7), 513–532. <https://doi.org/10.1038/nrd4233>
- Kalluri, R., & Zeisberg, M. (2006). Fibroblasts in cancer. *Nature Reviews Cancer* 2006 6:5, 6(5), 392–401. <https://doi.org/10.1038/nrc1877>
- Kamakura, D., Asano, R., & Yasunaga, M. (2021). T Cell Bispecific Antibodies: An Antibody-Based Delivery System for Inducing Antitumor Immunity. *Pharmaceuticals* 2021, Vol. 14, Page 1172, 14(11), 1172. <https://doi.org/10.3390/PH14111172>
- Kammula, U. S., Kuntz, E. J., Francone, T. D., Zeng, Z., Shia, J., Landmann, R. G., Paty, P. B., & Weiser, M. R. (2007). Molecular co-expression of the c-Met oncogene and hepatocyte growth factor in primary colon cancer predicts tumor stage and clinical outcome. *Cancer Letters*, 248(2), 219–228. <https://doi.org/10.1016/J.CANLET.2006.07.007>
- Kaplan, D. H., Shankaran, V., Dighe, A. S., Stockert, E., Aguet, M., Old, L. J., & Schreiber, R. D. (1998). Demonstration of an interferon γ -dependent tumor surveillance system in immunocompetent mice. *Proceedings of the National Academy of Sciences of the United States of America*, 95(13), 7556–7561. <https://doi.org/10.1073/PNAS.95.13.7556/ASSET/EDE174A5-CF98-408C-9AFD-91E390C365AE/ASSETS/GRAPHIC/PQ1281384004.JPEG>
- Karapetis, C. S., Khambata-Ford, S., Jonker, D. J., O'Callaghan, C. J., Tu, D., Tebbutt, N. C., Simes, R. J., Chalchal, H., Shapiro, J. D., Robitaille, S., Price, T. J., Shepherd, L., Au, H.-J., Langer, C., Moore, M. J., & Zalcborg, J. R. (2008). K-ras Mutations and Benefit from Cetuximab in Advanced Colorectal Cancer. *New England Journal of Medicine*, 359(17), 1757–1765. https://doi.org/10.1056/NEJMOA0804385/SUPPL_FILE/NEJM_KARAPETIS_1757SA1.PDF
- Kato, T., Noma, K., Ohara, T., Kashima, H., Katsura, Y., Sato, H., Komoto, S., Katsube, R., Ninomiya, T., Tazawa, H., Shirakawa, Y., & Fujiwara, T. (2018). Cancer-associated fibroblasts affect intratumoral CD8 β and Foxp3 β T cells via IL6 in the tumor microenvironment. *Clinical Cancer Research*, 24(19), 4820–4833. <https://doi.org/10.1158/1078-0432.CCR-18-0205/72949/AM/CANCER-ASSOCIATED-FIBROBLASTS-AFFECT-INTRATUMORAL>
- Katz, S. C., Burga, R. A., McCormack, E., Wang, L. J., Mooring, W., Point, G. R., Khare, P. D., Thorn, M., Ma, Q., Stainken, B. F., Assanah, E. O., Davies, R., Espat, N. J., & Junghans, R. P. (2015). Phase I hepatic immunotherapy for metastases study of intra-arterial chimeric antigen receptor-modified T-cell therapy for CEA+ liver metastases. *Clinical Cancer Research*, 21(14), 3149–3159. <https://doi.org/10.1158/1078-0432.CCR-14-1421/86470/AM/PHASE-I-HEPATIC-IMMUNOTHERAPY-FOR-METASTASES-STUDY>
- Kawalekar, O. U., O'Connor, R. S., Fraietta, J. A., Guo, L., McGettigan, S. E., Posey, A. D., Patel, P. R., Guedan, S., Scholler, J., Keith, B., Snyder, N., Blair, I., Milone, M. C., & June, C. H. (2016). Distinct Signaling of Coreceptors Regulates Specific Metabolism Pathways and Impacts Memory Development in CAR T Cells. *Immunity*, 44(2), 380–390. <https://doi.org/10.1016/J.IMMUNI.2016.01.021>

- Kehrl, J. H., Wakefield, L. M., Roberts, A. B., Jakowlew, S., Alvarez-Mon, M., Derynck, R., Sporn, M. B., & Fauci, A. S. (1986). Production of transforming growth factor β by human T lymphocytes and its potential role in the regulation of T cell growth. *Journal of Experimental Medicine*, *163*(5), 1037–1050. <https://doi.org/10.1084/jem.163.5.1037>
- Keir, M. E., Butte, M. J., Freeman, G. J., & Sharpe, A. H. (2008). PD-1 and Its Ligands in Tolerance and Immunity. <https://doi.org/10.1146/Annurev.Immunol.26.021607.090331>, *26*, 677–704. <https://doi.org/10.1146/ANNUREV.IMMUNOL.26.021607.090331>
- Keir, M. E., Freeman, G. J., & Sharpe, A. H. (2007). PD-1 Regulates Self-Reactive CD8+ T Cell Responses to Antigen in Lymph Nodes and Tissues. *The Journal of Immunology*, *179*(8), 5064–5070. <https://doi.org/10.4049/JIMMUNOL.179.8.5064>
- Keir, M. E., Liang, S. C., Guleria, I., Latchman, Y. E., Qipo, A., Albacker, L. A., Koulmanda, M., Freeman, G. J., Sayegh, M. H., & Sharpe, A. H. (2006). Tissue expression of PD-L1 mediates peripheral T cell tolerance. *Journal of Experimental Medicine*, *203*(4), 883–895. <https://doi.org/10.1084/JEM.20051776>
- Kelly, A., Gunaltay, S., McEntee, C. P., Shuttleworth, E. E., Smedley, C., Houston, S. A., Fenton, T. M., Levison, S., Mann, E. R., & Travis, M. A. (2018). Human monocytes and macrophages regulate immune tolerance via integrin $\alpha\beta 8$ -mediated TGF β activation. *Journal of Experimental Medicine*, *215*(11), 2725–2736. <https://doi.org/10.1084/JEM.20171491>
- Kerkar, S. P., Goldszmid, R. S., Muranski, P., Chinnasamy, D., Yu, Z., Reger, R. N., Leonardi, A. J., Morgan, R. A., Wang, E., Marincola, F. M., Trinchieri, G., Rosenberg, S. A., & Restifo, N. P. (2011). IL-12 triggers a programmatic change in dysfunctional myeloid-derived cells within mouse tumors. *The Journal of Clinical Investigation*, *121*(12), 4746–4757. <https://doi.org/10.1172/JCI58814>
- Kershaw, M. H., Westwood, J. A., Parker, L. L., Wang, G., Eshhar, Z., Mavroukakis, S. A., White, D. E., Wunderlich, J. R., Canevari, S., Rogers-Freezer, L., Chen, C. C., Yang, J. C., Rosenberg, S. A., & Hwu, P. (2006). A Phase I Study on Adoptive Immunotherapy Using Gene-Modified T Cells for Ovarian Cancer. *Clinical Cancer Research*, *12*(20), 6106–6115. <https://doi.org/10.1158/1078-0432.CCR-06-1183>
- Kim, C. G., Jang, M., Kim, Y., Leem, G., Kim, K. H., Lee, H., Kim, T. S., Choi, S. J., Kim, H. D., Han, J. W., Kwon, M., Kim, J. H., Lee, A. J., Nam, S. K., Bae, S. J., Lee, S. B., Shin, S. J., Park, S. H., Ahn, J. B., ... Shin, E. C. (2019). VEGF-A drives TOX-dependent T cell exhaustion in anti-PD-1-resistant microsatellite stable colorectal cancers. *Science Immunology*, *4*(41). https://doi.org/10.1126/SCIIMMUNOL.AAY0555/SUPPL_FILE/AAY0555_TABLE_S4.XLSX
- Kim, H., Phung, Y., & Ho, M. (2012). Changes in Global Gene Expression Associated with 3D Structure of Tumors: An Ex Vivo Matrix-Free Mesothelioma Spheroid Model. *PLOS ONE*, *7*(6), e39556. <https://doi.org/10.1371/JOURNAL.PONE.0039556>
- Kim, T. W., Lee, K. W., Ahn, J. B., Lee, J., Ryu, J., Oh, B., Ock, C.-Y., Hwang, S., Hahm, K. B., Kim, S.-J., & Park, Y. S. (2021). Efficacy and safety of vactosertib and pembrolizumab combination in patients with previously treated microsatellite

- stable metastatic colorectal cancer. *Journal of Clinical Oncology*, 39(15_suppl), 3573–3573. https://doi.org/10.1200/JCO.2021.39.15_SUPPL.3573
- Kim, Y. J., Stringfield, T. M., Chen, Y., & Broxmeyer, H. E. (2005). Modulation of cord blood CD8+ T-cell effector differentiation by TGF- β 1 and 4-1BB costimulation. *Blood*, 105(1), 274–281. <https://doi.org/10.1182/BLOOD-2003-12-4343>
- Kim, Y. S., Park, G. Bin, Lee, H.-K., Song, H., Choi, I.-H., Lee, W. J., & Hur, D. Y. (2008). Cross-Linking of B7-H1 on EBV-Transformed B Cells Induces Apoptosis through Reactive Oxygen Species Production, JNK Signaling Activation, and fasL Expression. *The Journal of Immunology*, 181(9), 6158–6169. <https://doi.org/10.4049/JIMMUNOL.181.9.6158>
- King, D. M., Albertini, M. R., Schalch, H., Hank, J. A., Gan, J., Surfus, J., Mahvi, D., Schiller, J. H., Warner, T., Kim, K. M., Eickhoff, J., Kendra, K., Reifeld, R., Gillies, S. D., & Sondel, P. (2004). Phase I clinical trial of the immunocytokine EMD 273063 in melanoma patients. *Journal of Clinical Oncology*, 22(22), 4463–4473. <https://doi.org/10.1200/JCO.2004.11.035>
- Kitadai, Y., Radinsky, R., Bucana, C. D., Takahashi, Y., Xie, K., Tahara, E., & Fidler, I. J. (1996). Regulation of Carcinoembryonic Antigen Expression in Human Colon Carcinoma Cells by the Organ Microenvironment. *American Journal of Pathology*, 149(4), 1157–1166.
- Kitano, S., Tsuji, T., Liu, C., Hirschhorn-Cymerman, D., Kyi, C., Mu, Z., Allison, J. P., Gnjjatic, S., Yuan, J. D., & Wolchok, J. D. (2013). Enhancement of tumor-reactive cytotoxic CD4+ T cell responses after ipilimumab treatment in four advanced melanoma patients. *Cancer Immunology Research*, 1(4), 235–244. <https://doi.org/10.1158/2326-6066.CIR-13-0068/470332/AM/ENHANCEMENT-OF-TUMOR-REACTIVE-CYTOTOXIC-CD4-T-CELL>
- Klinger, M., Brandl, C., Zugmaier, G., Hijazi, Y., Bargou, R. C., Topp, M. S., Gökbuget, N., Neumann, S., Goebeler, M., Viardot, A., Stelljes, M., Brüggemann, M., Hoelzer, D., Degenhard, E., Nagorsen, D., Baeuerle, P. A., Wolf, A., & Kufer, P. (2012). Immunopharmacologic response of patients with B-lineage acute lymphoblastic leukemia to continuous infusion of T cell-engaging CD19/CD3-bispecific BiTE antibody blinatumomab. *Blood*, 119(26), 6226–6233. <https://doi.org/10.1182/BLOOD-2012-01-400515>
- Knüpfner, H., & Preiss, R. (2010). Serum interleukin-6 levels in colorectal cancer patients—a summary of published results. *International Journal of Colorectal Disease*, 25(2), 135–140. <https://doi.org/10.1007/S00384-009-0818-8/TABLES/1>
- Ko, J. S., Zea, A. H., Rini, B. I., Ireland, J. L., Elson, P., Cohen, P., Golshayan, A., Rayman, P. A., Wood, L., Garcia, J., Dreicer, R., Bukowski, R., & Finke, J. H. (2009). Sunitinib mediates reversal of myeloid-derived suppressor cell accumulation in renal cell carcinoma patients. *Clinical Cancer Research*, 15(6), 2148–2157. <https://doi.org/10.1158/1078-0432.CCR-08-1332/350618/P/SUNITINIB-MEDIATES-REVERSAL-OF-MYELOID-DERIVED>
- Koeck, S., Kern, J., Zwierzina, M., Gamerith, G., Lorenz, E., Sopper, S., Zwierzina, H., & Amann, A. (2017). The influence of stromal cells and tumor-microenvironment-derived cytokines and chemokines on CD3+CD8+ tumor infiltrating lymphocyte subpopulations. *Oncolimmunology*, 6(6).

https://doi.org/10.1080/2162402X.2017.1323617/SUPPL_FILE/KONI_A_1323617_SM4682.DOCX

- Komoda, H., Tanaka, Y., Honda, M., Matsuo, Y., Hazama, K., & Takao, T. (1998). Interleukin-6 levels in colorectal cancer tissues. *World Journal of Surgery*, *22*(8), 895–898. <https://doi.org/10.1007/S002689900489/METRICS>
- Kong, J. C. H., Guerra, G. R., Millen, R. M., Roth, S., Xu, H., Neeson, P. J., Darcy, P. K., Kershaw, M. H., Sampurno, S., Malaterre, J., Liu, D. S. H., Pham, T. D., Narasimhan, V., Wang, M., Huang, Y.-K., Visvanathan, K., McCormick, J., Lynch, A. C., Warriar, S., ... Ramsay, R. G. (2018). Tumor-Infiltrating Lymphocyte Function Predicts Response to Neoadjuvant Chemoradiotherapy in Locally Advanced Rectal Cancer. *JCO Precision Oncology*, *2*, 1–15. <https://doi.org/10.1200/PO.18.00075>
- Koopman, M., Kortman, G. A. M., Mekenkamp, L., Ligtenberg, M. J. L., Hoogerbrugge, N., Antonini, N. F., Punt, C. J. A., & Van Krieken, J. H. J. M. (2009). Deficient mismatch repair system in patients with sporadic advanced colorectal cancer. *British Journal of Cancer* *2009 100:2*, *100*(2), 266–273. <https://doi.org/10.1038/sj.bjc.6604867>
- Kopetz, S., Desai, J., Chan, E., Hecht, J. R., O'Dwyer, P. J., Maru, D., Morris, V., Janku, F., Dasari, A., Chung, W., Issa, J. P. J., Gibbs, P., James, B., Powis, G., Nolop, K. B., Bhattacharya, S., & Saltz, L. (2015). Phase II Pilot Study of Vemurafenib in Patients With Metastatic BRAF-Mutated Colorectal Cancer. *Journal of Clinical Oncology*, *33*(34), 4032. <https://doi.org/10.1200/JCO.2015.63.2497>
- Kopetz, S., McDonough, S. L., Morris, V. K., Lenz, H.-J., Magliocco, A. M., Atreya, C. E., Diaz, L. A., Allegra, C. J., Wang, S. E., Lieu, C. H., Eckhardt, S. G., Semrad, T. J., Kaberle, K., Guthrie, K. A., & Hochster, H. S. (2017). Randomized trial of irinotecan and cetuximab with or without vemurafenib in BRAF-mutant metastatic colorectal cancer (SWOG 1406). *Journal of Clinical Oncology*, *35*(4_suppl), 520–520. https://doi.org/10.1200/JCO.2017.35.4_SUPPL.520
- Korinek, V., Barker, N., Morin, P. J., Van Wichen, D., De Weger, R., Kinzler, K. W., Vogelstein, B., & Clevers, H. (1997). Constitutive transcriptional activation by a β -catenin-Tcf complex in APC(-/-) colon carcinoma. *Science*, *275*(5307), 1784–1787. <https://doi.org/10.1126/SCIENCE.275.5307.1784/ASSET/ADCB468C-A233-4E01-AB4F-F6A6D22310FF/ASSETS/GRAPHIC/SE1274928004.JPEG>
- Kortylewski, M., Kujawski, M., Wang, T., Wei, S., Zhang, S., Pilon-Thomas, S., Niu, G., Kay, H., Mulé, J., Kerr, W. G., Jove, R., Pardoll, D., & Yu, H. (2005). Inhibiting Stat3 signaling in the hematopoietic system elicits multicomponent antitumor immunity. *Nature Medicine* *2005 11:12*, *11*(12), 1314–1321. <https://doi.org/10.1038/nm1325>
- Krangel, M. S. (2009). Mechanics of T cell receptor gene rearrangement. *Current Opinion in Immunology*, *21*(2), 133–139. <https://doi.org/10.1016/J.COI.2009.03.009>
- Krupka, C., Kufer, P., Kischel, R., Zugmaier, G., Lichtenegger, F. S., Köhnke, T., Vick, B., Jeremias, I., Metzeler, K. H., Altmann, T., Schneider, S., Fiegl, M., Spiekermann, K., Bauerle, P. A., Hiddemann, W., Riethmüller, G., & Subklewe, M.

- (2015). Blockade of the PD-1/PD-L1 axis augments lysis of AML cells by the CD33/CD3 BiTE antibody construct AMG 330: reversing a T-cell-induced immune escape mechanism. *Leukemia* 2016 30:2, 30(2), 484–491. <https://doi.org/10.1038/leu.2015.214>
- Kryczek, I., Zou, L., Rodriguez, P., Zhu, G., Wei, S., Mottram, P., Brumlik, M., Cheng, P., Curiel, T., Myers, L., Lackner, A., Alvarez, X., Ochoa, A., Chen, L., & Zou, W. (2006). B7-H4 expression identifies a novel suppressive macrophage population in human ovarian carcinoma. *Journal of Experimental Medicine*, 203(4), 871–881. <https://doi.org/10.1084/JEM.20050930>
- Kuang, D. M., Zhao, Q., Peng, C., Xu, J., Zhang, J. P., Wu, C., & Zheng, L. (2009a). Activated monocytes in peritumoral stroma of hepatocellular carcinoma foster immune privilege and disease progression through PD-L1. *Journal of Experimental Medicine*, 206(6), 1327–1337. <https://doi.org/10.1084/JEM.20082173>
- Kuang, D. M., Zhao, Q., Peng, C., Xu, J., Zhang, J. P., Wu, C., & Zheng, L. (2009b). Activated monocytes in peritumoral stroma of hepatocellular carcinoma foster immune privilege and disease progression through PD-L1. *Journal of Experimental Medicine*, 206(6), 1327–1337. <https://doi.org/10.1084/JEM.20082173>
- Kuboki, Y., Yaeger, R., Fakih, M., Strickler, J. H., Masuishi, T., Kim, E. J.-H., Bestvina, C. M., Langer, C. J., Krauss, J. C., Puri, S., Cardona, P., Chang, E. K., Tran, Q., & Hong, D. S. (2022). 45MO Sotorasib in combination with panitumumab in refractory KRAS G12C-mutated colorectal cancer: Safety and efficacy for phase Ib full expansion cohort. *Annals of Oncology*, 33, S1445–S1446. <https://doi.org/10.1016/j.annonc.2022.10.077>
- Kuczek, D. E., Larsen, A. M. H., Thorseth, M. L., Carretta, M., Kalvisa, A., Siersbæk, M. S., Simões, A. M. C., Roslind, A., Engelholm, L. H., Noessner, E., Donia, M., Svane, I. M., Straten, P. T., Grøntved, L., & Madsen, D. H. (2019). Collagen density regulates the activity of tumor-infiltrating T cells. *Journal for ImmunoTherapy of Cancer*, 7(1), 1–15. <https://doi.org/10.1186/S40425-019-0556-6/FIGURES/6>
- Kuen, J., Darowski, D., Kluge, T., & Majety, M. (2017). Pancreatic cancer cell/fibroblast co-culture induces M2 like macrophages that influence therapeutic response in a 3D model. *PLOS ONE*, 12(7), e0182039. <https://doi.org/10.1371/JOURNAL.PONE.0182039>
- Kuhnert, F., Davis, C. R., Wang, H.-T., Chu, P., Lee, M., Yuan, J., Nusse, R., & Kuo, C. J. (2004). Essential requirement for Wnt signaling in proliferation of adult small intestine and colon revealed by adenoviral expression of Dickkopf-1. *Proceedings of the National Academy of Sciences*, 101(1), 266–271. <https://doi.org/10.1073/pnas.2536800100>
- Kusmartsev, S., & Gabrilovich, D. I. (2005). STAT1 Signaling Regulates Tumor-Associated Macrophage-Mediated T Cell Deletion. *The Journal of Immunology*, 174(8), 4880–4891. <https://doi.org/10.4049/JIMMUNOL.174.8.4880>
- Kusmartsev, S., Nefedova, Y., Yoder, D., & Gabrilovich, D. I. (2004). Antigen-Specific Inhibition of CD8+ T Cell Response by Immature Myeloid Cells in Cancer Is

- Mediated by Reactive Oxygen Species. *The Journal of Immunology*, 172(2), 989–999. <https://doi.org/10.4049/JIMMUNOL.172.2.989>
- Laforêts, F., Kotantaki, P., Malacrida, B., Elorbany, S., Manchanda, R., Donnadieu, E., & Balkwill, F. (2023). Semi-supervised analysis of myeloid and T cell behavior in ex vivo ovarian tumor slices reveals changes in cell motility after treatments. *iScience*, 26(4), 106514. <https://doi.org/10.1016/J.ISCI.2023.106514>
- Lakins, M. A., Ghorani, E., Munir, H., Martins, C. P., & Shields, J. D. (2018). Cancer-associated fibroblasts induce antigen-specific deletion of CD8 + T Cells to protect tumour cells. *Nature Communications* 2018 9:1, 9(1), 1–9. <https://doi.org/10.1038/s41467-018-03347-0>
- Lamichhane, P., Karyampudi, L., Shreeder, B., Krempski, J., Bahr, D., Daum, J., Kalli, K. R., Goode, E. L., Block, M. S., Cannon, M. J., & Knutson, K. L. (2017). IL10 release upon PD-1 blockade sustains immunosuppression in ovarian cancer. *Cancer Research*, 77(23), 6667–6678. <https://doi.org/10.1158/0008-5472.CAN-17-0740/652867/AM/IL-10-RELEASE-UPON-PD-1-BLOCKADE-SUSTAINS>
- Lämmermann, T., Bader, B. L., Monkley, S. J., Worbs, T., Wedlich-Söldner, R., Hirsch, K., Keller, M., Förster, R., Crichtley, D. R., Fässler, R., & Sixt, M. (2008). Rapid leukocyte migration by integrin-independent flowing and squeezing. *Nature* 2008 453:7191, 453(7191), 51–55. <https://doi.org/10.1038/nature06887>
- Lan, Y., Zhang, D., Xu, C., Hance, K. W., Marelli, B., Qi, J., Yu, H., Qin, G., Sircar, A., Hernández, V. M., Jenkins, M. H., Fontana, R. E., Deshpande, A., Locke, G., Sabzevari, H., Radvanyi, L., & Lo, K. M. (2018). Enhanced preclinical antitumor activity of M7824, a bifunctional fusion protein simultaneously targeting PD-L1 and TGF-. *Science Translational Medicine*, 10(424), 5488. https://doi.org/10.1126/SCITRANSLMED.AAN5488/SUPPL_FILE/AAN5488_SM.PDF
- Lange, S. S., Takata, K. I., & Wood, R. D. (2011). DNA polymerases and cancer. *Nature Reviews Cancer* 2011 11:2, 11(2), 96–110. <https://doi.org/10.1038/nrc2998>
- Lanitis, E., Dangaj, D., Irving, M., & Coukos, G. (2017). Mechanisms regulating T-cell infiltration and activity in solid tumors. *Annals of Oncology*, 28, xii18–xii32. <https://doi.org/10.1093/ANNONC/MDX238>
- Larbi, A., Zelba, H., Goldeck, D., & Pawelec, G. (2010). Induction of HIF-1 α and the glycolytic pathway alters apoptotic and differentiation profiles of activated human T cells. *Journal of Leukocyte Biology*, 87(2), 265–273. <https://doi.org/10.1189/JLB.0509304>
- Larkin, J., Chiarion-Sileni, V., Gonzalez, R., Grob, J. J., Cowey, C. L., Lao, C. D., Schadendorf, D., Dummer, R., Smylie, M., Rutkowski, P., Ferrucci, P. F., Hill, A., Wagstaff, J., Carlino, M. S., Haanen, J. B., Maio, M., Marquez-Rodas, I., McArthur, G. A., Ascierto, P. A., ... Wolchok, J. D. (2015). Combined Nivolumab and Ipilimumab or Monotherapy in Untreated Melanoma. *New England Journal of Medicine*, 373(1), 23–34. https://doi.org/10.1056/NEJMOA1504030/SUPPL_FILE/NEJMOA1504030_DISCLOSURES.PDF
- Lau, T., Chan, E., Callow, M., Waaler, J., Boggs, J., Blake, R. A., Magnuson, S., Sambrone, A., Schutten, M., Firestein, R., Machon, O., Korinek, V., Choo, E.,

- Diaz, D., Merchant, M., Polakis, P., Holsworth, D. D., Krauss, S., & Costa, M. (2013). A novel tankyrase small-molecule inhibitor suppresses APC mutation-driven colorectal tumor growth. *Cancer Research*, *73*(10), 3132–3144. <https://doi.org/10.1158/0008-5472.CAN-12-4562/650978/AM/A-NOVEL-TANKYRASE-SMALL-MOLECULE-INHIBITOR>
- Lawand, M., Déchanet-Merville, J., & Dieu-Nosjean, M. C. (2017). Key features of gamma-delta T-cell subsets in human diseases and their immunotherapeutic implications. *Frontiers in Immunology*, *8*, 761. <https://doi.org/10.3389/FIMMU.2017.00761/BIBTEX>
- Lawrence, M. S., Stojanov, P., Polak, P., Kryukov, G. V., Cibulskis, K., Sivachenko, A., Carter, S. L., Stewart, C., Mermel, C. H., Roberts, S. A., Kiezun, A., Hammerman, P. S., McKenna, A., Drier, Y., Zou, L., Ramos, A. H., Pugh, T. J., Stransky, N., Helman, E., ... Getz, G. (2013). Mutational heterogeneity in cancer and the search for new cancer-associated genes. *Nature* *2013* 499:7457, *499*(7457), 214–218. <https://doi.org/10.1038/nature12213>
- Le, D. T., Durham, J. N., Smith, K. N., Wang, H., Bartlett, B. R., Aulakh, L. K., Lu, S., Kemberling, H., Wilt, C., Luber, B. S., Wong, F., Azad, N. S., Rucki, A. A., Laheru, D., Donehower, R., Zaheer, A., Fisher, G. A., Crocenzi, T. S., Lee, J. J., ... Diaz, L. A. (2017). Mismatch repair deficiency predicts response of solid tumors to PD-1 blockade. *Science*, *357*(6349), 409–413. https://doi.org/10.1126/SCIENCE.AAN6733/SUPPL_FILE/AAN6733_TABLES-S8-S9-S10.XLSX
- Le, D. T., Uram, J. N., Wang, H., Bartlett, B. R., Kemberling, H., Eyring, A. D., Skora, A. D., Luber, B. S., Azad, N. S., Laheru, D., Biedrzycki, B., Donehower, R. C., Zaheer, A., Fisher, G. A., Crocenzi, T. S., Lee, J. J., Duffy, S. M., Goldberg, R. M., de la Chapelle, A., ... Diaz, L. A. (2015). PD-1 Blockade in Tumors with Mismatch-Repair Deficiency. *New England Journal of Medicine*, *372*(26), 2509–2520. https://doi.org/10.1056/NEJMOA1500596/SUPPL_FILE/NEJMOA1500596_DISCLOSURES.PDF
- Lee, J. H., & Lee, S.-W. (2017). The Roles of Carcinoembryonic Antigen in Liver Metastasis and Therapeutic Approaches. *Gastroenterology Research and Practice*, *2017*, 7521987. <https://doi.org/10.1155/2017/7521987>
- Lee, J., Mehdizadeh, S., Tsai, K., Algazi, A., Rosenblum, M., Daud, A., & Bluestone, J. A. (2018). Immunological Insights Into Liver Metastasis Associated Resistance To Checkpoint Blockade Cancer Immunotherapy. *The Journal of Immunology*, *200*(1_Supplement), 122.26-122.26. <https://doi.org/10.4049/JIMMUNOL.200.SUPP.122.26>
- Lee, M. S., Loehrer, P. J., Imanirad, I., Cohen, S., Ciombor, K. K., Moore, D. T., Carlson, C. A., Sanoff, H. K., & McRee, A. J. (2021). Phase II study of ipilimumab, nivolumab, and panitumumab in patients with KRAS/NRAS/BRAF wild-type (WT) microsatellite stable (MSS) metastatic colorectal cancer (mCRC). *Journal of Clinical Oncology*, *39*(3_suppl), 7–7. https://doi.org/10.1200/JCO.2021.39.3_SUPPL.7
- Lehmann, B., Biburger, M., Brückner, C., Ipsen-Escobedo, A., Gordan, S., Lehmann, C., Voehringer, D., Winkler, T., Schaft, N., Dudziak, D., Sirbu, H., Weber, G. F., & Nimmerjahn, F. (2017). Tumor location determines tissue-specific recruitment of

tumor-associated macrophages and antibody-dependent immunotherapy response. *Science Immunology*, 2(7).
https://doi.org/10.1126/SCIIMMUNOL.AAH6413/SUPPL_FILE/AAH6413_SM.PDF

- Lehmann, S., Perera, R., Grimm, H. P., Sam, J., Colombetti, S., Fauti, T., Fahrni, L., Schaller, T., Freimoser-Grundschober, A., Zielonka, J., Stoma, S., Rudin, M., Klein, C., Umana, P., Gerdes, C., & Bacac, M. (2016). In Vivo Fluorescence Imaging of the Activity of CEA TCB, a Novel T-Cell Bispecific Antibody, Reveals Highly Specific Tumor Targeting and Fast Induction of T-Cell-Mediated Tumor Killing. *Clinical Cancer Research*, 22(17), 4417–4427.
<https://doi.org/10.1158/1078-0432.CCR-15-2622/128610/AM/IN-VIVO-IMAGING-OF-THE-ACTIVITY-OF-CEA-TCB-A-NOVEL>
- Lenz, H.-J., Parikh, A. R., Spigel, D. R., Cohn, A. L., Yoshino, T., Kochenderfer, M. D., Elez, E., Shao, S. H., Deming, D. A., Holdridge, R. C., Larson, T., Chen, E., Mahipal, A., Ucar, A., Cullen, D., Baskin-Bey, E. S., Ledezine, J.-M., Hammell, A., & Tabernero, J. (2022a). Nivolumab (NIVO) + 5-fluorouracil/leucovorin/oxaliplatin (mFOLFOX6)/bevacizumab (BEV) versus mFOLFOX6/BEV for first-line (1L) treatment of metastatic colorectal cancer (mCRC): Phase 2 results from CheckMate 9X8. *Journal of Clinical Oncology*, 40(4_suppl), 8–8.
https://doi.org/10.1200/JCO.2022.40.4_SUPPL.008
- Lenz, H.-J., Parikh, A. R., Spigel, D. R., Cohn, A. L., Yoshino, T., Kochenderfer, M. D., Elez, E., Shao, S. H., Deming, D. A., Holdridge, R. C., Larson, T., Chen, E., Mahipal, A., Ucar, A., Cullen, D., Baskin-Bey, E. S., Ledezine, J.-M., Hammell, A., & Tabernero, J. (2022b). Nivolumab (NIVO) + 5-fluorouracil/leucovorin/oxaliplatin (mFOLFOX6)/bevacizumab (BEV) versus mFOLFOX6/BEV for first-line (1L) treatment of metastatic colorectal cancer (mCRC): Phase 2 results from CheckMate 9X8. *Journal of Clinical Oncology*, 40(4_suppl), 8–8.
https://doi.org/10.1200/JCO.2022.40.4_SUPPL.008
- Letterio, J. J., & Roberts, A. B. (1998). REGULATION OF IMMUNE RESPONSES BY TGF- β . *Annual Review of Immunology*, 16, 137–161.
<https://doi.org/10.1146/ANNUREV.IMMUNOL.16.1.137>
- Lewis, J. S., Landers, R. J., Underwood, J. C. E., Harris, A. L., & Lewis, C. E. (n.d.). *Expression of vascular endothelial growth factor by macrophages is up-regulated in poorly vascularized areas of breast carcinomas*. <https://doi.org/10.1002/1096-9896>
- Li, B., Wang, F., Ma, C., Hao, T., Geng, L., & Jiang, H. (2019). Predictive value of IL-18 and IL-10 in the prognosis of patients with colorectal cancer. *Oncology Letters*, 18(1), 713–719. <https://doi.org/10.3892/OL.2019.10338/HTML>
- Li, J., Lee, Y., Li, Y., Jiang, Y., Lu, H., Zang, W., Zhao, X., Liu, L., Chen, Y., Tan, H., Yang, Z., Zhang, M. Q., Mak, T. W., Ni, L., & Dong, C. (2018). Co-inhibitory Molecule B7 Superfamily Member 1 Expressed by Tumor-Infiltrating Myeloid Cells Induces Dysfunction of Anti-tumor CD8⁺ T Cells. *Immunity*, 48(4), 773-786.e5.
<https://doi.org/10.1016/J.IMMUNI.2018.03.018>
- Li, J., Li, W., Huang, K., Zhang, Y., Kupfer, G., & Zhao, Q. (2018). Chimeric antigen receptor T cell (CAR-T) immunotherapy for solid tumors: lessons learned and strategies for moving forward. *Journal of Hematology & Oncology* 2018 11:1, 11(1), 1–18. <https://doi.org/10.1186/S13045-018-0568-6>

- Li, J., Stagg, N. J., Johnston, J., Harris, M. J., Menzies, S. A., DiCara, D., Clark, V., Hristopoulos, M., Cook, R., Slaga, D., Nakamura, R., McCarty, L., Sukumaran, S., Luis, E., Ye, Z., Wu, T. D., Sumiyoshi, T., Danilenko, D., Lee, G. Y., ... Junttila, T. T. (2017). Membrane-Proximal Epitope Facilitates Efficient T Cell Synapse Formation by Anti-FcRH5/CD3 and Is a Requirement for Myeloma Cell Killing. *Cancer Cell*, *31*(3), 383–395. <https://doi.org/10.1016/J.CCELL.2017.02.001>
- Li, J., Ybarra, R., Mak, J., Herault, A., De Almeida, P., Arrazate, A., Ziai, J., Totpal, K., Junttila, M. R., Walsh, K. B., & Junttila, T. T. (2018). IFN γ -induced Chemokines Are Required for CXCR3-mediated T-Cell Recruitment and Antitumor Efficacy of Anti-HER2/CD3 Bispecific Antibody. *Clinical Cancer Research*, *24*(24), 6447–6458. <https://doi.org/10.1158/1078-0432.CCR-18-1139/255691/AM/IFN-INDUCED-CHEMOKINES-ARE-REQUIRED-FOR-CXCR3>
- Li, M. O., Sanjabi, S., & Flavell, R. A. A. (2006). Transforming Growth Factor- β Controls Development, Homeostasis, and Tolerance of T Cells by Regulatory T Cell-Dependent and -Independent Mechanisms. *Immunity*, *25*(3), 455–471. <https://doi.org/10.1016/J.IMMUNI.2006.07.011>
- Li, M. O., Wan, Y. Y., Sanjabi, S., Robertson, A. K. L., & Flavell, R. A. (2006). TRANSFORMING GROWTH FACTOR- β REGULATION OF IMMUNE RESPONSES. *Annual Review of Immunology*, *24*, 99–146. <https://doi.org/10.1146/ANNUREV.IMMUNOL.24.021605.090737>
- Li, T., Yi, S., Liu, W., Jia, C., Wang, G., Hua, X., Tai, Y., Zhang, Q., & Chen, G. (2013). Colorectal carcinoma-derived fibroblasts modulate natural killer cell phenotype and antitumor cytotoxicity. *Medical Oncology*, *30*(3), 1–7. <https://doi.org/10.1007/S12032-013-0663-Z/TABLES/1>
- Li, Z. L., Wang, Z. J., Wei, G. H., Yang, Y., & Wang, X. W. (2020). Changes in extracellular matrix in different stages of colorectal cancer and their effects on proliferation of cancer cells. *World Journal of Gastrointestinal Oncology*, *12*(3), 267. <https://doi.org/10.4251/WJGO.V12.I3.267>
- Liao, D., Luo, Y., Markowitz, D., Xiang, R., & Reisfeld, R. A. (2009). Cancer Associated Fibroblasts Promote Tumor Growth and Metastasis by Modulating the Tumor Immune Microenvironment in a 4T1 Murine Breast Cancer Model. *PLOS ONE*, *4*(11), e7965. <https://doi.org/10.1371/JOURNAL.PONE.0007965>
- Lièvre, A., Bachet, J. B., Boige, V., Cayre, A., Le Corre, D., Buc, E., Ychou, M., Bouché, O., Landi, B., Louvet, C., André, T., Bibeau, F., Diebold, M. D., Rougier, P., Ducreux, M., Tomasic, G., Emile, J. F., Penault-Llorca, F., & Laurent-Puig, P. (2008). KRAS mutations as an independent prognostic factor in patients with advanced colorectal cancer treated with cetuximab. *Journal of Clinical Oncology*, *26*(3), 374–379. <https://doi.org/10.1200/JCO.2007.12.5906>
- Lin, H. H., Chen, J. H., Huang, C. C., & Wang, C. J. (2007). Apoptotic effect of 3,4-dihydroxybenzoic acid on human gastric carcinoma cells involving JNK/p38 MAPK signaling activation. *International Journal of Cancer*, *120*(11), 2306–2316. <https://doi.org/10.1002/IJC.22571>
- Lin, H., Wei, S., Hurt, E. M., Green, M. D., Zhao, L., Vatan, L., Szeliga, W., Herbst, R., Harms, P. W., Fecher, L. A., Vats, P., Chinnaiyan, A. M., Lao, C. D., Lawrence, T. S., Wicha, M., Hamanishi, J., Mandai, M., Kryczek, I., & Zou, W. (2018). Host

expression of PD-L1 determines efficacy of PD-L1 pathway blockade-mediated tumor regression. *The Journal of Clinical Investigation*, 128(2), 805–815. <https://doi.org/10.1172/JCI96113>

- List, T., & Neri, D. (2012). Biodistribution studies with tumor-targeting bispecific antibodies reveal selective accumulation at the tumor site. *MAbs*, 4(6), 775–783. https://doi.org/10.4161/MABS.22271/SUPPL_FILE/KMAB_A_10922271_SM0001.ZIP
- Liu, S. Q., Grantham, A., Landry, C., Granda, B., Chopra, R., Chakravarthy, S., Deutsch, S., Vogel, M., Russo, K., Seiss, K., Tschantz, W. R., Rejtar, T., Ruddy, D. A., Hu, T., Aardalen, K., Wagner, J. P., Dranoff, G., & D'Alessio, J. A. (2021). A CRISPR screen reveals resistance mechanisms to CD3-bispecific antibody therapy. *Cancer Immunology Research*, 9(1), 34–49. <https://doi.org/10.1158/2326-6066.CIR-20-0080/470971/AM/A-CRISPR-SCREEN-REVEALS-RESISTANCE-MECHANISMS-TO>
- Liu, V. C., Wong, L. Y., Jang, T., Shah, A. H., Park, I., Yang, X., Zhang, Q., Lonning, S., Teicher, B. A., & Lee, C. (2007). Tumor Evasion of the Immune System by Converting CD4+CD25– T Cells into CD4+CD25+ T Regulatory Cells: Role of Tumor-Derived TGF- β . *The Journal of Immunology*, 178(5), 2883–2892. <https://doi.org/10.4049/JIMMUNOL.178.5.2883>
- Liu, Y., Li, Q., & Zhu, L. (2012). Expression of the hepatocyte growth factor and c-Met in colon cancer: correlation with clinicopathological features and overall survival. *Tumori*, 98(1), 105–112. <https://doi.org/10.1177/030089161209800115>
- Liu, Y., Zeng, B., Zhang, Z., Zhang, Y., & Yang, R. (2008). B7-H1 on myeloid-derived suppressor cells in immune suppression by a mouse model of ovarian cancer. *Clinical Immunology*, 129(3), 471–481. <https://doi.org/10.1016/J.CLIM.2008.07.030>
- Liu, Z., Zhang, Y., Niu, Y., Li, K., Liu, X., Chen, H., & Gao, C. (2014). A Systematic Review and Meta-Analysis of Diagnostic and Prognostic Serum Biomarkers of Colorectal Cancer. *PLOS ONE*, 9(8), e103910. <https://doi.org/10.1371/JOURNAL.PONE.0103910>
- Llosa, N. J., Cruise, M., Tam, A., Wicks, E. C., Hechenbleikner, E. M., Taube, J. M., Blosser, R. L., Fan, H., Wang, H., Lubner, B. S., Zhang, M., Papadopoulos, N., Kinzler, K. W., Vogelstein, B., Sears, C. L., Anders, R. A., Pardoll, D. M., & Housseau, F. (2015). The vigorous immune microenvironment of microsatellite instable colon cancer is balanced by multiple counter-inhibitory checkpoints. *Cancer Discovery*, 5(1), 43–51. <https://doi.org/10.1158/2159-8290.CD-14-0863/42558/AM/THE-VIGOROUS-IMMUNE-MICROENVIRONMENT-OF>
- Longley, D. B., Harkin, D. P., & Johnston, P. G. (2003). 5-Fluorouracil: mechanisms of action and clinical strategies. *Nature Reviews Cancer* 2003 3:5, 3(5), 330–338. <https://doi.org/10.1038/nrc1074>
- Lowin, B., Hahne, M., Mattmann, C., & Tschopp, J. (1994). Cytolytic T-cell cytotoxicity is mediated through perforin and Fas lytic pathways. *Nature* 1994 370:6491, 370(6491), 650–652. <https://doi.org/10.1038/370650a0>

- Lu, P., Weaver, V. M., & Werb, Z. (2012). The extracellular matrix: A dynamic niche in cancer progression. *Journal of Cell Biology*, *196*(4), 395–406. <https://doi.org/10.1083/JCB.201102147>
- Ludvíksson, B. R., Seegers, D., Resnick, A. S., & Strober, W. (2000). The effect of TGF-beta on immune responses of naive versus memory CD4 + Th1/Th2 T cells. *European Journal of Immunology*, *30*(7), 2101–2111. <https://doi.org/10.1002/1521-4141>
- Lukashev, D., Klebanov, B., Kojima, H., Grinberg, A., Ohta, A., Berenfeld, L., Wenger, R. H., Ohta, A., & Sitkovsky, M. (2006). Cutting Edge: Hypoxia-Inducible Factor 1 α and Its Activation-Inducible Short Isoform I.1 Negatively Regulate Functions of CD4+ and CD8+ T Lymphocytes. *The Journal of Immunology*, *177*(8), 4962–4965. <https://doi.org/10.4049/JIMMUNOL.177.8.4962>
- Luke, J. J., Bao, R., Sweis, R. F., Spranger, S., & Gajewski, T. F. (2019). WNT/b-catenin pathway activation correlates with immune exclusion across human cancers. *Clinical Cancer Research*, *25*(10), 3074–3083. <https://doi.org/10.1158/1078-0432.CCR-18-1942/74038/AM/WNT-CATENIN-PATHWAY-ACTIVATION-CORRELATES-WITH>
- Lurquin, C., Van Pel, A., Mariamé, B., De Plaen, E., Szikora, J. P., Janssens, C., Reddehase, M. J., Lejeune, J., & Boon, T. (1989). Structure of the gene of tum-transplantation antigen P91A: The mutated exon encodes a peptide recognized with Ld by cytolytic T cells. *Cell*, *58*(2), 293–303. [https://doi.org/10.1016/0092-8674\(89\)90844-1](https://doi.org/10.1016/0092-8674(89)90844-1)
- Lutterbuese, R., Raum, T., Kischel, R., Hoffmann, P., Mangold, S., Rattel, B., Friedrich, M., Thomas, O., Lorenczewski, G., Rau, D., Schaller, E., Herrmann, I., Wolf, A., Urbig, T., Baeuerle, P. A., & Kufer, P. (2010). T cell-engaging BiTE antibodies specific for EGFR potentially eliminate KRAS- and BRAF-mutated colorectal cancer cells. *Proceedings of the National Academy of Sciences of the United States of America*, *107*(28), 12605–12610. https://doi.org/10.1073/PNAS.1000976107/SUPPL_FILE/PNAS.201000976SI.PDF
- Mace, T. A., Ameen, Z., Collins, A., Wojcik, S., Mair, M., Young, G. S., Fuchs, J. R., Eubank, T. D., Frankel, W. L., Bekaii-Saab, T., Bloomston, M., & Lesinski, G. B. (2013). Pancreatic cancer-associated stellate cells promote differentiation of myeloid-derived suppressor cells in a StAT3-dependent manner. *Cancer Research*, *73*(10), 3007–3018. <https://doi.org/10.1158/0008-5472.CAN-12-4601/651064/AM/PANCREATIC-CANCER-ASSOCIATED-STELLATE-CELLS>
- Majumder, B., Baraneedharan, U., Thiyagarajan, S., Radhakrishnan, P., Narasimhan, H., Dhandapani, M., Brijwani, N., Pinto, D. D., Prasath, A., Shanthappa, B. U., Thayakumar, A., Surendran, R., Babu, G. K., Shenoy, A. M., Kuriakose, M. A., Bergthold, G., Horowitz, P., Loda, M., Beroukhim, R., ... Majumder, P. K. (2015). Predicting clinical response to anticancer drugs using an ex vivo platform that captures tumour heterogeneity. *Nature Communications* *2015* 6:1, *6*(1), 1–14. <https://doi.org/10.1038/ncomms7169>
- Makino, Y., Nakamura, H., Ikeda, E., Ohnuma, K., Yamauchi, K., Yabe, Y., Poellinger, L., Okada, Y., Morimoto, C., & Tanaka, H. (2003). Hypoxia-Inducible Factor Regulates Survival of Antigen Receptor-Driven T Cells. *The Journal of*

Immunology, 171(12), 6534–6540.
<https://doi.org/10.4049/JIMMUNOL.171.12.6534>

- Mandel, J., Church, T., Bond, J., Ederer, F., Geisser, M., & Schuman, L. (2000). The Effect of Fecal Occult-Blood Screening on the Incidence of Colorectal Cancer. *The New England Journal of Medicine*, 343(22), 1603–1607.
<https://doi.org/10.1056/NEJM200011303432203>
- Mandikyan, D., Takahashi, N., Lo, A. A., Li, J., Eastham-Anderson, J., Slaga, D., Ho, J., Hristopoulos, M., Clark, R., Totpal, K., Lin, K., Joseph, S. B., Dennis, M. S., Prabhu, S., Junttila, T. T., & Boswell, C. A. (2018). Relative target affinities of T-cell-dependent bispecific antibodies determine biodistribution in a solid tumor mouse model. *Molecular Cancer Therapeutics*, 17(4), 776–785.
<https://doi.org/10.1158/1535-7163.MCT-17-0657/86779/AM/RELATIVE-TARGET-AFFINITIES-OF-T-CELL-DEPENDENT>
- Mantovani, A., Sica, A., Sozzani, S., Allavena, P., Vecchi, A., & Locati, M. (2004). The chemokine system in diverse forms of macrophage activation and polarization. *Trends in Immunology*, 25(12), 677–686. <https://doi.org/10.1016/J.IT.2004.09.015>
- Mantovani, A., Sozzani, S., Locati, M., Allavena, P., & Sica, A. (2002). Macrophage polarization: tumor-associated macrophages as a paradigm for polarized M2 mononuclear phagocytes. *Trends in Immunology*, 23(11), 549–555.
[https://doi.org/10.1016/S1471-4906\(02\)02302-5](https://doi.org/10.1016/S1471-4906(02)02302-5)
- Mariadason, J. M., Bordonaro, M., Aslam, F., Shi, L., Kuraguchi, M., Velcich, A., & Augenlicht, L. H. (2001). Down-Regulation of Catenin TCF Signaling Is Linked to Colonic Epithelial Cell Differentiation 1. *CANCER RESEARCH*, 61, 3465–3471.
<http://aacrjournals.org/cancerres/article-pdf/61/8/3465/3253673/ch080103465p.pdf>
- Mariathasan, S., Turley, S. J., Nickles, D., Castiglioni, A., Yuen, K., Wang, Y., Kadel, E. E., Koepfen, H., Astarita, J. L., Cubas, R., Jhunjunwala, S., Banchereau, R., Yang, Y., Guan, Y., Chalouni, C., Ziai, J., Şenbabaoğlu, Y., Santoro, S., Sheinson, D., ... Powles, T. (2018). TGFβ attenuates tumour response to PD-L1 blockade by contributing to exclusion of T cells. *Nature* 2018 554:7693, 554(7693), 544–548.
<https://doi.org/10.1038/nature25501>
- Marie, J. C., Letterio, J. J., Gavin, M., & Rudensky, A. Y. (2005). TGF-β1 maintains suppressor function and Foxp3 expression in CD4+CD25+ regulatory T cells. *Journal of Experimental Medicine*, 201(7), 1061–1067.
<https://doi.org/10.1084/JEM.20042276>
- Marin-Acevedo, J. A., Kimbrough, E. M. O., & Lou, Y. (2021). Next generation of immune checkpoint inhibitors and beyond. *Journal of Hematology & Oncology* 2021 14:1, 14(1), 1–29. <https://doi.org/10.1186/S13045-021-01056-8>
- Mariotti, L., Pollock, K., & Guettler, S. (2017). Regulation of Wnt/β-catenin signalling by tankyrase-dependent poly(ADP-ribosyl)ation and scaffolding. *British Journal of Pharmacology*, 174(24), 4611. <https://doi.org/10.1111/BPH.14038>
- Marshall, J. S., Warrington, R., Watson, W., & Kim, H. L. (2018). An introduction to immunology and immunopathology. *Allergy, Asthma and Clinical Immunology*, 14(2), 1–10. <https://doi.org/10.1186/S13223-018-0278-1/TABLES/4>

- Marshall, L. A., Marubayashi, S., Jorapur, A., Jacobson, S., Zibinsky, M., Robles, O., Hu, D. X., Jackson, J. J., Pookot, D., Sanchez, J., Brovarney, M., Wadsworth, A., Chian, D., Wustrow, D., Kassner, P. D., Cutler, G., Wong, B., Brockstedt, D. G., & Talay, O. (2020). Tumors establish resistance to immunotherapy by regulating Treg recruitment via CCR4. *Journal for ImmunoTherapy of Cancer*, 8(2), e000764. <https://doi.org/10.1136/JITC-2020-000764>
- Martelange, V., De Smet, C., De Plaen, E., Lurquin, C., & Boon, T. (2000). Identification on a Human Sarcoma of Two New Genes with Tumor-specific Expression 1. *CANCER RESEARCH*, 60, 3848–3855. <http://www-genome.wi.mit.edu/cgi-bin/contig/rhmapper.pl>.
- Martin, M. D., & Badovinac, V. P. (2018). Defining memory CD8 T cell. *Frontiers in Immunology*, 9(NOV), 2692. <https://doi.org/10.3389/FIMMU.2018.02692/BIBTEX>
- Maryanski, J. L., Marchand, M., Uyttenhove, C., & Boon, T. (1983). Immunogenic variants obtained by mutagenesis of mouse mastocytoma P815. VI. Occasional escape from host rejection due to antigen-loss secondary variants. *International Journal of Cancer*, 31(1), 119–123. <https://doi.org/10.1002/IJC.2910310119>
- Massagué, J. (2008). TGF β in Cancer. *Cell*, 134(2), 215–230. <https://doi.org/10.1016/J.CELL.2008.07.001>
- Matsumoto, K., Umitsu, M., De Silva, D. M., Roy, A., & Bottaro, D. P. (2017). Hepatocyte growth factor/MET in cancer progression and biomarker discovery. *Cancer Science*, 108(3), 296–307. <https://doi.org/10.1111/CAS.13156>
- Mattoo, H., Mahajan, V. S., Maehara, T., Deshpande, V., Della-Torre, E., Wallace, Z. S., Kulikova, M., Drijvers, J. M., Daccache, J., Carruthers, M. N., Castellino, F. V., Stone, J. R., Stone, J. H., & Pillai, S. (2016). Clonal expansion of CD4+ cytotoxic T lymphocytes in patients with IgG4-related disease. *Journal of Allergy and Clinical Immunology*, 138(3), 825–838. <https://doi.org/10.1016/J.JACI.2015.12.1330>
- Maude, S. L., Laetsch, T. W., Buechner, J., Rives, S., Boyer, M., Bittencourt, H., Bader, P., Verneris, M. R., Stefanski, H. E., Myers, G. D., Qayed, M., De Moerloose, B., Hiramatsu, H., Schlis, K., Davis, K. L., Martin, P. L., Nemecek, E. R., Yanik, G. A., Peters, C., ... Grupp, S. A. (2018). Tisagenlecleucel in Children and Young Adults with B-Cell Lymphoblastic Leukemia. *New England Journal of Medicine*, 378(5), 439–448. https://doi.org/10.1056/NEJMOA1709866/SUPPL_FILE/NEJMOA1709866_DISCLOSURES.PDF
- Mazanet, M. M., & Hughes, C. C. W. (2002). B7-H1 Is Expressed by Human Endothelial Cells and Suppresses T Cell Cytokine Synthesis. *The Journal of Immunology*, 169(7), 3581–3588. <https://doi.org/10.4049/JIMMUNOL.169.7.3581>
- Mazzolini, G., Narvaiza, I., Martinez-Cruz, L. A., Arina, A., Barajas, M., Galofré, J. C., Qian, C., Mato, J. M., Prieto, J., & Melero, I. (2003). Pancreatic cancer escape variants that evade immunogene therapy through loss of sensitivity to IFN γ -induced apoptosis. *Gene Therapy* 2003 10:13, 10(13), 1067–1078. <https://doi.org/10.1038/sj.gt.3301957>

- McCarthy, E. F. (2006). The Toxins of William B. Coley and the Treatment of Bone and Soft-Tissue Sarcomas. *The Iowa Orthopaedic Journal*, 26, 154.
/pmc/articles/PMC1888599/
- McGranahan, N., Furness, A. J. S., Rosenthal, R., Ramskov, S., Lyngaa, R., Saini, S. K., Jamal-Hanjani, M., Wilson, G. A., Birkbak, N. J., Hiley, C. T., Watkins, T. B. K., Shafi, S., Murugaesu, N., Mitter, R., Akarca, A. U., Linares, J., Marafioti, T., Henry, J. Y., Van Allen, E. M., ... Swanton, C. (2016). Clonal neoantigens elicit T cell immunoreactivity and sensitivity to immune checkpoint blockade. *Science*, 351(6280), 1463–1469.
https://doi.org/10.1126/SCIENCE.AAF1490/SUPPL_FILE/MCGRANAHAN-SM.PDF
- McKarns, S. C., Schwartz, R. H., & Kaminski, N. E. (2004). Smad3 Is Essential for TGF- β 1 to Suppress IL-2 Production and TCR-Induced Proliferation, but Not IL-2-Induced Proliferation. *The Journal of Immunology*, 172(7), 4275–4284.
<https://doi.org/10.4049/JIMMUNOL.172.7.4275>
- McKeown, S. R. (2014). Defining normoxia, physoxia and hypoxia in tumours - Implications for treatment response. *British Journal of Radiology*, 87(1035).
<https://doi.org/10.1259/BJR.20130676/ASSET/IMAGES/LARGE/BJR.20130676.G002.JPEG>
- Mckisic, M. D., Lancki, D. W., & Fitch3, F. W. (1993). Cytolytic activity of murine CD4+ T cell clones correlates with IFN-gamma production in mouse strains having a BALB/c background. *The Journal of Immunology*, 150(9), 3793–3805.
<https://doi.org/10.4049/JIMMUNOL.150.9.3793>
- Meder, L., Schuldt, P., Thelen, M., Schmitt, A., Dietlein, F., Klein, S., Borchmann, S., Wennhold, K., Vlastic, I., Oberbeck, S., Riedel, R., Florin, A., Golfmann, K., Schlößer, H. A., Odenthal, M., Buettner, R., Wolf, J., Hallek, M., Herling, M., ... Ullrich, R. T. (2018). Combined VEGF and PD-L1 blockade displays synergistic treatment effects in an autochthonous mouse model of small cell lung cancer. *Cancer Research*, 78(15), 4270–4281. <https://doi.org/10.1158/0008-5472.CAN-17-2176/653018/AM/COMBINED-VEGF-AND-PD-L1-BLOCKADE-DISPLAYS>
- Meric-Bernstam, F., Hurwitz, H., Raghav, K. P. S., McWilliams, R. R., Fakih, M., VanderWalde, A., Swanton, C., Kurzrock, R., Burris, H., Sweeney, C., Bose, R., Spigel, D. R., Beattie, M. S., Blotner, S., Stone, A., Schulze, K., Cuchelkar, V., & Hainsworth, J. (2019). Pertuzumab plus trastuzumab for HER2-amplified metastatic colorectal cancer (MyPathway): an updated report from a multicentre, open-label, phase 2a, multiple basket study. *The Lancet Oncology*, 20(4), 518–530. [https://doi.org/10.1016/S1470-2045\(18\)30904-5](https://doi.org/10.1016/S1470-2045(18)30904-5)
- Mestas, J., & Hughes, C. C. W. (2004a). Of Mice and Not Men: Differences between Mouse and Human Immunology. *The Journal of Immunology*, 172(5), 2731–2738.
<https://doi.org/10.4049/JIMMUNOL.172.5.2731>
- Mestas, J., & Hughes, C. C. W. (2004b). Of Mice and Not Men: Differences between Mouse and Human Immunology. *The Journal of Immunology*, 172(5), 2731–2738.
<https://doi.org/10.4049/JIMMUNOL.172.5.2731>
- Mettu, N. B., Ou, F. S., Zemla, T. J., Halfdanarson, T. R., Lenz, H. J., Breakstone, R. A., Boland, P. M., Crysler, O. V., Wu, C., Nixon, A. B., Bolch, E., Niedzwiecki, D.,

- Elsing, A., Hurwitz, H. I., Fakih, M. G., & Bekaii-Saab, T. (2022a). Assessment of Capecitabine and Bevacizumab With or Without Atezolizumab for the Treatment of Refractory Metastatic Colorectal Cancer: A Randomized Clinical Trial. *JAMA Network Open*, *5*(2), e2149040–e2149040. <https://doi.org/10.1001/JAMANETWORKOPEN.2021.49040>
- Mettu, N. B., Ou, F. S., Zemla, T. J., Halfdanarson, T. R., Lenz, H. J., Breakstone, R. A., Boland, P. M., Crysler, O. V., Wu, C., Nixon, A. B., Bolch, E., Niedzwiecki, D., Elsing, A., Hurwitz, H. I., Fakih, M. G., & Bekaii-Saab, T. (2022b). Assessment of Capecitabine and Bevacizumab With or Without Atezolizumab for the Treatment of Refractory Metastatic Colorectal Cancer: A Randomized Clinical Trial. *JAMA Network Open*, *5*(2), e2149040–e2149040. <https://doi.org/10.1001/JAMANETWORKOPEN.2021.49040>
- Meyers, D. E., & Banerji, S. (2020). Biomarkers of Immune Checkpoint Inhibitor Efficacy in Cancer. *Current Oncology* 2020, Vol. 27, Pages 106-114, *27*(s2), 106–114. <https://doi.org/10.3747/CO.27.5549>
- Mikhailov, A., Shinohara, M., & Rieder, C. L. (2004). Topoisomerase II and histone deacetylase inhibitors delay the G2/M transition by triggering the p38 MAPK checkpoint pathway. *Journal of Cell Biology*, *166*(4), 517–526. <https://doi.org/10.1083/JCB.200405167>
- Miller, J. C., Brown, B. D., Shay, T., Gautier, E. L., Jojic, V., Cohain, A., Pandey, G., Leboeuf, M., Elpek, K. G., Helft, J., Hashimoto, D., Chow, A., Price, J., Greter, M., Bogunovic, M., Bellemare-Pelletier, A., Frenette, P. S., Randolph, G. J., Turley, S. J., ... Benoist, C. (2012). Deciphering the transcriptional network of the dendritic cell lineage. *Nature Immunology* 2012 13:9, *13*(9), 888–899. <https://doi.org/10.1038/ni.2370>
- Mimura, K., Kono, K., Takahashi, A., Kawaguchi, Y., & Fujii, H. (2007). Vascular endothelial growth factor inhibits the function of human mature dendritic cells mediated by VEGF receptor-2. *Cancer Immunology, Immunotherapy*, *56*(6), 761–770. <https://doi.org/10.1007/S00262-006-0234-7/FIGURES/5>
- Mlecnik, B., Tosolini, M., Charoentong, P., Kirilovsky, A., Bindea, G., Berger, A., Camus, M., Gillard, M., Bruneval, P., Fridman, W. H., Pagès, F., Trajanoski, Z., & Galon, J. (2010). Biomolecular Network Reconstruction Identifies T-Cell Homing Factors Associated With Survival in Colorectal Cancer. *Gastroenterology*, *138*(4), 1429–1440. <https://doi.org/10.1053/J.GASTRO.2009.10.057>
- Mok, S., Koya, R. C., Tsui, C., Xu, J., Robert, L., Wu, L., Graeber, T. G., West, B. L., Bollag, G., & Ribas, A. (2014). Inhibition of CSF-1 receptor improves the antitumor efficacy of adoptive cell transfer immunotherapy. *Cancer Research*, *74*(1), 153–161. <https://doi.org/10.1158/0008-5472.CAN-13-1816/651228/AM/INHIBITION-OF-CSF1-RECEPTOR-IMPROVES-THE-ANTI>
- Molnár, Á., Theodoras, A. M., Zon, L. I., & Kyriakis, J. M. (1997). Cdc42Hs, but not Rac1, inhibits serum-stimulated cell cycle progression at G1/S through a mechanism requiring p38/RK. *Journal of Biological Chemistry*, *272*(20), 13229–13235. <https://doi.org/10.1074/jbc.272.20.13229>
- Molon, B., Ugel, S., Del Pozzo, F., Soldani, C., Zilio, S., Avella, D., De Palma, A., Mauri, P. L., Monegal, A., Rescigno, M., Savino, B., Colombo, P., Jonjic, N.,

- Pecanic, S., Lazzarato, L., Fruttero, R., Gasco, A., Bronte, V., & Viola, A. (2011). Chemokine nitration prevents intratumoral infiltration of antigen-specific T cells. *Journal of Experimental Medicine*, *208*(10), 1949–1962. <https://doi.org/10.1084/JEM.20101956>
- Monach, P. A., Meredith, S. C., T.Siegel, C., & Schreiber, H. (1995). A unique tumor antigen produced by a single amino acid substitution. *Immunity*, *2*(1), 45–59. [https://doi.org/10.1016/1074-7613\(95\)90078-0](https://doi.org/10.1016/1074-7613(95)90078-0)
- Morales-Kastresana, A., Catalán, E., Hervás-Stubbs, S., Palazón, A., Azpilikueta, A., Bolaños, E., Anel, A., Pardo, J., & Melero, I. (2013). Essential complicity of perforin-granzyme and FAS-L mechanisms to achieve tumor rejection following treatment with anti-CD137 mAb. *Journal for ImmunoTherapy of Cancer*, *1*(1), 3. <https://doi.org/10.1186/2051-1426-1-3>
- Morin, P. J., Sparks, A. B., Korinek, V., Barker, N., Clevers, H., Vogelstein, B., & Kinzler, K. W. (1997). Activation of β -Catenin-Tcf Signaling in Colon Cancer by Mutations in β -Catenin or APC. *Science*, *275*(5307), 1787–1790. <https://doi.org/10.1126/SCIENCE.275.5307.1787>
- Motz, G. T., Santoro, S. P., Wang, L. P., Garrabrant, T., Lastra, R. R., Hagemann, I. S., Lal, P., Feldman, M. D., Benencia, F., & Coukos, G. (2014). Tumor endothelium FasL establishes a selective immune barrier promoting tolerance in tumors. *Nature Medicine* *2014* *20*:6, *20*(6), 607–615. <https://doi.org/10.1038/nm.3541>
- Movahedi, K., Laoui, D., Gysemans, C., Baeten, M., Stangé, G., Van Bossche, J. Den, Mack, M., Pipeleers, D., In't Veld, P., De Baetselier, P., & Van Ginderachter, J. A. (2010). Different tumor microenvironments contain functionally distinct subsets of macrophages derived from Ly6C(high) monocytes. *Cancer Research*, *70*(14), 5728–5739. <https://doi.org/10.1158/0008-5472.CAN-09-4672/656065/P/DIFFERENT-TUMOR-MICROENVIRONMENTS-CONTAIN>
- Mujal, A. M., Delconte, R. B., & Sun, J. C. (2021). Natural Killer Cells: From Innate to Adaptive Features. *Annual Review of Immunology*, *39*, 417–447. <https://doi.org/10.1146/ANNUREV-IMMUNOL-101819-074948>
- Mumm, J. B., Emmerich, J., Zhang, X., Chan, I., Wu, L., Mauze, S., Blaisdell, S., Basham, B., Dai, J., Grein, J., Sheppard, C., Hong, K., Cutler, C., Turner, S., LaFace, D., Kleinschek, M., Judo, M., Ayanoglu, G., Langowski, J., ... Oft, M. (2011). IL-10 Elicits IFN γ -Dependent Tumor Immune Surveillance. *Cancer Cell*, *20*(6), 781–796. <https://doi.org/10.1016/J.CCR.2011.11.003>
- Murdoch, C., Muthana, M., Coffelt, S. B., & Lewis, C. E. (2008). The role of myeloid cells in the promotion of tumour angiogenesis. *Nature Reviews Cancer* *2008* *8*:8, *8*(8), 618–631. <https://doi.org/10.1038/nrc2444>
- Muz, B., Puente, P. de la, Azab, F., & Azab, A. K. (2015). The role of hypoxia in cancer progression, angiogenesis, metastasis, and resistance to therapy. *Hypoxia*, *3*, 83. <https://doi.org/10.2147/HP.S93413>
- Muzny, D. M., Bainbridge, M. N., Chang, K., Dinh, H. H., Drummond, J. A., Fowler, G., Kovar, C. L., Lewis, L. R., Morgan, M. B., Newsham, I. F., Reid, J. G., Santibanez, J., Shinbrot, E., Trevino, L. R., Wu, Y. Q., Wang, M., Gunaratne, P., Donehower, L. A., Creighton, C. J., ... Thomson, E. (2012). Comprehensive molecular

characterization of human colon and rectal cancer. *Nature* 2012 487:7407, 487(7407), 330–337. <https://doi.org/10.1038/nature11252>

- Myungjin Lee, J., Mhawech-Fauceglia, P., Lee, N., Cristina Parsanian, L., Gail Lin, Y., Andrew Gayther, S., & Lawrenson, K. (2013). A three-dimensional microenvironment alters protein expression and chemosensitivity of epithelial ovarian cancer cells in vitro. *Laboratory Investigation; a Journal of Technical Methods and Pathology*, 93(5), 528–542. <https://doi.org/10.1038/LABINVEST.2013.41>
- Nagarsheth, N., Peng, D., Kryczek, I., Wu, K., Li, W., Zhao, E., Zhao, L., Wei, S., Frankel, T., Vatan, L., Szeliga, W., Dou, Y., Owens, S., Marquez, V., Tao, K., Huang, E., Wang, G., & Zou, W. (2016). PRC2 epigenetically silences Th1-type chemokines to suppress effector T-cell trafficking in colon cancer. *Cancer Research*, 76(2), 275–282. <https://doi.org/10.1158/0008-5472.CAN-15-1938/652120/AM/PRC2-EPIGENETICALLY-SILENCES-TH1-TYPE-CHEMOKINES>
- Naing, A., Infante, J. R., Papadopoulos, K. P., Chan, I. H., Shen, C., Ratti, N. P., Rojo, B., Autio, K. A., Wong, D. J., Patel, M. R., Ott, P. A., Falchook, G. S., Pant, S., Hung, A., Pekarek, K. L., Wu, V., Adamow, M., McCauley, S., Mumm, J. B., ... Off, M. (2018). PEGylated IL-10 (Pegilodecakin) Induces Systemic Immune Activation, CD8+ T Cell Invigoration and Polyclonal T Cell Expansion in Cancer Patients. *Cancer Cell*, 34(5), 775-791.e3. <https://doi.org/10.1016/J.CCELL.2018.10.007>
- Naishiro, Y., Yamada, T., Takaoka, A. S., Hayashi, R., Hasegawa, F., Imai, K., & Hirohashi, S. (2001). Restoration of Epithelial Cell Polarity in a Colorectal Cancer Cell Line by Suppression of-catenin/T-Cell Factor 4-mediated Gene Transactivation 1. *CANCER RESEARCH*, 61, 2751–2758. <http://aacrjournals.org/cancerres/article-pdf/61/6/2751/3252535/ch060102751p.pdf>
- Nakagawa, Y., Negishi, Y., Shimizu, M., Takahashi, M., Ichikawa, M., & Takahashi, H. (2015). Effects of extracellular pH and hypoxia on the function and development of antigen-specific cytotoxic T lymphocytes. *Immunology Letters*, 167(2), 72–86. <https://doi.org/10.1016/J.IMLET.2015.07.003>
- Nakajima, C., Mukai, T., Yamaguchi, N., Morimoto, Y., Park, W.-R., Iwasaki, M., Gao, P., Ono, S., Fujiwara, H., & Hamaoka, T. (2002). Induction of the chemokine receptor CXCR3 on TCR-stimulated T cells: dependence on the release from persistent TCR-triggering and requirement for IFN- γ stimulation. *European Journal of Immunology*. <https://doi.org/10.1002/1521-4141>
- Naldini, A., Carraro, F., Silvestri, S., & Bocci, V. (1997). Hypoxia Affects Cytokine Production and Proliferative Responses by Human Peripheral Mononuclear Cells. *JOURNAL OF CELLULAR PHYSIOLOGY*, 173, 335–342. [https://doi.org/10.1002/\(SICI\)1097-4652\(199712\)173:3](https://doi.org/10.1002/(SICI)1097-4652(199712)173:3)
- Nap, M., Mollgard, K., Burtin, P., & Fleuren, G. J. (1988). Immunohistochemistry of Carcino-Embryonic Antigen in the Embryo, Fetus and Adult. *Tumor Biology*, 9(2–3), 145–153. <https://doi.org/10.1159/000217555>

- Naugler, W. E., & Karin, M. (2008). The wolf in sheep's clothing: the role of interleukin-6 in immunity, inflammation and cancer. *Trends in Molecular Medicine*, 14(3), 109–119. <https://doi.org/10.1016/J.MOLMED.2007.12.007>
- Nazareth, M. R., Broderick, L., Simpson-Abelson, M. R., Kelleher, R. J., Yokota, S. J., & Bankert, R. B. (2007). Characterization of Human Lung Tumor-Associated Fibroblasts and Their Ability to Modulate the Activation of Tumor-Associated T Cells. *The Journal of Immunology*, 178(9), 5552–5562. <https://doi.org/10.4049/JIMMUNOL.178.9.5552>
- Needham, D. J., Lee, J. X., & Beilharz, M. W. (2006). Intra-tumoural regulatory T cells: A potential new target in cancer immunotherapy. *Biochemical and Biophysical Research Communications*, 343(3), 684–691. <https://doi.org/10.1016/J.BBRC.2006.03.018>
- Nestle, F. O., Burg, G., Fähr, J., Wrone-Smith, T., & Nickoloff, B. J. (1997). Human sunlight-induced basal-cell-carcinoma-associated dendritic cells are deficient in T cell co-stimulatory molecules and are impaired as antigen-presenting cells. *The American Journal of Pathology*, 150(2), 641. [/pmc/articles/PMC1858265/?report=abstract](https://pubmed.ncbi.nlm.nih.gov/1158265/)
- Newey, A., Griffiths, B., Michaux, J., Pak, H. S., Stevenson, B. J., Woolston, A., Semiannikova, M., Spain, G., Barber, L. J., Matthews, N., Rao, S., Watkins, D., Chau, I., Coukos, G., Racle, J., Gfeller, D., Starling, N., Cunningham, D., Bassani-Sternberg, M., & Gerlinger, M. (2019). Immunopeptidomics of colorectal cancer organoids reveals a sparse HLA class I neoantigen landscape and no increase in neoantigens with interferon or MEK-inhibitor treatment. *Journal for ImmunoTherapy of Cancer*, 7(1), 1–15. <https://doi.org/10.1186/S40425-019-0769-8/FIGURES/5>
- Nguyen, H. H., Kim, T., Song, S. Y., Park, S., Cho, H. H., Jung, S. H., Ahn, J. S., Kim, H. J., Lee, J. J., Kim, H. O., Cho, J. H., & Yang, D. H. (2016). Naïve CD8+ T cell derived tumor-specific cytotoxic effectors as a potential remedy for overcoming TGF- β immunosuppression in the tumor microenvironment. *Scientific Reports* 2016 6:1, 6(1), 1–10. <https://doi.org/10.1038/srep28208>
- Nguyen, H. T., & Duong, H. Q. (2018). The molecular characteristics of colorectal cancer: Implications for diagnosis and therapy (review). *Oncology Letters*, 16(1), 9–18. <https://doi.org/10.3892/OL.2018.8679/HTML>
- Ni, C., Wu, P., Zhu, X., Ye, J., Zhang, Z., Chen, Z., Zhang, T., Zhang, T., Wang, K., Wu, D., Qiu, F., & Huang, J. (2013). IFN- γ selectively exerts pro-apoptotic effects on tumor-initiating label-retaining colon cancer cells. *Cancer Letters*, 336(1), 174–184. <https://doi.org/10.1016/J.CANLET.2013.04.029>
- Nicolas-Boluda, A., Vaquero, J., Vimeux, L., Guilbert, T., Barrin, S., Kantari-Mimoun, C., Ponzio, M., Renault, G., Deptula, P., Pogoda, K., Bucki, R., Cascone, I., Courty, J., Fouassier, L., Gazeau, F., & Donnadiou, E. (2021). Tumor stiffening reversion through collagen crosslinking inhibition improves t cell migration and anti-pd-1 treatment. *ELife*, 10. <https://doi.org/10.7554/ELIFE.58688>
- Nissen, N. I., Karsdal, M., & Willumsen, N. (2019). Collagens and Cancer associated fibroblasts in the reactive stroma and its relation to Cancer biology. *Journal of*

Experimental and Clinical Cancer Research, 38(1), 1–12.
<https://doi.org/10.1186/S13046-019-1110-6/TABLES/1>

- Nobuhiko Kayagaki, B., Kawasaki, A., Ebata, T., Ohmoto, H., Ikeda, S., Inoue, S., & Okumura, K. (1995). Metalloproteinase-mediated Release of Human Fas Ligand. *Journal of Experimental Medicine*. <http://rupress.org/jem/article-pdf/182/6/1777/1107323/1777.pdf>
- Noman, M. Z., Hasmim, M., Messai, Y., Terry, S., Kieda, C., Janji, B., & Chouaib, S. (2015). Hypoxia: A key player in antitumor immune response. A review in the theme: Cellular responses to hypoxia. *American Journal of Physiology - Cell Physiology*, 309(9), C569–C579.
<https://doi.org/10.1152/AJPCCELL.00207.2015/ASSET/IMAGES/LARGE/ZH00201578190003.JPEG>
- Öbrink, B. (1997). CEA adhesion molecules: multifunctional proteins with signal-regulatory properties. *Current Opinion in Cell Biology*, 9(5), 616–626.
[https://doi.org/10.1016/S0955-0674\(97\)80114-7](https://doi.org/10.1016/S0955-0674(97)80114-7)
- O’Connell, J. B., Maggard, M. A., & Ko, C. Y. (2004). Colon Cancer Survival Rates With the New American Joint Committee on Cancer Sixth Edition Staging. *JNCI: Journal of the National Cancer Institute*, 96(19), 1420–1425.
<https://doi.org/10.1093/JNCI/DJH275>
- Offner, S., Hofmeister, R., Romaniuk, A., Kufer, P., & Baeuerle, P. A. (2006). Induction of regular cytolytic T cell synapses by bispecific single-chain antibody constructs on MHC class I-negative tumor cells. *Molecular Immunology*, 43(6), 763–771.
<https://doi.org/10.1016/J.MOLIMM.2005.03.007>
- Oft, M. (2014). IL-10: Master Switch from Tumor-Promoting Inflammation to Antitumor Immunity. *Cancer Immunology Research*, 2(3), 194–199.
<https://doi.org/10.1158/2326-6066.CIR-13-0214>
- Oh, D. Y., Kwek, S. S., Raju, S. S., Li, T., McCarthy, E., Chow, E., Aran, D., Ilano, A., Pai, C. C. S., Rancan, C., Allaire, K., Burra, A., Sun, Y., Spitzer, M. H., Mangul, S., Porten, S., Meng, M. V., Friedlander, T. W., Ye, C. J., & Fong, L. (2020). Intratumoral CD4+ T Cells Mediate Anti-tumor Cytotoxicity in Human Bladder Cancer. *Cell*, 181(7), 1612-1625.e13. <https://doi.org/10.1016/J.CELL.2020.05.017>
- Ohta, A., Diwanji, R., Kini, R., Subramanian, M., Ohta, A., & Sitkovsky, M. (2011). In vivo T cell activation in lymphoid tissues is inhibited in the oxygen-poor microenvironment. *Frontiers in Immunology*, 2(JUL), 27.
<https://doi.org/10.3389/FIMMU.2011.00027/BIBTEX>
- Ohta, A., Ohta, A., Madasu, M., Kini, R., Subramanian, M., Goel, N., & Sitkovsky, M. (2009). A2A Adenosine Receptor May Allow Expansion of T Cells Lacking Effector Functions in Extracellular Adenosine-Rich Microenvironments. *The Journal of Immunology*, 183(9), 5487–5493. <https://doi.org/10.4049/JIMMUNOL.0901247>
- Okada-Iwasaki, R., Takahashi, Y., Watanabe, Y., Ishida, H., Saito, J. I., Nakai, R., & Asai, A. (2016). The Discovery and characterization of K-756, a Novel Wnt/b-Catenin pathway inhibitor targeting tankyrase. *Molecular Cancer Therapeutics*, 15(7), 1525–1534. <https://doi.org/10.1158/1535-7163.MCT-15-0938/86719/AM/THE-DISCOVERY-AND-CHARACTERIZATION-OF-K-756-A>

- Orimo, A., Gupta, P. B., Sgroi, D. C., Arenzana-Seisdedos, F., Delaunay, T., Naeem, R., Carey, V. J., Richardson, A. L., & Weinberg, R. A. (2005). Stromal Fibroblasts Present in Invasive Human Breast Carcinomas Promote Tumor Growth and Angiogenesis through Elevated SDF-1/CXCL12 Secretion. *Cell*, *121*(3), 335–348. <https://doi.org/10.1016/J.CELL.2005.02.034>
- Osada, T., Hsu, D., Hammond, S., Hobeika, A., Devi, G., Clay, T. M., Lysterly, H. K., & Morse, M. A. (2009). Metastatic colorectal cancer cells from patients previously treated with chemotherapy are sensitive to T-cell killing mediated by CEA/CD3-bispecific T-cell-engaging BiTE antibody. *British Journal of Cancer* *2010* *102*:1, *102*(1), 124–133. <https://doi.org/10.1038/sj.bjc.6605364>
- Osada, T., Patel, S. P., Hammond, S. A., Osada, K., Morse, M. A., & Lysterly, H. K. (2015). CEA/CD3-bispecific T cell-engaging (BiTE) antibody-mediated T lymphocyte cytotoxicity maximized by inhibition of both PD1 and PD-L1. *Cancer Immunology, Immunotherapy*, *64*(6), 677–688. <https://doi.org/10.1007/S00262-015-1671-Y/FIGURES/6>
- Otte, J. M., Schmitz, F., Kiehne, K., Stechele, H. U., Banasiewicz, T., Krokowicz, P., Nakamura, T., Fölsch, U. R., & Herzig, K. H. (2000). Functional Expression of HGF and Its Receptor in Human Colorectal Cancer. *Digestion*, *61*(4), 237–246. <https://doi.org/10.1159/000007764>
- Ozao-Choy, J., Ge, M., Kao, J., Wang, G. X., Meseck, M., Sung, M., Schwartz, M., Divino, C. M., Pan, P. Y., & Chen, S. H. (2009). The novel role of tyrosine kinase inhibitor in the reversal of immune suppression and modulation of tumor microenvironment for immune-based cancer therapies. *Cancer Research*, *69*(6), 2514–2522. <https://doi.org/10.1158/0008-5472.CAN-08-4709/655043/P/THE-NOVEL-ROLE-OF-TYROSINE-KINASE-INHIBITOR-IN-THE>
- Pagès, F., Mlecnik, B., Marliot, F., Bindea, G., Ou, F. S., Bifulco, C., Lugli, A., Zlobec, I., Rau, T. T., Berger, M. D., Nagtegaal, I. D., Vink-Börger, E., Hartmann, A., Geppert, C., Kolwelter, J., Merkel, S., Grützmann, R., Van den Eynde, M., Jouret-Mourin, A., ... Galon, J. (2018). International validation of the consensus Immunoscore for the classification of colon cancer: a prognostic and accuracy study. *The Lancet*, *391*(10135), 2128–2139. [https://doi.org/10.1016/S0140-6736\(18\)30789-X](https://doi.org/10.1016/S0140-6736(18)30789-X)
- Panda, S. K., & Colonna, M. (2019). Innate lymphoid cells in mucosal immunity. *Frontiers in Immunology*, *10*. <https://doi.org/10.3389/FIMMU.2019.00861/BIBTEX>
- Pandiyan, P., Zheng, L., Ishihara, S., Reed, J., & Lenardo, M. J. (2007). CD4+CD25+Foxp3+ regulatory T cells induce cytokine deprivation-mediated apoptosis of effector CD4+ T cells. *Nature Immunology* *2007* *8*:12, *8*(12), 1353–1362. <https://doi.org/10.1038/ni1536>
- Pankova, D., Chen, Y., Terajima, M., Schliekelman, M. J., Baird, B. N., Fahrenholtz, M., Sun, L., Gill, B. J., Vadakkan, T. J., Kim, M. P., Ahn, Y. H., Roybal, J. D., Liu, X., Cuentas, E. R. P., Rodriguez, J., Wistuba, I. I., Creighton, C. J., Gibbons, D. L., Hicks, J. M., ... Kurie, J. M. (2016). Cancer-associated fibroblasts induce a collagen cross-link switch in tumor stroma. *Molecular Cancer Research*, *14*(3), 287–295. <https://doi.org/10.1158/1541-7786.MCR-15-0307/80548/AM/CANCER-ASSOCIATED-FIBROBLASTS-INDUCE-A-COLLAGEN>

- Paraiso, K. H. T., & Smalley, K. S. M. (2013). Fibroblast-mediated drug resistance in cancer. *Biochemical Pharmacology*, *85*(8), 1033–1041. <https://doi.org/10.1016/J.BCP.2013.01.018>
- Park, J. R., DiGiusto, D. L., Slovak, M., Wright, C., Naranjo, A., Wagner, J., Meechoovet, H. B., Bautista, C., Chang, W. C., Ostberg, J. R., & Jensen, M. C. (2007). Adoptive Transfer of Chimeric Antigen Receptor Re-directed Cytolytic T Lymphocyte Clones in Patients with Neuroblastoma. *Molecular Therapy*, *15*(4), 825–833. <https://doi.org/10.1038/SJ.MT.6300104>
- Pasch, C. A., Favreau, P. F., Yueh, A. E., Babiarz, C. P., Gillette, A. A., Sharick, J. T., Karim, M. R., Nickel, K. P., DeZeeuw, A. K., Sprackling, C. M., Emmerich, P. B., DeStefanis, R. A., Pitera, R. T., Payne, S. N., Korkos, D. P., Clipson, L., Walsh, C. M., Miller, D., Carchman, E. H., ... Deming, D. A. (2019). Patient-derived cancer organoid cultures to predict sensitivity to chemotherapy and radiation. *Clinical Cancer Research*, *25*(17), 5376–5387. <https://doi.org/10.1158/1078-0432.CCR-18-3590/74108/AM/PATIENT-DERIVED-CANCER-ORGANOID-CULTURES-TO>
- Paszek, M. J., Zahir, N., Johnson, K. R., Lakins, J. N., Rozenberg, G. I., Gefen, A., Reinhart-King, C. A., Margulies, S. S., Dembo, M., Boettiger, D., Hammer, D. A., & Weaver, V. M. (2005). Tensional homeostasis and the malignant phenotype. *Cancer Cell*, *8*(3), 241–254. <https://doi.org/10.1016/J.CCR.2005.08.010>
- Patel, S. P., & Kurzrock, R. (2015). PD-L1 expression as a predictive biomarker in cancer immunotherapy. *Molecular Cancer Therapeutics*, *14*(4), 847–856. <https://doi.org/10.1158/1535-7163.MCT-14-0983/86482/AM/PD-L1-EXPRESSION-AS-A-PREDICTIVE-BIOMARKER-IN>
- Paz-Ares, L., Champiat, S., Lai, W. V., Izumi, H., Govindan, R., Boyer, M., Hummel, H.-D., Borghaei, H., Johnson, M. L., Steeghs, N., Blackhall, F., Dowlati, A., Reguart, N., Yoshida, T., He, K., Gadgeel, S. M., Felip, E., Zhang, Y., Pati, A., ... Owonikoko, T. K. (2023). Tarlatamab, a First-In-Class DLL3-Targeted Bispecific T-Cell Engager, in Recurrent Small Cell Lung Cancer: An Open-Label, Phase I Study. *Journal of Clinical Oncology: Official Journal of the American Society of Clinical Oncology*, JCO2202823. <https://doi.org/10.1200/JCO.22.02823>
- Pearce, O. M. T., Delaine-Smith, R. M., Maniati, E., Nichols, S., Wang, J., Böhm, S., Rajeeve, V., Ullah, D., Chakravarty, P., Jones, R. R., Montfort, A., Dowe, T., Gribben, J., Jones, J. L., Kocher, H. M., Serody, J. S., Vincent, B. G., Connelly, J., Brenton, J. D., ... Balkwill, F. R. (2018). Deconstruction of a metastatic tumor microenvironment reveals a common matrix response in human cancers. *Cancer Discovery*, *8*(3), 304–319. <https://doi.org/10.1158/2159-8290.CD-17-0284/333253/AM/DECONSTRUCTION-OF-A-METASTATIC-TUMOR>
- Peng, D., Kryczek, I., Nagarsheth, N., Zhao, L., Wei, S., Wang, W., Sun, Y., Zhao, E., Vatan, L., Szeliga, W., Kotarski, J., Tarkowski, R., Dou, Y., Cho, K., Hensley-Alford, S., Munkarah, A., Liu, R., & Zou, W. (2015). Epigenetic silencing of TH1-type chemokines shapes tumour immunity and immunotherapy. *Nature* *2015* *527*:7577, *527*(7577), 249–253. <https://doi.org/10.1038/nature15520>
- Peranzoni, E., Lemoine, J., Vimeux, L., Feuillet, V., Barrin, S., Kantari-Mimoun, C., Bercovici, N., Guérin, M., Biton, J., Ouakrim, H., Régnier, F., Lupo, A., Alifano, M., Damotte, D., & Donnadiou, E. (2018). Macrophages impede CD8 T cells from reaching tumor cells and limit the efficacy of anti-PD-1 treatment. *Proceedings of*

the National Academy of Sciences of the United States of America, 115(17), E4041–E4050.
https://doi.org/10.1073/PNAS.1720948115/SUPPL_FILE/PNAS.1720948115.SMO8.AVI

- Perera Molligoda Arachchige, A. S. (2021). Human NK cells: From development to effector functions. *Innate Immunity*, 27(3), 212.
<https://doi.org/10.1177/17534259211001512>
- Pfirschke, C., Engblom, C., Rickelt, S., Cortez-Retamozo, V., Garris, C., Pucci, F., Yamazaki, T., Poirier-Colame, V., Newton, A., Redouane, Y., Lin, Y. J., Wojtkiewicz, G., Iwamoto, Y., Mino-Kenudson, M., Huynh, T. G., Hynes, R. O., Freeman, G. J., Kroemer, G., Zitvogel, L., ... Pittet, M. J. (2016). Immunogenic Chemotherapy Sensitizes Tumors to Checkpoint Blockade Therapy. *Immunity*, 44(2), 343–354. <https://doi.org/10.1016/J.IMMUNI.2015.11.024>
- Philipson, B. I., O'Connor, R. S., May, M. J., June, C. H., Albelda, S. M., & Milone, M. C. (2020). 4-1BB costimulation promotes CAR T cell survival through noncanonical NF-κB signaling. *Science Signaling*, 13(625), 31.
https://doi.org/10.1126/SCISIGNAL.AAY8248/SUPPL_FILE/AAY8248_SM.PDF
- Pinchuk, I. V., Saada, J. I., Beswick, E. J., Boya, G., Qiu, S. M., Mifflin, R. C., Raju, G. S., Reyes, V. E., & Powell, D. W. (2008). PD-1 Ligand Expression by Human Colonic Myofibroblasts/Fibroblasts Regulates CD4+ T-Cell Activity. *Gastroenterology*, 135(4), 1228-1237.e2.
<https://doi.org/10.1053/J.GASTRO.2008.07.016>
- Pirtskhalaishvili, G., & Nelson, J. B. (2000). Endothelium-Derived Factors as Paracrine Mediators of Prostate Cancer Progression. *Prostate*, 44, 77–87.
<https://doi.org/10.1002/1097-0045>
- Pollard, J. W. (2004). Tumour-educated macrophages promote tumour progression and metastasis. *Nature Reviews Cancer*, 4(1), 71–78.
<https://doi.org/10.1038/nrc1256>
- Porębska, I., Harłodzińska, A., & Bojarowski, T. (2000). Expression of the Tyrosine Kinase Activity Growth Factor Receptors (EGFR, ERB B2, ERB B3) in Colorectal Adenocarcinomas and Adenomas. *Tumor Biology*, 21(2), 105–115.
<https://doi.org/10.1159/000030116>
- Postow, M. A., Chesney, J., Pavlick, A. C., Robert, C., Grossmann, K., McDermott, D., Linette, G. P., Meyer, N., Giguere, J. K., Agarwala, S. S., Shaheen, M., Ernstoff, M. S., Minor, D., Salama, A. K., Taylor, M., Ott, P. A., Rollin, L. M., Horak, C., Gagnier, P., ... Hodi, F. S. (2015). Nivolumab and Ipilimumab versus Ipilimumab in Untreated Melanoma. *New England Journal of Medicine*, 372(21), 2006–2017.
https://doi.org/10.1056/NEJMOA1414428/SUPPL_FILE/NEJMOA1414428_DISCLOSURES.PDF
- Powell, S. M., Zilz, N., Beazer-Barclay, Y., Bryan, T. M., Hamilton, S. R., Thibodeau, S. N., Vogelstein, B., & Kinzler, K. W. (1992). APC mutations occur early during colorectal tumorigenesis. *Nature* 1992 359:6392, 359(6392), 235–237.
<https://doi.org/10.1038/359235a0>
- Powles, T., Eder, J. P., Fine, G. D., Braithwaite, F. S., Loriot, Y., Cruz, C., Bellmunt, J., Burris, H. A., Petrylak, D. P., Teng, S. L., Shen, X., Boyd, Z., Hegde, P. S., Chen,

- D. S., & Vogelzang, N. J. (2014). MPDL3280A (anti-PD-L1) treatment leads to clinical activity in metastatic bladder cancer. *Nature* 2014 515:7528, 515(7528), 558–562. <https://doi.org/10.1038/nature13904>
- Price, T. J., Peeters, M., Kim, T. W., Li, J., Cascinu, S., Ruff, P., Suresh, A. S., Thomas, A., Tjulandin, S., Zhang, K., Murugappan, S., & Sidhu, R. (2014). Panitumumab versus cetuximab in patients with chemotherapy-refractory wild-type KRAS exon 2 metastatic colorectal cancer (ASPECCT): a randomised, multicentre, open-label, non-inferiority phase 3 study. *The Lancet Oncology*, 15(6), 569–579. [https://doi.org/10.1016/S1470-2045\(14\)70118-4](https://doi.org/10.1016/S1470-2045(14)70118-4)
- Principe, D. R., Park, A., Dorman, M. J., Kumar, S., Viswakarma, N., Rubin, J., Torres, C., McKinney, R., Munshi, H. G., Grippo, P. J., & Rana, A. (2019). TGF β blockade augments PD-1 inhibition to promote T-cell-mediated regression of pancreatic cancer. *Molecular Cancer Therapeutics*, 18(3), 613–620. <https://doi.org/10.1158/1535-7163.MCT-18-0850/87328/AM/TGF-BLOCKADE-AUGMENTS-PD-1-INHIBITION-TO-PROMOTE-T>
- Probst, H. C., McCoy, K., Okazaki, T., Honjo, T., & Van Den Broek, M. (2005). Resting dendritic cells induce peripheral CD8 $^{+}$ T cell tolerance through PD-1 and CTLA-4. *Nature Immunology* 2005 6:3, 6(3), 280–286. <https://doi.org/10.1038/ni1165>
- Proost, P., Mortier, A., Loos, T., Vandercappellen, J., Gouwy, M., Ronsse, I., Schutyser, E., Put, W., Parmentier, M., Struyf, S., & Van Damme, J. (2007). Proteolytic processing of CXCL11 by CD13/aminopeptidase N impairs CXCR3 and CXCR7 binding and signaling and reduces lymphocyte and endothelial cell migration. *Blood*, 110(1), 37–44. <https://doi.org/10.1182/BLOOD-2006-10-049072>
- Qi, L., Chen, J., Yang, Y., & Hu, W. (2020). Hypoxia Correlates With Poor Survival and M2 Macrophage Infiltration in Colorectal Cancer. *Frontiers in Oncology*, 10, 2491. <https://doi.org/10.3389/FONC.2020.566430/BIBTEX>
- Qin, S., Li, J., Wang, L., Xu, J., Cheng, Y., Bai, Y., Li, W., Xu, N., Lin, L. Z., Wu, Q., Li, Y., Yang, J., Pan, H., Ouyang, X., Qiu, W., Wu, K., Xiong, J., Dai, G., Liang, H., ... Liu, T. (2018). Efficacy and Tolerability of First-Line Cetuximab Plus Leucovorin, Fluorouracil, and Oxaliplatin (FOLFOX-4) Versus FOLFOX-4 in Patients With RAS Wild-Type Metastatic Colorectal Cancer: The Open-Label, Randomized, Phase III TAILOR Trial. *Journal of Clinical Oncology*, 36(30), 3031. <https://doi.org/10.1200/JCO.2018.78.3183>
- Quaranta, V., Rainer, C., Nielsen, S. R., Raymant, M. L., Ahmed, M. S., Engle, D. D., Taylor, A., Murray, T., Campbell, F., Palmer, D. H., Tuveson, D. A., Mielgo, A., & Schmid, M. C. (2018). Macrophage-derived granulins drive resistance to immune checkpoint inhibition in metastatic pancreatic cancer. *Cancer Research*, 78(15), 4253–4269. <https://doi.org/10.1158/0008-5472.CAN-17-3876/653353/AM/MACROPHAGE-DERIVED-GRANULIN-DRIVES-RESISTANCE-TO>
- Quezada, S. A., Simpson, T. R., Peggs, K. S., Merghoub, T., Vider, J., Fan, X., Blasberg, R., Yagita, H., Muranski, P., Antony, P. A., Restifo, N. P., & Allison, J. P. (2010). Tumor-reactive CD4 $^{+}$ T cells develop cytotoxic activity and eradicate large established melanoma after transfer into lymphopenic hosts. *Journal of Experimental Medicine*, 207(3), 637–650. <https://doi.org/10.1084/JEM.20091918>

- Ranges, G. E., Figari, I. S., Espevik, T., & Palladino, M. A. (1987). Inhibition of cytotoxic T cell development by transforming growth factor beta and reversal by recombinant tumor necrosis factor alpha. *Journal of Experimental Medicine*, *166*(4), 991–998. <https://doi.org/10.1084/JEM.166.4.991>
- Ranzani, V., Rossetti, G., Panzeri, I., Arrigoni, A., Bonnal, R. J. P., Curti, S., Gruarin, P., Provasi, E., Sugliano, E., Marconi, M., De Francesco, R., Geginat, J., Bodega, B., Abrignani, S., & Pagani, M. (2015). The long intergenic noncoding RNA landscape of human lymphocytes highlights the regulation of T cell differentiation by linc-MAF-4. *Nature Immunology* *2015* *16*:3, *16*(3), 318–325. <https://doi.org/10.1038/ni.3093>
- Ratta, M., Fagnoni, F., Curti, A., Vescovini, R., Sansoni, P., Oliviero, B., Fogli, M., Ferri, E., Cuna, G. R. Della, Tura, S., Baccarani, M., & Lemoli, R. M. (2002). Dendritic cells are functionally defective in multiple myeloma: the role of interleukin-6. *Blood*, *100*(1), 230–237. <https://doi.org/10.1182/BLOOD.V100.1.230>
- Ravichandran, G., Neumann, K., Berkhout, L. K., Weidemann, S., Langeneckert, A. E., Schwinge, D., Poch, T., Huber, S., Schiller, B., Hess, L. U., Ziegler, A. E., Oldhafer, K. J., Barikbin, R., Schramm, C., Altfeld, M., & Tiegs, G. (2019). Interferon- γ -dependent immune responses contribute to the pathogenesis of sclerosing cholangitis in mice. *Journal of Hepatology*, *71*(4), 773–782. <https://doi.org/10.1016/J.JHEP.2019.05.023>
- Ren, X., Ye, F., Jiang, Z., Chu, Y., Xiong, S., & Wang, Y. (2007). Involvement of cellular death in TRAIL/DR5-dependent suppression induced by CD4+CD25+ regulatory T cells. *Cell Death & Differentiation* *2007* *14*:12, *14*(12), 2076–2084. <https://doi.org/10.1038/sj.cdd.4402220>
- Renner, C., Held, G., Ohnesorge, S., Bauer, S., Gerlach, K., Pfitzenmeier, J. P., & Pfreundschuh, M. (1997a). Role of naive and memory T cells in tumor cell lysis mediated by Bi-specific antibodies. *Immunobiology*, *197*(1), 122–132. [https://doi.org/10.1016/S0171-2985\(97\)80062-9](https://doi.org/10.1016/S0171-2985(97)80062-9)
- Renner, C., Held, G., Ohnesorge, S., Bauer, S., Gerlach, K., Pfitzenmeier, J. P., & Pfreundschuh, M. (1997b). Role of perforin, granzymes and the proliferative state of the target cells in apoptosis and necrosis mediated by bispecific-antibody-activated cytotoxic T cells. *Cancer Immunology Immunotherapy*, *44*(2), 70–76. <https://doi.org/10.1007/S002620050357/METRICS>
- Ribas, A., & Wolchok, J. D. (2018). Cancer immunotherapy using checkpoint blockade. *Science*, *359*(6382), 1350–1355. https://doi.org/10.1126/SCIENCE.AAR4060/ASSET/97E659F6-3962-4E23-AF15-0FD114953352/ASSETS/GRAPHIC/359_1350_F3.JPEG
- Ribot, J. C., Lopes, N., & Silva-Santos, B. (2020). $\gamma\delta$ T cells in tissue physiology and surveillance. *Nature Reviews Immunology* *2020* *21*:4, *21*(4), 221–232. <https://doi.org/10.1038/s41577-020-00452-4>
- Richman, S. D., Southward, K., Chambers, P., Cross, D., Barrett, J., Hemmings, G., Taylor, M., Wood, H., Hutchins, G., Foster, J. M., Oumie, A., Spink, K. G., Brown, S. R., Jones, M., Kerr, D., Handley, K., Gray, R., Seymour, M., & Quirke, P. (2016). HER2 overexpression and amplification as a potential therapeutic target in colorectal cancer: analysis of 3256 patients enrolled in the QUASAR, FOCUS and

PICCOLO colorectal cancer trials. *The Journal of Pathology*, 238(4), 562–570.
<https://doi.org/10.1002/PATH.4679>

- Riesenberg, R., Weiler, C., Spring, O., Eder, M., Buchner, A., Popp, T., Castro, M., Kammerer, R., Takikawa, O., Hatz, R. A., Stief, C. G., Hofstetter, A., & Zimmermann, W. (2007). Expression of Indoleamine 2,3-Dioxygenase in Tumor Endothelial Cells Correlates with Long-term Survival of Patients with Renal Cell Carcinoma. *Clinical Cancer Research*, 13(23), 6993–7002.
<https://doi.org/10.1158/1078-0432.CCR-07-0942>
- Rizvi, N. A., Hellmann, M. D., Snyder, A., Kvistborg, P., Makarov, V., Havel, J. J., Lee, W., Yuan, J., Wong, P., Ho, T. S., Miller, M. L., Rekhtman, N., Moreira, A. L., Ibrahim, F., Bruggeman, C., Gasmi, B., Zappasodi, R., Maeda, Y., Sander, C., ... Chan, T. A. (2015). Mutational landscape determines sensitivity to PD-1 blockade in non-small cell lung cancer. *Science*, 348(6230), 124–128.
https://doi.org/10.1126/SCIENCE.AAA1348/SUPPL_FILE/RIZVI-SM.PDF
- Robbins, P. F., El-Gamil, M., Li, Y. F., Kawakami, Y., Loftus, D., Appella, E., & Rosenberg, S. A. (1996). A mutated beta-catenin gene encodes a melanoma-specific antigen recognized by tumor infiltrating lymphocytes. *Journal of Experimental Medicine*, 183(3), 1185–1192.
<https://doi.org/10.1084/JEM.183.3.1185>
- Robert, C., Schachter, J., Long, G. V., Arance, A., Grob, J. J., Mortier, L., Daud, A., Carlino, M. S., McNeil, C., Lotem, M., Larkin, J., Lorigan, P., Neyns, B., Blank, C. U., Hamid, O., Mateus, C., Shapira-Frommer, R., Kosh, M., Zhou, H., ... Ribas, A. (2015). Pembrolizumab versus Ipilimumab in Advanced Melanoma. *New England Journal of Medicine*, 372(26), 2521–2532.
https://doi.org/10.1056/NEJM0A1503093/SUPPL_FILE/NEJM0A1503093_DISCLOSURES.PDF
- Rodriguez, P. C., Zea, A. H., Culotta, K. S., Zabaleta, J., & Ochoa Augusto C Ochoa, J. B. (2002). Regulation of T cell receptor CD3 ζ chain expression by L-arginine. *Journal of Biological Chemistry*, 277(24), 21123–21129.
<https://doi.org/10.1074/jbc.M110675200>
- Rodríguez-Colman, M. J., Schewe, M., Meerlo, M., Stigter, E., Gerrits, J., Pras-Raves, M., Sacchetti, A., Hornsveld, M., Oost, K. C., Snippert, H. J., Verhoeven-Duif, N., Fodde, R., & Burgering, B. M. T. (2017). Interplay between metabolic identities in the intestinal crypt supports stem cell function. *Nature* 2017 543:7645, 543(7645), 424–427. <https://doi.org/10.1038/nature21673>
- Roelofs, H. M. J., te Morsche, R. H. M., van Heumen, B. W. H., Nagengast, F. M., & Peters, W. H. M. (2014). Over-expression of COX-2 mRNA in colorectal cancer. *BMC Gastroenterology*, 14(1), 1–6. <https://doi.org/10.1186/1471-230X-14-1/FIGURES/1>
- Roman, J., Rangasamy, T., Guo, J., Sugunan, S., Meednu, N., Packirisamy, G., Shimoda, L. A., Golding, A., Semenza, G., & Georas, S. N. (2010). T-Cell Activation under Hypoxic Conditions Enhances IFN- γ Secretion. *American Journal of Respiratory Cell and Molecular Biology*, 42(1), 123.
<https://doi.org/10.1165/RCMB.2008-0139OC>

- Rosales, C., & Uribe-Querol, E. (2017). Phagocytosis: A Fundamental Process in Immunity. *BioMed Research International*. <https://doi.org/10.1155/2017/9042851>
- Rosenberg, J. E., Hoffman-Censits, J., Powles, T., Van Der Heijden, M. S., Balar, A. V., Necchi, A., Dawson, N., O'Donnell, P. H., Balmanoukian, A., Loriot, Y., Srinivas, S., Retz, M. M., Grivas, P., Joseph, R. W., Galsky, M. D., Fleming, M. T., Petrylak, D. P., Perez-Gracia, J. L., Burris, H. A., ... Dreicer, R. (2016). Atezolizumab in patients with locally advanced and metastatic urothelial carcinoma who have progressed following treatment with platinum-based chemotherapy: a single-arm, multicentre, phase 2 trial. *The Lancet*, *387*(10031), 1909–1920. [https://doi.org/10.1016/S0140-6736\(16\)00561-4](https://doi.org/10.1016/S0140-6736(16)00561-4)
- Rosenberg, S. A., Sherry, R. M., Morton, K. E., Scharfman, W. J., Yang, J. C., Topalian, S. L., Royal, R. E., Kammula, U., Restifo, N. P., Hughes, M. S., Schwartzentruber, D., Berman, D. M., Schwarz, S. L., Ngo, L. T., Mavroukakis, S. A., White, D. E., & Steinberg, S. M. (2005). Tumor Progression Can Occur despite the Induction of Very High Levels of Self/Tumor Antigen-Specific CD8+ T Cells in Patients with Melanoma. *The Journal of Immunology*, *175*(9), 6169–6176. <https://doi.org/10.4049/JIMMUNOL.175.9.6169>
- Rosenberg, S. A., Yang, J. C., Sherry, R. M., Kammula, U. S., Hughes, M. S., Phan, G. Q., Citrin, D. E., Restifo, N. P., Robbins, P. F., Wunderlich, J. R., Morton, K. E., Laurencot, C. M., Steinberg, S. M., White, D. E., & Dudley, M. E. (2011). Durable complete responses in heavily pretreated patients with metastatic melanoma using T-cell transfer immunotherapy. *Clinical Cancer Research*, *17*(13), 4550–4557. <https://doi.org/10.1158/1078-0432.CCR-11-0116/84227/AM/DURABLE-COMplete-responses-in-heavily-pretreated>
- Rosenberg, S. A., Yang, J. C., Topalian, S. L., Schwartzentruber, D. J., Weber, J. S., Parkinson, D. R., Seipp, C. A., Einhorn, J. H., & White, D. E. (1994). Treatment of 283 Consecutive Patients With Metastatic Melanoma or Renal Cell Cancer Using High-Dose Bolus Interleukin 2. *JAMA*, *271*(12), 907–913. <https://doi.org/10.1001/JAMA.1994.03510360033032>
- Rossowska, J., Anger, N., Kicielińska, J., Pajtasz-Piasecka, E., Bielawska-Pohl, A., Wojas-Turek, J., & Duś, D. (2015). Temporary elimination of IL-10 enhanced the effectiveness of cyclophosphamide and BMDC-based therapy by decrease of the suppressor activity of MDSCs and activation of antitumour immune response. *Immunobiology*, *220*(3), 389–398. <https://doi.org/10.1016/J.IMBIO.2014.10.009>
- Rossowska, J., Anger, N., Szczygieł, A., Mierzejewska, J., & Pajtasz-Piasecka, E. (2018). Reprogramming the murine colon cancer microenvironment using lentivectors encoding shRNA against IL-10 as a component of a potent DC-based chemoimmunotherapy. *Journal of Experimental and Clinical Cancer Research*, *37*(1), 1–14. <https://doi.org/10.1186/S13046-018-0799-Y/FIGURES/5>
- Rowbottom, A. W., Lepper, M. W., Garland, R. J., Cox, C. V., Corley, E. G., Oakhill, A., & Steward, C. G. (1999). Interleukin-10-induced CD8 cell proliferation. *Immunology*, *98*(1), 80. <https://doi.org/10.1046/J.1365-2567.1999.00828.X>
- Roxburgh, C. S. D., & McMillan, D. C. (2012). The role of the in situ local inflammatory response in predicting recurrence and survival in patients with primary operable colorectal cancer. *Cancer Treatment Reviews*, *38*(5), 451–466. <https://doi.org/10.1016/J.CTRV.2011.09.001>

- Rubin, B. Y., Sekar, V., & Martimucci, W. A. (1983). Comparative antiproliferative efficacies of human α and γ interferons. *Journal of General Virology*, 64(8), 1743–1748. <https://doi.org/10.1099/0022-1317-64-8-1743/CITE/REFWORKS>
- Ruf, P., Kluge, M., Jäger, M., Burges, A., Volovat, C., Heiss, M. M., Hess, J., Wimberger, P., Brandt, B., & Lindhofer, H. (2010). Pharmacokinetics, immunogenicity and bioactivity of the therapeutic antibody catumaxomab intraperitoneally administered to cancer patients. *British Journal of Clinical Pharmacology*, 69(6), 617. <https://doi.org/10.1111/J.1365-2125.2010.03635.X>
- Ruffell, B., & Coussens, L. M. (2015). Macrophages and Therapeutic Resistance in Cancer. *Cancer Cell*, 27(4), 462–472. <https://doi.org/10.1016/J.CCELL.2015.02.015>
- Russell, J. H., & Ley, T. J. (2002). Lymphocyte-Mediated Cytotoxicity. *Annual Review of Immunology*, 20, 323–370. <https://doi.org/10.1146/ANNUREV.IMMUNOL.20.100201.131730>
- Sad, S., & Mosmann, T. R. (1994). Single IL-2-secreting precursor CD4 T cell can develop into either Th1 or Th2 cytokine secretion phenotype. *The Journal of Immunology*, 153(8), 3514–3522. <https://doi.org/10.4049/JIMMUNOL.153.8.3514>
- Saeed, A., Park, R., Dai, J., Al-Rajabi, R. M. T., Kasi, A., Saeed, A., Collins, Z., Thompson, K., Barbosa, L., Mulvaney, K., Manirad, V., Phadnis, M., Williamson, S. K., Baranda, J. C., & Sun, W. (2022). Phase II trial of cabozantinib (Cabo) plus durvalumab (Durva) in chemotherapy refractory patients with advanced mismatch repair proficient/microsatellite stable (pMMR/MSS) colorectal cancer (CRC): CAMILLA CRC cohort results. *Journal of Clinical Oncology*, 40(4_suppl), 135–135. https://doi.org/10.1200/JCO.2022.40.4_SUPPL.135
- Saito, H., Soma, Y., Koeda, J., Wada, T., Kawaguchi, H., Sobue, T., Aisawa, T., & Yoshida, Y. (1995). Reduction in risk of mortality from colorectal cancer by fecal occult blood screening with immunochemical hemagglutination test. A case-control study. *International Journal of Cancer*, 61(4), 465–469. <https://doi.org/10.1002/IJC.2910610406>
- Sakemura, R., Hefazi, M., Siegler, E. L., Cox, M. J., Larson, D. P., Hansen, M. J., Manriquez Roman, C., Schick, K. J., Can, I., Tapper, E. E., Horvei, P., Adada, M. M., Bezerra, E. D., Kankeu Fonkoua, L. A., Ruff, M. W., Nevala, W. K., Walters, D. K., Parikh, S. A., Lin, Y., ... Kenderian, S. S. (2022). Targeting cancer-associated fibroblasts in the bone marrow prevents resistance to CART-cell therapy in multiple myeloma. *Blood*, 139(26), 3708–3721. <https://doi.org/10.1182/BLOOD.2021012811>
- Saleh, R., & Elkord, E. (2019). Treg-mediated acquired resistance to immune checkpoint inhibitors. *Cancer Letters*, 457, 168–179. <https://doi.org/10.1016/J.CANLET.2019.05.003>
- Sallusto, F., & Lanzavecchia, A. (2000). Understanding dendritic cell and T-lymphocyte traffic through the analysis of chemokine receptor expression. *Immunological Reviews*, 177(1), 134–140. <https://doi.org/10.1034/J.1600-065X.2000.17717.X>
- Salmon, H., Franciszkiewicz, K., Damotte, D., Dieu-Nosjean, M. C., Validire, P., Trautmann, A., Mami-Chouaib, F., & Donnadieu, E. (2012). Matrix architecture defines the preferential localization and migration of T cells into the stroma of

human lung tumors. *The Journal of Clinical Investigation*, 122(3), 899.
<https://doi.org/10.1172/JCI45817>

- Sanjabi, S., Mosaheb, M. M., & Flavell, R. A. (2009). Opposing Effects of TGF- β and IL-15 Cytokines Control the Number of Short-Lived Effector CD8+ T Cells. *Immunity*, 31(1), 131–144. <https://doi.org/10.1016/J.IMMUNI.2009.04.020>
- Santin, A. D., Hermonat, P. L., Ravaggi, A., Bellone, S., Pecorelli, S., Roman, J. J., Parham, G. P., & Cannon, M. J. (2000). Interleukin-10 Increases Th1 Cytokine Production and Cytotoxic Potential in Human Papillomavirus-Specific CD8 + Cytotoxic T Lymphocytes. *Journal of Virology*, 74(10), 4729–4737. <https://doi.org/10.1128/JVI.74.10.4729-4737.2000/ASSET/81FE239C-23FD-442A-8BC6-92AFA507DC66/ASSETS/GRAPHIC/JV1002261008.JPEG>
- Santini, M. T., Rainaldi, G., Romano, R., Ferrante, A., Clemente, S., Motta, A., & Indovina, P. L. (2004). MG-63 human osteosarcoma cells grown in monolayer and as three-dimensional tumor spheroids present a different metabolic profile: a ¹H NMR study. *FEBS Letters*, 557(1–3), 148–154. [https://doi.org/10.1016/S0014-5793\(03\)01466-2](https://doi.org/10.1016/S0014-5793(03)01466-2)
- Sartore-Bianchi, A., Trusolino, L., Martino, C., Bencardino, K., Lonardi, S., Bergamo, F., Zagonel, V., Leone, F., Depetris, I., Martinelli, E., Troiani, T., Ciardiello, F., Racca, P., Bertotti, A., Siravegna, G., Torri, V., Amatu, A., Ghezzi, S., Marrapese, G., ... Siena, S. (2016). Dual-targeted therapy with trastuzumab and lapatinib in treatment-refractory, KRAS codon 12/13 wild-type, HER2-positive metastatic colorectal cancer (HERACLES): a proof-of-concept, multicentre, open-label, phase 2 trial. *The Lancet Oncology*, 17(6), 738–746. [https://doi.org/10.1016/S1470-2045\(16\)00150-9](https://doi.org/10.1016/S1470-2045(16)00150-9)
- Sato, T., Stange, D. E., Ferrante, M., Vries, R. G. J., Van Es, J. H., Van Den Brink, S., Van Houdt, W. J., Pronk, A., Van Gorp, J., Siersema, P. D., & Clevers, H. (2011). Long-term Expansion of Epithelial Organoids From Human Colon, Adenoma, Adenocarcinoma, and Barrett's Epithelium. *Gastroenterology*, 141(5), 1762–1772. <https://doi.org/10.1053/J.GASTRO.2011.07.050>
- Sauter, B., Albert, M. L., Francisco, L., Larsson, M., Somersan, S., & Bhardwaj, N. (2000). Consequences of Cell Death Exposure to Necrotic Tumor Cells, but Not Primary Tissue Cells or Apoptotic Cells, Induces the Maturation of Immunostimulatory Dendritic Cells. *Journal of Experimental Medicine*, 191(3), 423–434. <https://doi.org/10.1084/JEM.191.3.423>
- Schadendorf, D., Hodi, F. S., Robert, C., Weber, J. S., Margolin, K., Hamid, O., Patt, D., Chen, T. T., Berman, D. M., & Wolchok, J. D. (2015). Pooled analysis of long-term survival data from phase II and phase III trials of ipilimumab in unresectable or metastatic melanoma. *Journal of Clinical Oncology*, 33(17), 1889–1894. <https://doi.org/10.1200/JCO.2014.56.2736>
- Schilbach, K., Welker, C., Krickeberg, N., Kaißer, C., Schleicher, S., & Hashimoto, H. (2020). In the Absence of a TCR Signal IL-2/IL-12/18-Stimulated $\gamma\delta$ T Cells Demonstrate Potent Anti-Tumoral Function Through Direct Killing and Senescence Induction in Cancer Cells. *Cancers 2020*, Vol. 12, Page 130, 12(1), 130. <https://doi.org/10.3390/CANCERS12010130>

- Schmitt, E., Hoehn, P., Huels, C., Goedert, S., Palm, N., Rude, E., & Germann, T. (1994). T helper type 1 development of naive CD4+ T cells requires the coordinate action of interleukin-12 and interferon-gamma and is inhibited by transforming growth factor-beta. *European Journal of Immunology*, *24*(4), 793–798. <https://doi.org/10.1002/EJL.1830240403>
- Schmittnaegel, M., Rigamonti, N., Kadioglu, E., Cassarà, A., Rmili, C. W., Kiialainen, A., Kienast, Y., Mueller, H. J., Ooi, C. H., Laoui, D., & De Palma, M. (2017). Dual angiopoietin-2 and VEGFA inhibition elicits antitumor immunity that is enhanced by PD-1 checkpoint blockade. *Science Translational Medicine*, *9*(385). https://doi.org/10.1126/SCITRANSLMED.AAK9670/SUPPL_FILE/AAK9670_TABLES_S1_AND_S2.ZIP
- Schnalzger, T. E., Groot, M. H. de, Zhang, C., Mosa, M. H., Michels, B. E., Röder, J., Darvishi, T., Wels, W. S., & Farin, H. F. (2019). 3D model for CAR-mediated cytotoxicity using patient-derived colorectal cancer organoids. *The EMBO Journal*, *38*(12), e100928. <https://doi.org/10.15252/EMBJ.2018100928>
- Schroder, K., Hertzog, P. J., Ravasi, T., & Hume, D. A. (2004). Interferon- γ : an overview of signals, mechanisms and functions. *Journal of Leukocyte Biology*, *75*(2), 163–189. <https://doi.org/10.1189/JLB.0603252>
- Schuetz, V., Embgenbroich, M., Ulas, T., Welz, M., Schulte-Schrepping, J., Draffehn, A. M., Quast, T., Koch, K., Nehring, M., König, J., Zweynert, A., Harms, F. L., Steiner, N., Limmer, A., Förster, I., Berberich-Siebelt, F., Knolle, P. A., Wohlleber, D., Kolanus, W., ... Burgdorf, S. (2016). Mannose receptor induces T-cell tolerance via inhibition of CD45 and up-regulation of CTLA-4. *Proceedings of the National Academy of Sciences of the United States of America*, *113*(38), 10649–10654. https://doi.org/10.1073/PNAS.1605885113/SUPPL_FILE/PNAS.1605885113.SD01.XLSX
- Schwartz, R. H. (2003). T Cell Anergy. *Annual Review of Immunology*, *21*, 305–334. <https://doi.org/10.1146/ANNUREV.IMMUNOL.21.120601.141110>
- Schwartz, R. H., Mueller, D. L., Jenkins, M. K., & Quill, H. (1989). T-cell Clonal Anergy. *Cold Spring Harbor Symposia on Quantitative Biology*, *54*(2), 605–610. <https://doi.org/10.1101/SQB.1989.054.01.072>
- Segal, N. H., Logan, T. F., Hodi, F. S., McDermott, D., Melero, I., Hamid, O., Schmidt, H., Robert, C., Chiarion-Sileni, V., Ascierto, P. A., Maio, M., Urba, W. J., Gangadhar, T. C., Suryawanshi, S., Neely, J., Jure-Kunkel, M., Krishnan, S., Kohrt, H., Sznol, M., & Levy, R. (2017). Results from an integrated safety analysis of urelumab, an agonist anti-CD137 monoclonal antibody. *Clinical Cancer Research*, *23*(8), 1929–1936. <https://doi.org/10.1158/1078-0432.CCR-16-1272/274409/AM/RESULTS-FROM-AN-INTEGRATED-SAFETY-ANALYSIS-OF>
- Segura, E., Kapp, E., Gupta, N., Wong, J., Lim, J., Ji, H., Heath, W. R., Simpson, R., & Villadangos, J. A. (2010). Differential expression of pathogen-recognition molecules between dendritic cell subsets revealed by plasma membrane proteomic analysis. *Molecular Immunology*, *47*(9), 1765–1773. <https://doi.org/10.1016/J.MOLIMM.2010.02.028>

- Seki, N., Brooks, A. D., Carter, C. R. D., Back, T. C., Parsonneault, E. M., Smyth, M. J., Wiltrout, R. H., & Sayers, T. J. (2002). Tumor-Specific CTL Kill Murine Renal Cancer Cells Using Both Perforin and Fas Ligand-Mediated Lysis In Vitro, But Cause Tumor Regression In Vivo in the Absence of Perforin. *The Journal of Immunology*, *168*(7), 3484–3492. <https://doi.org/10.4049/JIMMUNOL.168.7.3484>
- Seliger, B., Harders, C., Wollscheid, U., Staeger, M. S., Reske-Kunz, A. B., & Huber, C. (1996). Suppression of MHC class I antigens in oncogenic transformants: association with decreased recognition by cytotoxic T lymphocytes. *Experimental Hematology*, *24*(11), 1275–1279. <https://europepmc.org/article/med/8862437>
- Sen, D. R., Kaminski, J., Barnitz, R. A., Kurachi, M., Gerdemann, U., Yates, K. B., Tsao, H. W., Godec, J., LaFleur, M. W., Brown, F. D., Tonnerre, P., Chung, R. T., Tully, D. C., Allen, T. M., Frahm, N., Lauer, G. M., Wherry, E. J., Yosef, N., & Haining, W. N. (2016). The epigenetic landscape of T cell exhaustion. *Science*, *354*(6316), 1165–1169. https://doi.org/10.1126/SCIENCE.AAE0491/SUPPL_FILE/AAE0491_TABLES7.TXT
- Shah, B. D., Ghobadi, A., Oluwole, O. O., Logan, A. C., Boissel, N., Cassaday, R. D., Leguay, T., Bishop, M. R., Topp, M. S., Tzachanis, D., O'Dwyer, K. M., Arellano, M. L., Lin, Y., Baer, M. R., Schiller, G. J., Park, J. H., Subklewe, M., Abedi, M., Minnema, M. C., ... Houot, R. (2021). KTE-X19 for relapsed or refractory adult B-cell acute lymphoblastic leukaemia: phase 2 results of the single-arm, open-label, multicentre ZUMA-3 study. *The Lancet*, *398*(10299), 491–502. [https://doi.org/10.1016/S0140-6736\(21\)01222-8](https://doi.org/10.1016/S0140-6736(21)01222-8)
- Shah, K., Al-Haidari, A., Sun, J., & Kazi, J. U. (2021). T cell receptor (TCR) signaling in health and disease. *Signal Transduction and Targeted Therapy* *2021 6:1*, *6*(1), 1–26. <https://doi.org/10.1038/s41392-021-00823-w>
- Shankaran, V., Ikeda, H., Bruce, A. T., White, J. M., Swanson, P. E., Old, L. J., & Schreiber, R. D. (2001). IFN γ and lymphocytes prevent primary tumour development and shape tumour immunogenicity. *Nature* *2001 410:6832*, *410*(6832), 1107–1111. <https://doi.org/10.1038/35074122>
- Shaukat, A., Mongin, S. J., Geisser, M. S., Lederle, F. A., Bond, J. H., Mandel, J. S., & Church, T. R. (2013). Long-Term Mortality after Screening for Colorectal Cancer. *New England Journal of Medicine*, *369*(12), 1106–1114. https://doi.org/10.1056/NEJMORA1300720/SUPPL_FILE/NEJMORA1300720_DISCLOSURES.PDF
- Shi, Z. R., Tsao, D., & Kim, Y. S. (1983). Subcellular Distribution, Synthesis, and Release of Carcinoembryonic Antigen in Cultured Human Colon Adenocarcinoma Cell Lines¹. *CANCER RESEARCH*, *43*, 4045–4049. <http://aacrjournals.org/cancerres/article-pdf/43/9/4045/2417020/cr0430094045.pdf>
- Shin, D. S., Zaretsky, J. M., Escuin-Ordinas, H., Garcia-Diaz, A., Hu-Lieskovan, S., Kalbasi, A., Grasso, C. S., Hugo, W., Sandoval, S., Torrejon, D. Y., Palaskas, N., Abril-Rodriguez, G., Parisi, G., Azhdam, A., Chmielowski, B., Cherry, G., Seja, E., Berent-Maoz, B., Shintaku, I. P., ... Ribas, A. (2017). Primary resistance to PD-1 blockade mediated by JAK1/2 mutations. *Cancer Discovery*, *7*(2), 188–201. <https://doi.org/10.1158/2159-8290.CD-16-1223/333268/AM/PRIMARY-RESISTANCE-TO-PD-1-BLOCKADE-MEDIATED-BY>

- Shojaei, F., Wu, X., Zhong, C., Yu, L., Liang, X. H., Yao, J., Blanchard, D., Bais, C., Peale, F. V., Van Bruggen, N., Ho, C., Ross, J., Tan, M., Carano, R. A. D., Meng, Y. G., & Ferrara, N. (2007). Bv8 regulates myeloid-cell-dependent tumour angiogenesis. *Nature* 2007 450:7171, 450(7171), 825–831. <https://doi.org/10.1038/nature06348>
- Shrimali, R. K., Yu, Z., Theoret, M. R., Chinnasamy, D., Restifo, N. P., & Rosenberg, S. A. (2010). Antiangiogenic agents can increase lymphocyte infiltration into tumor and enhance the effectiveness of adoptive immunotherapy of cancer. *Cancer Research*, 70(15), 6171–6180. <https://doi.org/10.1158/0008-5472.CAN-10-0153/656120/P/ANTIANGIOGENIC-AGENTS-CAN-INCREASE-LYMPHOCYTE>
- Shuford, W. W., Klussman, K., Tritchler, D. D., Loo, D. T., Chalupny, J., Siadak, A. W., Brown, T. J., Emswiler, J., Raecho, H., Larsen, C. P., Pearson, T. C., Ledbetter, J. A., Aruffo, A., & Mittler, R. S. (1997). 4-1BB Costimulatory Signals Preferentially Induce CD8+ T Cell Proliferation and Lead to the Amplification In Vivo of Cytotoxic T Cell Responses. *Journal of Experimental Medicine*, 186(1), 47–55. <https://doi.org/10.1084/JEM.186.1.47>
- Shukla, S. A., Rooney, M. S., Rajasagi, M., Tiao, G., Dixon, P. M., Lawrence, M. S., Stevens, J., Lane, W. J., Dellagatta, J. L., Steelman, S., Sougnez, C., Cibulskis, K., Kiezun, A., Hacohen, N., Brusic, V., Wu, C. J., & Getz, G. (2015). Comprehensive analysis of cancer-associated somatic mutations in class I HLA genes. *Nature Biotechnology* 2015 33:11, 33(11), 1152–1158. <https://doi.org/10.1038/nbt.3344>
- Shussman, N., & Wexner, S. D. (2014). Colorectal polyps and polyposis syndromes. *Gastroenterology Report*, 2(1), 1–15. <https://doi.org/10.1093/GASTRO/GOT041>
- Sibille, C., Chomez, P., Wildmann, C., Van Pel, A., De Plaen, E., Maryanski, J. L., de Bergeyck, V., & Boon, T. (1990). Structure of the gene of tum- transplantation antigen P198: a point mutation generates a new antigenic peptide. *Journal of Experimental Medicine*, 172(1), 35–45. <https://doi.org/10.1084/JEM.172.1.35>
- Siena, S., Sartore-Bianchi, A., Di Nicolantonio, F., Balfour, J., & Bardelli, A. (2009). Biomarkers Predicting Clinical Outcome of Epidermal Growth Factor Receptor–Targeted Therapy in Metastatic Colorectal Cancer. *JNCI: Journal of the National Cancer Institute*, 101(19), 1308–1324. <https://doi.org/10.1093/JNCI/DJP280>
- Singh, N., Lee, Y. G., Shestova, O., Ravikumar, P., Hayer, K. E., Hong, S. J., Lu, X. M., Pajarillo, R., Agarwal, S., Kuramitsu, S., Orlando, E. J., Mueller, K. T., Good, C. R., Berger, S. L., Shalem, O., Weitzman, M. D., Frey, N. V., Maude, S. L., Grupp, S. A., ... Ruella, M. (2020). Impaired death receptor signaling in leukemia causes antigen-independent resistance by inducing CAR T-cell dysfunction. *Cancer Discovery*, 10(4), 552–567. <https://doi.org/10.1158/2159-8290.CD-19-0813/333456/AM/IMPAIRED-DEATH-RECEPTOR-SIGNALING-IN-LEUKEMIA>
- Śledzińska, A., Vila de Mucha, M., Bergerhoff, K., Hotblack, A., Demane, D. F., Ghorani, E., Akarca, A. U., Marzolini, M. A. V., Solomon, I., Vargas, F. A., Pule, M., Ono, M., Seddon, B., Kassiotis, G., Ariyan, C. E., Korn, T., Marafioti, T., Lord, G. M., Stauss, H., ... Quezada, S. A. (2020). Regulatory T Cells Restrain Interleukin-2- and Blimp-1-Dependent Acquisition of Cytotoxic Function by CD4+ T Cells. *Immunity*, 52(1), 151-166.e6. <https://doi.org/10.1016/J.IMMUNI.2019.12.007>

- Smith, L. K., Boukhaled, G. M., Condotta, S. A., Mazouz, S., Guthmiller, J. J., Vijay, R., Butler, N. S., Bruneau, J., Shoukry, N. H., Krawczyk, C. M., & Richer, M. J. (2018). Interleukin-10 Directly Inhibits CD8+ T Cell Function by Enhancing N-Glycan Branching to Decrease Antigen Sensitivity. *Immunity*, *48*(2), 299-312.e5. <https://doi.org/10.1016/J.IMMUNI.2018.01.006>
- Smyth, M. J., Strobl, S. L., Young, H. A., Ortaldo, J. R., & Ochoa, A. C. (1991). Regulation of lymphokine-activated killer activity and pore-forming protein gene expression in human peripheral blood CD8+ T lymphocytes. Inhibition by transforming growth factor-beta. *The Journal of Immunology*, *146*(10), 3289–3297. <https://doi.org/10.4049/JIMMUNOL.146.10.3289>
- Sojka, D. K., Huang, Y. H., & Fowell, D. J. (2008). Mechanisms of regulatory T-cell suppression – a diverse arsenal for a moving target. *Immunology*, *124*(1), 13. <https://doi.org/10.1111/J.1365-2567.2008.02813.X>
- Song, M., Ping, Y., Zhang, K., Yang, L., Li, F., Zhang, C., Cheng, S., Yue, D., Maimela, N. R., Qu, J., Liu, S., Sun, T., Li, Z., Xia, J., Zhang, B., Wang, L., & Zhang, Y. (2019). Low-dose IFN γ induces tumor cell stemness in tumor microenvironment of non-small cell lung cancer. *Cancer Research*, *79*(14), 3737–3748. <https://doi.org/10.1158/0008-5472.CAN-19-0596/653746/AM/LOW-DOSE-IFN-INDUCES-TUMOR-CELL-STEMNESS-IN-THE>
- Souglakos, J., Philips, J., Wang, R., Marwah, S., Silver, M., Tzardi, M., Silver, J., Ogino, S., Hooshmand, S., Kwak, E., Freed, E., Meyerhardt, J. A., Saridaki, Z., Georgoulas, V., Finkelstein, D., Fuchs, C. S., Kulke, M. H., & Shivdasani, R. A. (2009). Prognostic and predictive value of common mutations for treatment response and survival in patients with metastatic colorectal cancer. *British Journal of Cancer* *2009 101:3*, *101*(3), 465–472. <https://doi.org/10.1038/sj.bjc.6605164>
- Sow, H. S., Ren, J., Camps, M., Ossendorp, F., & Ten Dijke, P. (2019). Combined Inhibition of TGF- β Signaling and the PD-L1 Immune Checkpoint Is Differentially Effective in Tumor Models. *Cells* *2019, Vol. 8, Page 320*, *8*(4), 320. <https://doi.org/10.3390/CELLS8040320>
- Spees, A. M., Kingsbury, D. D., Wangdi, T., Xavier, M. N., Tsohis, R. M., & Bäumlner, A. J. (2014). Neutrophils are a source of gamma interferon during acute Salmonella enterica serovar typhimurium colitis. *Infection and Immunity*, *82*(4), 1692–1697. https://doi.org/10.1128/IAI.01508-13/SUPPL_FILE/ZII999090581SO1.PDF
- Spranger, S., Bao, R., & Gajewski, T. F. (2015). Melanoma-intrinsic β -catenin signalling prevents anti-tumour immunity. *Nature* *2015 523:7559*, *523*(7559), 231–235. <https://doi.org/10.1038/nature14404>
- Spranger, S., Dai, D., Horton, B., & Gajewski, T. F. (2017). Tumor-Residing Batf3 Dendritic Cells Are Required for Effector T Cell Trafficking and Adoptive T Cell Therapy. *Cancer Cell*, *31*(5), 711-723.e4. <https://doi.org/10.1016/j.ccell.2017.04.003>
- Stalder, T., Hahn, S., & Erb, P. (1994). Fas antigen is the major target molecule for CD4+ T cell-mediated cytotoxicity. *The Journal of Immunology*, *152*(3), 1127–1133. <https://doi.org/10.4049/JIMMUNOL.152.3.1127>
- Stanilov, N., Miteva, L., Deliysky, T., Jovchev, J., & Stanilova, S. (2010). Advanced Colorectal Cancer Is Associated With Enhanced IL-23 and IL-10 Serum Levels.

Laboratory Medicine, 41(3), 159–163.
<https://doi.org/10.1309/LM7T43AQZIUPIOWZ>

- Stein, A., Binder, M., Goekkurt, E., Lorenzen, S., Riera-Knorrenschild, J., Depenbusch, R., Ettrich, T. J., Doerfel, S., Al-Batran, S.-E., Karthaus, M., Pelzer, U., Simnica, D., Waberer, L., Hinke, A., Bokemeyer, C., & Hegewisch-Becker, S. (2020). Avelumab and cetuximab in combination with FOLFOX in patients with previously untreated metastatic colorectal cancer (MCRC): Final results of the phase II AVETUX trial (AIO-KRK-0216). *Journal of Clinical Oncology*, 38(4_suppl), 96–96. https://doi.org/10.1200/JCO.2020.38.4_SUPPL.96
- Steinbrink, K., Graulich, E., Kubsch, S., Knop, J., & Enk, A. H. (2002). CD4(+) and CD8(+) anergic T cells induced by interleukin-10-treated human dendritic cells display antigen-specific suppressor activity. *Blood*, 99(7), 2468–2476. <https://doi.org/10.1182/BLOOD.V99.7.2468>
- Steinbrink, K., Jonuleit, H., Müller, G., Schuler, G., Knop, J., & Enk, A. H. (1999). Interleukin-10–Treated Human Dendritic Cells Induce a Melanoma–Antigen–Specific Anergy in CD8+ T Cells Resulting in a Failure to Lyse Tumor Cells. *Blood*, 93(5), 1634–1642. <https://doi.org/10.1182/BLOOD.V93.5.1634>
- Steinbrink, K., Wolfl, M., Jonuleit, H., Knop, J., & Enk, A. H. (1997). Induction of tolerance by IL-10-treated dendritic cells. *The Journal of Immunology*, 159(10), 4772–4780. <https://doi.org/10.4049/JIMMUNOL.159.10.4772>
- Stockinger, B., & Omenetti, S. (2017). The dichotomous nature of T helper 17 cells. *Nature Reviews Immunology* 2017 17:9, 17(9), 535–544. <https://doi.org/10.1038/nri.2017.50>
- Strickler, J., Cercek, A., Siena, S., André, T., Ng, K., Van Cutsem, E., Wu, C., Paulson, A., Hubbard, J., Coveler, A., Fountzilias, C., Kardosh, A., Kasi, P., Lenz, H., Ciombor, K., Elez, E., Bajor, D., Stecher, M., Feng, W., & Bekaii-Saab, T. (2022). LBA-2 Primary analysis of MOUNTAINEER: A phase 2 study of tucatinib and trastuzumab for HER2-positive mCRC. *Annals of Oncology*, 33, S375–S376. <https://doi.org/10.1016/j.annonc.2022.04.440>
- Stüber, T., Monjezi, R., Wallstabe, L., Kühnemundt, J., Nietzer, S. L., Dandekar, G., Wöckel, A., Einsele, H., Wischhusen, J., & Hudecek, M. (2020). Inhibition of TGF-β-receptor signaling augments the antitumor function of ROR1-specific CAR T-cells against triple-negative breast cancer. *Journal for ImmunoTherapy of Cancer*, 8(1), e000676. <https://doi.org/10.1136/JITC-2020-000676>
- Subramanian, A., Tamayo, P., Mootha, V. K., Mukherjee, S., Ebert, B. L., Gillette, M. A., Paulovich, A., Pomeroy, S. L., Golub, T. R., Lander, E. S., & Mesirov, J. P. (2005). Gene set enrichment analysis: A knowledge-based approach for interpreting genome-wide expression profiles. *Proceedings of the National Academy of Sciences of the United States of America*, 102(43), 15545–15550. https://doi.org/10.1073/PNAS.0506580102/SUPPL_FILE/06580FIG7.JPG
- Sullivan, K. M., Jiang, X., Guha, P., Lausted, C., Carter, J. A., Hsu, C., Labadie, K. P., Kohli, K., Kenerson, H. L., Daniel, S. K., Yan, X., Meng, C., Abbasi, A., Chan, M., Seo, Y. D., Park, J. O., Crispe, I. N., Yeung, R. S., Kim, T. S., ... Pillarisetty, V. G. (2023). Blockade of interleukin 10 potentiates antitumour immune function in

human colorectal cancer liver metastases. *Gut*, 72(2), 325–337.
<https://doi.org/10.1136/GUTJNL-2021-325808>

- Sullivan, K. M., Jiang, X., Seo, Y. D., Kenerson, H. L., Yan, X., Lausted, C., Meng, C., Jabbari, N., Labadie, K. P., Daniel, S. K., Tian, Q., Kim, T. S., Yeung, R. S., & Pillarisetty, V. G. (2019). Abstract 4489: IL-10 blockade reactivates antitumor immunity in human colorectal cancer liver metastases. *Cancer Research*, 79(13_Supplement), 4489–4489. <https://doi.org/10.1158/1538-7445.AM2019-4489>
- Sutherland, R. M., McCredie, J. A., & Inch, W. R. (1971). Growth of Multicell Spheroids in Tissue Culture as a Model of Nodular Carcinomas. *JNCI: Journal of the National Cancer Institute*, 46(1), 113–120. <https://doi.org/10.1093/JNCI/46.1.113>
- Svane, I. M., Engel, A. M., Nielsen, M. B., Ljunggren, H. G., Rygaard, J., & Werdelin, O. (1996). Chemically induced sarcomas from nude mice are more immunogenic than similar sarcomas from congenic normal mice. *European Journal of Immunology*, 26(8), 1844–1850. <https://doi.org/10.1002/EJI.1830260827>
- Szabo, P. A., Levitin, H. M., Miron, M., Snyder, M. E., Senda, T., Yuan, J., Cheng, Y. L., Bush, E. C., Dogra, P., Thapa, P., Farber, D. L., & Sims, P. A. (2019). Single-cell transcriptomics of human T cells reveals tissue and activation signatures in health and disease. *Nature Communications* 2019 10:1, 10(1), 1–16. <https://doi.org/10.1038/s41467-019-12464-3>
- Tabernero, J., Grothey, A., van Cutsem, E., Yaeger, R., Wasan, H., Yoshino, T., Desai, J., Ciardiello, F., Loupakis, F., Hong, Y. S., Steeghs, N., Guren, T. K., Arkenau, H. T., Garcia-Alfonso, P., Elez, E., Gollerkeri, A., Maharry, K., Christy-Bittel, J., & Kopetz, S. (2021). Encorafenib plus cetuximab as a new standard of care for previously treated BRAF V600E-mutant metastatic colorectal cancer: Updated survival results and subgroup analyses from the BEACON study. *Journal of Clinical Oncology*, 39(4), 273–284. <https://doi.org/10.1200/JCO.20.02088>
- Tabernero, J., Melero, I., Ros, W., Argiles, G., Marabelle, A., Rodriguez-Ruiz, M. E., Albanell, J., Calvo, E., Moreno, V., Cleary, J. M., Eder, J. P., Karanikas, V., Bouseida, S., Sandoval, F., Sabanes, D., Sreckovic, S., Hurwitz, H., Paz-Ares, L. G., Suarez, J. M. S., & Segal, N. H. (2017). Phase Ia and Ib studies of the novel carcinoembryonic antigen (CEA) T-cell bispecific (CEA CD3 TCB) antibody as a single agent and in combination with atezolizumab: Preliminary efficacy and safety in patients with metastatic colorectal cancer (mCRC). *Journal of Clinical Oncology*, 35(15_suppl), 3002–3002. https://doi.org/10.1200/JCO.2017.35.15_SUPPL.3002
- Tabernero, J., Yoshino, T., Cohn, A. L., Obermannova, R., Bodoky, G., Garcia-Carbonero, R., Ciuleanu, T. E., Portnoy, D. C., Van Cutsem, E., Grothey, A., Prausová, J., Garcia-Alfonso, P., Yamazaki, K., Clingan, P. R., Lonardi, S., Kim, T. W., Simms, L., Chang, S. C., & Nasroulah, F. (2015). Ramucirumab versus placebo in combination with second-line FOLFIRI in patients with metastatic colorectal carcinoma that progressed during or after first-line therapy with bevacizumab, oxaliplatin, and a fluoropyrimidine (RAISE): a randomised, double-blind, multicentre, phase 3 study. *The Lancet Oncology*, 16(5), 499–508. [https://doi.org/10.1016/S1470-2045\(15\)70127-0](https://doi.org/10.1016/S1470-2045(15)70127-0)
- Taga, K., Mostowski, H., & Tosato, G. (1993). Human interleukin-10 can directly inhibit T-cell growth. *Blood*, 81(11), 2964–2971. <https://doi.org/10.1182/BLOOD.V81.11.2964.2964>

- Takahashi, H., Sakakura, K., Kudo, T., Toyoda, M., Kaira, K., Oyama, T., & Chikamatsu, K. (2017). Cancer-associated fibroblasts promote an immunosuppressive microenvironment through the induction and accumulation of protumoral macrophages. *Oncotarget*, *8*(5), 8633. <https://doi.org/10.18632/ONCOTARGET.14374>
- Takenaka, K., Moriguchi, T., & Nishida, E. (1998). Activation of the Protein Kinase p38 in the Spindle Assembly Checkpoint and Mitotic Arrest. *Science*, *280*(5363), 599–661. <https://doi.org/10.1126/SCIENCE.280.5363.599>
- Tang, D., & Kang, R. (2022). Glimmers of hope for targeting oncogenic KRAS-G12D. *Cancer Gene Therapy 2022 30:3*, *30*(3), 391–393. <https://doi.org/10.1038/s41417-022-00561-3>
- Tang, N., Cheng, C., Zhang, X., Qiao, M., Li, N., Mu, W., Wei, X. F., Han, W., & Wang, H. (2020). TGF- β inhibition via CRISPR promotes the long-term efficacy of CAR T cells against solid tumors. *JCI Insight*, *5*(4). <https://doi.org/10.1172/JCI.INSIGHT.133977>
- Tang, P. A., Cohen, S. J., Kollmannsberger, C., Bjarnason, G., Virik, K., MacKenzie, M. J., Lourenco, L., Wang, L., Chen, A., & Moore, M. J. (2012). Phase II clinical and pharmacokinetic study of aflibercept in patients with previously treated metastatic colorectal cancer. *Clinical Cancer Research*, *18*(21), 6023–6031. <https://doi.org/10.1158/1078-0432.CCR-11-3252/84880/AM/PHASE-II-CLINICAL-AND-PHARMACOKINETIC-STUDY-OF>
- Tang, Y., Xu, X., Guo, S., Zhang, C., Tang, Y., Tian, Y., Ni, B., Lu, B., & Wang, H. (2014). An Increased Abundance of Tumor-Infiltrating Regulatory T Cells Is Correlated with the Progression and Prognosis of Pancreatic Ductal Adenocarcinoma. *PLOS ONE*, *9*(3), e91551. <https://doi.org/10.1371/JOURNAL.PONE.0091551>
- Tannenbaum, C. S., Tubbs, R., Armstrong, D., Finke, J. H., Bukowski, R. M., & Hamilton, T. A. (1998). The CXC Chemokines IP-10 and Mig Are Necessary for IL-12-Mediated Regression of the Mouse RENCA Tumor. *The Journal of Immunology*, *161*(2), 927–932. <https://doi.org/10.4049/JIMMUNOL.161.2.927>
- Taube, J. M., Anders, R. A., Young, G. D., Xu, H., Sharma, R., McMiller, T. L., Chen, S., Klein, A. P., Pardoll, D. M., Topalian, S. L., & Chen, L. (2012). Colocalization of Inflammatory Response with B7-H1 Expression in Human Melanocytic Lesions Supports an Adaptive Resistance Mechanism of Immune Escape. *Science Translational Medicine*, *4*(127), 127ra37. <https://doi.org/10.1126/SCITRANSLMED.3003689>
- Taube, J. M., Klein, A., Brahmer, J. R., Xu, H., Pan, X., Kim, J. H., Chen, L., Pardoll, D. M., Topalian, S. L., & Anders, R. A. (2014). Association of PD-1, PD-1 ligands, and other features of the tumor immune microenvironment with response to anti-PD-1 therapy. *Clinical Cancer Research*, *20*(19), 5064–5074. <https://doi.org/10.1158/1078-0432.CCR-13-3271/176301/AM/ASSOCIATION-OF-PD-1-PD-1-LIGANDS-AND-OTHER>
- Tauriello, D. V. F., Palomo-Ponce, S., Stork, D., Berenguer-Llargo, A., Badia-Ramentol, J., Iglesias, M., Sevillano, M., Ibiza, S., Cañellas, A., Hernando-Momblona, X., Byrom, D., Matarin, J. A., Calon, A., Rivas, E. I., Nebreda, A. R.,

- Riera, A., Attolini, C. S. O., & Batlle, E. (2018). TGF β drives immune evasion in genetically reconstituted colon cancer metastasis. *Nature* 2018 554:7693, 554(7693), 538–543. <https://doi.org/10.1038/nature25492>
- Tawbi, H. A., Schadendorf, D., Lipson, E. J., Ascierto, P. A., Matamala, L., Castillo Gutiérrez, E., Rutkowski, P., Gogas, H. J., Lao, C. D., De Menezes, J. J., Dalle, S., Arance, A., Grob, J.-J., Srivastava, S., Abaskharoun, M., Hamilton, M., Keidel, S., Simonsen, K. L., Sobiesk, A. M., ... Long, G. V. (2022). Relatlimab and Nivolumab versus Nivolumab in Untreated Advanced Melanoma. *New England Journal of Medicine*, 386(1), 24–34. https://doi.org/10.1056/NEJMOA2109970/SUPPL_FILE/NEJMOA2109970_DATA-SHARING.PDF
- Tecchio, C., Micheletti, A., & Cassatella, M. A. (2014). Neutrophil-derived cytokines: Facts beyond expression. *Frontiers in Immunology*, 5. <https://doi.org/10.3389/FIMMU.2014.00508/BIBTEX>
- Tesniere, A., Schlemmer, F., Boige, V., Kepp, O., Martins, I., Ghiringhelli, F., Aymeric, L., Michaud, M., Apetoh, L., Barault, L., Mendiboure, J., Pignon, J. P., Jooste, V., Van Endert, P., Ducreux, M., Zitvogel, L., Piard, F., & Kroemer, G. (2009). Immunogenic death of colon cancer cells treated with oxaliplatin. *Oncogene* 2010 29:4, 29(4), 482–491. <https://doi.org/10.1038/onc.2009.356>
- Textor, A., Listopad, J. J., Wührmann, L. Le, Perez, C., Kruschinski, A., Chmielewski, M., Abken, H., Blankenstein, T., & Charo, J. (2014). Efficacy of CAR T-cell therapy in large tumors relies upon stromal targeting by IFN γ . *Cancer Research*, 74(23), 6796–6805. <https://doi.org/10.1158/0008-5472.CAN-14-0079/657677/AM/EFFICACY-OF-CAR-T-CELL-THERAPY-IN-LARGE-TUMORS>
- Thakur, A., Schalk, D., Sarkar, S. H., Al-Khadimi, Z., Sarkar, F. H., & Lum, L. G. (2012). A Th1 cytokine-enriched microenvironment enhances tumor killing by activated T cells armed with bispecific antibodies and inhibits the development of myeloid-derived suppressor cells. *Cancer Immunology, Immunotherapy*, 61(4), 497–509. <https://doi.org/10.1007/S00262-011-1116-1/FIGURES/6>
- Thakur, A., Schalk, D., Tomaszewski, E., Kondadasula, S. V., Yano, H., Sarkar, F. H., & Lum, L. G. (2013). Microenvironment generated during EGFR targeted killing of pancreatic tumor cells by ATC inhibits myeloid-derived suppressor cells through COX2 and PGE2 dependent pathway. *Journal of Translational Medicine*, 11(1), 1–10. <https://doi.org/10.1186/1479-5876-11-35/FIGURES/5>
- Thomas, D. A., & Massagué, J. (2005). TGF- β directly targets cytotoxic T cell functions during tumor evasion of immune surveillance. *Cancer Cell*, 8(5), 369–380. <https://doi.org/10.1016/J.CCR.2005.10.012>
- Thomassen, M. J., Divis, L. T., & Fisher, C. J. (1996). Regulation of Human Alveolar Macrophage Inflammatory Cytokine Production by Interleukin-10. *Clinical Immunology and Immunopathology*, 80(3), 321–324. <https://doi.org/10.1006/CLIN.1996.0130>
- Tiriác, H., Belleau, P., Engle, D. D., Plenker, D., Deschênes, A., Somerville, T. D. D., Froeling, F. E. M., Burkhart, R. A., Denroche, R. E., Jang, G. H., Miyabayashi, K., Young, C. M., Patel, H., Ma, M., Lacombe, J. F., Palmaira, R. L. D., Javed, A. A., Huynh, J. C., Johnson, M., ... Tuveson, D. A. (2018). Organoid profiling identifies

common responders to chemotherapy in pancreatic cancer. *Cancer Discovery*, 8(9), 1112–1129. <https://doi.org/10.1158/2159-8290.CD-18-0349/42871/AM/ORGANOID-PROFILING-IDENTIFIES-COMMON-RESPONDERS-TO>

- Tivol, E. A., Borriello, F., Schweitzer, A. N., Lynch, W. P., Bluestone, J. A., & Sharpe, A. H. (1995). Loss of CTLA-4 leads to massive lymphoproliferation and fatal multiorgan tissue destruction, revealing a critical negative regulatory role of CTLA-4. *Immunity*, 3(5), 541–547. [https://doi.org/10.1016/1074-7613\(95\)90125-6](https://doi.org/10.1016/1074-7613(95)90125-6)
- Todaro, M., Zerilli, M., Ricci-Vitiani, L., Bini, M., Alea, M. P., Florena, A. M., Miceli, L., Condorelli, G., Bonventre, S., Di Gesù, G., De Maria, R., & Stassi, G. (2006). Autocrine Production of Interleukin-4 and Interleukin-10 Is Required for Survival and Growth of Thyroid Cancer Cells. *Cancer Research*, 66(3), 1491–1499. <https://doi.org/10.1158/0008-5472.CAN-05-2514>
- Tokunaga, R., Zhang, W., Naseem, M., Puccini, A., Berger, M. D., Soni, S., McSkane, M., Baba, H., & Lenz, H. J. (2018). CXCL9, CXCL10, CXCL11/CXCR3 axis for immune activation – A target for novel cancer therapy. *Cancer Treatment Reviews*, 63, 40–47. <https://doi.org/10.1016/J.CTRV.2017.11.007>
- Tone, Y., Furuuchi, K., Kojima, Y., Tykocinski, M. L., Greene, M. I., & Tone, M. (2007). Smad3 and NFAT cooperate to induce Foxp3 expression through its enhancer. *Nature Immunology* 2007 9:2, 9(2), 194–202. <https://doi.org/10.1038/ni1549>
- Topalian, S. L., Hodi, F. S., Brahmer, J. R., Gettinger, S. N., Smith, D. C., McDermott, D. F., Powderly, J. D., Carvajal, R. D., Sosman, J. A., Atkins, M. B., Leming, P. D., Spigel, D. R., Antonia, S. J., Horn, L., Drake, C. G., Pardoll, D. M., Chen, L., Sharfman, W. H., Anders, R. A., ... Sznol, M. (2012). Safety, Activity, and Immune Correlates of Anti-PD-1 Antibody in Cancer. *New England Journal of Medicine*, 366(26), 2443–2454. https://doi.org/10.1056/NEJMOA1200690/SUPPL_FILE/NEJMOA1200690_DISCLOSURES.PDF
- Topp, M. S., Kufer, P., Gökbüget, N., Goebeler, M., Klinger, M., Neumann, S., Horst, H. A., Raff, T., Viardot, A., Schmid, M., Stelljes, M., Schaich, M., Degenhard, E., Köhne-Volland, R., Brüggemann, M., Ottmann, O., Pfeifer, H., Burmeister, T., Nagorsen, D., ... Bargou, R. C. (2011). Targeted therapy with the T-cell - Engaging antibody blinatumomab of chemotherapy-refractory minimal residual disease in B-lineage acute lymphoblastic leukemia patients results in high response rate and prolonged leukemia-free survival. *Journal of Clinical Oncology*, 29(18), 2493–2498. <https://doi.org/10.1200/JCO.2010.32.7270>
- Torre, L. A., Bray, F., Siegel, R. L., Ferlay, J., Lortet-Tieulent, J., & Jemal, A. (2015). Global cancer statistics, 2012. *CA: A Cancer Journal for Clinicians*, 65(2), 87–108. <https://doi.org/10.3322/CAAC.21262>
- Tournigand, C., André, T., Achille, E., Lledo, G., Flesh, M., Mery-Mignard, D., Quinaux, E., Couteau, C., Buyse, M., Ganem, G., Landi, B., Colin, P., Louvet, C., & De Gramont, A. (2004). FOLFIRI followed by FOLFOX6 or the reverse sequence in advanced colorectal cancer: A randomized GERCOR study. *Journal of Clinical Oncology*, 22(2), 229–237. <https://doi.org/10.1200/JCO.2004.05.113>

- Townsend, A. R. M., Rothbard, J., Gotch, F. M., Bahadur, G., Wraith, D., & McMichael, A. J. (1986). The epitopes of influenza nucleoprotein recognized by cytotoxic T lymphocytes can be defined with short synthetic peptides. *Cell*, *44*(6), 959–968. [https://doi.org/10.1016/0092-8674\(86\)90019-X](https://doi.org/10.1016/0092-8674(86)90019-X)
- Tran, B., Horvath, L., Dorff, T., Rettig, M., Lolkema, M. P., Machiels, J.-P., Rottey, S., Autio, K., Greil, R., Adra, N., Lemech, C., Minocha, M., Cheng, F.-C., Kouros-Mehr, H., & Fizazi, K. (2020). 609O Results from a phase I study of AMG 160, a half-life extended (HLE), PSMA-targeted, bispecific T-cell engager (BiTE®) immune therapy for metastatic castration-resistant prostate cancer (mCRPC). *Annals of Oncology*, *31*, S507. <https://doi.org/10.1016/J.ANNONC.2020.08.869>
- Tran, E., Robbins, P. F., Lu, Y.-C., Prickett, T. D., Gartner, J. J., Jia, L., Pasetto, A., Zheng, Z., Ray, S., Groh, E. M., Kriley, I. R., & Rosenberg, S. A. (2016). T-Cell Transfer Therapy Targeting Mutant KRAS in Cancer. *New England Journal of Medicine*, *375*(23), 2255–2262. https://doi.org/10.1056/NEJMOA1609279/SUPPL_FILE/NEJMOA1609279_DISCLOSURES.PDF
- Travis, M. A., & Sheppard, D. (2014). TGF- β Activation and Function in Immunity. *Annual Review of Immunology*, *32*, 51–82. <https://doi.org/10.1146/ANNUREV-IMMUNOL-032713-120257>
- Triebel, F., Jitsukawa, S., Baixeras, E., Roman-Roman, S., Genevee, C., Viegas-Pequignot, E., & Hercend, T. (1990). LAG-3, a novel lymphocyte activation gene closely related to CD4. *Journal of Experimental Medicine*, *171*(5), 1393–1405. <https://doi.org/10.1084/JEM.171.5.1393>
- Troy, A., Davidson, P., Atkinson, C., & Hart, D. (1998). PHENOTYPIC CHARACTERISATION OF THE DENDRITIC CELL INFILTRATE IN PROSTATE CANCER. *The Journal of Urology*, *160*(1), 214–219. [https://doi.org/10.1016/S0022-5347\(01\)63093-3](https://doi.org/10.1016/S0022-5347(01)63093-3)
- Troy, A. J., Summers, K. L., Davidson, P. J. T., Atkinson, C. H., Hart, D. N. J., Immunology, H. /, & Group, R. (1998). *Minimal Recruitment and Activation of Dendritic Cells within Renal Cell Carcinoma*. *4*, 585–593. <http://aacrjournals.org/clincancerres/article-pdf/4/3/585/2069875/585.pdf>
- Tsai, S., McOlash, L., Palen, K., Johnson, B., Duris, C., Yang, Q., Dwinell, M. B., Hunt, B., Evans, D. B., Gershan, J., & James, M. A. (2018). Development of primary human pancreatic cancer organoids, matched stromal and immune cells and 3D tumor microenvironment models. *BMC Cancer*, *18*(1), 1–13. <https://doi.org/10.1186/S12885-018-4238-4/FIGURES/6>
- Tsukamoto, H., Nishikata, R., Senju, S., & Nishimura, Y. (2013). Myeloid-derived suppressor cells attenuate TH1 development through IL-6 production to promote tumor progression. *Cancer Immunology Research*, *1*(1), 64–76. <https://doi.org/10.1158/2326-6066.CIR-13-0030/471013/P/MYELOID-DERIVED-SUPPRESSOR-CELLS-ATTENUATE-TH1>
- Tumeh, P. C., Harview, C. L., Yearley, J. H., Shintaku, I. P., Taylor, E. J. M., Robert, L., Chmielowski, B., Spasic, M., Henry, G., Ciobanu, V., West, A. N., Carmona, M., Kivork, C., Seja, E., Cherry, G., Gutierrez, A. J., Grogan, T. R., Mateus, C., Tomasic, G., ... Ribas, A. (2014). PD-1 blockade induces responses by inhibiting

- adaptive immune resistance. *Nature* 2014 515:7528, 515(7528), 568–571. <https://doi.org/10.1038/nature13954>
- Türeci, Ö., Sahin, U., Zwick, C., Koslowski, M., Seitz, G., & Pfreundschuh, M. (1998). Identification of a meiosis-specific protein as a member of the class of cancer/testis antigens. *Proceedings of the National Academy of Sciences of the United States of America*, 95(9), 5211. <https://doi.org/10.1073/PNAS.95.9.5211>
- Upadhyay, R., Boiarsky, J. A., Pantsulaia, G., Svensson-Arvelund, J., Lin, M. J., Wroblewska, A., Bhalla, S., Scholler, N., Bot, A., Rossi, J. M., Sadek, N., Parekh, S., Lagana, A., Baccarini, A., Merad, M., Brown, B. D., & Brody, J. D. (2021). A critical role for fas-mediated off-target tumor killing in T cell immunotherapy. *Cancer Discovery*, 11(3), 599. <https://doi.org/10.1158/2159-8290.CD-20-0756>
- Valle, L., Vilar, E., Tavtigian, S. V., & Stoffel, E. M. (2019). Genetic predisposition to colorectal cancer: syndromes, genes, classification of genetic variants and implications for precision medicine. *The Journal of Pathology*, 247(5), 574–588. <https://doi.org/10.1002/PATH.5229>
- Van Cutsem, E., Cervantes, A., Nordlinger, B., Arnold, D., & The ESMO Guidelines Working Group. (2014). Metastatic colorectal cancer: ESMO clinical practice guidelines for diagnosis, treatment and follow-up. *Annals of Oncology*, 25, iii1–iii9. <https://doi.org/10.1093/annonc/mdu260>
- Van Cutsem, E., Köhne, C.-H., Hitre, E., Zaluski, J., Chang Chien, C.-R., Makhson, A., D’Haens, G., Pintér, T., Lim, R., Bodoky, G., Roh, J. K., Folprecht, G., Ruff, P., Stroh, C., Tejpar, S., Schlichting, M., Nippgen, J., & Rougier, P. (2009). Cetuximab and Chemotherapy as Initial Treatment for Metastatic Colorectal Cancer. *New England Journal of Medicine*, 360(14), 1408–1417. https://doi.org/10.1056/NEJMOA0805019/SUPPL_FILE/NEJM_VAN_CUTSEM_1408SA1.PDF
- Van Cutsem, E., Tabernero, J., Lakomy, R., Prenen, H., Prausová, J., Macarulla, T., Ruff, P., Van Hazel, G. A., Moiseyenko, V., Ferry, D., McKendrick, J., Polikoff, J., Tellier, A., Castan, R., & Allegra, C. (2012). Addition of aflibercept to fluorouracil, leucovorin, and irinotecan improves survival in a phase III randomized trial in patients with metastatic colorectal cancer previously treated with an oxaliplatin-based regimen. *Journal of Clinical Oncology*, 30(28), 3499–3506. <https://doi.org/10.1200/JCO.2012.42.8201>
- Van Den Eynde, B., Lethé, B., Van Pel, A., De Plaen, E., & Boon, T. (1991). The gene coding for a major tumor rejection antigen of tumor P815 is identical to the normal gene of syngeneic DBA/2 mice. *Journal of Experimental Medicine*, 173(6), 1373–1384. <https://doi.org/10.1084/JEM.173.6.1373>
- Van der Bruggen, P., Zhang, Y., Chaux, P., Stroobant, V., Panichelli, C., Schultz, E. S., Chapiro, J., Van den Eynde, B. J., Brossmer, F., & Boon, T. (2002). Tumor-specific shared antigenic peptides recognized by human T cells. *Immunological Reviews*, 188(1), 51–64. <https://doi.org/10.1034/J.1600-065X.2002.18806.X>
- van der Burg, S. H., & Melief, C. J. M. (2011). Therapeutic vaccination against human papilloma virus induced malignancies. *Current Opinion in Immunology*, 23(2), 252–257. <https://doi.org/10.1016/J.COI.2010.12.010>

- Van Elsas, A., Hurwitz, A. A., & Allison, J. P. (1999). Combination Immunotherapy of B16 Melanoma Using Anti-Cytotoxic T Lymphocyte-Associated Antigen 4 (Ctla-4) and Granulocyte/Macrophage Colony-Stimulating Factor (Gm-Csf)-Producing Vaccines Induces Rejection of Subcutaneous and Metastatic Tumors Accompanied by Autoimmune Depigmentation. *Journal of Experimental Medicine*, *190*(3), 355–366. <https://doi.org/10.1084/JEM.190.3.355>
- Van Laarhoven, H. W. M., Kaanders, J. H. A. M., Lok, J., Peeters, W. J. M., Rijken, P. F. J. W., Wiering, B., Ruers, T. J. M., Punt, C. J. A., Heerschap, A., & Van Der Kogel, A. J. (2006). Hypoxia in relation to vasculature and proliferation in liver metastases in patients with colorectal cancer. *International Journal of Radiation Oncology*Biophysics*, *64*(2), 473–482. <https://doi.org/10.1016/J.IJROBP.2005.07.982>
- Van Rooij, N., Van Buuren, M. M., Philips, D., Velds, A., Toebes, M., Heemskerk, B., Van Dijk, L. J. A., Behjati, S., Hilkmann, H., El Atmioui, D., Nieuwland, M., Stratton, M. R., Kerkhoven, R. M., Keşmir, C., Haanen, J. B., Kvistborg, P., & Schumacher, T. N. (2013). Tumor exome analysis reveals neoantigen-specific T-cell reactivity in an ipilimumab-responsive melanoma. *Journal of Clinical Oncology*, *31*(32). <https://doi.org/10.1200/JCO.2012.47.7521>
- Vaupel, P. (2004). Tumor microenvironmental physiology and its implications for radiation oncology. *Seminars in Radiation Oncology*, *14*(3), 198–206. <https://doi.org/10.1016/J.SEMRADONC.2004.04.008>
- Venook, A. P., Niedzwiecki, D., Lenz, H.-J., Innocenti, F., Fruth, B., Meyerhardt, J. A., Schrag, D., Greene, C., O'neil, B. H., James, J., Atkins, N., Berry, S., Polite, B. N., O'reilly, E. M., Goldberg, R. M., Hochster, H. S., Schilsky, R. L., Bertagnolli, M. M., El-Khoueiry, A. B., ... Venook, A. (2017). Effect of First-Line Chemotherapy Combined With Cetuximab or Bevacizumab on Overall Survival in Patients With KRAS Wild-Type Advanced or Metastatic Colorectal Cancer: A Randomized Clinical Trial. *JAMA*, *317*(23), 2392–2401. <https://doi.org/10.1001/JAMA.2017.7105>
- Vermeulen, L., De Sousa E Melo, F., van der Heijden, M., Cameron, K., de Jong, J. H., Borovski, T., Tuynman, J. B., Todaro, M., Merz, C., Rodermond, H., Sprick, M. R., Kemper, K., Richel, D. J., Stassi, G., & Medema, J. P. (2010). Wnt activity defines colon cancer stem cells and is regulated by the microenvironment. *Nature Cell Biology*, *12*(5), 468–476. <https://doi.org/10.1038/ncb2048>
- Vlachogiannis, G., Hedayat, S., Vatsiou, A., Jamin, Y., Fernández-Mateos, J., Khan, K., Lampis, A., Eason, K., Huntingford, I., Burke, R., Rata, M., Koh, D. M., Tunariu, N., Collins, D., Hulkki-Wilson, S., Ragulan, C., Spiteri, I., Moorcraft, S. Y., Chau, I., ... Valeri, N. (2018). Patient-derived organoids model treatment response of metastatic gastrointestinal cancers. *Science*, *359*(6378), 920–926. https://doi.org/10.1126/SCIENCE.AAO2774/SUPPL_FILE/AAO2774_VLACHOGIANNIS_SM_TABLES_S1_AND_S3_TO_S8.XLSX
- von Boehmer, L., Mattle, M., Bode, P., Landshammer, A., Schäfer, C., Nuber, N., Ritter, G., Old, L., Moch, H., Schäfer, N., Jäger, E., Knuth, A., & van den Broek, M. (2013). NY-ESO-1-specific immunological pressure and escape in a patient with metastatic melanoma. *Cancer Immunity*, *13*(3). <https://doi.org/10.1158/1424-9634.DCL-12.13.3>

- Voron, T., Colussi, O., Marcheteau, E., Pernot, S., Nizard, M., Pointet, A. L., Latreche, S., Bergaya, S., Benhamouda, N., Tanchot, C., Stockmann, C., Combe, P., Berger, A., Zinzindohoue, F., Yagita, H., Tartour, E., Taieb, J., & Terme, M. (2015). VEGF-A modulates expression of inhibitory checkpoints on CD8+ T cells in tumors. *Journal of Experimental Medicine*, *212*(2), 139–148. <https://doi.org/10.1084/JEM.20140559>
- Waal Malefyt, R. De, Haanen, J., Spits, H., Koncarolo, M. G., Te Velde, A., Figdor, C., Johnson, K., Kastelein, R., Yssel, H., & De Vries, J. E. (1991). Interleukin 10 (IL-10) and viral IL-10 strongly reduce antigen-specific human T cell proliferation by diminishing the antigen-presenting capacity of monocytes via downregulation of class II major histocompatibility complex expression. *Journal of Experimental Medicine*, *174*(4), 915–924. <https://doi.org/10.1084/JEM.174.4.915>
- Waalder, J., Machon, O., Tumova, L., Dinh, H., Korinek, V., Wilson, S. R., Paulsen, J. E., Pedersen, N. M., Eide, T. J., Machonova, O., Gradl, D., Voronkov, A., Von Kries, J. P., & Krauss, S. (2012). A novel tankyrase inhibitor decreases canonical Wnt signaling in colon carcinoma cells and reduces tumor growth in conditional APC mutant mice. *Cancer Research*, *72*(11), 2822–2832. <https://doi.org/10.1158/0008-5472.CAN-11-3336/650166/AM/A-NOVEL-TANKYRASE-INHIBITOR-DECREASES-CANONICAL>
- WADA, J., SUZUKI, H., FUCHINO, R., YAMASAKI, A., NAGAI, S., YANAI, K., KOGA, K., NAKAMURA, M., TANAKA, M., MORISAKI, T., & KATANO, M. (2009). The Contribution of Vascular Endothelial Growth Factor to the Induction of Regulatory T-Cells in Malignant Effusions. *Anticancer Research*, *29*(3).
- Waldhauer, I., Gonzalez-Nicolini, V., Freimoser-Grundschober, A., Nayak, T. K., Fahrni, L., Hosse, R. J., Gerrits, D., Geven, E. J. W., Sam, J., Lang, S., Bommer, E., Steinhart, V., Husar, E., Colombetti, S., Van Puijenbroek, E., Neubauer, M., Cline, J. M., Garg, P. K., Dugan, G., ... Klein, C. (2021). Simlukafusp alfa (FAP-IL2v) immunocytokine is a versatile combination partner for cancer immunotherapy. *MAbs*, *13*(1). https://doi.org/10.1080/19420862.2021.1913791/SUPPL_FILE/KMAB_A_1913791_SM0281.DOCX
- Waldner, M. J., & Neurath, M. F. (2009). Colitis-associated cancer: The role of T cells in tumor development. *Seminars in Immunopathology*, *31*(2), 249–256. <https://doi.org/10.1007/S00281-009-0161-8/FIGURES/1>
- Wallin, J., Pishvaian, M. J., Hernandez, G., Yadav, M., Jhunjunwala, S., Delamarre, L., He, X., Powderly, J., Lieu, C., Eckhardt, S. G., Hurwitz, H., Hochster, H. S., Murphy, J., Leveque, V., Cha, E., Funke, R., Waterkamp, D., Hegde, P., & Bendell, J. (2016). Abstract 2651: Clinical activity and immune correlates from a phase Ib study evaluating atezolizumab (anti-PDL1) in combination with FOLFOX and bevacizumab (anti-VEGF) in metastatic colorectal carcinoma. *Cancer Research*, *76*(14_Supplement), 2651–2651. <https://doi.org/10.1158/1538-7445.AM2016-2651>
- Wang, D., & DuBois, R. N. (2018). Role of prostanoids in gastrointestinal cancer. *The Journal of Clinical Investigation*, *128*(7), 2732–2742. <https://doi.org/10.1172/JCI97953>

- Wang, T., Niu, G., Kortylewski, M., Burdelya, L., Shain, K., Zhang, S., Bhattacharya, R., Gabrilovich, D., Heller, R., Coppola, D., Dalton, W., Jove, R., Pardoll, D., & Yu, H. (2003). Regulation of the innate and adaptive immune responses by Stat-3 signaling in tumor cells. *Nature Medicine* 2004 10:1, 10(1), 48–54. <https://doi.org/10.1038/nm976>
- Waterhouse, P., Penninger, J. M., Timms, E., Wakeham, A., Shahinian, A., Lee, K. P., Thompson, C. B., Griesser, H., & Mak, T. W. (1995). Lymphoproliferative Disorders with Early Lethality in Mice Deficient in Ctl α -4. *Science*, 270(5238), 985–988. <https://doi.org/10.1126/SCIENCE.270.5238.985>
- Weaver, V. M., Lelièvre, S., Lakins, J. N., Chrenek, M. A., Jones, J. C. R., Giancotti, F., Werb, Z., & Bissell, M. J. (2002). β 4 integrin-dependent formation of polarized three-dimensional architecture confers resistance to apoptosis in normal and malignant mammary epithelium. *Cancer Cell*, 2(3), 205–216. [https://doi.org/10.1016/S1535-6108\(02\)00125-3](https://doi.org/10.1016/S1535-6108(02)00125-3)
- Weber, J., Salgaller, M., Samid, D., Johnson, B., Herlyn, M., Lassam, N., Treisman, J., & Rosenberg, S. (1994). Expression of the MAGE-1 Tumor Antigen Is Up-Regulated by the Demethylating Agent 5-Aza-2'-Deoxycytidine. *Cancer Research*, 54(7), 1766–1771. <https://aacrjournals.org/cancerres/article/54/7/1766/501036/Expression-of-the-MAGE-1-Tumor-Antigen-Is-Up>
- Wei, S. C., Levine, J. H., Cogdill, A. P., Zhao, Y., Anang, N. A. A. S., Andrews, M. C., Sharma, P., Wang, J., Wargo, J. A., Pe'er, D., & Allison, J. P. (2017). Distinct Cellular Mechanisms Underlie Anti-CTLA-4 and Anti-PD-1 Checkpoint Blockade. *Cell*, 170(6), 1120-1133.e17. <https://doi.org/10.1016/J.CELL.2017.07.024>
- Weide, B., Eigentler, T. K., Pflugfelder, A., Zelba, H., Martens, A., Pawelec, G., Giovannoni, L., Ruffini, P. A. delchi, Elia, G., Neri, D., Gutzmer, R., Becker, J. C., & Garbe, C. (2014). Intralesional treatment of stage III metastatic melanoma patients with L19-IL2 results in sustained clinical and systemic immunologic responses. *Cancer Immunology Research*, 2(7), 668–678. <https://doi.org/10.1158/2326-6066.CIR-13-0206/466982/AM/INTRALESIONAL-TREATMENT-OF-STAGE-III-METASTATIC>
- Weigelin, B., & Friedl, P. (2010). A three-dimensional organotypic assay to measure target cell killing by cytotoxic T lymphocytes. *Biochemical Pharmacology*, 80(12), 2087–2091. <https://doi.org/10.1016/J.BCP.2010.09.004>
- Westendorf, A. M., Skibbe, K., Adamczyk, A., Buer, J., Geffers, R., Hansen, W., Pastille, E., & Jendrossek, V. (2017). Hypoxia Enhances Immunosuppression by Inhibiting CD4+ Effector T Cell Function and Promoting Treg Activity. *Cellular Physiology and Biochemistry*, 41(4), 1271–1284. <https://doi.org/10.1159/000464429>
- Whiteside, T. L. (2002a). Apoptosis of immune cells in the tumor microenvironment and peripheral circulation of patients with cancer: implications for immunotherapy. *Vaccine*, 20(SUPPL. 4), A46–A51. [https://doi.org/10.1016/S0264-410X\(02\)00387-0](https://doi.org/10.1016/S0264-410X(02)00387-0)

- Whiteside, T. L. (2002b). Tumor-induced death of immune cells: Its mechanisms and consequences. *Seminars in Cancer Biology*, 12(1), 43–50. <https://doi.org/10.1006/SCBI.2001.0402>
- Wilcox, R. A., Tamada, K., Flies, D. B., Zhu, G., Chapoval, A. I., Blazar, B. R., Kast, W. M., & Chen, L. (2004). Ligation of CD137 receptor prevents and reverses established anergy of CD8+ cytolytic T lymphocytes in vivo. *Blood*, 103(1), 177–184. <https://doi.org/10.1182/BLOOD-2003-06-2184>
- Wing, K., Onishi, Y., Prieto-Martin, P., Yamaguchi, T., Miyara, M., Fehervari, Z., Nomura, T., & Sakaguchi, S. (2008). CTLA-4 control over Foxp3+ regulatory T cell function. *Science*, 322(5899), 271–275. https://doi.org/10.1126/SCIENCE.1160062/SUPPL_FILE/WING.SOM.PDF
- Witko-Sarsat, V., Rieu, P., Descamps-Latscha, B., Lesavre, P., & Halbwachs-Mecarelli, L. (2000). Neutrophils: Molecules, Functions and Pathophysiological Aspects. *Laboratory Investigation* 2000 80:5, 80(5), 617–653. <https://doi.org/10.1038/labinvest.3780067>
- Wolf, A. M., Wolf, D., Steurer, M., Gastl, G., Gunsilius, E., & Grubeck-Loebenstien, B. (2003). Increase of Regulatory T Cells in the Peripheral Blood of Cancer Patients. *Clinical Cancer Research*, 9(2), 606–612. <http://aacrjournals.org/clincancerres/article-pdf/9/2/606/2086643/df0203000606.pdf>
- Wolf, E., Hofmeister, R., Kufer, P., Schlereth, B., & Baeuerle, P. A. (2005). BiTEs: bispecific antibody constructs with unique anti-tumor activity. *Drug Discovery Today*, 10(18), 1237–1244. [https://doi.org/10.1016/S1359-6446\(05\)03554-3](https://doi.org/10.1016/S1359-6446(05)03554-3)
- Wolf, K., Müller, R., Borgmann, S., Bröcker, E. B., & Friedl, P. (2003). Amoeboid shape change and contact guidance: T-lymphocyte crawling through fibrillar collagen is independent of matrix remodeling by MMPs and other proteases. *Blood*, 102(9), 3262–3269. <https://doi.org/10.1182/BLOOD-2002-12-3791>
- Wölfel, T., Hauer, M., Schneider, J., Serrano, M., Wölfel, C., Klehmann-Hieb, E., De Plaen, E., Hankeln, T., Meyer Zum Büschenfelde, K. H., & Beach, D. (1995). A p16INK4a-Insensitive CDK4 Mutant Targeted by Cytolytic T Lymphocytes in a Human Melanoma. *Science*, 269(5228), 1281–1284. <https://doi.org/10.1126/SCIENCE.7652577>
- Wolk, K., Kunz, S., Asadullah, K., & Sabat, R. (2002). Cutting Edge: Immune Cells as Sources and Targets of the IL-10 Family Members? *The Journal of Immunology*, 168(11), 5397–5402. <https://doi.org/10.4049/JIMMUNOL.168.11.5397>
- Woo, S. R., Turnis, M. E., Goldberg, M. V., Bankoti, J., Selby, M., Nirschl, C. J., Bettini, M. L., Gravano, D. M., Vogel, P., Liu, C. L., Tansombatvisit, S., Grosso, J. F., Netto, G., Smeltzer, M. P., Chaux, A., Utz, P. J., Workman, C. J., Pardoll, D. M., Korman, A. J., ... Vignali, D. A. A. (2012). Immune inhibitory molecules LAG-3 and PD-1 synergistically regulate T-cell function to promote tumoral immune escape. *Cancer Research*, 72(4), 917–927. <https://doi.org/10.1158/0008-5472.CAN-11-1620/649950/AM/IMMUNE-INHIBITORY-MOLECULES-LAG-3-AND-PD-1>
- Woolston, A., Khan, K., Spain, G., Barber, L. J., Griffiths, B., Gonzalez-Exposito, R., Hornsteiner, L., Punta, M., Patil, Y., Newey, A., Mansukhani, S., Davies, M. N., Furness, A., Sclafani, F., Peckitt, C., Jiménez, M., Kouvelakis, K., Ranftl, R.,

- Begum, R., ... Gerlinger, M. (2019). Genomic and Transcriptomic Determinants of Therapy Resistance and Immune Landscape Evolution during Anti-EGFR Treatment in Colorectal Cancer. *Cancer Cell*, *36*(1), 35-50.e9. <https://doi.org/10.1016/J.CCELL.2019.05.013>
- Workman, C. J., Cauley, L. S., Kim, I.-J., Blackman, M. A., Woodland, D. L., & Vignali, D. A. A. (2004). Lymphocyte Activation Gene-3 (CD223) Regulates the Size of the Expanding T Cell Population Following Antigen Activation In Vivo. *The Journal of Immunology*, *172*(9), 5450–5455. <https://doi.org/10.4049/JIMMUNOL.172.9.5450>
- Workman, C. J., & Vignali, D. A. A. (2005). Negative Regulation of T Cell Homeostasis by Lymphocyte Activation Gene-3 (CD223). *The Journal of Immunology*, *174*(2), 688–695. <https://doi.org/10.4049/JIMMUNOL.174.2.688>
- Xie, Y., Akpinarli, A., Maris, C., Hipkiss, E. L., Lane, M., Kwon, E. K. M., Muranski, P., Restifo, N. P., & Antony, P. A. (2010). Naive tumor-specific CD4+ T cells differentiated in vivo eradicate established melanoma. *Journal of Experimental Medicine*, *207*(3), 651–667. <https://doi.org/10.1084/JEM.20091921>
- Xu, Y., Chaudhury, A., Zhang, M., Savoldo, B., Metelitsa, L. S., Rodgers, J., Yustein, J. T., Neilson, J. R., & Dotti, G. (2016). Glycolysis determines dichotomous regulation of T cell subsets in hypoxia. *The Journal of Clinical Investigation*, *126*(7), 2678–2688. <https://doi.org/10.1172/JCI85834>
- Yamada, A., Arakaki, R., Saito, M., Kudo, Y., & Ishimaru, N. (2017). Dual role of Fas/FasL-mediated signal in peripheral immune tolerance. *Frontiers in Immunology*, *8*(APR), 403. <https://doi.org/10.3389/FIMMU.2017.00403/BIBTEX>
- Yan, C., Hu, Y., Zhang, B., Mu, L., Huang, K., Zhao, H., Ma, C., Li, X., Tao, D., Gong, J., & Qin, J. (2016). The CEA-*lo* colorectal cancer cell population harbors cancer stem cells and metastatic cells. *Oncotarget*, *7*(49), 80700. <https://doi.org/10.18632/ONCOTARGET.13029>
- Yang, L., DeBusk, L. M., Fukuda, K., Fingleton, B., Green-Jarvis, B., Shyr, Y., Matrisian, L. M., Carbone, D. P., & Lin, P. C. (2004). Expansion of myeloid immune suppressor Gr+CD11b+ cells in tumor-bearing host directly promotes tumor angiogenesis. *Cancer Cell*, *6*(4), 409–421. <https://doi.org/10.1016/J.CCR.2004.08.031>
- Yang, R., Peng, Y., Pi, J., Liu, Y., Yang, E., Shen, X., Yao, L., Shen, L., Modlin, R. L., Shen, H., Sha, W., & Chen, Z. W. (2021). A CD4+CD161+ T-Cell Subset Present in Unexposed Humans, Not Tb Patients, Are Fast Acting Cells That Inhibit the Growth of Intracellular Mycobacteria Involving CD161 Pathway, Perforin, and IFN- γ /Autophagy. *Frontiers in Immunology*, *12*, 599641. <https://doi.org/10.3389/FIMMU.2021.599641/BIBTEX>
- Yang, R., Yang, E., Shen, L., Modlin, R. L., Shen, H., & Chen, Z. W. (2018). IL-12+IL-18 Cossignaling in Human Macrophages and Lung Epithelial Cells Activates Cathelicidin and Autophagy, Inhibiting Intracellular Mycobacterial Growth. *The Journal of Immunology*, *200*(7), 2405–2417. <https://doi.org/10.4049/JIMMUNOL.1701073>
- Yang, X., Letterio, J. J., Lechleider, R. J., Chen, L., Hayman, R., Gu, H., Roberts, A. B., Deng, C., Yang, X., & Letterio, J. J. (1999). Targeted disruption of SMAD3 results

- in impaired mucosal immunity and diminished T cell responsiveness to TGF- β . *The EMBO Journal*, 18(5), 1280–1291. <https://doi.org/10.1093/EMBOJ/18.5.1280>
- Yee, A. S., Paulson, E. K., McDevitt, M. A., Rieger-Christ, K., Summerhayes, I., Berasi, S. P., Kim, J., Huang, C. Y., & Zhang, X. (2004). The HBP1 transcriptional repressor and the p38 MAP kinase: unlikely partners in G1 regulation and tumor suppression. *Gene*, 336(1), 1–13. <https://doi.org/10.1016/J.GENE.2004.04.004>
- Yi, M., Wu, Y., Niu, M., Zhu, S., Zhang, J., Yan, Y., Zhou, P., Dai, Z., & Wu, K. (2022). Original research: Anti-TGF- β /PD-L1 bispecific antibody promotes T cell infiltration and exhibits enhanced antitumor activity in triple-negative breast cancer. *Journal for Immunotherapy of Cancer*, 10(12), 5543. <https://doi.org/10.1136/JITC-2022-005543>
- Yi, M., Zhang, J., Li, A., Niu, M., Yan, Y., Jiao, Y., Luo, S., Zhou, P., & Wu, K. (2021). The construction, expression, and enhanced anti-tumor activity of YM101: a bispecific antibody simultaneously targeting TGF- β and PD-L1. *Journal of Hematology and Oncology*, 14(1), 1–22. <https://doi.org/10.1186/S13045-021-01045-X/FIGURES/11>
- Yin, J., & Ferguson, T. A. (2009). Identification of an IFN- γ -Producing Neutrophil Early in the Response to *Listeria monocytogenes*. *The Journal of Immunology*, 182(11), 7069–7073. <https://doi.org/10.4049/JIMMUNOL.0802410>
- Yokota, T., Ura, T., Shibata, N., Takahari, D., Shitara, K., Nomura, M., Kondo, C., Mizota, A., Utsunomiya, S., Muro, K., & Yatabe, Y. (2011). BRAF mutation is a powerful prognostic factor in advanced and recurrent colorectal cancer. *British Journal of Cancer* 2011 104:5, 104(5), 856–862. <https://doi.org/10.1038/bjc.2011.19>
- Yonesaka, K., Zejnullahu, K., Okamoto, I., Satoh, T., Cappuzzo, F., Souglakos, J., Ercan, D., Rogers, A., Roncalli, M., Takeda, M., Fujisaka, Y., Philips, J., Shimizu, T., Maenishi, O., Cho, Y., Sun, J., Destro, A., Taira, K., Takeda, K., ... Jänne, P. A. (2011). Activation of ERBB2 signaling causes resistance to the EGFR-directed therapeutic antibody cetuximab. *Science Translational Medicine*, 3(99). https://doi.org/10.1126/SCITRANSLMED.3002442/SUPPL_FILE/3-99RA86_SM.PDF
- Yu, M., Guo, G., Huang, L., Deng, L., Chang, C. S., Achyut, B. R., Canning, M., Xu, N., Arbab, A. S., Bollag, R. J., Rodriguez, P. C., Mellor, A. L., Shi, H., Munn, D. H., & Cui, Y. (2020). CD73 on cancer-associated fibroblasts enhanced by the A2B-mediated feedforward circuit enforces an immune checkpoint. *Nature Communications*, 11(1), 1–17. <https://doi.org/10.1038/s41467-019-14060-x>
- Yu, Q., Sharma, A., Oh, S. Y., Moon, H. G., Hossain, Z. M., Salay, T. M., Leeds, K. E., Du, H., Wu, B., Waterman, M. L., Zhu, Z., & Sen, J. M. (2009). T cell factor 1 initiates the T helper type 2 fate by inducing the transcription factor GATA-3 and repressing interferon- γ . *Nature Immunology* 2009 10:9, 10(9), 992–999. <https://doi.org/10.1038/ni.1762>
- Yu, S., Li, A., Liu, Q., Li, T., Yuan, X., Han, X., & Wu, K. (2017). Chimeric antigen receptor T cells: a novel therapy for solid tumors. *Journal of Hematology & Oncology* 2017 10:1, 10(1), 1–13. <https://doi.org/10.1186/S13045-017-0444-9>

- Zacharakis, N., Chinnasamy, H., Black, M., Xu, H., Lu, Y. C., Zheng, Z., Pasetto, A., Langhan, M., Shelton, T., Prickett, T., Gartner, J., Jia, L., Trebska-McGowan, K., Somerville, R. P., Robbins, P. F., Rosenberg, S. A., Goff, S. L., & Feldman, S. A. (2018). Immune recognition of somatic mutations leading to complete durable regression in metastatic breast cancer. *Nature Medicine* 24:6, 24(6), 724–730. <https://doi.org/10.1038/s41591-018-0040-8>
- Zaretsky, J. M., Garcia-Diaz, A., Shin, D. S., Escuin-Ordinas, H., Hugo, W., Hu-Lieskovan, S., Torrejon, D. Y., Abril-Rodriguez, G., Sandoval, S., Barthly, L., Saco, J., Homet Moreno, B., Mezzadra, R., Chmielowski, B., Ruchalski, K., Shintaku, I. P., Sanchez, P. J., Puig-Saus, C., Cherry, G., ... Ribas, A. (2016). Mutations Associated with Acquired Resistance to PD-1 Blockade in Melanoma. *New England Journal of Medicine*, 375(9), 819–829. https://doi.org/10.1056/NEJMOA1604958/SUPPL_FILE/NEJMOA1604958_DISCLOSURES.PDF
- Zaunders, J. J., Dyer, W. B., Wang, B., Munier, M. L., Miranda-Saksena, M., Newton, R., Moore, J., Mackay, C. R., Cooper, D. A., Saksena, N. K., & Kelleher, A. D. (2004). Identification of circulating antigen-specific CD4+ T lymphocytes with a CCR5+, cytotoxic phenotype in an HIV-1 long-term nonprogressor and in CMV infection. *Blood*, 103(6), 2238–2247. <https://doi.org/10.1182/BLOOD-2003-08-2765>
- Zhang, C., Wang, Z., Yang, Z., Wang, M., Li, S., Li, Y., Zhang, R., Xiong, Z., Wei, Z., Shen, J., Luo, Y., Zhang, Q., Liu, L., Qin, H., Liu, W., Wu, F., Chen, W., Pan, F., Zhang, X., ... Qian, C. (2017). Phase I Escalating-Dose Trial of CAR-T Therapy Targeting CEA+ Metastatic Colorectal Cancers. *Molecular Therapy*, 25(5), 1248–1258. <https://doi.org/10.1016/J.YMTHE.2017.03.010>
- Zhang, F., Liu, G., Li, D., Wei, C., & Hao, J. (2018). DDIT4 and Associated IncDDIT4 Modulate Th17 Differentiation through the DDIT4/TSC/mTOR Pathway. *The Journal of Immunology*, 200(5), 1618–1626. <https://doi.org/10.4049/JIMMUNOL.1601689>
- Zhang, L., Conejo-Garcia, J. R., Katsaros, D., Gimotty, P. A., Massobrio, M., Regnani, G., Makrigiannakis, A., Gray, H., Schlienger, K., Liebman, M. N., Rubin, S. C., & Coukos, G. (2003). Intratumoral T Cells, Recurrence, and Survival in Epithelial Ovarian Cancer. *New England Journal of Medicine*, 348(3), 203–213. https://doi.org/10.1056/NEJMOA020177/SUPPL_FILE/NEJM_ZHANG_203SA1-4.PDF
- Zhang, Q. wen, Liu, L., Gong, C. yang, Shi, H. shan, Zeng, Y. hui, Wang, X. ze, Zhao, Y. wei, & Wei, Y. quan. (2012). Prognostic Significance of Tumor-Associated Macrophages in Solid Tumor: A Meta-Analysis of the Literature. *PLOS ONE*, 7(12), e50946. <https://doi.org/10.1371/JOURNAL.PONE.0050946>
- Zhang, R., Qi, F., Zhao, F., Li, G., Shao, S., Zhang, X., Yuan, L., & Feng, Y. (2019). Cancer-associated fibroblasts enhance tumor-associated macrophages enrichment and suppress NK cells function in colorectal cancer. *Cell Death & Disease*, 10(4). <https://doi.org/10.1038/S41419-019-1435-2>
- Zhao, S., Wu, D., Wu, P., Wang, Z., Huang, J., & Gao, J. X. (2015). Serum IL-10 Predicts Worse Outcome in Cancer Patients: A Meta-Analysis. *PLOS ONE*, 10(10), e0139598. <https://doi.org/10.1371/JOURNAL.PONE.0139598>

- Zhao, X., Yang, J., Zhang, X., Lu, X. A., Xiong, M., Zhang, J., Zhou, X., Qi, F., He, T., Ding, Y., Hu, X., De Smet, F., Lu, P., & Huang, X. (2020). Efficacy and Safety of CD28- or 4-1BB-Based CD19 CAR-T Cells in B Cell Acute Lymphoblastic Leukemia. *Molecular Therapy - Oncolytics*, *18*, 272–281. <https://doi.org/10.1016/j.omto.2020.06.016>
- Zheng, C., Zheng, L., Yoo, J. K., Guo, H., Zhang, Y., Guo, X., Kang, B., Hu, R., Huang, J. Y., Zhang, Q., Liu, Z., Dong, M., Hu, X., Ouyang, W., Peng, J., & Zhang, Z. (2017). Landscape of Infiltrating T Cells in Liver Cancer Revealed by Single-Cell Sequencing. *Cell*, *169*(7), 1342-1356.e16. <https://doi.org/10.1016/J.CELL.2017.05.035>
- Zhong, B., Cheng, B., Huang, X., Xiao, Q., Niu, Z., Chen, Y. feng, Yu, Q., Wang, W., & Wu, X. J. (2021). Colorectal cancer-associated fibroblasts promote metastasis by up-regulating LRG1 through stromal IL-6/STAT3 signaling. *Cell Death & Disease* *2021 13:1*, *13*(1), 1–15. <https://doi.org/10.1038/s41419-021-04461-6>
- Zhong, W., Myers, J. S., Wang, F., Wang, K., Lucas, J., Rosfjord, E., Lucas, J., Hooper, A. T., Yang, S., Lemon, L. A., Guffroy, M., May, C., Bienkowska, J. R., & Rejto, P. A. (2020). Comparison of the molecular and cellular phenotypes of common mouse syngeneic models with human tumors. *BMC Genomics* *2019 21:1*, *21*(1), 1–17. <https://doi.org/10.1186/S12864-019-6344-3>
- Zhou, H., Stanners, C. P., & Fuks2, A. (1993). Specificity of Anti-Carcinoembryonic Antigen Monoclonal Antibodies and Their Effects on CEA-mediated Adhesion1. *Cancer Research*, 3817–3822. <http://aacrjournals.org/cancerres/article-pdf/53/16/3817/2450853/cr0530163817.pdf>
- Zhu, G., Pei, L., Xia, H., Tang, Q., & Bi, F. (2021). Role of oncogenic KRAS in the prognosis, diagnosis and treatment of colorectal cancer. *Molecular Cancer* *2021 20:1*, *20*(1), 1–17. <https://doi.org/10.1186/S12943-021-01441-4>
- Zhu, X., & Zhu, J. (2020). CD4 T Helper Cell Subsets and Related Human Immunological Disorders. *International Journal of Molecular Sciences* *2020, Vol. 21, Page 8011*, *21*(21), 8011. <https://doi.org/10.3390/IJMS21218011>
- Zhu, Y., Knolhoff, B. L., Meyer, M. A., Nywening, T. M., West, B. L., Luo, J., Wang-Gillam, A., Goedegebuure, S. P., Linehan, D. C., & De Nardo, D. G. (2014). CSF1/CSF1R blockade reprograms tumor-infiltrating macrophages and improves response to T-cell checkpoint immunotherapy in pancreatic cancer models. *Cancer Research*, *74*(18), 5057–5069. <https://doi.org/10.1158/0008-5472.CAN-13-3723/657718/AM/CSF1-CSF1R-BLOCKADE-REPROGRAMS-TUMOR-INFILTRATING>
- Ziani, L., Chouaib, S., & Thiery, J. (2018). Alteration of the antitumor immune response by cancer-associated fibroblasts. *Frontiers in Immunology*, *9*(MAR), 414. <https://doi.org/10.3389/FIMMU.2018.00414/BIBTEX>
- Ziogas, A. C., Gavalas, N. G., Tsiatas, M., Tsitsilonis, O., Politi, E., Terpos, E., Rodolakis, A., Vlahos, G., Thomakos, N., Haidopoulos, D., Antsaklis, A., Dimopoulos, M. A., & Bamias, A. (2012). VEGF directly suppresses activation of T cells from ovarian cancer patients and healthy individuals via VEGF receptor Type 2. *International Journal of Cancer*, *130*(4), 857–864. <https://doi.org/10.1002/IJC.26094>

Zocche, D. M., Ramirez, C., Fontao, F. M., Costa, L. D., & Redal, M. A. (2015). Global impact of KRAS mutation patterns in FOLFOX treated metastatic colorectal cancer. *Frontiers in Genetics*, 6(MAR), 116.
<https://doi.org/10.3389/FGENE.2015.00116/BIBTEX>